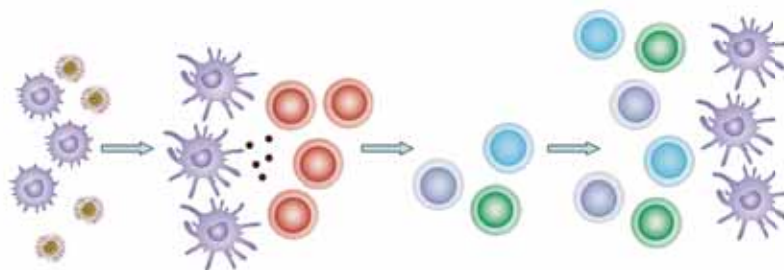
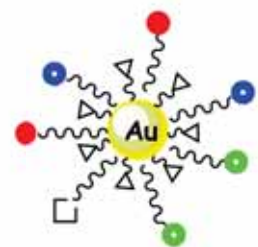
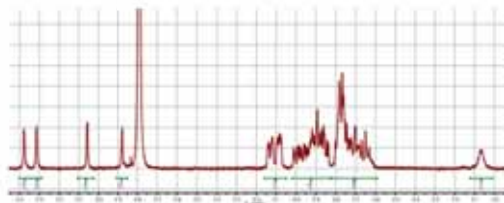
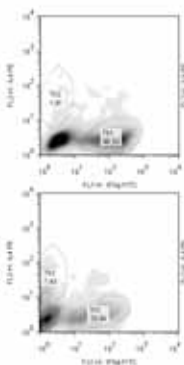


Gold Glyconanoparticles as Multivalent Nanocarriers for Carbohydrate-Antigens

Fabrizio Chiodo

2013



Gold glyco-nanoparticles as multivalent nanocarriers for carbohydrate-antigens.

Fabrizio Chiodo

Glyco-Nanotechnology Laboratory, Biofunctional Nanomaterials Unit,
CIC biomaGUNE.

2013

ANEXO X

AUTORIZACIÓN DEL DIRECTOR O DIRECTORA DE LA TESIS DOCTORAL PARA SU PRESENTACIÓN

Prof. Soledad Pénades Ullate con N.I.F 02683273R y Dr. Marco Marradi con N.I.E. X-7352065T como Directores de la Tesis Doctoral: Gold glyco-nanoparticles as multivalent nanocarriers for carbohydrate-antigens, realizada en el Glyconanotechnology Laboratory en el Centro de Investigación Cooperativa en Biomateriales (CIC biomaGUNE) y desarrollada en el Programa de Doctorado en Química Aplicada y Materiales Poliméricos, por el Doctorando Don Fabrizio Chiodo, autorizamos la presentación de la citada Tesis Doctoral, dado que reúne las condiciones necesarias para su defensa.

En San Sebastian, a de de 2013

EL/LA DIRECTOR/A DE LA TESIS

Fdo.: Soledad Pénades Ullate

Fdo.: Marco Marradi

1959-1960



Universidad
del País Vasco

Euskal Herriko
Unibertsitatea

ANEXO XI

AUTORIZACIÓN DE LA COMISIÓN ACADÉMICA DEL PROGRAMA DE DOCTORADO

La Comisión Académica del Programa de Doctorado en Química Aplicada y Materiales Poliméricos en reunión celebrada el día ____ de _____ de 2013, ha acordado dar la conformidad a la presentación de la Tesis Doctoral titulada: Gold glyco-nanoparticles as multivalent nanocarriers for carbohydrate-antigens, dirigida por: Prof. Soledad Pénades Ullate y Dr. Marco Marradi y presentada por Don Fabrizio Chiodo_e inscrita en el Departamento de Ciencia y Tecnología de Polímeros

En _____ a ____ de _____ de _____

EL COORDINADOR O COORDINADORA DEL PROGRAMA DE DOCTORADO

Fdo.: _____

1959-1960



Universidad del País Vasco
Euskal Herriko Unibertsitatea

ANEXO XII

ACTA DE GRADO DE DOCTOR O DOCTORA ACTA DE DEFENSA DE TESIS DOCTORAL

DOCTORANDO: Don Fabrizio Chiodo.

TITULO DE LA TESIS: Gold glyco-nanoparticles as multivalent nanocarriers for carbohydrate-antigens

El Tribunal designado por la Subcomisión de Doctorado de la UPV/EHU para calificar la Tesis Doctoral arriba indicada y reunido en el día de la fecha, una vez efectuada la defensa por el doctorando y contestadas las objeciones y/o sugerencias que se le han formulado, ha otorgado por _____ la calificación de:
unanimidad ó mayoría

--

APTO o NO APTO

Idioma/s de defensa (en caso de más de un idioma, especificar apartados o porcentaje defendido en cada idioma): _____

En _____ a _____ de _____ de _____

EL/LA PRESIDENTE/A,

EL/LA SECRETARIO/A,

Fdo.:

Fdo.:

Dr/a: _____

Dr/a: _____

VOCAL 1º,

VOCAL 2º,

VOCAL 3º,

Fdo.:

Fdo.:

Fdo.:

Dr/a: _____ Dr/a: _____ Dr/a: _____

EL/LA DOCTORANDO/A,

Fdo.: _____

1959-1960



Universidad del País Vasco
Euskal Herriko Unibertsitatea



**AUTORIZACION DEL PONENTE DE TESIS
PARA SU PRESENTACION**

Prof. Dr/a. Isabel Goñi Echave, como Ponente de la Tesis Doctoral:

Gold glyco-nanoparticles as multivalent nanocarriers for carbohydrate-antigens, realizada en el Laboratorio de Gliconanotecnología en el Centro de Investigación Cooperativa en Biomateriales (CIC biomaGUNE) y presentada en el Departamento de Ciencia y Tecnología de Polímeros por el Doctorando Don Fabrizio Chiodo, y dirigida por Prof. Soledad Pénades Ullate y Dr. Marco Marradi, autorizo la presentación de la citada Tesis Doctoral, dado que reúne las condiciones necesarias para su defensa.

En _____ a _____ de _____ de 2013

EL PONENTE DE LA TESIS

Fdo.: _____



CONFORMIDAD DEL DEPARTAMENTO

El Consejo del Departamento de Ciencia y Tecnología de Polímeros
en reunión celebrada el día de de 2013 ha acordado dar la conformidad a
la admisión a trámite de presentación
de la Tesis Doctoral titulada: Gold glyco-nanoparticles as multivalent nanocarriers for
carbohydrate-antigens, dirigida por: Prof. Soledad Pénades Ullate y Dr. Marco Marradi
y presentada por Don Fabrizio Chiodo_ante este Departamento.

En _____ a _____ de _____ de 2013.

Vº Bº DIRECTOR/A DEL DEPARTAMENTO SECRETARIO/A DEL DEPARTAMENTO

Fdo.: _____

Fdo.: _____

This Thesis has been carried out in the Laboratory of Glyconanotechnology, Biofunctional Nanomaterials Unit at Centro de Investigación Cooperativa en Biomateriales, CIC biomaGUNE, in San Sebastian, País Vasco, Spain.

The research developed during this Thesis was financially supported by a European pre-doctoral Marie Curie Fellowship (Glycogold project) and a fellowship from the Spanish Ministry of Science and Innovation (BES-2009-025533) associated to the project NANOBIOCEL (CTQ-2008-04638).

Abstract:

Gold glyco-nanoparticles as multivalent nanocarriers for carbohydrate-antigens.

Fabrizio Chiodo

Glyco-Nanotechnology Laboratory, Biofunctional Nanomaterials Unit, CIC
biomaGUNE.

Carbohydrates are one of the major classes of molecules exploited by evolution to maintain the complexity of life. Linked to proteins or lipids, carbohydrates are one of the main components of the outer surface of cells where they are involved in many cellular processes. There are many approaches to understand and intervene in carbohydrate-mediated interactions: One strategy consists in the design and preparation of synthetic chemical tools able to mimic the natural glycans presentation.

In this Thesis, multivalent and multifunctional gold nanoparticles coated with thiol-ending glycosides and/or drugs have been prepared to contribute in different biomedical fields where carbohydrates are involved. Gold nanoparticles coated with carbohydrate-antigens related to human immunodeficiency virus (HIV), *Streptococcus pneumoniae* and other parasites have been designed and prepared as biomimetic synthetic macromolecules for mimicking the carbohydrate presentation of these pathogens.

These gold glyco-nanoparticles have been exploited as drug delivery system against HIV, as carrier for carbohydrate-based vaccines against HIV and *S. pneumoniae* and as new and sensitive tool for the detection of biomarkers involved in parasitic infections. In addition, these biocompatible nanomaterials have been explored to study the role of different carbohydrates (non-self and self) in the dendritic cells-mediated innate immunity.

The results of this Thesis encourage the exploitation of gold glyco-nanoparticles in different field of glyco-science ranging from biomarkers detection to adaptive and innate immune response against carbohydrates.

Abstract

Resumen Tesis Fabrizio Chiodo:

Gold glyco-nanoparticles as multivalent nanocarriers for carbohydrate-antigens.

Los carbohidratos son una de las principales clases de moléculas empleadas en la evolución para mantener la complejidad de la vida. Conjugados a proteínas o lípidos, los carbohidratos son uno de los componentes principales de la membrana externa de las células sobre la cual participan en multitud de procesos celulares. Existen múltiples enfoques para comprender y actuar sobre las interacciones mediadas por carbohidratos: Una de estas estrategias consiste en el diseño y elaboración de herramientas químicas sintéticas capaces de imitar la presentación natural de dichos carbohidratos.

En este contexto, el objetivo principal de esta tesis consiste en explorar la potencialidad de la glico-nanotecnología para actuar sobre los procesos biológicos donde los carbohidratos están involucrados, mediante el diseño y la preparación de nanopartículas de oro polivalentes y multifuncionales recubiertas con carbohidratos (gliconanopartículas, GNPs) y otras moléculas (fármacos o péptidos).

Esta tesis se centra en dos importantes procesos que afectan a la salud humana: La infección por el virus de la inmunodeficiencia humana (VIH) y la neumonía bacteriana

causada por *Streptococcus pneumoniae*. El papel funcional de los carbohidratos en estos procesos será estudiado a nivel molecular y se desarrollarán algunas aplicaciones empleando las gliconanopartículas como herramientas químicas.

Los objetivos de la tesis se pueden resumir en dos partes. La primera parte (Parte-1) se refiere a la potencialidad de las GNPs como vehículos para medicamentos contra el VIH y como vehículos para antígenos basados en carbohidratos. Esta parte incluye la aplicación de las GNPs en diferentes estrategias para luchar contra las infecciones parasitarias. GNPs que portan medicamentos contra el VIH se explorarán como sistema de administración de fármacos contra el VIH (Capítulo-1); GNPs que llevan antígenos basados en carbohidratos se evaluarán como base para vacunas contra el VIH (Capítulo-2) y *S. pneumoniae* (Capítulo-3) y como herramientas sensibles para detectar marcadores biológicos implicados en infecciones parasitarias (Capítulo-4).

A continuación se describirá en detalle cada uno de los objetivos.

El primer objetivo de esta tesis es el desarrollo de gliconanopartículas de oro como herramienta química para abordar alternativas a las diferentes estrategias desarrolladas en los últimos años contra el virus de la inmunodeficiencia humana (VIH). La estrategia para alcanzar este objetivo incluye la preparación de GNPs: i) como sistema de administración de fármacos anti-VIH; ii) como replicas de los clústeres de carbohidratos ricos en manosa que cubren la glicoproteína gp120 de la envoltura de VIH para emplear las GNPs como potenciales vehículos de vacunas contra el VIH.

Este trabajo está relacionado con el proyecto europeo CHAARM, que tiene por objetivo el desarrollo de microbicidas para prevenir la infección por VIH (Capítulo-1).

El segundo tipo de gliconanopartículas se ha diseñado para elucidar los procesos donde están implicados los carbohidratos en la infección por VIH. Los glicanos con alto contenido en manosa (por ejemplo, el oligomanosido $\text{Man}_9\text{GlcNAc}_2$) de la glicoproteína gp120 de VIH (una de las proteínas más altamente glicosilada en la naturaleza) tienen un papel importante durante la infección viral y presentan una clase conservada de epítomos que se podría ser de utilidad en el diseño de vacunas contra el VIH. El diseño racional de estas gliconanopartículas tiene su origen en el descubrimiento del anticuerpo 2G12 que es capaz de interactuar con ramas de los oligomanosidos presente en la superficie de VIH. Por esa razón se han preparado GNPs recubiertas de oligomanosidos sintéticos como imitación de los grupos de carbohidratos ricos en manosa de la gp120. Estas GNPs se han utilizado para estudiar las interacciones moleculares del 2G12 por diferentes técnicas como por ejemplo Resonancia Magnética Nuclear (RMN). Basándose en estos resultados estructurales, los mejores oligomanosidos se han utilizado para preparar nanopartículas de oro como vehículos de vacunas contra el VIH. Con este propósito, un epítomo de las células T se ha añadido a la superficie de las GNPs para evocar una respuesta inmune adaptativa específica (Capítulo-2).

Una estrategia similar se ha extendido también a otros parásitos. Así, nanopartículas de oro fueron diseñadas también como vehículos de antígenos de *Streptococcus pneumoniae*. Esta bacteria está cubierta por un polisacárido capsular que es una molécula inmuno-activa capaz de inducir la producción de anticuerpos. Uno de los epítomos basados en carbohidratos de este polisacárido es un tetrasacárido ramificado que se ha conjugado con éxito a las GNPs para obtener vacunas sintéticas contra S.

pneumoniae. Se prepararon GNPs con una relación diferente entre el tetrasacárido sintético relacionado con el polisacárido capsular tipo *S. pneumoniae* 14 y el epítipo de células T y se ensayaron en ratones para estudiar la producción de anticuerpos contra el tetrasacárido. La inmunización de los ratones se realizó en el marco del proyecto europeo Glyco-gold. Los resultados de esta investigación se presentaran en el Capítulo-3.

En otro objetivo y con la idea de aumentar la sensibilidad de los métodos ya establecidos para la detección de anticuerpos frente a carbohidratos, se ha desarrollado un nuevo Enzyme-linked immunosorbent assay (ELISA) basado en la adsorción directa de GNPs sobre placas de ELISA. Este enfoque se extendió también a otros biomarcadores importantes relacionados con los carbohidratos y los resultados de este estudio se presentaran en el capítulo-4. La simplicidad, alta sensibilidad y versatilidad de este método puede facilitar los estudios básicos de interacciones proteína-carbohidrato que aportan información sobre los epítopos de carbohidratos que participan en el reconocimiento celular. Este método podría ser también útil para el desarrollo de vacunas basad en carbohidratos.

La segunda parte de la tesis (Parte-2) se compone de dos capítulos que abordar el papel de los carbohidratos en la inmunidad innata. Nanopartículas de oro recubiertas con carbohidratos han sido también empleadas para estudiar la influencia de la presentación multivalente de estos carbohidratos que se encuentran tanto en humanos como en parásitos, en la inmunidad innata mediada por células dendríticas.

GNPs cubiertas de galactofuranosa, oligomanosídeos o antígeno de Lewis se utilizaron para estudiar los marcadores de maduración y la producción de interleucinas en las células dendríticas. Las interacciones entre las células dendríticas y las células T

también fueron estudiadas. Los experimentos celulares se llevaron a cabo durante un período de seis meses de estancia en el Departamento de Biología Celular y Inmunología Molecular (MCBI) en la Vrije University Medical Center (VUmc) de Amsterdam. Los resultados de estos estudios biológicos se presentarán en el Capítulo-5 y 6 de esta Tesis.

Los resultados de esta tesis pretenden fomentar el uso de las gliconanopartículas en diferentes campos de la glicociencia, desde su uso para la detección de biomarcadores hasta el estudio de la respuesta inmune adaptativa e innata contra carbohidratos.

List of abbreviations

3TC: Lamivudine
ABC: Abacavir
AIDS: Acquired immunodeficiency syndrome
APC: antigen-presenting cells
AZT: Zidovudine
BSA: Bovine serum albumin
CLR: C-type lectin receptors
ConA: concanavalin-A
CRM₁₉₇: cross-reacting material of diphtheria toxin
DC: dendritic cell
DC-SIGN: Dendritic Cell-Specific Intercellular adhesion molecule-3-Grabbing Non-integrin
DDS: drug delivery system
DMAP: 4-dimethylaminopyridine
DNA: Deoxyribonucleic acid
EDC: ethyl-3-(3-(dimethylamino)-propyl)carbodiimide
EGTA: ethylene glycol tetra acetic acid
ELISA: Enzyme-Linked ImmunoSorbent Assay
Fab: fragment antigen binding
GNP: glyconanoparticle
HAART: highly active antiretroviral therapy
HIV: human immunodeficiency virus
HPLC: High-performance liquid chromatography
HRP: horseradish peroxidase
IC₅₀: half maximal inhibitory concentration
Ig: immunoglobulin
IL: interleukin
K_D: Dissociation constant
LAL: *Limulus* Amoebocyte Lysate
Lewis^X or Le^X: (Galβ1-4[Fucα1-3]GlcNAcβ1)
LPE: ligand place exchange
LPS: Lipopolysaccharide
MHC: major-histocompatibility complex
MLR: mixed leukocyte reaction
moDC: monocyte-derived dendritic cell
MPL: Monophosphoryl Lipid A
MW: molecular weight
NMR: Nuclear magnetic resonance
NNRTI: non-nucleoside RT inhibitor
NRTI: nucleoside analog reverse transcriptase inhibitor
PAMP: pathogen-associated molecular pattern
PBL: peripheral blood leucocytes
PBMC: peripheral blood mononuclear cell
PBS: Phosphate buffered saline
PC: phosphatidylcholine
Pn14PS: capsular polysaccharide of *S. pneumoniae* type 14
PRR: pattern recognition receptor

PX: Polymyxin B
RT: reverse transcriptase
SAM: self-assembled monolayer
SPR: Surface Plasmon Resonance
STD-NMR: Saturation Transfer Difference NMR spectroscopy
TACA: tumor-associated carbohydrate antigens
TBC: tuberculosis
TCR: T-cell receptor
TEM: Transmission electron microscopy
TetraPn: Gal(β 1-4)Glc(β 1-6)[Gal(β 1-4)] β GlcNAc
Th: T-helper cell
TLR: Toll-like receptor
TMB: 3,3',5,5'-Tetramethylbenzidine
TNF- α : Tumor necrosis factor-alpha
TSP: Trimethylsilyl propionate
Treg: T-regulatory cells
UV: ultraviolet

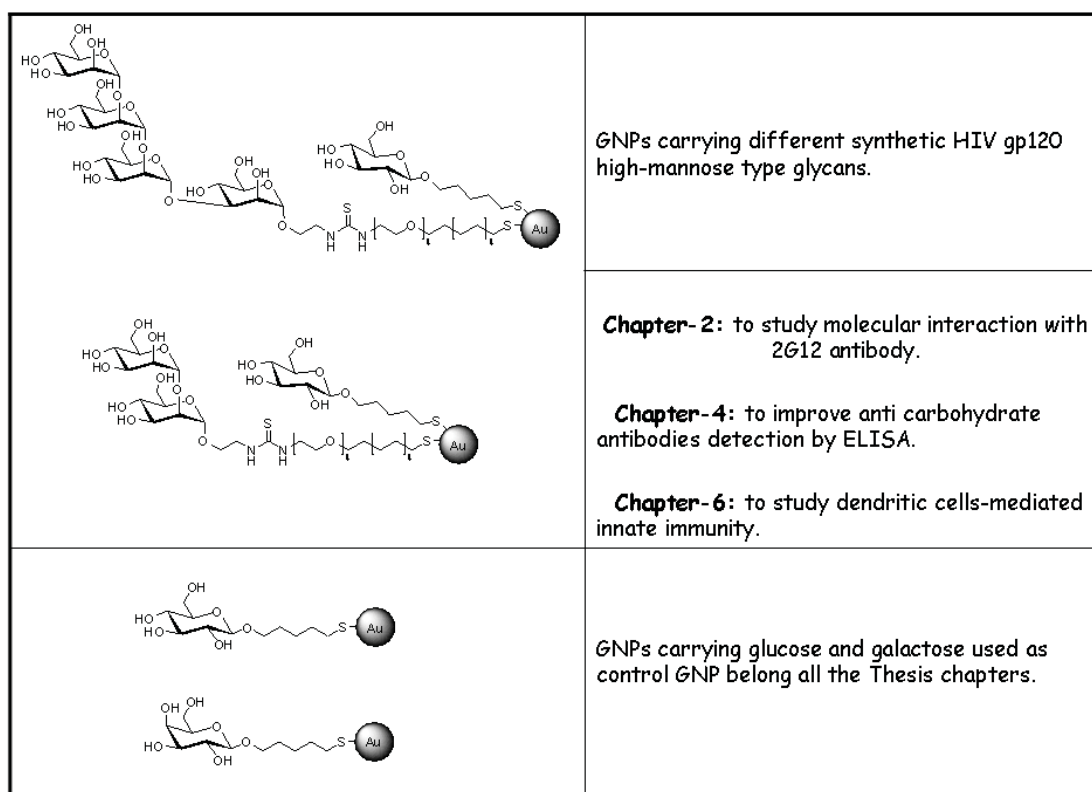
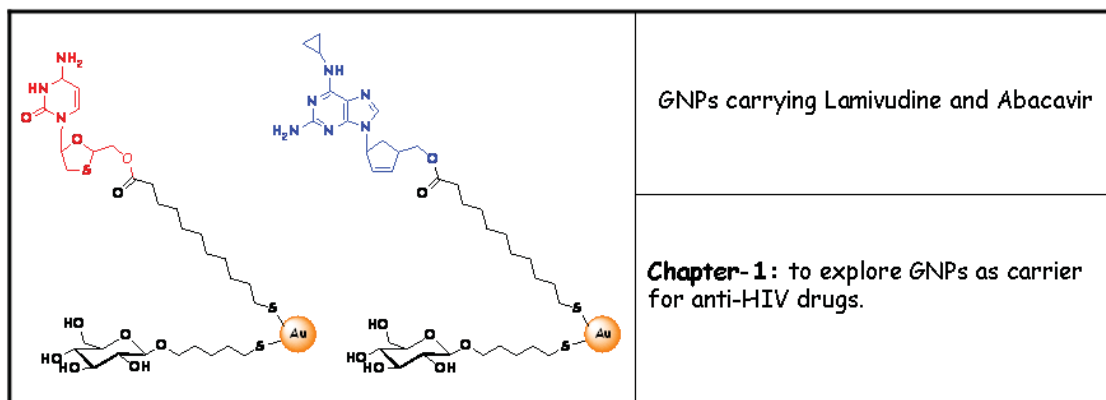
*Per chi mi ha Motivato, senza esserci piú...
Per Mamma e Yuri...*

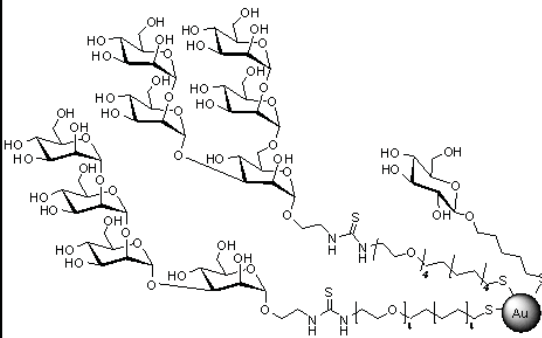
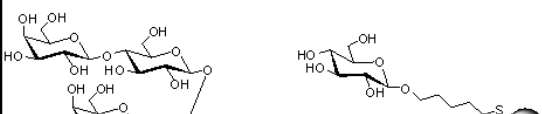
Per te, Agnese, ogni cosa bella...

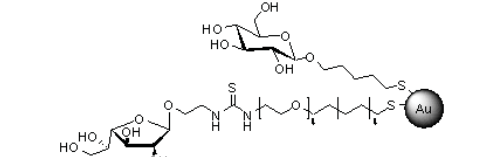
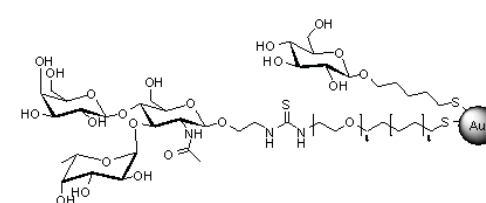
CONTENTS

General Introduction:	1
The role of carbohydrate conjugates in biology and the chemical tools to mimic them	
Part-1 (Introduction):	19
Exploring Glyconanoparticles as multivalent tools to fight pathogens	
Chapter-1:	29
Gold nanoparticles as carriers for anti-HIV prodrugs (drug delivery strategy)	
Chapter-2:	47
Gold nanoparticles as carriers for HIV carbohydrate antigens (the vaccine approach)	
<u>2.1</u> Anti-HIV carbohydrate-based vaccine rational design	
<u>2.2</u> Looking for the 2G12 minimum carbohydrate epitope on GNPs by different techniques	
<u>2.3</u> “Dissecting” the selectivity of the binding of oligomannosides to 2G12 by STD-NMR and glycan array	
<u>2.4</u> Assembling different antennas of the gp120 high-mannose-type glycan to re-build the complete Man9 on the gold GNPs	
<u>2.5</u> Immunization studies with Te/P/OVA-GNPs	
Chapter-3:	85
Gold nanoparticles as carriers for a fully synthetic <i>Streptococcus pneumoniae</i> type 14 vaccine candidate	
Chapter-4:	103
Multivalent Glyconanoparticles allow high sensitive detection of carbohydrate binding proteins on an ELISA-based solid phase assay	
Part-2 (Introduction):	123
GNPs as tool to study the role of carbohydrates in the dendritic cell-mediated innate immunity	
Chapter-5:	131
Gold nanoparticles coated with galactofuranose elicit a pro-inflammatory response in human monocytes-derived dendritic cells and interact with C-type lectins	
Chapter-6:	153
Gold glyconanoparticles bearing Lewis and high- mannoses type self-glycans for the modulation of T-cell responses	
Appendix	177
1. Design, preparation and characterization of Gold Glyco Nanoparticles	
2. Synthesis of oligomannosides	

Glyconanoparticles prepared in this Thesis and their applications



	<p>GNPs carrying different synthetic HIV gp120 high-mannose type glycans.</p>
	<p>Chapter- 2: to study molecular interaction with 2G12 antibody and for <i>in vivo</i> immunization studies to explore GNPs as carrier for carbohydrate-based vaccine against HIV.</p>
	<p>GNPs carrying a small immunogenic fragment of the <i>S. pneumoniae</i> type 14 capsular polysaccharide.</p>
	<p>Chapter- 3: to explore GNPs as carrier for carbohydrate-based vaccine against <i>S. pneumoniae</i>. Chapter- 4: to improve anti carbohydrate antibodies detection by ELISA.</p>

	<p>GNPs carrying the non-self galactofuranose.</p>
	<p>Chapter- 5: to study the role of galactofuranose during the interaction with dendritic cells.</p>
	<p>GNPs carrying the self carbohydrate-Lewis X.</p>
	<p>Chapter- 6: to study the role of carbohydrates in the dendritic cells-mediated innate immune response.</p>

General Introduction

**The role of carbohydrate conjugates in
biology and the chemical tools to mimic
them**

Evolution makes use of different molecules to allow for organisms reproduction and thus transmission of the information corresponding to their highly ordered structure.¹ Nucleic acids, proteins, lipids and carbohydrates are the essential molecules of life and are exploited by evolution to maintain the complexity of living systems. (Fig. 1) Life is the results of all the combinations and interactions of these molecules.

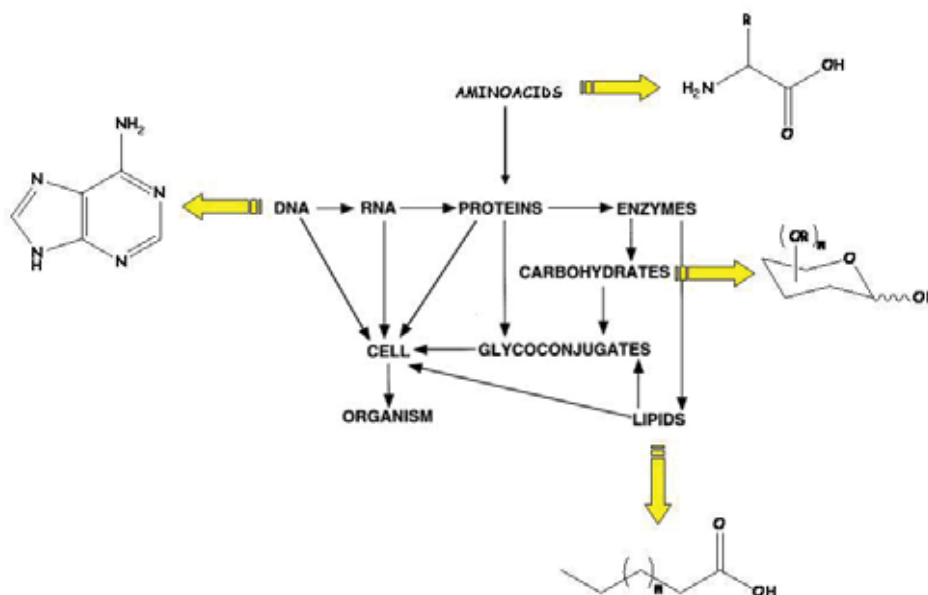


Figure 1: Nucleobases, amino acids, carbohydrates, and lipids are the molecules for life. Cellular role of carbohydrates: protein and lipid glycoconjugates play a key role in the cellular life maintaining the complex and elegant code of life. Adenine was selected to represent one of the four nucleobases. Picture adapted from: Varki A, Cummings R, Esko J, et al., editors. *Essentials of Glycobiology*. Cold Spring Harbor (NY): Historical Background and Overview.

Once thought to be only energetic sources or structural molecules protecting the cell surface, carbohydrates are nowadays recognized as an essential signalling class of molecules for life. Linked to proteins or lipids ("glycoconjugates"), carbohydrates are the major component of the outer surface, the glycocalyx, of almost every living cell (Fig. 2).² In the glycocalyx, carbohydrates appear mainly as clustered glycoconjugates to develop their biological function. Glycoproteins, glycolipids and proteoglycans are involved in many biological processes including cell-cell adhesion, immune responses, cell growth, viral replication, parasitic infection, fertilization and inflammation.³ Glycoscience (the study of the complex

¹ Chance and Necessity: An Essay on the Natural Philosophy of Modern Biology by Jacques Monod, New York, Alfred A. Knopf, 1971, ISBN 0-394-46615-2.

² Dwek R. A., *Glycobiology: Toward Understanding the Function of Sugars*, Chem. Rev. 1996, 96, 683-720.

³ Varki A., Cummings R., Esko J., et al., editors. *Essentials of Glycobiology*. Cold Spring Harbor (NY): Cold Spring Harbor Laboratory Press; 1999. Historical Background and Overview.

carbohydrates on the surface of proteins and lipids)⁴, which includes carbohydrate chemistry and glycobiology⁵ tries to understand the physiological role of carbohydrates in living systems starting from their structures and biosynthesis.

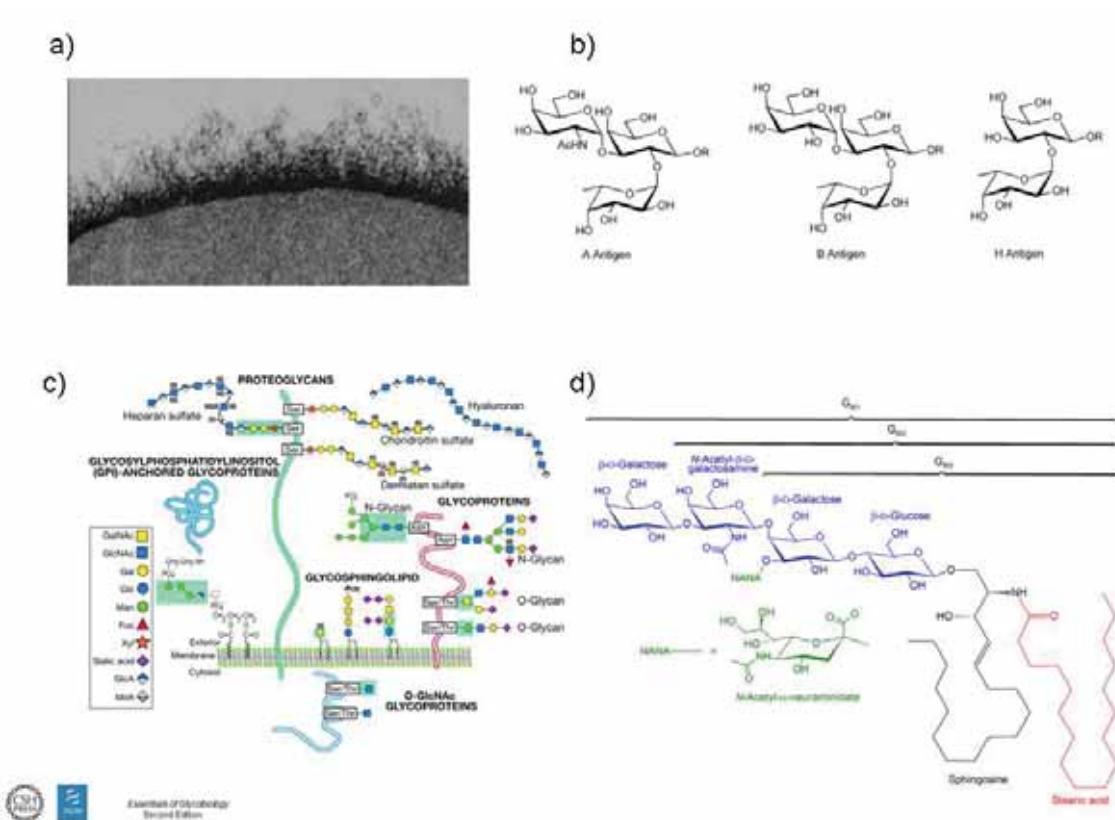


Figure 2: Significant examples of different carbohydrates structures on the cellular glycocalyx : **a)** Historical electron micrograph of red blood cell glycocalyx. **b)** ABO antigens are a well known class of glycoconjugates discovered by K. Landsteiner in 1918⁶. The ABO blood group system is the most important blood type system (or blood group system) in human blood transfusion. **c)** Schematic picture of cellular glycocalyx: carbohydrates appear mainly as glycoproteins, glycolipids and proteoglycans glycoconjugates. Picture taken from Varki A., Cummings R., Esko J., et al., editors. *Essentials of Glycobiology*. Cold Spring Harbor (NY): 1999. Historical Background and Overview. **d)** General picture of an important class of glycoconjugates: gangliosides. They are found predominantly in the nervous system where they constitute 6% of all phospholipids and they are involved in many biological processes. They are specific determinants in cellular recognition and cell-to-cell communication.

Carbohydrate structural diversity, the variability of sugar–units sequence (linkage points, stereochemistry of stereogenic centers, alpha or beta anomeric configuration) and the chemical

⁴ Merry A. H., Merry C. L., *Glycoscience finally comes of age*, *EMBO reports* 2005, 6, 900-903.

⁵ Rademacher T. W., R. B. Parekh R. B., Dwek R. A., *Glycobiology*, *Annu. Rev. Biochem.* 1988, 57, 785–838.

⁶ Landsteiner K., Lampl H., *Concerning the dependence of serological specificity on the chemical structure. Depiction of antigens with familiar chemical constitutions of the specific group*, *Biochemische Zeitschrift* 1918, 86, 343-394.

modification with different functional groups (phosphate, sulphate, *N*-acetyl) as well as the three-dimensional structures that they can adopt depending on the environments (differential conformer selection),⁷ create a unique level of diversity in the glyco-code. This code determines the mechanism of carbohydrates interaction with lectins (specific carbohydrate binding-proteins), enzymes or antibodies. Due to the extremely large information capacity of the glyco-code,⁸ the complexity of the glycome, “*the entire complement of sugars, whether free or present in more complex molecules, of an organism*”⁹ is much higher than that of the genome (the entirety of an organism's hereditary information) and proteome (the entire set of proteins expressed by a genome, cell, tissue or organism). Thirteen monosaccharides constitute the glycome alphabet and can give a number of combinations much higher than the one of the four nucleic bases that constitute the DNA alphabet (Fig. 3).¹⁰

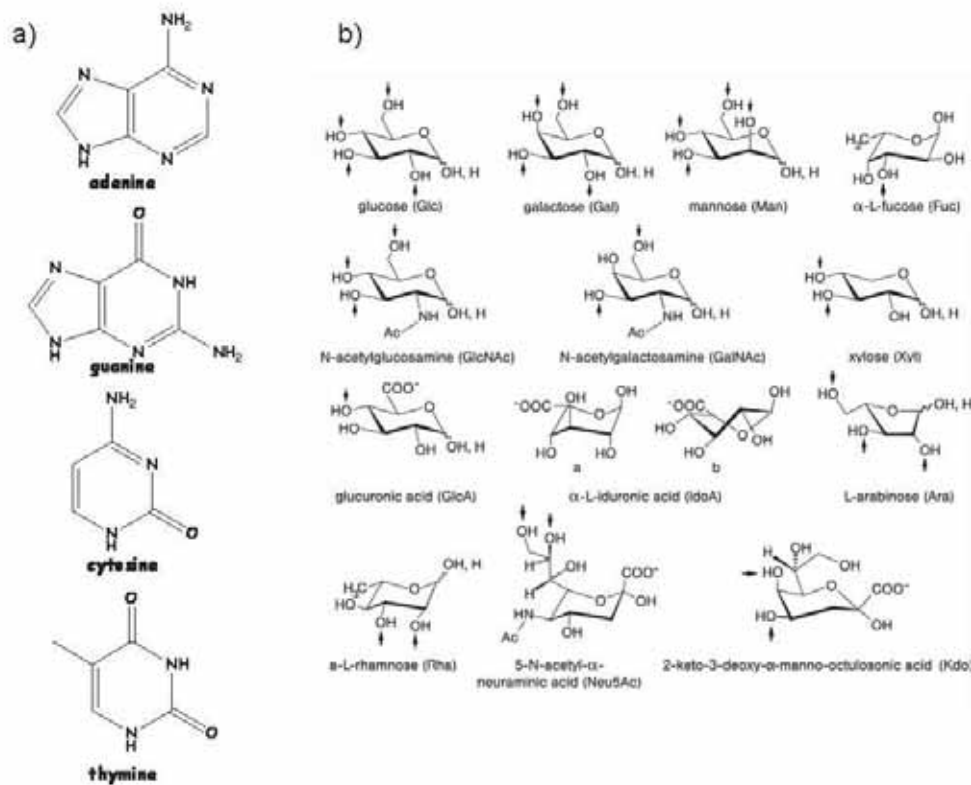


Figure 3: a) Constituent of the DNA alphabet: adenine and guanine are the two purine bases found in the DNA. Cytosine and thymine are the complementary pyrimidine bases. b) Alphabet of the sugar-code: Structural representation, name and symbol as well as the set of known acceptor positions (arrows) in glycoconjugates. Figure adapted from reference 10.

⁷ Gabius H. J., Siebert H. C., André S., Jiménez-Barbero J., Rüdiger H., Chemical biology of the sugar code, ChemBioChem 2004, 5, 740-764.

⁸ The Sugar Code, Gabius H. J. (ed.), Wiley-VCH, Weinheim

⁹ Feizi T., Progress in deciphering the information content of the 'glycome'--a crescendo in the closing years of the millennium, Glycoconjugate J. 2000, 17, 553-565.

¹⁰ Rudiger H. and Gabius H. J. (2009) The biochemical basis and coding capacity of the sugar code. In: Gabius, H.-J. (Ed.) The Sugar Code. Fundamentals of glycosciences. pp. 3–13, Wiley-VCH, Weinheim

The complexity of the glyco-code in comparison to the protein-code, can be exemplified in the formation of an hexasaccharide from six monosaccharides versus an hexapeptide from six aminoacids. Six monosaccharides can be arrange 10^{12} combinations¹¹, including branched forms, while six aminoacids can be arranged in “only” 10^4 combinations to form an hexapeptide (Fig. 4). With this in mind, it is important to remember that the four nucleotides that compose the DNA and their 64 combinations are enough to write the entire genetic-code (genome). The genome is then decoded during protein bio-synthesis, where 22 amino acids can be assembled in different ways to expressing the proteome.

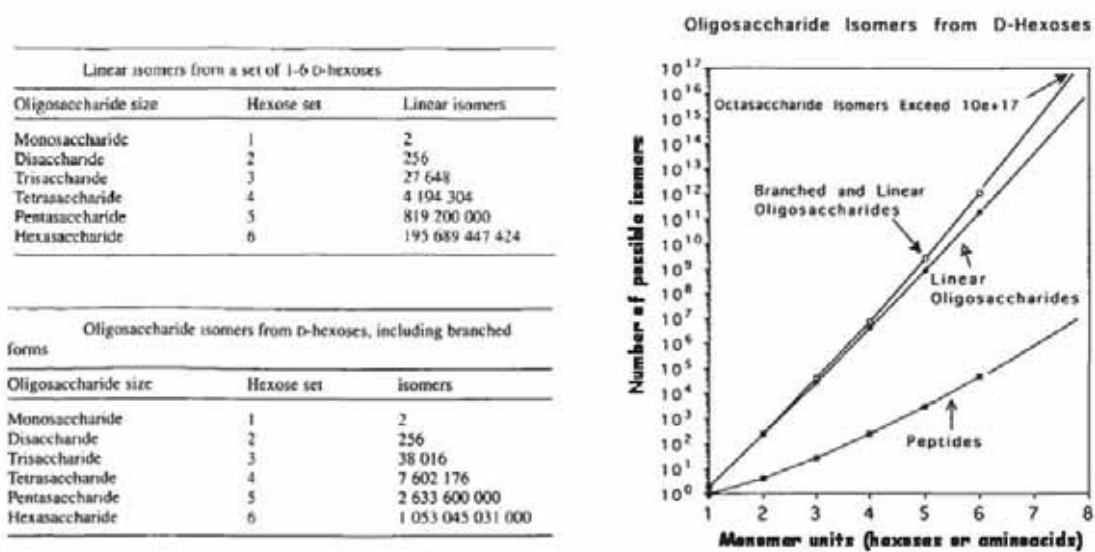


Figure 4: Possible oligosaccharide isomers: Glyco-code is more complex and dynamic respect to the peptide-code. The figure is adapted from reference 11.

Carbohydrate-mediated interactions are generally very weak and the low affinity is compensated by the multivalent presentation of glycans.¹² The cluster-glycoside effect was defined as “the binding affinity enhancement exhibited by a multivalent carbohydrate ligand over and beyond that from the concentration increase resulting from its multivalency”.¹³

¹¹ Laine R. A., A calculation of all possible oligosaccharide isomers both branched and linear yields 1.05×10^{12} structures for a reducing hexasaccharide: the Isomer Barrier to development of single-method saccharide sequencing or synthesis systems, *Glycobiology* 1994, 4, 759-767.

¹² Lee Y. C., Lee R. T., Carbohydrate-protein interactions: basis of glycobiology, *Acc. Chem. Res.* 1995, 28, 321-327 and Lundquist J. J., Toone E. J., The cluster glycoside effect, *Chem. Rev.* 2002, 102, 555–578.

¹³ Lee Y. C., Lee R. T., Enhanced biochemical affinities of multivalent neoglycoconjugates, in *Neoglycoconjugates: Preparation and Applications*, ed. Y. C. Lee and R. T. Lee, Academic Press, London, 1994, chapter 2, p.46.

Ligand–receptor polyvalent interactions are characterized by the simultaneous binding of multiple ligands on one biological entity to multiple receptors on another biological entity and can be cooperatively much stronger than the corresponding monovalent interactions (see Fig. 5).^{14, 15} Multivalency has been attributed to either the increase of structural complementarities between ligand and receptors or to a statistical effect such as effective concentrations and statistical rebinding.¹⁶ These interactions are ubiquitous in biology and include both cellular signalling and matching contacts of viral and bacterial surfaces to host cells.

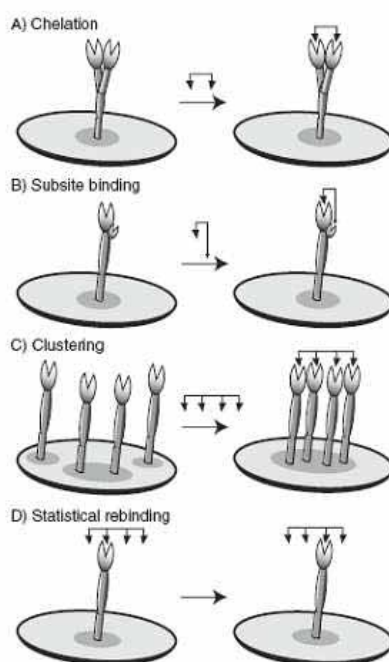


Figure 5: Receptors binding mechanisms that are involved in their interactions with multivalent systems. Figure 5 is taken from reference 15.

Chemical approaches to glycobiology can provide valuable tools to intervene in carbohydrate-mediated processes¹⁷, but these approaches have to take into account the weak affinity and the multivalency of carbohydrate interactions. The design and development of glycomimics, can be used to interfere with cellular interactions, carbohydrate biosynthesis and processing

¹⁴ Mammen M., Choi S.K., Whitesides G. M., Polyvalent interactions in biological systems: Implications for design and use of multivalent ligands and inhibitors, *Angew. Chem. Int. Ed.* 1998, 37, 2754-2794.

¹⁵ Kiessling L. L., Gestwicki J. E., Strong L. E., Synthetic multivalent ligands as probes of signal transduction, *Angew. Chem. Int. Ed.* 2006, 45, 2348-2368.

¹⁶ Pieters R. J., Maximising multivalency effects in protein-carbohydrate interactions. *Org. Biomol. Chem.* 2009, 7, 2013-2025.

¹⁷ Kiessling L. L., Splain R. A., Chemical approaches to glycobiology, *Annu. Rev. Biochem.* 2010, 79, 619-653.

pathways.¹⁸ As a result of this knowledge, the definition of carbohydrate-based drugs for therapeutic purposes has become widespread in recent years.¹⁹ Unfortunately, the isolation of biological relevant oligosaccharides from natural sources yields small amounts of the desired glycan and rarely provides high degree of purity. The solution to this drawback is undoubtedly to increase the efficiency of traditional solution phase synthesis and automated solid phase synthesis²⁰ of complex glycoconjugates, which will benefit glycoscience progression.

“While the synthesis and semisynthesis of defined glycans is a Herculean task, it represents one of the important research areas where chemists can contribute in a unique way to glycobiology. The preparation of pure samples of chemically defined structures is the surest way of establishing critical structure–function relationships and unambiguously confirming the identity of glycans and glycoconjugates from complex biological samples”.[from Editorial of B. Imperiali, reference number 21].

To understand the molecular basis of carbohydrate-mediated interactions and gain the ability to manipulate them, several strategies have been designed and developed to mimic the carbohydrate multivalent presentation of the glycocalyx. Haywoods pioneering work in 1974, led to the preparation of phosphatidylcholine(PC)-cholesterol liposomes incorporating a bovine ganglioside as model-systems to mimic the glycolipid presentation in the cellular membrane. This system was explored to study the behaviour of Sendai virus, a paramyxovirus known as murine parainfluenza virus type 1 or hemagglutinating virus of Japan.²² Sendai virus was the target pathogen because of its capability to adsorb to red cells. Viral surface glycoprotein spikes interact with neuraminic acid moieties on erythrocytes membrane causing the hemagglutination of blood cells. The ganglioside liposomes provided artificial receptors for Sendai virus as they could efficiently capture it. On the contrary, no detectable amount of virus was adsorbed to neutral liposomes which contained only PC and cholesterol, or to liposomes containing cerebroside (glycolipids that do not contain Neu5Ac). The virus-mediated agglutination of erythrocytes was then studied by using liposomes with different Neu5Ac:PC ratios to analyze the effect of surface density of the ganglioside. It was found that ~3% of

¹⁸ Bertozzi C. R., Kiessling L. L., Chemical glycobiology, Science 2001, 291, 2357-2364.

¹⁹ Doores K. J., Gamblin D. P., Davis B. G., Exploring and exploiting the therapeutic potential of glycoconjugates, Chem. Eur. J. 2006, 12, 656-665 and Ernst B., Magnani J. L., From carbohydrate leads to glycomimetic drugs, Nat. Rev. Drug Discov. 2009, 8, 661-677.

²⁰ Stallforth P., Lepenies B., Adibekian A., Seeberger P. H., Carbohydrates: a frontier in medicinal chemistry, J. Med. Chem. 2009, 52, 5561-5577.

²¹ Imperiali B., J. Am. Chem. Soc. 2012, 134, 17835–17839.

ganglioside on liposomes is the minimum amount necessary to inhibit Sendai virus attachment. Furthermore, the free gangliosides were not able to inhibit the hemagglutination. These “glycomembrane” models evidenced the importance of the multivalent presentation of specific carbohydrates to interfere with carbohydrate-mediated biological processes. In 1982, Lee and co-workers demonstrated with a synthetic glyco-peptide that the functional affinity of carbohydrate-protein interactions increases with the number of carbohydrate residues involved.²³ Since these two seminal works, several synthetic multivalent systems such as glycoliposomes,²⁴ glycopeptides and glycoproteins,²⁵ glycopolymers,²⁶ glycodendrimers,²⁷ glyco-DNA,²⁸ glyco-fullerenes,²⁹ glyco-cyclodextrins,³⁰ glyco-nanotubes³¹ and glyco-self-assembled monolayers (SAMs)³² have been developed to multimerise biologically relevant carbohydrates and address carbohydrate-protein interaction questions (Fig. 6).

²² Haywood A.M., Characteristics of sendai virus receptors in a model membrane, *J. Mol. Biol.* 1974, 83, 427-436.

²³ Connolly D. T., Townsend R. R., Kawaguchi K., Bell W. R., Lee Y. C., Binding and endocytosis of cluster glycosides by rabbit hepatocytes. Evidence for a short-circuit pathway that does not lead to degradation, *J. Biol. Chem.*, 1982, 257, 939-945.

²⁴ Marradi M., Chiodo F., García I., Penadés S., Glycoliposomes and metallic glyconanoparticles in glycoscience, in *Synthesis and biological applications of glycoconjugates*, Edited by O. Renaudet; Co-Edited by N. Spinelli, Bentham eBooks, 2010, ISBN: 978-1-60805-277-6, chapter 10.

²⁵ Gamblin D. P., Scanlan E. M., Davis B. G., Glycoprotein synthesis: an update, *Chem. Rev.* 2009, 109, 131-163 and Davis B. G., *Synthesis of glycoproteins*, *Chem. Rev.*, 2002, 102, 579-602.

²⁶ Bovin N. V., Gabius H. J., Polymer-immobilized carbohydrate ligands: Versatile chemical tools for biochemistry and medical sciences, *Chem. Soc. Rev.* 1995, 24, 413-421.

²⁷ Chabre Y. M., Roy R., Design and creativity in synthesis of multivalent neoglycoconjugates, *Adv. Carbohydr. Chem. Biochem.* 2010, 63, 165-393.

²⁸ Spinelli N., Defrancq E., Oligonucleotide-Carbohydrate Conjugates, in *Synthesis and biological applications of glycoconjugates*, 2010, Edited by O. Renaudet; Co-Edited by N. Spinelli, Bentham eBooks, ISBN: 978-1-60805-277-6, Chapter 9.

²⁹ Chabre Y. M., Roy R., Solving Promiscuous Protein Carbohydrate Recognition Domains with Multivalent Glycofullerenes, in *Synthesis and biological applications of glycoconjugates*, 2010, Edited by O. Renaudet; Co-Edited by N. Spinelli, Bentham eBooks, ISBN: 978-1-60805-277-6, chapter 4.

³⁰ André S., Kaltner H., Furuike T., Nishimura S., Gabius H. J., Persubstituted cyclodextrin-based glycoclusters as inhibitors of protein-carbohydrate recognition using purified plant and mammalian lectins and wild-type and lectin-gene-transfected tumor cells as targets, *Bioconjugate Chem.* 2004, 15, 87-98.

³¹ Gattuso G., Menzer S., Nepogodiev S. A., Fraser Stoddart J., David. J. Williams D. J., Carbohydrate Nanotubes, *Angew. Chem. Int. Ed.*, 1997, 36, 1451-1454.

³² Smith E. A., Thomas W.D., Kiessling L. L., Corn R. M., Surface plasmon resonance imaging studies of protein-carbohydrate interactions, *J. Am. Chem. Soc.* 2003, 125, 6140-6148.

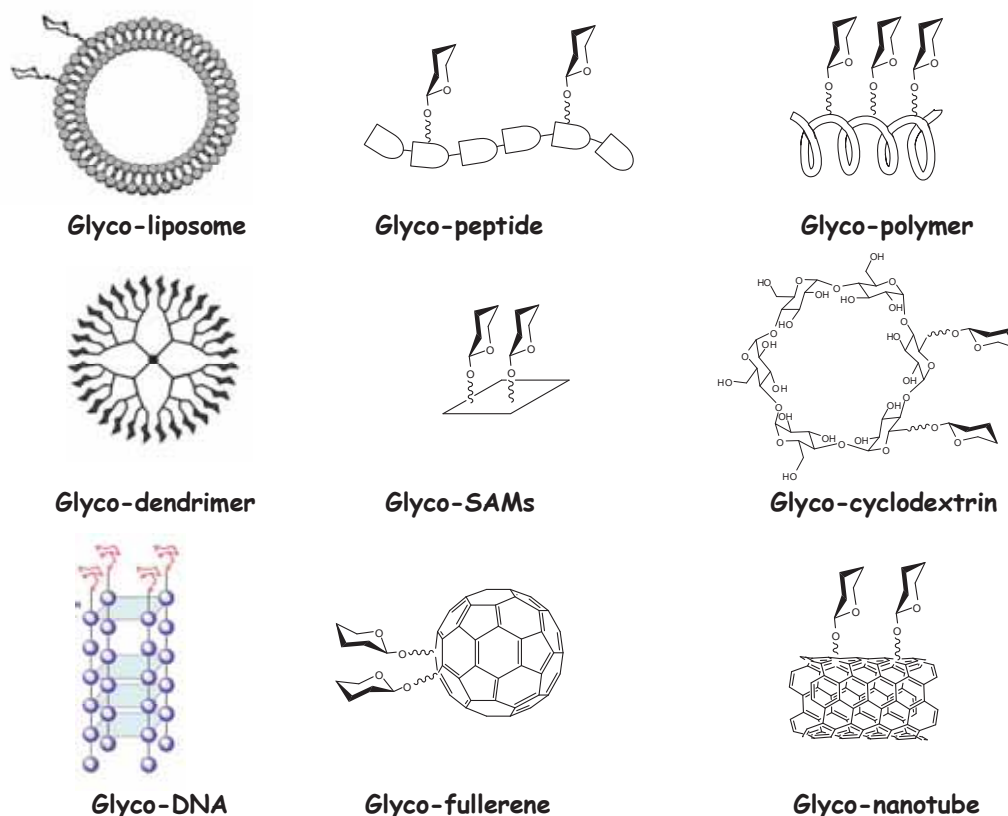


Figure 6: Synthetic multivalent systems which have been proposed to mimic the natural clustered presentation of glycans at cell surface: From the first glyco-liposome (1974), scientists have been developed different strategies to mimic the natural glycans presentation.

Nanotechnology has allowed the development of novel nanomaterials which have opened new perspectives in different research and applicative fields, especially in nanomedicine.³³ The integration of biomolecules to nanostructured materials has produced novel organic-inorganic hybrid nano(bio)materials with properties and functions that have found applications in bioassays and bioelectronic devices (biosensing), as well as in therapeutics and diagnostics.³⁴ The size of biofunctional nanomaterials, in the same order of magnitude of proteins and nucleic acids, allows their use for bio-mimetic purposes and to intervene in bio-recognition processes at molecular level. The chemical stability of gold colloids has been exploited to create nanoparticles of different size, structure and shape.³⁵ The binding between noble metals and biomolecules can be easily achieved by means of self-assembled monolayers

³³ Vogel V. Nanotechnology, Vol. 5; Wiley-VCH Verlag GmbH & Co. KGaA: Weinheim, 2009.

³⁴ You C. C., Chompoosor A., Rotello V. M., The biomacromolecule-nanoparticle interface, *Nano Today* 2007, 2, 34-43.

³⁵ Turkevich J., Colloidal Gold Part I: Historical and Preparative Aspects, Morphology and Structure, *Gold Bull.* 1985, 18, 86-91.

(SAMs) of thiol-armed biomolecules onto the metal surface.³⁶ The formation of SAMs onto bidimensional surfaces can be translated to three-dimensional surface of metal nanoclusters. The incorporation of functionalized biological ligands onto gold nanoparticles is an example of promising newborn tools for medicinal applications.³⁷

To understand and intervene in these carbohydrate-mediated interactions, our group developed a chemical strategy at the interface carbohydrate chemistry-nanotechnology that was named glyconanotechnology.³⁸ Glyconanotechnology can be seen as a synergy between glycoscience and nanotechnology because it profits from concepts and developments of both areas. Glyconanotechnology allows the generation of SAMs of different types of carbohydrates onto metal-based nanoclusters to give glyconanoparticles (GNPs), i.e. three dimensional water-soluble polyvalent systems constituted by a metallic core and a carbohydrate shell (Fig. 7). GNPs constitute a good bio-mimetic model of carbohydrate presentation at cell surface, providing a glycocalyx-like shell with globular shape and chemically defined composition.³⁸ This technology allows also the preparation of gold GNPs carrying different ligands, such as fluorophores, peptides, DNA and with different ratio between these molecules.³⁹ Linkers of varying length can be also used to present the molecules (ligands) in different ways, depending of the biological processes that have to be approached (Fig. 7).

³⁶ Love J. C., Estroff L. A. Kriebel J. K., Nuzzo R. G., Whitesides G. M., Self-assembled monolayers of thiolates on metals as a form of nanotechnology, *Chem. Rev.* 2005, 105, 1103-1169.

³⁷ Boisselier E., Astruc D., Gold nanoparticles in nanomedicine: preparations, imaging, diagnostics, therapies and toxicity, *Chem. Soc. Rev.* 2009, 38, 1759-1782.

³⁸ de la Fuente J. M., Penadés S., Understanding carbohydrate-carbohydrate interactions by means of glyconanotechnology, *Glycoconj. J.* 2004, 21, 149-163.

³⁹ Marradi M., Martín-Lomas M., Penadés S., Glyconanoparticles polyvalent tools to study carbohydrate-based interaction, *Adv. Carbohydr. Chem. Biochem.* 2010, 64, 211-290.

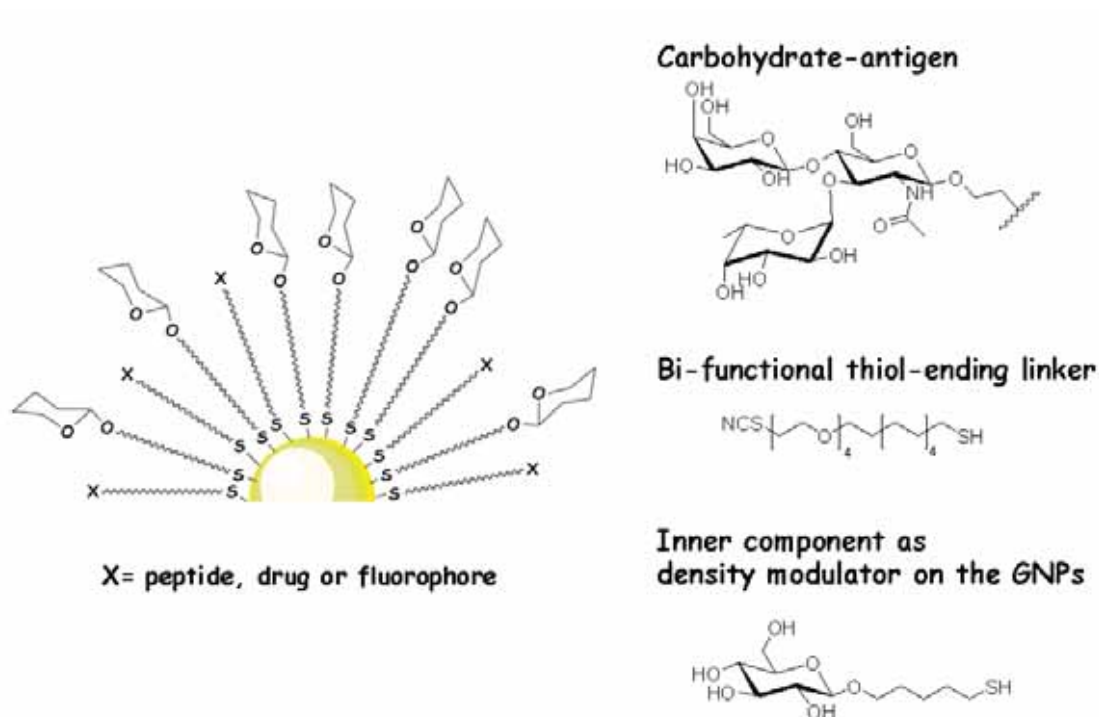


Figure 7: General GNPs picture: SAMs of thiol-armed molecules onto the gold surface. Carbohydrate-antigens are functionalized by a “long” bi-functional thiol ending linker through an isothiocyanate (–SCN) group. A glucose thiol-ending conjugate was exploited as modulator of the ligands density on the GNPs and its “short” linker allows the carbohydrate-antigens to protrude from the GNPs. Lewis X was selected as example of carbohydrate-antigen used in this Thesis.

Glyconanotechnology has introduced new methods to prepare multivalent and multifunctional tools designed to address and study different carbohydrate related biological and biomedical topics.⁴⁰ GNPs coated with the trisaccharide determinant Lewis^X (Gal β 1-4[Fuc α 1-3]GlcNAc β 1) were the first “glycocalyx model” to demonstrate and quantify the calcium-dependent self-aggregation (carbohydrate-carbohydrate interaction) of this antigen determinant.⁴¹ Many current challenges in glycoscience still need systematic approaches to be addressed and glyconanotechnology offers the opportunity to face such challenges through the use of a versatile nanoplatform as the GNPs.

⁴⁰ García I., Marradi M., Penadés S., Glyconanoparticles: multifunctional nanomaterials for biomedical applications, *Nanomedicine* 2010, 5, 777-792.

⁴¹ de la Fuente, J. M., Barrientos A. G., Rojas T. C., Rojo J.; Cañada J.; Fernández A.; Penadés S., Gold glyconanoparticles as water-soluble polyvalent models to study carbohydrate interactions, *Angew. Chem. Int. Ed.* 2001, 40, 2258-2261.

General procedure for glycoconjugation

In this Thesis, a general method to link different carbohydrates on the GNPs has been used (Fig. 8). Protected glycans have been synthesized with benzyl *N*-(2-hydroxyethyl)carbamate as aglycon. After deprotection, the glycan amino-derivative is coupled with a long amphiphilic bifunctional isothiocyanate/thiol-protected linker. The insertion of the thiol group is fundamental to link the glycans on the gold surface of GNPs. After the deprotection of the thiol group, the thiol-ending neoglyconconjugates are ready for the preparation of GNPs by the methodology described before.

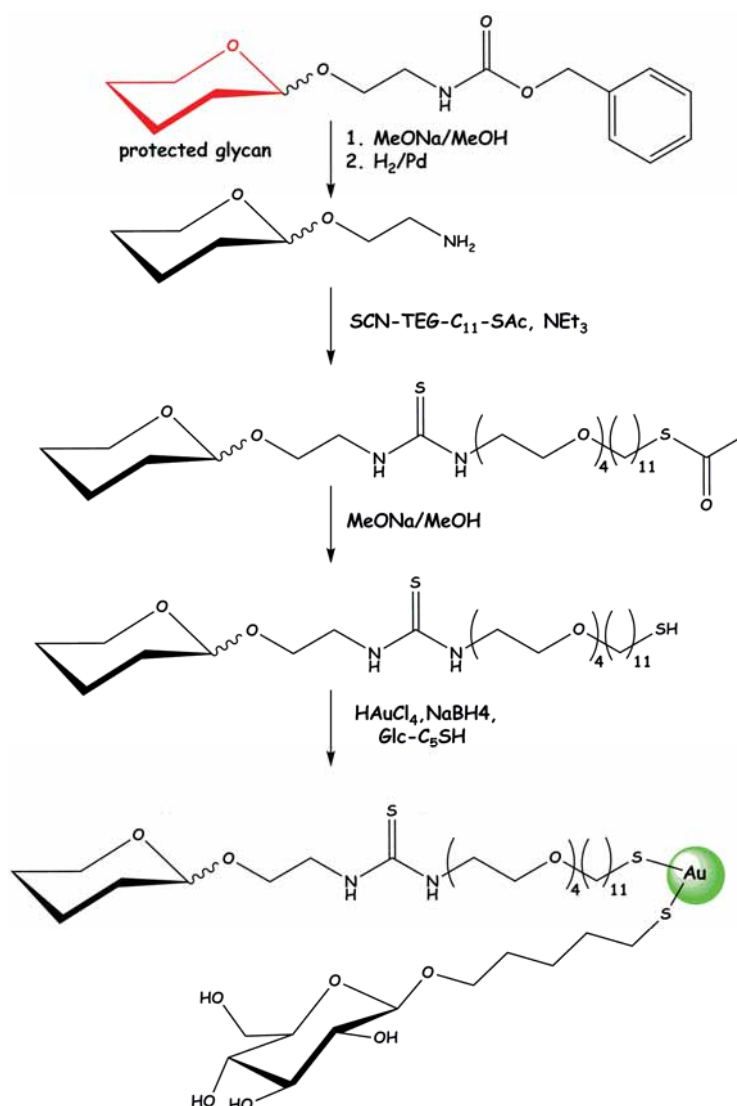
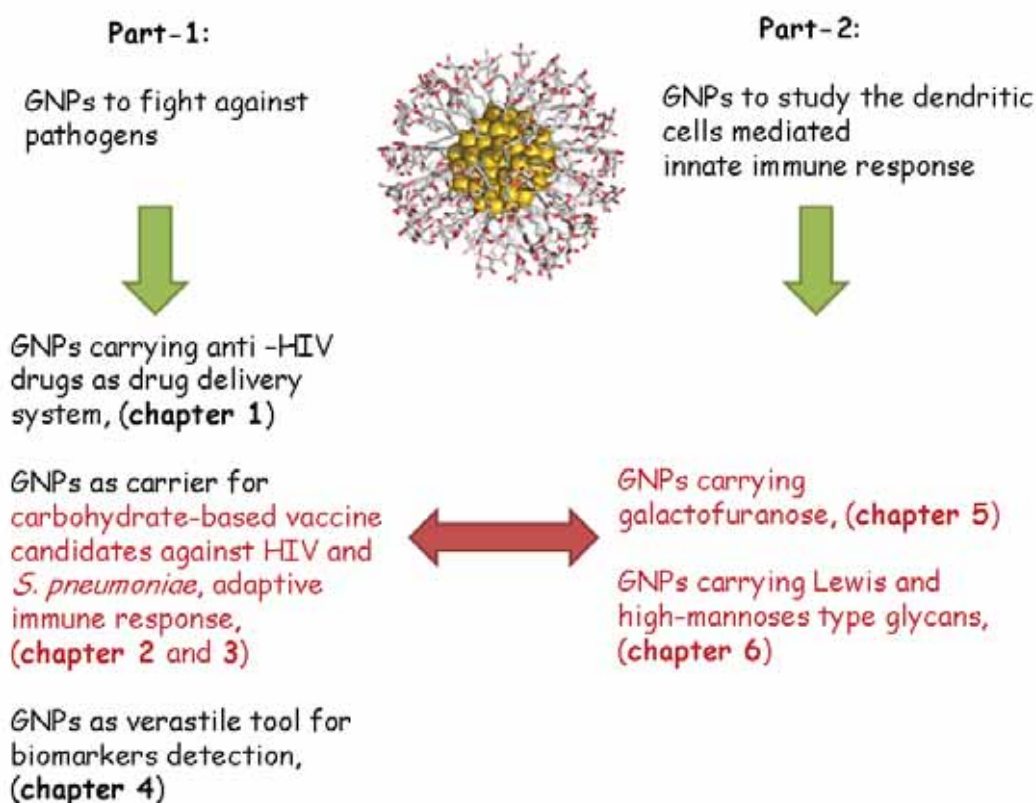


Figure 8: General method of glycoconjugation used in this Thesis to link thiol-ending glycans to gold nanoparticles.

Scope and aims of this Thesis

The main aim of this Thesis is to explore the potentiality of glyconanotechnology by designing and preparing multivalent and multifunctional gold nanoparticles coated with carbohydrates and/or other molecules (Glyconanoparticles, GNPs) in order to intervene in biological processes where carbohydrates are involved. This Thesis focuses in two important processes that affect human health: Infection by the human immunodeficiency virus (HIV) and bacteria *Streptococcus pneumoniae*, and the associated innate immune response produced by pathogen-associated glycans. With gold glyconanoparticles as chemical tools, the functional role of glycans in these processes can be interrogated at molecular level and some applications will be developed.

The objectives of the Thesis can be gathered in two different parts (Scheme 1). The first part (Part-1) deals with the potentiality of GNPs as carrier for anti HIV drugs and carbohydrate antigens: this part includes the application of GNPs in different strategies to fight parasitic infections. The GNPs bearing anti-HIV drugs will be explored as drug delivery system against HIV (**chapter-1**); those carrying carbohydrate-antigens will be explored as carbohydrate-based vaccines candidates against HIV (**chapter-2**) and *S. pneumoniae* (**chapter-3**) and as sensitive tools to detect biomarkers involved in parasitic infections (**chapter-4**).



Scheme 1: Schematic representation of the aims and chapters of this Thesis.

In the second part (Part-2) these multivalent carbohydrate systems carrying self or non-self glycans will be exploited to study the dendritic cells-mediated innate immune response (**chapter 5 and 6**).

The first objective of this Thesis is to develop gold glyconanoparticles as a chemical tool to approach alternatives to the different strategies developed in the last years against the human immunodeficiency virus (HIV). The strategy to achieve this objective includes the preparation of GNPs: i) as drug delivery system for anti-HIV pro-drugs; ii) as mimetic of the high-mannose glycan clusters that cover the HIV envelop glycoprotein gp120 to exploit GNPs as carrier for anti-carbohydrate HIV vaccine.

Exploiting the conjugation of different antiretroviral drugs on the same GNP, a high local drug concentration can be achieved improving the activity of the drugs (**drug delivery system**). This work was related to the European project CHAARM (Combined Highly Active Anti-Retroviral Microbicides) that aims at developing microbicides to prevent HIV sexual infection (**chapter-1**).

The second type of glyconanoparticles is designed to elucidate carbohydrate-mediated processes involved in the HIV infection. The high-mannose type glycans ($\text{Man}_9\text{GlcNAc}_2$) of the HIV envelope glycoprotein gp120 (one of the most highly glycosylated protein in nature)⁴² play an important role during viral infection and are a conserved class of epitopes that could be exploited in a vaccine design against HIV. The rational design of these glyconanoparticles takes origins from the discovery of the human broadly neutralizing antibody 2G12 isolated from infected patient that was able to interact with clusters of the high-mannose glycan present on the HIV surface.⁴³ For that reason, GNPs carrying synthetic oligomannosides that are partial structures of the high-mannose type glycans will be prepared as **mimetic of the high-mannose glycan clusters of gp120**. These GNPs will be used to study the molecular interactions with antibody 2G12 by different techniques. The interactions between the oligomannoside-conjugates selected to prepare the GNPs and 2G12 will be studied by NMR and printed glycan array analysis to have a deeper insight on the molecular basis of the 2G12/oligomannoside interactions. Based on these structural results, the best oligomannosides will be used to prepare gold nanoparticles **as carrier for anti-carbohydrate HIV vaccines**. For this purpose, a T-cell epitope will be added to the surface of oligomannoside-coated GNPs to evoke a specific adaptive immune response (**chapter-2**).

⁴² Wyatt R., Kwong P. D., Desjardins E., Sweet R. W., Robinson J., Hendrickson W. A., Sodroski J. G., The antigenic structure of the HIV gp120 envelope glycoprotein, *Nature* 1998, 393, 705–711.

A similar strategy has been also extended to other parasites. Gold nanoparticles were also designed as carriers for *Streptococcus pneumoniae* antigens. This bacterium is covered by a capsular polysaccharide that is one of the immuno-active macromolecule able to elicit production of antibodies.⁴⁴ The minimum carbohydrate epitope of this polysaccharide is a branched tetrasaccharide⁴⁵ and the strategy of attaching it on the GNPs has been used to obtain **synthetic vaccines candidate** against *S. pneumoniae*. GNPs with different ratio of the synthetic tetrasaccharide epitope related to the *S. pneumoniae* type 14 capsular polysaccharide and a T-cell epitope will be prepared and tested in mice for antibodies production. Mice immunization was performed in the frame of the European project Glyco-gold. The results of this research are presented in **chapter-3**.

With the idea to increase the sensitivity of well-established analytical methods to detect anti-carbohydrate antibodies, we developed a new Enzyme-Linked ImmunoSorbent Assay (ELISA) coating based on the direct adsorption of GNPs on the plates (GNP-ELISA). This approach was also extended to other important biomarkers related with carbohydrates and the results of this GNPs-ELISA are presented in **chapter-4**. The simplicity, high sensitivity and versatility of GNP-ELISA could facilitate basic studies of protein-carbohydrate interactions giving information on carbohydrate epitopes that participate in cellular recognition. This method could be also useful in carbohydrate-based vaccines development, pathogen infection studies and in the identification of important glycan-associated biomarkers.

The second part of the thesis is made up of two chapters that address the role of carbohydrates in innate immunity. Carbohydrate-coated gold nanoparticles have been also employed to study the influence of multivalent presentation of carbohydrates present in human (self-glycan) and in parasites (self and non-self glycans) in the **innate** immunity mediated by dendritic cells (DC). GNPs carrying galactofuranose (non-self carbohydrate antigen presented on the cell wall of different parasites) and high-mannoses and Lewis type glycans (self-carbohydrate antigens present in human and in some parasites) were used to study the maturation markers and interleukins production on human DCs. The cross-talk

⁴³ Doores K. J., Fulton Z., Huber M., Wilson I. A., Burton D. R., Antibody 2G12 Recognizes Di-Mannose Equivalently in Domain- and Nondomain-Exchanged Forms but Only Binds the HIV-1 Glycan Shield if Domain Exchanged, *J. Virol.* 2010 84, 10690-10699

⁴⁴ Avery O. T., Goebel W. F., Chemo-immunological studies on conjugated carbohydrate-proteins : V. The immunological specificity of an antigen prepared by combining the capsular polysaccharide of type III pneumococcus with foreign protein, *J. Exp. Med.* 1931, 54, 437-447.

⁴⁵ Mawas F., Niggemann J., Jones C., Corbel M. J., Kamerling J. P., Vliegenthart J. F. G., Immunogenicity in a mouse model of a conjugate vaccine made with a synthetic single repeating unit of type 14 pneumococcal polysaccharide coupled to CRM197, *Infect. Immun.* 2002, 70, 5107-5114.

between the DCs and T cells was also studied. The cellular experiments were performed during a six months stay in the Molecular Cell Biology and Immunology Department (MCBI) of Vrije University Medical Center (VUmc) in the groups of Irma van Die and Yvette van Kooyk (Amsterdam). The results of these biological studies are presented in chapter-5 and 6 (Part-2) of this Thesis.

Nowadays, the most efficient treatments against infectious diseases are based on drugs (antibiotics, antivirals), microbicides and vaccines (either therapeutic or preventive). The aim of this PhD Thesis was to explore the potential of the glyconanoparticle platform in these areas. Thus a series of gold glyconanoparticles incorporating specific antiviral and oligosaccharide molecules have been prepared as:

- Anti retroviral drug delivery system against HIV (Chapter-1)
- Multivalent carbohydrate tool for elucidating carbohydrate-antibody interactions involved in the immune response of HIV (Chapter-2)
- Carrier for anti-carbohydrate vaccine candidates against HIV (Chapter-2)
- Carrier for anti-carbohydrate vaccine candidates against *S. pneumoniae* (adaptive immune response, Chapter-3)
- Multivalent scaffold to improve the detection of important biomarkers (Chapter-4)
- Multivalent carbohydrate systems to study dendritic cell-mediate innate immune response (Chapter-5 and Chapter-6)

Part-1

Exploring Glyconanoparticles as multivalent tools to fight pathogens

Introduction

This part of the Thesis focuses on multifunctional gold glyconanoparticles (GNPs) that have been designed and prepared to understand and intervene in the mechanism of pathogen infection where the interaction between specific glycans on the pathogen and receptors on the cells are involved. The targeted pathogens are the human immunodeficiency virus (HIV) and the bacteria *Streptococcus pneumoniae*, two pathogens that infect cells by interaction of glycans expressed at their surface with specific receptors on the host cell.

Infectious diseases caused more than 14 million deaths in 2002, being the cause of 26% off all human deaths.¹ The top three parasites killers are the human immunodeficiency virus (HIV), the *Mycobacterium tuberculosis* and the *Plasmodium falciparum*. While the number of deaths due to the majority of parasitic diseases decreased, deaths due to the acquired immunodeficiency syndrome (HIV/AIDS) have increased four times in the last 5 years. In addition, pneumococcal disease is a major public health problem, and it is estimated that 1.6 million people die each year from this infection.² People with HIV/AIDS or people who have suffered organ transplants and are taking immunosuppressive drugs are also at high risk of getting this disease.

Nowadays, the most used treatments against infectious diseases are based on drugs (anti-biotic and anti-viral drugs) and vaccination.

A series of GNPs were prepared with the idea to intervene in the glycan-mediate mechanism that pathogens use to infect cells and provoke AIDS in the case of HIV, and pneumonia in the case of the *S. pneumoniae*. The GNPs were designed as tools to approach the strategies used to fight pathogens, **the drugs** and **vaccination strategies**, but we have also employed the GNPs as a **diagnostic tool** to develop a test for a sensitive detection of anti-carbohydrate antibodies in serum.

In the **drugs approach** (chapter-1) we have used the GNPs as carrier of HIV antiretrovirals that are well known to be highly active in therapy. Indeed, the highly active antiretroviral therapy (HAART)

¹ World health report 2004, statistical annex, table 2, pag. 120-125.

² WHO, 2007. Wkly. Epidemiol. Rec. 82: 93-104.

is the only regimen approved to treat people infected with HIV.³ The introduction of HAART in 1996 transformed AIDS to a chronic pathology with an impressive decrease in mortality of HIV-infected patients. However, HAART has not allowed the cure of HIV infection.⁴ Nowadays, selected HAART drugs are also being used as a new class of anti-viral compounds called microbicides to prevent sexual infection.⁵ These molecules can be applied inside the vagina or rectum to protect against sexually transmitted infections including HIV. The multifunctionality of the gold nanoparticles allowed us to design multi-component GNPs where each ligand on the gold surface could act in different steps of viral replication. The “drug” entities selected for the design of complex GNPs, were the HIV antiretrovirals Zidovudine (AZT), Abacavir (ABC) and Lamivudine (3TC) that are nucleoside analog reverse transcriptase inhibitors (NRTIs). These inhibitors have been modified as pro-drugs before to attach them to the GNPs. We expected that the high local concentration of the drugs on the GNPs will increase their activity and stability. The chemo-enzymatic hydrolysis of the pro-drugs will release the drug in the cellular milieu validating the inhibitor-GNPs as a new drug delivery system of anti HIV drugs (Fig. 1).

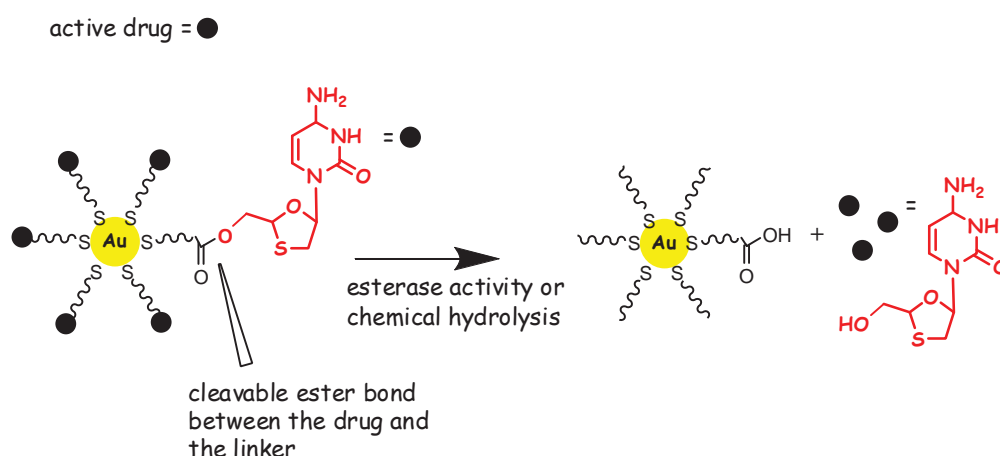


Figure 1: Anti HIV drug delivery system based on GNPs. Cleavable drugs were linked on the GNPs and will be released under chemical or enzymatic hydrolysis. Lamivudine (3TC) is used in this figure as example of anti-HIV drug. In this Thesis Zidovudine (AZT), Abacavir (ABC) and Lamivudine (3TC) will be used as anti-HIV drugs to decorate GNPs.

³ De Clercq E., Antiretroviral drugs, *Curr. Opin. Pharmacol.* 2010, 10, 507-515.

⁴ Le Douce V., Janossy A., Hallay H., Ali S., Riclet R., Rohr O., Schwartz C., Achieving a cure for HIV infection: do we have reasons to be optimistic? *J. Antimicrob. Chemother.* 2012, 67, 1063–1074.

⁵ Balzarini J., Van Damme L., Microbicide drug candidates to prevent HIV infection, *Lancet* 2007, 369, 787–797.

The **vaccination strategy** (approached in chapter-2 and chapter-3) against pathogens is probably one of the most exciting and successfully scientific goals of science. There are several types of vaccines in use: Attenuated, inactivated, sub-unit, toxoid, DNA, recombinant vector and conjugate vaccines. Capsular polysaccharides are the major virulence factor of bacteria and they can be exploited to evoke protection against a bacterium. However, carbohydrates are usually poorly immunogenic and strategies have been developed to improve their immune response.⁶ With the exception of zwitterionic polysaccharides^{7, 8} carbohydrates are T cell independent antigens and conjugate vaccines convert the immune response into one with a T cell dependent character.⁹ Conjugation of polysaccharides to an immunogenic protein (conjugate vaccines) solved two drawbacks related with a polysaccharide vaccine: The induction of immunological memory and the low antibody response in infants.¹⁰ Although carbohydrate conjugate vaccines have been prepared against malaria¹¹ and prostate cancer,¹² only a few have been successfully used to prevent invasive pneumococcal¹³ and *Haemophilus* type b¹⁴ diseases. There are still many

⁶ Astronomo R. D, Burton D. R., Carbohydrate vaccines: Developing sweet solutions to sticky situations? Nat. Rev. Drug Discov. 2010, 9, 308–324.

⁷ Kalka-Moll W. M., Tzianabos A. O., Bryant P. W., Niemayer M., Ploegh H. L., Kasper D. L., Zwitterionic polysaccharides stimulate T cells by MHL class II-dependent interactions, J. Immunol. 2002, 169, 6149–6153.

⁸ Avci F. Y., Kasper D. L., How Bacterial Carbohydrates Influence the Adaptive Immune System. Annu. Rev. Immunol. 2010, 28, 107–130.

⁹ Pena Icart L., Fernández-Santana V., Veloso R. C. et al.: Protective immunity of pneumococcal glycoconjugates. In: Carbohydrate-Based Vaccines (Volume 989). René Roy (Ed.), ACS Symposium Series, American Chemical Society, Washington, DC, USA, 1–19 (2008).

¹⁰ Rijkers G. T, van Mens S. P., van Velzen-Blad H., What do the next 100 years hold for pneumococcal vaccination?, Expert Rev. Vaccines 2010, 9, 1241-1244.

¹¹ Schofield L., Hewitt M. C., Evans K., Siomos M. A., Seeberger P. H., Synthetic GPI as a candidate anti-toxic vaccine in a model of malaria, Nature 2002, 418, 785–789.

¹² Slovin S. F, Ragupathi G., Adluri S., Ungers G., Terry K., Kim S., Spassova M., Bornmann W. G., Fazzari M., Dantis L., Olkiewicz K., Lloyd K. O., Livingston P. O., Danishefsky S. J., Scher H. I., Carbohydrate vaccines in cancer: Immunogenicity of a fully synthetic globo H hexasaccharide conjugate in man, Proc. Natl. Acad. Sci. USA 1999, 96, 5710–5715.

¹³ Whitney C. G., Farley M. M., Hadler J., Harrison L. H., Bennett N. M., Lynfield R., Reingold A., Cieslak P. R., Pilishvili T., Jackson D., Facklam R. R., Jorgensen J. H., Schuchat A., Decline in invasive pneumococcal disease after the introduction of protein-polysaccharide conjugate vaccine, New Engl. J. Med. 2003, 348, 1737–1746.

¹⁴ Verez-Bencomo V., Fernández-Santana V., Hardy E., Toledo M. E., Rodríguez M. C., Heynngnezz L., Rodríguez A., Baly A., Herrera L., Izquierdo M., Villar A., Valdés Y., Cosme K., Deler M. L., Montane M., Garcia E., Ramos A., Aguilar A., Medina E., Toraño G., Sosa I., Hernandez I., Martínez R., Muzachio A., Carmenates

challenges and problems to be addressed in the area of carbohydrate vaccine design. One of these challenges is related to the elucidation of the mechanism of glycoconjugate vaccine activation of adaptive immune system.¹⁵ A main concern for synthetic conjugate vaccines is the risk of an unspecific immune response against the immunogenic protein (carrier-induced epitopic suppression).¹⁶ Current advances in the identification of the smallest protective carbohydrate epitopes for many pathogens and their synthesis have opened new ways to rationalize carbohydrate vaccine design.¹⁷ Several approaches for the production of synthetic carbohydrate-based vaccines have been developed to overcome the hurdles encountered with the use of protein carriers and complex bacterial capsular polysaccharides.¹⁸ These approaches include the use of liposomes,¹⁹ dendrimers,²⁰ peptides,²¹ micrometric beads,²² and polymeric nanoparticles,²³ as scaffolds to obtain multivalent conjugate vaccines. Curiously, in 1931 organic colloidal particles were used as carrier for bacterial polysaccharides trying to improve their immunogenic

A., Costa L., Cardoso F., Campa C., Diaz M., Roy R., A synthetic conjugate polysaccharide vaccine against *Haemophilus influenzae* type b, *Science* 2004, 305, 522-525.

¹⁵ Avci F. Y., Li X., Tsuji M., Kasper D. L., A mechanism for glycoconjugate vaccine activation of the adaptive immune system and its implications for vaccine design, *Nat. Med.* 2011, 17, 1602-1609.

¹⁶ Schutze M. P., Leclerc C., Jolivet M., Audibert F., Chedid L., Carrier-induced epitopic suppression, a major issue for future synthetic vaccines, *J. Immunol.* 1985, 135, 2319-2322.

¹⁷ Stallforth P., Lepenies B., Adibekian A., Seeberger P. H., Carbohydrates: a frontier in medicinal chemistry, *J. Med. Chem.* 2009, 52, 5561-5577.

¹⁸ Keding S. J., Danishefsky S., Synthetic Carbohydrate-based Vaccines. In: *Carbohydrate-Based Drug Discovery*. Chi-Huey Wong (Ed.), Wiley-VCH Verlag, 381-406 (2003).

¹⁹ Ingale S., Wolfert M. A., Gaekwad J., Buskas T., Boons G. J., Robust immune responses elicited by a fully synthetic three-component vaccine, *Nat. Chem. Biol.* 2007, 3, 663-667 and Hassane F. S., Phalipon A., Tanguy M. et al., Rational design and immunogenicity of liposome-based diepitope constructs: Application to synthetic oligosaccharides mimicking the *Shigella flexneri* 2a O-antigen, *Vaccine* 2009, 27, 5419-5426.

²⁰ Wang S. K., Liang P. H., Astronomo R. D., Hsu T. L., et al., Targeting the carbohydrates on HIV-1: Interaction of oligomannose dendrons with human monoclonal antibody 2G12 and DC-SIGN. *Proc. Natl. Acad. Sci. USA* 2008, 105, 3690-3695.

²¹ Joyce J. G., Krauss I. J., Song H. C. et al., An oligosaccharide-based HIV-1 2G12 mimotope vaccine induces carbohydrate-specific antibodies that fail to neutralize HIV-1 virions, *Proc. Natl. Acad. Sci. USA* 2008, 105, 15684-15689.

²² Song E. H., Osanya A. O., Petersen C. A., Pohl N. L., Synthesis of multivalent tuberculosis and Leishmania-associated capping carbohydrates reveals structure-dependent responses allowing immune evasion, *J. Am. Chem. Soc.* 2010, 132, 11428-11430.

²³ Fahmy T. M., Demento S. L., Caplan M. J., Mellman I., Saltzman W. M., Design opportunities for actively targeted nanoparticle vaccines. *Nanomedicine* 2008, 3, 343-355.

properties.²⁴ The adsorption of these polysaccharides to the colloid surface was exploited to have an “adjuvant-effect” of these colloids. Although this seminal work lacks of information on the molecular mechanism, it showed for the first time that polysaccharides can be rendered immunogenic by adsorption on colloid carrier.

In our vaccine strategy, we have constructed a fully synthetic vaccine using gold colloid as carrier for the vaccine components. Gold GNPs carrying a B cell epitope (carbohydrate antigens of HIV or *Streptococcus pneumoniae*) and a T cell epitope immunogenic peptide (tetanus toxoide or OVA₃₂₃₋₃₃₉ peptide) were designed and prepared (Fig. 2). This approach has been developed during this Thesis preparing GNPs bearing oligomannosides of the HIV envelop protein gp120 and a tetrasaccharide of the capsular polysaccharide of the *S. pneumoniae* Type 14 as anti-carbohydrate vaccine candidates.

²⁴ Zozaya J., Combination of bacterial polysaccharides and collodion particles as antigens, Science 1931, 74, 270-271.

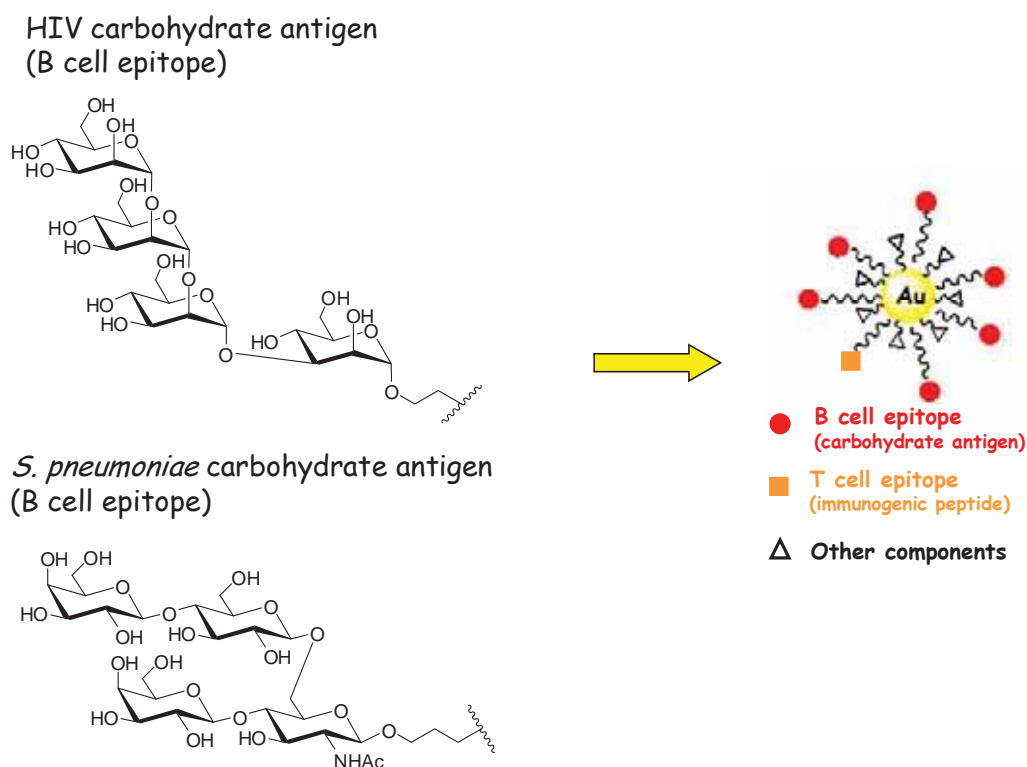


Figure 2: GNPs as a new carrier for carbohydrate-based vaccines. The multifunctionality of GNPs has been exploited to incorporate carbohydrate-antigens from HIV or *S. pneumoniae* and T cell epitopes.

In the **diagnostic strategy** (chapter-4), the GNPs that were prepared as anti-carbohydrate vaccine candidates have been used as a multivalent chemical tool to detect antibodies triggered by parasitic infections. The detection of serum antibodies as biomarkers is a methodology used in the clinic to identify cancer cells or parasites infection and consequently select the correct therapeutic strategy. Enzyme-linked immunosorbent assay (ELISA) is one of the most useful techniques for biomarker detection. New versatile and low cost methods that improve sensitive for clinical diagnostic are highly desirable. GNPs allow the presence of a high number of carbohydrates on a nanometric gold scaffold (60-100 molecules) and their high molecular weight (around 50-100 kDa) make them suitable for ELISA plates coating, improving the sensitivity of the anti-carbohydrates antibodies detection (Fig. 3). This GNP-ELISA coating approach has been employed in this Thesis

for the detection of specific immunoglobulins IgGs in the nanomolar range and for studying carbohydrate-mediated interactions with lectins and cells.

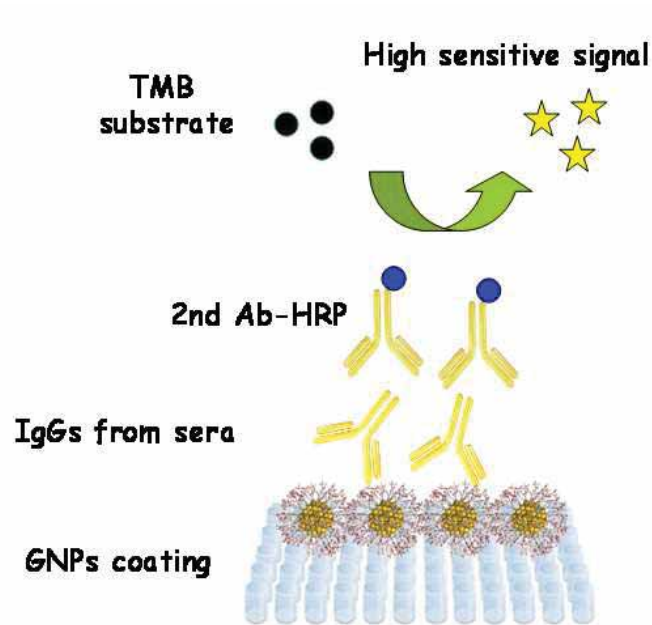


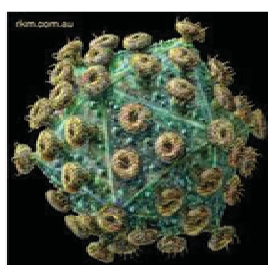
Figure 3: GNP-ELISA. Commercial NUNC Maxisorp ELISA plates have been coated with GNPs carrying carbohydrate antigens for the detection of specific anti-carbohydrates antibodies.

Chapter-1

Gold nanoparticles as carriers for anti-HIV prodrugs (drug delivery strategy)

In the frame of CHAARM project

Acquired immune deficiency syndrome (AIDS) is mainly caused by human immunodeficiency virus type-1 (HIV-1)¹ and continues to be a major leading pandemic disease worldwide with approximately 34 million people living with HIV.² Due to its incredible genetic variance and the specificity for CD4⁺ T cells, this virus is the responsible of 800.000 deaths per year. In addition to **sexual preventions**, the strategies used to inhibit viral replication in human CD4⁺ T cells consist on the combinational **highly active antiretroviral therapy** (HAART) and the design of a **vaccine** that should protect people among all the different HIV strains.³ Although great results have been obtained by the use of the HAART regimes since 1996, there are still several problems to solve, such as toxic side-effects of the HAART drugs and the emergence of multi-drug resistance. After more than 25 years of intensive research, the **vaccine strategy** has not been able to design an efficient vaccine against HIV. The natural variability of HIV provides a drawback for understanding the complex biology of this virus and for the design of a universal vaccine against it.⁴ Figure 1 shows the strengths of virus HIV that avoid the development of an anti HIV vaccine. Recently, the results of the RV144 Thai trial released in September 2009 have brought new optimism to the HIV vaccine field. This study employed envelope-based immunogens delivered as a priming vaccination with a recombinant poxvirus vector and boosting with recombinant proteins. Although neutralizing antibodies were not induced in the RV144 study, considerable titers of binding antibodies to HIV-1 viral envelope were evoked.⁵



Sequence diversity due to an high propensity for recombination and a rapid <i>in vivo</i> turnover.
Infection of critical immune cells like CD4 ⁺ T cells that are fundamental for coordinating effective immune responses.
Immune avoidance due to the different viral proteins: Nef viral protein down-regulates the major histocompatibility complex (MHC) molecules that are crucial for the T cell recognition of the infected cells and surface envelope proteins that avoid the antibody recognition.
Masking of neutralization epitopes exploiting an highly glycosilation pathway of the human host.
Latent reservoir of infected cells by integration of its gentic material into the host chromosome.

Figure 1: Left: Artistic HIV representation from Russell Kightley scientific illustrator (rkm.com.au). HIV envelope shows the gp120 trimers as spikes on the viral surface. Right: properties of HIV that hinder vaccine development.⁶

¹ Gallo R. C., Montagnier L., The discovery of HIV as the cause of AIDS, N. Engl. J. Med. 2003; 349, 2283-2285.

² <http://www.who.int/hiv/data/en/>

³ <http://www.avert.org/hiv-types.htm>

⁴ Korber B., Gaschen B., Yusim K., Thakallapally R., Kesmir C., Detours V., Evolutionary and immunological implications of contemporary HIV-1 variation, Br. Med. Bull. 2001, 58, 19-42.

⁵ Munier C. M., Andersen C. R., Kelleher A. D., HIV vaccines: progress to date, Drugs. 2011 71, 387-414.

⁶ Walker B. D., Burton D. R., Toward an AIDS vaccine, Science 2008, 320, 760-764.

Nowadays the safest **prevention** against **sexual infection** relies on physical barriers, but recently a new type of protection based on microbicides has started to be developed. **Microbicides** are a new class of chemical-physical barrier in clinical development that can be directly applied to the vagina or rectum before sexual intercourses in order to prevent the transmission of HIV.⁷ Some microbicides candidate (Carraguard®, Cyanoviran®, cellulose sulphate, PRO 2000®) provide a physical barrier that avoids HIV and other pathogens reaching the target cells, but these microbicides have shown some drawbacks like tissues inflammation and mucosa damages. Recently, the conventional anti-HIV drugs used for HAART are also being exploited as potential microbicides. A gel formulation containing 1% of the reverse transcriptase inhibitor Tenofovir (CAPRISA 004 gel) is a new microbicide that has showed good results in prevention HIV infections in South African women.⁸ At the moment there are 23 microbicides in various stages of clinical development.⁹ The development of efficient, widely available, and low-cost microbicides to prevent sexually transmitted HIV infections is a high priority in the fight against HIV.

Based on this problematic issue, we aim at approaching the different strategies in the fight against HIV by exploiting the potential of GNPs technology that allows the combination of different molecules on the same platform. We reasoned that the presence of multiple anti-retroviral molecules on the GNPs, could lead to a drug **delivery system** and/or **microbicides** able to inhibit viral replication or to prevent sexual infection.

To take advantage of the multifunctionality of the GNPs, active molecules against HIV used in the HAART therapy were linked to the gold surface. These anti-HIV drugs are compounds that can also be directly applied to the vagina or rectum before sexual intercourses in order to prevent the transmission of HIV (**microbicides**). These molecules can be formulated as a gel, cream, as already mention in the case of Tenofovir.

⁷ Balzarini J., Van Damme L., Microbicide drug candidates to prevent HIV infection, *Lancet* 2007, 369, 787–797.

⁸ Abdool Karim Q., Abdool Karim S. S., Frohlich J. A., Grobler A. C., Baxter C., Mansoor L. E., Kharsany A. B., Sibeko S., Mlisana K. P., Omar Z., Gengiah T. N., Maarschalk S., Arulappan N., Mlotshwa M., Morris L. et. al, Effectiveness and safety of tenofovir gel, an antiretroviral microbicide, for the prevention of HIV infection in women, *Science* 2010, 329, 1168-1174.

⁹ <http://www.who.int/hiv/topics/microbicides/microbicides/en/>

One of the greatest challenges of anti-retroviral therapies is developing of drug delivery systems (DDSs) that have a high efficacy and therapeutic selectivity.¹⁰ The application of gold nanoparticles as a DDS is an expanding field due to the inert properties of the gold core, their controlled fabrication, and multifunctionality.¹¹ This multifunctionality allows the design of particles containing multiple chemotherapeutics and a targeting moiety. In addition, the metallic core seems to be non-toxic and biocompatible.¹²

Gold nanoparticles offer a multivalent scaffold that can be exploited to carry different molecules with anti HIV activity. We have previously described the usefulness of gold nanoparticles as a carrier for different structures related to HIV. GNPs coated with oligomannosides of the gp120 (*manno*-GNPs) were able to inhibit the DC-SIGN-mediated HIV-1 *trans*-infection of human T-cells¹³ and multivalent gold nanoparticles coated with sulfated ligands showed to interfere with the adhesion/fusion of HIV during its entry.¹⁴

With the idea to have multiple copies of different anti-retroviral molecules on the same GNP, we decided to investigate the usefulness of gold nanoparticles as carrier for anti-HIV drugs. The use of gold GNP as scaffolds for the anti-viral drugs could bring some important benefits such as improve the solubility in water and biological media of the drugs and increase their local concentration on the gold surface. In addition, the introduction of targeted molecules (like antibodies) on the GNPs could offer also the possibility to delivery the drug to the HIV reservoirs.

As anti-viral drugs, the nucleoside analog reverse transcriptase inhibitors (NRTIs) Zidovudine (AZT), Abacavir (ABC) and Lamivudine (3TC) were selected and used in the form of drugs derivatives to prepare GNPs as drug delivery system (Fig. 2). The combination of these three inhibitors is used as protocol of HAART and this combination is also available as fixed-dose combination in a single pill and from 2000 is licensed as Trizivir.¹⁵ HIV-1 reverse transcriptase

¹⁰ Allen T. M., Cullis P.R., Drug delivery systems: entering the mainstream, *Science* 2004, 303, 1818-1822.

¹¹ Duncan B., Kim C., Rotello V. M., Gold nanoparticle platforms as drug and biomacromolecule delivery systems, *J. Control. Release* 2010, 148, 122-127.

¹² Connor E. E., Mwamuka J., Gole A., Murphy C. J., Wyatt M. D., Gold nanoparticles are taken up by human cells but do not cause acute cytotoxicity, *Small* 2005, 1, 325-327.

¹³ Martínez-Ávila, O., Bedoya L. M., Marradi M., Clavel, C., Alcamí J., Penadés S., Multivalent manno-glyconanoparticles inhibit DC-SIGN-mediated HIV-1 *trans*-infection of human T cells, *Chembiochem* 2009, 10, 1806-1809.

¹⁴ Di Gianvincenzo P., Marradi M., Martínez-Avila O. M., Bedoya L. M., Alcamí J., Penadés S., Gold nanoparticles capped with sulfate-ended ligands as anti-HIV agents, *Bioorg Med Chem Lett.* 2010, 20, 2718-2721.

¹⁵ <http://www.emea.europa.eu/ema/>

(RT) is one of the crucial enzymes in the replication of the virus, being responsible for the conversion of the viral RNA into DNA. HIV-1 RT inhibitors are classified as nucleotide RT inhibitors (NRTIs) and non-nucleoside RT inhibitors (NNRTIs). NRTIs have to be phosphorylated intracellularly before the 5'-triphosphate nucleotide analog can interact with the HIV reverse transcriptase as an alternate substrate/competitive inhibitor, while NNRTIs are non-competitive inhibitors.¹⁶ NRTIs compete as triphosphates with normal nucleoside substrates acting as chain terminators in the DNA polymerisation reaction catalyzed by HIV-1 RT.¹⁷ When bound in the active site, they stop polymerization because they lack a 3' hydroxyl group.¹⁸

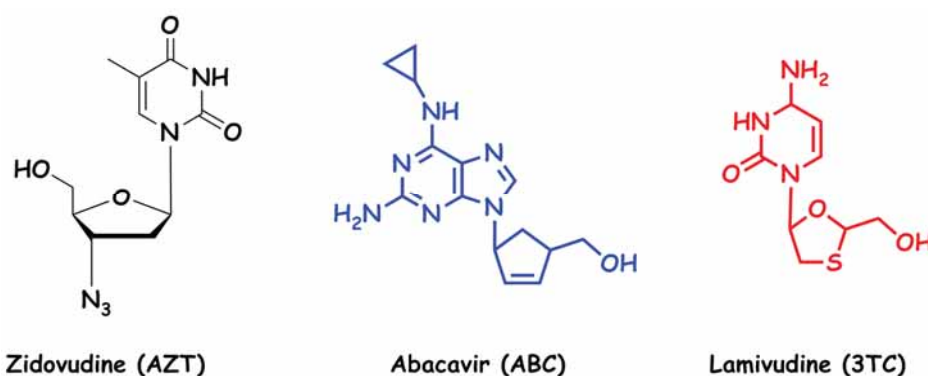


Figure 2: The nucleoside reverse transcriptase inhibitors (NRTIs) Zidovudine (AZT), Abacavir (ABC), and lamiduvine (3TC) were selected in this Thesis to prepare the drug delivery glyconanoparticles (DDS-GNPs).

The preparation and characterization of ABC-GNPs and 3TC-GNPs as well as their application as HIV-1 inhibitors in cellular model is the object of the next sections of this Thesis.

¹⁶ De Clercq E., The history of antiretrovirals: key discoveries over the past 25 years, *Rev. Med. Virol.* 2009, 19, 287–299.

¹⁷ De Clercq E., Antiretroviral drugs, *Curr. Opin. Pharmacol.* 2010, 10, 507-515.

¹⁸ Otto M., New nucleoside reverse transcriptase inhibitors for the treatment of HIV infections, *Curr. Opin. Pharmacol.* 2004, 4, 431-436.

Preparation of anti-HIV prodrug-GNPs

In 2009 gold nanoparticles were used for the first time as carrier for an anti-HIV entry inhibitor drug. An inactive derivative of the inhibitor entry TAK-779 (the active part of the drug was modified to link it to the gold surface) was multimerized on the gold nanoparticle.¹⁹ These nanoparticles coated with the inactive derivative of TAK-779 showed surprisingly anti-HIV activity, probably due to the high-local concentration of the drug derivative on the gold surface. At this time, we were trying to introduce the protease inhibitor Saquinavir on the GNPs, but we encountered chemical problems related with the high lipophilicity of this drug. We decided then to introduce the well known NRTI, Zidovudine (AZT). To link the AZT to the gold surface, chemical modifications of the drug were needed, which can influence the final drug activity. A bifunctional linker bearing an alkyne at a terminal position and a thiol-protected at the other terminus was prepared and used as a molecular bridge between the AZT drug and the gold nanoparticles (Fig. 3). The linker was reacted by click chemistry with the azide group in 3 position of the AZT ribose ring, which is an important group for the activity of AZT. After removal of the thiol-protecting group, the thiol functionality was employed for the formation of the S-Au bond in the preparation of GNPs. GNPs carrying 20 and 50% of this AZT-thiol conjugate were prepared by reducing a water soluble gold salt in presence of NaBH₄. In this reaction, the thiol AZT derivative was mixed with different ratio of a glucose derivative (5-(thio)pentyl β-D-glucopyranoside) which worked as biocompatible component able to modulate the density of the drug on the GNPs. After the AZT-GNPs preparation and characterization we tested their anti-viral activity in cellular experiments. In the tested conditions and at the tested concentrations (from 0.04 to 42 μM in terms of AZT), the AZT-GNPs were not able to improve the free AZT drug antiviral activity which showed a strong inhibition activity at 0.01 μM. The AZT-GNPs failure can thus be ascribed to different reasons. As we have evidence that this type of GNPs are easily uptaken by cells,²⁰ it can be supposed that either the kinases are not able to phosphorylate properly the AZT-derivative on the nanoparticles or the reverse transcriptase does not recognize the AZT-GNPs as substrate.

¹⁹ Bowman M. C., Ballard T. E., Ackerson C. J., Feldheim D. L., Margolis D. M., Melander C., Inhibition of HIV fusion with multivalent gold nanoparticles, *J. Am. Chem. Soc.* 2008, 130, 6896-6897.

²⁰ Arnáiz B., Martínez-Ávila O., Falcon-Perez J. M., Penadés S., Cellular uptake of gold nanoparticles bearing HIV gp120 oligomannosides, *Bioconjug Chem.* 2012, 23, 814-825.

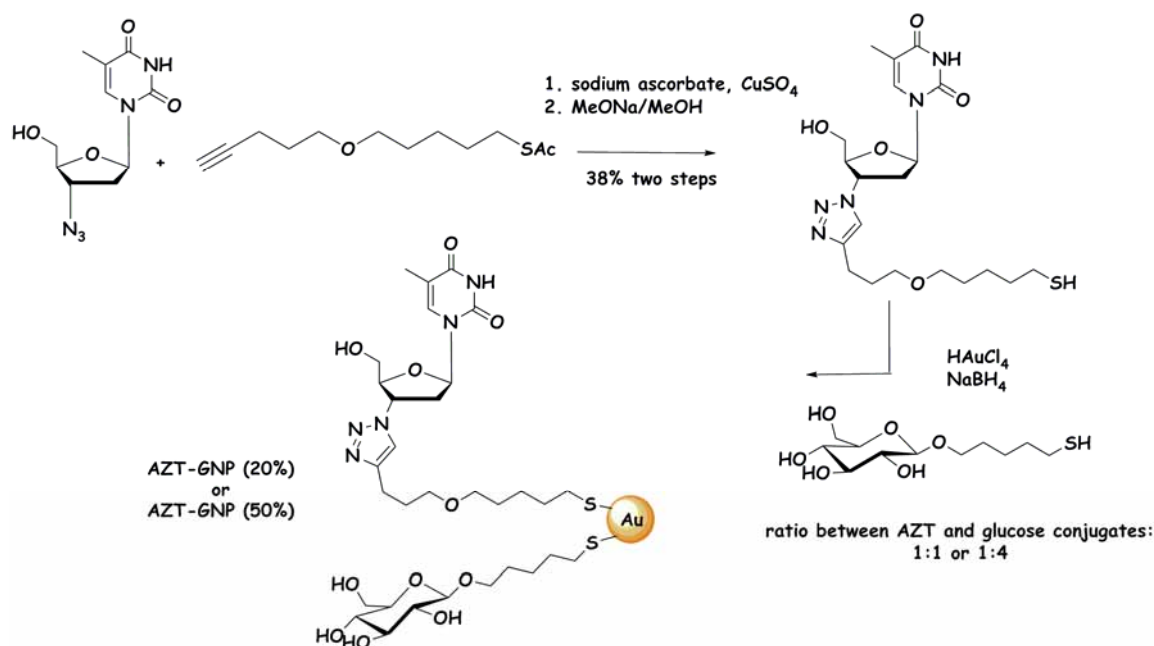


Figure 3: Synthesis of AZT derivative and its multimerization on GNPs. AZT was coupled with a bifunctional alkyne-thiol ending linker by click chemistry. After thiol deprotection, the AZT-thiol conjugate was mixed with different amount of a glucose thiol-ending derivative (used as biocompatible density modulator molecule) in the presence of water soluble gold salt (HAuCl_4) and NaBH_4 in order to prepare the GNPs. After 2h the experimental conditions allowed the formation of water soluble GNPs containing 20 or 50% of AZT and 80 or 50% of the glucose derivative.

Another strategy was then designed for the preparation of drugs containing GNPs: Prodrugs with an easy hydrolysable group that allows the release of the drug from the prepared GNPs by enzymatic/or pH mediated hydrolysis were prepared. We decided to functionalize Abacavir (ABC) and Lamivudine (3TC) at the hydroxyl primary groups through an ester bond to avoid the manipulation of key functionalities that could alter the drug activity. Exploiting the esterase activity or the acid conditions in the cellular medium, it is expected that gold nanoparticles can delivery the drug acting as a drug delivery system for anti-HIV drugs.

In order to obtain the ester prodrugs, ABC and 3TC were reacted with 11-(acetylthio)undecanoic acid, a bifunctional linear aliphatic spacer which has a terminal carboxyl group by one side and a thiol-protected functionality at the other terminus. The resulting drug-conjugates were then deacetylated with hydrazine acetate to give the conjugate prodrugs of ABC and 3TC (Fig. 4)

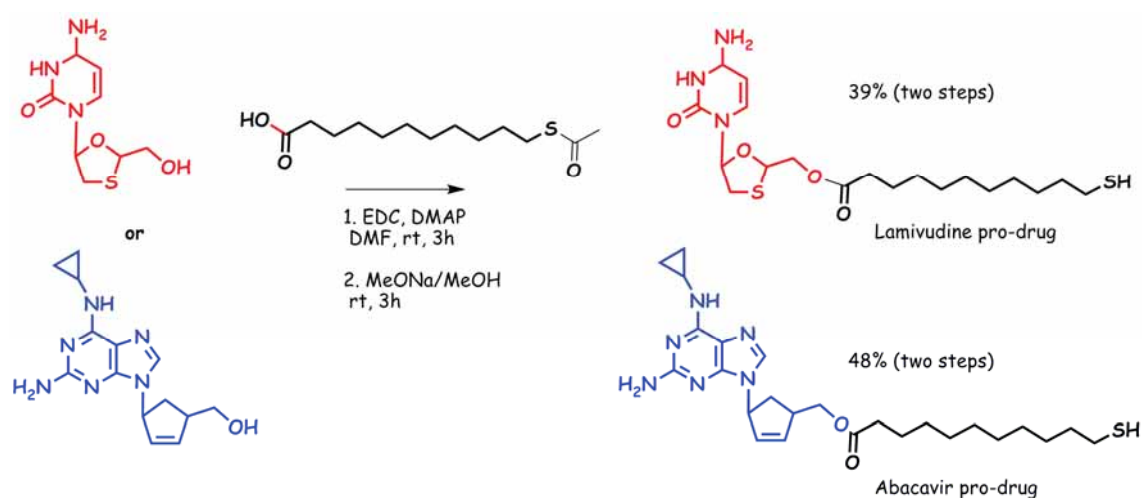


Figure 4: Synthesis of Abacavir and Lamivudine prodrug conjugates. Ester coupling was performed in DMF in presence of ethyl-3-(3-(dimethylamino)-propyl)carbodiimide (EDC) and 4-dimethylaminopyridine (DMAP). After purification, the protecting group of the thiol was removed with MeONa to give the corresponding ester prodrugs with a free thiol ending group. The compounds are depicted as thiol (SH) derivatives for clarity reasons, but in solution they exist as a mixture of thiol and corresponding disulfide (S-S).

Due to the presence of an ester group in the prepared drug derivatives, NaBH_4 could not be used as reducing agent for the *in situ* preparation of these gold nanoparticles. The ABC- and 3TC-GNPs were then prepared by the so-called “thiol-for-thiol” ligand place exchange (LPE) reaction²¹. The LPE reaction methodology allows the insertion of thiol ending ligands (in our case, the thiol-ending prodrugs) on pre-formed GNPs (in our case, GNPs fully covered by a glucose conjugate) by a “thiol for thiol” exchange on the gold surface (Fig. 5). Pre-formed GlcC_5 -GNPs were incubated with ABC and/or 3TC conjugate (0.2 equivalents respect to the glucose conjugates on the GNP). After purification, water soluble GNPs with around 10% of ABC and/or 3TC were obtained and analyzed by HPLC and MS spectrometry to estimate their drug content (see next section).

²¹ Hostetler M. J., Templeton A. C., Murray R. W., Dynamics of place-exchange reactions on monolayer-protected gold cluster molecules, *Langmuir* 1999, 15, 3782-3789.

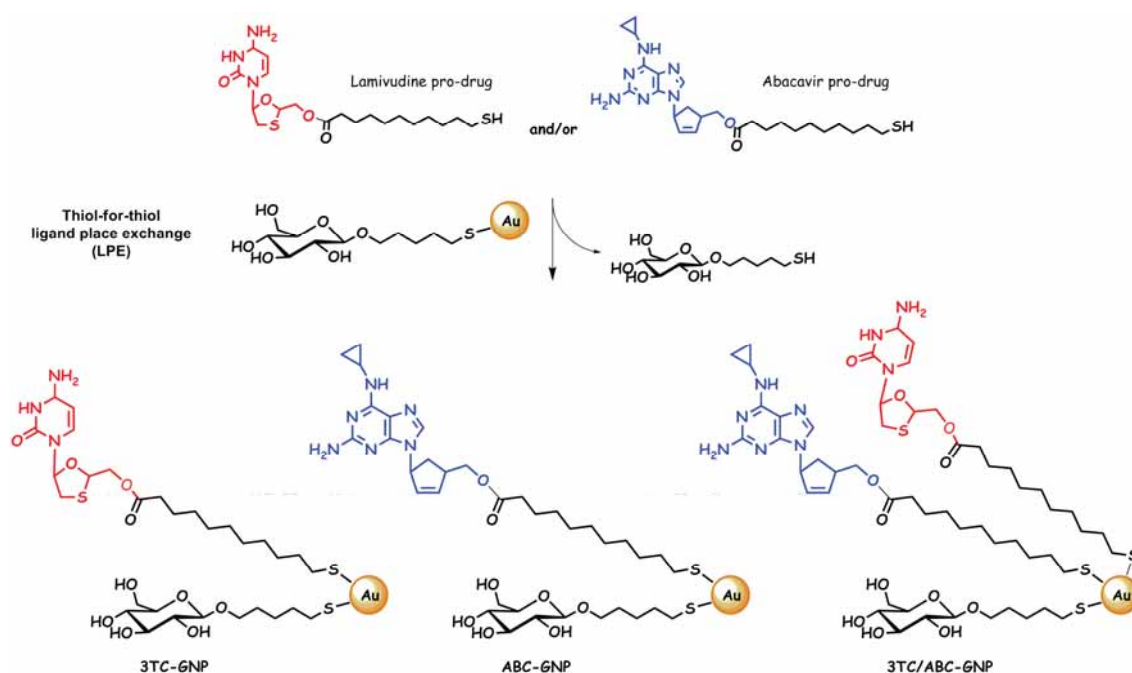


Figure 5: 3TC and ABC-GNPs were prepared by ligand place exchange (LPE) reactions. Glc-GNPs were incubated for 24h with 0.2 eq of the ABC or 3TC thiol-ending prodrugs. The reaction conditions allowed the thiol by thiol ligand exchange on the gold surface allowing the drug inclusion on the GNPs by replacing some glucose ligands on the Glc-GNPs.

Drug quantification and release from the GNPs

To quantify the amount of drug on nanoparticles and to determine the release of the drug from the nanoparticles, first an UV calibration curve of the free drug in the same release conditions was performed. We studied the stability of the GNPs containing ABC or 3TC (around 10%) in HCl 1N at different times by HPLC-MS (Fig. 6). A solution of drugs-GNPs (2mg/mL) in water was treated with HCl 1N and 1:1000 dilution aliquots (10 μ L) of the GNPs-solution were injected at different time in HPLC detecting the free drug by mass spectrometry and quantifying it by UV detection.

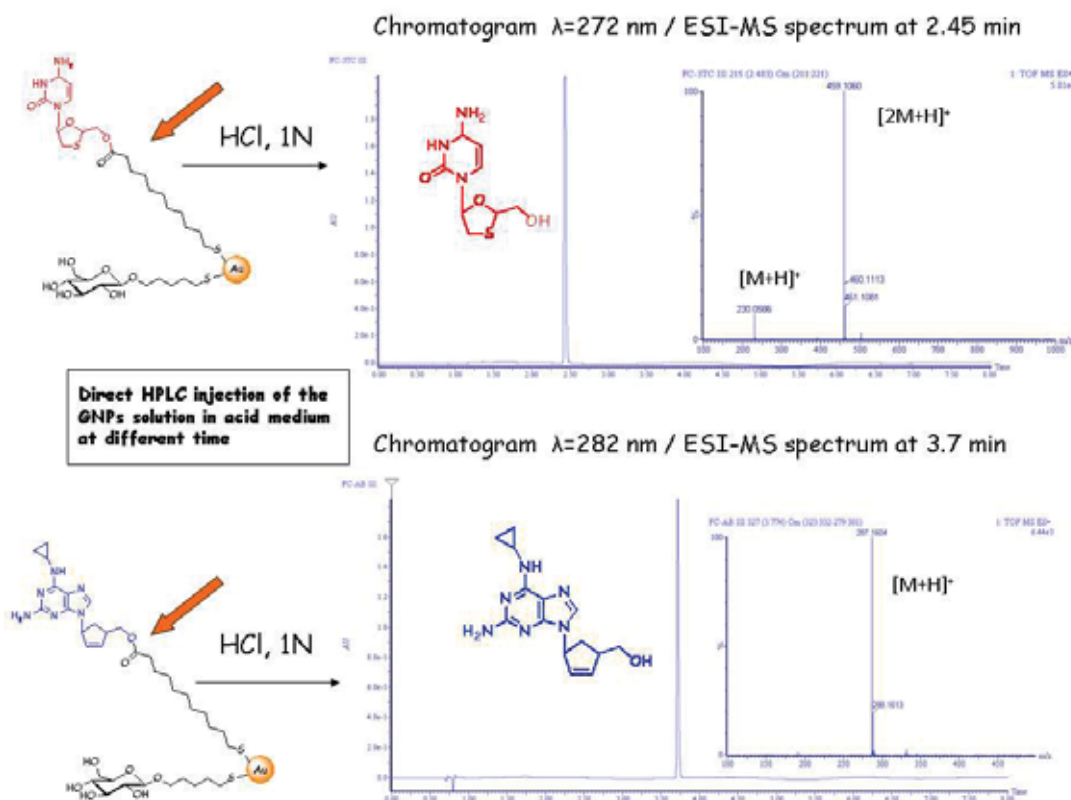


Figure 6: 3TC and ABC-GNPs were treated with HCl 1N at room temperature and aliquots of the GNPs solution were injected in HPLC at different times. The free drug was detected by MS and quantified by UV detection. Upper panel: HPLC chromatogram from 3TC-GNPs injection after 3h in HCl 1N. The peak at 272nm is related with the free 3TC released by the GNPs and its mass was detected by ESI-MS. Lower panel: HPLC chromatogram from ABC-GNPs injection after 3h in HCl 1N. The peak at 282nm is related with the free ABC released by the GNPs and its mass was detected by ESI-MS. In the absence of HCl the GNPs solution shows no peaks in the chromatogram at these wavelengths.

The pH mediated-delivery of the drugs from the GNPs was followed for 2-3 days until a plateau in the kinetic curve of the drug release (Fig. 7). The release of the drug from a $2\mu\text{g/mL}$ GNPs dilution after 150 h was around 200 nM (for ABC-GNPs). Since the concentration of drug in 2mg/mL of ABC-GNPs was estimated to be $200\mu\text{M}$, the pH mediated-release results confirmed the estimation of 10% of the drug on the gold surface and the validity of the system as pH mediated-DDS. The release results fitted with the estimated amount of drug entered on the gold surface after the ligand place exchange reaction and from these results the estimated amount of drug per 1mg of GNPs is $0.1\mu\text{moles}$.

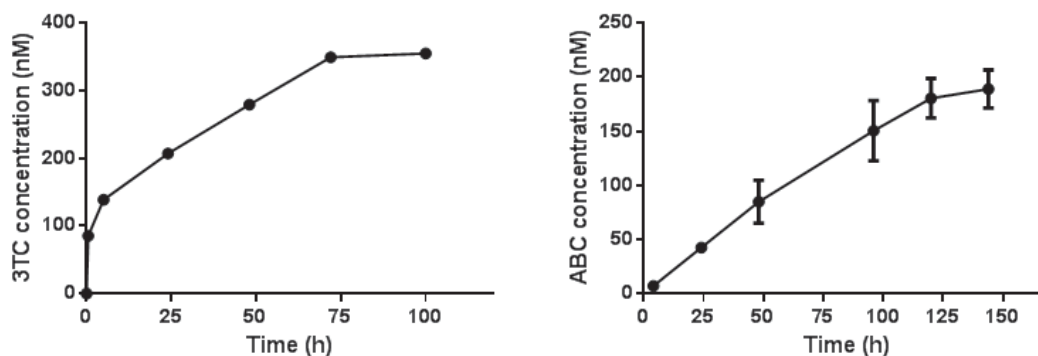


Figure 7: Time course release of free 3TC and ABC from the corresponding GNPs in HCl 1N, followed by HPLC-MS. Left: Release of 3TC from 2 µg/mL 3TC-GNPs for 100h; error bars are not visible. Right: release of ABC from 2 µg/mL ABC-GNPs for 150h until a stable drug concentration in the release medium is reached. Both experiments were performed in triplicate.

Cellular experiments with Lamivudine (3TC) and Abacavir (ABC)-GNPs

To evaluate the anti viral activity of the glyconanoparticles bearing Abacavir or Lamivudine drug conjugates (ABC-GNPs and 3TC-GNPs), cellular experiments were performed in collaboration with Dr Eloisa Yuste (Retrovirology and Viral Immunopathology, IDIBAPS, Hospital Clinic). TZM-bl cells (derived HeLa-cell immortalized cell line that express high levels of CD4 and co-receptors CXCR4 and CCR5) were incubated for 30min with different amount of drug-GNPs (drug concentration from 0.1 to 10 µM), followed by the addition of NL4-3 HIV virus that encodes for luciferase used as reporter gene in the medium. The viral replication was followed by the luciferase activity setting 100% of viral replication (luciferase activity) for the TZM-bl cells treated in the absence of GNPs. A schematic overview of the experiment and a hypothetical mechanism of action of the drug-GNPs is depicted in figure 8.

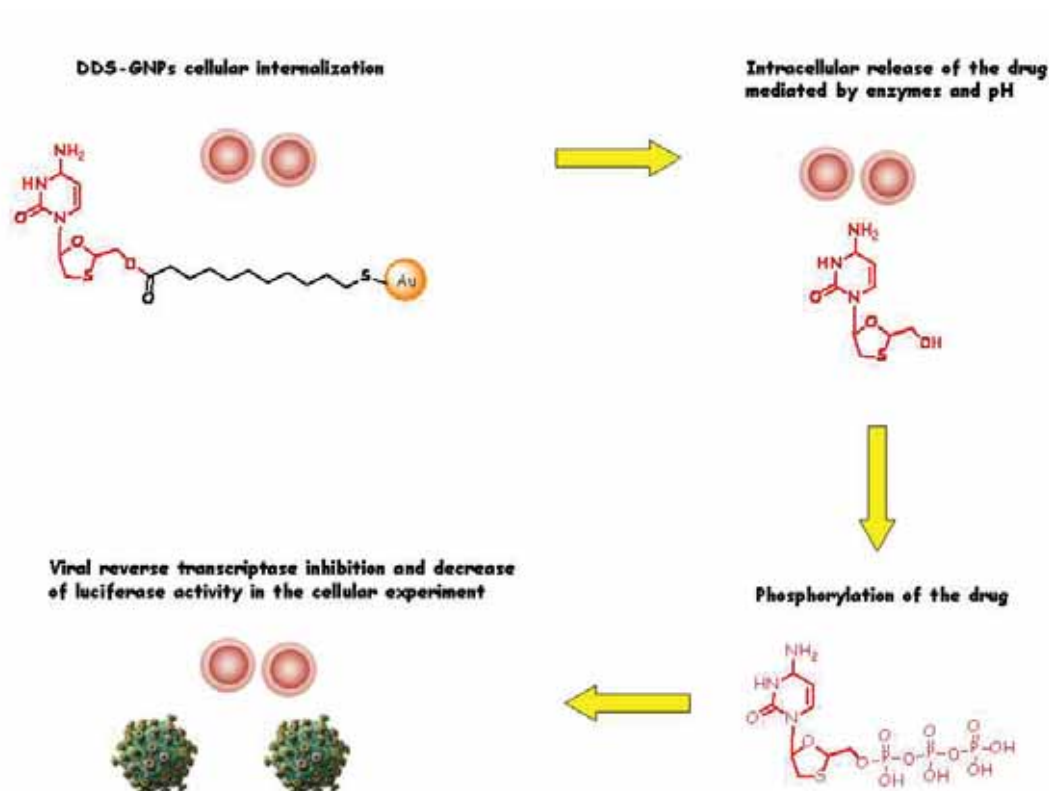


Figure 8: Hypothetical drug-GNPs mechanism of action. The GNPs carrying the drug have first to be up-taken and internalized by the cells. Once in the cellular cytoplasm, intracellular esterase and low pH will hydrolyze the ester bond between the drug and the GNP releasing the free drug. To inhibit the viral reverse transcriptase, the free drug has to be phosphorylated on the free -OH of the ribose-like ring. Once phosphorylated, the drug can irreversibly block the viral enzyme decreasing virus reproduction. The virus, cells and GNPs are not in scale.

Figure 9 shows the decrease of viral replication (correlated with the percentage of luciferase activity) of the Lamivudine GNPs and Abacavir GNPs. Free Lamivudine (Fig. 9 upper panel) showed an IC_{50} of $0.35\mu M$ and its corresponding GNPs showed an IC_{50} of $1\mu M$. Free Abacavir showed an IC_{50} of $5\mu M$ and its corresponding GNPs showed an IC_{50} of $8\mu M$ (Fig. 9 bottom panel). The GNPs carrying both drugs (ABC/3TC-GNPs) showed an IC_{50} of $5\mu M$, very similar to the GNPs carrying only one type of drug. The IC_{50} of the anti-viral activity of the free drugs and the drugs-GNPs were similar. Glc-GNPs were not able to exhibit any anti-viral activity at the tested concentrations.

GNP	IC ₅₀
Glc-GNPs	90 μM
Abacavir	5 μM
Abacavir prodrug	Active
Abacavir GNPs	8 μM
Lamivudine	0.35 μM
Lamivudine prodrug	0.2 μM
Lamivudine GNPs	1 μM
Abacavir/Lamivudine-GNPs	5 μM

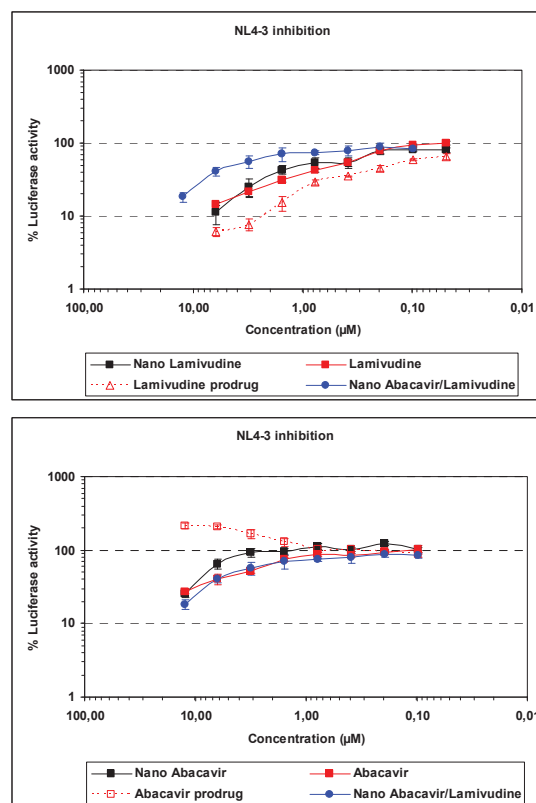


Figure 9: Cellular experiment: Left: The table shows the IC₅₀ of the GNPs in terms of drug concentration. The GNPs containing the prodrugs shows a clear anti viral activity with a similar IC₅₀ of the free drug. Right: The two graphs show the percentage of luciferase activity decreases in the presence of increasing amount of GNPs. 3TC and ABC-GNPs showed an anti viral activity (upper and bottom panel) with an IC₅₀ similar to the free drug.

After only 30min of pre-incubation with TZM-bl cells, these GNPs seem to release the drugs inside the cells and show an NRTi activity as the free drugs at similar concentration. These drugs inhibit the HIV reverse transcriptase enzyme competitively and act as a chain terminator of DNA synthesis. As mentioned before, the lack of a 3'-OH group in the incorporated nucleoside analogue prevents the formation of the 5' to 3' phosphodiester linkage essential for DNA chain elongation and therefore the viral DNA growth is terminated. The activity result suggests that the drug is delivered by the GNPs into the TZM-bl cells where it is triphosphorylated to active metabolites that can compete with the natural substrate of RT avoiding the RNA transcription, e.g. the viral replication (Fig. 8).

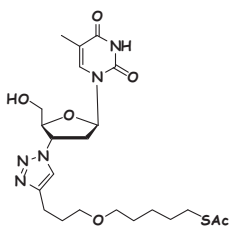
Conclusions

The cellular results indicate that the GNPs were able to inhibit viral replication supporting the strategy for the design of a drug delivery system based on the coupling of ester prodrugs onto gold nanoparticles (DDS-GNPs). We can suppose that the inhibitory activity is due to the cellular internalization of the GNPs and subsequent intracellular release of the drug (Fig. 8). These preliminary results allow us to re-design more complex GNPs with improved activity carrying at the same time different inhibitors able to inhibit viral replication. In addition, complex GNPs carrying other type of molecules, able to block different steps of the viral replication, can be introduced as previously showed with the microbicide candidates sulfate⁻¹⁴ and *manno*-GNPs¹³.

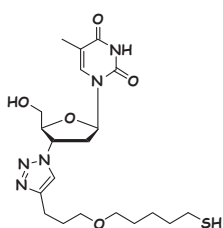
GNPs can also be prepared with higher copies of drugs (more than 10%) on the gold surface although they could result water insoluble. However, in a topical formulation of DDS for vagina or rectum drug release, the solubility of the system in water is not a key feature and the acidic vagina pH could be exploited to release the drug in a sustainable and controlled way.

Experimental section

Zidovudine (AZT) derivative synthesis and AZT-GNPs preparation



S-acetyl protected AZT derivative: Bifunctional alkyne linker (27mg, 0.2mmol) was dissolved in THF (1mL). Then 80 μ L of a 7.5% water solution of CuSO₄ and 94 μ L of sodium ascorbate (1M in water) were added to the linker solution. After 10min stirring AZT (32mg, 0.12mmol) was added to the mixture followed by the addition of 200 μ L of tert-butanol and 200 μ L of water to improve the solubility of the compound in the reaction mixture. The reaction was stirred for 48h, concentrated and purified by column chromatography on silica gel (gradient AcOEt/MeOH 20/1 to AcOEt/MeOH 10/1) to obtain the *S*-acetyl protected AZT derivative as a white solid (31mg, 0.06mmol, 54%). ¹H NMR (500 MHz, CDCl₃) δ = 9.35 (bs, 1H), 7.53 (s, 1H), 7.51 (s, 1H), 6.26 (t, J=6.6, 1H), 5.47-5.43 (m, 1H), 4.42-4.39 (m, 1H), 3.89 (AB system, 2H), 3.45 (t, J=6.2, 2H), 3.39 (t, J = 6.5, 2H), 2.95-2.90 (m, 2H), 2.85 (t, J=7.3, 2H), 2.80 (t, J=7.3, 2H), 2.31 (s, 3H, SAc), 1.97-1.91 (m, 2H), 1.90 (s, 3H, CH₃), 1.61-1.54 (m, 4H), 1.44-1.38 (m, 2H), 1.25 (t, J=7.7, 1H).



AZT derivative (thiol-ending AZT): *S*-acetyl protected AZT derivative (31mg, 0.06mmol) was dissolved in MeOH (2mL) and stirred in presence of MeONa (1.7mg, 0.03mmol). After 2h the reaction was quenched thought Amberlite and the residue was purified by size-exclusion chromatography Sephadex LH-20 (MeOH/H₂O 9/1) to give the unprotected AZT derivative (20mg, 0.045mmol, 71%). ¹H NMR (500 MHz, MeOD) δ = 9.13 (bs, 1H),

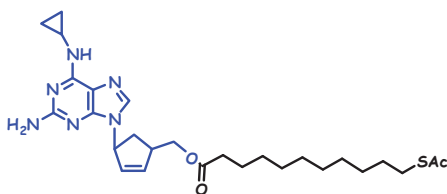
7.52 (s, 1H), 7.47 (s, 1H), 6.23 (t, J=6.6, 1H), 5.48-5.42 (m, 1H), 4.44-4.38 (m, 1H), 3.91 (AB system, 2H), 3.47 (t, J=6.2, 2H), 3.42 (t, J = 6.5, 2H), 2.99-2.91 (m, 2H), 2.82 (t, J=7.6, 2H), 2.53 (q, J=6.2, 2H), 1.98-1.92 (m, 2H), 1.92 (s, 3H, CH₃), 1.66-1.55 (m, 4H), 1.48-1.42 (m, 2H), 1.35 (t, J=7.7, 1H). High resolution mass spectrometry: theoretical [M+H] m/z: 454.2124, experimental 454.2129, deviation 1.1 ppm.

AZT-GNPs (20% and 50%): Reaction of a 1:4 or 1:1 mixture of AZT-derivative (4 or 9mg) and Glc-C₅SH (9.9 or 5.6mg) with HAuCl₄ and NaBH₄ gave 1.5 or 1.8mg of AZT-GNPs as brown solid. TEM (average diameter): ~1.5 or 1.8nm. Molar ratio of conjugates per nanoparticle was determined by analyzing the mixtures using NMR before and after nanoparticles formation.

AZT-GNPs 20%: ¹H NMR for AZT-GNPs 20% (500 MHz, D₂O ws): Only significant peaks are reported: δ = 7.94 (bd, 2H, from aromatic protons of AZT conjugate), 6.51 (bs, 1H, AZT conjugate proton), 5.52 (bs, 1H, AZT conjugate proton), 4.49 (bs, 5H, from anomeric proton of glucose conjugate). Ratio between AZT-Cd and Glucose signals ~1:5.7. These results are in agreement with the estimation of 20% of AZT on the GNPs. UV/Vis (H₂O, 0.1 mg/mL): surface plasmon band not observed.

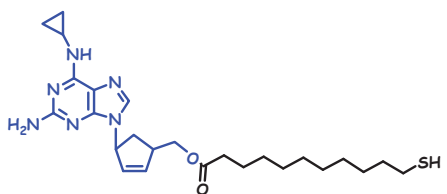
AZT-GNPs 50%: ¹H NMR for AZT-GNPs 50% (500 MHz, D₂O ws): Only significant peaks are reported: δ = 7.70 (bd, 2H, from aromatic protons of AZT conjugate), 6.27 (bs, 1H, AZT conjugate proton), 5.26 (bs, 1H, AZT conjugate proton), 4.25 (bs, 1H, from anomeric proton of glucose conjugate). Ratio between AZT-Cd and Glucose signals ~1:2.3. These results are in agreement with the estimation of 50% of AZT on the GNPs. UV/Vis (H₂O, 0.1 mg/mL): surface plasmon band not observed.

Abacavir (ABC) derivative synthesis and Abacavir-GNPs preparation



Protected Abacavir conjugate: Abacavir (63mg, 0.2mmol) was dissolved in dry DMF (3mL) followed by the addition of the bifunctional acid linker (89mg, 0.3mmol) and DMAP (54mg, 0.4mmol). The solution was put at 0 °C in ice bath and EDC (84mg, 0.4mmol) was added. After 5h the reaction was diluted with

AcOEt and wash with water (4X5mL). The organic phase was dried over Na₂SO₄ and purified by column chromatography on silica gel (gradient MeOH/CH₂Cl₂ 1/20 to MeOH/CH₂Cl₂ 1/9) to obtain the protected Abacavir derivative as a clear oil (100mg, 0.12mmol, 85%). ¹H NMR (500 MHz, MeOD) δ = 7.68 (s, 1H), 6.15-6.12 (m, 1H), 5.97-5.94 (m, 1H), 5.52-5.49 (m, 1H), 4.19-4.11 (m, 2H), 3.20-3.13 (m, 1H), 2.95-2.87 (m, 1H), 2.86-2.79 (m, 1H), 2.29 (s, 3H, SAc), 1.68-1.63 (m, 1H), 1.56-1.49 (m, 4H), 1.35-1.20 (m, 12H), 0.86-0.82 (m, 2H), 0.62-0.59 (m, 2H).



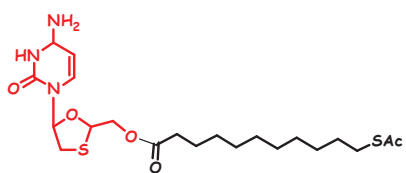
Abacavir derivative (ester prodrug): acetyl protected Abacavir derivative (65mg, 0.12mmol) was dissolved in MeOH (3mL) and stirred in presence of hydrazine acetate (35mg, 0.3mmol). After 24h the reaction was diluted with AcOEt, neutralized with HCl 0.1M and washed with water (5X8mL). The organic phase was

dried over Na₂SO₄ and the residue was purified by size-exclusion chromatography Sephadex LH-20 (MeOH/H₂O 9/1) to give the unprotected Abacavir derivative (34mg, 56%). ¹H NMR (500 MHz, MeOD) δ = 7.69 (s, 1H), 6.17-6.13 (m, 1H), 5.99-5.95 (m, 1H), 5.53-5.50 (m, 1H), 4.20-4.11 (m, 2H), 3.20-3.12 (m, 1H), 2.96-2.87 (m, 1H), 2.83-2.79 (m, 1H), 2.65 (t, J = 7.2, disulfide ~10%), 2.47 (t, J=7.1, 2H, thiol ~90%), 2.31-2.27 (m, 2H), 1.69-1.64 (m, 1H), 1.59-1.53 (m, 4H),

1.40-1.19 (m, 12H), 0.92-0.80 (m, 2H), 0.65-0.57 (m, 2H). High resolution mass spectrometry, theoretical $[M+H]^+$ m/z : 487.2856, experimental 487.2854, deviation < 1 ppm.

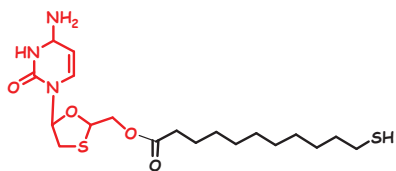
Abacavir GNPs: 1mg of Glc-GNPs were dissolved in a mixture $H_2O/MeOH$ (140 μ L). 0.046mg of Abacavir ester prodrug (0.2eq respect to the Glc-GNPs ligands, 90% thiol, 10% disulphide checked by NMR) in MeOH solution were added to the Glc-GNPs. After 22h of shaking at room temperature the GNPs were precipitated with EtOH and washed 5 times (5x1mL EtOH). The final dark solid was then dissolved in 450 μ L of H_2O + 50 μ L of DMSO. TEM (average gold diameter): 2.9 \pm 0.9 (Fig. 10); UV/Vis ($H_2O/DMSO$, 0.1 mg/mL): surface plasmon band not observed.

Lamivudine (3TC) derivative synthesis and Lamivudine-GNPs preparation



Protected Lamivudine derivative: Lamivudine (12mg, 0.05mmol) was dissolved in dry DMF (3mL) followed by the addition of the bifunctional acid linker (20mg, 0.07mmol) and DMAP (12.5mg, 0.1mmol). The solution was put at 0 $^{\circ}C$ in ice bath and EDC (19.5mg, 0.1mmol) was added. After

3h the reaction was diluted with AcOEt and wash with water (4X5mL). The organic phase was dried over Na_2SO_4 and purified by column chromatography on silica gel (gradient MeOH/ CH_2Cl_2 1/40 to MeOH/ CH_2Cl_2 1/10) to obtain the protected Abacavir derivative as a clear oil (8mg, 70%). 1H NMR (500 MHz, MeOD) δ = 7.88 (d, $J=7.5$, 1H), 6.29 (t, $J=4.9$, 1H), 5.90 (d, $J=7.5$, 1H), 5.44-5.42 (m, 1H), 4.61-4.58 (m, 1H), 4.49 (AB system, 2H), 3.54 (dd, $J=12.0$, 5.4, 1H), 3.15 (dd, $J=12.0$, 4.6, 1H), 2.85 (t, $J=7.3$, 2H), 2.39 (t, $J=7.3$, 2H), 2.30 (s, 3H, SAC), 1.67-1.61 (m, 2H), 1.58-1.52 (m, 2H), 1.38-1.26 (m, 12H).



Lamivudine derivative (ester prodrug): Protected Lamivudine derivative (4mg, 0.007mmol) was dissolved in MeOH (2mL) and stirred in presence of hydrazine acetate (2mg, 0.02mmol). After 3h the reaction was diluted with AcOEt, neutralized with HCl 0.1M and washed with water (4X4mL). The organic phase was dried over Na_2SO_4 and the

residue was purified by size-exclusion chromatography Sephadex LH-20 (MeOH/ H_2O 9/1) to give the unprotected Abacavir derivative (2mg, 56%). 1H NMR (500 MHz, MeOD) δ = 7.88 (d, $J=7.5$, 1H), 6.29 (t, $J=5.0$, 1H), 5.91 (d, $J=7.5$, 1H), 5.44-5.42 (m, 1H), 4.49 (AB system, 2H), 3.54 (dd, $J=12.0$, 5.4, 1H), 3.15 (dd, $J=12.0$, 4.6, 1H), 2.48 (t, $J=7.1$, 2H), 2.39 (t, $J=7.3$, 2H), 1.69-1.53 (m, 4H), 1.43-1.25 (m, 12H). High resolution mass spectrometry, theoretical $[M+H]^+$ m/z : 430.1834, experimental 430.1809, deviation 5.8 ppm.

Lamivudine GNPs: 1mg of Glc-GNPs was dissolved in a mixture $H_2O/MeOH$ (140 μ L). 0.040mg of Lamivudine ester prodrug (0.2eq respect to the Glc-GNPs ligands, 90% thiol, 10% disulphide checked by NMR) in MeOH solution were added to the Glc-GNPs. After 22h of shaking at room temperature the GNPs were precipitated with EtOH and washed 5 times (5x1mL EtOH). The final dark solid was then dissolved in 450 μ L of H_2O + 50 μ L of DMSO. TEM (average gold diameter): 3.0 \pm 1.2 nm (Fig. 10); UV/Vis ($H_2O/DMSO$, 0.1 mg/mL): surface plasmon band not observed.

Abacavir/Lamivudine-GNPs preparation: 1mg of Glc-GNPs were dissolved in a mixture H₂O/MeOH (140μL). 0.05mg of Abacavir ester prodrug (0.1eq respect to the Glc-GNPs ligands, 90% thiol, 10% disulphide checked by NMR) in MeOH solution and 0.04mg of Lamivudine ester prodrug (0.1eq respect to the Glc-GNPs ligands, 90% thiol, 10% disulphide checked by NMR) in MeOH solution were added to the Glc-GNPs. After 22h of shaking at room temperature the GNPs were precipitated with EtOH and washed 5 times (5x1mL EtOH). The final dark solid was then dissolved in 450μL of H₂O + 50 μL of DMSO. TEM (average gold diameter): 3.0±1.3 nm (Fig. 10); UV/Vis (H₂O/DMSO, 0.1 mg/mL): surface plasmon band not observed.

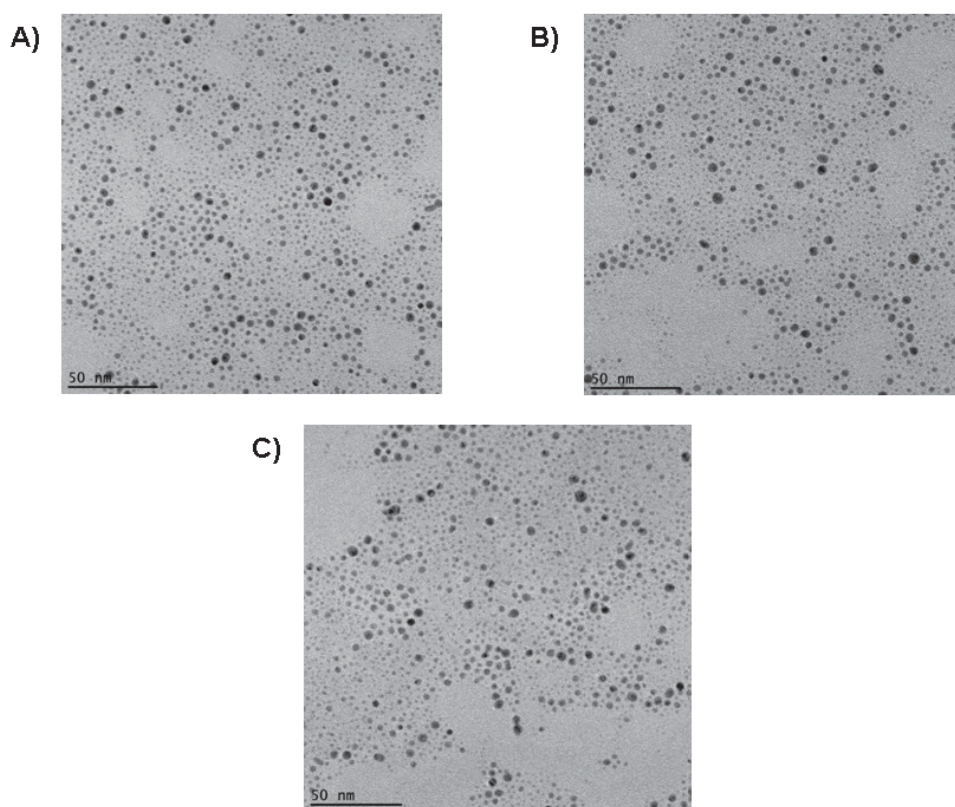


Figure 10: TEM micrographs of the drugs GNPs. **A)** GNPs bearing ABC conjugate, **B)** GNPs bearing 3TC conjugate, **C)** GNPs bearing ABC and 3TC conjugates.

Chapter-2

Gold nanoparticles as carrier for HIV carbohydrate antigens (the vaccine approach)

In the frame of Glyco-HIV project

As we mentioned in the introduction to this part of the Thesis, the highly active antiretroviral therapy (HAART) is the only regimen approved to treat people infected by human immunodeficiency virus (HIV). Although several progresses in the development of anti-HIV vaccines have been recently achieved, no effective vaccines or microbicides against this virus are currently available. A deeper understanding of molecular basis of HIV infection and the design of new chemical tools that could contribute to improve the anti-HIV therapy are really necessary. By combining simultaneously on the GNPs carbohydrate antigens of the HIV envelop protein gp120 with T-helper peptides, we expected to obtain **anti-carbohydrate vaccine candidates** able to evoke specific and functional IgG antibodies against the virus (see Fig. 2 in the Introduction to Part-1).

Being a virus, HIV needs the host cells biochemical pathways to reproduce its genome. For example, during the assembly in the host CD4⁺ T cells, the viral surface protein gp120 is highly glycosylated by the host cellular system exploiting the host Golgi pathway. Evolution maintain this carbohydrate pathway and HIV takes reproductive advantages from it: The carbohydrates mask the viral surface for immune recognition¹, trigger an immunosuppressive response on the T cells and help HIV in the dendritic cells (DC)-mediated *trans*-infection.¹ HIV gp120 is one of the most glycosylated proteins present in nature: Around 50% of its mass is composed by high-mannose type glycans that are human self-carbohydrates.²

Clusters of self high-mannose glycans are one of the conserved patterns on HIV surface that can be exploited and studied in the design of an effective vaccine against HIV. Broadly neutralizing antibodies were found in some HIV-infected individuals and they were able to provide protection against viral challenge in animal models.³ One of these broadly neutralizing anti-HIV antibodies, 2G12, is able to recognize clusters of high-mannose *N*-glycans present on the viral envelope glycoprotein gp120.⁴ Crystal structures of the complex between 2G12 with the dimannoside Man α 1 \rightarrow 2Man and the triantennary undecasaccharide Man₉GlcNAc₂ (Fig.1,

¹ Walker B. D., Burton D. R., Toward an AIDS vaccine, *Science* 2008, 320, 760-764 and Yuste E., Bixby J., Lifson J., Sato S., Johnson W., Desrosiers R., Glycosylation of gp41 of simian immunodeficiency virus shields epitopes that can be targets for neutralizing antibodies, *J Virol.* 2008, 82, 12472-12486.

² Barin F., McLane M. F., Allan J. S., Lee T. H., Groopman J. E., Essex M., Virus envelope protein of HTLV-III represents major target antigen for antibodies in AIDS patients, *Science* 1985, 228, 1094-1096.

³ Mascola J. R., Montefiori D. C., The role of antibodies in HIV vaccines, *Annu. Rev. Immunol.* 2010, 28, 413-444.

⁴ Sanders R. W., Venturi M., Schiffner L., Kalyanaraman R., Katinger H., Lloyd K. O., Kwong P. D., Moore J. P., The mannose-dependent epitope for neutralizing antibody 2G12 on human immunodeficiency virus type 1 glycoprotein gp120, *J. Virol.* 2002, 76, 7293-7305.

right) showed that the antibody has a peculiar shape in which two fragment antigen binding sections (Fab) are swapped (Fig. 1, left). A molecular model for the 2G12/gp120 interaction was proposed: Three separate **Man₉GlcNAc₂** glycans seem to mediate the binding of 2G12 to gp120 opening the way for new strategies in the design of carbohydrate-based anti-HIV vaccines.⁵

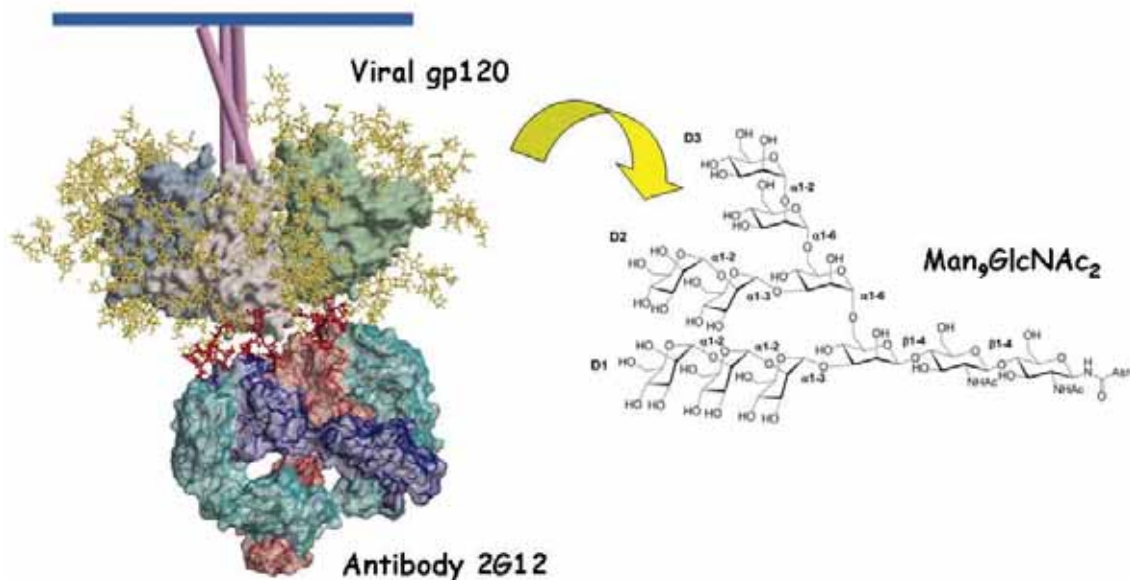


Figure 1: Left: A model of mAb 2G12 Fab2 bound to the HIV-1 gp120 Env spike, showing the multivalent interaction of the clusters of high-mannose glycans (**Man₉GlcNAc₂**) with the 2G12. From: Burton D R et al. PNAS 2005; 102:14943-14948. Right: **Man₉GlcNAc₂** structure presents on the viral gp120, showing the D1, D2 and D3 oligomannoside antennas (or arms).

Recently, new broadly neutralizing antibodies called PGT 125-128 were found in several donors providing broad protection at low concentrations by neutralizing 50% of the tested HIV clades.⁶ Some of these antibodies competed with 2G12 in gp120 competition assay suggesting that a carbohydrate epitope was recognized. A glycan microarray was then performed revealing that the antibodies called PGT 125-128 recognized the nonamannoside **Man₉** and **Man₉GlcNAc₂**. The binding of PGT antibodies to gp120 was competed by **Man₉**, but, unlike 2G12, was not competed by the tetramannoside **Man₄** (D1 arm of **Man₉GlcNAc₂**, also called Te

⁵ Calarese D. A., Scanlan C. N., Zwick M. B., Deechongkit S., Mimura Y., Kunert R., Zhu P., Wormald M. R., Stanfield R. L., Roux K. H., Kelly J. W., Rudd P. M., Dwek R. A., Katinger H., Burton D. R., Wilson I. A., Antibody domain exchange is an immunological solution to carbohydrate cluster recognition, Science 2003, 300, 2065-2071.

⁶ Walker L.M., Huber M., Doores K. J., Falkowska E., Pejchal R., Julien J. P., Wang S. K., Ramos A., Chan-Hui P. Y., Moyle M., Mitcham J. L., Hammond P. W., Olsen O. A., Phung P., Fling S., Wong C. H., Phogat S., Wrin T., Simek M. D., Protocol G Principal Investigators, Koff W. C., Wilson I. A., Burton D. R., Poignard P., Broad neutralization coverage of HIV by multiple highly potent antibodies, Nature 2011, 477, 466-470.

in this chapter). This study revealed new anti-carbohydrate antibodies against HIV and molecular studies have given a deeper knowledge about the carbohydrate epitopes of these antibodies.⁷

The way to get a carbohydrate-based vaccine against HIV is still long and a lot of research has to be done revealing the molecular mechanisms of antibody recognition and immune response against the high-mannose clusters of the HIV gp120. Carbohydrates are usually poorly immunogenic, but it seems that the presentation as clusters of high-mannose *N*-glycans of the viral envelope glycoprotein gp120 evokes an immune response able to raise specific anti-carbohydrate IgG antibodies as the 2G12. The multivalent nature of the 2G12-oligomannosides interactions inspired scientist to multimerise the undecasaccharide Man₉GlcNAc₂ and/or its partial structures onto different scaffolds in order to mimic the natural multivalent presentation of the gp120-high-mannose glycans.^{8, 9} Wang's,^{10, 11} Wong, Burton and colleagues',^{12, 13} Danishefsky's,^{14, 15} and Rappuoli's¹⁶ groups, have multimerized high mannose-

⁷ Pejchal R., Doores K. J., Walker L. M., Khayat R., Huang P. S., Wang S. K., Stanfield R. L., Julien J. P., Ramos A., Crispin M., Depetris R., Katpally U., Marozsan A., Cupo A., Malveste S., Liu Y., McBride R., Ito Y., Sanders R. W., Ogohara C., Paulson J. C., Feizi T., Scanlan C. N., Wong C. H., Moore J. P., Olson W. C., Ward A. B., Pognard P., Schief W. R., Burton D. R., Wilson I. A, A potent and broad neutralizing antibody recognizes and penetrates the HIV glycan shield, *Science* 2011, 334, 1097-1103.

⁸ L.-X. Wang, Carbohydrate-Based Vaccines against HIV/AIDS in *Carbohydrate Drug Design*, Eds: A. A. Klyosov, Z. J. Witzczak, D. Platt; ACS Symposium Series 932, 2006, Chapter 6, pp 133-160.

⁹ D. Calarese, C. Scanlan, H.-K. Lee, P. Rudd, C.-H. Wong, R. Dwek, D. Burton, and I. A. Wilson, Toward a Carbohydrate-Based HIV-1 Vaccine, in *Carbohydrate Drug Design*, Eds: A. A. Klyosov, Z. J. Witzczak, D. Platt; ACS Symposium Series 932, 2006, Chapter 7, pp 161-185

¹⁰ Wang J., Li H., Zou G., Wang L. X., Novel template-assembled oligosaccharide clusters as epitope mimics for HIV-neutralizing antibody 2G12. Design, synthesis, and antibody binding study, *Org. Biomol. Chem.* 2007, 5, 1529-1540.

¹¹ Ni J., Song H., Wang Y., Stamatou N. M., Wang L. X., Toward a carbohydrate-based HIV-1 vaccine: synthesis and immunological studies of oligomannose-containing glycoconjugates, *Bioconjugate Chem.*, 2006, 17, 493-500.

¹² Astronomo R.D., Kaltgrad E., Udit A. K., Wang S. K., Doores K. J., Huang C. Y., Pantophlet R., Paulson J. C., Wong C. H., Finn M. G., Burton D. R., Defining criteria for oligomannose immunogens for HIV using icosahedral virus capsid scaffolds, *Chem. Biol.* 2010, 17, 357-370.

¹³ Astronomo R. D., Lee H. K., Scanlan C. N., Pantophlet R., Huang C. Y., Wilson I. A., Blixt O., Dwek R. A., Wong C. H., Burton D. R., A glycoconjugate antigen based on the recognition motif of a broadly neutralizing human immunodeficiency virus antibody, 2G12, is immunogenic but elicits antibodies unable to bind to the self glycans of gp120, *J. Virol.* 2008, 82, 6359-6368.

¹⁴ Krauss I. J., Joyce J. G., Finnefrock A. C., Song H. C., Dudkin V. Y., Geng X., Warren J. D., Chastain M., Shiver J. W., Danishefsky S. J., Fully synthetic carbohydrate HIV antigens designed on the logic of the 2G12 antibody, *J. Am. Chem. Soc.* 2007, 129, 11042-11044.

¹⁵ Joyce J. G., Krauss I. J., Song H. C., Opalka D. W., Grimm K. M., Nahas D. D., Esser M. T., Hrin R., Feng M., Dudkin V. Y., Chastain M., Shiver J. W., Danishefsky S. J., An oligosaccharide-based HIV-1 2G12

type oligosaccharides onto different synthetic scaffolds. The incorporation of T-helper epitope peptides¹¹ or antigenic carrier proteins^{10, 14, 16} onto these scaffolds enhanced the poor immunogenicity of the oligosaccharides. Although most of these systems were able to induce a carbohydrate-specific immune response in animals, the IgG antibodies, however, were unable to bind to gp120 or neutralize the virus.^{11, 12, 13, 15, 16} These results highlight the difficulty to obtain specific IgG antibodies against HIV and the need for new carbohydrate multivalent systems, which can help in the fight against HIV. To elicit high titers of antibodies against the 2G12 epitope remains a still open challenge for synthetic carbohydrate-based vaccines against HIV.

In this part of the Thesis, we have tried to design and prepare anti-HIV carbohydrate vaccines based on GNPs. We have addressed first the study of the molecular interactions between multivalent GNPs carrying synthetic oligomannoside branches of Man₉ oligosaccharide and 2G12 by means of several techniques such as Surface Plasmon Resonance (SPR), Saturation Transfer Difference NMR spectroscopy (STD-NMR), printed microarrays, and cellular assays. The aim was to identify the minimal carbohydrate epitopes able to mimic the interaction of high-mannoses clusters on the gp120 with 2G12. Based on these results, we have prepared GNPs carrying the best 2G12 oligomannoside ligands as anti carbohydrate-based vaccine candidates against HIV and tested them *in vivo* (mice) as immunogens.

2.1 Anti-HIV carbohydrate-based vaccine rational design

Our group had previously prepared a small library of GNPs coated with oligomannosides that are partial structures of the gp120 undecasaccharide Man₉GlcNAc₂ (Fig. 2). These nanoparticles, named *manno*-GNPs were prepared as microbicides candidates.¹⁷ The *manno*-GNPs were designed to target the mannose-binding lectin DC-SIGN (Dendritic Cell-Specific

mimotope vaccine induces carbohydrate-specific antibodies that fail to neutralize HIV-1 virions, Proc. Natl. Acad. Sci. USA 2008, 105, 15684-15689.

¹⁶ Kabanova A., Adamo R., Proietti D., Berti F., Tontini M., Rappuoli R., Costantino P., Preparation, characterization and immunogenicity of HIV-1 related high-mannose oligosaccharides-CRM197 glycoconjugates, Glycoconj. J. 2010, 27, 501-513.

¹⁷ Martínez-Ávila O., Hijazi K., Marradi M., Clavel, C., Campion, C., Kelly C., Penadés S., Gold manno-glyconanoparticles: multivalent systems to block HIV-1 gp120 binding to the lectin DC-SIGN, Chem. Eur. J. 2009, 15, 9874-9888.

Intercellular adhesion molecule-3-Grabbing Non-integrin), a surface receptor of dendritic cells (DCs), which mediates the interaction between gp120 glycans and DCs.¹⁸ DCs are antigen-presenting cells (APC) exploited by the virus to infect T lymphocytes where viral replication mainly occurs. This DC-HIV interaction is mediated by the high-mannose-type glycans of gp120 and DC-SIGN expressed on DCs. The multivalent *manno*-GNPs inhibited the binding of DC-SIGN to gp120 at sub-micromolar level, showing enhanced activity respect to the corresponding monovalent mannosides (millimolar range).¹⁷ Furthermore, cellular experiments demonstrated that *manno*-GNPs were able to inhibit *in vitro* DC-SIGN-mediated HIV-1 *trans*-infection of human T cells.¹⁹ The *trans*-infection is one of the proposed mechanisms that HIV exploits to infect T lymphocytes, where viral replication occurs.²⁰ The obtained results suggested that *manno*-GNPs are good candidates as an antiadhesive barrier to prevent early stage of HIV infection. Based on these results and knowing that one of the human broadly neutralizing antibody against HIV-1, namely IgG 2G12 (Fig.1), recognizes clusters of high-mannose glycans of HIV envelope gp120, we used the *manno*-GNPs to develop anti-HIV vaccine candidates with the expectation that they could be able to evoke 2G12-like antibodies (vaccine approach). The GNP technology provides control over the density and conformational flexibility of the attached glycans on the GNPs. A correct mimicking system of the gp120 glycans should be able to evoke neutralizing 2G12-like antibodies. The *manno*-GNPs could offer a valid and versatile alternative in this direction, similarly as the strategies that have been applied by different researchers towards the design of HIV carbohydrate-based vaccines.^{8,9}

The investigation of the selectivity of the distinct *manno*-GNPs for the 2G12 antibody was the first step to design an anti-HIV carbohydrate vaccine. A small library of thiol-ending oligomannoside conjugates and the corresponding *manno*-GNPs (Fig. 2) with varying density of oligomannosides were prepared by *in situ* synthesis as already described.¹⁷

¹⁸ van Kooyk Y., Geijtenbeek T. B. H., DC-SIGN: escape mechanism for pathogens, Nat. Rev. Immunol. 2003, 3, 697-709.

¹⁹ Martínez-Ávila, O., Bedoya L. M., Marradi M., Clavel, C., Alcamí J., Penadés S., Multivalent manno-glyconanoparticles inhibit DC-SIGN-mediated HIV-1 *trans*-infection of human T cells, Chembiochem 2009, 10, 1806-1809.

²⁰ Geijtenbeek T. B. H., Kwon D. S., Torensma R., van Vliet S. J., van Duijnhoven G. C. F., Middel J., Cornelissen I., Nottet H., KewalRamani V. N., Littman D. R., Figdor C. G., van Kooyk Y., DC-SIGN, a dendritic cell-specific HIV-1-binding protein that enhances *trans*-infection of T cells, Cell 2000, 100, 587-597.

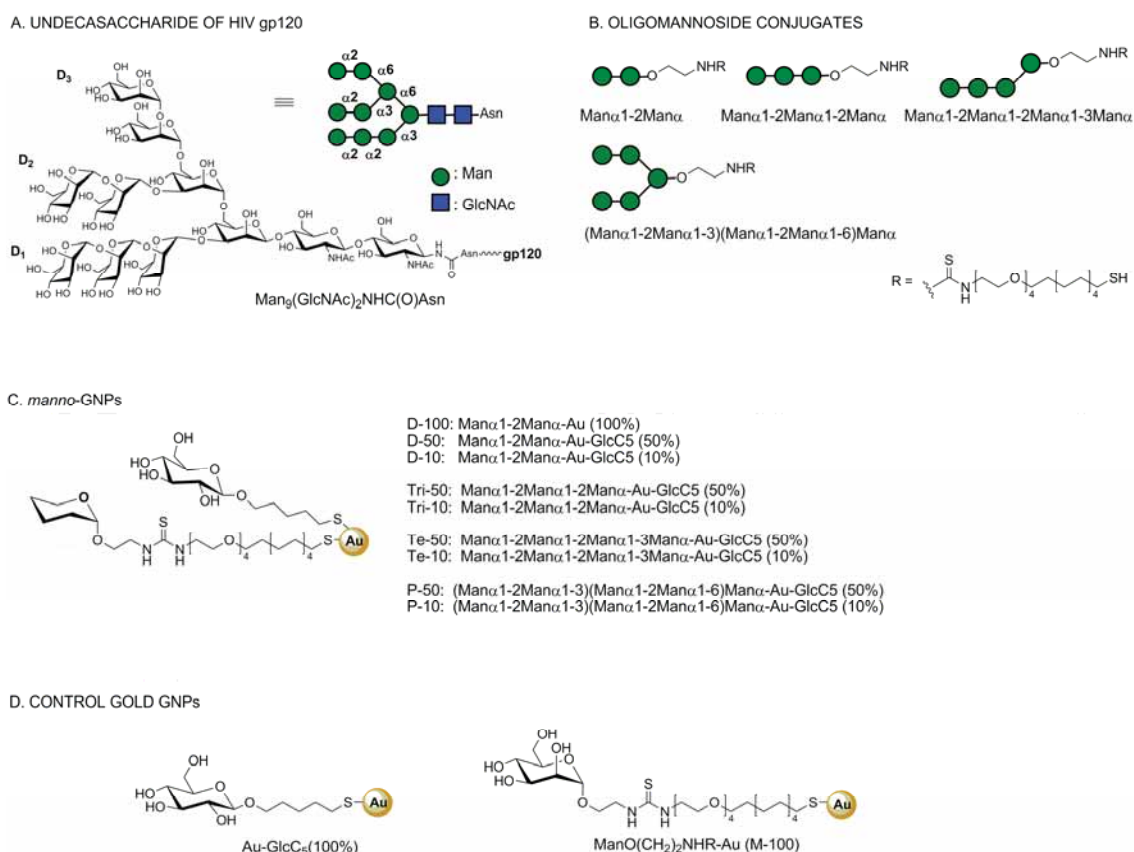


Figure 2: **A)** The structure of gp120 *high-mannose* undecasaccharide Man₉GlcNAc₂ glycan; **B)** thiol-terminating oligomannosides conjugates synthesized and used for GNP preparation; **C)** prepared GNPs bearing varying density of selected oligomannoside constituents of the D1, D2, and D3 arms of the undecasaccharide Man₉GlcNAc₂ (e.g. D-100 means GNP bearing 100% density of the dimannoside); **D)** GNPs bearing glucose and mannose conjugates prepared as control.

The GNP ability to bind directly 2G12 and to inhibit 2G12/gp120 binding was studied by different techniques (Fig. 3). The direct interactions between *manno*-GNPs and 2G12 were studied by SPR (Fig. 3a) and competition experiments between 2G12 bound to the oligomannosides and the *manno*GNPs were carried out by STD-NMR (Fig. 3b). Furthermore SPR-inhibition experiments of the 2G12/gp120 interaction were performed (Fig. 3c). The best GNP candidates were then applied to an *in vitro* cellular model of HIV infection (Fig. 3d). To have a better molecular knowledge of the interactions of the monomeric oligomannosides with 2G12, printed glycan-microarray (Fig. 3e) and STD-NMR experiments (Fig. 3b) were also performed.

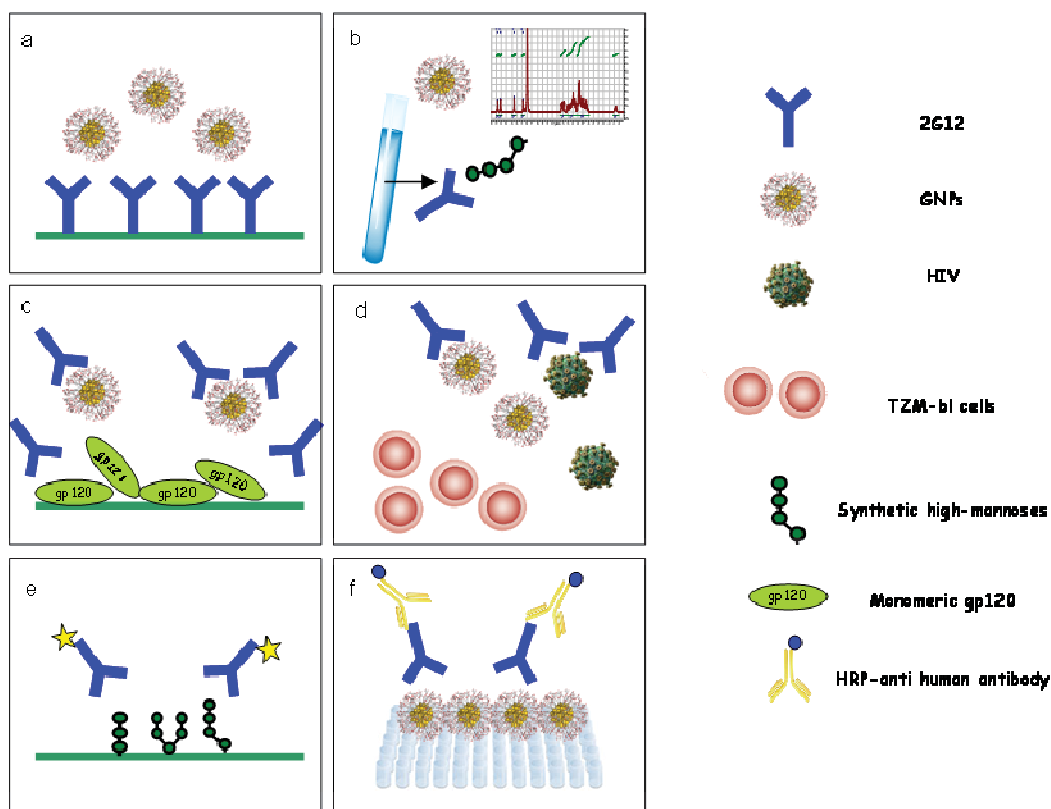


Figure 3: General overview on the techniques employed to study the 2G12/*manno*-GNP and oligomannoside interactions. **a)** Biosensors: GNPs were flowed on a 2G12 functionalized chip detecting the SPR differences triggered by these interactions. **b)** STD-NMR solution experiments to determine at molecular level the specificity of the interaction between 2G12 and *manno*-GNPs or synthetic oligomannosides. **c)** Biosensors: SPR inhibition experiments were performed to study the potency of *manno*-GNPs to inhibit the binding of 2G12 to gp120. **d)** Cellular neutralization assay was performed to study the ability of GNPs to compete with HIV for the 2G12 antibody. **e)** Printed glycan array was performed to study the interaction between synthetic oligomannosides printed on a glass slide and 2G12. **f)** GNP-ELISA approach (described in chapter 4) to detect anti-carbohydrate antibodies 2G12 after *in vivo* immunization experiments.

The interaction between the described *manno*-GNPs and 2G12 was finally optimized by assembling different high-mannose arms on the same GNPs to re-build the Man₉ on the GNPs. Following the results from all these approaches, GNPs carrying selected high-mannose-type oligosaccharides of gp120 and a T cell epitope were prepared for *in vivo* immunization studies. The screening of the antibodies evoked in mice by the best gp120 mimetic GNPs was carried out by a classic ELISA experiment, but to improve the sensitivity of the anti-carbohydrate antibodies detection, a new ELISA approach based on the direct coating of the plates with the *manno*-GNPs was developed (Fig. 3f). A detailed report on this GNP-ELISA technique will be presented in the chapter 4 of this part of the Thesis.

2.2. Looking for the 2G12 minimum carbohydrate epitope on GNPs by different techniques

(Part of this work was published in *J. Mol. Biol.* 2012, 410, 798-810 – Gold nanoparticles coated with oligomannosides of HIV-1 glycoprotein gp120 mimic the carbohydrate epitope of antibody 2G12)

Thiol-ending oligomannoside conjugates and the corresponding *manno*-GNPs have been prepared as mimetic system of the viral gp120 high-mannose clusters and are depicted in Chart 1. The preparation of the oligomannosides-conjugates is reported in Appendix 2 and *manno*-GNPs were prepared as already described.¹⁷

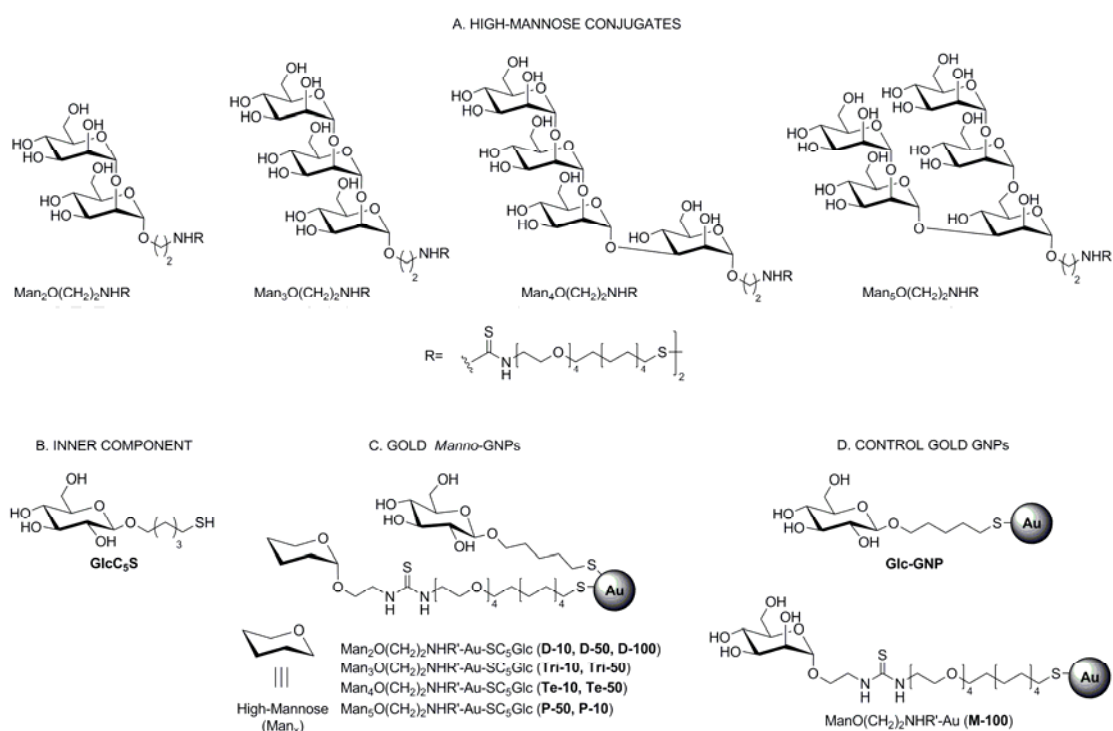


Chart 1: **A)** Structures of the high-mannose-type oligosaccharides (structural motifs of Man₅GlcNAc₂) used for the preparation of *manno*-GNPs. **B)** Glucose conjugate used as an inner component of *manno*-GNPs. **C)** Schematic representation of different *manno*-GNPs. Numbers indicate the percentages of the (oligo)mannosides on *manno*-GNPs. **D)** Schematic representation of GNPs 100% coated with glucose or mannose conjugates used as negative controls.

Binding studies by SPR. Antibody 2G12 was immobilized on the sensor chip and increasing concentrations of *manno*-GNPs were flowed over the chip. High affinity was reached depending on the oligomannoside and its density on the gold surface. Unlike Te-GNPs, GNPs carrying the dimannoside (D or Man₂), trimannoside (Tri or Man₃) or the pentamannoside (P or Man₅), which showed slightly lower affinities for 2G12 than Man₄ as free ligands, were able to bind to 2G12 only when the oligomannoside density on the gold nanoparticles was higher than

10% as measure by SPR binding assay (direct binding of *manno*-GNPs to immobilized 2G12). These results highlight the importance of carbohydrate presentation of synthetic glycoconjugates.

Inhibition studies by SPR. After analyzing the direct binding of *manno*-GNPs to immobilized 2G12, we also performed inhibition experiments. In these experiments, gp120 was immobilized on the sensor chip and *manno*-GNPs were used to inhibit the binding between 2G12 and gp120. The biosensor chip was functionalized with gp120 and increasing amounts of the multivalent *manno*-GNPs, pre-mixed with a fixed concentration of 2G12, were then co-injected (Fig. 4).

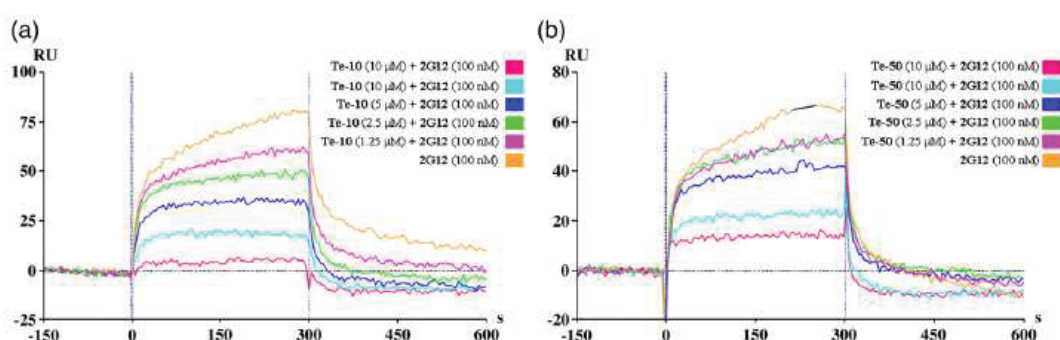


Figure 4: Sensorgrams of the inhibition of binding between 2G12 (100 nM) and gp120 (immobilized on the sensor chip) by different concentrations of **a)** Te-10 (0 μ M, 0.625 μ M, 1.25 μ M, 2.5 μ M, 5 μ M, and 10 μ M, referring to Man₄) and **b)** Te-50 (0 μ M, 0.625 μ M, 1.25 μ M, 2.5 μ M, 5 μ M, and 10 μ M, referring to Man₄).

In the presence of Te-10 and Te-50 carrying 10% and 50% concentration of Man₄, the 2G12 binding response decreased with increasing concentrations of these GNPs indicating a dose-dependent inhibition of 2G12 binding to gp120 immobilized on the surface (Fig. 5a and b). Te-10 and Te-50-GNPs inhibited the binding between 2G12 and gp120 with IC₅₀ values in the micromolar range (Te concentration).

Cellular experiments. Selected *manno*-GNPs (Te-10 and Te-50-GNPs) from the SPR screening were able to interfere with the binding of 2G12 with a recombinant virus as evaluated in competition neutralization assays (Fig. 3d) under conditions in which normal antibodies inhibit infection. These cellular experiments were performed in collaboration with Dr Eloisa Yuste (Retrovirology and Viral Immunopathology, IDIBAPS, Hospital Clinic). GNPs Te-10 and Te-50 caused a reproducible and concentration-dependent inhibition of 2G12 neutralization of the virus within the micromolar range in cellular models (TZM-bl cells). The highest effect blocking 2G12 was observed when a concentration of 11 μ M of Te-10 (74 μ M in Man₄) or 4 μ M of Te-50

(229 μM in Man_4) were used: The amount of antibody 2G12 required to inhibit 50% of the infectivity (IC_{50}) was 7 times and 13 times higher (respectively) than the amount of 2G12 used in the absence of *manno*-GNPs. The *in vitro* screening of *manno*-GNPs demonstrated that these *manno*-GNPs mimic the oligomannoside-rich spikes of viral envelope and could be further explored for synthetic carbohydrate-based vaccines against HIV. The validation of *manno*-GNPs as 2G12 ligands was a necessary step prior to a rational design of gold nanoparticles as anti-HIV carbohydrate vaccine and gave a deeper insight on the molecular interactions between oligomannosides and 2G12 antibody.

The results of this work, presented in detail in the publication Marradi et. al. 2011,²¹ show that the most potent ligand for 2G12 is the GNP incorporating 10 or 50 % density of tetramannosides.

²¹ Marradi M., Di Gianvincenzo P., Enríquez-Navas P. M., Martínez-Ávila O. M., Chiodo F., Yuste E., Angulo J., Penadés S., Gold nanoparticles coated with oligomannosides of HIV-1 glycoprotein gp120 mimic the carbohydrate epitope of antibody 2G12, J. Mol. Biol. 2011, 410, 798-810.

2.3. “Dissecting” the selectivity of the binding of oligomannosides to 2G12 by STD-NMR and glycan array

(Part of this work was published in *ChemBioChem* 2012, 13, 1357-1365 – STD NMR study of the interactions between antibody 2G12 and synthetic oligomannosides that mimic selected branches of gp120 glycans)

To have a deeper insight on the binding selectivity between selected branched of the gp120 high-mannose glycan and 2G12, we have further dissected the Man₉ antennas as shown in Figure 5. The pentamannoside P (Man₅) was dissected in the trisaccharides Man α 1-2Man α 1-3Man (**Tri-1**) and Man α 1-2Man α 1-6Man (**Tri-2**), while the non-natural heptamannoside H was dissected into the natural D1 arm tetramannoside (Man α 1-2Man α 1-2Man α 1-3Man, Te=Man₄) and the non-natural Te-4 (Man α 1-2Man α 1-2Man α 1-6Man,) (Fig. 5). To find the better ligands for 2G12, the binding of these epitope mimics was studied by STD-NMR and printed glycan micro array.

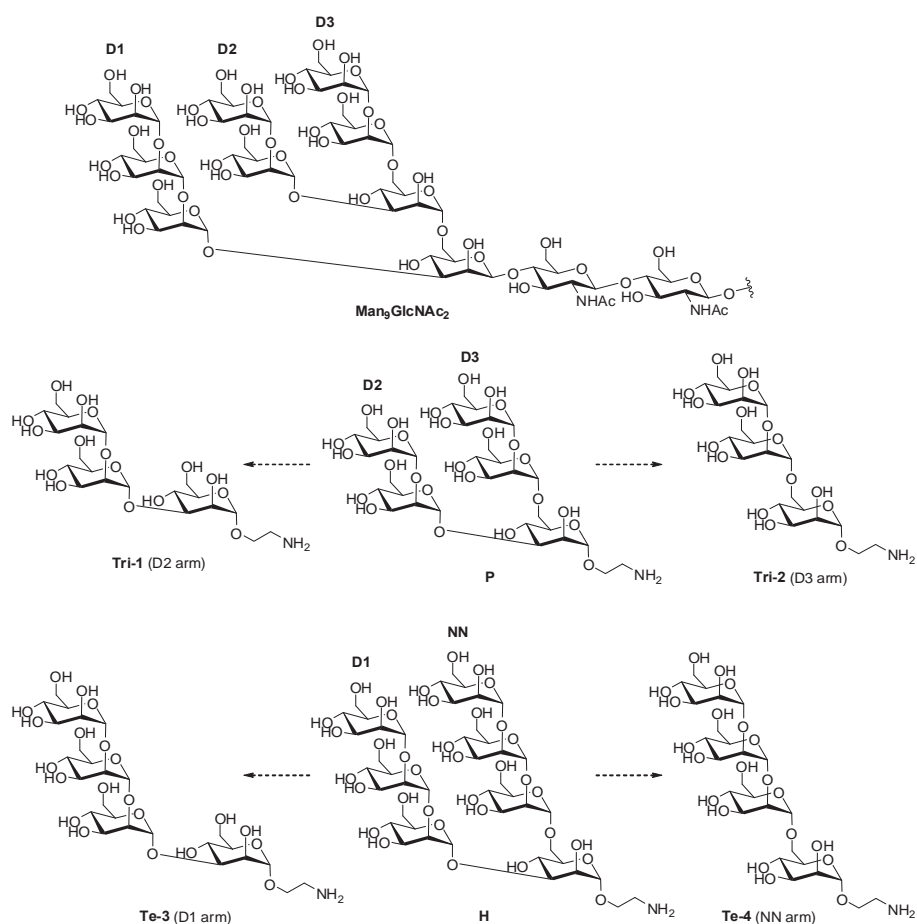


Figure 5: Structures of undecasaccharide $\text{Man}_9\text{GlcNAc}_2$ present at the surface of the HIV gp120, branched pentamannoside P, non-natural heptamannoside H, and trimannosides (Tri-1 and Tri-2) and tetramannosides (Te-3 and Te-4) prepared in this part of the Thesis. Tri-1 mimics the D2 arm, Tri-2 the D3 arm, Te-3 the D1 arm of Man_9 , and Te-4 is a non-natural (NN) branch.

Previously, our group studied by STD-NMR and transferred NOE experiments²² the interactions of 2G12 with the linear tetramannoside Te-3 (D1-arm) the branched pentamannoside P (containing both D2 and D3 arms of the natural high-mannose), and the non natural heptamannoside H (composed by the repetition of two Man α 1-2Man α 1-2Man trimannosides). It was found that Te-3 was recognized in a single binding mode by 2G12, in agreement with the crystal structures.^{5, 23} However, the branched pentamannoside P showed a different behavior. Besides the conformation observed in the solid-state between 2G12 and D3 arm, in the STD-NMR study the antibody also recognizes the D2-like arm of the pentamannoside P. In the case of the branched and non-natural heptamannoside H, the antibody preferentially recognizes its D1-like arm although the structural motif Man α 1 2Man α 1 2Man is repeated in both arms. These results indicate that there is still much to do in order to understand the interaction of 2G12 and its epitopes and for this reason we dissected both Penta (P) and Heptamannoside (H).

The interaction of the constitutive trisaccharides of the pentamannoside P (Tri-1 and Tri-2) towards 2G12 was similar, as measured by STD-NMR in isotropic solution (Fig. 6). The binding affinity to 2G12 of individual ligands Tri-1 and Tri-2 is in good agreement with our previous observation (Table 1).²² On the other hand, the tetramannosides Te-3 (previously called Te or Man₄) and Te-4 fragments of the dissected heptamannoside H notably show different affinities to 2G12 (Table 1). Te-3 shows higher affinity than Te-4 as measured in solution by STD. The only structural difference between Te-3 and Te-4 is the linkage α 1,3 or α 1,6 of non-reducing trisaccharide to the reducing mannose (Fig. 5).

²² Enríquez-Navas P.M., Marradi M., Padro D., Angulo J., Penadés S., A solution NMR study of the interactions of oligomannosides and the anti-HIV-1 2G12 antibody reveals distinct binding modes for branched ligands, *Chem. Eur. J.* 2011, 17, 1369-1707.

²³ Calarese D. A., Lee H. K., Huang C. Y., Best M. D., Astronomo R. D., Stanfield R. L., Katinger H., Burton D. R., Wong C. H., Wilson I. A., Dissection of the carbohydrate specificity of the broadly neutralizing anti-HIV-1 antibody 2G12, *Proc. Natl. Acad. Sci. USA* 2005, 102, 13372-13377.

Table 1: Dissociation constants (K_D) of the interactions of the dissected oligomannosides with antibody 2G12. Affinities were calculated by using the STD-AF initial slopes approach.²⁴

Ligand	K_D [mM]
Tri-1	3.0±1
Tri-2	3.8±0.3
Te-3	0.4±0.1
Te-4	2.2±0.3
P	3.0±0.2
H	0.8±0.08

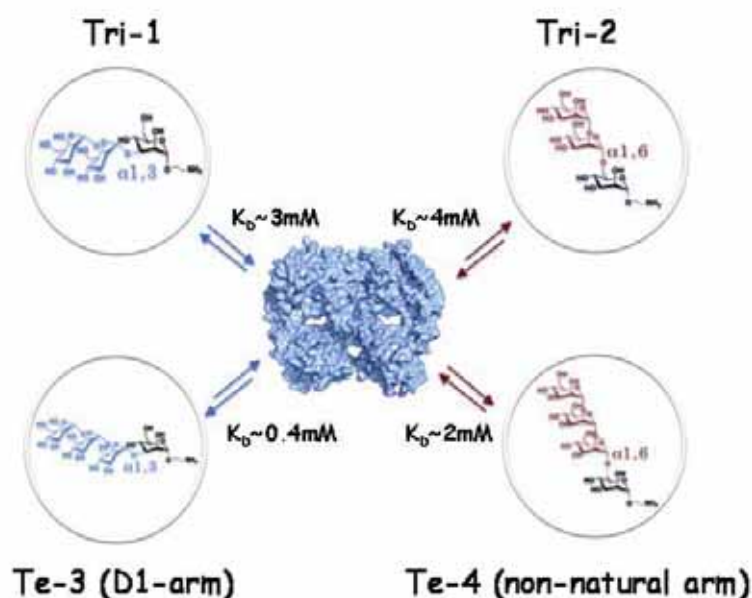


Figure 6: Different oligomannosides structures related to the gp120 Man₉ clusters and their interaction with 2G12. Tri-1 mimics the D2 arm of Man₉, Tri-2 the D3 arm, Te-3 the D1 arm, and Te-4 is a non-natural (NN) branch. The interactions between the depicted oligomannosides and 2G12 were studied in solution by STD-NMR and the dissociation constant K_D was calculated. Te-3 showed the better K_D (0.4mM), while Te-4, Tri-1 and Tri-2 showed a K_D higher than 2mM.

²⁴ Angulo J., Enríquez-Navas P. M., Nieto P. M., Ligand-receptor binding affinities from saturation transfer difference (STD) NMR spectroscopy: the binding isotherm of STD initial growth rates, Chem. Eur. J., 2010, 16, 7803-7812.

Our previous STD-NMR data (above-mentioned) show that linear trisaccharide Man₃ (Man α 1-2 Man α 1-2Man α , Chart 1) is a better ligand for 2G12 than dimannoside Man₂ (K_D 0.4 \pm 0.2 mM) and similar to the Te-3,²² which has a further α 1-3-linked mannoside at the reducing end respect to Man₃. On the contrary, the α 1-6-linked trimannoside in the non natural tetrasaccharide Te-4 (NN arm) shows a lower affinity for 2G12 (K_D Te-4 = 2.2 \pm 0.3 mM). This is a key result in terms of structure–binding relationships for this oligomannoside series, highlighting that a simple structural change at the reducing end of the two tetrasaccharides (α 1,6 linkage in Te-4 versus α 1,3 in Te-3) has a significant impact on the energetics of the molecular recognition process, but not in the mode of binding.

To compare the NMR results obtained in solution with a solid-phase assay, we performed printed glycan microarray experiments detecting the 2G12 interactions by fluorescence. Before testing their interaction of Te-3 and Te-4 with 2G12, the array functionalization was confirmed with fluorescently labeled concanavalin-A (ConA), a lectin specific for mannose (Fig. 7).

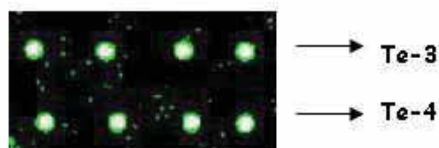


Figure 7: Microarray image showing the interaction between fluorescently labeled ConA with different Te-3 and Te-4 concentrations (from left to right 25, 50, 100, and 200 μ M). The fluorescence signal indicates a successful functionalization of the microarray slides with the oligomannosides.

To evaluate the interaction between the oligomannosides and 2G12 antibody, fluorescently labeled 2G12 (2G12*) was prepared following a standard methodology.²⁵ The tetrasaccharide Te-4 was not at all recognized on the printed array, while Te-3 showed a good binding with the antibody (Fig. 8). This result might be attributed to a different presentation of the oligomannoside on the surface.

²⁵ 2G12 was labeled with Hilyte Plus™ 555 protein labeling kit from AnaSpec, (Freemont, USA) according to the instructions of the manufacturer.

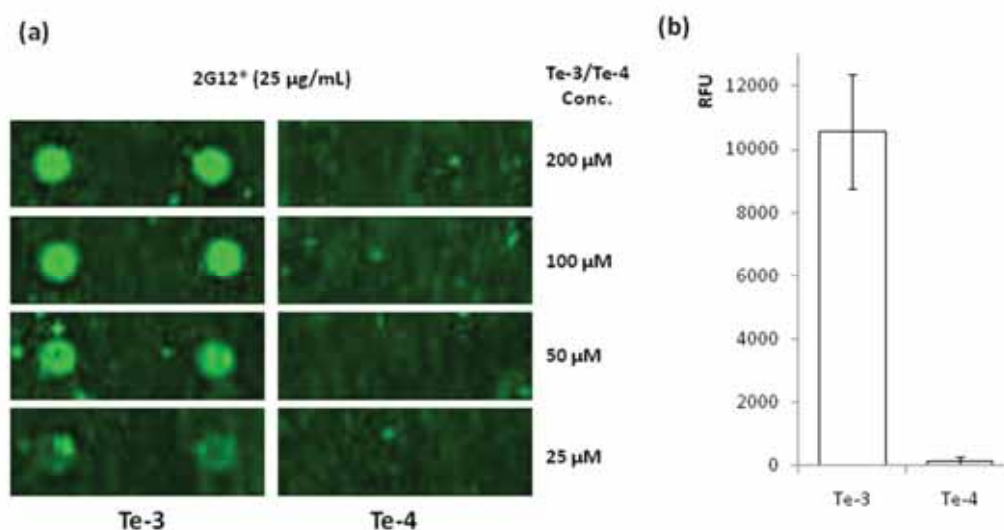


Figure 8. Microarray analysis of the interaction between fluorescently labeled 2G12 (2G12*) with Te-3 and Te-4. **a)** Microarray image of the interaction between fluorescently labeled 2G12 with different Te-3 and Te-4 concentrations (from bottom to top 25, 50, 100, and 200 µM). **b)** Interaction between 25 µg/mL of 2G12* with 100 µM of printed Te-3 or Te-4, expressed in relative fluorescent units (RFU).

Comparing the STD-NMR and the microarray results, it is notable that the monomeric trimannosides Tri-1 and Tri-2 and the non-natural tetramannoside (Te-4) with K_D 2-4mM in solution, are not recognized in the microarray surface at the printed concentrations. On the contrary, Te-3 that has a K_D 0.4mM (as measured by STD) is well recognized by the antibody 2G12 also in the glycan array. The α 1-6-linkage in the non natural tetrasaccharide Te-4 seems to affect the interactions with 2G12 respect to the Te-3 decreasing its affinity for the antibody. The results of this work, presented in a publication,²⁶ indicate that the tetramannoside Te-3 is the best ligand for 2G12.

Altogether, the study presented in this part of the Thesis confirms the distinct preferences of 2G12 for the oligomannoside branches of Man₉. The results expand our comprehension of the molecular basis of 2G12/gp120 interaction, affording key structural information for the development of an anti-HIV carbohydrate-based vaccine.

²⁶ Enríquez-Navas P. M., Chiodo F., Marradi M., Angulo J., Penadés S., STD NMR study of the interactions between antibody 2G12 and synthetic oligomannosides that mimic selected branches of gp120 glycans, *Chembiochem*, 2012, 13, 1357-1365.

2.4. Assembling different antennas of the gp120 high-mannose-type glycan to re-build the complete Man₉ on the gold GNPs

Based on the previous studies, we have selected the tetramannosides Te-3 as the main component to generate more complex multivalent *manno*-GNPs towards a carbohydrate-based vaccine candidate. The idea was to assemble the three arms of Man₉, D1 arm (Te-3) and D2 and D3 arms (pentamannoside P) on the gold surface to obtain a glyconanoparticle (Te/P-GNP) that re-builds the complete Man₉ in a multivalent fashion for better mimic the viral carbohydrate envelope (Fig. 9). The insertion of the three antennas of Man₉ was possible by exploiting one of the characteristic of glyconanotechnology, i. e. the simultaneous insertion of multifunctionality in a one-pot fashion.

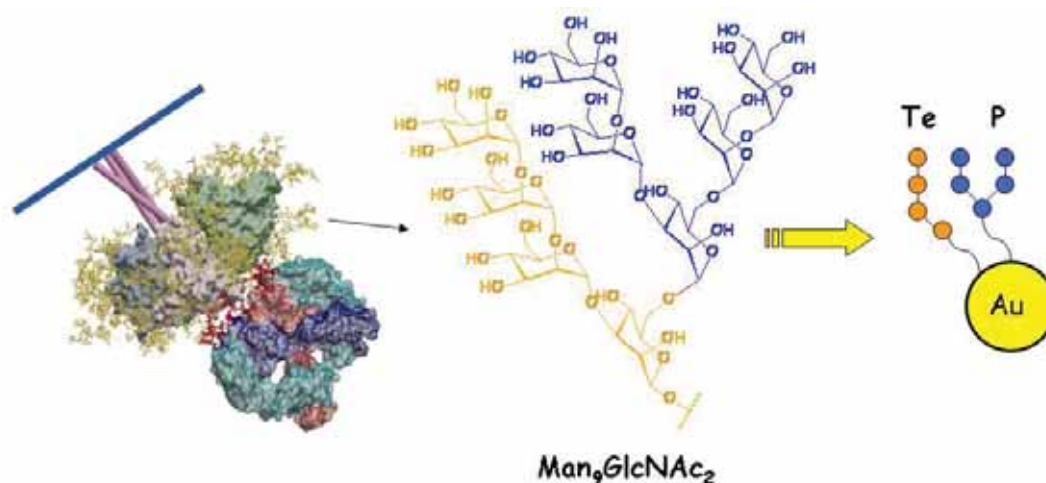


Figure 9: Left: Representation of the interaction of the high-mannose glycan clusters of the HIV envelope glycoprotein gp120 and the antibody 2G12. Middle: The structure of the high-mannose glycan Man₉GlcNAc₂. Right: Te/P-GNP bearing the tetramannosides Te (in orange) and the pentasaccharide P (in blue) designed and prepared in order to have a better mimicking system of the high-mannose clusters on the viral gp120.

We previously showed that increasing the percentage of tetramannoside Te from 10% to 50% did not increase the potency of GNPs to inhibit the 2G12-gp120 binding, thus 10% of tetramannoside Te (Man₄) on the gold surface (GNP Te-10) was good enough to obtain an efficient 2G12 binding. The pentamannoside P (Man₅), previously multimerised on the gold nanoparticles, showed poor interaction with 2G12 at the tested concentrations.²¹ We have prepared Te/P-GNPs, maintaining 10% of final oligomannoside-concentration on the gold nanoparticles (5% of Te + 5% of P). The interaction between Te/P-GNPs and 2G12 was studied by SPR and STD-NMR (Fig 3 a-c). We want to test if the co-presence of a strong 2G12 ligand (Te) and a less efficient one (P), on the same GNP was able to synergistically improve the binding between 2G12 and Te-GNPs. In a previous work, Wong and co-workers studied how

the co-presence of two strong 2G12 interacting molecules (Man_9 and Man_4) in different ratio in hybrid glyco-dendrimers influences the interaction with 2G12.²⁷ They found that the dendrimer containing 5 molecules of Man_4 and 4 molecules of Man_9 showed a two fold increase of 2G12 interaction in comparison with the glyco-dendrimer containing 9 molecules of Man_9 . This interesting work showed for the first time the role of neighboring glycans in the interaction of 2G12 with high-mannose multivalent systems.

Design and synthesis of Te/P-GNPs

The Te/P-GNPs were prepared by standard procedure.¹⁷ The average numbers of oligomannosides on the gold surface was calculated by quantitative NMR (qNMR) integrating the carbohydrate anomeric signals with an internal standard (Trimethylsilyl propionate, TSP). Figure 10 shows the ^1H NMR of Te/P-GNPs where the signals from Te and P are clearly detectable in the anomeric proton region. The approximate 1:1 ratio confirms the equimolar incorporation of Te and P on gold surface. NMR analysis of the oligomannoside mixture before and after the nanoparticles preparation was also performed to verify that the ligands ratio is maintained.

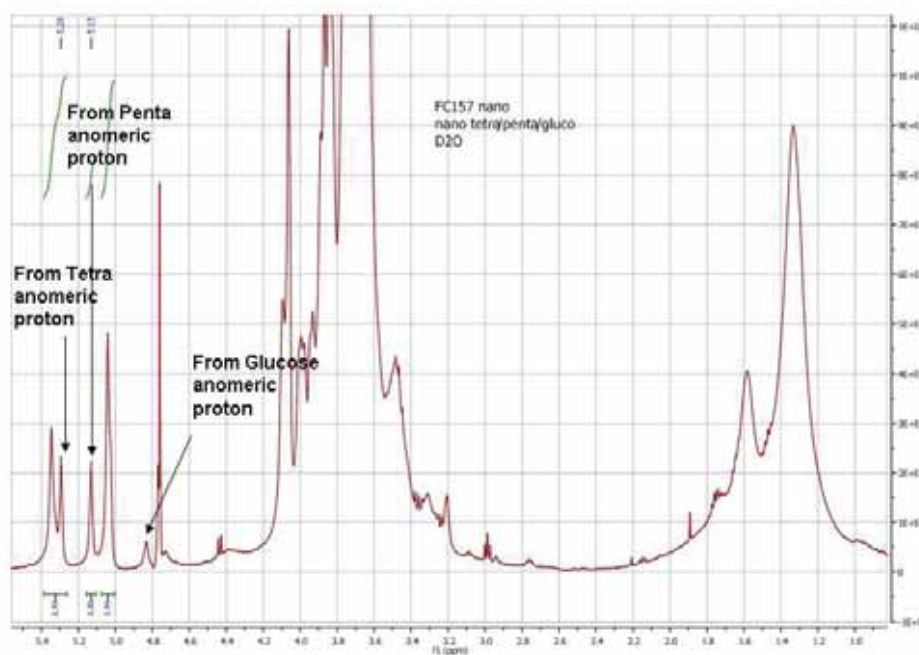


Figure 10: ^1H NMR spectrum of Te/P-GNPs in D_2O at 500 MHz. The signals from the anomeric protons of the oligomannosides are clearly observed between 5.0 and 5.5 ppm.

²⁷ Liang C. H., Wang S. K., Lin C. W., Wang C. C., Wong C. H., Wu C. Y., Effects of neighboring glycans on antibody-carbohydrate interaction, *Angew Chem Int Ed.* 2011, 50, 1608-1612.

TEM microscopy was used to determine the GNPs size, which was approximately 2 nm in terms of gold core diameter (Fig. 11). The TEM micrographs showed that Te/P-GNPs were highly monodispersed. UV-Vis spectra were also recorded in water and showed no surface plasmon band of gold – usually found around 520 nm – confirming that the gold nanoparticles are less than 2 nm in average size. These nanoparticles were highly soluble in water and stable for long times in solution and/or after freeze-drying processes.

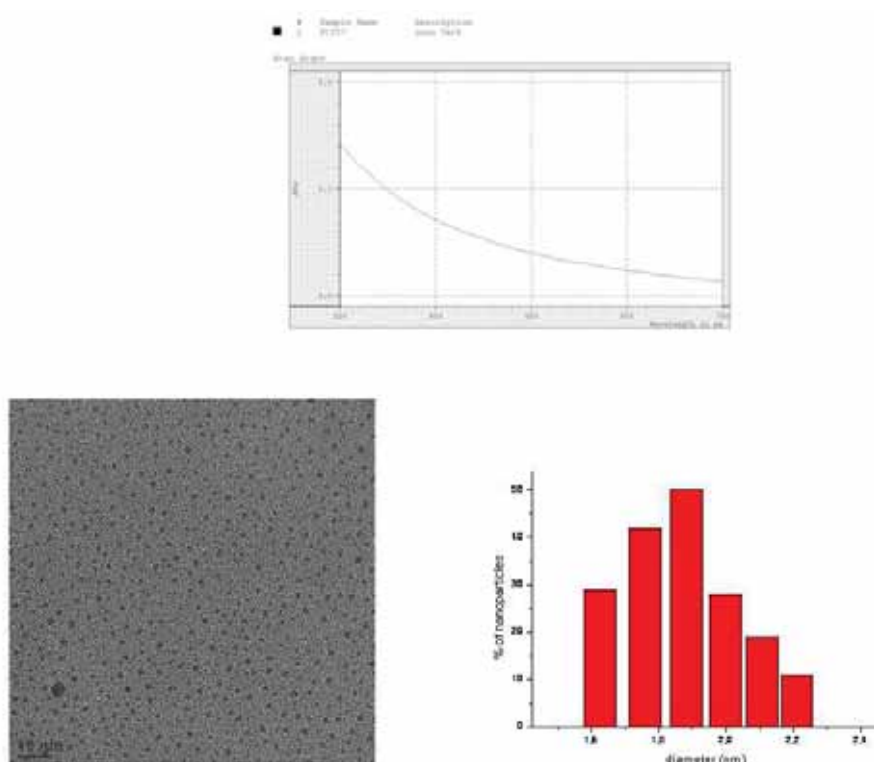


Figure 11. Characterization of Te/P-GNPs: A) UV-Vis spectra of a 0.1 mg/mL solution of the Te/P-GNPs in water; B) TEM micrograph; C) size-distribution histogram obtained from analysis of TEM micrograph reported in B.

Table 2 resumes the chemical properties of Te-GNP and Te/P-GNP.

Table 2: Average molecular formula of GNPs molecular weight (MW) and the corresponding oligomannosides content as estimated from the TEM and qNMR data.

GNP	Average MW ^[a]	Average molecular formula ^[a]	Average mannoside chains for GNP ^[a]	Oligomannosides per 1mg of GNPs ^[b]
Te-GNP	47KDa	Au ₁₁₆ Te ₇ Glc ₅₉	7	0.21μmol
Te/P-GNP	67KDa	Au ₂₀₁ Te ₄ P ₄ Glc ₆₄	8	0.12μmol

^[a] Calculated following the procedure reported in the Appendix 1; ^[b] As measured by qNMR

Direct binding of Te/P-GNP to 2G12 by SPR

The binding of Te/P-GNPs bearing a total 10% of both oligomannosides to 2G12 was evaluated by SPR. 2G12 was immobilized on a sensor chip. Figure 11A shows selected SPR sensorgrams of the direct binding of Te/P-GNP to 2G12 and the binding of Te-GNPs in a mixture with P-, D- and Glc-GNPs (final [GNPs]=10 $\mu\text{g}/\text{mL}$).

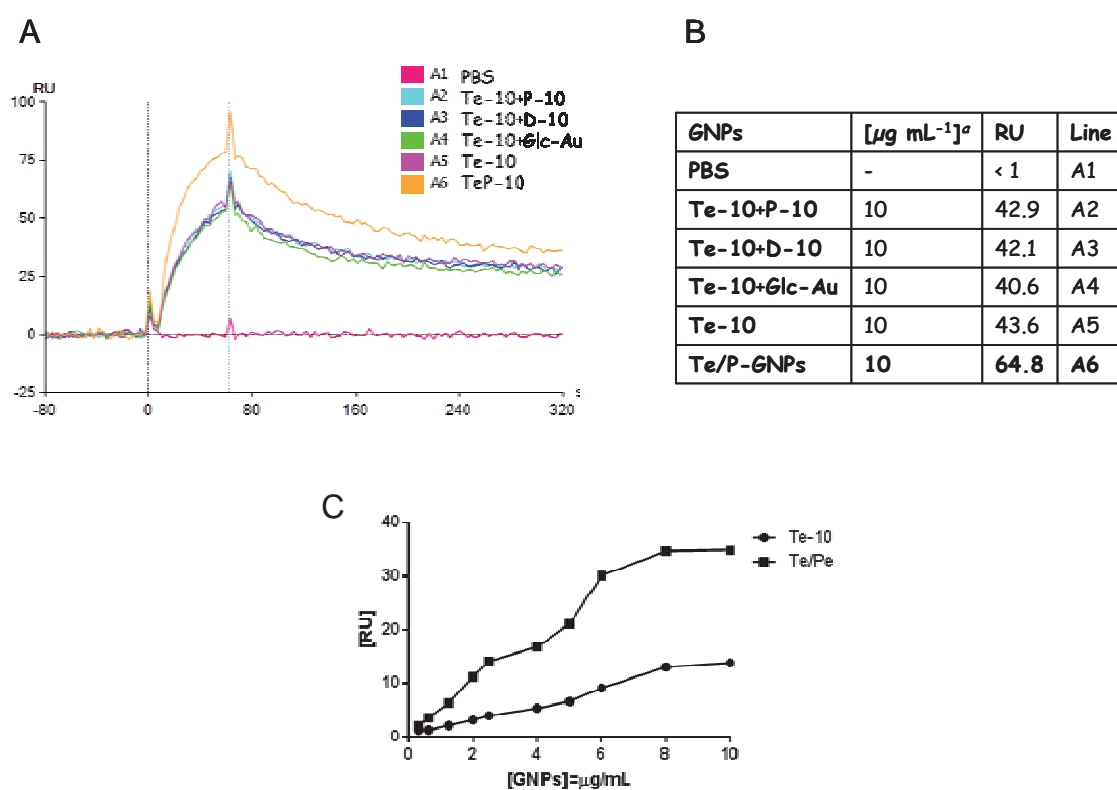


Figure 11: **A)** Selected SPR sensorgrams of the direct binding of Te/P-GNP to 2G12 and of Te-GNPs in cocktail with P, D and Glc-GNPs. Te/P-GNPs shows the best interaction with 2G12 (line A6); **B)** Table shows the response units (RU) at 80s related to the interaction between the tested GNPs (10 $\mu\text{g}/\text{mL}$) and 2G12 printed on the SPR chip. **C)** Dose-response curves between serial dilution of Te-10 and Te/Pe-GNPs and RU at 80s.

At the tested concentration, the GNPs showed different SPR binding curves and the Te/P-GNPs showed the best binding (line A6). Mixtures of Te-10 GNPs with P, D or Glc-GNPs did not improve the Te-10 GNP binding to 2G12 in the SPR experiments (Fig. 11A and B). Serial GNP dilutions from 10 to 0.31 $\mu\text{g}/\text{mL}$ were also screened on the SPR chip coated with 2G12 and the RU response at 80s has been used to construct a dose-response curve (Fig. 11C). Glc-GNPs were used as negative control. GNPs carrying 10% of P are not able to bind 2G12 on SPR experiments at the tested concentrations (from 10 to 0.31 $\mu\text{g}/\text{mL}$ ²¹).

Te-GNP gave a response of 12RU at 10 μ g/mL, while the Te/P-GNP gave a response of 35RU at the same concentration (Fig. 11C). Although the SPR direct binding could be affected by the different GNPs molecular weight, we performed these experiments to make a first screening of the ability of Te/P-GNP to bind 2G12.

Inhibition of 2G12/gp120 binding by Te/P-GNP as observed by SPR experiments

After analyzing the direct binding of Te and Te/P-GNPs to the antibody 2G12, we performed experiments where the interaction of 2G12 with gp120 on the SPR surface was affected by the nanoparticles. The biosensor chip was functionalized with monomeric gp120 and a fixed concentration of 2G12 incubated with increasing amounts of the multivalent GNPs were then co-injected. Figure 12A shows selected sensorgrams of the inhibition binding between 2G12 (400nM) and gp120 in presence of different concentrations (10 or 3 μ g/mL, line A5 and A3) of GNPs: again Te/P-GNP seems to be the best GNPs able to decrease the interaction between 2G12 and gp120.

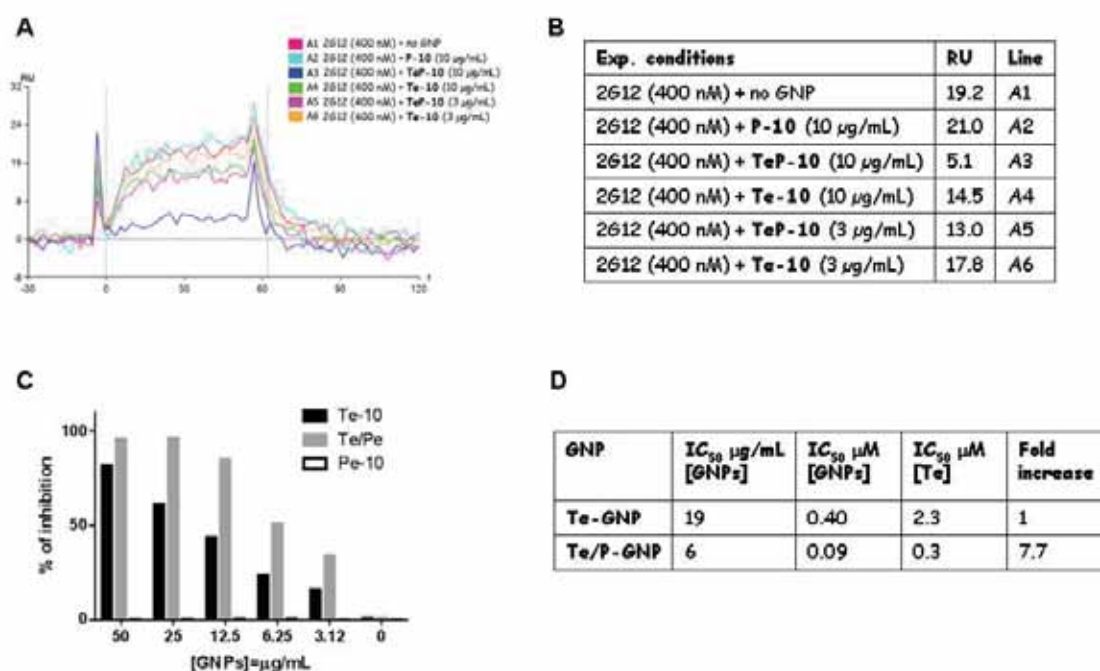


Figure 12: **A)** Selected sensorgrams of the inhibition binding between 2G12 (400nM) and gp120 in presence of different concentrations (10 or 3 μ g/mL) of GNPs. **B)** Table shows the response units (RU) at 80s related to the interaction between 2G12 (pre-incubated with GNPs) and the gp120 printed on the SPR chip. **C)** Dose-response curves between serial dilution of Te-10, Te/Pe and Pe-10-GNPs and % of gp120 binding inhibition. **D)** IC₅₀ values calculated from the dose-response curves

In the presence of Te-10 and Te/P-GNPs, the 2G12 binding response decreased with increasing concentrations of these GNPs, indicating a dose-dependent inhibition of the 2G12 binding to the gp120-immobilised surface (Figure 12B). From the analysis of the concentration-response curves, it was possible to estimate a half maximal inhibitory concentration (IC_{50}) for Te and Te/P-GNPs (Fig. 12D). The IC_{50} values were expressed both in terms of concentrations of GNP and tetramannoside (Te) by taking into consideration the average molecular weights of the GNPs and the number of tetramannosides per nanoparticle. These GNPs proved to be inhibitors of 2G12/gp120 interaction with IC_{50} values in the sub-micromolar range in terms of GNPs concentrations and micromolar in terms of tetramannoside concentration.

These competition experiments confirmed that **Te/P-GNP is a better ligand for 2G12 than Te-GNP**. In spite of the fact that the amount of Man_4 on Te/P-GNP is lower than that on Te-GNP, we showed a cooperative effect between Man_4 and Man_5 on the GNPs that increased the affinity for Te/P-GNPs to 2G12. As showed in Figure 12C, Man_5 at this concentration is not able to influence alone the 2G12/gp120 binding when multimerized on the GNP. In the inhibition of 2G12-gp120 interaction, Te-GNP carrying on its surface 10% of tetramannoside showed an IC_{50} of 2.3 μ M in terms of Te concentration. Te/P-GNP, carrying 5% of tetramannoside Te and 5% of pentamannoside P, showed approximately an 8 times fold decrease of IC_{50} respect to Te-10. The final concentration of high mannoses on this GNP was 10% and the co-presence of Te and P clearly affected the 2G12 interaction, although P-GNPs showed no inhibition activity at these concentrations. The assembly of different high mannoses on the same gold nanoparticle is a good strategy to “build” Man_9 -like clusters exploiting the role of neighboring glycans on the GNPs.

Study of the Te/P-GNP/2G12 interaction by STD-NMR

In order to get a deeper insight on the molecular interactions between Te/P-GNPs and 2G12, saturation Transfer Difference (STD) NMR competition experiments were carried out in a similar way to section 2.2. A sample containing 2G12 (25 μ M) and the aminoethyl tetramannoside Te (in a ratio Te/2G12, 320) was treated with increasing concentrations of Te/P-GNPs (2.1, 4.2, 8.6, 22.3, 31.1, 39.5, and 47 μ M in Man_4). In order to calculate the affinity of GNP for 2G12, the H1A proton of free Te (as monovalent ligand) was monitored. All protons of the Te showed the same trend, but only H1A values were followed because the signal of this proton is well resolved in all spectra.

The STD signal intensity of H1A of free aminoethyl tetramannoside decreased up to 45% of its original value in a dose-dependent way after addition of Te/P-GNPs (Fig. 13), while approximately only a 60% decrease was observed by titration with Te-10 and Te-50 GNPs. This result indicates that Te/P-GNPs displace the free tetramannoside ligand from the binding site of 2G12 more efficiently than Te-10 and Te-50 GNPs and agree with the results obtained in the SPR experiments.

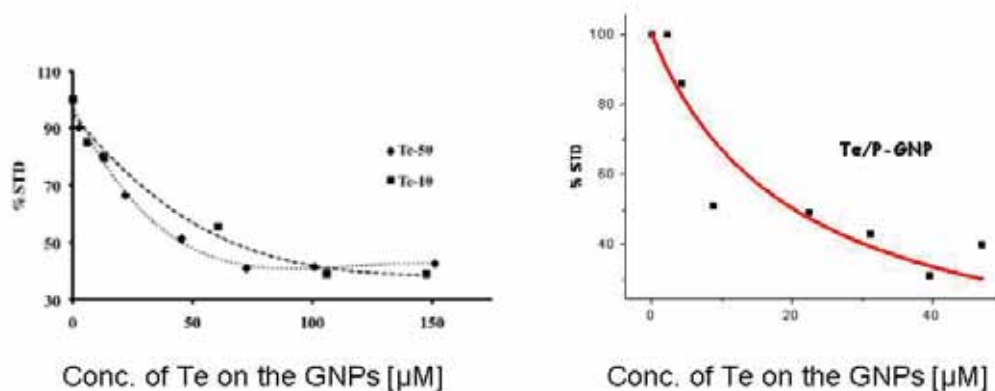


Figure 13: Competitive titration curves of 2G12/monovalent Te (Man_4) complex with Te-10, Te-50 (Left) and Te/P (Right)-GNPs.

Table 3 shows the %STD values obtained in the titration experiments with Te/P-GNP.

Table 3: STD values from H1A proton of free aminoethyl tetramannoside Te during its interaction in solution with 2G12 after addition of increasing concentrations of Te/P-GNPs expressed as concentration of Te (Man_4)

		Concentration of Te (Man_4) on the Te/P-GNPs [μM]							
		0	2.15	4.29	8.69	22.39	31.18	39.57	47
Man₄ as free ligand (8 mM)	STD H1A	2.18	2.18	1.88	1.9	1.08	0.93	0.97	1
	%STD H1A	100	100	86	87	49	43	44	46

The dissociation constant K_D was calculated from the decrease of the STD signal of H1A of tetramannoside fitted to an experimental equation,²⁸ previously also used to obtain the dissociation constant of several nanoparticles (see experimental). This obtained K_D for Te/P-GNP is $1\mu\text{M}$, 4 times lower than the Te-GNP with higher number of Man_4 copies and 400 times than the tetramannoside as monovalent ligand.

By increasing the Te/P-GNP concentration during the STD-NMR titration experiments a precipitate was observed. We observed a decrease of the 2G12 antibody NMR signals with increase GNPs concentration that correlates with the observed precipitation. We also confirmed that neither the antibody nor the nanoparticles precipitated in the same buffer conditions. Although different nanoparticles (Te and P-GNPs) and conditions have been previously used in the titration of with 2G12²¹ (see section 2.2), this was the first time that aggregation between 2G12 and a GNP was observed. This aggregation was forced by leaving the NMR tube in the fridge overnight in presence of 2G12 and Te or Te/P-GNPs. This result can be explained by the formation of cluster complexes between 2G12 and the multivalent GNPs that might produce agglutination.

From all these result, **Te/P-GNPs seem to be the best candidate for mice immunization studies**. In SPR experiments, the co-presence of Man_4 and Man_5 decreased 7.8 times the IC_{50} in comparison with the GNPs containing only Man_4 . In addition to SPR experiments, STD-NMR confirmed the same behavior of the Te/Pe-GNP: a 4 times better K_D was calculated in comparison with the Te-GNPs.

While P-GNP shows no-binding to 2G12 as measured by SPR and STD-NMR, the combination of the “inert” Man_5 and Man_4 on GNP (Te/P-GNP) showed an interesting synergetic effect between the oligomannosides, which results in a GNP with higher affinity for 2G12 than the cocktail of Te-GNP and P-GNP.

²⁸ Benie A. J, Moser R., Bäuml E., Blaas D., Peters T., Virus-ligand interactions: identification and characterization of ligand binding by NMR spectroscopy, *J. Am. Chem. Soc.* 2003, 125, 14-15 and Cheng Y., Prusoff W. H., Relationship between the inhibition constant (K_1) and the concentration of inhibitor which causes 50 per cent inhibition (I_{50}) of an enzymatic reaction, *Biochem. Pharmacol.* 1973, 22, 3099-3108.

2.5. Immunization studies with Te/P/OVA-GNPs

The Te/P-GNP can be considered a good GNP candidate to evoke 2G12 like antibodies against HIV gp120. A preliminary immunization study was performed using GNPs carrying tetramannoside Te and a peptide from tetanus toxoide as T-cell epitope (Te/Tetanus GNP, Fig. 14A). Te/Tetanus GNP was tested to evaluate the potency for inducing an adaptative immune response by generation of specific and functional antibodies against HIV in a murine model (BALB/c mice) in collaboration with the group AMRg-IQAC CIBER-BBN in the frame of Glyco-HIV project. The results obtained showed no adaptive immune response of the host animals (mice) towards the tested GNP as no anti-Te IgGs were founded in the immunized mice sera. These results suggested that Te/Tetanus-GNP lacks of the expected immunogenic capacity, and needs some improvements.

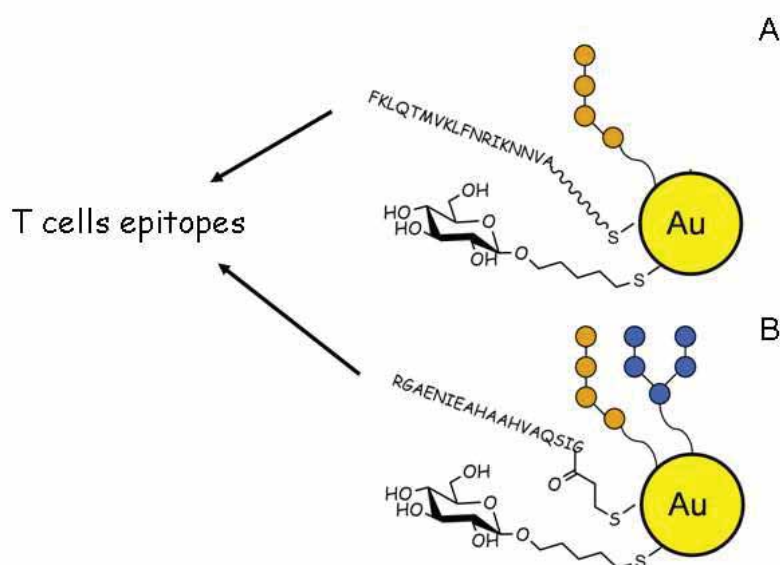


Figure 14: GNPs carrying carbohydrates and T cell epitopes prepared for immunization studies in mice. A) GNPs carrying the D1 arm of gp120 Man₉ and the T cell epitope Tetanus toxoide. B) Te/P-GNPs carrying the T cell epitope OVA₃₂₃₋₃₃₉.

For the *in vivo* experiments a new Te/P-GNP incorporating the T cell epitope OVA₃₂₃₋₃₃₉ for was prepared (Te/P/OVA-GNPs, Fig. 14B) and mice were subcutaneously immunized with 50µg of Te/P/OVA-GNPs in presence of adjuvants (10µg of Monophosphoryl Lipid A, MPL and 20µg of

Quil-A) following a described protocol.²⁹ After 30 days mice were boosted with other 50 μ g of Te/P/OVA-GNPs and after 40 days from the primary immunization, mice were sacrificed and sera collected for antibodies analysis. To detect the presence of anti-carbohydrates antibodies evoked by the immunization with Te/P/OVA-GNP, a new ELISA assay was used. This new ELISA approach for the detection of anti-carbohydrates antibodies in sera will be fully described in the chapter 4. ELISA plates were coated with 50 μ L (15 μ g /mL) of Te/P/OVA-GNP and other GNPs carrying the tetramannoside (Te-GNP), glucose (Glc-GNP), and glucose and the OVA peptide (Glc/OVA-GNP). This ELISA approach allows the detection of specific IgGs against carbohydrates epitopes linked on the GNPs. A significant response (OD~0.25) at 450 nm of mice sera was obtained with the Te-GNPs on the ELISA plate. No IgGs were detected against Glc-GNP and Glc/OVA-GNP or monomeric recombinant gp120. Sera from control mice (no immunized) did not show any answer against Te- and Te/P/OVA-GNPs. Although the Te/P/OVA-GNP was not able to evoke IgGs against the gp120 (like as other similar published works⁸), it was able to evoke a significant response (IgGs production) against the Te and Te/P present as antigens onto the GNPs (Fig. 14).

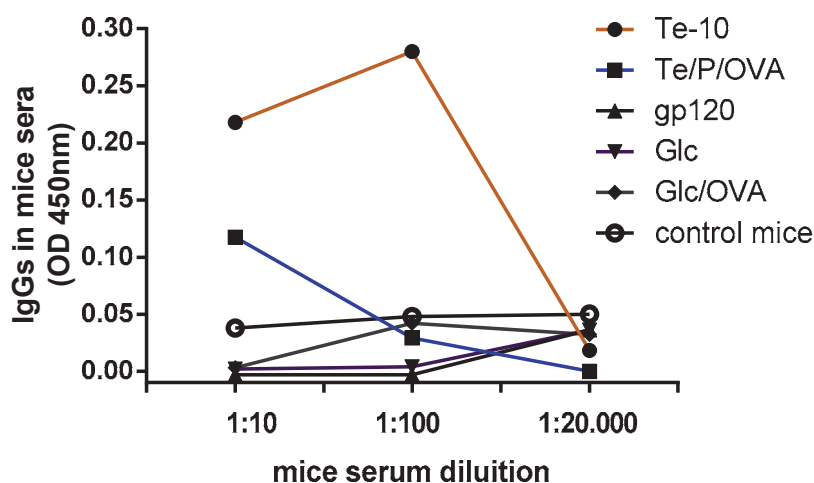


Figure 14: Specific IgGs in the mice immunized with Te/P/OVA-GNPs were detected by GNP-ELISA. Sera were diluted 1:10, 1:100 and 1:20.000. IgGs against the carbohydrates-epitopes present on GNPs were detected by OD at 450nm. A clear and significant IgGs response against Te and Te/P/OVA-GNPs was detected at 1:10 sera dilution. At 1:100 only Te was recognized by the evoked IgGs. Control mice show no IgGs production against the GNPs on the ELISA plates.

²⁹ Safari D., Marradi M., Chiodo F., Th Dekker H. A., Shan Y., Adamo R., Oscarson S., Rijkers G. T., Lahmann M., Kamerling J. P., Penadés S., Snippe H., Gold nanoparticles as carriers for a synthetic *Streptococcus pneumoniae* type 14 conjugate vaccine, *Nanomedicine UK* 2012, 7, 651-662.

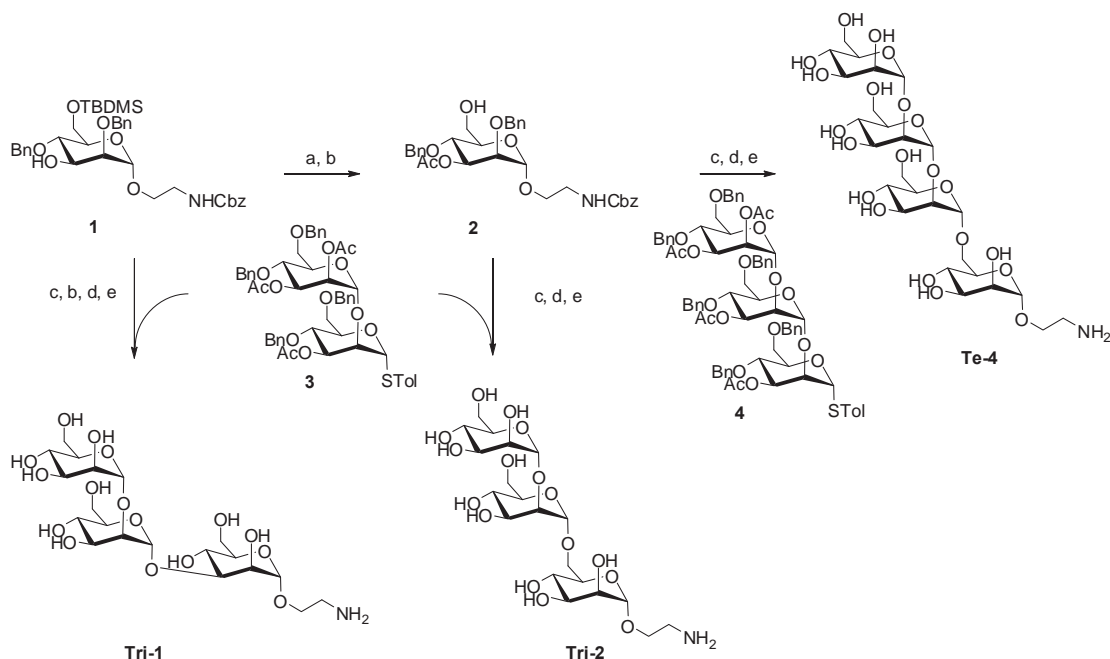
Conclusions

We have explored GNPs as potential anti-carbohydrate-based vaccines against HIV. We have first investigated by different techniques (SPR, STD-NMR and printed glycan array) the best oligomannoside epitope able to mimic the gp120 high-mannose clusters (Sections 2.1-2.4). The combination of the tetramannoside Te and the pentamannoside P on the same gold nanocluster (Te/P-GNP) showed the best affinity to the 2G12 antibody. This GNP was selected for the *in vivo* immunization studies by adding on the Te/P-GNP the T-cell epitope OVA₃₂₃₋₃₃₉. We have explored the potential of this structure to evoke specific anti-carbohydrates antibodies against HIVgp120 and obtained a weak but significant IgG production in mice. Although different functional assays are necessary to better understand the behavior of the evoked IgGs, the result with Te/P/OVA-GNPs has opened the way to explore GNPs as carriers for anti-carbohydrates vaccine. In **chapter 3** this approach will be exploited for the design of GNPs as carrier for anti-carbohydrate vaccine candidates against *Streptococcus pneumoniae*.

Experimental section

Synthesis of high mannoses conjugates: see Appendix 2.

Intermediates for the synthesis of high-mannose-type aminoethyl oligosaccharides Tri-1, Tri-2, and Te-4 (scheme 1)

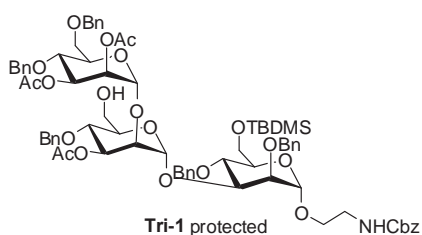


Scheme 1: Reagents and conditions for the synthesis of Tri-1, Tri-2, and Te-4: (a) Ac_2O , DMAP, Py, rt, 12 h, 93%; (b) TBAF, THF, rt, 15 h; (c) NIS, TfOH, CH_2Cl_2 dry, $-10\text{ }^\circ\text{C}$, 2 h; (d) MeONa, MeOH, rt, 48 h; (e) H_2 / Pd, MeOH, rt, 12 h.

Synthesis of Acceptor 2. Acceptor **1** was prepared as previously described^{17, 30} (see Appendix 2) and acetylated by treatment with Ac_2O . In order to obtain acceptor **2**, Acceptor **1** (349 mg, 0.535 mmol) was dissolved in pyridine (9 mL) and then Ac_2O (203 μL , 4 equiv.) and a catalytic amount of DMAP were added. The reaction was stirred overnight at rt. Quenching and washing with HCl 1M (4 x 20 mL) led to acetylated acceptor **1** (346 mg, 0.498 mmol, 93%) which was directly used for the next reaction. Acetylated acceptor **1** (346 mg, 0.498 mmol) was dissolved in dry THF (2 mL) followed by the addition of TBAF (1M in THF, 1.25 mL, 2.5 equiv.). The mixture was stirred at rt for 17 h before dilution with CH_2Cl_2 and concentration. The crude was purified by column chromatography on silica gel (gradient AcOEt/Hexane 1/1 to AcOEt/Hexane 2/1) to obtain acceptor **2** as a clear oil (193 mg, 0.333 mmol, 67%).

³⁰ Lee H. K., Scanlan C. N., Huang C. Y., Chang A. Y., Calarese D. A., Dwek R. A., Rudd P. M., Burton D. R., Wilson I. A., Wong C. H., Reactivity-based one-pot synthesis of oligomannoses: defining antigens recognized by 2G12, a broadly neutralizing anti-HIV-1 antibody, *Angew. Chem. Int. Ed.* 2004, 43, 1000-1003.

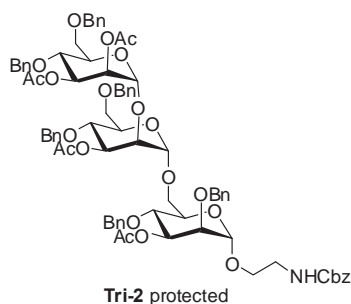
^1H NMR (500 MHz, CDCl_3) δ 7.38 – 7.27 (m, 15H), 5.20 (dd, J = 9.6, 3.3, 1H, H-3), 5.16 – 5.11 (m, 1H, NH), 5.10 (s, 2H), 4.80 (bs, 1H, H-1), 4.72 – 4.56 (m, 4H), 3.99 (t, J = 9.6, 1H, H-4), 5.20 (dd, J = 3.3, 2.0, 1H, H-2), 3.85 – 3.65 (m, 4H), 3.53 – 3.47 (m, 1H), 3.46 – 3.26 (m, 2H, CH_2NHZ), 1.97 (s, 3H, COCH_3), OH not detected. ^{13}C NMR (125 MHz, CDCl_3) δ = 170.2 (s, 1C, COCH_3), 156.4 (s, 1C, NHCO), 138.0 (s, 1C), 137.8 (s, 1C), 136.4 (s, 1C), 128.5, 128.4, 128.1, 127.9, 127.8, 127.7, 98.1 (d, 1C, C-1), 75.9 (d, 1C, C-2), 74.8 (t, 1C), 73.6 (d, 1C, C-3), 73.2 (t, 1C), 73.1 (d, 1C, C-4), 72.2 (d, 1C, C-5), 67.0 (t, 1C, $\text{OCH}_2\text{CH}_2\text{NHZ}$), 66.7 (t, 1C, $\text{NHC(O)OCH}_2\text{Ph}$), 61.9 (t, 1C, C-6), 40.6 (t, 1C, CH_2NHZ), 21.2 (q, 1C, COCH_3). IR (KBr): ν_{max} ~3600-3050 (broad), 3064, 3032, 2919, 2871, 1741 (strong), 1696, 1526, 1455, 1368, 1264, 1230. HR-MS for $\text{C}_{32}\text{H}_{37}\text{NO}_9$: Calcd. 618.210 $[\text{M}+\text{K}]^+$. Found 618.212 $[\text{M}+\text{K}]^+$.



Synthesis of Tri-1 protected. Acceptor **1** (scheme 1) (57 mg, 0.087 mmol) and disaccharide building block **3**³⁰ (98 mg, 0.105 mmol, 1.2 equiv.) were dissolved in anhydrous CH_2Cl_2 (1.5 mL) and stirred in presence of 4Å molecular sieves (480 mg) at rt for 2h. The reaction mixture was then cooled at -10°C before addition of *N*-iodosuccinimide (NIS) (25.4 mg, 0.113 mmol, 1.3 equiv.)

and trifluoromethanesulfonic acid (TfOH) (1 μL , 0.011 mmol, 0.13 equiv.). After 4 h, the reaction was quenched with sat. NaHCO_3 (aq) and left to reach rt. The reaction mixture was diluted with CH_2Cl_2 (3 mL) and was filtered through celite. The organic layer was washed with sat. $\text{Na}_2\text{S}_2\text{O}_3$ (aq) (10 mL x 4) and then dried over anhydrous Na_2SO_4 . The solvent was removed under reduced pressure to give colourless oil. The oil was purified by column chromatography (AcOEt/Toluene 7/100 to AcOEt/Toluene 30/100) to give fully protected **Tri-1** as a colourless oil (122 mg, 0.083 mmol, 95%).

^1H NMR (500 MHz, CDCl_3) δ 7.37 – 7.11 (m, 35H), 5.38 (d, J = 3.1, 1H), 5.36 (d, J = 3.1, 1H), 5.32 (dd, J = 3.3, 1.9, 1H), 5.24 (bt, J = 5.8, 1H), 5.21 (s, 1H), 5.05 (s, 2H), 4.86 – 4.33 (m, 12H), 4.76 (s, 1H), 4.73 (s, 1H), 4.10 – 3.97 (m, 5H), 3.91 – 3.82 (m, 3H), 3.74–3.48 (m, 9H), 3.33 – 3.19 (m, 2H, CH_2NHZ), 2.13 (s, 3H, COCH_3), 2.00 (s, 3H, COCH_3), 1.97 (s, 3H, COCH_3), 0.83 (s, 9H, $\text{Si}(\text{CH}_3)_2^t\text{Bu}$), -0.01 (s, 3H, $\text{Si}(\text{CH}_3)_2^t\text{Bu}$), -0.02 (s, 3H, $\text{Si}(\text{CH}_3)_2^t\text{Bu}$). ^{13}C NMR (125 MHz, CDCl_3) δ 170.2, 156.0, 137.5, 136.2, 128.1, 127.9, 127.5, 127.4, 100.6 (d, 1C), 99.2 (d, 1C), 97.4 (d, 1C), 80.2 (d, 1C), 77.7 (d, 1C), 77.4 (d, 1C), 75.1 (t, 1C), 75.0 (t, 1C), 74.7 (t, 1C), 74.6 (d, 1C), 73.7 (d, 1C), 73.5 (d, 1C), 73.3 (d, 1C), 73.3 (t, 1C), 73.1 (t, 1C), 72.2 (d, 3C), 71.9 (t, 1C), 71.6 (d, 1C), 70.1 (d, 1C), 69.5 (t, 1C), 68.3 (t, 1C), 67.6 (t, 1C), 66.4 (t, 1C), 62.6 (t, 1C), 40.9 (t, 1C, CH_2NHZ), 25.9 (q, 3C, $\text{Si-C}(\text{CH}_3)_3$), 21.2 (q, 1C, COCH_3), 21.1 (q, 2C, 2 x COCH_3), 18.1 (s, 1C, $\text{Si-C}(\text{CH}_3)_3$), -5.3 (q, 2C, $\text{Si}(\text{CH}_3)_2^t\text{Bu}$). MALDI-TOF for $\text{C}_{82}\text{H}_{99}\text{NO}_{21}\text{Si}$: Calcd. 1479.6 $[\text{M}+\text{NH}_4]^+$; Found 1480.6 $[\text{M}+\text{NH}_4]^+$.

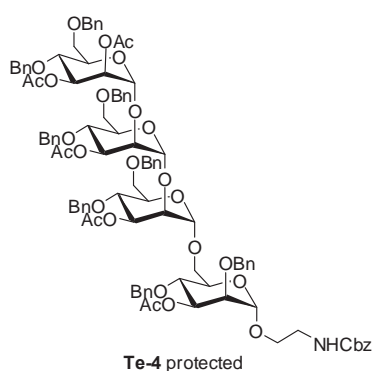


Synthesis of Tri-2 protected. Acceptor **2** (77 mg, 0.133 mmol) and disaccharide building block **3** (150 mg, 0.16 mmol, 1.2 equiv.) were dissolved in anhydrous CH_2Cl_2 (1.5 mL) and stirred in presence of 4Å molecular sieves (480 mg) at rt for 2h under Ar atmosphere. The reaction mixture was then cooled at -10°C before addition of NIS (38.9 mg, 0.173 mmol, 1.3 equiv.) and TfOH (1 μL , 0.017 mmol, 0.13 equiv.). After 3 h, the reaction was quenched with sat. NaHCO_3 (aq) and left to reach rt. The reaction mixture was diluted with CH_2Cl_2 (3 mL) and then filtered through celite. The organic layer was washed with sat.

$\text{Na}_2\text{S}_2\text{O}_3$ (aq) (10 mL x 4) and then dried over anhydrous Na_2SO_4 . The solvent was removed under reduced pressure to give colorless oil. The oil was purified by column chromatography

(gradient AcOEt/toluene 5/100 to AcOEt/toluene 50/100) to give a colorless oil (93 mg, 0.07 mmol, 51%).

^1H NMR (500 MHz, CDCl_3) δ 7.37 – 7.14 (m, 35H), 5.41 (dd, $J = 9.6, 3.2$, 1H), 5.35 (bs, 1H), 5.34 (s, 2H), 5.31 (dd, $J = 9.6, 3.2$, 1H), 5.18 (dd, $J = 8.9, 3.1$, 1H), 5.08 (s, 2H), 5.02 (s, 1H), 4.80 (s, 1H), 4.76 (s, 1H), 4.70 – 4.42 (m, 12H), 4.08 – 3.58 (m, 14H), 3.50 – 3.43 (m, 1H), 3.42 – 3.35 (m, 2H, CH_2NHZ), 2.12 (s, 3H, COCH_3), 1.99 (s, 3H, COCH_3), 1.97 (s, 3H, COCH_3), 1.93 (s, 3H, COCH_3). ^{13}C NMR (125 MHz, CDCl_3) δ 170.5 (s, 1C, COCH_3), 170.2 (s, 1C, COCH_3), 170.1 (s, 1C, COCH_3), 169.8 (s, 1C, COCH_3), 156.5 (s, 1C, NHCO), 138.3 (s, 1C), 138.2 (s, 3C), 138.0 (s, 1C), 137.9 (s, 1C), 136.7 (s, 1C), 128.5, 128.4, 128.3, 128.1, 127.9, 127.8, 127.7, 127.6, 127.4, 99.5 (d, 1C, C-1), 98.5 (d, 1C, C-1), 97.8 (d, 1C, C-1), 77.8, 75.8, 74.9, 74.7, 74.6, 73.7, 73.4, 73.2, 73.1, 73.0, 71.9, 71.7, 71.6, 71.3, 70.2, 68.8, 68.6, 66.6 (t, 1C, $\text{NHC(O)OCH}_2\text{Ph}$), 66.6 (t, 1C, $\text{OCH}_2\text{CH}_2\text{NHZ}$), 66.4, 40.4 (t, 1C, CH_2NHZ), 21.0 (q, 1C, COCH_3), 20.9 (q, 3C, 3 x COCH_3). MALDI-TOF: for $\text{C}_{78}\text{H}_{87}\text{NO}_{22}$: Calcd. 1412.6 $[\text{M}+\text{Na}]^+$. Found 1412.4 $[\text{M}+\text{Na}]^+$.



Synthesis of Te-4 protected. Acceptor **2** (36 mg, 0.062 mmol) and trisaccharide building block **4** (see Appendix 2) (97.8 mg, 0.074 mmol, 1.2 equiv.) were dissolved in anhydrous CH_2Cl_2 (1 mL) and stirred in presence of 4Å molecular sieves (400 mg) at rt for 2h under Ar atmosphere. The reaction mixture was then cooled at -10°C before addition of NIS (18.1 mg, 0.08 mmol, 1.3 equiv.) and TfOH (1 μL , 0.008 mmol, 0.13 equiv.). After 3 h, the reaction was quenched with sat. NaHCO_3 (aq) and left to reach rt. The reaction mixture was diluted with CH_2Cl_2 (3 mL) and then filtered through celite. The organic layer was

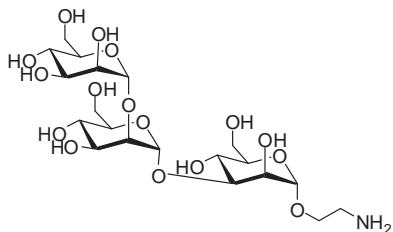
washed with sat. $\text{Na}_2\text{S}_2\text{O}_3$ (aq) (10 mL x 4) and then dried over anhydrous Na_2SO_4 . The solvent was removed under reduced pressure to give colorless oil. The oil was purified by column chromatography (AcOEt/Toluene 5/100 to AcOEt/Toluene 50/100) to give a colorless oil (70 mg, 0.039 mmol, 63%).

^1H NMR (500 MHz, CDCl_3) δ 7.41 – 7.07 (m, 45H), 5.39 (bt, 1H, NH), 5.38 (dd, $J = 9.4, 3.4$, 1H), 5.36 – 5.27 (m, 3H), 5.16 (m, 1H), 5.06 (s, 2H), 5.03 (s, 1H), 4.97 (s, 1H), 4.89 (s, 1H), 4.74 (s, 1H), 4.71 – 4.37 (m, 16H), 4.16 (bt, 1H), 4.10-3.98 (m, 3H), 3.97 – 3.85 (m, 3H), 3.83-3.73 (m, 5H), 3.71 – 3.52 (m, 8H), 3.50 – 3.42 (m, 1H), 3.40-3.30 (m, 2H), 2.15 (s, 3H, COCH_3), 2.05 (s, 3H, COCH_3), 1.98 (s, 6H, 2 x COCH_3), 1.91 (s, 3H, COCH_3). ^{13}C NMR (125 MHz, CDCl_3) δ 170.5 (s, 1C, COCH_3), 170.4 (s, 1C, COCH_3), 170.2 (s, 1C, COCH_3), 170.1 (s, 1C, COCH_3), 169.7 (s, 1C, COCH_3), 156.5 (s, 1C, NHCO), 138.5 (s, 1C), 138.3 (s, 1C), 138.2 (s, 1C), 138.1 (s, 1C), 138.0 (s, 2C), 137.9 (s, 1C), 137.8 (s, 1C), 136.7 (s, 1C), 134.5 (s, 1C), 129.8, 129.0, 128.5, 128.4, 128.3, 128.0, 127.9, 127.8, 127.7, 127.6, 127.5, 127.3, 100.6 (d, 1C, C-1), 99.1 (d, 1C, C-1), 98.4 (d, 1C, C-1), 97.6 (d, 1C, C-1), 75.8, 74.8, 74.5, 74.4, 74.0, 73.7, 73.6, 73.4, 73.3, 73.2, 73.0, 72.8, 71.9, 71.7, 71.6, 71.1, 70.2, 69.0, 68.8, 68.2, 66.6 (t, 1C, $\text{OCH}_2\text{CH}_2\text{NHZ}$), 66.5 (t, 1C, $\text{NHC(O)OCH}_2\text{Ph}$), 40.3 (t, 1C, CH_2NHZ), 21.0 (q, 3C, 3 x COCH_3), 20.9 (q, 2C, 2 x COCH_3), 14.2. MALDI TOF: for $\text{C}_{100}\text{H}_{111}\text{NO}_{28}$ Calcd. 1796.7 $[\text{M}+\text{Na}]^+$. Found 1796.8 $[\text{M}+\text{Na}]^+$

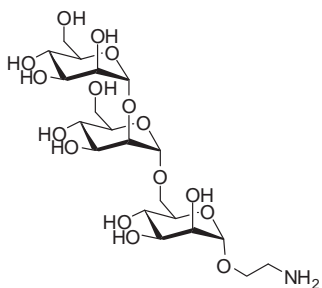
Synthesis of aminoethyl oligomannosides Tri-1, Tri-2, and Te-4

Tetramannoside **Te-3** was prepared according to the literature³⁰(see also Appendix 2). Aminoethyloligomannosides **Tri-1**, **Tri-2**, and **Te-4** were obtained by deprotection of the corresponding fully protected parent compounds whose preparation from acceptor **1** and acceptor **2** was described before. *General procedure:* The fully protected oligomannosides (0.06 mmol) were dissolved in MeOH (3 mL) and NaOMe (1 equiv., 3.6 mg, 0.06 mmol) was added to solution. The solution was stirred at rt for 48 h and then it was brought to pH~7 with Amberlite IR-120 (**Tri-1** and **Tri-2**) or to pH~2 with HCl 1M (**Te-4**). The solvent was removed

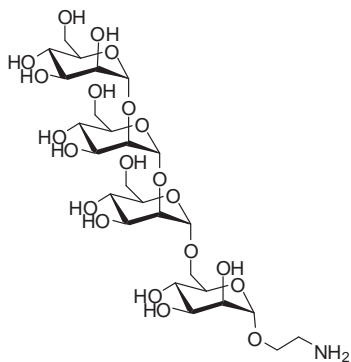
under reduced pressure to give a residue. The oligomannoside was dissolved in MeOH/HCOOH (v/v = 95/5) (3 mL) and 1.5 mass equiv. Pd-Black was added to the solution. The reaction mixture was flushed with H₂ (3 times) and stirred at rt under H₂ for 12 h. The reaction mixture was diluted with MeOH and filtered through Celite. The solvent was removed under reduced pressure. The resulting residue was purified by size-exclusion chromatography Sephadex LH-20 (MeOH/H₂O 9/1). After freeze-drying, the desired products were collected as white solids.



Tri-1: (yield 72%). ¹H NMR (500 MHz, D₂O) δ 8.45 (s, 1H, HCOO⁻), 5.38 (d, 1H, *J*=1.4, H1B), 5.05 (d, 1H, *J*=1.6, H1A), 4.89 (d, 1H, *J*=1.6, H1C), 4.14 (dd, 1H, *J*=3.2, 1.6, H2C), 4.10 (dd, 1H, *J*=3.2, 1.7, H2B), 4.07 (dd, 1H, *J*=3.3, 1.8, H2A), 4.06 – 4.01 (m, 1H, OCH₂CH₂NH₃⁺), 3.99 (dd, 1H, *J*=9.6, 3.3, H3B), 3.94 – 3.62 (m, 15H), 3.43 – 3.30 (m, 2H, CH₂NH₃⁺). HSQC NMR (125 MHz, D₂O) δ 102.3 (d, 1C, C1A), 100.7 (d, 1C, C1B), 99.7 (d, 1C, C1C), 78.4 (d, 1C, C2B), 78.1, 73.2, 73.1, 70.2, 69.9, 69.8 (d, 1C, C2A), 69.3 (d, 1C, C2C), 66.8, 65.8, 60.9, 60.8, 61.4 (d, 1C, OCH₂CH₂NH₃⁺), 56.3 (t, 1C, CH₂NH₃⁺). IR (KBr): ν[~] ~3600-3050 (broad), 2934, 2885, 1593 (strong), 1385, 1344, 1131, 1054, 1033. HR-MS: Calcd. for C₂₀H₃₇NO₁₆Na⁺ 570.201 [M-HCOOH+Na]⁺; Found 570.198. [α]_d²⁰ = +30 (c = 0.1, H₂O)



Tri-2: (yield 78%). ¹H NMR (500 MHz, D₂O) δ 8.48 (s, 1H, HCOO⁻), 5.17 (d, 1H, *J*=1.4, H1D), 5.04 (d, 1H, *J*=1.5, H1E), 4.90 (d, *J*=1.5, 1H, H1C), 4.09 (dd, 1H, *J*=3.2, 1.5), 4.03 – 3.67 (m, 18H), 3.63 (t, *J*=9.8, 1H), 3.28 – 3.21 (m, 2H, CH₂NH₃⁺). HSQC NMR (125 MHz, D₂O) δ 102.3 (d, 1C, C1E), 100.1 (d, 1C, C1C), 97.9 (d, 1C, C1D), 78.7 (d, 1C), 73.2 (d, 1C), 72.7 (d, 1C), 71.1 (d, 1C), 70.6 (d, 1C), 70.3 (d, 1C), 70.2 (d, 1C), 69.9 (d, 1C), 69.7 (d, 1C), 66.9 (d, 2C), 66.4 (d, 1C), 65.7 (t, 1C), 63.4 (t, 1C), 61.1 (t, 1C), 60.9 (t, 1C), 39.0 (t, 1C, CH₂NH₃⁺). IR (KBr): ν[~] ~3600-3050 (broad), 2937, 1591 (strong), 1386, 1345, 1125, 1090, 1062. HR-MS: Calcd. for C₂₀H₃₇NO₁₆Na⁺ 570.201 [M-HCOOH+Na]⁺; Found 570.199. [α]_d²⁰ = +9 (c = 0.5, H₂O)



Te-4: (yield 75%). ¹H NMR (500 MHz, D₂O) δ 5.30 (s, 1H, *J*=1.4, H1E), 5.15 (s, 1H, *J*=1.4, H1D), 5.06 (s, 1H, *J*=1.5, H1Z), 4.90 (s, 1H, *J*=1.5, H1C), 4.12 (dd, 1H, *J*=3.0, 1.4, H2E), 4.08 (dd, *J* = 3.3, 1.5, 1H, H2Z), 4.03 – 3.59 (m, 24H), 3.19 (m, 2H, CH₂NH₃⁺). HSQC NMR (125 MHz, D₂O) δ 102.1 (d, 1C, C1Z), 100.6 (d, 1C, C1E), 100.1 (d, 1C, C1C), 98.0 (d, 1C, C1D), 78.8, 78.4 (d, 1C, C2E), 73.1, 72.8, 70.9, 70.3, 69.8 (d, 1C, C2Z), 66.9, 66.8, 65.9, 61.0, 39.2 (t, 1C, CH₂NH₃⁺). IR (KBr): ν[~] ~3600-3050 (broad), 2925, 2877, 1131, 1058. HR-MS: Calcd. for C₂₆H₄₈NO₂₁⁺: 710.272 [M-Cl]⁺; Found 732.252. Calcd. for C₂₆H₄₇NO₂₁Na⁺: 732.254 [M-HCl+Na]⁺; Found 732.252. [α]_D²⁰ = +5 (c = 0.5, H₂O)

STD-NMR spectroscopy aminoethyl oligosaccharides **Tri-1**, **Tri-2**, and **Te-4**

For the preparation of the NMR samples, first, the majority of maltose present in the antibody batch was removed, and the sample buffer exchanged, by dialysis with a membrane of 20 kDa (Spectra/Por, Medicell International Ltd.). All the ligands were lyophilized against 99% D₂O twice and once with 99.99% D₂O from Sigma–Aldrich. All the samples were prepared in 10 mM phosphate deuterated buffer solution at pH 6.7. The ¹H NMR signals of each ligand were assigned by employing a combination of COSY, TOCSY, NOESY, and HSQC experiments performed on a Bruker DRX (500 MHz) spectrometer. For STD NMR experiments, the temperature was 298 K for all experiments. The experiments were performed without suppression of the residual HDO signal. The broad signals of the antibody were deleted by adding a T1ρ filter to the STD NMR pulse sequence. All the STD NMR experiments were carried out with 1 K scans. The build-up curves were obtained by using seven saturation times (0.5, 0.75, 1, 1.5, 2, 2.5, and 3 s) varying the relaxation delay (with a minimum of 0.1 s) inversely to the saturation time for each experiment, keeping the total experimental time constant. Each saturation time was composed by a train of Gaussian-shaped pulses of 50 ms. Off- and on-resonance frequencies of 40 and 0.86 ppm (antibody aliphatic region), respectively, were used for the STD NMR build-up curves. For the titration experiments, antibody/ligand molar ratios were increased from 1:11 to 1:200 by adding different aliquots of the ligand to the NMR sample from high concentration stocks of each ligand. For each ratio an STD build-up curve was calculated to obtain the initial slopes (STD₀) by a mathematical fitting.³¹

Dissociation constants (K_D) for each oligomannoside were obtained by fitting every isotherm made of initial slopes from the STD NMR build-up curves to a Langmuir equation of the kind $(B_{\max} \cdot [L]) / (K_D + [L])$. The binding epitopes of the ligands were obtained at the largest antibody/ligand ratios reached in the experimental setup by normalizing the STD-AF₀ values for each ligand against the largest value, to which a value of 100% was arbitrarily assigned.

In the competitive experiments between **Te-3** and **Te-4**, the sample was prepared in the same buffer that those for the STD NMR build-up curves, but the concentrations were [2G12] = 25 μM and [**Te-4**] = 1 mM. Afterwards, **Te-3**, was added to this sample, obtaining a sample in which both tetramannosides were in the same concentration with antibody-to-ligand ratio of 1: 40.

The described STD-NMR experiments were performed by Dr. P. M. Enríquez-Navas under the supervision of Dr. J. Angulo.

Microarrays

Microarrays were printed on glass slides employing a robotic non-contact spotter Piezorray from Perkin Elmer, Shelton, USA. NHS activated glass slides Nexterion[®] H were purchased from Schott AG, Mainz, Germany. 2G12* and ConA* incubations were performed using the Fast Frame[®] incubation chambers from Whatman, Kent, UK. Fluorescence measurements were performed in an Agilent G265BA microarray scanner system, Agilent Technologies, Santa Clara, USA. Quantification was achieved by ProScanArray Express software from Perkin Elmer, Shelton, USA.

Buffered solutions (200 μL, 300 mM, pH 8.5) of **Tri-1**, **Tri-2**, **Te-3**, **Te-4**, and aminoethyl glucoside were placed into a 384-well source plate and arrayed onto NHS functionalized glass

³¹ Angulo J., Enríquez-Navas P. M., Nieto P. M., Ligand-receptor binding affinities from saturation transfer difference (STD) NMR spectroscopy: the binding isotherm of STD initial growth rates, Chem. Eur. J. 2010, 16, 7803-7812.

slides. Volumes (0.7 nL) of the buffered solutions were spotted in 8 replicates. After printing, the slides were placed in a 75% humidity chamber (saturated NaCl solution) at 25 °C for 18 hours. The remaining NHS groups were quenched by placing the slides in a 50 mM solution of ethanolamine in sodium borate buffer 50 mM, pH 9.0, for 1h. Then, the slides were washed with a standard protocol and dried in a slide spinner. A buffered solution (100 µL) of fluorescently labeled 2G12 (25 µg/mL) was incubated in the dark over each microarray for 1 hour at room temperature. After washing and drying, the fluorescence was analyzed with a microarray scanner. Ligand solutions (Tri-1, Tri-2, Te-3, Te-4, and aminoethyl glucoside) were prepared from stock solutions (1 mM in water) by dilution with sodium phosphate buffer (300 mM, pH 8.5, 0.005% Tween 20) to a final concentration of 25, 50, 100, and 200 µM. These solutions (20 µL) were placed into a 384-well source plate and spatially arrayed onto NHS functionalized glass slides. Volumes (0.7 nL) of the glycan buffered solutions were spotted in 8 replicates. After printing, the slides were placed in a 75% humidity chamber (saturated NaCl solution) at 25 °C for 18 hours. The remaining NHS groups were quenched by placing the slides in a 50 mM solution of ethanolamine in sodium borate buffer 50 mM, pH 9.0, for 1h. The standard washing of the slides was performed with PBST (phosphate buffered saline (PBS) solution containing 0.5% Tween 20), PBS and water. The slides were dried in a slide spinner.

Test for biofunctionality of the printed ligands using ConA*: Concanavalin A (ConA) was purchased from Vector laboratories, Burlingame, USA and labeled with Hilyte Plus™ 555 protein labeling kit from AnaSpec, Fremont, USA. The microarrays were compartmentalized with a 16-well gasket. Solutions (100 µL) of fluorescently labeled Concanavalin A (ConA*), a well-characterized α -mannose selective lectin ³²(ConA-555, 50 µg/mL) were incubated in the dark over each sub-array for 1h at room temperature. The slide was washed under standard conditions, dried with a slide spinner and the fluorescence was analyzed with a microarray scanner. ConA solution was prepared in PBST (PBS with 0.05% Tween-20) with CaCl₂ (1 mM) and MgCl₂ (1 mM). Results confirmed the correct functionalization of the slides with all the glycans (data not shown). The functionalization of the slides with Te-3 and Te-4 is shown in Figure 7. This is consistent with the known α -mannose binding preferences of ConA.

Binding of the printed ligands with 2G12*: HIV-1 gp120 Monoclonal Antibody 2G12 was kindly supplied by Dr D. Katinger (Polymun Scientific, Vienna, Austria). 2G12 was labeled with Hilyte Plus™ 555 protein labeling kit from AnaSpec, (Fremont, USA) according to the instructions of the manufacturer. The microarray was compartmentalized with a 16-well gasket. Solutions (100 µL) of fluorescently labeled 2G12 (25 µg/mL in PBS with 0.05% Tween-20) were incubated in the dark over each sub-array for 1h at room temperature. The slide was washed under standard conditions, dried with a slide spinner and the fluorescence was analyzed with a microarray scanner. Figure 8 shows the result after incubation with 2G12*.

These experiments were performed with the help of Dr. S. Serna and J. Echevarria.

GNPs preparation and characterization:

Te/P-GNPs: Reaction of a 0.5:0.5:9 mixture of 2mg of Te, 2.29mg of P conjugate and 4mg of GlcC₅S with HAuCl₄ and NaBH₄ gave 1.6mg of Te/P -GNPs as a dark-brown powder. TEM (average diameter and number of gold atoms): ~1.8 nm. Quantitative ¹H NMR: 0.83mg of Te/P-GNPs were dissolved in 830µL of 0.75% TSP in D₂O and 0.03µmoles of Te and 0.03 µmoles of P were founded. ¹H NMR: (500 MHz, D₂O, water suppression) only significant peaks are

³² Shimura K., Kasai K., Determination of the affinity constants of concanavalin A for monosaccharides by fluorescence affinity probe capillary electrophoresis, *Anal. Biochem.* 1995, 227, 186–194.

reported: $\delta = 5.35$ (bs, from 2 anomeric protons), 5.29 (s, from Te anomeric proton), 5.13 (s, from P anomeric proton), 5.04 (bs, from 3 anomeric protons), 4.83 (s, from glucose anomeric proton); two anomeric protons below water signal (4.75).

Ratio between Te and P signals $\sim 1:1$. These results are in agreement with the estimation of 5% of Te and 5% of P on the GNPs. Molar ratio of conjugates per nanoparticle was also determined by analyzing the mixtures using NMR before and after nanoparticle formation. Estimated average molecular weight for $(C_{46}H_{85}N_2O_{25}S_2)_4(C_{52}H_{95}N_2O_{30}S_2)_4(C_{11}H_{21}O_6S)_{64}Au_{201}$: ~ 67 kDa. IR (KBr): $\nu = \sim 3300\text{--}3200$ (br), 2900, 2850, 1100. UV/Vis (H_2O , 0.1 mg/mL): surface plasmon band not observed.

Te/Tetanus-GNPs: Tetanus toxoide (1.02 mg, 0.37 μmol) was dissolved in CF_3COOD (50 μL) and dried under air stream until formation of an oil. **GlcC₅S** (1.03 mg, 3.7 μmol) and Te (3.72 mg, 3.29 μmol) were added to the oil and the mixture was dissolved in CD_3OD (600 μL). The 1H NMR spectrum showed a ratio 10:9:1 between the signals of **GlcC₅S**, tetramannoside conjugate Te and Tetanus toxoide. The solution was diluted with MeOH to a 0.012 M concentration of organic material and pH was adjusted to 1 by addition of CF_3COOH . An aqueous solution of $HAuCl_4$ (58.4 μL , 0.025M) was added; then 31 μL of 1 M aqueous $NaBH_4$ solution were added to the mixture under rapid shaking. The black suspension was shaken for 2h and the methanolic supernatant was separated by decantation. The black solid was washed with EtOH (3 mL) and MeOH (3 mL), dissolved in water (5 mL) and purified by dialysis (Slide-A-Lyzer Dialysis casset, 10,000 MWCO). UV/Vis (H_2O , 0.1 mg/mL): surface Plasmon band not observed. TEM: average gold diameter 1.9 nm. 1H NMR (500 MHz, D_2O) $\delta = 7.30$ (m), 5.35 (d, $J=27.3$), 5.07 (s), 4.86 (bs), 4.20 – 3.21 (m), 2.84–2.63 (m), 1.86 – 1.11 (m).

Figure 15 shows the thiol-ending conjugates of the peptides used for the preparation of Te/Tetanus-GNPs and Te/P/OVA-GNPs

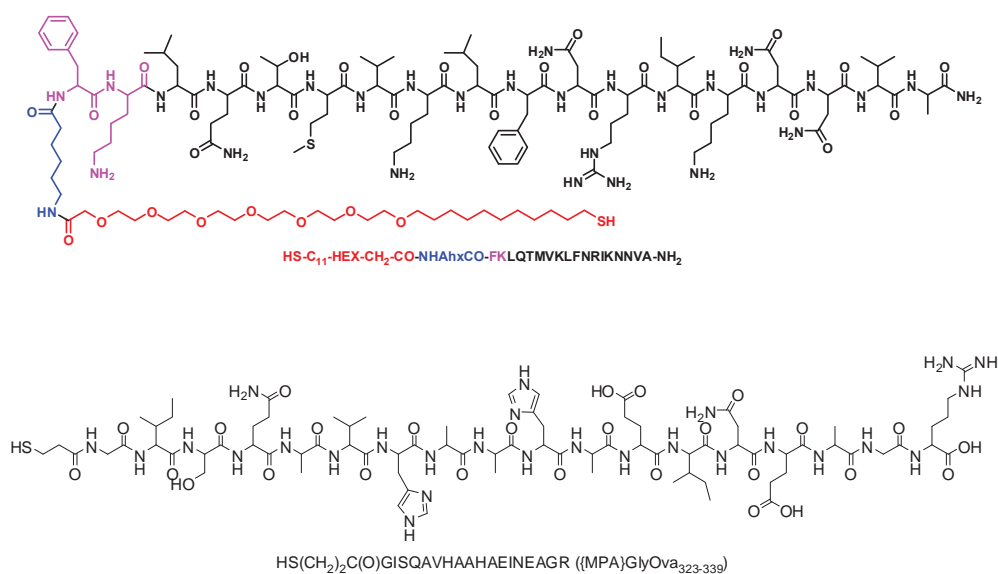


Figure 15: Thiol-ending T-helper peptides tailored into the GNPs with the aim of evoking anti-carbohydrate adaptive responses. *Up*: thiol-ending derivative of a Tetanus toxoide peptide; *Bottom*: OVA₃₂₃₋₃₃₉ peptide-derivative from Ovalbumin.

Te/P/OVA-GNPs: Reaction of a 1:1:7.5:0.5 mixture of 0.89mg of Te conjugate, 1.02mg of P conjugate, 1.67mg of GlcC₅S and 0.76mg of OVA₃₂₃₋₃₃₉ conjugate with $HAuCl_4$ and $NaBH_4$ gave 0.5mg of Te/P/OVA-GNPs as a dark-brown powder. TEM (average diameter): $1.7\pm 0.3\text{nm}$. NMR: (500 MHz, D_2O) only significant peaks are reported: $\delta = 5.30$ (bs, from 2 anomeric protons),

5.23 (bs, from Te anomeric proton), 5.07 (bs, from P anomeric proton), 4.98 (bs, from 3 anomeric protons), 4.37 (bs, from glucose anomeric proton); 0.81 (bs from OVA₃₂₃₋₃₃₉ Valine signals) ratio between Te:P:Glc:OVA signals $\sim 0.87:1:10:0.4$.

These results are in agreement with the estimation of 10% of Te, 10% of P and 5% of OVA₃₂₃₋₃₃₉ on the GNPs. Molar ratio of conjugates per nanoparticle was also determined by analyzing the mixtures using NMR before and after nanoparticle formation. UV/Vis (H₂O, 0.1 mg/mL): surface plasmon band not observed.

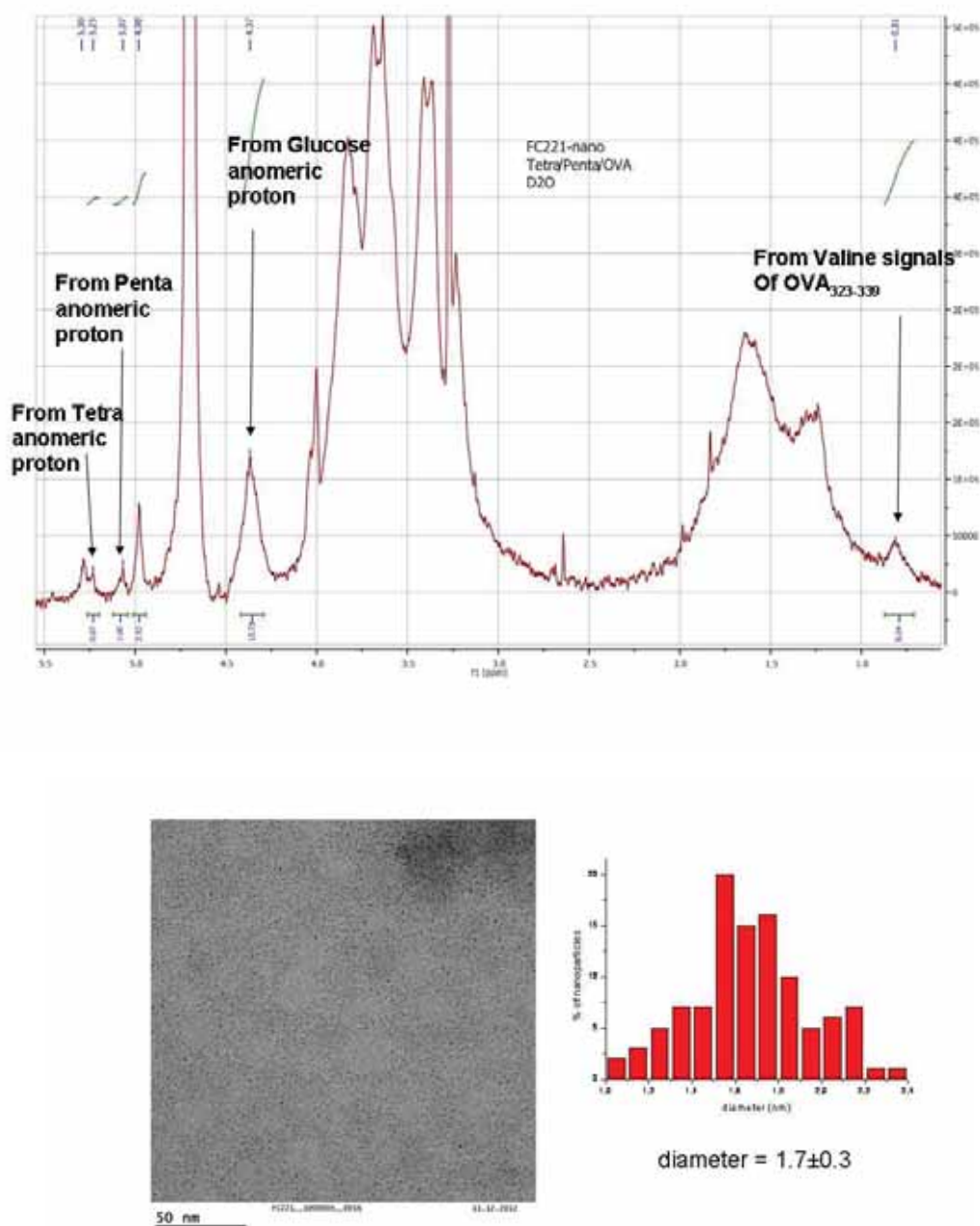


Figure 16: Characterization of Te/P/OVA-GNPs: *Upper panel:* ¹H NMR spectrum of Te/P/OVA-GNPs in D₂O at 500 MHz. *Bottom panel:* Left: TEM micrograph; Right: size-distribution histogram obtained from analysis of TEM micrographs.

Biosensors: Surface plasmon resonance (SPR) experiments with Te/P-GNPs

SPR analyses were performed at 25 °C using a ProteOn™ XPR36 Protein Interaction Array System (Bio-Rad Laboratories, Inc.) with research-grade GLC sensor chips. 2G12 and gp120 were immobilized using the standard amine coupling chemistry according to the manufacturer's instructions.

Binding Studies. 2G12 was immobilized on a GLC sensor chip using the ProteOn™ amine coupling kit at a level of 2,600 Response Units (RU) using PBST as running buffer, i.e. phosphate buffered saline (PBS: Na₃PO₄ 10 mM, NaCl 150 mM, pH 7.4) with 0.005% of the surfactant Tween 20. The carboxylic groups of two different channels on the chip surface were activated by injecting 30 µL (contact time: 60 s; flow rate: 30 µL min⁻¹) of a 1:1 by volume mixture of EDAC (16 mM) and Sulfo-NHS (4 mM). One of the channels was further injected with 120 µL (240 s; 30 µL min⁻¹) of a 2G12 solution in acetate buffer (50 µg mL⁻¹, 10 mM, pH 5.5). Only PBST was flown into the other channel which was thus used as a reference. The surface of both channels was then saturated by 100 µL of 1 M ethanolamine HCl (200 s; 30 µL min⁻¹). Binding experiments were carried out in tris(hydroxymethyl)aminomethane (TRIS) buffered saline (TRIS 10 mM, NaCl 150 mM, pH 7.4), containing 0.005% of Tween 20.

The sensorgrams were obtained after injection of the analytes (high mannose oligosaccharides, *manno*-GNPs, and control GNPs) at 25 °C (flow rate: 30 µL min⁻¹; contact time: 300 s; dissociation: 300 s) by automatic subtraction of the reference surface signal from the 2G12 surface signal. The sensor surface between runs was regenerated with a short pulse (flow rate: 100 µL min⁻¹; contact time: 300 s) of 3.5 M MgCl₂. Glycoprotein gp120 was tested to verify that 2G12 maintains its recognition properties after immobilization. 2G12 activity slightly decreased during the experiments due to the regeneration conditions and to the instability of the antibody at 25 °C for long periods.

Inhibition Studies. Glycoprotein gp120 was immobilized on a GLC sensor-chip at a level of 8,000 RU using the methodology described above for 2G12. TRIS buffered saline was used as running buffer. The sensor surface between runs was regenerated with a short pulse of 0.1 M HCl. Antibody 2G12 (final concentration 100 nM) was pre-incubated with different concentrations of *manno*-GNPs for ~10 min at 25 °C in TRIS buffered saline and the mixture was then co-injected onto the gp120-functionalized sensor chip (flow rate: 30 µL min⁻¹, contact time: 300 s, dissociation: 300 s). In each experiment, six different concentrations of *manno*-GNPs (including a control channel where 2G12 was added with buffer) were used. During the experiments, gp120 shows a slight loss of activity due to HCl regeneration phases.

STD-NMR spectroscopy experiments with *manno*-GNPs

In a typical experiment, special NMR tubes (3 mm x 100 mm, Bruker) adaptable to a Bruker MATCH™ holder were charged with 180 µL containing 2G12 (25 µM) and aminoethyl tetramannoside (8 mM) in 10 mM deuterated potassium phosphate buffer (pH 6.7). The high ligand/antibody ratio was set up so that more than 90% of the 2G12 binding sites were occupied, fulfilling the condition of competitive inhibition titrations.²⁸ Increasing volumes (0.6, 2.46, 6.33, 7.85, 9.0 and 18.0 µL) of solution of Te-50 GNP (733 µM in tetramannoside) in D₂O were added to the 180 µL solution of 2G12/aminoethyl tetramannoside mixture. For more details see the publication Marradi *et al.* 2011.²¹ These NMR experiments were performed by Dr. P. M. Enríquez-Navas under the supervision of Dr. J. Angulo.



Gold Nanoparticles Coated with Oligomannosides of HIV-1 Glycoprotein gp120 Mimic the Carbohydrate Epitope of Antibody 2G12

Marco Marradi^{1,2*}, Paolo Di Gianvincenzo^{1†}, Pedro M. Enríquez-Navas^{1†}, Olga M. Martínez-Ávila¹, Fabrizio Chiodo¹, Eloísa Yuste^{3,4}, Jesús Angulo⁵ and Soledad Penadés^{1,2*}

¹Laboratory of GlycoNanotechnology, Biofunctional Nanomaterials Unit, CIC biomaGUNE, Paseo Miramón 182, E-20009 San Sebastián, Spain

²Biomedical Research Networking Center in Bioengineering, Biomaterials, and Nanomedicine (CIBER-BBN), Paseo Miramón 182, E-20009 San Sebastián, Spain

³Retrovirology and Viral Immunopathology Laboratory, IDIBAPS, Hospital Clínic, University of Barcelona, Barcelona, Spain

⁴HIVACAT, Hospital Clínic, Faculty of Medicine, University of Barcelona, Barcelona, Spain

⁵Department of Bioorganic Chemistry, Instituto de Investigaciones Químicas (CSIC-US), Américo Vespucio 49, E-41092 Sevilla, Spain

Received 1 February 2011;
received in revised form

18 March 2011;
accepted 18 March 2011

Available online
25 March 2011

Edited by M. F. Summers

Keywords:

multivalent gold glyconanoparticles; high-mannose-type oligosaccharides; surface plasmon resonance; NMR spectroscopy; 2G12/gp120 inhibition

After three decades of research, an effective vaccine against the pandemic AIDS caused by human immunodeficiency virus (HIV) is not still available, and a deeper understanding of HIV immunology, as well as new chemical tools that may contribute to improve the currently available arsenal against the virus, is highly wanted. Among the few broadly neutralizing human immunodeficiency virus type 1 (HIV-1) monoclonal antibodies, 2G12 is the only carbohydrate-directed one. 2G12 recognizes a cluster of high-mannose glycans on the viral envelope glycoprotein gp120. This type of glycan has thus been envisaged as a target to develop an HIV vaccine that is capable of eliciting 2G12-like antibodies. Herein we show that gold nanoparticles coated with self-assembled monolayers of synthetic oligomannosides [*manno*-gold glyconanoparticles (GNPs)], which are present in gp120, are able to bind 2G12 with high affinity and to interfere with 2G12/gp120 binding, as determined by surface plasmon resonance and saturation transfer difference NMR spectroscopy. Cellular neutralization assays demonstrated that GNPs coated with a linear tetramannoside could block the 2G12-mediated neutralization of a replication-competent virus under conditions that resemble the ones in which normal serum prevents infection of the target cell. Dispersibility in water and physiological media, absence of cytotoxicity, and the possibility of inserting more than one component into the same nanoparticle make *manno*-GNPs versatile, polyvalent, and

*Corresponding authors. Laboratory of GlycoNanotechnology, Biofunctional Nanomaterials Unit, CIC biomaGUNE, San Sebastián, Spain. E-mail addresses: mmarradi.ciber-bbn@cicbiomagune.es; spenades@cicbiomagune.es.

† P.D.G. and P.M.E.-N. contributed equally to this work.

Abbreviations used: HIV, human immunodeficiency virus; HIV-1, human immunodeficiency virus type 1; GNP, gold glyconanoparticle; mAb, monoclonal antibody; SPR, surface plasmon resonance; STD, saturation transfer difference; GlcC₅S, 5-(thio)pentyl β-D-glucopyranoside; RU, response unit; PBS, phosphate-buffered saline.

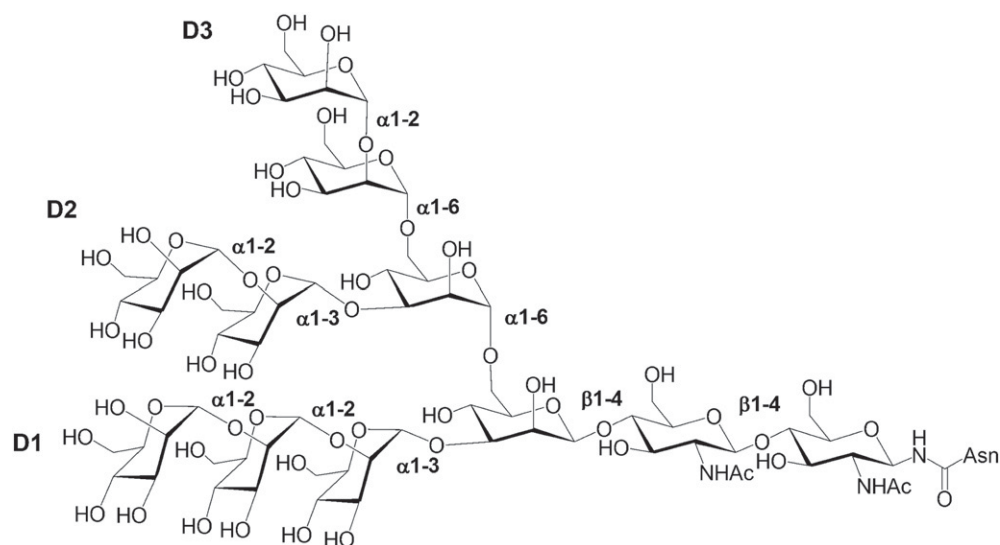
multifunctional systems that may aid efforts to develop new multifaceted strategies against HIV.

© 2011 Elsevier Ltd. All rights reserved.

Introduction

To date, highly active antiretroviral therapy is the only regimen approved to treat people infected with human immunodeficiency virus (HIV).¹ The use of antiretroviral drugs presents some inconveniences such as viral resistance to therapy, adverse effects, and high costs, which make this strategy unfeasible for application in poor countries where HIV-induced acquired immunodeficiency syndrome (AIDS) still kills hundreds of thousands of patients every year. Alternative strategies directed at also protecting HIV-negative people from becoming infected or getting sick have been proposed. Nevertheless, attempts to generate effective microbicides and vaccines against HIV have failed, so that integrated systems and new strategies are urgently needed.^{2,3} The lack of an HIV vaccine is due to a series of extraordinary obstacles,⁴ and a deeper understanding of HIV molecular biology is required. Much of the effort in human immunodeficiency virus type 1 (HIV-1; the worldwide predominant virus type) research has been dedicated to immunogens that are able to elicit antibodies against HIV-1 primary isolates. One approach is to produce epitope mimics of the broadly neutralizing monoclonal antibodies (mAbs) isolated from patients. The outer envelope glycoprotein gp120 of HIV is highly glycosylated.⁵ This dense carbohydrate array is composed by immunogenically silent "self"-glycans that are used by the virus as a defence mechanism to evade host

immune attacks.⁶⁻⁸ In spite of the poor immunogenicity of these "self"-glycans, the broadly neutralizing mAb 2G12 exclusively targets the carbohydrates of HIV gp120,⁹ namely a cluster of high-mannose oligosaccharides.¹⁰ Crystal structures of 2G12 and its complexes with the dimannose Man α 1-2Man and the undecasaccharide Man₉(GlcNAc)₂ (Scheme 1) revealed a two-domain-swapped fragment antigen binding as the prevalent form by which 2G12 recognizes gp120 and confirmed a multivalent interaction with a conserved cluster of Man α 1-2Man-linked high-mannose-type carbohydrates of gp120.¹¹ On the basis of these data, a molecular model for the 2G12/gp120 interaction in which three separate Man₉(GlcNAc)₂ mediate the binding of 2G12 to gp120 was proposed. The terminal Man α 1-2Man α residues of the D1 arm of Man₉(GlcNAc)₂ account for most of the contacts with the fragment antigen binding, although Man α 1-2Man by itself is less potent than the complete glycan in binding to 2G12. The relatively conserved nature of the 2G12 epitope and the protective role of viral envelope glycans against antibodies make the gp120 carbohydrates a tempting target for drug and vaccine design.^{12,13} A very recent article by Doores *et al.* showed that Man α 1-2Man-terminating glycans of the type recognized by 2G12 are 3-fold more abundant on the HIV-1 native envelope than on the recombinant monomer and are also found on isolates not neutralized by 2G12.¹⁴ Nevertheless, there are still no examples of synthetic immunogens



Scheme 1. Structure of high-mannose Man₉(GlcNAc)₂ present in the envelope glycoprotein gp120.

based on carbohydrates that can elicit effective antibodies against HIV-1.

The critical role of multivalency within the 2G12/gp120 interaction was demonstrated by different research groups.^{15–25} Synthetic Man α 1–2Man-containing oligomannosides were tested as inhibitors of 2G12 binding to gp120 in ELISAs.²⁶ Man α 1–2Man α 1–2Man α 1–3Man (Man₄) and Man α 1–2Man α 1–3[Man α 1–2Man α 1–6]Man (Man₅) derivatives were identified as being as effective as Man₉ in inhibiting 2G12/gp120 interaction.²⁶ This result was confirmed by microarray-based studies.¹⁵ In particular, a multivalent presentation of Man₄ and Man₅ on microtiter plates afforded an ~10,000-fold enhancement of binding to 2G12 compared to the solution-phase ELISAs of the monomers.¹⁵ Microarrays of Man₉ conjugates and related substructures corroborated the ligand specificity of 2G12 for Man α 1–2Man terminal oligosaccharides and the importance of multivalency.^{16–19} These studies evidenced that more complex oligomannosides (Man₆, Man₇, and Man₈) are also good synthetic mimics of 2G12 epitope but do not generally improve the affinity for 2G12 with respect to Man₄. The multimerization of high-mannose-type oligosaccharides by chemical systems has been achieved using galactose,²⁰ cholic acid,²¹ peptide scaffolds,^{22–24} dendrons,^{25,27} and icosahedral virus capsides.²⁸ These synthetic oligomannoside clusters were able to mimic the carbohydrate epitope of 2G12, being effective in binding the antibody at micromolar and submicromolar ranges (the gp120 affinity for 2G12 being at a nanomolar level). The incorporation of T-helper epitope peptides²⁹ or antigenic carrier proteins^{23,24,27} into these scaffolds enhanced the poor immunogenicity of the oligosaccharides. Although most of these systems were able to induce a carbohydrate-specific immune response in animals, the IgG antibodies were unable to bind to gp120 or to neutralize the virus.^{27–31} Strategies that are not based on synthetic chemistry have also been proposed: Man₈-reach mutant strains of a yeast glycoprotein elicited mannose-specific gp120-binding antibodies that anyway were practically unable to neutralize the virus,^{32,33} unless virions forced to exclusively express high-mannose N-linked glycans were used.³⁴ The difficulty of eliciting high titers of antibodies to the 2G12 epitope remains a still-open challenge in search for carbohydrate-based vaccines against HIV.

Our group has demonstrated that gold glyconanoparticles (GNPs) (i.e., three-dimensional sugar-coated gold nanoclusters) are multivalent³⁵ and multifunctional³⁶ systems that can be straightforwardly prepared in a controlled way and used to study carbohydrate-based interactions.³⁷ GNPs are water dispersible and nontoxic to different cellular lines and to mice.³⁸ We have recently reported the preparation of multivalent gold nanoparticles coated with sets of different structural motifs of high-

mannose-type glycans of gp120 (*manno*-GNPs).³⁹ We have shown in cellular models that *manno*-GNPs inhibit the DC-SIGN (*dendritic-cell-specific intercellular-adhesion-molecule-grabbing nonintegrin*)-mediated HIV-1 transinfection of T cells⁴⁰ at nanomolar concentrations.⁴¹ The interaction of synthetic oligomannose dendrons with DC-SIGN has been also reported.^{25,42} It is in fact known that the high-mannose clusters of gp120 not only play a crucial role in HIV immunity but are also involved in different steps of viral infection through interaction with dendritic cells.⁴³

We have previously demonstrated that selected *manno*-GNPs are promising HIV prophylactic anti-viral agents.⁴¹ We herein describe the validation of these glyconanoparticles as synthetic mimics of the 2G12 epitope using surface plasmon resonance (SPR) technology and saturation transfer difference (STD) NMR spectroscopy. *manno*-GNPs were able to bind 2G12 and to inhibit 2G12/gp120 binding, proving that the oligomannosides maintain their functionality and enhance their ability to interact with this antibody when clustered onto gold nanoparticles. Depending on the oligomannoside and its density on the gold surface, high levels of affinity were reached. The capability of selected *manno*-GNPs to interfere with the binding of 2G12 with a recombinant virus was evaluated in competition neutralization assays. These results may validate GNPs as tools for developing new strategies in the fight against HIV.

Results and Discussion

Design and synthesis

Gold nanoparticles coated with synthetic (oligo)mannosides were prepared in one step from mixtures of the high-mannose-type oligosaccharide conjugates 23,23'-Dithiobis[N-(ethyl α -D-Manp-(1-2)- α -D-Manp), N'-(3,6,9,12-tetraoxa-tricosanyl)thiourea] (5), 23,23'-Dithiobis[N-(ethyl α -D-Manp-(1-2)- α -D-Manp-(1-2)- α -D-Manp), N'-(3,6,9,12-tetraoxa-tricosanyl)thiourea] (6), 23,23'-Dithiobis[N-(ethyl α -D-Manp-(1-2)- α -D-Manp-(1-2)- α -D-Manp-(1-3)- α -D-Manp), N'-(3,6,9,12-tetraoxa-tricosanyl)thiourea] (7), and 23,23'-Dithiobis [N-[ethyl (bis(α -D-Manp-(1-2)- α -D-Manp-(1-3,6))- α -D-Manp)], N'-(3,6,9,12-tetraoxa-tricosanyl)thiourea] (8) and 5-(thio)pentyl β -D-glucopyranoside (GlcC₅S), as previously described (*manno*-GNPs; Fig. 1).³⁹ In this way, oligomannosides 5–8 were incorporated (in different and defined proportions with respect to the GlcC₅S conjugate) into the same gold nanoparticles, allowing the control of their density loading. Some of the synthetic oligomannosides used in this work have comparable affinities for 2G12 as that of Man₉,^{16,18,20,22,26} for this reason, they were selected for assembling onto the gold nanoplatform.

Table 1. Binding of GNPs ($1 \mu\text{g mL}^{-1}$) and gp120 ($1.6 \mu\text{g mL}^{-1}$) to 2G12

Entry	<i>manno</i> -GNP	Binding (RU) ^a	Mannoside chains ^b	GNP concentration (μM) ^c	Mannoside concentration (μM) ^d
1	D-10	<2	9	0.014	0.13
2	D-50	77	22	0.025	0.55
3	D-100	26	59	0.016	0.94
4	Tri-10	<5	13	0.012	0.16
5	Tri-50	66	62	0.010	0.62
6	Te-10	85	7	0.021	0.15
7	Te-50	113	56	0.008	0.45
8	P-10	<5	5	0.017	0.09
9	P-50	39	28	0.010	0.28
10	gp120	20 ^e	— ^f	0.011	—
11	M-100	0	40	0.024	0.96
12	Au-SC ₅ Glc	0	0	0.027	0

^a Taken at 150 s in the association phase of the sensorgrams.

^b Taken from Martínez-Ávila *et al.*³⁹

^c Calculated using the average molecular formulas (see Table S1).

^d Calculated from the number of oligomannosides per GNP (see Table S1).

^e The SPR values of gp120 are not directly comparable with those of *manno*-GNPs: although the molecular weights are in the same ranges (e.g., Te-50 and gp120 have nearly the same molecular weight), the lower SPR response of gp120 with respect to *manno*-GNPs can be due to the gold colloid SPR-enhancing effects.⁴⁴

^f The glycoprotein gp120 used in this work was recently part of an immunogenicity study.⁴⁵ This included a glycan analysis that showed mostly Man₃—but some Man₉—structures. It is assumed that all 23 sites are occupied, and there is no complex glycan from the insect cell source.

The (oligo)mannosides were functionalized with a long amphiphilic linker in order to allow a proper presentation of the antigens, while GlcC₅S, containing a short aliphatic linker, was used as inner component. The aliphatic part of the linkers allows good self-assembled monolayers packaging and confers rigidity to the inner organic shell to protect the gold core, while the external polyether moiety, due to its flexibility upon solvation in water, ensures accessibility to the (oligo)mannosides, assists water solubility, and prevents nonspecific adsorption of proteins.³⁹

The nanometric gold platform is a rigid core that displays a large number of carbohydrates in a three-dimensional arrangement on a reduced surface with a high local concentration of sugars (~100 molecules on a 2-nm-diameter core gold).³⁹ The average number of (oligo)mannosides per GNP and their average molecular weights were calculated from elemental analysis and gold cluster size (1–2 nm, as determined by transmission electron microscopy; see Table S1).

Nanoparticle Au-SC₅Glc that is 100% coated with GlcC₅S and M-100 bearing an α -mannose conjugate functionalized with the same amphiphilic linker as the oligomannosides were used as controls (Fig. 1d).

Studies of *manno*-GNP binding to 2G12 by SPR experiments

SPR was used to study the binding of *manno*-GNPs to 2G12 covalently immobilized on a sensor chip (see Materials and Methods). GNP serial dilutions from $1 \mu\text{g mL}^{-1}$ to $0.03125 \mu\text{g mL}^{-1}$ (six different concentrations) were made to study binding to 2G12 (Figs. S1–S10). The response at 150 s in the

association phase of the sensorgrams using $1 \mu\text{g mL}^{-1}$ *manno*-GNPs, negative controls (M-100 and Au-SC₅Glc), and positive control (gp120)[‡] is reported in Table 1. The sensorgrams of GNPs at this concentration are shown in Fig. 2a. At $1 \mu\text{g mL}^{-1}$, the GNPs coated with 50% dimannoside 5 (D-50) and 100% dimannoside 5 (D-100) showed apparent binding to 2G12 immobilized on the chip surface (Table 1, entries 2–3), while D-10 did not give any apparent response neither at this concentration (entry 1) nor at $10 \mu\text{g mL}^{-1}$ (data not shown). Although it is known that 2G12 needs terminal Man α 1–2Man-linked moieties for effective recognition,^{10,11} synthetic multivalent systems functionalized with the basic Man α 1–2Man α unit have not been tested so far. Our result demonstrates that 2G12 recognizes high-affinity Man α 1–2Man α units when presented in adequate density onto a gold nanocluster.

D-100 gave a response of 26 response units (RU) (Table 1, entry 3), a value that is lower than the one (77 RU) obtained with D-50 (Table 1, entry 2). It has to be considered that the concentration of these GNPs ($1 \mu\text{g mL}^{-1}$) corresponds to a molarity of dimannoside 5 that is much higher for D-100 than for D-50 and D-10 ($0.94 \mu\text{M}$ versus $0.55 \mu\text{M}$ and $0.13 \mu\text{M}$, respectively; see Table 1). A comparison between the response units of *manno*-GNPs at the same concentration of dimannoside ($0.1 \mu\text{M}$) is

[‡] In analogous SPR experiments, a response of around 170RU was found for gp120 (at $5 \mu\text{g mL}^{-1}$, 30s) binding to 2G12 (10,000RU immobilization levels); see Dudkin *et al.*²³ Under our conditions (2G12 at 2600RU immobilization levels), gp120 (at $6.4 \mu\text{g mL}^{-1}$, 150s) gave 56RU.

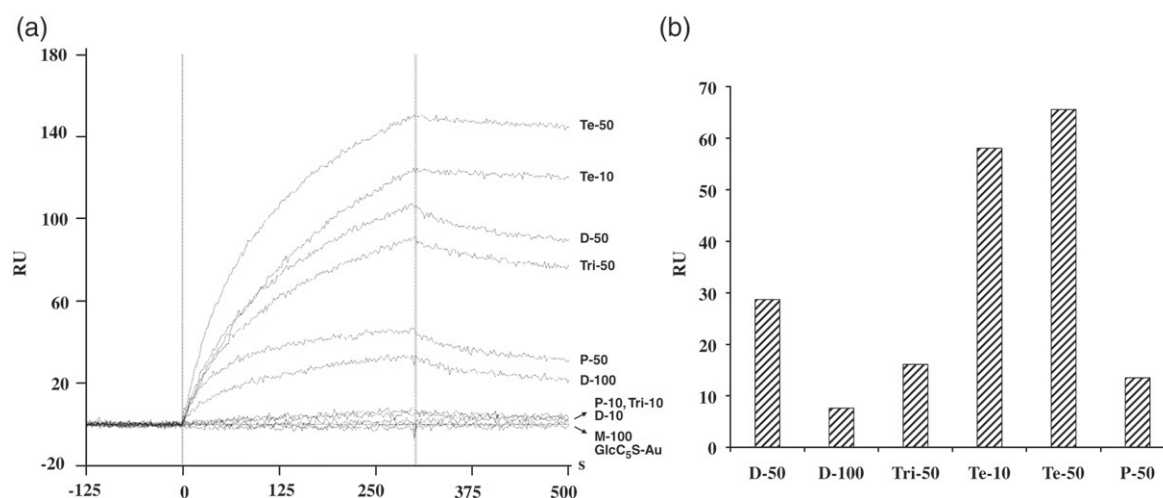


Fig. 2. Biosensor binding analyses. (a) Selected SPR sensorgrams of the binding of *manno*-GNPs at $1 \mu\text{g mL}^{-1}$ passing over a GLC chip channel functionalized with 2600 RU of 2G12. (b) Binding of *manno*-GNPs to 2G12, interpolated at $0.1 \mu\text{M}$ of the corresponding oligomannoside (see Scheme S1).

reported in Fig. 2b and confirms that the affinity for 2G12 is D-50 > D-100. These data show that a 100% coverage of dimannoside 5 on GNPs does not improve the binding affinity, presumably because of steric hindrance. The demonstration that 50% oligomannoside loading is able to achieve efficient recognition by 2G12 opens up the opportunity for further functionalization of the same gold nanocluster with other molecules. Thus, we carried out 2G12 binding studies and 2G12/gp120 inhibition screenings with GNPs functionalized with 50% and 10% densities of oligomannosides (Table 1).

Among the tested *manno*-GNPs with a 10% density of oligomannoside, Te-10 was the only nanoparticle that showed strong binding to 2G12 at $1 \mu\text{g mL}^{-1}$ (85 RU; Table 1, entry 6). This concentration corresponds to a tetramannoside molarity around $0.15 \mu\text{M}$. The bar diagrams in Fig. 2b show a comparison of the binding of GNPs at $0.1 \mu\text{M}$ in terms of the corresponding oligomannoside and confirm that Te-10 has a very high affinity for 2G12. This result is in agreement with previous findings that Man₄ is an excellent epitope mimic,²⁶ and a multivalent display of this antigen results in a high affinity for 2G12^{15,18,19} and efficiency to interfere in the 2G12/gp120 interaction.^{18,24,25} All the 50% density *manno*-GNPs gave an apparent response at $1 \mu\text{g mL}^{-1}$ (~ 0.3 – $0.6 \mu\text{M}$ oligomannoside). Te-10 and Te-50 have the highest and similar binding affinities for 2G12 (Fig. 2a; Table 1, entries 6 and 7, respectively), as confirmed by interpolation at $0.1 \mu\text{M}$ oligomannoside (Fig. 2b; Scheme S1). In all cases, the association and dissociation do not follow ideal Langmuir curves, in agreement with the results obtained for other multivalent systems.^{22–24}

As control experiments, GNPs coated with a 100% density of α -mannose conjugate (M-100; Fig. 1d) and

β -glucose conjugate (Au-SC₅Glc; Fig. 1d) were also tested by SPR experiments. These GNPs gave no response at $1 \mu\text{g mL}^{-1}$ (Fig. 2a; Figs. S1 and S11), demonstrating that neither gold nor the amphiphilic linker or the glucose conjugate is involved in binding to 2G12. The divalent oligomannoside conjugates 5–8 (disulfides) were also submitted to biosensor analysis (see Supplementary Data). Tetramannoside 7 did not give an appreciable response at $1 \mu\text{g mL}^{-1}$ ($0.44 \mu\text{M}$); a response of 76 RU was observed, but only at $10 \mu\text{M}$ ($20 \mu\text{M}$ Man₄) (Figs. S13–S16). Injection of up to $100 \mu\text{M}$ solution of monovalent aminoethyl oligomannosides 2-(α -D-Manp-(1–2)- α -D-Manp)ethanamine (1), 2-(α -D-Manp-(1–2)- α -D-Manp-(1–2)- α -D-Manp)ethanamine (2), 2-(α -D-Manp-(1–2)- α -D-Manp-(1–2)- α -D-Manp-(1–3)- α -D-Manp)ethanamine (3), 2-[bis(α -D-Manp-(1–2)- α -D-Manp-(1–3,6)]- α -D-Manp)ethanamine (4) resulted in no measurable response (data not shown). Although a comparison in terms of response units between gold *manno*-GNPs and the corresponding monovalent compounds 1–4 and divalent compounds 5–8 is not possible due to the colloidal gold enhancement of SPR signal,⁴⁴ these data confirm that multimerization of oligomannosides 5–8 onto gold nanoparticles results in enhanced SPR responses.

Inhibition of 2G12/gp120 interaction by *manno*-GNPs as observed by SPR experiments

After analyzing the binding of *manno*-GNPs to the antibody 2G12, we also studied the interaction of 2G12 with gp120 in competition with the nanoparticles. The biosensor chip was functionalized with gp120, and increasing amounts of the multivalent GNPs, together with a fixed concentration of 2G12, were then coinjected (see Materials

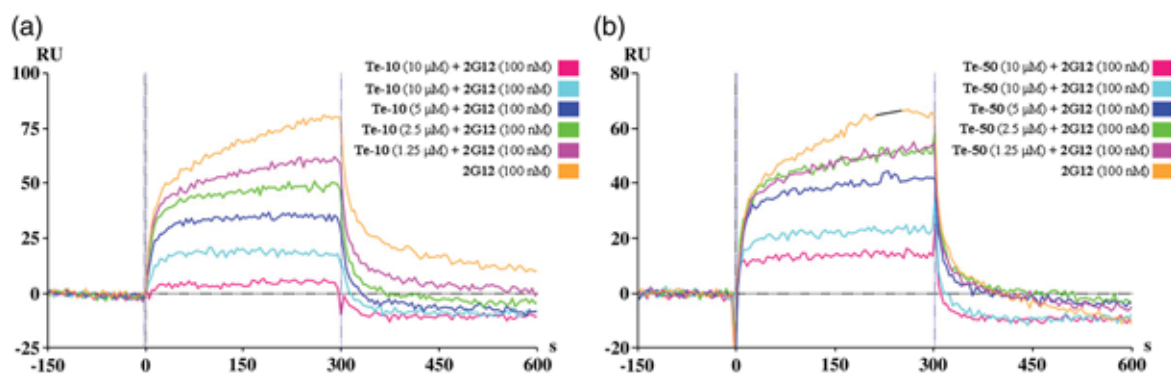


Fig. 3. Sensorgrams of the inhibition of binding between 2G12 (100 nM) and gp120 (immobilized at 8000 RU on the sensor chip) by different concentrations of (a) Te-10 (0 μM , 0.625 μM , 1.25 μM , 2.5 μM , 5 μM , and 10 μM , referring to Man_4) and (b) Te-50 (0 μM , 0.625 μM , 1.25 μM , 2.5 μM , 5 μM , and 10 μM , referring to Man_4). The black line in the orange curve of (b) was obtained using the artifact removal function of the ProteOn Manager Software in order to remove a spike from this sensorgram.

and Methods). In the presence of Te-10 and Te-50, the 2G12 binding response decreased with increasing concentrations of these GNPs, indicating a dose-dependent 2G12 binding inhibition with the gp120-immobilized surface (Fig. 3a and b). From the analysis of concentration–response curves, it was possible to estimate a half-maximal inhibitory concentration (IC_{50}) for Te-10 and Te-50. The IC_{50} values were expressed in terms of the concentrations of GNP and tetramannoside by taking into consideration the average molecular weights of the GNPs and the number of tetramannosides per nanoparticle. These *manno*-GNPs proved to be potent inhibitors of 2G12/gp120 interaction, with IC_{50} values in the submicromolar range in terms of GNP concentrations [$\text{IC}_{50}(\text{Te-10})=17.5 \mu\text{g mL}^{-1}$ (0.37 μM); $\text{IC}_{50}(\text{Te-50})=8.6 \mu\text{g mL}^{-1}$ (0.07 μM)] and in the micromolar range in terms of tetramannoside concentrations [$\text{IC}_{50}(\text{Man}_4)=2.6 \mu\text{M}$ for Te-10 and $\text{IC}_{50}(\text{Man}_4)=3.9 \mu\text{M}$ for Te-50] (Fig. S25). GNP Te-10, which incorporates an average of seven units of tetramannoside conjugate 7, displayed inhibition potency as good as Te-50 (56 units of Compound 7), indicating that a low-grade multimerization of Compound 7 is enough to reach a strong inhibition of the binding of 2G12 to gp120.

The other *manno*-GNPs showed slight effects (D-50 and Tri-50) to moderate effects (D-100 and P-50) at the tested concentrations (up to 20 μM oligomannoside) and were not able to reach levels of inhibition to estimate an IC_{50} (Figs. S19, S20, S22, and S24). GNPs D-10, Tri-10, and P-10 were not able at all to influence the binding of 2G12 to gp120 at the concentrations tested (Figs. S18, S21, and S23). This result was expected from the 2G12 binding data (Fig. 2a; Table 1, entries 1, 4, and 8), and it is further evidence that neither gold nor glucose conjugate is able to interfere with the interaction of 2G12 with gp120.

Titration experiments by NMR techniques

The interactions between *manno*-GNPs and 2G12 were also investigated in isotropic solution by STD-NMR. In this technique,⁴⁶ signals are caused by magnetization transfer from the protons of a large receptor (such as a protein or an antibody) to the protons of the corresponding ligand (a small or medium molecule). During the residence time of the ligand in the binding pocket of the receptor, the protons of the small molecule that make closer contacts with the receptor yield more intense signals than remote protons in the final difference spectrum. Recently, we reported a systematic study of molecular recognition in the solution of synthetic aminoethyl oligomannosides 1–4 (Fig. 1) by 2G12 (large receptor) using STD-NMR.⁴⁷ In that work, the dissociation constants (K_d) in the solution of oligomannosides 1–4 as monovalent ligands were obtained following a protocol based on the initial slopes of the buildup curves of the STD amplification factor against ligand concentration. This protocol has been validated for well-studied systems and has successfully increased the accuracy of K_d determination by STD-NMR.⁴⁸

Although STD-NMR cannot give details of the direct interaction of *manno*-GNPs with 2G12 as both are large molecular systems, affinities can be obtained by indirect measurements through competitive titrations. Competition experiments have been extensively used since the early days of STD-NMR spectroscopy to obtain dissociation constants of unknown ligands from their IC_{50} values obtained after competition with known ligands.⁴⁹ In these experiments, a sample containing a receptor and the known ligand is titrated with the unknown one, and the STD signal of the first one is monitored. The displacement of the first ligand from the receptor binding site translates into a significant

reduction of its STD signal. The decaying curve is fitted to a Cheng–Prusoff equation, which allows us to obtain the K_d value from the experimentally determined IC_{50} .

We have carried out competitive titrations of the previously characterized 2G12/trimannoside **2** system or 2G12/tetramannoside **3** system and the corresponding GNPs (Tri-10, Tri-50, Te-10, and Te-50). In each case, a sample containing 2G12 (micromolar range) and a large excess of ligand **2** or ligand **3** (millimolar range) was titrated by increasing concentrations of a given GNP. We monitored the decay of the STD signals of the monovalent oligomannosides (Fig. S27) while displaced from the antibody binding pockets (see Materials and Methods). Aminoethyl oligomannosides **2** and **3** were selected as monovalent ligands for the inhibition experiments because they displayed a higher affinity for 2G12 ($K_d \sim 400 \mu\text{M}$) than dimannoside **1** and pentamannoside **4** ($K_d > 2 \text{ mM}$).⁴⁷ The high concentrations of Compounds **1** and **4** required to saturate the binding pocket of 2G12 could give rise to nonspecific contacts with the antibody.

Figure 4a shows the decrease in the STD signal intensity of the proton H1 at the nonreducing mannose A (see Fig. 1) of the monovalent ligand **3** after addition of increasing amounts of Te-10 and Te-50. The decrease in the STD signal is related to the efficiency of GNPs in displacing Compound **3** from the binding sites of 2G12. In agreement with the SPR results, Te-10 and Te-50 efficiently inhibited the interaction between Compound **3** and 2G12. At 100 μM , in terms of Man_4 ($268 \mu\text{g mL}^{-1}$ and $340 \mu\text{g mL}^{-1}$ for Te-50 and Te-10, respectively), these GNPs were able to displace from the binding sites up to 60% of Compound **3** used at a concentration of 8 mM.

GNPs Tri-10 and Tri-50 could not displace Compound **2** from 2G12 binding sites even at high concentrations (up to 50 μM Man_3 on GNP) (Fig. 4b). Although both Compound **2** and Compound **3** display the $\text{Man}\alpha 1\text{-}2\text{Man}\alpha 1\text{-}2\text{Man}\alpha$ unit and showed approximately the same affinity for 2G12,⁴⁷ the multimerization of trimannoside conjugate **6** into gold nanoparticles does not lead to a favorable multivalent effect, which, in contrast, has been evidenced by two-dimensional microarrays.¹⁶ However, when Te-10 ($\sim 100 \mu\text{M}$ Man_4) was added to the sample containing the 2G12/**2** complex, Tri-10, and Tri-50, the STD intensity of the proton H1 of mannose A of Compound **2** decreased by up to 50% of the initial value (Fig. S31). This result is analogous to the one obtained with Te-10 to displace Compound **3** (Fig. 4a) and confirms that Te-10 interacts with 2G12 with higher affinity than Tri-10 and Tri-50. The competition between Te-10 and Compound **2** or Compound **3** resulted in comparable STD intensities for the monovalent ligands, confirming that Compounds **2** and **3** have similar affinities for 2G12 in solution and that an $\alpha 1\text{-}3\text{Man}$ extension at the nonreducing end of Compound **2** does not improve the binding affinity for 2G12.⁴⁷ GNPs P-10, P-50, D-10, and D-50 were not able to generate any significant decrease in the STD signals of aminoethyl oligomannosides (Figs. S28 and S30). GNP Au- SC_5Glc , used as negative control, confirmed that neither GlcC_5S nor gold interacts with the antibody (Fig. S29).

The STD data obtained from the titrations experiments with Te-10 and Te-50 were mathematically fitted to a competitive model (Eq. (S1))⁵⁰ derived from the seminal Cheng–Prusoff equation⁵¹ to obtain the inhibition constant (K_i) of the studied

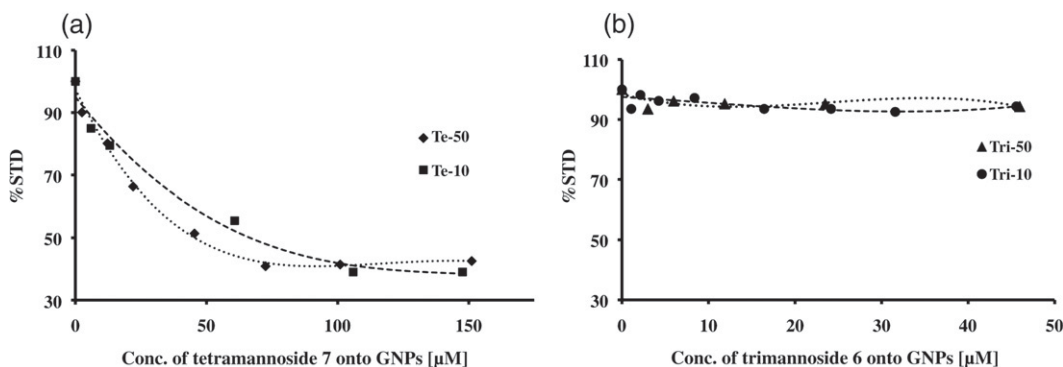


Fig. 4. (a) Competitive titration of 2G12/monovalent aminoethyl tetramannoside **3** complex with Te-10 and Te-50. The decrease in the STD intensity of the anomeric proton H1 of the mannose ring at the nonreducing end of Compound **3** (mannose A) is monitored as a function of the GNP concentration expressed in terms of tetramannoside conjugate **7**. (b) Competitive titration of the 2G12/monovalent aminoethyl trimannoside **2** complex with Tri-10 and Tri-50. The STD intensity of the anomeric proton H1 of the mannose ring at the nonreducing end of Compound **2** (mannose A) is monitored as a function of the GNP concentration expressed in terms of trimannoside conjugate **6**, and no decrease is observable. In these experiments, the concentration of the monovalent aminoethyl oligomannoside **2** or **3** was set to 8 mM. Symbols correspond to experimental data. Lines represent a three-order polynomial fitting (for visualization purposes).

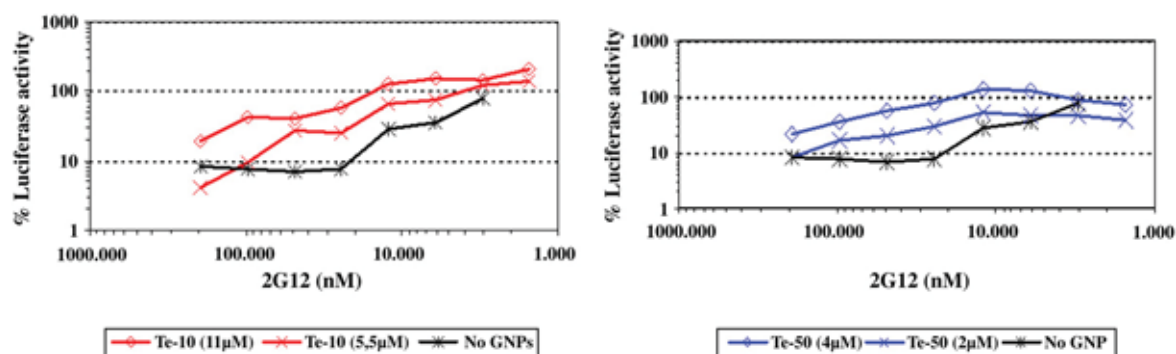


Fig. 5. Inhibition of the 2G12-mediated neutralization of the HIV infection of TZM-bl cells by Te-10 at 11 μM and 5.5 μM , and by Te-50 at 4 μM and 2 μM (see also Fig. S33).

GNP. Inhibition constants of $4.2 \pm 0.5 \mu\text{M}$ and $3.6 \pm 0.6 \mu\text{M}$ (expressed in terms of Man_4) were obtained for Te-10 and Te-50, respectively. The affinity of Compound 3 for 2G12 ($K_d \sim 400 \mu\text{M}$)⁴⁷ was ~ 100 -fold enhanced by the multimerization of Man_4 onto gold nanoparticles. In agreement with the SPR data and with the model of recognition of the antibody 2G12,¹¹ NMR results point out that an increase in the loading of tetramannoside onto GNPs does not necessarily involve an enhancement of the affinity for 2G12.

Effect of selected *manno*-GNPs on HIV-1 neutralization by 2G12

The inhibitory effect of the GNPs coated with tetramannoside conjugate 7 (Te-10 and Te-50) on the 2G12-mediated neutralization of the HIV-1 infection of TZM-bl cells (Table S3 and Fig. S32) was evaluated. Briefly, these GNPs were preincubated with 2G12 and then added to HIV-1 (NL4-3 strain). The GNP–2G12–HIV mixture was then incubated with TZM-bl cells, and neutralization activity was reported as the percentage of luciferase activity measured from cell lysates (see Materials and Methods). Te-10 and Te-50 caused a reproducible inhibition of 2G12 neutralization within the micromolar range in experiments using TZM-bl cells. At 5.5 μM , Te-10 could block the neutralization of the NL4-3 strain by 2G12 (Fig. 5 and Table 2). At this concentration of Te-10, the amount of 2G12 required

to reduce 50% of viral infectivity (IC_{50}) is three times higher (13.3 nM) than the concentration required when no GNP is blocking the antibody (4.3 nM). The highest effect to block 2G12 was observed when a concentration of 11 μM was used. At this concentration of Te-10, the amount of antibody required to inhibit 50% of the infectivity is seven times higher (30 nM). At 1.4 μM (0.06 mg mL^{-1}), Te-10 was not able to increase the IC_{50} of 2G12 (Fig. 5; Table S4). When Te-50 was used, similar results were observed. In this case, the 2G12-blocking effect was even higher, with an IC_{50} 13 times higher when the antibody was preincubated with this GNP at a concentration of 4 μM (Fig. 5 and Table 2).

No significant effect of these GNPs tested on viral infectivity was observed (data not shown). Au- SC_5Glc was also tested as a negative control for nonspecific blocking of 2G12 neutralization. No inhibition of neutralization was observed when Au- SC_5Glc was used even at the highest concentration tested (0.5 mg mL^{-1} , 13.5 μM).

Conclusions

GNPs Te-10 and Te-50 inhibited the binding between 2G12 and gp120 with IC_{50} values in the micromolar range (Man_4 concentration), as measured by SPR technology and STD-NMR spectroscopy. Synthetic oligomannosides, which are known

Table 2. Inhibition of the 2G12-mediated neutralization (IC_{50}) of the HIV infection of TZM-bl cells by Te-10 at 11 μM and 5.5 μM , and by Te-50 at 4 μM and 2 μM

Te-10			IC_{50} (2G12) ^a		Te-50			IC_{50} (2G12) ^a	
mg mL^{-1}	μM	μM (Man_4)	$\mu\text{g mL}^{-1}$	nM	mg mL^{-1}	μM	μM (Man_4)	$\mu\text{g mL}^{-1}$	nM
0.5	11	74	4.5	30	0.5	4	229	9.0	60
0.25	5.5	37	2.0	13.3	0.25	2	114	2.0	13.3
0	0	0	0.65	4.3	0	0	0	0.7	4.7

^a Concentration of 2G12 required to inhibit 50% of viral infectivity.

to interact with 2G12, improve their affinity when tailored into a nanometric gold core. Furthermore, lowering the tetramannoside density onto the gold nanoplatform up to 10% does not affect the high-affinity recognition of these GNPs towards 2G12, as observed by SPR and NMR experiments. On the contrary, GNPs decorated with trimannoside Man₃ or pentamannoside Man₅, which showed slightly lower affinities for 2G12 than Man₄ as free ligands, were not capable of generating such result. The inhibitory effect of Te-10 and Te-50 on the 2G12-mediated neutralization of a replication-competent HIV infection of TZM-bl cells was also demonstrated under conditions in which normal antibodies inhibit infection.

The *in vitro* screening of *manno*-GNPs, which mimic the oligomannoside-rich spikes of a viral envelope, adds information on some key molecular requirements for the exploration of synthetic carbohydrate-based vaccines against HIV. The validation of *manno*-GNPs as efficient 2G12 ligands represents a necessary step prior to increasing the degree of complexity of the gold nanoparticles to obtain improved synthetic anti-HIV agents. Besides the sugars, additional components (adjuvants, immunogenic peptides, and/or anti-HIV molecules) can be inserted into the same nanocluster in order to create synergetic effects. Due to their versatile, polyvalent, and multifunctional characteristics, *manno*-GNPs may supply an alternative to other synthetic systems that have been used for mimicking the gp120 glycan shield and may offer novel strategies against HIV.

Materials and Methods

SPR experiments

SPR analyses were performed at 25 °C using the ProteOn™ XPR36 Protein Interaction Array System (Bio-Rad Laboratories, Inc.) with research-grade GLC sensor chips. 2G12 and gp120 were immobilized using standard amine coupling chemistry, according to the manufacturer's instructions.

Binding studies

2G12 was immobilized on a GLC sensor chip with the ProteOn™ amine coupling kit (for details, see [Supplementary Data](#)) at a level of 2600 RU using phosphate-buffered saline (PBS)-Tween 20 as running buffer [i.e., PBS (10 mM Na₃PO₄ and 150 mM NaCl, pH 7.4) with 0.005% of the surfactant Tween 20]. The carboxylic groups of two different channels on the chip surface were activated by injecting 30 μL (contact time: 60 s; flow rate: 30 μL min⁻¹) of a 1:1 (by volume) mixture of 1-ethyl-3-(3-dimethylaminopropyl)carbodiimide (16 mM) and *N*-hydroxysulfosuccinimide (4 mM). One of the channels was further injected with

120 μL (240 s, 30 μL min⁻¹) of a 2G12 solution in acetate buffer (50 μg mL⁻¹, 10 mM, pH 5.5). Only PBS-Tween 20 was flown into the other channel, which was thus used as reference. The surface of both channels was then saturated by 100 μL of 1 M ethanolamine HCl (200 s, 30 μL min⁻¹). Binding experiments were carried out in tris(hydroxymethyl)aminomethane (Tris)-buffered saline [10 mM Tris and 150 mM NaCl (pH 7.4)] containing 0.005% Tween 20.

The sensorgrams were obtained after injection of the analytes (high-mannose oligosaccharides, *manno*-GNPs, and control GNPs) at 25 °C (flow rate: 30 μL min⁻¹; contact time: 300 s; dissociation: 300 s) by automatic subtraction of the reference surface signal from the 2G12 surface signal. The sensor surface between runs was regenerated with a short pulse (flow rate: 100 μL min⁻¹; contact time: 300 s) of 3.5 M MgCl₂. Glycoprotein gp120 was tested to verify that 2G12 maintains its recognition properties after immobilization. 2G12 activity slightly decreased during the experiments due to the regeneration conditions and the instability of the antibody at 25 °C for long periods.

Inhibition studies

Glycoprotein gp120 was immobilized on a GLC sensor chip at a level of 8000 RU using the methodology described above for 2G12. Tris-buffered saline was used as running buffer. The sensor surface between runs was regenerated with a short pulse of 0.1 M HCl. Antibody 2G12 (final concentration, 100 nM) was preincubated with different concentrations of *manno*-GNPs for ~10 min at 25 °C in Tris-buffered saline, and the mixture was then coinjected into the gp120-functionalized sensor chip (flow rate: 30 μL min⁻¹; contact time: 300 s; dissociation: 300 s). In each experiment, six different concentrations of *manno*-GNPs (including a control channel where 2G12 was added with buffer) were used. During the experiments, gp120 shows a slight loss of activity due to HCl regeneration phases.

NMR experiments

NMR experiments were carried out using a Bruker DRX 500-MHz spectrometer with a broadband inverse probe at 25 °C. STD-NMR experiments were carried out by selective irradiation of the aromatic side chains of 2G12 using a typical train of 50 ms Gaussian pulses, each one⁴⁶ with a total saturation time of 2 s. The absence of aromatic protons in the oligomannoside-containing *manno*-GNPs allowed the selective excitation of antibody ¹H resonances without affecting the signals of any of the ligands (Fig. S26). Blank experiments were carried out in the absence of the antibody 2G12 to confirm that the ligands were not indirectly saturated when the aromatic zone of the spectrum was selectively irradiated.

Monovalent ligands 2 and 3, 2G12, and GNPs were lyophilized twice against D₂O (99.9% purity). The competitive titrations were carried out in 10 mM potassium phosphate buffer (pH 6.7). The samples were prepared with a concentration of monovalent ligand enough to occupy more than 90% of the binding sites of the antibody, fulfilling the condition of competitive inhibition titrations.⁵¹ Thus, the concentrations of

ligands **2** and **3** were set to 8 mM, and the antibody/ligand ratio was 1:320 for each sample. All the tested *manno*-GNPs were used in competitive titrations against Compound **3**, except for Tri-10 and Tri-50, which were used against Compound **2**.

Competition neutralization assay

The ability of selected *manno*-GNPs to block the 2G12 neutralization of HIV-1 infection was tested using a luciferase reporter cell line (TZM-bl).^{52–54} TZM-bl is a HeLa cell line that stably expresses CD4, CCR5, and CXCR4 (viral receptor and coreceptors). These cells also contain separate integrated copies of the luciferase and β -galactosidase genes under the control of the HIV-1 promoter. This neutralization assay has been previously validated by comparison with the current standardized pseudotype assays, and a good agreement was found.^{55,56} GNPs Te-10 and Te-50 were preincubated with 2G12 antibody in triplicate for 30 min at 37 °C. The GNP–2G12 solution was added (1:1, by volume) to the HIV-1 virus (NL4-3 strain), and the mixture was incubated for 1 h at 37 °C. The virus–GNP–antibody mixture was added (1:1, by volume) to 10,000 TZM-bl cells. The plate was then placed in a humidified chamber within a CO₂ incubator at 37 °C. Luciferase activity was measured from cell lysates when levels were sufficiently over background to give reliable measurements (at least 10-fold) using the Luciferase Assay System (Promega) and following the manufacturer's recommendations. Virus equivalent to 4 ng of the p24 capsid protein (quantified by an antigen-capture assay; Innogenetics, Belgium) of the NL4-3 strain of HIV-1 was chosen as the lowest level of viral input sufficient to give a clear luciferase signal within the linear range on day 3 postinfection. Neutralization activity was measured in triplicate and reported as the percentage of luciferase activity compared to the luciferase activity corresponding to the wells with virus and no antibody. The 2G12 concentration required to inhibit 50% of viral infectivity (IC₅₀) was determined for each GNP at different concentrations. Competition was observed when the addition of GNP resulted in a decrease in the neutralizing capacity of the antibody (higher IC₅₀).

Acknowledgements

This work was supported by the Spanish Ministry of Science and Innovation MICINN (grant CTQ2008-04638/BQU), the European Union (CHAARM grant Health-F3-2009-242135), and the Department of Industry of the Basque Country (grant ETOR-TEK2009). TZM-bl was obtained from Dr. John C. Kappes, Dr. Xiaoyun Wu, and Tranzyme, Inc., through the National Institutes of Health AIDS Research and Reference Reagent Program, Division of AIDS, National Institute of Allergy and Infectious Diseases, National Institutes of Health. HIV-1 gp120 mAb 2G12 was kindly supplied by Dr. D. Katinger

(Polymun Scientific, Vienna, Austria). Recombinant gp120 from the HIV-1 CN54 clone (repository reference ARP683) was obtained from the Program EVA Center for AIDS Reagents, National Institute for Biological Standards and Control, UK (supported by the EC FP6/7 Europrise Network of Excellence, the AVIP and NGIN consortia, and the Bill and Melinda Gates GHRC-CAVD Project), and was donated by Prof. Ian Jones (Reading University, UK). Prof. Ian Jones is also acknowledged for the information on HIV-1 gp120 used in this work. J.A. acknowledges financial support from the Ministerio de Ciencia e Innovación through the Ramon y Cajal program. E.Y. acknowledges financial support from FIPSE 36780/08.

Supplementary Data

Supplementary data associated with this article can be found, in the online version, at [doi:10.1016/j.jmb.2011.03.042](https://doi.org/10.1016/j.jmb.2011.03.042)

References

1. De Clercq, E. (2010). Antiretroviral drugs. *Curr. Opin. Pharmacol.* **10**, 507–515.
2. Haase, A. T. (2010). Targeting early infection to prevent HIV-1 mucosal transmission. *Nature*, **464**, 217–223.
3. Balzarini, J. & Van Damme, L. (2007). Microbicide drug candidates to prevent HIV infection. *Lancet*, **369**, 787–797.
4. Barouch, D. H. (2008). Challenges in the development of an HIV-1 vaccine. *Nature*, **455**, 613–619.
5. Mizuochi, T., Spellman, M. W., Larkin, M., Solomon, J., Basa, L. J. & Feizi, T. (1988). Carbohydrate structures of the human-immunodeficiency-virus (HIV) recombinant envelope glycoprotein gp120 produced in Chinese-hamster ovary cells. *Biochem. J.* **254**, 599–603.
6. Reitter, J. N., Means, R. E. & Desrosiers, R. C. (1998). A role of carbohydrates in immune evasion in AIDS. *Nat. Med.* **4**, 679–684.
7. Wyatt, R., Kwong, P. D., Desjardins, E., Sweet, R. W., Robinson, J., Hendrickson, W. A. & Sodroski, J. G. (1998). The antigenic structure of the HIV gp120 envelope glycoprotein. *Nature*, **393**, 705–711.
8. Wei, X., Decker, J. M., Wang, S., Hui, H., Kappes, J. C., Wu, X. *et al.* (2003). Antibody neutralization and escape by HIV-1. *Nature*, **422**, 307–312.
9. Trkola, A., Purtscher, M., Muster, T., Ballaun, C., Buchacher, A., Sullivan, N. *et al.* (1996). Human monoclonal antibody 2G12 defines a distinctive neutralization epitope on the gp120 glycoprotein of human immunodeficiency virus type 1. *J. Virol.* **70**, 1100–1108.
10. Scanlan, C. N., Pantophlet, R., Wormald, M. R., Ollmann Saphire, E., Stanfield, R., Wilson, I. A. *et al.* (2002). The broadly neutralizing anti-human immunodeficiency virus type 1 antibody 2G12 recognizes a

- cluster of $\alpha 1 \rightarrow 2$ mannose residues on the outer face of gp120. *J. Virol.* **76**, 7306–7321.
11. Calarese, D. A., Scanlan, C. N., Zwicky, M. B., Deechongkit, S., Mimura, Y., Kunert, R. *et al.* (2003). Antibody domain exchange is an immunological solution to carbohydrate cluster recognition. *Science*, **300**, 2065–2071.
 12. Wang, L. X. (2006). Carbohydrate-based vaccines against HIV/AIDS. In *Carbohydrate Drug Design* (Klyosov, A. A., Witczak, Z. J. & Platt, D., eds), pp. 133–160, ACS Symposium Series, No. 932, Washington, DC, USA.
 13. Pashov, A., Perry, M., Dyar, M., Chow, M. & Kieber-Emmons, T. (2007). Defining carbohydrate antigens as HIV vaccine candidates. *Curr. Pharm. Des.* **13**, 185–201.
 14. Doores, K. J., Bonomelli, C., Harveyc, D. J., Vasiljevic, S., Dwek, R. A., Burton, D. R. *et al.* (2010). Envelope glycans of immunodeficiency virions are almost entirely oligomannose antigens. *Proc. Natl Acad. Sci. USA*, **107**, 13800–13805.
 15. Bryan, M. C., Fazio, F., Lee, H. K., Huang, C. Y., Chang, A., Best, M. D. *et al.* (2004). Covalent display of oligosaccharide arrays in microtiter plates. *J. Am. Chem. Soc.* **126**, 8640–8641.
 16. Adams, E. W., Ratner, D. M., Bokesch, H. R., McMahon, J. B., O'Keefe, B. R. & Seeberger, P. H. (2004). Oligosaccharide and glycoprotein microarrays as tools in HIV glycochemistry: glycan-dependent gp120/protein interactions. *Chem. Biol.* **11**, 875–881.
 17. Blixt, O., Head, S., Mondala, T., Scanlan, C., Huflejt, M. E., Alvarez, R. *et al.* (2004). Printed covalent glycan array for ligand profiling of diverse glycan binding proteins. *Proc. Natl Acad. Sci. USA*, **101**, 17033–17038.
 18. Calarese, D. A., Lee, H. K., Huang, C. Y., Best, M. D., Astronomo, R. D., Stanfield, R. L. *et al.* (2005). Dissection of the carbohydrate specificity of broadly neutralizing anti-HIV-1 antibody 2G12. *Proc. Natl Acad. Sci. USA*, **102**, 13372–13377.
 19. Liang, P. H., Wang, S. K. & Wong, C. H. (2007). Quantitative analysis of carbohydrate–protein interactions using glycan microarrays: determination of surface and solution dissociation constants. *J. Am. Chem. Soc.* **129**, 11177–11184.
 20. Wang, L. X., Ni, J., Singh, S. & Li, H. (2004). Binding of high-mannose-type oligosaccharides and synthetic oligomannose clusters to human antibody 2G12: implications for HIV-1 vaccine design. *Chem. Biol.* **11**, 127–134.
 21. Li, H. & Wang, L. X. (2004). Design and synthesis of a template-assembled oligomannose cluster as an epitope mimic for human HIV-neutralizing antibody 2G12. *Org. Biomol. Chem.* **2**, 483–488.
 22. Dudkin, V. Y., Orlova, M., Geng, X., Mandal, M., Olson, W. C. & Danishefsky, S. J. (2004). Toward fully synthetic carbohydrate-based HIV antigen design: on the critical role of bivalency. *J. Am. Chem. Soc.* **126**, 9560–9562.
 23. Krauss, I. J., Joyce, J. G., Finnefrock, A. C., Song, H. C., Dudkin, V. Y., Geng, X. *et al.* (2007). Fully synthetic carbohydrate HIV antigens designed on the logic of the 2G12 antibody. *J. Am. Chem. Soc.* **129**, 11042–11044.
 24. Wang, J., Li, H., Zou, G. & Wang, L. X. (2007). Novel template-assembled oligosaccharide clusters as epitope mimics for HIV-neutralizing antibody 2G12. Design, synthesis, and antibody binding study. *Org. Biomol. Chem.* **5**, 1529–1540.
 25. Wang, S. K., Liang, P. H., Astronomo, R. D., Hsu, T. L., Hsieh, S. L., Burton, D. R. & Wong, C. H. (2008). Targeting the carbohydrates on HIV-1: interaction of oligomannose dendrons with human monoclonal antibody 2G12 and DC-SIGN. *Proc. Natl Acad. Sci. USA*, **105**, 3690–3695.
 26. Lee, H. K., Scanlan, C. N., Huang, C. Y., Chang, A. Y., Calarese, D. A., Dwek, R. A. *et al.* (2004). Reactivity-based one-pot synthesis of oligomannoses: defining antigens recognized by 2G12, a broadly neutralizing anti-HIV-1 antibody. *Angew. Chem. Int. Ed.* **43**, 1000–1003.
 27. Kabanova, A., Adamo, R., Proietti, D., Berti, F., Tontini, M., Rappuoli, R. & Costantino, P. (2010). Preparation, characterization and immunogenicity of HIV-1 related high-mannose oligosaccharides–CRM₁₉₇ glycoconjugates. *Glycoconjugate J.* **27**, 501–513.
 28. Astronomo, R. D., Kaltgrad, E., Udit, A. K., Wang, S. K., Doores, K. J., Huang, C. Y. *et al.* (2010). Defining criteria for oligomannose immunogens for HIV using icosahedral virus capsid scaffolds. *Chem. Biol.* **17**, 357–370.
 29. Ni, J., Song, H., Wang, Y., Stamatou, N. M. & Wang, L. X. (2006). Toward a carbohydrate-based HIV-1 vaccine: synthesis and immunological studies of oligomannose-containing glycoconjugates. *Bioconjugate Chem.* **17**, 493–500.
 30. Astronomo, R. D., Lee, H. K., Scanlan, C. N., Pantophlet, R., Huang, C. Y., Wilson, I. A. *et al.* (2008). A glycoconjugate antigen based on the recognition motif of a broadly neutralizing human immunodeficiency virus antibody, 2G12, is immunogenic but elicits antibodies unable to bind to the self glycans of gp120. *J. Virol.* **82**, 6359–6368.
 31. Joyce, J. G., Krauss, I. J., Song, H. C., Opalka, D. W., Grimm, K. M., Nahas, D. D. *et al.* (2008). An oligosaccharide-based HIV-1 2G12 mimotope vaccine induces carbohydrate-specific antibodies that fail to neutralize HIV-1 virions. *Proc. Natl Acad. Sci. USA*, **105**, 15684–15689.
 32. Luallen, R. J., Lin, J., Fu, H., Cai, K. K., Agrawal, C., Mboudjeka, I. *et al.* (2008). An engineered *Saccharomyces cerevisiae* strain binds the broadly neutralizing human immunodeficiency virus type 1 antibody 2G12 and elicits mannose-specific gp120-binding antibodies. *J. Virol.* **82**, 6447–6457.
 33. Dunlop, D. C., Bonomelli, C., Mansab, F., Vasiljevic, S., Doores, K. J., Wormald, M. R. *et al.* (2010). Polysaccharide mimicry of the epitope of the broadly neutralizing anti-HIV antibody, 2G12, induces enhanced antibody responses to self oligomannose glycans. *Glycobiology*, **20**, 812–823.
 34. Agrawal-Gamse, C., Luallen, R. J., Liu, B., Fu, H., Lee, F. H., Geng, Y. & Doms, R. W. (2011). Yeast-elicited cross-reactive antibodies to HIV env glycans efficiently neutralize virions expressing exclusively high-mannose N-linked glycans. *J. Virol.* **85**, 470–480.
 35. de La Fuente, J. M., Barrientos, A. G., Rojas, T. C., Rojo, J., Cañada, J., Fernández, A. & Penadés, S.

- (2001). Gold glyconanoparticles as water-soluble polyvalent models to study carbohydrate interactions. *Angew. Chem. Int. Ed. Engl.* **40**, 2257–2261.
36. Barrientos, A. G., de la Fuente, J. M., Rojas, T. C., Fernández, A. & Penadés, S. (2003). Gold glyconanoparticles: synthetic polyvalent ligands mimicking glycolyx-like surfaces as tools for glycobiological studies. *Chem. Eur. J.* **9**, 1909–1921.
37. Marradi, M., Martín-Lomas, M. & Penadés, S. (2010). Glyconanoparticles: polyvalent tools to study carbohydrate-based interactions. *Adv. Carbohydr. Chem. Biochem.* **64**, 211–290.
38. Rojo, J., Diaz, V., de la Fuente, J. M., Segura, I., Barrientos, A. G., Riese, H. H. *et al.* (2004). Gold glyconanoparticles as new tools in antiadhesive therapy. *ChemBioChem*, **5**, 291–297.
39. Martínez-Ávila, O., Hijazi, K., Marradi, M., Clavel, C., Campion, C., Kelly, C. & Penadés, S. (2009). Gold *manno*-glyconanoparticles: multivalent systems to block HIV-1 gp120 binding to the lectin DC-SIGN. *Chem. Eur. J.* **15**, 9874–9888.
40. Geijtenbeek, T. B. H., Kwon, D. S., Torensma, R., van Vliet, S. J., van Duijnhoven, G. C. F., Middel, J. *et al.* (2000). DC-SIGN, a dendritic cell-specific HIV-1-binding protein that enhances trans-infection of T cells. *Cell*, **100**, 587–597.
41. Martínez-Ávila, O., Bedoya, L. M., Marradi, M., Clavel, C., Alcamí, J. & Penadés, S. (2009). Multivalent *manno*-glyconanoparticles inhibit DC-SIGN-mediated HIV-1 trans-infection of human T cells. *ChemBioChem*, **10**, 1806–1809.
42. Sattin, S., Daggetti, A., Thépaut, M., Berzi, A., Sánchez-Navarro, M., Tabarani, G. *et al.* (2010). Inhibition of DC-SIGN-mediated HIV infection by a linear trimannoside mimic in a tetravalent presentation. *Chem. Biol.* **5**, 301–312.
43. Feinberg, H., Mitchell, D. A., Drickamer, K. & Weis, W. I. (2001). Structural basis for selective recognition of oligosaccharides by DC-SIGN and DC-SIGNR. *Science*, **294**, 2163–2166.
44. He, L., Musick, M. D., Nicewarner, S. R., Salinas, F. G., Benkovic, S. J., Natan, M. J. & Keating, C. D. (2000). Colloidal Au-enhanced surface plasmon resonance for ultrasensitive detection of DNA hybridization. *J. Am. Chem. Soc.* **122**, 9071–9077.
45. Kong, L., Sheppard, N. C., Stewart-Jones, G. B. E., Robson, C. L., Chen, H., Xu, X. *et al.* (2010). Expression-system-dependent modulation of HIV-1 envelope glycoprotein antigenicity and immunogenicity. *J. Mol. Biol.* **403**, 131–147.
46. Mayer, M. & Meyer, B. (1999). Characterization of ligand binding by saturation transfer difference NMR spectra. *Angew. Chem. Int. Ed.* **38**, 1784–1788.
47. Enríquez-Navas, P. M., Marradi, M., Padro, D., Angulo, J. & Penadés, S. (2011). A solution NMR study of the interactions of oligomannosides and the anti-HIV-1 2G12 antibody reveals distinct binding modes for branched ligands. *Chem. Eur. J.* **17**, 1369–1707.
48. Angulo, J., Enríquez-Navas, P. M. & Nieto, P. M. (2010). Ligand–receptor binding affinities from saturation transfer difference (STD) NMR spectroscopy: the binding isotherm of STD initial growth rates. *Chem. Eur. J.* **16**, 7803–7812.
49. Mayer, M. & Meyer, B. (2001). Group epitope mapping by saturation transfer difference NMR to identify segments of a ligand in direct contact with a protein receptor. *J. Am. Chem. Soc.* **123**, 6108–6117.
50. Benie, A. J., Moser, R., Bäuml, E., Blaas, D. & Peters, T. (2003). Virus–ligand interactions: identification and characterization of ligand binding by NMR spectroscopy. *J. Am. Chem. Soc.* **125**, 14–15.
51. Cheng, Y. C. & Prusoff, W. H. (1973). Relationship between the inhibition constant (K_i) and the concentration of inhibitor which causes 50 per cent inhibition (I_{50}) of an enzymatic reaction. *Biochem. Pharmacol.* **22**, 3099–3108.
52. Derdeyn, C. A., Decker, J. M., Sfakianos, J. N., Wu, X., O'Brien, W. A., Ratner, L. *et al.* (2000). Sensitivity of human immunodeficiency virus type 1 to the fusion inhibitor T-20 is modulated by coreceptor specificity defined by the V3 loop of gp120. *J. Virol.* **74**, 8358–8367.
53. Platt, E. J., Wehrly, K., Kuhmann, S. E., Chesebro, B. & Kabat, D. (1998). Effects of CCR5 and CD4 cell surface concentrations on infections by macrophagetropic isolates of human immunodeficiency virus type 1. *J. Virol.* **72**, 2855–2864.
54. Wei, X., Decker, J. M., Liu, H., Zhang, Z., Arani, R. B., Kilby, J. M. *et al.* (2002). Emergence of resistant human immunodeficiency virus type 1 in patients receiving fusion inhibitor (T-20) monotherapy. *Antimicrob. Agents Chemother.* **46**, 1896–1905.
55. Fenyo, E. M., Heath, A., Dispinseri, S., Holmes, H., Lusso, P., Zolla-Pazner, S. *et al.* (2009). International network for comparison of HIV neutralization assays: the NeutNet report. *PLoS One*, **4**, e4505.
56. Garcia-Perez, J., Sanchez-Palomino, S., Perez-Olmeda, M., Fernandez, B. & Alcamí, J. (2007). A new strategy based on recombinant viruses as a tool for assessing drug susceptibility of human immunodeficiency virus type 1. *J. Med. Virol.* **79**, 127–137.

STD NMR Study of the Interactions between Antibody 2G12 and Synthetic Oligomannosides that Mimic Selected Branches of gp120 Glycans

Pedro M. Enríquez-Navas,^[a, d] Fabrizio Chiodo,^[a] Marco Marradi,^[a, b] Jesús Angulo,^{*,[c]} and Soledad Penadés^[a, b]

The human immunodeficiency virus type-1 (HIV-1) is able to shield immunogenic peptide epitopes on its envelope spike (a trimer of two glycoproteins, gp120 and gp41) by presenting numerous host-derived N-linked glycans. Nevertheless, broadly neutralizing antibodies against gp120 and gp41 have been isolated from HIV-1-infected patients and provide protection against viral challenge in animal models. Among these, the monoclonal antibody 2G12 binds to clusters of high-mannose-type glycans that are present on the surface of gp120. These types of glycans have thus been envisaged as target structures for the development of synthetic agents capable of eliciting 2G12-like antibodies. High-resolution structural studies of 2G12 and chemically defined glycan-type ligands, including crystallographic data, have been performed to gain an insight into this interaction. Further studies are still required to design a carbo-

hydrate-based vaccine for HIV. Our previous NMR studies highlighted different recognition modes of two branched synthetic oligosaccharides, a penta- and a heptamannoside, by 2G12 in solution. In order to clarify the underlying structural reasons for such different behaviors, we have herein “dissected” the branches into the linear tri- and tetra- oligomannosides by chemical synthesis and studied their interactions with 2G12 in solution by saturation transfer difference (STD) NMR spectroscopy. The results confirm the distinct preferences of 2G12 for the studied branches and afford explanations for the observed differences. This study provides important structural information for further ligand optimizations. Possible effects of structural modifications on the solvent-exposed end of the ligands are also discussed.

Introduction

The development of an efficient vaccine against pandemic acquired immunodeficiency syndrome (AIDS) caused by human immunodeficiency virus (HIV) is one of the unaccomplished challenges of the last decades.^[1] Some HIV-infected individuals produce potent broadly neutralizing antibodies^[2] that are able to provide protection against viral challenge in animal models.^[3] Investigations of these types of antibodies can aid in the rational design of a vaccine by affording key structural information.^[3,4] Among these anti-HIV antibodies, 2G12 recognizes a cluster of high-mannose N-glycans present on the “silent face” of the viral envelope glycoprotein gp120.^[5] Crystal structures of complexes of 2G12 with the dimannoside Man α 1–2Man and with the triantennary undecasaccharide Man $_9$ GlcNAc $_2$ (Scheme 1) showed that the antibody has a peculiar shape in which two fragment antigen binding (Fab) sections are exchanged.^[6] On the basis of these data, a molecular model for the 2G12–gp120 interaction was proposed in which up to three separate Man $_9$ GlcNAc $_2$ glycans mediate the binding of 2G12 to gp120.^[6] The terminal Man α 1–2Man disaccharide moiety at the non-reducing end of the D1 arm of Man $_9$ GlcNAc $_2$ (Scheme 1) is responsible for most of the contacts with the Fab.^[7] Nevertheless, the undecasaccharide Man $_9$ GlcNAc $_2$ inhibits binding of 2G12 to gp120 ~50-fold better than the disaccharide Man α 1–2Man.^[7]

The multivalent nature of the 2G12–oligomannosides interactions, and the importance of the type of mannoside frag-

ments involved, have pushed several groups to multimerize Man $_9$ GlcNAc $_2$ and/or its constituent arms onto different scaffolds in order to mimic the multivalent presentation of the 2G12 epitope on gp120.^[8,9] In some of these works, in vivo immunization experiments were carried out in order to evoke 2G12-like antibodies. However, either ineffective or low titers of gp120-binding antibodies were raised, and they were unable to neutralize the virus.^[8,9–15] These results highlight that

[a] Dr. P. M. Enríquez-Navas,[†] F. Chiodo,[†] Dr. M. Marradi, Prof. Dr. S. Penadés
Laboratory of GlycoNanotechnology
Biofunctional Nanomaterial Unit, CIC biomaGUNE
Paseo de Miramón 182, 20009 San Sebastián (Spain)

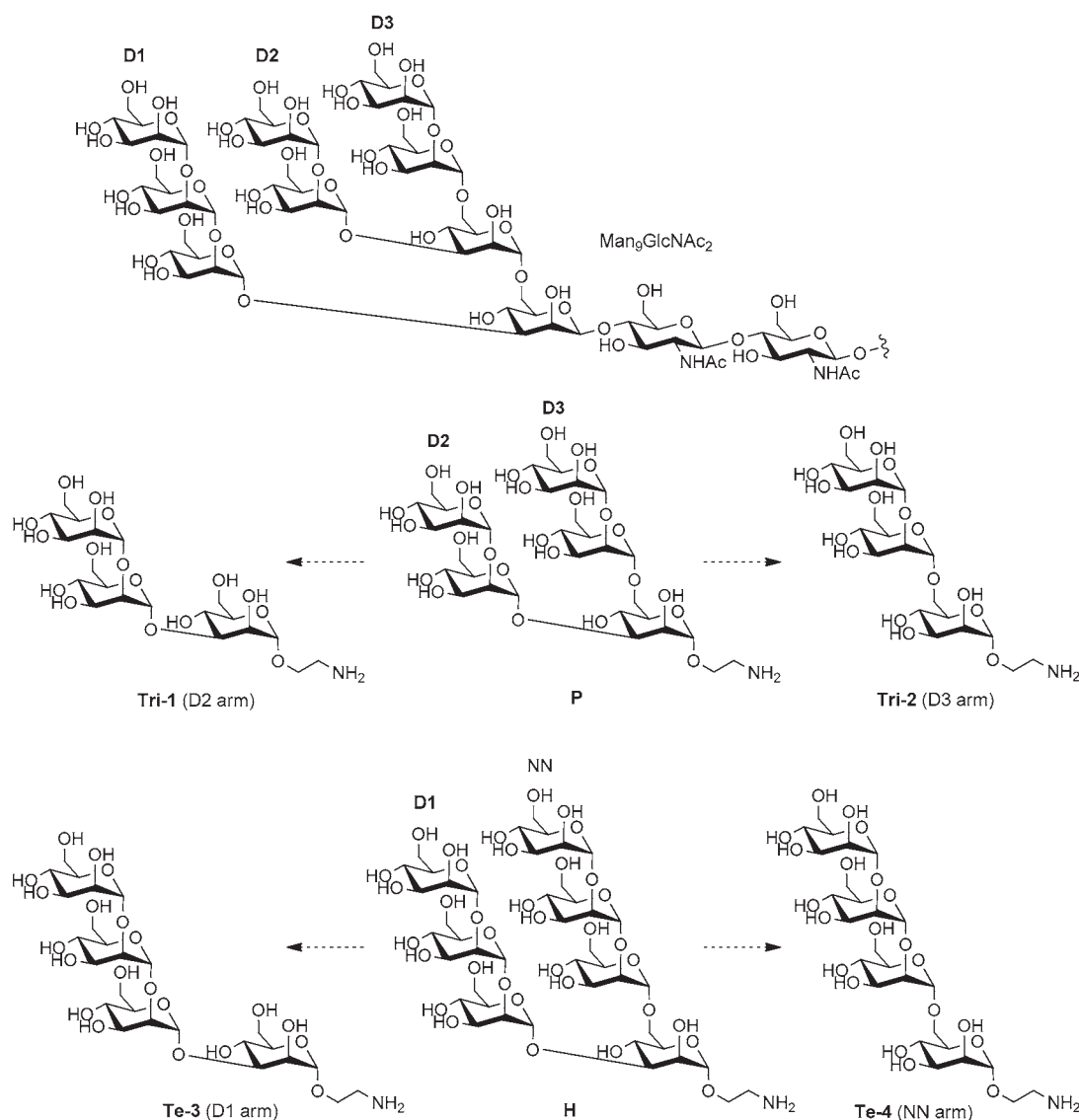
[b] Dr. M. Marradi, Prof. Dr. S. Penadés
Biomedical Research Networking Center in Bioengineering, Biomaterials
and Nanomedicine (CIBER-BBN)
Paseo Miramón 182, 20009 San Sebastián (Spain)

[c] Dr. J. Angulo
Department of Bioorganic Chemistry
Instituto de Investigaciones Químicas (CSIC-US)
Américo Vespucio, 49, 41092 Sevilla (Spain)
E-mail: jesus@iiq.csic.es

[d] Dr. P. M. Enríquez-Navas[†]
Present address: Nanobiotechnology Research Section
Andalusian Centre for Nanomedicine and Biotechnology (BIONAND)
Málaga (Spain)

[*] These authors contributed equally to this work.

Supporting information for this article is available on the WWW under <http://dx.doi.org/10.1002/cbic.201200119>.



Scheme 1. Structures of the undecasaccharide $\text{Man}_9\text{GlcNAc}_2$, representative of the high-mannose glycans present at the surface of the HIV glycoprotein gp120, the branched pentamannoside **P**, the non-natural heptamannoside **H**, trimannosides **Tri-1** and **Tri-2**, and tetramannosides **Te-3** and **Te-4**. **Tri-1** mimics the D2 arm of Man_9 , **Tri-2** the D3 arm, **Te-3** the D1 arm, and **Te-4** is a non-natural (NN) branch.

important structural details are still lacking for a full understanding of the molecular basis of the 2G12–gp120 interaction.^[16]

Recently, we reported an NMR study in solution of the interactions between structural motifs of $\text{Man}_9\text{GlcNAc}_2$ and the antibody 2G12.^[17] Saturation transfer difference (STD) NMR^[18a] and transferred NOE^[18b] experiments revealed that the branched pentamannoside **P** (D2 + D3 arms, Scheme 1) shows similar affinity for 2G12 as the corresponding monovalent $\text{Man}\alpha 1\text{--}2\text{Man}$ moiety, while the non-natural branched heptamannoside **H** shows less affinity than $\text{Man}\alpha 1\text{--}2\text{Man}\alpha 1\text{--}2\text{Man}$, despite the divalent presentation of this latter motif (Scheme 1).^[17] Additionally, these studies unveiled distinct binding modes for the two branched oligomannosides **P** and **H**. Pentamannoside **P** shows two alternate binding modes for the same binding site of 2G12 involving both the D3-like and the D2-like arms. In contrast, the heptamannoside **H** preferentially interacts with

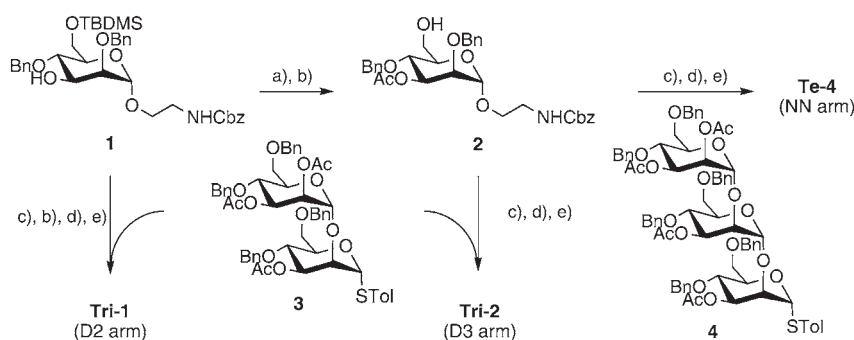
2G12 through the structural motif $\text{Man}\alpha 1\text{--}2\text{Man}\alpha 1\text{--}2\text{Man}$ at position 3 of the mannose at the reducing end (i.e., the D1-like arm), although this motif is repeated at position 6 (the non-natural arm, Scheme 1).^[17]

In order to gain a deeper insight into the interactions of the oligomannosides **P** and **H** with the human monoclonal antibody 2G12, we have synthetically “dissected” these Man_9 -like branched oligomannosides onto their constituent arms (Scheme 1). The interactions of the aminoethyl α -oligomannosides **Tri-1**, **Tri-2**, and **Te-4** with 2G12, as well as the competition between ligand **Te-4** and the previously studied **Te-3**,^[17] were investigated in isotropic solution by STD NMR spectroscopy. The present NMR study affords further structural information on the molecular recognition processes underlying the broad neutralization of the virus by 2G12 that may contribute to the design of an appropriate synthetic epitope for a carbohydrate-based vaccine against HIV.

Results

Synthesis of oligomannosides

The aminoethyl α -oligomannosides **Tri-1**, **Tri-2**, and **Te-4** were prepared by modification of the methodology proposed by Wong (Scheme 2).^[19] The donor disaccharide **3** was coupled to



Scheme 2. Reagents and conditions for the synthesis of **Tri-1**, **Tri-2**, and **Te-4**: a) Ac_2O , DMAP, Py, RT, 12 h, 93%; b) TBAF, THF, RT, 15 h; c) NIS, TFOH, CH_2Cl_2 dry, -10°C , 2 h; d) MeONa, MeOH, RT, 48 h; e) H_2/Pd , MeOH, RT, 12 h.

acceptor **1** and then deprotected by sequential methanolysis and Pd/C-catalyzed hydrogenation to afford trimannoside **Tri-1** (D2 arm) in 68% overall yield. In order to synthesize the trimannoside **Tri-2** (D3 arm) and the non-natural **Te-4** (NN arm), acceptor **1** was acetylated at position 3 (93% yield) and then desilylated at position 6 (67% yield) to obtain acceptor **2** with overall 62% yield. Donors **3** and **4** were coupled to acceptor **2** and then deprotected to give trimannoside **Tri-2** (D3 arm) and tetramannoside **Te-4** (NN arm) in 40 and 47% overall yields, respectively. Details of the synthesis (Scheme 2) are given in the Supporting Information.

STD NMR experiments

In STD NMR spectroscopy, protein–ligand binding events lead to magnetization transfer from the protons of the large receptor (antibody 2G12, in this case) to the protons of the corresponding ligand (the oligomannosides). The protons of the small molecule in close contact with the receptor in the bound state yield intense signals in the final difference spectrum, whereas remote protons show lower or null STD intensities. In this way, the analysis of STD NMR intensities of the proton signals allows the identification of the ligand-binding epitope. In addition, as the magnitude of the STD signal is proportional to the concentration of complex in solution, it is possible to evaluate the affinity of each ligand from titration experiments after appropriate treatment.^[20]

Addition of increasing concentrations of the oligomannosides **Tri-1**, **Tri-2** or **Te-4** to a solution of 2G12 led to the observation of STD NMR signals in the corresponding difference spectra. For each different antibody-to-ligand ratio used in the various samples (1:11 to 1:200), an STD build-up curve was obtained by increasing the saturation time (from 0.5 to 3 s). Next,

the experimental data were fitted to a mono-exponential asymptotic function:

$$\text{STD}(t_{\text{sat}}) = \text{STD}_{\text{max}}[1 - \exp(-k_{\text{sat}}t_{\text{sat}})] \quad (1)$$

From Equation (1), we obtained the initial slope of each build-up curve (STD_0) by the product: $k_{\text{sat}} \cdot \text{STD}_{\text{max}}$. We used the initial slopes of the STD build-up curves, instead of the STD intensities themselves, to avoid some of the factors that can affect proper determination of both the ligand-binding epitopes and the dissociation constants (K_D) when using STD NMR spectroscopy.^[20,21] The ligand binding epitopes reflect the main contacts of the ligand with the antibody in the bound state and are obtained by normalizing the STD_0 values for each ligand against the largest STD value, which is arbitrarily assigned as 100%.

Figure 1 shows expansions of the anomeric region (H1 protons) of the ^1H STD NMR spectra of **Tri-1** in the presence of 2G12 at different saturation times (from 0.5 to 3 s). As saturation time increases, saturation transfer of the anomeric proton at the non-reducing end is higher than the others ($\text{H1-A} > \text{H1-B} \gg \text{H1-C}$). In order to obtain the best signal-to-noise ratio in the STD spectra, the binding epitopes of the oligomannosides were obtained at the largest antibody-to-ligand ratios reached in the experimental setup (1:200; $25 \mu\text{M}$ 2G12). Figure 2 shows the spectra and Scheme 3 the relative percentages of STD for **Tri-1**, **Tri-2**, and **Te-4**, respectively. The corresponding STD build-up curves (i.e., reporting the experimental values at different saturation times) are in the Supporting Information.

In particular, STD intensities of the H1 protons at the non-reducing end rings (mannoses A, E, and Z for **Tri-1**, **Tri-2**, and **Te-4**, respectively, see Figure 2) are stronger than for the other H1 protons, indicating a similar binding mode. The same distribution of STD intensities along the different rings of the ligands was also observed in all other protons, whose STD signals could be unambiguously integrated (Figures S1–S3), showing monotonically decreasing STD values from the non-reducing to the reducing end of the oligosaccharide chain. For the sake of simplicity, the analysis here focuses on the anomeric protons, as they show good chemical shift dispersion in the spectra (Figure 1).

In order to obtain the affinities of the ligands towards 2G12, the dissociation constants (K_D) of **Tri-1**, **Tri-2**, and **Te-4** were experimentally determined by using the recently developed STD-AF initial slopes approach.^[20] By using the so-called STD amplification factor^{18b} at saturation time zero (STD-AF_0) versus the ligand concentration, and by fitting the experimental values to a Langmuir equation, it was possible to obtain the K_D . The results are reported in Table 1. For the sake of comparison, the



Figure 1. Anomeric region of the ^1H STD NMR spectra at increasing saturation times for a sample containing **Tri-1** (residues A–C, named in Scheme 3) in the presence of 2G12 (antibody-to-ligand ratio 1:200; antibody concentration $25\ \mu\text{M}$). The bottom spectrum is the reference ^1H NMR of **Tri-1** in the presence of 2G12.

K_D of **Te-3**, **P**, and **H**, determined in a previous work,^[17] are also shown in Table 1.

STD NMR competition experiments

The significant differences in affinities towards 2G12 between the tetramannosides **Te-3** and **Te-4** (Table 1), which are structural analogues (Scheme 1), prompted us to carry out a competition STD NMR experiment between both oligomannosides in the presence of 2G12. **Te-4** was added to a sample containing 2G12 ($25\ \mu\text{M}$) and **Te-3** ($1\ \text{mM}$), obtaining a final sample in which both ligands were in equimolar conditions. If competition for the ligand binding site occurs between these oligomannosides, **Te-4** should displace **Te-3** from the 2G12 binding pocket but, due to the higher affinity of **Te-3** towards the antibody, this displacement should be of less than 50% of the original fraction of **Te-3** bound to 2G12.

Table 1. Dissociation constants of the interactions of **Tri-1**, **Tri-2**, and **Te-4** with antibody 2G12. Affinities were calculated by using the STD-AF initial slopes approach.^[20]

Ligand	Tri-1	Tri-2	Te-4	Te-3 ^[a]	P ^[a]	H ^[a]
K_D [mM]	$3.0(\pm 1)$	$3.8(\pm 0.3)$	$2.2(\pm 0.3)$	$0.4(\pm 0.1)$	$3.0(\pm 0.2)$	$0.8(\pm 0.08)$
[a] Obtained from ref. [17].						

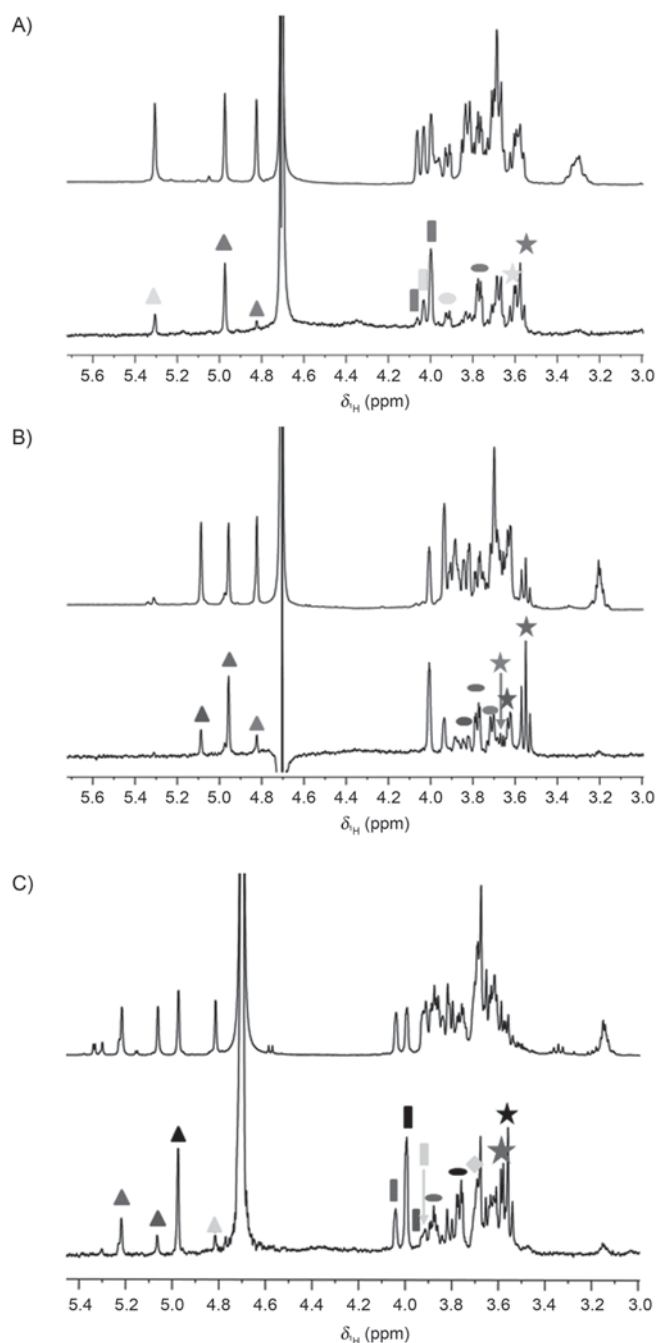
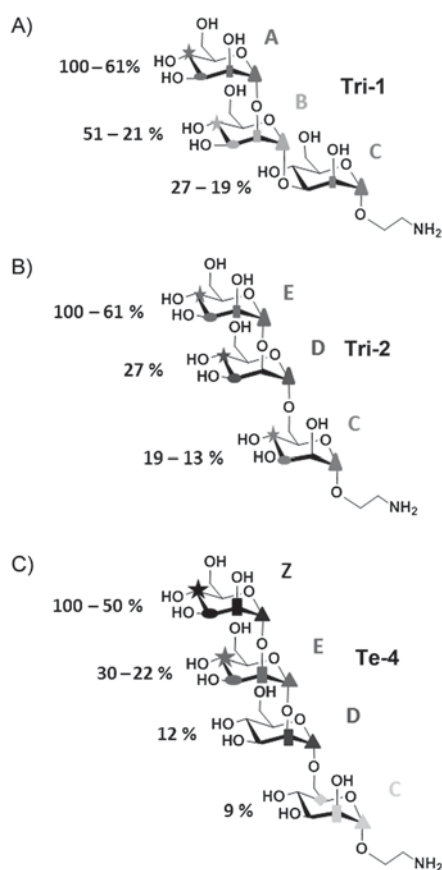


Figure 2. ^1H NMR (top) of aminoethyl oligomannosides A) **Tri-1**, B) **Tri-2**, and C) **Te-4**, and corresponding ^1H STD NMR spectra (bottom) obtained following their addition to 2G12 solutions. Symbols on the proton signals correspond to those on the structures in Scheme 3.

The STD NMR competition experiment showed reduction in the intensities of the STD signals of **Te-3** upon addition of the other ligand, but this reduction was significantly less than half of the original STD intensities. Moreover, in a sample contain-



Scheme 3. Schematic representations of the oligomannosides with the binding epitopes expressed as percentage ranges per mannosyl moiety (relative STD values). Symbols on the chemical structures correspond to the proton signals that were unambiguously integrated into the NMR spectra.

ing equimolar concentrations of both ligands, the STD signals corresponding to protons of **Te-3** were higher in intensity (Figure 3). As both ligands, **Te-3** and **Te-4**, are recognized by 2G12 in the same binding mode (Figures 3 and 4; cf. Figure 1 in ref. [17]), the observed differences in intensities are direct indications of their differences in affinities, confirming that **Te-3** is preferentially recognized by the antibody 2G12. This result is in good agreement with the previous study of the interaction between the antibody and the whole branched heptamannoside **H**, in which it was shown that the antibody preferentially recognizes the D1-like ramification (mimicked by **Te-3**).

Glycan microarray analysis

The synthesized oligomannosides **Tri-1**, **Tri-2**, **Te-3**, and **Te-4** were printed on a microarray slide at different concentrations (25, 50, 100, and 200 μM) following a reported methodology.^[22] The maintenance of glycan functionality after printing was checked by using fluorescently labeled ConA (Supporting Information). Solutions (100 μL) of fluorescently-labeled 2G12 (2G12*; 25 $\mu\text{g mL}^{-1}$) were incubated in the dark over each microarray for 1 h at room temperature following a reported protocol.^[23] Figure 4 shows that 2G12 (25 $\mu\text{g mL}^{-1}$) interacts with **Te-3** at all tested concentrations, while no interaction was de-

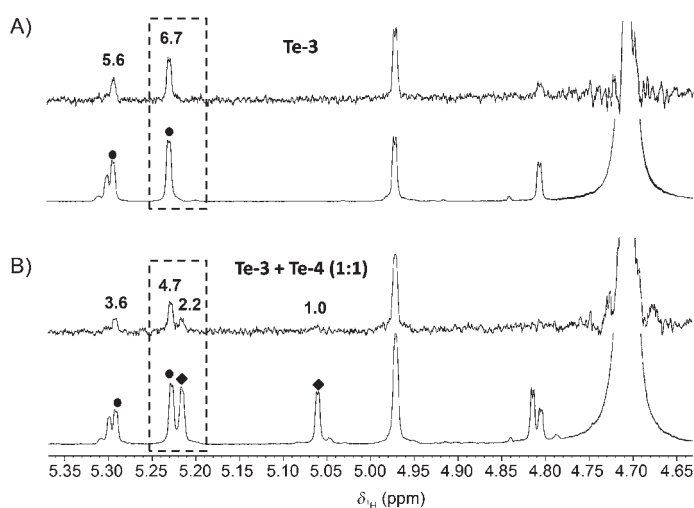


Figure 3. Competition between **Te-3** and **Te-4** for 2G12 antibody. A) ^1H NMR spectrum (bottom) and STD NMR spectrum (top) of 2G12 and **Te-3** (circles, anomeric protons). B) ^1H NMR spectrum (bottom) and STD NMR spectrum (top) of a sample of 2G12 and equimolar concentrations of **Te-3** (●) and **Te-4** (◆). Dashed boxes highlight key signals confirming that 2G12 preferentially recognizes **Te-3** in the presence of **Te-4**.

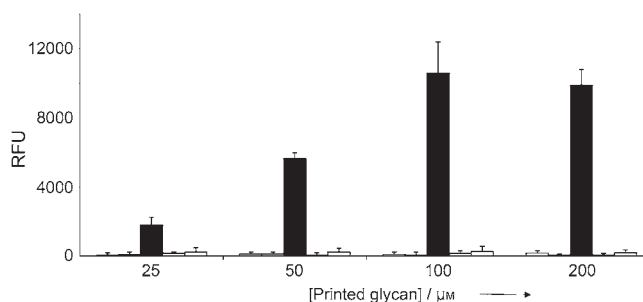


Figure 4. Microarray analysis of the interaction between fluorescently labeled 2G12 (25 $\mu\text{g mL}^{-1}$) and printed **Tri-1** (□), **Tri-2** (□), **Te-3** (■), **Te-4** (□), and the aminoethyl β -glucoside control (□). Histograms represent average relative fluorescent units (RFU) for eight replicated spots.

tected with **Tri-1**, **Tri-2**, and **Te-4**. An aminoethyl β -glucoside was used as negative control.

Discussion

The broadly neutralizing human anti-HIV-1 antibody 2G12 recognizes a cluster of $\alpha 1,2$ -linked mannose residues on the outer face of the viral glycoprotein gp120.^[24] A previous NMR study showed that the minimum epitope with good affinity for 2G12 in solution is the trisaccharide sequence $\text{Man}\alpha 1\text{-}2\text{Man}\alpha 1\text{-}2\text{Man}$ present on the D1 arm of the $\text{Man}_9(\text{GlcNAc})_2$ glycan of gp120.^[17] Very recently, Doores et al. showed that HIV-1 native envelope gp120 trimers mainly display $\text{Man}\alpha 1\text{-}2\text{Man}$ -terminating N-glycans ($\text{Man}_{6-9}(\text{GlcNAc})_2$) of the type recognized by 2G12 (high-mannose glycans) and an almost complete lack of complex-type glycans, in contrast to recombinant gp120.^[25]

We attempted to understand the importance of each branch present in the high-mannose $\text{Man}_9(\text{GlcNAc})_2$ structure for the interaction with 2G12, with the aim of gaining a better com-

prehension of the molecular basis of the 2G12–gp120 interactions. We used the ligand-based spectroscopic technique STD NMR to study the interactions in solution between the 2G12 antibody and oligomannosides **Tri-1**, **Tri-2**, **Te-3**, and **Te-4**. These oligomannosides mimic the arms of the branched ligands **P** and **H** (Scheme 1), which were studied previously.^[17] STD NMR build-up curves allowed the determination of their binding epitopes and, following a recently developed protocol,^[20] it was possible to obtain the dissociation constant (K_D) of each oligomannoside. We compared the affinities and epitopes of the branched oligomannosides **P** and **H**,^[17] with those of their constitutive linear oligomannosides (**P** was dissected into **Tri-1** and **Tri-2**, and **H** into **Te-3** and **Te-4**, Scheme 1).

Trimannosides **Tri-1** and **Tri-2** of pentamannoside **P**

Both trimannosides **Tri-1** and **Tri-2** (D2- and D3-like branches of pentamannoside **P**) interact with 2G12 by the terminal moiety Man α 1–2Man at the non-reducing end (Scheme 3) with similar binding modes. This is in very good agreement with the previous NMR study regarding 2G12 recognition of the entire pentamannoside **P** (K_D value of 3 mM). The antibody recognizes both **P** branches in alternate binding modes in the same binding pocket with a slight preference for the D3-type branch (Scheme 1).^[17] In the case of the trisaccharides (**Tri-1** and **Tri-2**) mimicking the individual ramifications of **P**, 2G12 recognizes the D2-like trimannoside **Tri-1** with similar affinity to the D3-like **Tri-2** (Table 1). The affinities of **Tri-1** and **Tri-2** are on the same order of magnitude as that of the entire pentamannoside **P** (Table 1),^[17] confirming that the repetition of Man α 1–2Man motifs in the structure of the pentamannoside **P** does not improve the affinity of this ligand towards the antibody 2G12.

Tetramannosides **Te-3** and **Te-4** of the non-natural heptamannoside **H**

STD NMR data confirm that tetramannoside **Te-4** is recognized by the antibody 2G12 primarily through the non-reducing end (mannose Z, Scheme 3), while the reducing end (mannose C, Scheme 3) is mostly solvent exposed in the bound state. This binding mode is reminiscent of that of the natural D1-like tetramannoside **Te-3**, a constituent arm of heptamannoside **H**. The binding of tetramannoside **Te-3** has been extensively studied by using different techniques (X-ray,^[6] ELISA,^[7] microarrays,^[7,26–28] and NMR^[17]). Among the three branches of the natural high-mannose glycan Man₉, this tetramannoside is preferentially recognized by 2G12 ($K_D=0.4$ mM).^[8f,17] In contrast, the tetramannoside **Te-4** studied here shows a fivefold decrease in affinity towards 2G12 ($K_D=2.2$ mM, Table 1) in comparison to natural **Te-3**. This is in good agreement with the previously observed preferential recognition of the D1-type arm over the non-natural branch in the entire heptamannoside **H**.^[17] Furthermore, this is a key result in terms of structure–binding relationships for this oligomannoside series, highlighting that a simple structural change at the reducing end of the two tetrasaccharides (α 1,6 linkage in **Te-4** versus α 1,3 in **Te-3**, Scheme 1) has

a significant impact on the energetics of the molecular recognition process, but not in the mode of binding. In addition, the STD NMR competitive experiment between oligomannosides **Te-3** and **Te-4** in the presence of the antibody 2G12 (Figure 3) confirms that the antibody preferentially recognizes **Te-3**, even though 2G12 recognizes both tetramannosides with the same binding mode, as deduced from the epitopes as determined by STD. NMR data indicates that the reducing end of **Te-4** makes some contacts with the protein (Scheme 3), which most likely restrict the conformational freedom characteristic of a flexible α 1,6-linkage in the bound state, leading to a greater entropy penalty upon binding in comparison to the most rigid α 1,3-linkage of **Te-3**.

Microarray technologies are being widely used to map the interactions between carbohydrates and proteins.^[26] With regard to high-mannose-type oligosaccharides, different groups have employed glycan microarrays to screen their affinity to 2G12, reinforcing the importance of multivalency in this interaction.^[7,19,23] The results of glycan microarray analysis show that 2G12 strongly interacts with **Te-3** at the tested concentrations but not with the other oligomannosides studied in this work. This is in agreement with previous findings, which demonstrate that **Te-3** is an excellent mimic of the 2G12 epitope,^[7,19,23,29] and a multivalent display of this antigen results in a high affinity^[15,19,29] and efficiency for interference in the 2G12–gp120 interaction.^[24] The **Tri-1**–2G12 interaction was also studied by using a glycan microarray; however, no interaction was detected,^[26] in agreement with our results.^[29] The **Tri-2** and **Te-4** oligomannosides have not been previously tested as 2G12 ligands.

The arrangement of the oligomannosides onto a printed array is not directly comparable with the NMR studies, which are performed in isotropic solution. Furthermore, a cluster effect, which is absent in the NMR solution of free ligands, has also to be taken into consideration with microarray slides. However, the interactions between the oligomannosides and 2G12 in solution follow the same trend of the microarray analysis. Upon comparison of **Te-3** and **Te-4**, both techniques suggest that the α 1,6-linkage at the non-reducing end strongly influences the interaction with 2G12. During the preparation of this manuscript, Walker et al.^[30] reported that pentamannoside Man α 1–3(Man α 1–2Man α 1–2Man α 1–6)Man, which corresponds to **Te-4** but incorporates a further mannose unit at position 3 of its reducing end, did not specifically bind to antibody 2G12 as measured by glycan array analysis, in contrast to previous findings.^[26] Multimerization of this type of oligomannoside onto a surface does not always result in an increase in binding. For example, gold nanoparticles incorporating multiple copies of the trimannoside Man α 1–2Man α 1–2Man, which was shown to be a good 2G12 epitope as measured by STD,^[17] were not able to displace the trimannoside from 2G12 binding sites even at high concentrations.^[29] Although microarray analysis is straightforward, and profits of multivalent interactions are similar to nanoparticles, the avidities and selectivity of specific interactions may depend on the density of the carbohydrates on the array and on the nature of the spacer which links the carbohydrate to the scaffold.

Conclusion

We have characterized the molecular recognition by the human anti-HIV-1 antibody 2G12 of the biologically relevant trimannosides **Tri-1** and **Tri-2**, and tetramannosides **Te-3** and **Te-4**. By studying these ligands, we have provided important structural information to clarify the molecular recognition by 2G12 of previously characterized branched oligomannoside constituents of the triantennary high-mannose Man₉GlcNAc₂ glycan: the pentamannoside **P**, containing both the D2 and D3 arms of the natural high-mannose, and the heptamannoside **H**, composed by the repetition of two Man α 1–2Man α 1–2Man trimannosides, the minimum structural requirements to yield good affinity towards 2G12.^[17]

The affinities of the constitutive fragments of pentamannoside **P** (e.g., **Tri-1** and **Tri-2**) are about the same. The binding to 2G12 of individual ligands **Tri-1** and **Tri-2** is in good agreement with the previous observation of a bimodal binding of the entire pentamannoside **P**. On the other hand, dissection of heptamannoside **H** leads to the tetramannosides **Te-3** and **Te-4**, which show notably different affinities to 2G12. In particular, **Te-3** shows higher affinity than **Te-4**. The only difference between **Te-3** and **Te-4** resides in the α 1,3- versus α 1,6-linkage between the reducing mannose and the trisaccharide at the non-reducing end (Scheme 1).

Although 85% of the contacts between antibody 2G12 and the gp120 high-mannose glycans occur through the non-reducing Man α 1–2Man motif of the D1 arm,^[6] our experimental results indicate that the mannose ring of the internal core can have a key influence in the interaction with 2G12. These results expand our comprehension of the molecular basis of the 2G12–gp120 interaction, affording key structural information for the development of an HIV carbohydrate-based vaccine.

Experimental Section

General: All chemicals were purchased as reagent grade from Sigma–Aldrich and used without further purification, unless otherwise stated. CH₂Cl₂ was distilled from calcium hydride before use. Dry MeOH was kept over 3 Å molecular sieves. TLC was performed on 0.25 mm pre-coated silica gel glass plates or aluminum-backed sheets (Merck silica gel 60 F₂₅₄) with detection by UV-light (254 nm) and/or heating at >200 °C after staining either with 10% H₂SO₄ (aqueous solution) or *p*-anisaldehyde solution [*p*-anisaldehyde (25 mL), H₂SO₄ (25 mL), EtOH (450 mL), and CH₃COOH (1 mL)]. Organic solvents were removed by rotary evaporation under reduced pressure at approximately 40 °C (water bath). Silica gel (0.041–0.063 mm, Amicon; 0.063–0.200 mm, Merck) was used for flash column chromatography (FCC). Size-exclusion column chromatography was performed on a Sephadex LH-20 (GE Healthcare). NMR spectra were recorded at 500 MHz (Bruker, ¹H) or 125 MHz (¹³C) at 25 °C. If not otherwise stated, chemical shifts are given relative to the residual solvent signal. Infrared spectra (IR) were recorded from 4000 to 400 cm⁻¹ with a Nicolet 6700 FTIR spectrometer (Thermo Spectra-Tech); solids were pressed into KBr pellets. Optical rotations were determined with a Perkin–Elmer 341 polarimeter. Mass spectrometric data was obtained from a Waters LCT Premier XE instrument with a standard ESI source by direct injection. The instrument was operated with a capillary voltage of 1.0 kV and a cone

voltage of 200 V. Cone and desolvation gas flow were set to 50 and 500 Lh⁻¹, respectively; source and desolvation temperatures were 100 °C. High-resolution mass was determined by using glycolic acid (Sigma) as an internal standard ([2M+Na]⁺, *m/z* 953.6058). MALDI-ToF spectra were recorded on a Bruker Reflex IV with 2',4',6'-trihydroxy-acetophenone monohydrate (THAP) as a matrix. HIV-1 gp120 monoclonal antibody 2G12 was kindly supplied by Dr. Dietmar Katinger (Polymun Scientific, Vienna, Austria).

Synthesis of aminoethyl oligomannosides: Tetramannoside **Te-3** was prepared according to the literature.³¹ Aminoethyloligomannosides **Tri-1**, **Tri-2**, and **Te-4** were obtained by deprotection of the corresponding fully protected parent compounds whose preparations from acceptor **1** and acceptor **2** is reported in the Supporting Information. **General procedure:** The fully protected oligomannosides (0.06 mmol) were dissolved in MeOH (3 mL), and NaOMe (1 equiv, 3.6 mg, 0.06 mmol) was added to the solution. The solution was stirred at room temperature for 48 h and was brought to pH~7 with Amberlite IR-120 (**Tri-1** and **Tri-2**) or to pH~2 with HCl (1 M; **Te-4**). The solvent was removed under reduced pressure to yield a residue. The oligomannoside was dissolved in MeOH/HCOOH (95:5, v/v, 3 mL) and 1.5 mass equiv Pd-Black was added to the solution. The reaction mixture was flushed with H₂ (three times) and stirred at room temperature under H₂ for 12 h. The reaction mixture was diluted with MeOH and filtered through Celite. The solvent was removed under reduced pressure. The resulting residue was purified by size-exclusion chromatography on a Sephadex LH-20 (MeOH/H₂O 9:1). After freeze-drying, the desired products were collected as white solids.

Tri-1 formate salt: (yield 72%); [α]_D²⁰ = +30 (*c* = 0.1, H₂O); ¹H NMR (500 MHz, D₂O): δ = 8.45 (s, 1H; HCOO⁻), 5.38 (d, *J* = 1.4 Hz, 1H; H1B), 5.05 (d, *J* = 1.6 Hz, 1H; H1A), 4.89 (d, *J* = 1.6 Hz, 1H; H1C), 4.14 (dd, *J* = 3.2, 1.6 Hz, 1H; H2C), 4.10 (dd, *J* = 3.2, 1.7 Hz, 1H; H2B), 4.07 (dd, *J* = 3.3, 1.8 Hz, 1H; H2A), 4.06–4.01 (m, 1H; OCH₂CH₂NH₃⁺), 3.99 (dd, *J* = 9.6, 3.3 Hz, 1H; H3B), 3.94–3.62 (m, 15H), 3.43–3.30 (m, 2H; CH₂NH₃⁺); ¹H,¹³C HSQC NMR (125 MHz, D₂O): δ = 102.3 (d, 1C, C1A), 100.7 (d, 1C, C1B), 99.7 (d, 1C, C1C), 78.4 (d, 1C, C2B), 78.1, 73.2, 73.1, 70.2, 69.9, 69.8 (d, 1C, C2A), 69.3 (d, 1C, C2C), 66.8, 65.8, 60.9, 60.8, 61.4 (d, 1C, OCH₂CH₂NH₃⁺), 56.3 (t, 1C, CH₂NH₃⁺); IR (KBr): $\tilde{\nu}$ = ~3600–3050 (br), 2934, 2885, 1593 (s), 1385, 1344, 1131, 1054, 1033; HR-MS: calcd for C₂₀H₃₇NO₁₆Na⁺: 570.201 [M–HCOOH+Na]⁺; found: 570.198.

Tri-2 formate salt: (yield 78%); [α]_D²⁰ = +9 (*c* = 0.5, H₂O) ¹H NMR (500 MHz, D₂O): δ = 8.48 (s, 1H; HCOO⁻), 5.17 (d, *J* = 1.4 Hz, 1H; H1D), 5.04 (d, *J* = 1.5 Hz, 1H; H1E), 4.90 (d, *J* = 1.5 Hz, 1H; H1C), 4.09 (dd, *J* = 3.2 Hz, 1H; 1.5), 4.03–3.67 (m, 18H), 3.63 (t, *J* = 9.8 Hz, 1H), 3.28–3.21 (m, 2H; CH₂NH₃⁺); ¹H,¹³C HSQC NMR (125 MHz, D₂O): δ = 102.3 (d, 1C, C1E), 100.1 (d, 1C, C1C), 97.9 (d, 1C, C1D), 78.7 (d, 1C), 73.2 (d, 1C), 72.7 (d, 1C), 71.1 (d, 1C), 70.6 (d, 1C), 70.3 (d, 1C), 70.2 (d, 1C), 69.9 (d, 1C), 69.7 (d, 1C), 66.9 (d, 2C), 66.4 (d, 1C), 65.7 (t, 1C), 63.4 (t, 1C), 61.1 (t, 1C), 60.9 (t, 1C), 39.0 (t, 1C, CH₂NH₃⁺); IR (KBr): $\tilde{\nu}$ = ~3600–3050 (br), 2937, 1591 (s), 1386, 1345, 1125, 1090, 1062; HR-MS: calcd for C₂₀H₃₇NO₁₆Na⁺: 570.201 [M–HCOOH+Na]⁺; found 570.199.

Te-4 chloride salt: (yield 75%); [α]_D²⁰ = +5 (*c* = 0.5, H₂O); ¹H NMR (500 MHz, D₂O): δ = 5.30 (s, *J* = 1.4 Hz, 1H; H1E), 5.15 (s, *J* = 1.4 Hz, 1H; H1D), 5.06 (s, *J* = 1.5 Hz, 1H; H1Z), 4.90 (s, *J* = 1.5 Hz, 1H; H1C), 4.12 (dd, *J* = 3.0, 1.4 Hz, 1H; H2E), 4.08 (dd, *J* = 3.3, 1.5 Hz, 1H; H2Z), 4.03–3.59 (m, 24H), 3.19 (m, 2H; CH₂NH₃⁺); ¹H,¹³C HSQC NMR (125 MHz, D₂O): δ = 102.1 (d, 1C, C1Z), 100.6 (d, 1C, C1E), 100.1 (d, 1C, C1C), 98.0 (d, 1C, C1D), 78.8, 78.4 (d, 1C, C2E), 73.1, 72.8, 70.9, 70.3, 69.8 (d, 1C, C2Z), 66.9, 66.8, 65.9, 61.0, 39.2 (t,

^1C , CH_2NH_3^+); IR (KBr): $\tilde{\nu} = \sim 3600\text{--}3050$ (br), 2925, 2877, 1131, 1058; HR-MS: calcd for $\text{C}_{26}\text{H}_{48}\text{NO}_{21}^+$: 710.272 $[\text{M}-\text{Cl}]^+$; found 732.252; calcd for $\text{C}_{26}\text{H}_{47}\text{NO}_{21}\text{Na}^+$: 732.254 $[\text{M}-\text{HCl}+\text{Na}]^+$; found 732.252.

NMR spectroscopy: For preparation of NMR samples, the majority of maltose present in the antibody batch was first removed and the sample buffer was exchanged by dialysis with a 20 kDa membrane (Spectra/Por, Medicell International Ltd.). All the ligands were lyophilized against 99% D_2O twice and once with 99.99% D_2O from Sigma-Aldrich. All samples were prepared in 10 mM phosphate-deuterated buffer solution at pH 6.7. The ^1H NMR signals of each ligand were assigned by employing a combination of COSY, TOCSY, NOESY, and ^1H , ^{13}C HSQC experiments performed on a Bruker DRX (500 MHz) spectrometer. The temperature was 298 K for all STD NMR experiments. The experiments were performed without suppression of the residual HDO signal. The broad signals of the antibody were deleted by adding a T1p filter to the STD NMR pulse sequence. All STD NMR experiments were carried out with 1 K scans. Build-up curves were obtained by using seven saturation times (0.5, 0.75, 1, 1.5, 2, 2.5, and 3 s) varying the relaxation delay (with a minimum of 0.1 s) inversely to the saturation time for each experiment and keeping the total experimental time constant. Each saturation time was composed of a train of Gaussian-shaped pulses of 50 ms. Off- and on-resonance frequencies of 40 and 0.86 ppm (antibody aliphatic region), respectively, were used for the STD NMR build-up curves. To check the selectivity of the experimental setup, STD NMR "blank" experiments were carried out for each ligand on samples without protein. For the titration experiments, antibody:ligand molar ratios were increased from 1:11 to 1:200 by adding different aliquots of the ligand to the NMR sample from high concentration stocks of each ligand. For each ratio, an STD build-up curve was calculated to obtain the initial slopes (STD_0) by mathematical fitting to Equation (1).

Dissociation constants (K_D) for each oligomannoside were obtained by fitting every isotherm composed of initial slopes from the STD NMR build-up curves to a Langmuir equation of the type $(B_{\text{max}}[\text{L}])/(K_D+[\text{L}])$.^[20] The binding epitopes of the ligands were obtained at the largest antibody:ligand ratios reached in the experimental setup by normalizing the STD-AF_0 values for each ligand against the largest STD value, which was arbitrarily assigned as 100%.

In the competitive experiments between **Te-3** and **Te-4**, the sample was prepared in the same buffer as those for the STD NMR build-up curves, but the concentrations were $[\text{2G12}] = 25 \mu\text{M}$ and $[\text{Te-3}] = 1 \text{ mM}$. Afterwards, **Te-4** was added, obtaining a sample in which both tetramannosides were in the same concentration with antibody-to-ligand ratios of 1:40. These experiments were carried out on a 600 MHz NMR Bruker spectrometer.

Microarrays: Microarrays were printed on glass slides employing a robotic noncontact spotter Piezorray (PerkinElmer). NHS-activated Nexterion H glass slides were purchased from Schott AG, Mainz, Germany. 2G12* and ConA* incubations were performed in Fast Frame incubation chambers (Whatman, Maidstone, UK). Fluorescence measurements were performed in an Agilent G265BA microarray scanner system (Agilent Technologies). Quantification was achieved by ProScanArray Express software from PerkinElmer.

Buffered solutions (200 μL , 300 mM, pH 8.5) of **Tri-1**, **Tri-2**, **Te-3**, **Te-4**, and aminoethyl β -glucoside were placed into a 384-well source plate and arrayed onto NHS-functionalized glass slides. Volumes (0.7 nL) of the buffered solutions were spotted in eight replicates. After printing, the slides were placed in a 75% humidity chamber

(saturated NaCl solution) at 25 °C for 18 h. The remaining NHS groups were quenched by placing the slides in a 50 mM solution of ethanolamine in sodium borate buffer (50 mM, pH 9.0) for 1 h. The slides were then washed with a standard protocol and dried in a slide spinner. A buffered solution (100 μL) of fluorescently-labeled 2G12 (25 $\mu\text{g mL}^{-1}$) was incubated in the dark over each microarray for 1 h at room temperature. After washing and drying, fluorescence was analyzed with a microarray scanner. For more details, see the Supporting Information.

Acknowledgements

This work was supported by the Spanish Ministry of Science and Innovation MICINN (grant CTQ2011-27268), EU (grant CHARM Health-F3-2009-242135), and the Department of Industry of the Basque Country (grant ETORTEK 2009 IE09-257). HIV-1 gp120 monoclonal antibody 2G12 was kindly supplied by Dr. D. Katinger (Polymun Scientific, Vienna, Austria). F.C. thanks the MICINN for a PhD. grant. J.A. acknowledges financial support from the MICINN through the Ramon y Cajal program. We thank BIO-NAND research center for NMR measurements at 600 MHz spectrometer. The authors are grateful to Dr. Sonia Serna and Dr. Juan Echevarria for their help and careful proofreading of the glycan microarray portion of this manuscript. Dr. Javier Calvo is gratefully acknowledged for mass spectrometry analyses.

Keywords: high-mannose-type oligosaccharides • HIV broadly neutralizing monoclonal antibody 2G12 • microarrays • NMR spectroscopy • protein-carbohydrate interactions

- [1] M. J. McElrath, B. F. Haynes, *Immunity* **2010**, *33*, 542–554.
- [2] J. R. Mascola, D. C. Montefiori, *Annu. Rev. Immunol.* **2010**, *28*, 413–444.
- [3] F. Ferrantelli, R. M. Ruprecht, *Curr. Opin. Immunol.* **2002**, *14*, 495–502.
- [4] D. R. Burton, R. A. Weiss, *Science* **2010**, *329*, 770–773.
- [5] a) A. Trkola, A. B. Pomales, H. Yuan, B. Korber, P. J. Maddon, G. P. Allaway, H. Katinger, C. F. Barbas III, D. R. Burton, D. D. Ho, J. P. Moore, *J. Virol.* **1995**, *69*, 6609–6617; b) A. Trkola, M. Purtscher, T. Muster, C. Ballaun, A. Buchacher, N. Sullivan, K. Srinivasan, J. Sodroski, J. P. Moore, H. Katinger, *J. Virol.* **1996**, *70*, 1100–1108; c) R. W. Sanders, M. Venturi, L. Schiffer, R. Kalyanaraman, H. Katinger, K. O. Lloyd, P. D. Kwong, J. P. Moore, *J. Virol.* **2002**, *76*, 7293–7305.
- [6] D. A. Calarese, C. N. Scanlan, M. B. Zwick, S. Deechongkit, Y. Mimura, R. Kunert, P. Zhu, M. R. Wormald, R. L. Stanfield, K. H. Roux, J. W. Kelly, P. M. Rudd, R. A. Dwek, H. Katinger, D. R. Burton, I. A. Wilson, *Science* **2003**, *300*, 2065–2071.
- [7] D. A. Calarese, H. K. Lee, C. Y. Huang, M. D. Best, R. D. Astronomo, R. L. Stanfield, H. Katinger, D. R. Burton, C.-H. Wong, I. A. Wilson, *Proc. Natl. Acad. Sci. USA* **2005**, *102*, 13372–13377.
- [8] a) L. X. Wang, J. Ni, S. Singh, H. Li, *Chem. Biol.* **2004**, *11*, 127–134; b) H. Li, L. X. Wang, *Org. Biomol. Chem.* **2004**, *2*, 483–488; c) V. Y. Dudkin, M. Orlova, X. Geng, M. Mandal, W. C. Olson, S. J. Danishefsky, *J. Am. Chem. Soc.* **2004**, *126*, 9560–9562; d) I. J. Krauss, J. G. Joyce, A. C. Finnefrock, H. C. Song, V. Y. Dudkin, X. Geng, J. D. Warren, M. Chastain, J. W. Shiver, S. J. Danishefsky, *J. Am. Chem. Soc.* **2007**, *129*, 11042–11044; e) J. Wang, H. Li, G. Zou, L. X. Wang, *Org. Biomol. Chem.* **2007**, *5*, 1529–1540; f) S. K. Wang, P. H. Liang, R. D. Astronomo, T. L. Hsu, S. L. Hsieh, D. R. Burton, C.-H. Wong, *Proc. Natl. Acad. Sci. USA* **2008**, *105*, 3690–3695; g) A. Kabanova, R. Adamo, D. Proietti, F. Berti, M. Tontini, R. Rappuoli, P. Costantino, *Glycoconjugate J.* **2010**, *27*, 501–513.
- [9] R. D. Astronomo, E. Kaltgrad, A. K. Udit, S. K. Wang, K. J. Doores, C. Y. Huang, R. Pantophlet, J. C. Paulson, C.-H. Wong, M. G. Finn, D. R. Burton, *Chem. Biol.* **2010**, *17*, 357–370.

- [10] J. Ni, H. Song, Y. Wang, N. M. Stamatou, L. X. Wang, *Bioconjugate Chem.* **2006**, *17*, 493–500.
- [11] R. D. Astronomo, H. K. Lee, C. N. Scanlan, R. Pantophlet, C. Y. Huang, I. A. Wilson, O. Blixt, R. A. Dwek, C.-H. Wong, D. R. Burton, *J. Virol.* **2008**, *82*, 6359–6368.
- [12] J. G. Joyce, I. J. Krauss, H. C. Song, D. W. Opalka, K. M. Grimm, D. D. Nahas, M. T. Esser, R. Hrin, M. Feng, V. Y. Dudkin, M. Chastain, J. W. Shiver, S. J. Danishefsky, *Proc. Natl. Acad. Sci. USA* **2008**, *105*, 15684–15689.
- [13] R. J. Luallen, J. Lin, H. Fu, K. K. Cai, C. Agrawal, I. Mboudjeka, F. H. Lee, D. Montefiori, D. F. Smith, R. W. Doms, Y. Geng, *J. Virol.* **2008**, *82*, 6447–6457.
- [14] D. C. Dunlop, C. Bonomelli, F. Mansab, S. Vasiljevic, K. J. Doores, M. R. Wormald, A. S. Palma, T. Feizi, D. J. Harvey, R. A. Dwek, M. Crispin, C. N. Scanlan, *Glycobiology* **2010**, *20*, 812–823.
- [15] C. Agrawal-Gamse, R. J. Luallen, B. Liu, H. Fu, F. H. Lee, Y. Geng, R. W. Doms, *J. Virol.* **2011**, *85*, 470–480.
- [16] R. C. Desrosiers, *Nat. Med.* **2004**, *10*, 221–223.
- [17] P. M. Enríquez-Navas, M. Marradi, D. Padro, J. Angulo, S. Penadés, *Chem. Eur. J.* **2011**, *17*, 1547–1560.
- [18] a) M. Mayer, B. Meyer, *Angew. Chem.* **1999**, *111*, 1902–1906; *Angew. Chem. Int. Ed.* **1999**, *38*, 1784–1788; b) B. Meyer, T. Peters, *Angew. Chem.* **2003**, *115*, 890–918; *Angew. Chem. Int. Ed.* **2003**, *42*, 864–891.
- [19] H. K. Lee, C. N. Scanlan, C. Y. Huang, A. Y. Chang, D. A. Calarese, R. A. Dwek, P. M. Rudd, D. R. Burton, I. A. Wilson, C.-H. Wong, *Angew. Chem.* **2004**, *116*, 1018–1021; *Angew. Chem. Int. Ed.* **2004**, *43*, 1000–1003.
- [20] J. Angulo, P. M. Enríquez-Navas, P. M. Nieto, *Chem. Eur. J.* **2010**, *16*, 7803–7812.
- [21] M. Mayer, T. L. James, *J. Am. Chem. Soc.* **2004**, *126*, 4453–4460.
- [22] S. Serna, J. Etxebarria, N. Ruiz, M. Martín-Lomas, N. C. Reichardt, *Chem. Eur. J.* **2010**, *16*, 13163–13175.
- [23] E. W. Adams, D. M. Ratner, H. R. Bokesch, J. B. McMahon, B. R. O'Keefe, P. H. Seeberger, *Chem. Biol.* **2004**, *11*, 875–881.
- [24] C. N. Scanlan, R. Pantophlet, M. R. Wormald, E. OllmannSaphire, R. Stanfield, I. A. Wilson, H. Katinger, R. A. Dwek, P. M. Rudd, D. R. Burton, *J. Virol.* **2002**, *76*, 7306–7321.
- [25] K. J. Doores, C. Bonomelli, D. J. Harvey, S. Vasiljevic, R. A. Dwek, D. R. Burton, M. Crispin, C. N. Scanlan, *Proc. Natl. Acad. Sci. USA* **2010**, *107*, 13800–13805.
- [26] O. Blixt, S. Head, T. Mondala, C. Scanlan, M. E. Huflejt, R. Alvarez, M. C. Bryan, F. Fazio, D. Calarese, J. Stevens, N. Razi, D. J. Stevens, J. J. Skehel, I. van Die, D. R. Burton, I. A. Wilson, R. Cummings, N. Bovin, C.-H. Wong, J. C. Paulson, *Proc. Natl. Acad. Sci. USA* **2004**, *101*, 17033–17038.
- [27] M. C. Bryan, F. Fazio, H.-K. Lee, C.-Y. Huang, A. Chang, M. D. Best, D. A. Calarese, O. Blixt, J. C. Paulson, D. Burton, I. A. Wilson, C.-H. Wong, *J. Am. Chem. Soc.* **2004**, *126*, 8640–8641.
- [28] P.-H. Liang, S.-K. Wang, C.-H. Wong, *J. Am. Chem. Soc.* **2007**, *129*, 11177–11184.
- [29] M. Marradi, P. Di Gianvincenzo, P. M. Enríquez-Navas, O. Martínez-Ávila, F. Chiodo, E. Yuste, J. Angulo, S. Penadés, *J. Mol. Biol.* **2011**, *410*, 798–810.
- [30] L. M. Walker, M. Huber, K. J. Doores, E. Falkowska, R. Pejchal, J.-P. Julien, S.-K. Wang, A. Ramos, P.-Y. Chan-Hui, M. Moyle, J. L. Mitcham, P. W. Hammond, O. A. Olsen, P. Phung, S. Fling, C.-H. Wong et al., *Nature* **2011**, *477*, 466–470.
- [31] O. Martínez-Ávila, K. Hijazi, M. Marradi, C. Clavel, C. Champion, C. Kelly, S. Penadés, *Chem. Eur. J.* **2009**, *15*, 9874–9888.

Received: February 17, 2012

Published online on May 24, 2012

Chapter-3

Gold nanoparticles as carriers for a fully synthetic *Streptococcus pneumoniae* type 14 vaccine candidate

In the frame of GlycoGold EU project

Pneumococcal pneumonia is a severe systematic disease that mainly causes illness in children younger than 5 years old and adults 65 years of age or older.¹ In addition, people with chronic heart, lung, or liver diseases are also at risk for getting pneumococcal pneumonia. People with HIV/AIDS or people who have had organ transplants and are taking immunosuppressive drugs are also at high risk of getting this disease.¹ Pneumococcal disease is a major public health problem, and it is estimated that 1.6 million people die each year from this infection.² Capsular polysaccharides are the major virulence factor of *Streptococcus pneumoniae* and they have been exploited to evoke protection against this bacterium. However, capsular polysaccharides are poorly immunogenic and strategies to increase an effective immune response have been developed. Conjugation of polysaccharides to protein carriers solved two drawbacks related with a polysaccharide vaccine: The induction of immunological memory and the antibody response in infants.³ The seminal work on **conjugate carbohydrate-vaccines** was described by Avery and Goebel in 1931. In this enthusiastic work, it was described for the first time that “*Type-specific antipneumococcus immunity has been induced in rabbits by immunization with antigen prepared by combining a specific derivative of the capsular polysaccharide of type III Pneumococcus with globulin from horse serum*”⁴. Due to the advent of antibiotics, it took 50 years before the principles of Avery were re-discovered and exploited for the preparation of polysaccharides conjugate vaccines. One of the most exciting work in this field was the large-scale synthesis and clinical evaluation of a conjugate vaccine based on a synthetic capsular polysaccharide antigen of *Haemophilus influenzae type b (Hib)*⁵. This vaccine was evaluated in clinical trials in Cuba showing long-term protective antibody titers. This extraordinary work demonstrated that the access to synthetic complex carbohydrate-based vaccines is possible, providing a basis for further

¹ <http://www.niaid.nih.gov/topics/pneumonia/pages/default.aspx>

² WHO, 2007. Wkly. Epidemiol. Rec. 82: 93-104

³ Rijkers G. T, van Mens S. P., van Velzen-Blad H., What do the next 100 years hold for pneumococcal vaccination?, Expert Rev. Vaccines 2010, 9, 1241-1244.

⁴ Avery O. T., Goebel W. F., Chemo-immunological studies on conjugated carbohydrate-proteins : V. The immunological specificity of an antigen prepared by combining the capsular polysaccharide of type III pneumococcus with foreign protein, J. Exp. Med. 1931, 54, 437-447.

⁵ Verez-Bencomo V., Fernández-Santana V., Hardy E., Toledo M. E., Rodríguez M. C., Heynngnezz L., Rodríguez A., Baly A., Herrera L., Izquierdo M., Villar A., Valdés Y., Cosme K., Deler M. L., Montane M., Garcia E., Ramos A., Aguilar A., Medina E., Toraño G., Sosa I., Hernandez I., Martínez R., Muzachio A., Carmenates A., Costa L., Cardoso F., Campa C., Diaz M., Roy R., A synthetic conjugate polysaccharide vaccine against *Haemophilus influenzae type b*, Science 2004, 305, 522-525.

development of similar approaches with other human pathogens. The passage from conjugate vaccines, in which naturally-derived glycans are conjugated to immunogenic carrier proteins, to synthetic carbohydrate vaccines (see Part-1, Introduction) has already started in spite of the ongoing controversy on the best strategy to follow.⁶ The aim is to elicit a strong, specific and long-lived antibody response against sugars by means of fully synthetic carbohydrate vaccines avoiding the problems of costs, availability and purity of key antigens, batch-to-batch variability, and the use of co-administered adjuvants.

In search for new fully synthetic conjugate vaccines not based on protein carriers, gold nanoclusters were exploited in this Thesis as a versatile platform to construct a potential carbohydrate-based vaccine against *S. pneumoniae* type 14. The capsular polysaccharide of *S. pneumoniae* type 14 (Pn14PS) consists of biosynthetic repeating units of the tetrasaccharide {6)-[β -D-Galp(1-4)]- β -D-GlcpNAc-(1-3)- β -D-Galp(1-4)- β -D-Glcp(1-)}_n (Figure 1). The synthetic branched tetrasaccharide (TetraPn or Tetra in this chapter) was identified as the smallest structure capable of evoking opsonophagocytic antibodies against *S. pneumoniae* type 14 when conjugated to the immunogenic cross-reactive material of diptheria toxin (CRM₁₉₇).⁷

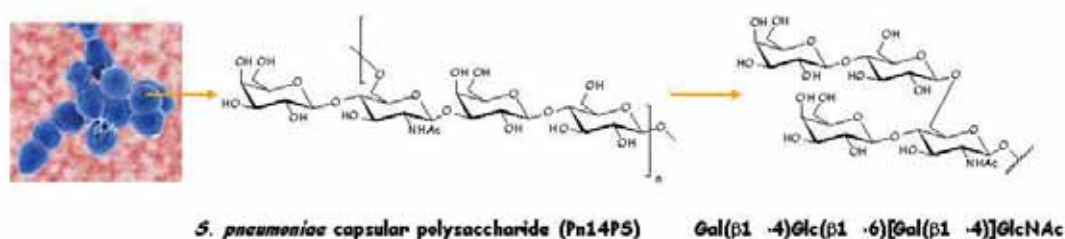


Figure 1: The synthetic branched tetrasaccharide Gal(β1-4)Glc(β1-6)[Gal(β1-4)]βGlcNAc (TetraPn) is a single repeating unit of the *S. pneumoniae* type 14 capsular polysaccharide (Pn14PS). This TetraPn was used in this Thesis as the smallest immunogenic structure related with Pn14PS.

⁶ Peri F., Clustered carbohydrates in synthetic vaccines, Chem. Soc. Rev. 2013, DOI: 10.1039/c2cs35422e.

⁷ Safari D., Dekker H. A., Joosten J. A., Michalik D., de Souza A. C., Adamo R., Lahmann M., Sundgren A., Oscarson S., Kamerling J. P., Snippe H., Identification of the smallest structure capable of evoking opsonophagocytic antibodies against *Streptococcus pneumoniae* type 14, Infect Immun. 2008, 76, 4615-4623..

A main concern for synthetic vaccines is the risk of carrier-induced epitopic suppression⁸. In the field of carbohydrate-based vaccines, different strategies have been developed (see intro part-1 of this Thesis). Nanotechnology can offer an alternative to conventional vaccine technologies and can improve vaccine development. The use of gold glyconanoparticles was explored by the group of Scrimin to mimic the capsular polysaccharide of *Neisseria meningitides* with the aim to obtain specific anti-polysaccharide antibodies after mice immunization.⁹ Recently, the same group studied the factors that affect the T cell responses induced by the GNPs coated with *N. meningitides* antigens (without T-epitopes on the GNPs).¹⁰ Another approach for the development of carbohydrate vaccines based on gold nanoparticles has been reported by Barchi and collaborators.¹¹ Several nanoparticles carrying glycopeptides bearing tumor-associated carbohydrate antigens (TACAs) were prepared and the immune response was evaluated in mice immunization with no additional adjuvants administered in cocktail with the GNPs during the immunization.

Our aim was to exploit gold nanoparticles as carrier for *S. pneumoniae* antigens avoiding the coupling of the antigenic carbohydrate with an immunogenic protein. To trigger the desired anti-carbohydrate immune response, we attached on the same GNPs the carbohydrate epitope mimic (TetraPn) and a small peptide (17 aminoacids) from albumin. The latter ovalbumin peptide-fragment OVA₃₂₃₋₃₃₉ (OVA) is a well known immunodominant T-cell epitope. Tetrasaccharide TetraPn, peptide OVA₃₂₃₋₃₃₉, and glucose (Glc) were functionalized with a thiol-ending linker and used for the construction of hybrid gold glyconanoparticles (Fig. 2). A series of gold nanoparticles coated with varying ratio of the three ligands (TetraPn, OVA and Glc) were prepared and characterized following a previously reported single-step procedure¹²(Fig. 3). Glucose bearing a short (five carbon atoms) thiol-ending aliphatic linker was used as inner component to assist water

⁸ Schutze M. P., Leclerc C., Jolivet M., Audibert F., Chedid L., Carrier-induced epitopic suppression, a major issue for future synthetic vaccines, *J. Immunol.* 1985, 135, 2319–2322.

⁹ Manea F., Bindoli C., Fallarini S., Lombardi G., Polito L., Lay L., Bonomi R., Mancin F., Scrimin P., Multivalent, saccharide-functionalized gold nanoparticles as fully synthetic analogs of type A *Neisseria meningitidis* antigens, *Adv. Mater.*, 2008, 20, 4348-4352.

¹⁰ Fallarini S., Paoletti T., Battaglini C. O., Ronchi P., Lay L., Bonomi R., Jha S., Mancin F., Scrimin P., Lombardi G., Factors affecting T cell responses induced by fully synthetic glyco-gold-nanoparticles, *Nanoscale*, 2012, 5, 390-400.

¹¹ Brinäs R. P., Sundgren A., Sahoo P., Morey S., Rittenhouse-Olson K., Wilding G. E., Deng W., Barchi J. J. Jr., Design and synthesis of multifunctional gold nanoparticles bearing tumor-associated glycopeptide antigens as potential cancer vaccines, *Bioconjug. Chem.* 2012, 23, 1513-1523.

¹² Ojeda R., de Paz J. L., Barrientos A. G., Martín-Lomas M., Penadés S., Preparation of multifunctional glyconanoparticles as a platform for potential carbohydrate-based anticancer vaccines, *Carbohydr. Res.* 2007 342, 448-459.

dispersibility and biocompatibility and to allow the tetrasaccharide moiety, armed with a long amphiphilic linker, to protrude above the organic shell of GNPs.

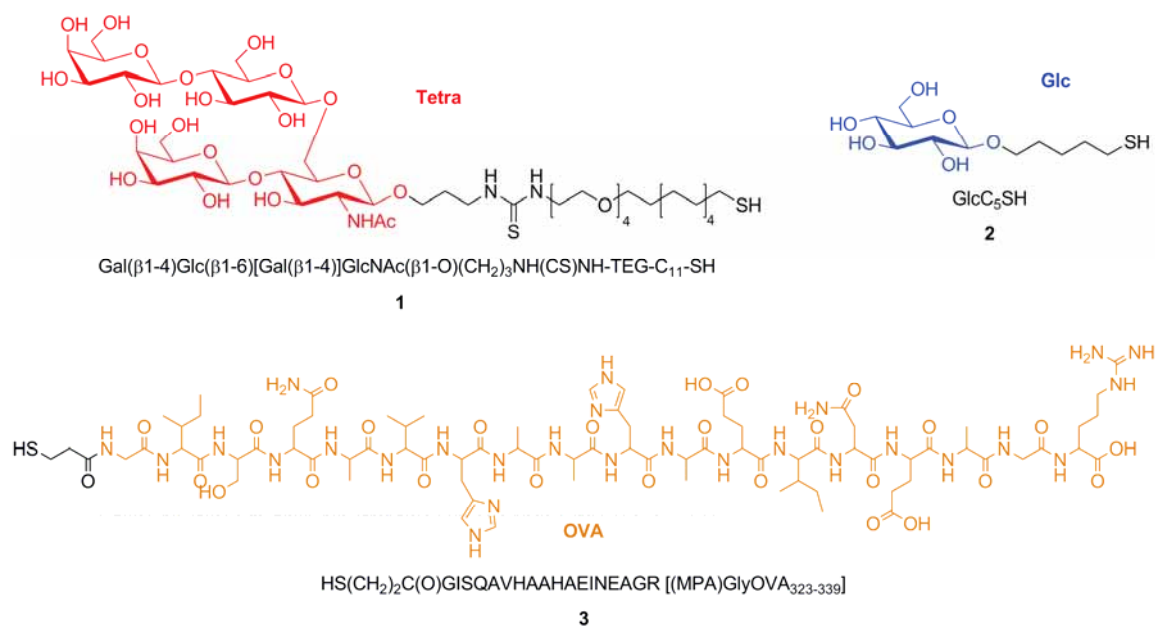


Figure 2: Conjugates used for the preparation of GNPs. Tetrasaccharide (TetraPn) β-D-Galp-(1→4)-β-D-Glcp-(1→6)-[β-D-Galp-(1→4)-]β-D-GlcpNAc (Gal-Glc-(Gal-)GlcNAc) conjugate **1**, D-glucose (Glc) conjugate **2**, and OVA₃₂₃₋₃₃₉ peptide (OVA) conjugate **3**. For clarity reasons, all conjugates are depicted as thiols.

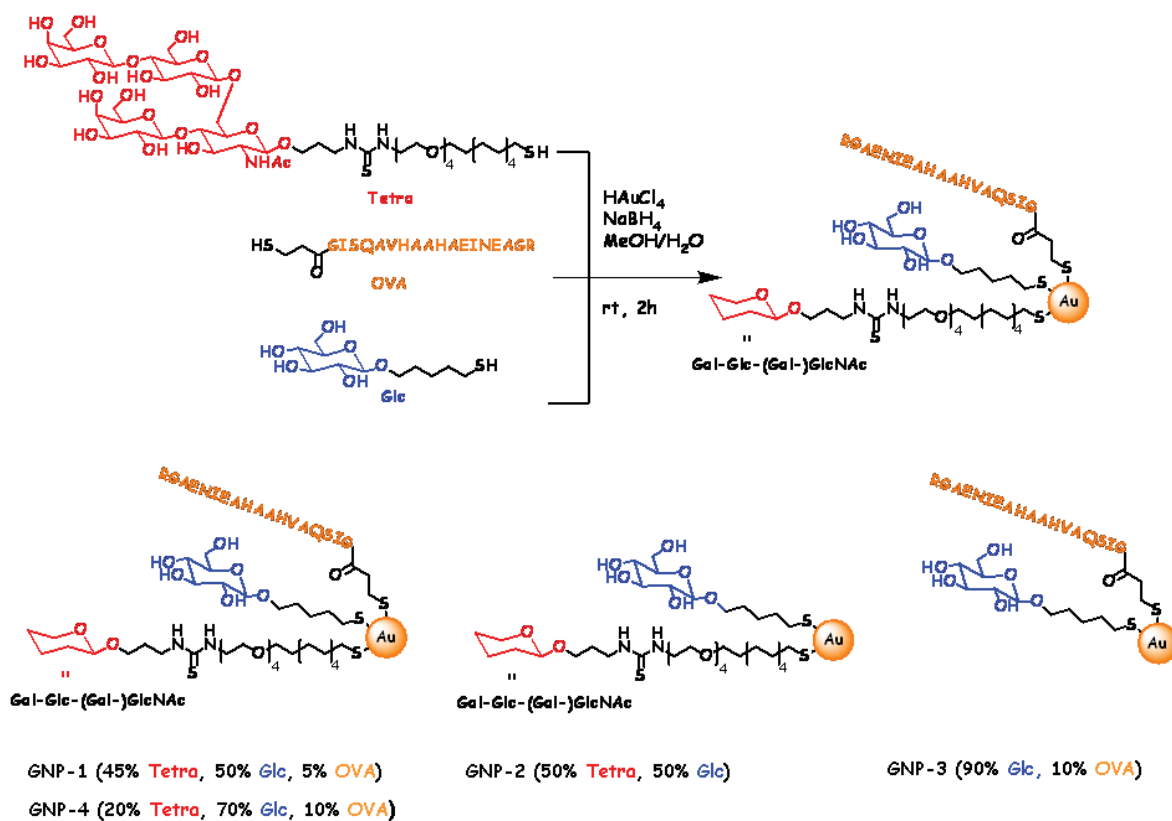


Figure 3: A small library of GNPs carrying different ratio of the antigenic tetrasaccharide TetraPn, ovalbumin peptide-fragment OVA₃₂₃₋₃₃₉ and glucose conjugates was prepared.

In collaboration with the Department of Medical Microbiology of the University Medical Center in Utrecht, these biofunctional GNPs having average gold core diameters of 2 nm were used to immunize intracutaneously BALB/c mice. The key points of this work can be summarized as follows:

- Depending on the density of the different ligands, GNPs coated with the tetrasaccharide conjugate (TetraPn) induced significant levels of specific IgG antibodies that recognize both the native polysaccharide of Pn14 and the branched tetrasaccharide fragment of Pn14PS (TetraPn) as determined by ELISA.
- The copresence of the T-cell-stimulating OVA₃₂₃₋₃₃₉ peptide and the tetrasaccharide antigen on the same gold nanoparticles was a prerequisite for the induction of the anti-Pn14PS IgG antibodies.

- The molar ratio between tetrasaccharide, OVA₃₂₃₋₃₃₉ and glucose on the gold nanoparticles was critical for optimal immunogenicity.
- The OVA₃₂₃₋₃₃₉ (T-cell epitope) on the nanoparticle does not lead to antibodies against the peptide and this avoids the risk of epitope suppression.
- The cytokine study confirmed that GNPs led to helper Th cell activation.
- The phagocytic study demonstrated that the antibodies in sera of mice immunized with GNP carrying TetraPn:Glc:OVA₃₂₃₋₃₃₉ = 45:50:5) were able to coat heat-inactivated fluorescein isothiocyanate-labeled *S. pneumoniae* type 14 and make the bacteria critically susceptible to the action of human polymorphonuclear leukocytes (opsonophagocytosis).

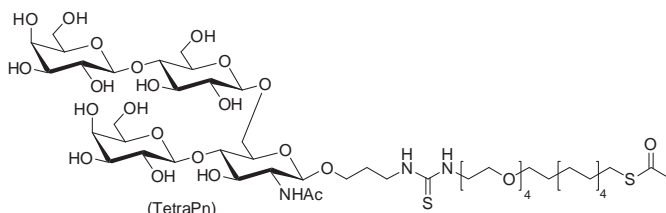
The experiments for evaluating the type-specific antibodies, opsonophagocytosis and cytokine levels after spleen cell stimulation are described in the attached publication Safari et al. 2012.¹³ These results confirm that a suitable presentation of antigenic carbohydrates is essential to induce a specific immune response and should encourage the use of gold GNPs as new systems in the development of a synthetic carbohydrate-based pneumococcal vaccine. This work was performed in the frame of the EU Research Training Network “GlycoGold” (MRTN-CT-2004-005645).

¹³ Safari D., Marradi M., Chiodo F., Th Dekker H. A., Shan Y., Adamo R., Oscarson S., Rijkers G. T., Lahmann M., Kamerling J. P., Penadés S., Snippe H., Gold nanoparticles as carriers for a synthetic *Streptococcus pneumoniae* type 14 conjugate vaccine, *Nanomedicine UK*, 2012, 7, 651-662.

Experimental section

Preparation and characterization of the glycoconjugates for GNPs preparation:

S-Acetylated tetrasaccharide conjugate.

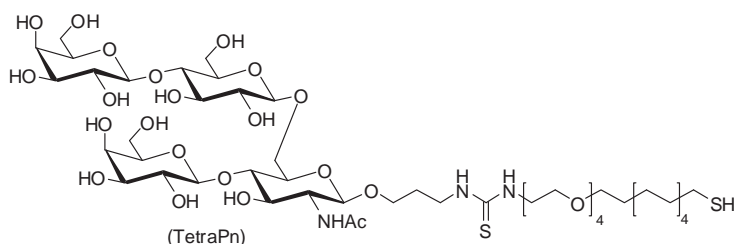


A solution of thiol-ending isothiocyanate linker SCN-TEG-C₁₁-SAC (12.1 mg, 26.1 μ mol, 1.8 equiv.) in H₂O-*i*-PrOH-CH₃CN (1:1:1, v/v/v, 0.6 mL) was added to a solution of 3-aminopropyl tetrasaccharide (prepared by M. Lahmann group) (11.62 mg, 14.5 μ mol, 1 equiv.) in

H₂O-*i*-PrOH-CH₃CN (1:1:1, v/v/v, 1.8 mL) and the pH was set to basic by addition of triethylamine (18 μ L, 130 μ mol, 9 equiv.). The mixture was stirred at room temperature for 17 h and then evaporated. The crude material was kept in high vacuum to remove the residual triethylamine and then triturated with Et₂O (4 x 2 mL) in order to get rid of the excess of the linker. The insoluble solid was purified by Sephadex LH-20 chromatography (column: diameter = 2 cm; height = 45 cm) using as eluent MeOH/H₂O = 9/1 to afford the *S*-acetyl protected tetrasaccharide conjugate as a white solid after lyophilization (12.6 mg, 10.3 μ mol, 71%).

¹H NMR (D₂O) δ 4.61-4.52 (m, 3H, 3xH-1); 4.48 (br d, 1H, J = 7.6 Hz, H-1); 4.31 (d, 1H, J = 10.2 Hz); 4.03-3.60 (m, 40H); 3.57 (m, 2H, 2xH-2); 3.50 (br t, 2H, J = 6.0 Hz, OCH₂CH₂CH₂); 3.41 (br t, 1H, J = 7.6 Hz, H-2); 2.88 (t, 2H, J = 7.1 Hz, CH₂SAC); 2.35 (s, 3H, SAC), 2.07 and 2.06 (s, 3H, NAc); 1.91-1.82 (m, 2H, OCH₂CH₂CH₂N); 1.65-1.53 (m, 4H, CH₂CH₂SAC and OCH₂CH₂CH₂); 1.44-1.26 (m, 14H, (CH₂)₇). ¹³C NMR (D₂O) δ 102.9 (d, 2C, C-1); 102.4 (d, 1C, C-1); 101.1 (d, 1C, C-1); 78.4; 77.8; 75.3; 74.7; 74.2; 73.4; 72.7; 72.6 (d, 1C, C-2); 72.5; 72.3; 71.0 (t, 1C, OCH₂CH₂CH₂); 70.9 (d, 2C, 2xC-2); 70.3; 70.0; 69.8; 69.7; 68.6; 67.3; 67.2 (d, 1C); 61.0; 60.9; 60.2; 43.7 (br t; CH₂NH); 30.2 (q, 1C, SC(O)CH₃); 29.7-29.0 and 25.8 (t, 9C, (CH₂)₉); 28.8 (t, 1C, CH₂SAC); 28.3 (t, 1C, OCH₂CH₂CH₂N); 22.2 (q, 1C, NC(O)CH₃); C=S and C=O undetected. IR (KBr): ν 3424 (broad), 2925, 2850, 1745, 1655, 1374, 1232, 1068 cm⁻¹. HR-MS for C₅₁H₉₃N₃O₂₆S₂: Calcd. 1250.5381 [M+Na]⁺, 1228.5561 [M+H]⁺. Found 1250.5468 [M + Na]⁺ \pm 6.9 ppm, 1228.5591 [M + H]⁺ \pm 2.4 ppm. [α]_D²⁹ = -8.1 (c = 0.4; H₂O).

Branched tetrasaccharide (TetraPn) conjugate 1.



Sodium methoxide (0.5 mg, 9.2 μ mol, 1 equiv.) was added to a solution of *S*-acetyl protected tetrasaccharide conjugate (11.28 mg, 9.2 μ mol, 1 equiv.) in MeOH (5 mL). The mixture was stirred at room temperature for 4 hours and then evaporated. The crude

material was concentrated and purified by Sephadex LH-20 chromatography (column: diameter = 2 cm; height = 45 cm) using as eluent MeOH/ H₂O = 9/1 to afford the tetrasaccharide conjugate **1** (TetraPn) (~2.5:1 mixture of disulfide and thiol) as a white solid after lyophilisation (8.8 mg, 7.4 μ mol (considered as thiol), 81%).

¹H NMR (D₂O) δ 4.60-4.52 (m, 3H, 3xH-1); 4.48 (br d, 1H, H-1, J = 7.3 Hz); 4.30 (br d, 1H, J = 9.9 Hz); 4.03-3.59 (m, 40H); 3.57 (m, 2H, 2xH-2); 3.53-3.46 (m, 2H, OCH₂CH₂CH₂); 3.42 (br t, 1H, J = 7.6 Hz,

H-2); 2.76-2.68 (br signal, ~1.4H, CH_2SS); 2.57-2.51 (br signal, ~0.6H, CH_2SH); 2.07 and 2.05 (s, 3H, NAc) 1.90-1.82 (m, 2H, $\text{OCH}_2\text{CH}_2\text{CH}_2\text{N}$); 1.77-1.68 (m, 1.5H, $\text{CH}_2\text{CH}_2\text{SS}$); 1.65-1.55 (m, 2.5H, $\text{CH}_2\text{CH}_2\text{SH}$ and $\text{OCH}_2\text{CH}_2\text{CH}_2$); 1.50-1.22 (m, 14H, $(\text{CH}_2)_7$). ^{13}C NMR (D_2O) δ 103.0 (d, 1C, C-1); 102.8 (d, 2C, C-1); 101.2 (d, 1C, C-1); 78.6; 77.8; 75.3; 74.7; 74.2; 72.5 (d, 1C, C-2); 72.3; 71.1 (t, 1C, $\text{OCH}_2\text{CH}_2\text{CH}_2$); 71.0; 70.9 (d, 2C, 2xC-2); 70.0; 68.4; 67.3 (d, 1C); 67.2; 61.0; 60.1; 43.7 (br t; CH_2NH); 38.8 (t, ~0.7C, CH_2SS); 24.4 (t, ~0.3C, CH_2SH); 29.1 (t, 2C, $\text{CH}_2\text{CH}_2\text{S}$ and $\text{OCH}_2\text{CH}_2\text{CH}_2$); 29.7-28.8 and 25.9 (t, 9C, $(\text{CH}_2)_9$); 28.2 (t, 1C, $\text{OCH}_2\text{CH}_2\text{CH}_2\text{N}$); 22.3 (q, 1C, $\text{NC}(\text{O})\text{CH}_3$); C=S and C=O undetected. IR (KBr): ν ~ 3369 (broad), 2925, 2854, 1654, 1564, 1381, 1075, 1047. HR-MS for $\text{C}_{49}\text{H}_{91}\text{N}_3\text{O}_{25}\text{S}_2$: Calcd. 1208.5275 [M+Na] $^+$. Found 1208.5261 [M+Na] $^+ \pm 1.2$ ppm.

Preparation and characterization of hybrid gold nanoparticles

GNP-1 (TetraPn:Glc:OVA = 45:50:5). Two different batches (GNP-1 and GNP-1b) were prepared. OVA peptide conjugate **3** (0.34 mg, 0.18 μmol) (Fig. 2) was dissolved in CF_3COOD (50 μL) and dried under air stream until formation of an oil. Tetrasaccharide conjugate **1** (1.89 mg, 1.6 μmol) and glucose conjugate **2** (0.5 mg, 1.8 μmol) were then added and the mixture was dissolved in $\text{CD}_3\text{OD}-\text{D}_2\text{O}$ (1:1, v/v, 600 μL). ^1H NMR analysis of the mixture showed a **1:2:3** ratio of ~9:10:1 (Fig. 4). After evaporation of the solvent, MeOH was added up to a 0.012 M concentration of organic material, and the pH was adjusted to 1 by addition of CF_3COOH . An aqueous solution of HAuCl_4 (28.3 μL , 0.025 M) was then added, followed by an aqueous NaBH_4 solution (15 μL , 1 M) under rapid shaking. The black suspension was shaken for 2 h, and the supernatant was separated by decantation. The black solid was washed with EtOH (4 x 1 mL) and MeOH (3 x 1 mL), dissolved in Nanopure water (0.5 mL) and purified by centrifugal filtering (AMICON MWCO 10.000, 50 min, 10.000 rpm). The residue in the AMICON filter was dissolved in 0.5 mL of Nanopure water and lyophilized to afford 0.7 mg of GNP-1.

UV/Vis (H_2O , 0.1 mg/mL): surface plasmon band not observed. TEM: average gold diameter 1.8 ± 0.5 nm (Fig. 8). Average molecular formula estimated based on the size of the cluster obtained from the TEM micrographs: $\text{Au}_{201}(\text{C}_{49}\text{H}_{90}\text{N}_3\text{O}_{25}\text{S}_2)_{32}(\text{C}_{11}\text{H}_{21}\text{O}_6\text{S})_{35}(\text{C}_{79}\text{H}_{126}\text{N}_{27}\text{O}_{27}\text{S})_4$ (MW 95 KDa). ^1H NMR (500 MHz, $\text{CD}_3\text{OD}:\text{D}_2\text{O} = 1:1$) of the mixture used to prepare GNP and ^1H NMR (500 MHz, D_2O) of the GNP and are reported in Figure 4.

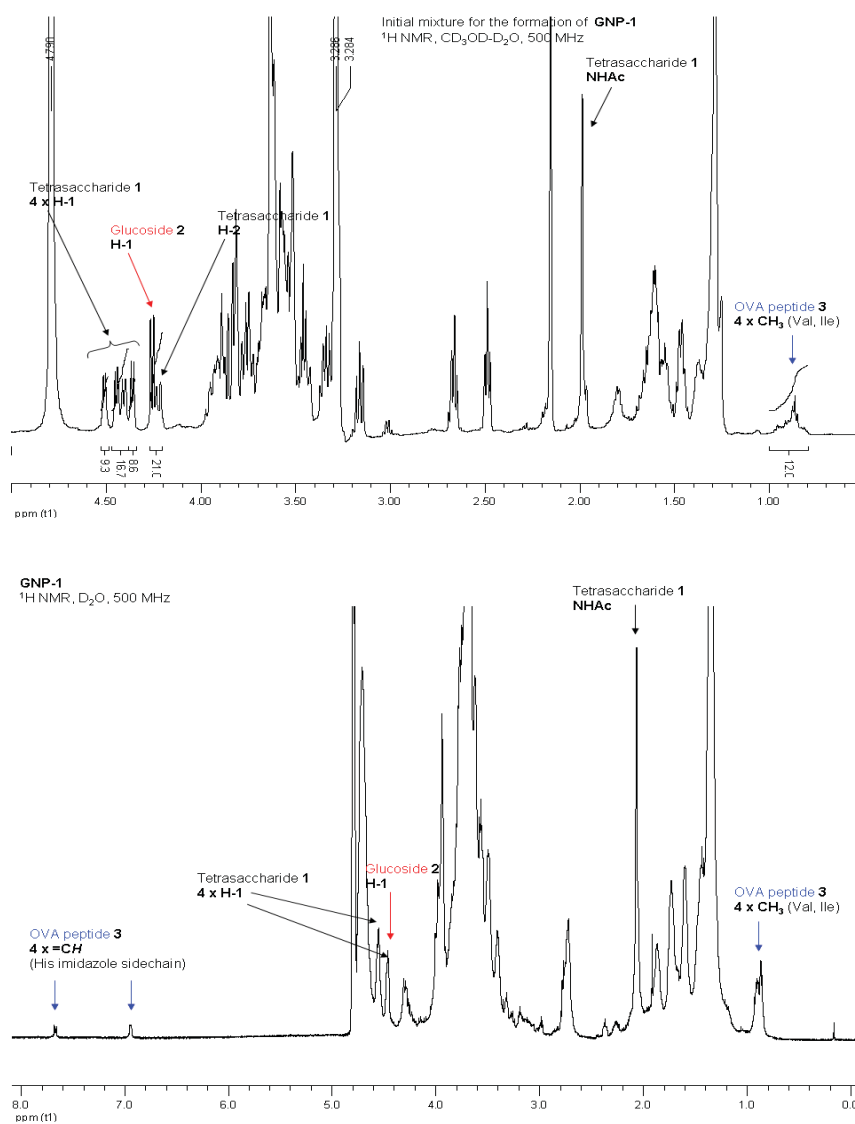


Figure 4: *Top panel:* ^1H NMR (500 MHz, $\text{CD}_3\text{OD}:\text{D}_2\text{O} = 1:1$) of the mixture used to prepare GNP-1. Integration of selected signals shows that the ratio between tetrasaccharide 1, glucose conjugate 2, and OVA peptide conjugate 3 is about 9:10:1. *Bottom panel:* ^1H NMR (500 MHz, D_2O , water suppression) of GNP-1. The selected signals show the presence of all three components (tetrasaccharide 1, glucose conjugate 2, and OVA peptide derivative 3) in the same nanoparticle.

GNP-2 (TetraPn:Glc = 50:50). Tetrasaccharide conjugate **1** (TetraPn)(4.6 mg, 3.9 μmol) and glucose conjugate **2** (1.1 mg, 3.9 μmol) were dissolved in D_2O (656 μL). ^1H NMR analysis of the mixture showed a ~1:1 ratio of **1** and **2** (Fig. 5). After evaporation of the solvent, MeOH was added up to a 0.012 M concentration of organic material. Next, an aqueous solution of HAuCl_4 (62.8 μL , 0.025 M) was added, followed by an aqueous NaBH_4 solution (33 μL , 1 M) under rapid shaking. The black suspension was shaken for 2 h, and then the supernatant was separated by decantation. The black solid was washed with EtOH (4 x 1 mL) and MeOH (3 x 1 mL), dissolved in Nanopure water (0.5 mL) and purified by centrifugal filtering (AMICON MWCO 10.000, 50 min, 10.000 rpm). The residue in the AMICON filter was dissolved in 0.5 mL of Nanopure water and lyophilized to afford 0.86 mg of GNP-2.

UV/Vis (H_2O , 0.1 mg/mL): surface plasmon band not observed. TEM: average gold diameter 1.9 ± 0.3 nm (Fig. 8). Average molecular formula: $\text{Au}_{225}(\text{C}_{49}\text{H}_{90}\text{N}_3\text{O}_{25}\text{S}_2)_{36}(\text{C}_{11}\text{H}_{21}\text{O}_6\text{S})_{35}$ (97 KDa). ^1H NMR (500 MHz, $\text{CD}_3\text{OD}:\text{D}_2\text{O} = 1:1$) of the mixture used to prepare GNP and ^1H NMR (500 MHz, D_2O) of the GNP and are reported in Figure 5.

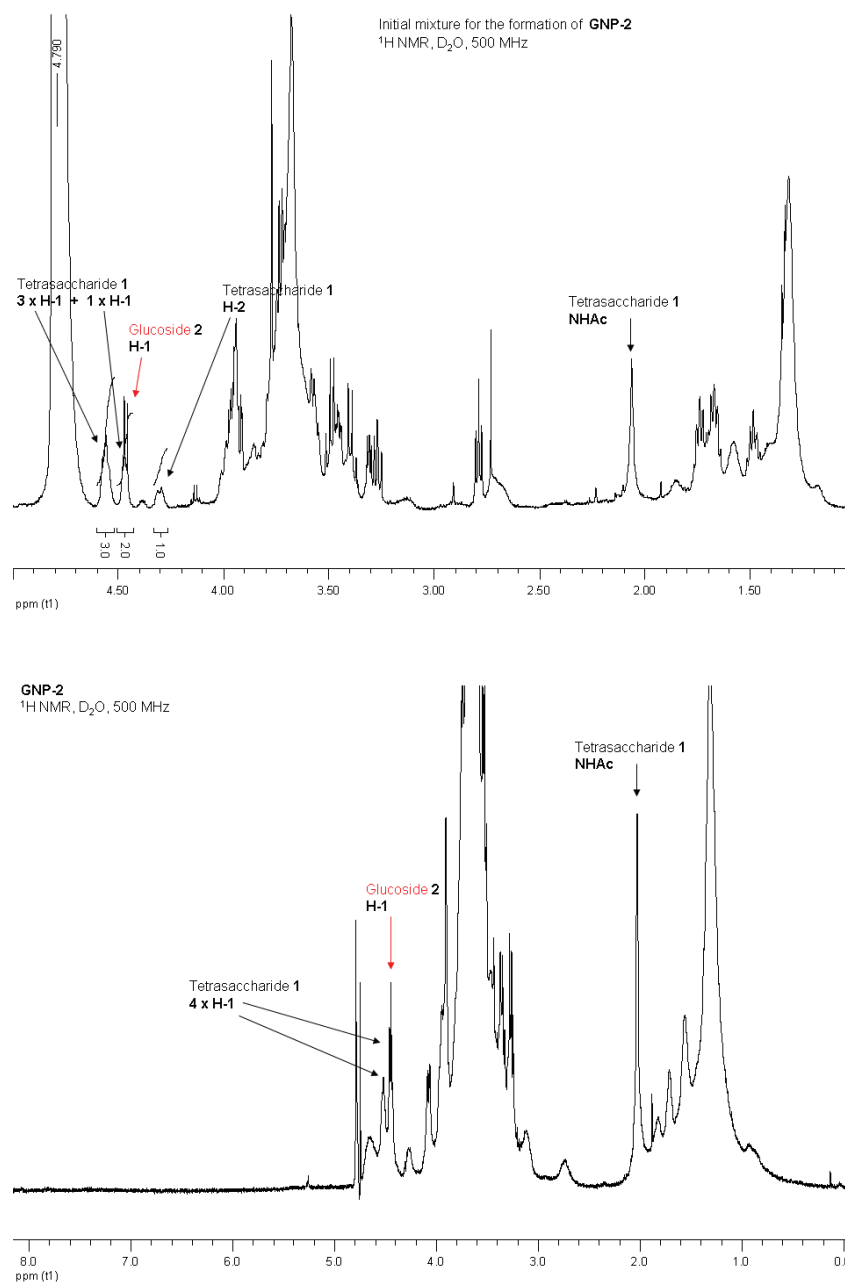


Figure 5: *Top panel:* $^1\text{H NMR}$ (500 MHz, D_2O) of the mixture used to prepare GNP-2. Integration of selected signals shows that the ratio between tetrasaccharide **1** and glucose conjugate **2** is about 1:1. *Bottom panel:* $^1\text{H NMR}$ (500 MHz, D_2O , water suppression) of GNP-2. The selected signals show the presence of both tetrasaccharide **1** and glucose conjugate **2** in the same nanoparticle.

GNP-3 (Glc:OVA = 90:10). OVA peptide derivative **3** (1.68 mg, 0.87 μmol) was dissolved in CF_3COOD (100 μL) and dried under air stream until formation of an oil. Glucose conjugate **2** (2.2 mg, 7.8 μmol) was then added and the mixture was dissolved in $\text{CD}_3\text{OD-D}_2\text{O}$ (1:1) (600 μL). ^1H NMR analysis of the mixture showed a compound **2:3** ratio of $\sim 9:1$ (Fig. 6). After evaporation of the solvent, MeOH was added up to a 0.012 M concentration of organic material. An aqueous solution of HAuCl_4 (70 μL , 0.025 M) was added, followed by an aqueous NaBH_4 solution (37 μL , 1 M) under rapid shaking. The black suspension was shaken for 2 h, and then the supernatant was separated by decantation. The black solid was washed with EtOH (4 x 1 mL) and MeOH (3 x 1 mL), dissolved in Nanopure water (3 mL) and purified by dialysis (Slide-A-Lyzer Dialysis cassette, Pierce, 10.000 MWCO) against 3 L of distilled water, recharging with fresh distilled water every 3–4 h over the course of 72 h. The solution in the membrane was then lyophilized to regain 0.60 mg of GNP-3. UV/Vis (H_2O , 0.1 mg/mL): surface plasmon band not observed. TEM: average gold diameter 1.9 ± 0.5 nm (Fig. 8). Average molecular formula: $\text{Au}_{225}(\text{C}_{11}\text{H}_{21}\text{O}_6\text{S})_{64}(\text{C}_{79}\text{H}_{126}\text{N}_{27}\text{O}_{27}\text{S})_7$ (76 KDa). ^1H NMR (500 MHz, $\text{CD}_3\text{OD:D}_2\text{O} = 1:1$) of the mixture used to prepare GNP and ^1H NMR (500 MHz, D_2O) of the GNP and are reported in Figure 6.

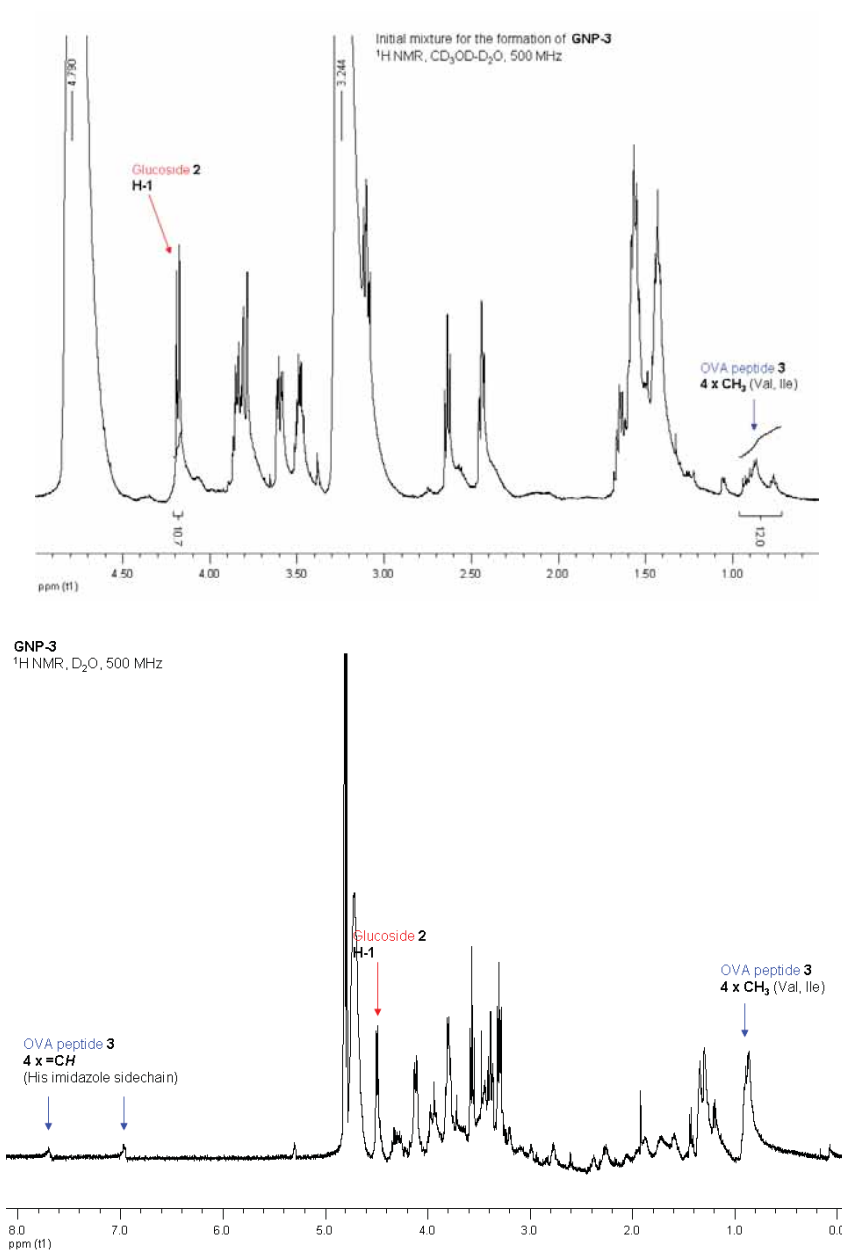


Figure 6: *Top panel:* $^1\text{H NMR}$ (500 MHz, $\text{CD}_3\text{OD:D}_2\text{O} = 1:1$) of the mixture used to prepare GNP-3. Integration of selected signals shows that the ratio between glucose conjugate **2** and OVA peptide derivative **3** is about 9:1. *Bottom panel:* $^1\text{H NMR}$ (500 MHz, D_2O , water suppression) of GNP-3. The selected signals show the presence of both glucose conjugate **2** and OVA peptide derivative **3** in the same nanoparticle.

GNP-4 (TetraPn:Glc:OVA = 20:70:10). OVA peptide derivative **3** (0.38 mg, 0.20 μmol) was dissolved in CF_3COOD (50 μL) and dried under air stream until formation of an oil. Tetrasaccharide conjugate **1** (TetraPn)(0.48 mg, 0.40 μmol) and glucose conjugate **3** (0.395 mg, 1.4 μmol) were added to the oil, and the mixture was dissolved in CD_3OD (600 μL). ^1H NMR analysis of the mixture showed a compound **1:2:3** ratio of $\sim 2:7:1$ (Fig. 7). After evaporation of the solvent, MeOH was added up to a 0.012 M concentration of organic material, and the pH was adjusted to 1 by addition of CF_3COOH . An aqueous solution of HAuCl_4 (16 μL , 0.025 M) was added, followed by an aqueous NaBH_4 solution (9 μL , 1 M) under rapid shaking. The black suspension was shaken for 2 h, and then the supernatant was separated by decantation. The black solid was washed with EtOH (4 x 1 mL) and MeOH (3 x 1 mL), dissolved in Nanopure water (0.5 mL) and purified by centrifugal filtering (AMICON MWCO 10.000, 50 min., 10.000 rpm). The residue in the AMICON filter was dissolved in 0.5 mL of water and lyophilized to afford 0.8 mg of GNP-4.

UV/Vis (H_2O , 0.1 mg/mL): surface plasmon band not observed. TEM: average gold diameter 1.7 ± 0.7 nm (Fig. 8). Average molecular formula: $\text{Au}_{201}(\text{C}_{49}\text{H}_{90}\text{N}_3\text{O}_{25}\text{S}_2)_{14}(\text{C}_{11}\text{H}_{21}\text{O}_6\text{S})_{50}(\text{C}_{79}\text{H}_{126}\text{N}_{27}\text{O}_{27}\text{S})_7$ (84 kDa). ^1H NMR (500 MHz, $\text{CD}_3\text{OD}:\text{D}_2\text{O} = 1:1$) of the mixture used to prepare GNP and ^1H NMR (500 MHz, D_2O) of the GNP and are reported in Figure 7.

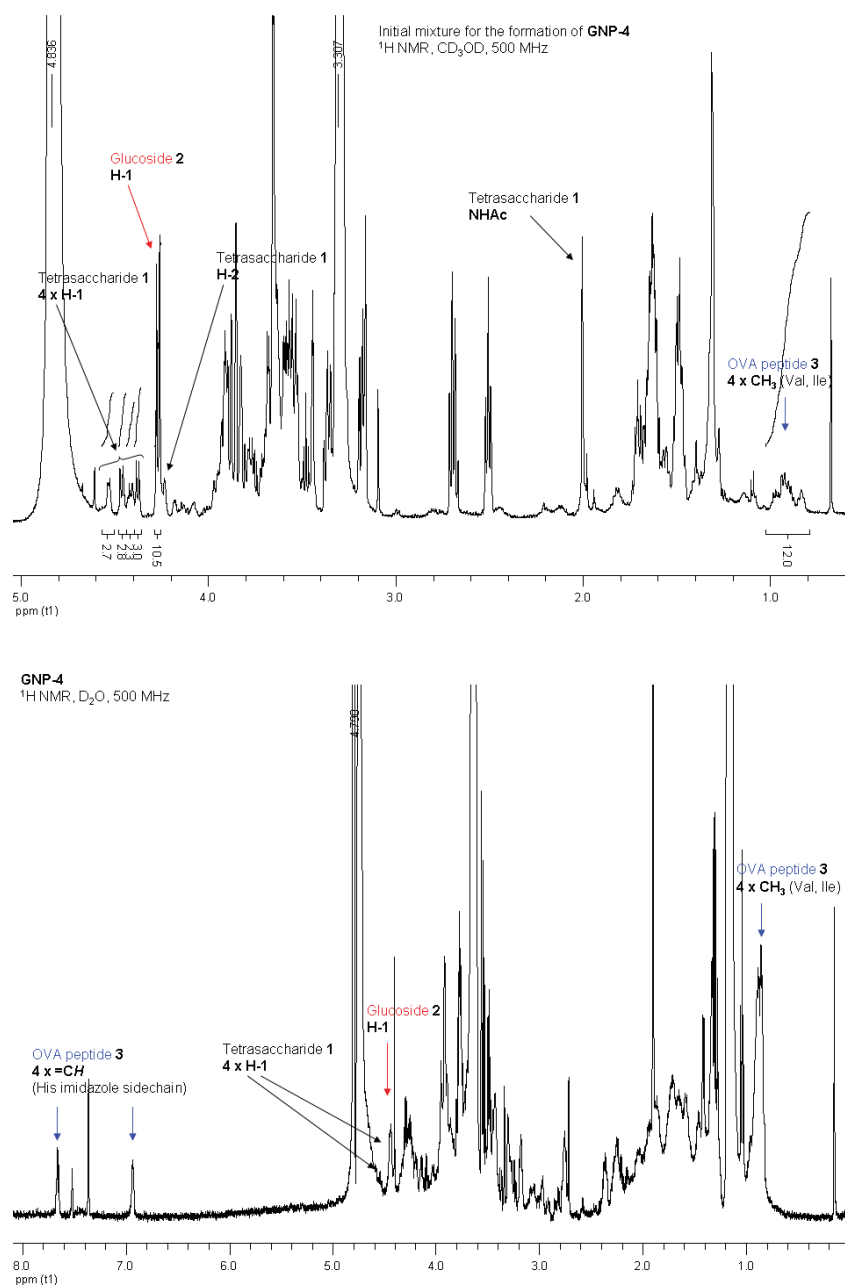


Figure 7: *Top panel:* $^1\text{H NMR}$ (500 MHz, CD_3OD) of the mixture used to prepare GNP-4. Integration of selected signals shows that the ratio between tetrasaccharide 1, glucose conjugate 2, and OVA peptide derivative 3 is about 2:7:1. *Bottom panel:* $^1\text{H NMR}$ (500 MHz, D_2O , water suppression) of GNP-4. The selected signals show the presence of all three components (tetrasaccharide 1, glucose conjugate 2, and OVA peptide derivative 3) in the same nanoparticle.

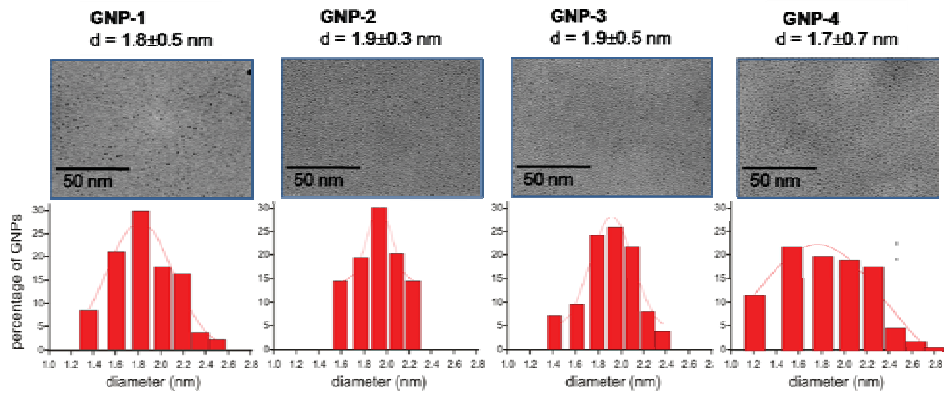


Figure 8: TEM micrographs and histograms of size distribution of gold GNPs.

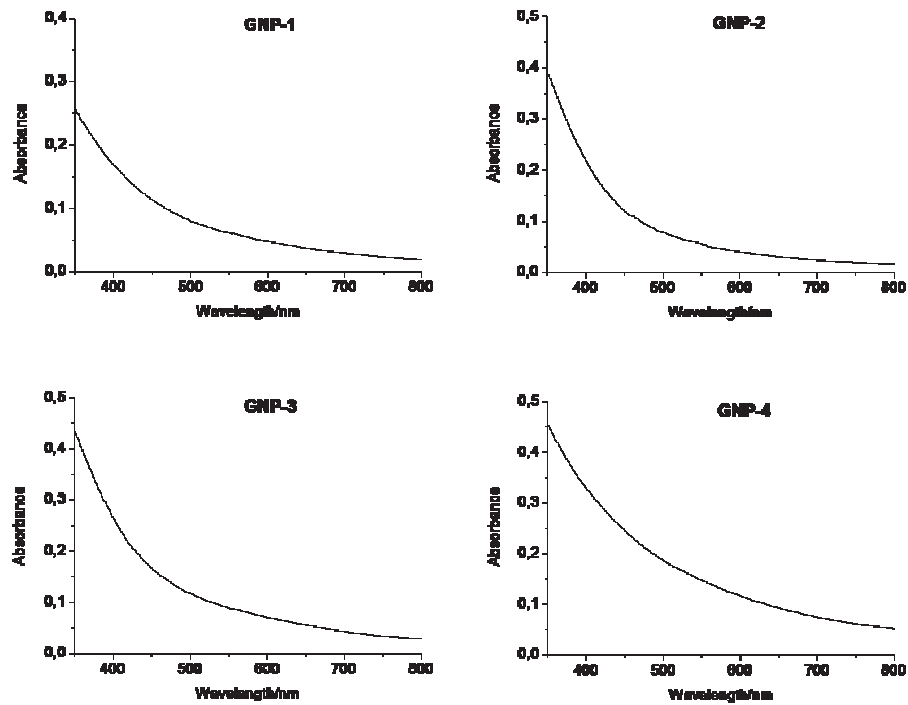


Figure 9: UV-visible adsorption spectra of gold GNPs at 0.1 mg/mL.



For reprint orders, please contact: reprints@futuremedicine.com

Gold nanoparticles as carriers for a synthetic *Streptococcus pneumoniae* type 14 conjugate vaccine

Aims: Coupling of capsular polysaccharides of pathogens to immunogenic protein carriers (conjugate vaccines) improves carbohydrate immune response. Our idea is to explore gold nanoclusters as carriers to prepare fully synthetic carbohydrate vaccines. **Materials & methods:** Gold glyconanoparticles bearing a synthetic tetrasaccharide epitope related to the *Streptococcus pneumoniae* type 14 capsular polysaccharide (Pn14PS), the T-helper ovalbumin 323–339 peptide (OVA_{323–339}), and D-glucose were prepared by a one-pot method. Their immunogenicity was tested in mice. Cytokine levels after spleen cell stimulation with OVA_{323–339} were analyzed using a luminex-multiplex cytokine assay. The capacity of the evoked antibodies to promote the uptake of *S. pneumoniae* type 14 by leukocytes was assessed. **Results & discussion:** Glyconanoparticles containing 45% of tetrasaccharide and 5% OVA_{323–339} triggered specific anti-Pn14PS IgG antibodies. Cytokine levels confirmed that glyconanoparticles led to T-helper cell activation. The anti-saccharide antibodies promoted the phagocytosis of type 14 bacteria by human leukocytes, indicating the functionality of the antibodies. **Conclusion:** Gold nanoparticles have great potential as carriers for the development of a great diversity of fully synthetic carbohydrate-based vaccines.

Original submitted 17 May 2011; Revised submitted 27 July 2011

KEYWORDS: antibody • gold nanoparticle • mice immunization • OVA_{323–339} peptide • *Streptococcus pneumoniae* • synthetic carbohydrate vaccine

Dodi Safari, Marco Marradi, Fabrizio Chiodo, Huberta A Th Dekker, Yulong Shan, Roberto Adamo, Stefan Oscarson, Ger T Rijkers, Martina Lahmann, Johannis P Kamerling, Soledad Penadés[‡] & Harm Snippe^{*‡}

^{*}Author for correspondence: Department of Medical Microbiology, University Medical Center Utrecht, Utrecht, The Netherlands
Tel.: +31 8875 53890
Fax: +31 3025 41770
h.snippe@umcutrecht.nl
[‡]Authors contributed equally
For a full list of affiliations please see page 662

Since carbohydrates are usually poorly immunogenic, strategies have been developed to improve their immune response [1]. One such strategy is the coupling of capsular polysaccharides of pathogens to suitable immunogenic protein carriers (conjugate vaccines) [2]. Although carbohydrate conjugate vaccines have been used to successfully prevent invasive pneumococcal infection [3] and the first synthetic human vaccine against *Haemophilus influenzae* type b has been approved [4], there are still many challenges and problems to be addressed in the area of carbohydrate vaccine design. One of these is the identification of the smallest protective epitopes for many pathogens. Furthermore, a main concern for synthetic vaccines is the risk of carrier-induced epitopic suppression [5].

Current advances in the identification and synthesis of carbohydrate epitopes have opened new ways to rationalize vaccine design [6]. Several strategies for the production of synthetic carbohydrate-based vaccines have been developed to overcome the hurdles encountered with the use of protein carriers and complex bacterial capsular polysaccharides [2,7]. These strategies include the use of liposomes [8,9], dendrimers [10], peptides [11] and micrometric beads [12] as scaffolds to obtain multivalent conjugate

vaccines [2]. Three-component synthetic vaccines containing a tumor-associated glycopeptide, a peptide T-helper epitope, and a Toll-like receptor 2 agonist [8] or L-rhamnose [13] were found to elicit high titers of IgG antibodies in mice.

Nanotechnology offers an alternative to conventional vaccine technologies and can improve vaccine development [14,15]. The conjugation of biomolecules to gold nanoparticles has been extensively explored because of their relative inertness, low toxicity and the chemistry of their surface is easy to control [16]. The opportunity of modifying the surface of nanoparticles to achieve simultaneous antigen-loading, adjuvant codelivery, improved circulation times and targeting properties has increased the interest in nanoparticle-based vaccines [14]. Micrometric gold particles have been used to administer DNA vaccines directly into human skin cells by 'gene gun' inoculations [17] that facilitate DNA delivery and gene expression in order to induce protective levels of antibody against hepatitis B virus [18] and influenza [19]. Metallic nanoparticles (5–10 nm) coated with tiopronine [20] or Cys-modified peptides [21] can trigger macrophage activation *in vitro*, demonstrating the possibility to modulate cell-mediated immune responses with suitable nanotools.

This study explores the potential application of gold glyconanoparticles (GNPs) as a carrier for vaccine candidates against *Streptococcus pneumoniae*, a major cause of invasive respiratory tract infections in both infants and the elderly [22]. A nonconjugated polysaccharide vaccine against the 23 most prevalent pneumococcal serotypes is currently available [23]. However, this vaccine elicits a poor antibody response in high-risk groups, especially neonates and children. Three polysaccharide–protein conjugate vaccines against *S. pneumoniae* are currently licensed. Conjugate vaccines of natural capsular polysaccharides coupled to the carrier protein CRM₁₉₇ (cross-reacting material, a nontoxic variant of diphtheria toxin) are immunogenic in young children and protect against invasive pneumococcal disease [22,24]. In subsequent studies, synthetic oligosaccharide fragments of *S. pneumoniae* capsular polysaccharides conjugated to protein carriers have been investigated for their effectiveness as vaccine candidates [22]. The synthetic branched tetrasaccharide β -D-Galp-(1–4)- β -D-Glcp-(1–6)-[β -D-Galp-(1–4)-] β -D-GlcpNAc-(1-) (Tetra), which corresponds to a single repeating unit of the *S. pneumoniae* type 14 capsular polysaccharide (Pn14PS), was identified as the smallest structure capable of evoking opsonophagocytic antibodies against *S. pneumoniae* type 14 when conjugated to CRM₁₉₇ protein [25,26].

We have previously developed a simple and versatile method to prepare sugar-functionalized gold nanoclusters with a polyvalent carbohydrate display and a globular shape [27,28]. This method allows the generation of complex gold GNPs by combining different molecules on the same nanoplatfrom in a controlled fashion [29]. GNPs are water-soluble, noncytotoxic, and stable under physiological conditions and have turned out to be useful tools with which to study and intervene in carbohydrate-mediated biological processes [30,31]. Based on our experience in the preparation of multicomponent biofunctional gold nanoclusters [29], we reasoned that a synthetic vaccine could also be constructed using gold nanoparticles as carriers of the vaccine components. Our aim was to develop new carbohydrate vaccines by functionalizing covalently the surface of gold nanoparticles with sugar antigens and T-helper peptides.

Herein, a series of 2-nm hybrid gold nanoparticles (GNP-1–4) displaying different ratios of the branched tetrasaccharide unit of Pn14PS [26], the T-helper ovalbumin 323–339 peptide (OVA_{323–339}) [32,33], and the

monosaccharide D-glucose, were prepared (FIGURE 1). The immunogenicity of the GNPs was studied in BALB/c mice.

Materials & methods

■ Preparation of thiol-ending conjugates

The synthesis of 1-(3-[β -D-Galp-(1–4)- β -D-Glcp-(1–6)-[β -D-Galp-(1–4)-] β -D-GlcpNAc]propyl)-3-(23-mercapto-3,6,9,12-tetraoxatricosyl)thiourea (1) has been carried out following a modified protocol [34] and is reported in the SUPPLEMENTARY MATERIAL (see online, www.futuremedicine.com/doi/suppl/10.2217/nnm.11.151).

5-(Thio)pentyl β -D-glucopyranoside (2) was synthesized as previously described [28].

The OVA_{323–339} peptide with an additional glycine and mercapto-propionic acid linker at the N-terminus HS(CH₂)₂C(O)GISQAVHAAHAEINEAGR (3) was obtained from GenScript Corp (Piscataway, NJ, USA).

■ Preparation of hybrid gold nanoparticles

A slight modification of an earlier reported single-step procedure [29] was applied to prepare the GNPs. A solution of tetrachloroauric acid (HAuCl₄, Strem Chemicals, 0.025 M, 1 equivalent) in water was added to a 0.012 M (five equivalents) methanolic solution of the mixture of thiol-ending conjugates 1, 2 and 3 (FIGURE 1 & SUPPLEMENTARY FIGURE 1) in different ratios. An aqueous solution of NaBH₄ 1 M (21 equivalents) was then added in four portions, with vigorous shaking. The black suspension formed was shaken for an additional 2 h at 25°C after which the supernatant was removed and analyzed. The residue was dissolved in a minimal volume of Nanopure® water and purified by dialysis or by centrifugal filtering. For the ligand analysis, proton nuclear magnetic resonance (¹H NMR) spectra of the initial mixture and of the supernatant after GNP formation were recorded (SUPPLEMENTARY FIGURES 3–6). The ratio of the ligands in the GNPs (TABLE 1) was evaluated by integrating the signals of the anomeric protons of tetrasaccharide 1, the anomeric proton of glucoside 2 and the methyl groups of isoleucine and valine of OVA_{323–339} peptide conjugate 3. The particle size distribution (average gold diameter) of the gold nanoparticles was determined from the transmission electron microscopy (TEM) micrographs (SUPPLEMENTARY FIGURE 9). The average number of gold atoms were calculated on the basis of the average diameter obtained by TEM micrographs, and molecular formulas of the GNPs were estimated according to previous work

(TABLE 1) [35]. Details of the chemical syntheses and analytical data (^1H NMR, infrared spectroscopy, TEM and UV–visible spectrophotometry) of the hybrid GNPs are provided in the SUPPLEMENTARY MATERIAL.

■ Mouse immunization studies

Inbred 6-week-old female BALB/c mice were immunized intracutaneously with a series of GNPs (6 μg), which contained the tetrasaccharide (approximately 3 μg per dose) and/or OVA_{323–339} peptide (approximately 3 μg per dose), using a mixture of monophosphoryl lipid-A and Quilaja purified saponin (Quil-A) as adjuvants (10 μg monophosphoryl lipid-A [derived from *Salmonella minnesota* R595 LPS; Ribi ImmunoChem Research Inc., Hamilton, MT, USA] and 20 μg Quil-A [Quil-A was a gift from Erik B Lindblad, Brenntag Biosector, Vedbaek, Denmark]) as described previously (SUPPLEMENTARY TABLE 1) [26]. The GNPs were injected at four different sites in the proximity of the lymph nodes of the axillae and the groins. The following antigens served as positive controls: *S. pneumoniae* type 14 polysaccharide conjugated to CRM₁₉₇ (Pn14PS-CRM₁₉₇; Wyeth Research, Pearl River, NY, USA, 2.5 μg of carbohydrate), free OVA_{323–339} peptide (2.5 μg), and OVA_{323–339} peptide conjugated to CRM₁₉₇ protein (OVA_{323–339} peptide-CRM₁₉₇, 50 μg). The OVA_{323–339} peptide-CRM₁₉₇ was constructed by coupling of the OVA_{323–339} peptide to CRM₁₉₇ protein as described previously [26]. All control antigens were injected into mice in combination with the adjuvants mentioned above (SUPPLEMENTARY TABLE 1). All booster immunizations were given without adjuvant and were performed on weeks 5 and 10. Blood samples were taken before and after the booster and the sera were stored at -20°C .

■ Measurement of type-specific antibodies & phagocytosis titer

The ELISA was performed to measure the antibodies to native Pn14PS, to the synthetic branched tetrasaccharide, and to OVA as described previously [26].

The opsonophagocytosis assay was performed by using human polymorphonuclear leukocytes isolated from the peripheral blood of healthy donors, as previously described [26,36]. Details of the protocol are provided in the SUPPLEMENTARY MATERIAL.

■ *In vitro* spleen cell stimulation

Mouse spleens ($n = 2$) were isolated 3 weeks after the second booster immunization. Spleen

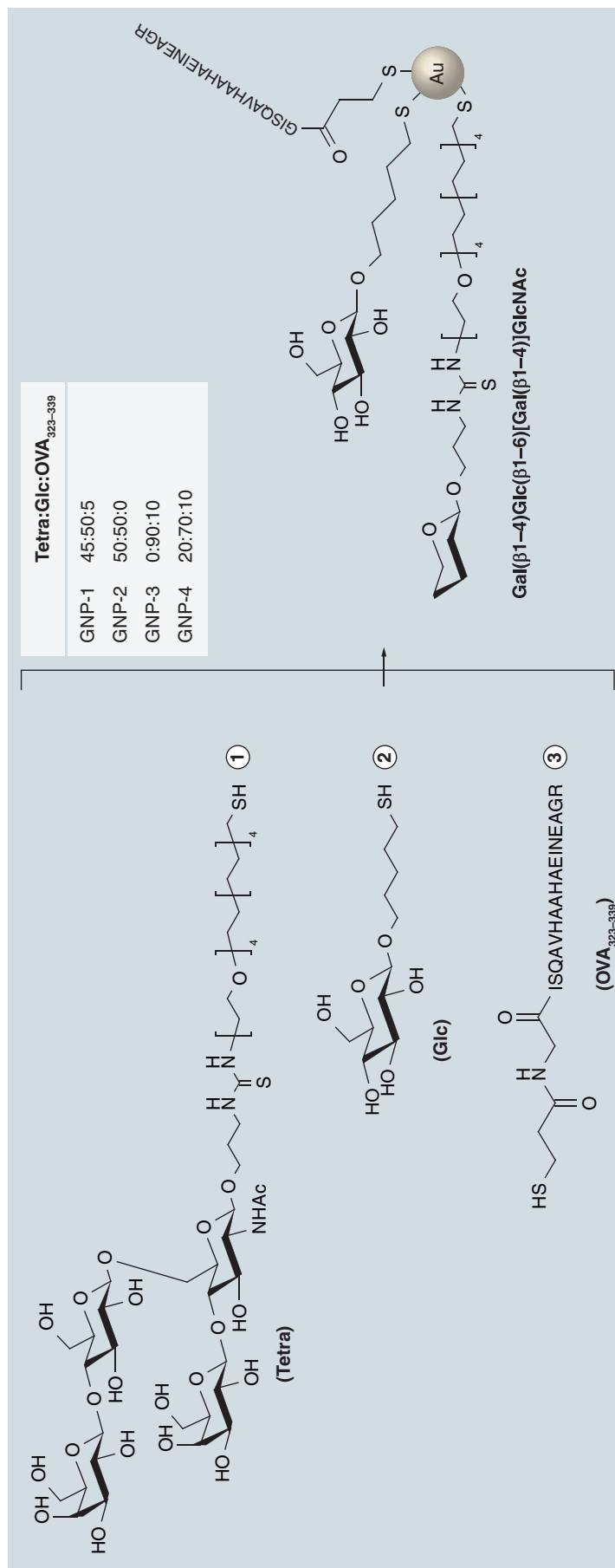


Figure 1. One-step synthesis of hybrid gold glyconanoparticles incorporating different molar ratios of branched tetrasaccharide 1 (Tetra = Gal-Glc-[Gal]-GlcNac), D-glucose (Glc) conjugate 2, and OVA_{323–339} peptide conjugate 3. Reagents and conditions for the one-step preparation of GNPs: HAuCl₄, NaBH₄; H₂O/MeOH; 2 h; 25°C. For clarity, all conjugates are depicted as thiols. The dimension of the gold nanoclusters is approximately 2 nm and is not in scale with the size of the conjugates. GNP: Glyconanoparticle; OVA: Ovalbumin.

Table 1. Physicochemical properties of the hybrid gold nanoparticles prepared in this study.

GNPs	Mean metal core diameter (nm) [†]	Average number of gold atoms [‡]	Average molecular weight (kDa)	Molar ratio of Tetra:Glc:OVA _{323–339} [§]	Estimated average molecular formula
GNP-1 [¶]	1.8 ± 0.5	201	95	45:50:5	Au ₂₀₁ (Tetra) ₃₂ (Glc) ₃₅ (OVA _{323–339}) ₄
GNP-2	1.9 ± 0.3	225	97	50:50:0	Au ₂₂₅ (Tetra) ₃₆ (Glc) ₃₅
GNP-3	1.9 ± 0.5	225	76	0:90:10	Au ₂₂₅ (Glc) ₆₄ (OVA _{323–339}) ₇
GNP-4	1.7 ± 0.7	201	84	20:70:10	Au ₂₀₁ (Tetra) ₁₄ (Glc) ₅₀ (OVA _{323–339}) ₇

[†]Diameter of the gold nanocluster (as measured by transmission electron microscopy).

[‡]Average number of gold atoms per nanoparticle was calculated from the size of the gold cluster obtained by transmission electron microscopy, as reported previously [35].

[§]Molar ratio of conjugates per nanoparticle was determined by analyzing the mixtures using NMR before and after nanoparticle formation (SUPPLEMENTARY MATERIAL,

METHODS SECTION).

[¶]Two different batches of GNP-1 were independently prepared and displayed the same physicochemical and immunochemical properties.

GNP: Glyconanoparticle; OVA: Ovalbumin.

cell suspensions (10⁷ cells/ml) were stimulated with OVA_{323–339} peptide (10 µg) in Roswell Park Memorial Institute 1640 tissue culture medium supplemented with 10% fetal calf serum and gentamycin. The cells were cultured at 37°C, in 100% relative humidity, and with 5% CO₂ in air. Finally, the supernatants were collected at 72 h after initiation of the cultures, and stored at -70°C until use. Six different cytokines were selected to screen the supernatants: IL-2 (171-G5003M), TNF-α (171-G5023M), and IFN-γ (171-G5017M) as Th1 cytokines; IL-4 (171-G5005M) and IL-5 (171-G5006) as Th2 cytokines; and IL-17 as Th17 marker (171-G50013M). We used a luminex-multiplex cytokine assay, following the manufacturer's instructions (Bio-Rad, Hercules, CA, USA). The lower limits of detection were 0.31 pg/ml (IL-2), 0.71 pg/ml (IL-4), 0.24 pg/ml (IL-5), 0.20 pg/ml (IL-17), 0.48 pg/ml (IFN-γ), and 5.2 pg/ml (TNF-α).

■ Statistical methods

Unpaired *t*-test was used to determine differences in antibody titer or cytokine level with a *p*-value ≤0.05 considered to be statistically significant (Graphad Prism 5.00).

■ Other methods

General information about chemicals and techniques, and details of the synthesis of branched tetrasaccharide conjugate 1, the preparation and characterization of hybrid gold nanoparticles GNP-1–4, detection of type-specific antibodies by ELISA and phagocytosis titers can be found in the SUPPLEMENTARY MATERIAL.

Results

■ Preparation & characterization of hybrid gold GNPs

Hybrid gold GNPs (GNP1–4) used in this study were prepared by *in situ* reduction of an Au(III) salt in the presence of mixtures of thiol-ending conjugates 1, 2 and 3, as gold binds thiols with a high

affinity [37]. Conjugates 1, 2 and 3 are constituted by the synthetic branched tetrasaccharide β-D-Galp-(1–4)-β-D-Glcp-(1–6)-[β-D-Galp-(1–4)-β-D-GlcpNAc-(1–), D-glucose, and the OVA_{323–339} peptide and thiol-ending linkers of different length and nature (FIGURE 1). The conjugates were used in excess with respect to the Au(III) salt in order to assure full coverage of the nascent gold nanoclusters and to ensure that their molar ratios in solution are maintained on the nanoparticles surface. The one-step method, which has been used, allows the incorporation of the conjugates in different and defined proportions on the same gold nanoparticles [28,29]. GNP-1 and GNP-4 were prepared from mixtures of 1, 2 and 3 in 45:50:5 and 20:70:10 molar ratios, respectively. The preparation of GNP-1 was also repeated using a different batch of tetrasaccharide conjugate 1. The resulting nanoparticles (GNP-1b) showed the same physicochemical properties and elicited a similar immune response (see below), indicating that the methodology is reproducible. GNP-2, containing tetrasaccharide conjugate 1 and glucose conjugate 2 in 50:50 ratio, was prepared to study the immune response to the tetrasaccharide in the absence of the immunodominant OVA peptide conjugate 3. GNP-3, containing ~10% of OVA peptide 3 and ~90% of glucose conjugate 2, served as the control system. The presence of conjugates on the GNPs was assessed qualitatively by comparing the ¹H NMR spectra of the initial mixtures and the formed GNPs (SUPPLEMENTARY FIGURES 3–6). The GNPs were monodisperse and showed exceptionally small gold core diameters, ranging from 1.7 to 1.9 nm (assuming a spherical shape), as demonstrated by TEM analysis (SUPPLEMENTARY FIGURE 9). The lack of a gold surface plasmon band at 520 nm in the UV–visible spectra (SUPPLEMENTARY FIGURE 10) confirmed the small core size of the GNPs. All of the prepared GNPs were water-soluble and stable for months in solution. Moreover, they survived freeze-drying processes and could be redispersed in water

without losing their physicochemical properties and integrity. Average molecular formulae and weights of the GNPs were estimated according to the literature [35], and are given in TABLE 1.

■ The immunogenicity of hybrid gold GNPs

Specific IgG antibodies against the native Pn14PS, the synthetic branched tetrasaccharide, and the OVA₃₂₃₋₃₃₉ peptide were determined in the sera of the immunized mice using ELISA. The IgG antibodies induced by GNP-1 (Tetra:Glc:OVA₃₂₃₋₃₃₉ = 45:50:5) bound to native Pn14PS (FIGURE 2A), but the titer was one log₁₀ lower than the response to the positive control antigen Pn14PS-CRM₁₉₇. Immunization with GNP-2 (Tetra:Glc = 50:50) or with GNP-3 (Glc:OVA₃₂₃₋₃₃₉ = 90:10), did not elicit any specific IgG antibodies against Pn14PS (FIGURE 2A). When GNP-2 + GNP-3 were admixed a marginal response was obtained. Immunization with GNP-4 (Tetra:Glc:OVA₃₂₃₋₃₃₉ = 20:70:10) elicited an even lower level of specific IgG antibodies against Pn14PS than GNP-1, bearing twice as much tetrasaccharide (FIGURE 2A & SUPPLEMENTARY TABLE 1). It can thus be concluded that the presence of the T-cell epitope OVA₃₂₃₋₃₃₉ peptide in the GNP is a prerequisite for the induction of an antibody response to the tetrasaccharide. The anti-Pn14PS IgG subclass

antibodies distribution was also investigated. Immunization with GNP-1 or GNP-4 elicited anti-Pn14PS IgG₁, IgG_{2b} and IgG₃ antibodies (FIGURE 2B). The titer of IgG_{2a} antibody against Pn14PS was not detected in the mice group immunized with GNP comparing to the ones immunized with Pn14PS-CRM₁₉₇ (FIGURE 2B).

The antibody response to the tetrasaccharide was determined on the conjugate constructed from the branched tetrasaccharide and bovine serum albumin protein. Sera obtained from mice immunized with GNP-1 (Tetra:Glc:OVA₃₂₃₋₃₃₉ = 45:50:5) recognized the branched tetrasaccharide structure (FIGURE 3B).

The OVA₃₂₃₋₃₃₉ peptide, a T-cell epitope of the OVA protein, when exposed on GNPs preparations elicited negligible levels of IgG antibodies against OVA (FIGURE 3A). Similar results [SAFARI D ET AL., UNPUBLISHED DATA] were obtained by ELISAs using plates coated with the OVA₃₂₃₋₃₃₉ peptide conjugated to bovine serum albumin. Overall, these data indicate that immunization with OVA₃₂₃₋₃₃₉-containing GNPs (GNP-1, GNP-3 and GNP-4) did not induce antibodies against the complete OVA protein or against this specific peptide (FIGURE 3A). In control groups of mice, significant specific IgG antibodies to OVA were induced with the OVA-CRM₁₉₇ conjugate and to a lesser degree with the peptide alone (FIGURE 3A).

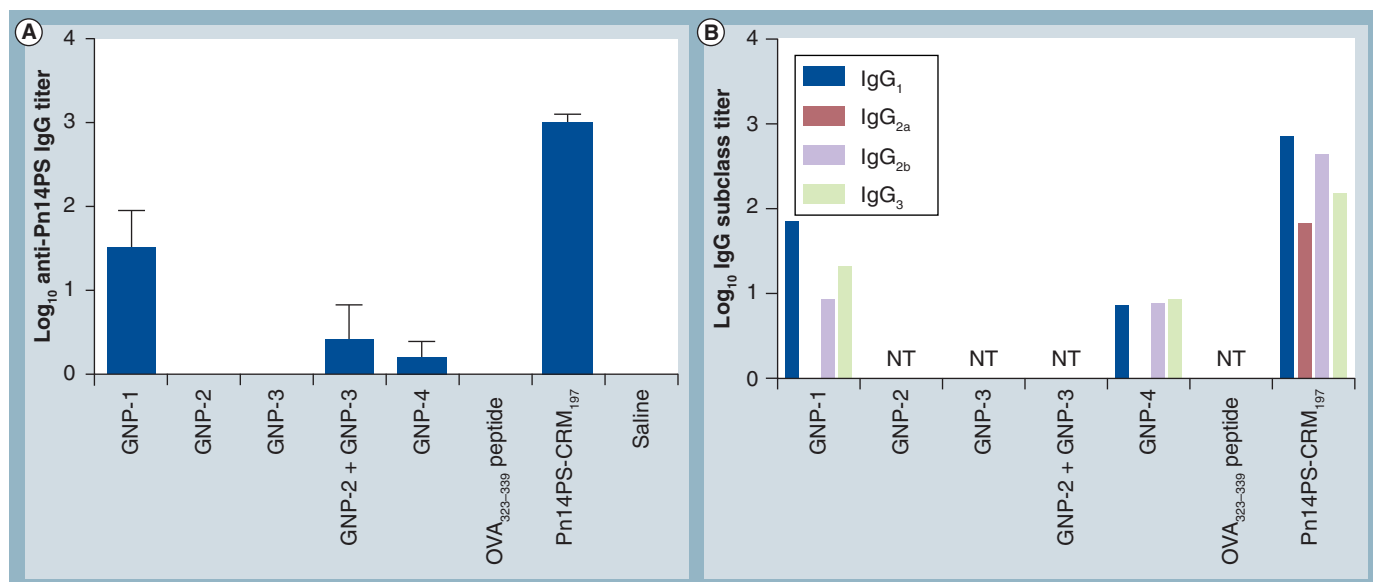


Figure 2. Specific anti-*Streptococcus pneumoniae* type 14 polysaccharide IgG total and IgG subclass distribution antibodies.

Groups of mice were immunized with series of GNPs with adjuvant coadministration at the primary injection and sera were collected 2 weeks after the second booster injection, which was given without adjuvant (for more details, see SUPPLEMENTARY TABLE 1). The GNPs differed in their tetrasaccharide:glucose:OVA-peptide molar ratio (TABLE 1). Pn14PS-CRM₁₉₇ and saline buffer immunization served as the positive and negative control, respectively. ELISA was performed to measure the (A) specific anti-Pn14PS IgG total and (B) the IgG subclass distribution antibodies with the native polysaccharide of Pn14PS as a coating material.

CRM: Cross-reactive material; GNP: Glyconanoparticle; NT: Not tested; OVA: Ovalbumin; Pn14PS: *Streptococcus pneumoniae* type 14 capsular polysaccharide.

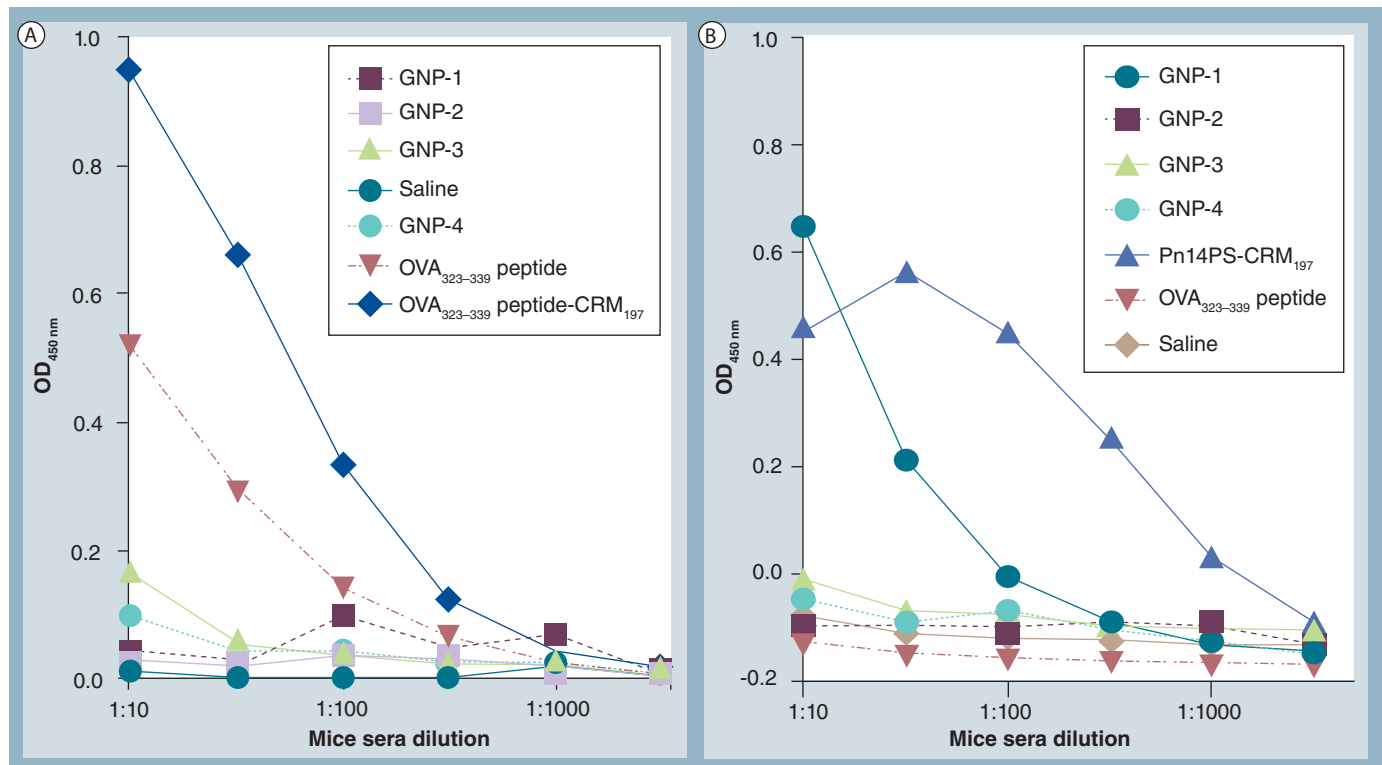


Figure 3. Level of antibodies against the ovalbumin protein and branched oligosaccharides fragment Gal-Glc-(Gal)-GlcNAc-Gal structure of Pn14PS. Pooled mice sera were tested by ELISA for the presence of (A) IgG antibodies against OVA protein and (B) the branched oligosaccharides structure of Pn14PS. The sera were obtained from mice previously immunized with a series of GNPs and control sera were obtained from mice immunized with CRM₁₉₇-OVA₃₂₃₋₃₃₉ peptide and free OVA₃₂₃₋₃₃₉ peptide. The level of antibodies was expressed as OD at 450 nm. CRM: Cross-reactive material; GNP: Glyconanoparticle; OD: Optical density; OVA: Ovalbumin; Pn14PS: *Streptococcus pneumoniae* type 14 capsular polysaccharide.

■ Phagocytic capacity of sera obtained from the GNPs immunization

An opsonophagocytosis assay that serves as a correlate of protection for candidate vaccines was used to test the functionality of the anti-saccharide antibodies. To that end, the activity of sera from mice immunized with different GNPs was tested in a phagocytosis assay using *S. pneumoniae* type 14 bacteria and human polymorphonuclear cells. Sera obtained from mice immunized with GNP-1 were able to opsonize *S. pneumoniae* type 14 bacteria, although in a lower fashion than sera from mice immunized with Pn14PS-CRM₁₉₇. The other GNPs, including GNP-4 and the mixture of GNP-2 + GNP-3, were not capable of inducing *S. pneumoniae* type 14-opsonizing antibodies (FIGURE 4).

■ Cytokine levels after spleen cell stimulation

To investigate whether OVA₃₂₃₋₃₃₉ peptide-containing GNPs can actually lead to T-lymphocyte activation, spleen cells from mice treated with GNP-1, GNP-2, GNP-3, and a

mixture of GNP-2+GNP-3 were (re)stimulated *in vitro* with the OVA₃₂₃₋₃₃₉ peptide and the cytokine levels were measured. Cytokines are important mediators of a number of critical steps during the immune response [38,39]. Spleen cells of mice previously immunized with OVA₃₂₃₋₃₃₉ peptide-containing GNPs (GNP-1, GNP-3 or the combination GNP-2+GNP-3) did respond to *in vitro* restimulation by producing IL-2, IL-4, IL-17 and IFN- γ (FIGURE 5). Induction of IL-5 occurred only in the cells from mice immunized with GNP-1, which correlates with the production of specific IgG antibodies to Pn14PS *in vivo* (FIGURES 2 & 5C). *In vitro* stimulation with the complete OVA protein led to a lower but otherwise similar cytokine-production profile [SAFARI D ET AL., UNPUBLISHED DATA]. Overall, the data indicate that immunization with either GNP-1, GNP-3, or the combination GNP-2 + GNP-3 always resulted in the activation of T cells, but that specific antibody production to the branched tetrasaccharide structure or native Pn14PS only occurred, if both the tetrasaccharide and OVA₃₂₃₋₃₃₉ peptide (GNP-1) were presented on the same gold GNP.

Discussion

Metal-based GNPs are biofunctional nanomaterials that combine the unique physical, chemical and optical properties of the metallic nucleus with the characteristics of the carbohydrate coating [30,31]. In this study, we propose gold nanoclusters as a versatile carrier to incorporate the varying density of the synthetic branched tetrasaccharide β -D-Galp-(1-4)- β -D-Glcp-(1-6)-[β -D-Galp-(1-4)-] β -D-GlcpNAc-(1-), related to Pn14PS, OVA₃₂₃₋₃₃₉ peptide and glucose. In order to prepare the gold GNPs, spacers ended in a thiol group were conjugated to the branched tetrasaccharide, D-glucose or OVA₃₂₃₋₃₃₉ (FIGURE 1). The nature and length of the spacers have been selected to control the presentation of the tetrasaccharide on the cluster surface. The glucose conjugate 2 was used as an inner component to assist water dispersibility and biocompatibility. The short linker (five aliphatic carbon atoms) of 2 was chosen to allow the tetrasaccharide fragment moiety to protrude above the glucose shell of GNPs. The tetrasaccharide was conjugated to a longer amphiphilic linker (eleven aliphatic carbon atoms + tetra-ethylene glycol). The aliphatic part of the linkers allows good self-assembled monolayer packaging and confers rigidity to the inner organic shell to protect the gold core, while the external polyether moiety, due to its flexibility upon solvation in water, assists water solubility and prevents nonspecific adsorption of proteins [28,40].

In this study, a combination of two adjuvants (monophosphoryl lipid-A and Quil-A) was given at the time of primary immunization. In the booster immunizations no adjuvants were added. We selected these two adjuvants because of their excellent performance in previous studies from our group [41].

We found that GNPs coated with the tetrasaccharide and OVA₃₂₃₋₃₃₉ peptide induce specific IgG antibodies that recognize the branched tetrasaccharide homologue β -D-Galp-(1-4)- β -D-Glcp-(1-6)-[β -D-Galp-(1-4)-] β -D-GlcpNAc-(1-3)- β -D-Gal-(1-) [26] and the native polysaccharide of Pn14PS. The different molar ratio of tetrasaccharide conjugate 1, glucose conjugate 2, and OVA₃₂₃₋₃₃₉ peptide conjugate 3 in the GNPs has a key effect on the immunogenic response. The GNP-4 with a molar ratio Tetra:Glc:OVA₃₂₃₋₃₃₉ = 20:70:10 induced a very low titer of anti-Pn14PS IgG antibodies compared with the GNP-1, which has a molar ratio Tetra:Glc:OVA₃₂₃₋₃₃₉ = 45:50:5. These experimental data indicate that the

tetrasaccharide:peptide ratio on the gold surface is of crucial importance to obtain significant levels of IgG antibodies. GNPs bearing a 40:10 tetrasaccharide: peptide ratio did not improve the immune response either against the tetrasaccharide or the Pn14PS [SAFARI D ET AL., UNPUBLISHED DATA]. Attempts to increase the amount of peptide up to 20% on the gold surface resulted in water-insoluble GNPs. The ligand density and the nature of spacers used to separate a selected ligand from the gold cluster are also important factors for immunogenicity.

It is worth mentioning that a different batch of GNP-1 (named GNP-1b) was also used in mice immunization (SUPPLEMENTARY FIGURE 11). While the primary immunizations were always performed with 6 μ g of these nanoparticles, the booster dosage of GNP-1b was augmented fivefold (30 μ g) with respect to GNP-1 (6 μ g). Following this, an increase in the level of specific antibodies induced by GNP-1b against Pn14PS was observed [SAFARI D ET AL., UNPUBLISHED DATA].

Another finding is that the presence of the T-cell-stimulating peptide OVA₃₂₃₋₃₃₉ in the hybrid GNPs was crucial for the induction of specific carbohydrate-directed IgG antibodies. We found that GNPs that do not contain OVA₃₂₃₋₃₃₉ peptide (GNP-2) were not able to elicit

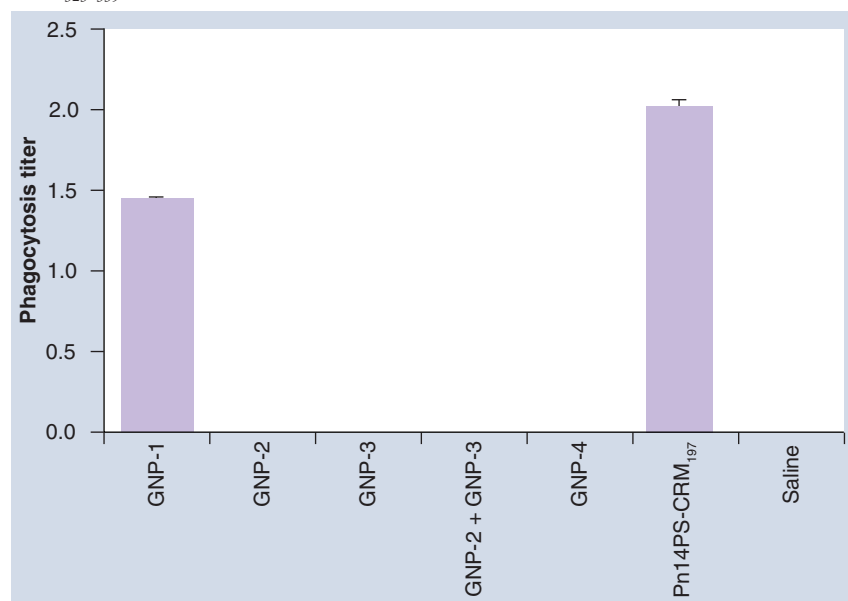


Figure 4. Phagocytosis titer. The phagocytic capacity of sera was measured using fluorescein isothiocyanate (FITC)-labeled heat-inactivated *Streptococcus pneumoniae* type 14 bacteria and polymorphonuclear leukocytes. Sera were collected 1 week after the second booster injection. Pn14PS-CRM₁₉₇ and saline buffer immunization served as a positive and negative control, respectively. The sera were heat inactivated and supplemented with 2% complement. The titers are expressed as the log₁₀ of the serum dilution during phagocytosis resulting in 25% of polymorphonuclear leukocytes being positive for FITC. CRM: Cross-reactive material; GNP: Glyconanoparticle; Pn14PS: *Streptococcus pneumoniae* type 14 capsular polysaccharide.

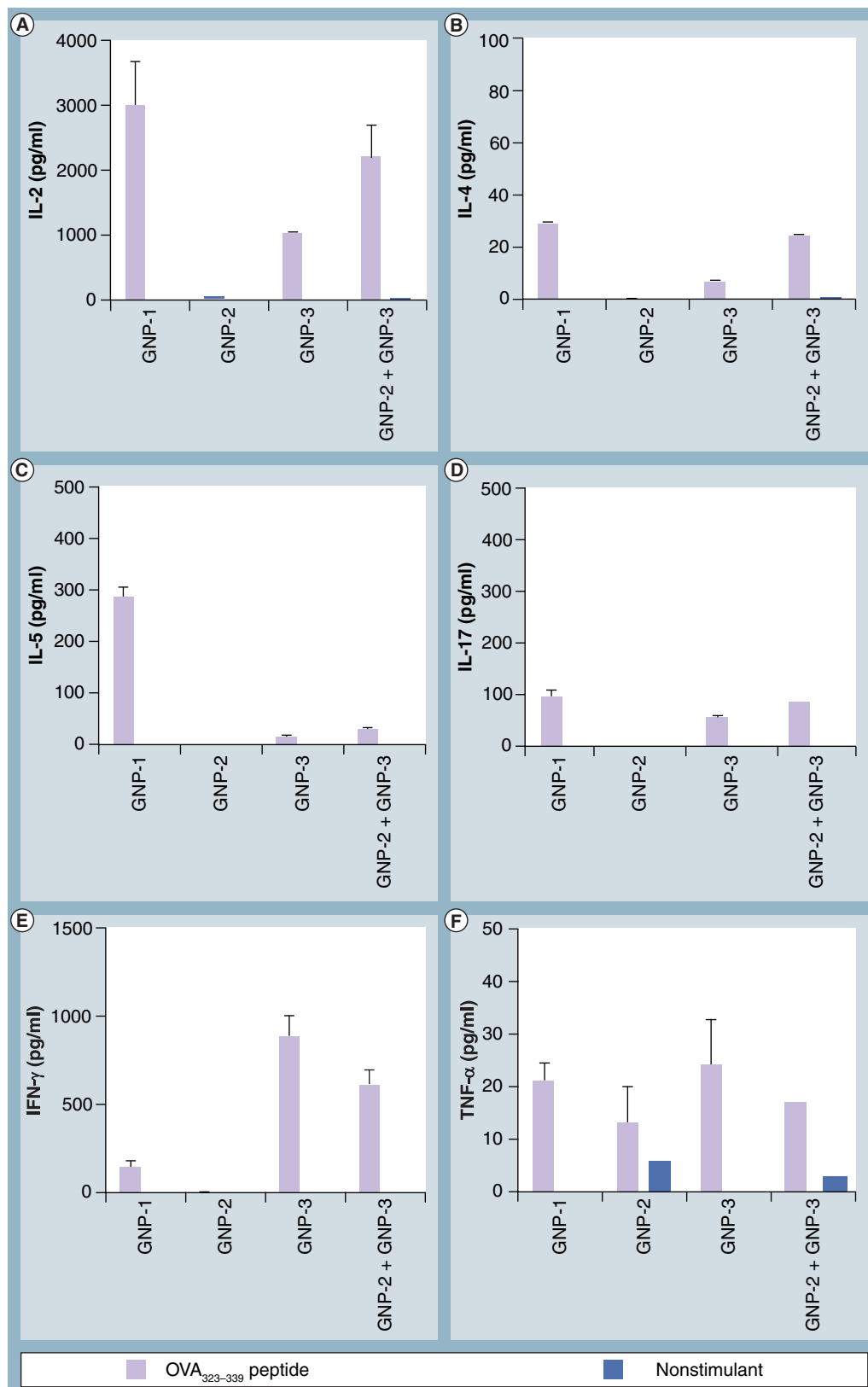


Figure 5. Cytokine production profiles after *in vitro* stimulation of spleen cells. Spleens were obtained 2 weeks after the second booster injection and spleen cells (10^7 cells/ml) were stimulated *in vitro* for 72 h with $10 \mu\text{g}$ OVA₃₂₃₋₃₃₉ peptide or medium. Levels of (A) IL-2, (B) IL-4, (C) IL-5, (D) IL-17, (E) IFN- γ and (F) TNF- α in cell-free culture supernatants were measured using the luminex-multiplex cytokine assay. GNP: Glyconanoparticle; OVA: Ovalbumin.

either anti-tetrasaccharide antibodies (FIGURE 3B) or anti-Pn14PS IgG antibodies (FIGURE 2A). The presence of the peptide was essential to evoke anti-saccharide antibodies, but it did not lead to anti-peptide antibodies and thereby avoids the risk of epitope suppression [5].

The activation of memory T cells was demonstrated by the cytokines' profiles after *in vitro* OVA₃₂₃₋₃₃₉ peptide-mediated (re)stimulation of the spleen cells from immunized mice. The induction of IL-2 (FIGURE 5A) is significant because it is the major growth factor for T cells, including regulatory T cells [42]. It is important to note that spleen cells derived from mice immunized with GNPs containing the OVA₃₂₃₋₃₃₉ peptide-produced cytokine IL-4, when stimulated by OVA₃₂₃₋₃₃₉ peptide. This indicates a Th2 response to the peptide. These T cells provide help in the B-cell response (antibody formation) to the saccharide moiety on GNP-1. Induction of IL-5 occurred only in those cells from animals previously immunized with GNPs, which contain tetrasaccharide and peptide (GNP-1 and FIGURE 5C) and correlates with the production of specific anti-Pn14PS IgG antibodies *in vivo*. In fact, IL-5 produced by Th2 cells acts as a B-cell differentiation factor by stimulating activated B cells to secrete antibodies [43]. These results are in line with other immunization studies in which the same synthetic tetrasaccharide was conjugated to the CRM₁₉₇ [26]. In human vaccination trials with the pneumococcal conjugate vaccine, an enhanced IL-5 secretion was observed in response to the carrier protein [44]. While cytokines IL-4 and IL-5 are well known Th2 markers, TNF- α (regulatory cytokine), IFN- γ (Th1 marker) and IL-17 (Th17 marker and regulatory cytokine) were studied because they play a key role in influencing the migration and pathogenic behavior during inflammatory diseases [45]. In particular, IL-17 has recently attracted much attention because of its role in protection against invasive pneumococcal infections [46,47].

The presentation of both the antigenic carbohydrate and the T-helper peptide on the same gold nanopatform seems to be crucial for eliciting a significant antibody response, even though the T-helper peptide and the B-cell epitope are not covalently linked. This observation is substantiated by the fact that the cocktail of GNP-2 (lacking OVA₃₂₃₋₃₃₉) and GNP-3 (lacking tetrasaccharide) elicited a much lower level of specific IgG antibodies against Pn14PS than GNP-1 that simultaneously present both OVA₃₂₃₋₃₃₉ and tetrasaccharide. Hassane

et al. have reported similar observations: liposomes displaying a pentadecasaccharide (B-cell epitope) and a Th epitope noncovalently linked induced an IgG-mediated immune response [9].

In phagocytosis assays, only antibodies in the sera of mice immunized with GNP-1 were able to render *S. pneumoniae* type 14 bacteria critically susceptible to the action of human polymorphonuclear leukocytes (FIGURE 4). Although the phagocytic titer was lower than the one obtained with Pn14PS-CRM₁₉₇, this result indicates that GNP-1 is a promising *S. pneumoniae* type 14 vaccine candidate. No opsonophagocytosis of the bacteria was promoted by the sera from mice immunized with the other GNPs, including the cocktail of GNP-2 and GNP-3.

Conclusion & future perspective

Hybrid gold nanoparticles coated with a synthetic branched tetrasaccharide antigen, OVA₃₂₃₋₃₃₉ peptide, and glucose are capable of inducing IgG antibodies against native polysaccharide of *S. pneumoniae* type 14. The molar ratio between tetrasaccharide and peptide in the hybrid gold nanoparticles turned out to be critical for optimal immunogenicity: gold nanoparticles containing 45% tetrasaccharide, 5% peptide and glucoconjugate as inner components were able to trigger specific anti-Pn14PS antibodies. Three main factors emerged for the induction of a robust carbohydrate-directed immune response with GNPs:

- The tetrasaccharide:peptide ratio on the gold nanopatform;
- The presence of the T-cell-stimulating peptide OVA₃₂₃₋₃₃₉ on the GNP;
- The simultaneous presence of a combination of both T-helper peptide and B-cell sugar epitopes on the same GNP.

Although further optimization of vaccine efficacy is necessary, this study presents the first example of a fully synthetic carbohydrate vaccine based on gold nanoclusters that is able to induce specific IgG antibodies that react with native capsular polysaccharide of *S. pneumoniae*. The current results demonstrate the usefulness of gold nanoparticles as a versatile platform for the development of a great diversity of synthetic carbohydrate-based vaccines. New GNPs, incorporating mannose instead of glucose, are being prepared for targeting dendritic cells to increase their immunogenicity.

Colloidal gold have been used in humans since the 1950s [48], but many concerns regarding the translation to clinic have still to be carefully addressed. Retention in organs (especially liver) and nanotoxicity [49] are the main concerns against systemic administration of metallic nanoparticles.

Risk–benefit analysis may suggest that nanotechnology-based tools could be admitted for one-off or limited administration such as primary immunization/boosters for vaccination, diagnostics and thermal cancer treatments [50].

The opportunity of easily producing stable conjugate vaccines bearing arrays of carbohydrate antigens and simultaneously targeting various bacterial structures arranged on a single gold nanoparticle open new perspectives in the vaccine field and thus may promote gold nanoparticles to the frontline for tailor-made polyvalent carbohydrate vaccine candidates.

Financial & competing interests disclosure

This research was supported by the European Union (grant GlycoGold, MRTN-CT-2004-005645), the Spanish

Ministry of Science and Innovation, MICINN (grant CTQ2008-04638), and the Department of Industry of the Basque Country (grant ETORTEK2009). The authors have no other relevant affiliations or financial involvement with any organization or entity with a financial interest in or financial conflict with the subject matter or materials discussed in the manuscript apart from those disclosed.

Writing assistance was utilized in the production of this manuscript. Writing assistance was provided by Laura Cobb, Culemborg, The Netherlands. Funding for this assistance was received from the University Medical Center, Utrecht, The Netherlands.

Ethical conduct of research

All immunization studies were approved by the Ethics Committee on Animal Experiments of Utrecht University, Utrecht, The Netherlands. The authors state that they have obtained appropriate institutional review board approval or have followed the principles outlined in the Declaration of Helsinki for all human or animal experimental investigations. In addition, for investigations involving human subjects, informed consent has been obtained from the participants involved.

Executive summary

- The preparation by a one-pot method of small (~2 nm) hybrid gold glyconanoparticles (GNPs) coated with a conjugate of the branched tetrasaccharide β -D-Galp-(1–4)- β -D-Glcp-(1–6)-[β -D-Galp-(1–4)-] β -D-GlcpNAc-(1–), which corresponds to a single repeating unit of Pn14PS, a conjugate of the ovalbumin 323–339 peptide (OVA_{323–339}), and a conjugate of D-glucose is reported.
- Immunogenicity studies in BALB/c mice showed that specific IgG antibodies against *Streptococcus pneumoniae* type 14 capsular polysaccharide (Pn14PS) were induced by the GNPs.
 - The copresence of the T-cell-stimulating OVA_{323–339} peptide and the tetrasaccharide antigen on the gold nanoparticles was a prerequisite for the induction of the anti-Pn14PS IgG antibodies.
 - The molar ratio between tetrasaccharide, OVA_{323–339} and glucose on the gold nanoparticles was critical for optimal immunogenicity.
 - The OVA_{323–339} (T-cell epitope) on the nanoparticle does not lead to antibodies against the peptide and this avoids the risk of epitope suppression.
- In the cytokine study, *in vitro* stimulation with the OVA_{323–339} peptide of spleen cells from immunized mice revealed cytokine levels (especially IL-5), which confirmed that GNPs led to helper Th cell activation.
- A phagocytic study demonstrated that the antibodies in sera of mice immunized with GNP-1 (tetrasaccharide:Glc:OVA_{323–339} = 45:50:5) were able to coat heat-inactivated fluorescein isothiocyanate-labeled *S. pneumoniae* type 14 and make the bacteria critically susceptible to the action of human polymorphonuclear leukocytes (opsonophagocytosis).
- This is the first example of a fully synthetic carbohydrate vaccine candidate based on gold nanoparticles capable of evoking specific antibodies against *S. pneumoniae* type 14.

References

Papers of special note have been highlighted as:

- of interest
- of considerable interest

- 1 Pena Icart L, Fernández-Santana V, Veloso RC *et al.* Protective immunity of pneumococcal glycoconjugates. In: *Carbohydrate-Based Vaccines (Volume 989)*. René Roy (Ed.). ACS Symposium Series, American Chemical Society, Washington, DC, USA, 1–19 (2008).
- 2 Astronomo RD, Burton DR. Carbohydrate vaccines: developing sweet solutions to sticky situations? *Nat. Rev. Drug Discov.* 9, 308–324 (2010).
- 3 Whitney CG, Farley MM, Hadler J *et al.* Decline in invasive pneumococcal disease after the introduction of protein–polysaccharide conjugate vaccine. *N. Engl. J. Med.* 348, 1737–1746 (2003).
- 4 Verez-Bencomo V, Fernández-Santana V, Hardy E *et al.* A synthetic conjugate polysaccharide vaccine against *Haemophilus influenzae* type b. *Science* 305, 522–525 (2004).
- 5 Schutze MP, Leclerc C, Jolivet M, Audibert F, Chedid L. Carrier-induced epitopic suppression, a major issue for future synthetic vaccines. *J. Immunol.* 135, 2319–2322 (1985).
- 6 Stallforth P, Lepenies B, Adibekian A, Seeberger PH. Carbohydrates: a frontier in medicinal chemistry. *J. Med. Chem.* 52, 5561–5577 (2009).

- 7 Keding SJ, Danishefsky S. Synthetic Carbohydrate-Based Vaccines. In: *Carbohydrate-Based Drug Discovery*. Chi-Huey Wong (Ed.), Wiley-VCH Verlag, Berlin, Germany, 381–406 (2003).
- 8 Ingale S, Wolfert MA, Gaekwad J, Buskas T, Boons GJ. Robust immune responses elicited by a fully synthetic three-component vaccine. *Nat. Chem. Biol.* 3, 663–667 (2007).
- **An elegant synthetic approach based on liposomes to circumvent immune suppression caused by carrier proteins or linker regions in classical conjugate vaccines.**
- 9 Hassane FS, Phalipon A, Tanguy M *et al.* Rational design and immunogenicity of liposome-based diepitope constructs: application to synthetic oligosaccharides mimicking the Shigella flexneri 2a O-antigen. *Vaccine* 27, 5419–5426 (2009).
- **An example of liposome-based carbohydrate vaccines where B-cell and Th epitopes are not covalently linked.**
- 10 Wang SK, Liang PH, Astronomo RD, Hsu TL *et al.* Targeting the carbohydrates on HIV-1: interaction of oligomannose dendrons with human monoclonal antibody 2G12 and DC-SIGN. *Proc. Natl Acad. Sci. USA* 105, 3690–3695 (2008).
- 11 Joyce JG, Krauss IJ, Song HC *et al.* An oligosaccharide-based HIV-1 2G12 mimotope vaccine induces carbohydrate-specific antibodies that fail to neutralize HIV-1 virions. *Proc. Natl Acad. Sci. USA* 105, 15684–15689. (2008).
- **A work that highlights one of the big HIV challenges: the induction of high levels of carbohydrate-specific antibodies is necessary, but is not a sufficient condition en route to a carbohydrate-based vaccine against HIV.**
- 12 Song EH, Osanya AO, Petersen CA, Pohl NL. Synthesis of multivalent tuberculosis and *Leishmania*-associated capping carbohydrates reveals structure-dependent responses allowing immune evasion. *J. Am. Chem. Soc.* 132, 11428–11430 (2010).
- 13 Sarkar S, Lombardo SA, Herner DN, Talan RS, Wall KA, Sucheck SJ. Synthesis of single-molecules L-rhamnose-containing three-component vaccine and evaluation of antigenicity in the presence of anti-L-rhamnose antibodies. *J. Am. Chem. Soc.* 132, 17236–17246 (2010).
- **A paper showing the increase in effectiveness of a cancer vaccine by conjugation of L-rhamnose to a carbohydrate antigen and a T-helper epitope.**
- 14 Fahmy TM, Demento SL, Caplan MJ, Mellman I, Saltzman WM. Design opportunities for actively targeted nanoparticle vaccines. *Nanomedicine* 3, 343–355 (2008).
- 15 Krishnamachari Y, Geary SM, Lemke CD, Salem AK. Nanoparticle delivery systems in cancer vaccines. *Pharm. Res.* 28, 215–236 (2011).
- 16 Boisselier E, Astruc D. Gold nanoparticles in nanomedicine: preparations, imaging, diagnostics, therapies and toxicity *Chem. Soc. Rev.* 38, 1759–1782 (2009).
- 17 Yang NS, Burkholder J, Roberts B, Martinell B, McCabe D. *In vivo* and *in vitro* gene transfer to mammalian somatic cells by particle bombardment. *Proc. Natl Acad. Sci. USA* 87, 9568–9572 (1990).
- 18 Roya MJ, Wua MS, Barra LJ *et al.* Induction of antigen-specific CD8⁺ T cells, T helper cells, and protective levels of antibody in humans by particle-mediated administration of a hepatitis B virus DNA vaccine. *Vaccine* 19, 764–778 (2001).
- 19 Drape RJ, Macklin MD, Barr LJ, Jones S, Haynes JR, Dean HJ. Epidermal DNA vaccine for influenza is immunogenic in humans. *Vaccine* 24, 4475–4481 (2006).
- 20 Castillo PM, Herrera JL, Fernandez-Montesinos R *et al.* Tiopronin monolayer-protected silver nanoparticles modulate IL-6 secretion mediated by Toll-like receptor ligands. *Nanomedicine* 3, 627–635 (2008).
- 21 Bastús NG, Sánchez-Tilló E, Pujals S *et al.* Peptides conjugated to gold nanoparticles induce macrophage activation. *Mol. Immunol.* 46, 743–748 (2009).
- 22 Snippe H, Jansen WTM, Kamerling JP. Immunology of Experimental Synthetic Carbohydrate-Protein Conjugate Vaccines Against *Streptococcus pneumoniae* Serotypes. In: *Carbohydrate-Based Vaccines (Volume 989)*. René Roy (Ed.). ACS Symposium Series, American Chemical Society, Washington, DC, USA, 85–104 (2008).
- 23 Rijkers GT, van Mens SP, van Velzen-Blad H. What do the next 100 years hold for pneumococcal vaccination? *Expert Rev. Vaccines* 9, 1241–1244 (2010).
- 24 Veenhoven R, Bogaert D, Uiterwaal C *et al.* Effect of conjugate pneumococcal vaccine followed by polysaccharide pneumococcal vaccine on recurrent acute otitis media: a randomised study. *Lancet* 361, 2189–2195 (2003).
- 25 Mawas F, Niggemann J, Jones C, Corbel MJ, Kamerling JP, Vliegenthart JFG. Immunogenicity in a mouse model of a conjugate vaccine made with a synthetic single repeating unit of type 14 pneumococcal polysaccharide coupled to CRM₁₉₇. *Infect. Immun.* 70, 5107–5114 (2002).
- 26 Safari D, Dekker HAT, Joosten JAF *et al.* Identification of the smallest structure capable of evoking opsonophagocytic antibodies against *Streptococcus pneumoniae* type 14. *Infect. Immun.* 76, 4615–4623 (2008).
- **A study that highlights the importance of individuating the minimum antigenic oligosaccharide fragment of a capsular polysaccharide in order to induce functional antibodies by conjugate vaccines.**
- 27 Barrientos AG, de la Fuente JM, Rojas TC, Fernandez A, Penadés S. Gold glyconanoparticles: synthetic polyvalent ligands mimicking glycocalyx-like surfaces as tools for glycobiological studies. *Chem. Eur. J.* 9, 1909–1921 (2003).
- 28 Martínez-Ávila O, Hijazi K, Marradi M *et al.* Gold manno-glyconanoparticles: multivalent systems to block HIV-1 gp120 binding to the lectin DC-SIGN. *Chem. Eur. J.* 15, 9874–9888 (2009).
- 29 Ojeda R, de Paz JL, Barrientos AG, Martín-Lomas M, Penadés S. Preparation of multifunctional glyconanoparticles as a platform for potential carbohydrate-based anticancer vaccines. *Carbohydr. Res.* 342, 448–459 (2007).
- **The first preparation of complex gold nanoparticles comprising up to four components (including carbohydrate antigens and T-cell helper peptides) with well-defined average chemical composition.**
- 30 Marradi M, Martín-Lomas M, Penadés S. Glyconanoparticles: polyvalent tools to study carbohydrate-based interactions. *Adv. Carbohydr. Chem. Biochem.* 64, 211–290 (2010).
- 31 García I, Marradi M, Penadés S. Glyconanoparticles: multifunctional nanomaterials for biomedical applications. *Nanomedicine* 5, 777–792 (2010).
- 32 Buus S, Colon S, Smith C, Freed JH, Miles C, Grey HM. Interaction between a ‘processed’ ovalbumin peptide and Ia molecules. *Proc. Natl Acad. Sci. USA* 83, 3968–3971 (1986).
- 33 Renz H, Bradley K, Larsen GL, McCall C, Gelfand EW. Comparison of the allergenicity of ovalbumin and ovalbumin peptide 323–339. Differential expansion of V beta-expressing T cell populations. *J. Immunol.* 151, 7206–7213 (1993).
- 34 Sundgren A, Lahmann M, Oscarson S. Block synthesis of *Streptococcus pneumoniae* type 14 capsular polysaccharide structures. *J. Carbohydr. Chem.* 24, 379–391 (2005).
- 35 Hostetler MJ, Wingate JE, Zhong C-J *et al.* Alkanethiolate gold cluster molecules with core diameters from 1.5 to 5.2 nm: core and monolayer properties as a function of core size. *Langmuir* 14, 17–30 (1998).

- 36 Jansen WTM, Gootjes J, Zelle M *et al.* Use of highly encapsulated *Streptococcus pneumoniae* strains in a flow-cytometric assay for assessment of the phagocytic capacity of serotype-specific antibodies. *Clin. Diagn. Lab. Immunol.* 5, 703–710 (1998).
- 37 Love JC, Estroff LA, Kriebel JK, Nuzzo RG, Whitesides GM. Self-assembled monolayers of thiolates on metals as a form of nanotechnology. *Chem. Rev.* 105, 1103–1169 (2005).
- 38 Svetic A, Finkelman FD, Jian YC *et al.* Cytokine gene expression after *in vivo* primary immunization with goat antibody to mouse IgD antibody. *J. Immunol.* 147, 2391–2397 (1991).
- 39 Svetic A, Jian YC, Lu P, Finkelman FD, Gause WC. *Brucella abortus* induces a novel cytokine gene expression pattern characterized by elevated IL-10 and IFN- γ in CD4⁺ T cells. *Int. Immunol.* 5, 877–883 (1993).
- 40 Mrksich M, Whitesides GM. Using self-assembled monolayers to understand the interactions of man-made surfaces with proteins and cells. *Annu. Rev. Biophys. Biomol. Struct.* 25, 55–78 (1996).
- 41 Safari D, Dekker HAT, Rijkers G, Snippe H. Codelivery of adjuvants at the primary immunization site is essential for evoking a robust immune response to neoglycoconjugates. *Vaccine* 29, 849–854 (2011).
- 42 Smith KA. Interleukin-2: inception, impact, and implications. *Science* 240, 1169–1176 (1988).
- 43 Randall TD, Lund FE, Brewer JW, Aldridge C, Wall R, Corley RB. Interleukin-5 (IL-5) and IL-6 define two molecularly distinct pathways of B-cell differentiation. *Mol. Cell. Biol.* 13, 3929–3936 (1993).
- 44 Wuorimaa T, Käyhty H, Eskola J, Bloigu A, Leroy O, Surcel HM. Activation of cell-mediated immunity following immunization with pneumococcal conjugate or polysaccharide vaccine. *Scand. J. Immunol.* 53, 422–428 (2001).
- 45 Cox CA, Shi G, Yin H *et al.* Both Th1 and Th17 are immunopathogenic but differ in other key biological activities. *J. Immunol.* 180, 7417–7422 (2008).
- 46 Lu Y, Gross J, Bogaert D *et al.* Interleukin IL-17A mediates acquired immunity to pneumococcal colonization. *PLoS Pathog.* 4, e1000159 (2008).
- 47 Zhang Z, Clarke TB, Weiser JN. Cellular effectors mediating Th17-dependent clearance of pneumococcal colonization in mice. *J. Clin. Invest.* 119, 1899–1909 (2009).
- 48 Baker WS. Carcinoma of the uterine cervix: Interstitial radioactive colloidal gold therapy of the lateral pelvic nodes. *Calif. Med.* 92, 25–30 (1960).
- 49 Hall JB, Dobrovolskaia MA, Patri AK, McNeil SE. Characterization of nanoparticles for therapeutics. *Nanomedicine* 2, 789–803 (2007).
- 50 Kennedy LC, Bickford LR, Lewinski NA *et al.* New era for cancer treatment: gold-nanoparticle-mediated thermal therapies. *Small* 7, 169–183 (2011).

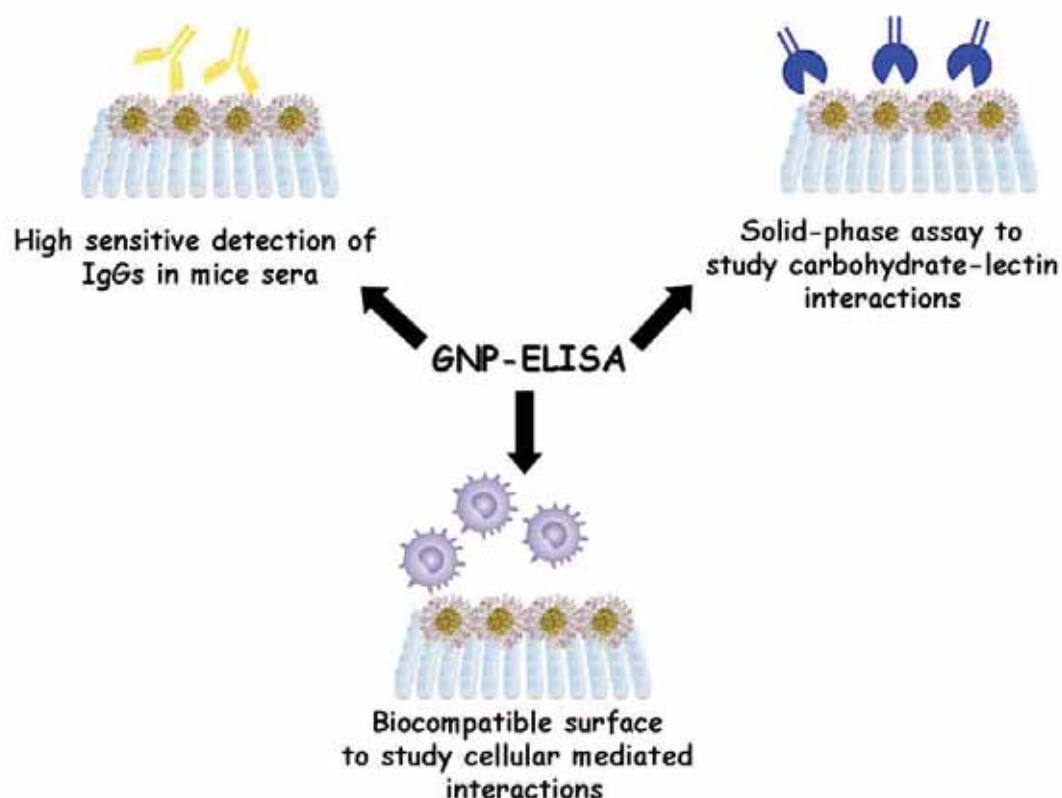
Affiliations

- **Dodi Safari**
Department of Medical Microbiology, University Medical Center Utrecht, Utrecht, The Netherlands
- **Marco Marradi**
Laboratory of GlycoNanotechnology, Biofunctional Nanomaterials Unit, CIC biomaGUNE, San Sebastián, Spain and Networking Research Centre on Bioengineering, Biomaterials and Nanomedicine (CIBER-BBN), San Sebastián, Spain
- **Fabrizio Chiodo**
Laboratory of GlycoNanotechnology, Biofunctional Nanomaterials Unit, CIC biomaGUNE, San Sebastián, Spain
- **Huberta A Th Dekker**
Department of Medical Microbiology, University Medical Center Utrecht, Utrecht, The Netherlands
- **Yulong Shan**
School of Chemistry, Bangor University, Bangor, UK
- **Roberto Adamo**
Bijvoet Center, Department of Bio-Organic Chemistry, Utrecht University, Utrecht, The Netherlands
- **Stefan Oscarson**
Center for Synthesis and Chemical Biology, University College Dublin, Belfield, Dublin 4, Ireland
- **Ger T Rijkers**
Department of Medical Microbiology and Immunology, St Antonius Hospital, Nieuwegein, The Netherlands
- **Martina Lahmann**
School of Chemistry, Bangor University, Bangor, UK
- **Johannis P Kamerling**
Bijvoet Center, Department of Bio-Organic Chemistry, Utrecht University, Utrecht, The Netherlands
- **Soledad Penadés**
Laboratory of GlycoNanotechnology, Biofunctional Nanomaterials Unit, CIC biomaGUNE, San Sebastián, Spain and Networking Research Centre on Bioengineering, Biomaterials and Nanomedicine (CIBER-BBN), San Sebastián, Spain
- **Harm Snippe**
Department of Medical Microbiology, University Medical Center Utrecht, Utrecht, The Netherlands
Tel.: +31 (0) 887553890
Fax: +31 (0) 302541770
h.snippe@umcutrecht.nl

Chapter-4

Multivalent glyconanoparticles allow high sensitive detection of carbohydrate binding proteins on an ELISA-based solid phase assay

Improved detection of anti-carbohydrate antibodies is a need in clinical identification of biomarkers for cancer cells or pathogens. Here, we report a new ELISA approach for the detection of specific immunoglobulins (IgGs) against carbohydrates. Two nanometer gold glyconanoparticles bearing oligosaccharide epitopes of HIV or *Streptococcus pneumoniae* were used as antigens to coat ELISA-plates. A ~3,000-fold improved detection of specific IgGs in mice immunized against *S. pneumoniae* respect to the well known BSA-glycoconjugate ELISA was achieved. Moreover, these multivalent glyconanoparticles have been employed in solid phase assays to detect the carbohydrate-dependent binding of human dendritic cells and lectin DC-SIGN. Multivalent glyconanoparticles in ELISA provides a versatile, easy and highly sensitive method to detect and quantify the binding of glycan to proteins and to facilitate the identification of biomarkers.



The detection of anti-glycan antibodies in serum is of mounting interest for the evaluation of carbohydrate-based vaccines and pathogen infection as well as for the detection of biomarkers in diseases like cancer. The profiling of human serum antibodies has shown that a substantial part of circulating antibodies is directed against carbohydrates.¹ The affinity of anti-

¹Oyelaran O., McShane L. M., Dodd L., Gildersleeve J.C., Profiling human serum antibodies with a carbohydrate antigen microarray, J. Proteome Res. 2009, 8, 4301-4310.

carbohydrate antibodies towards their epitopes, demands a multivalent presentation of the carbohydrate-ligands and highly sensitive screening methods. Furthermore, the low abundance of anti-carbohydrates antibodies in serum during pathological states and/or early infection hampers their use as biomarkers for prompt diagnosis. The coupling of carbohydrates on a scaffold (carrier) allows the multiple presentation of these antigens in an enzyme-linked immunosorbent assay (ELISA).² However, while protein coating of ELISA plates is a well-established methodology, equivalent strategies for the direct coating of carbohydrates have been hampered by technical limitations. Early attempts to detect antibodies against bacterial polysaccharides by ELISA showed the difficulty to absorb carbohydrates to the supporting materials. This problem was solved by conjugation of the polysaccharides to positive charged poly-lysine scaffold, which allowed the immobilization of the resulting neoglycoconjugate to ELISA plates.³ Soon afterwards, glycolipids were effectively employed to coat ELISA surfaces for a *Mycobacterium leprae*-specific serodiagnostic test.^{4,5,6} With the identification and characterization of oligosaccharide antigen structures, chemical strategies were developed to conjugate the carbohydrate antigen to proteins (bovine or human serum albumin), polymers (acrylamide derivatives)^{7,8} and dendrimers⁹ in order to enhance the number carbohydrate epitopes on the ELISA surface and improve the sensitivity of the assay.

The relatively recent introduction of glycan microarray technology also provided a platform for high throughput screening, yielding information about the specificity of glycan-binding proteins.^{10,11} Although novel applications of glycan microarrays are emerging, including vaccine development and identification of disease specific biomarkers, ELISA is still the most

² Gervay J., McReynolds K. D., Utilization of ELISA technology to measure biological activities of carbohydrates relevant in disease states, *Curr. Med. Chem.* 1999, 6, 129-153.

³ Gray B. M., ELISA methodology for polysaccharides antigens: protein coupling of polysaccharides for adsorption to plastic tubes, *J. Immun. Meth.* 1979, 28, 187-192.

⁴ Reggiardo Z., Vazquez E., Schnaper L., ELISA tests for antibodies against mycobacterial glycolipids, *J. Immunol. Methods* 1980, 34, 55-60.

⁵ Young D. B., Buchanan T. M., A serological test for leprosy with glycolipid specific for *Mycobacterium leprae*, *Science* 1983, 221, 1057-1059.

⁶ Spencer J. S., Brennan P. J., The role of *Mycobacterium leprae* phenolic glycolipid (PGL-I) in serodiagnosis and in pathogenesis of leprosy, *Lepr. Rev.* 2011, 82, 344-357.

⁷ Mariño-Albernas J., Verez-Bencomo V., Gonzalez-Rodriguez L., Perez-Martinez C. S., Gonzalez-Abreu Castell E., Gonzalez-Segredo A., Chemical synthesis of an artificial antigen containing the trisaccharide hapten of *Mycobacterium leprae*, *Carbohydr. Res.* 1988, 183, 175-182.

⁸ Galanina O. E., Mecklenburg M., Nifantiev N. E., Pazynina G. V., Bovin N.V., GlycoChip: multiarray for the study of carbohydrate-binding proteins, *Lab Chip.* 2003, 3, 260-265.

⁹ Wang S. K., Liang P. H., Astronomo R. D., Hsu T. L., Hsieh S. L., Burton D. R., Wong C. H., Targeting the carbohydrates on HIV-1: Interaction of oligomannose dendrons with human monoclonal antibody 2G12 and DC-SIGN, *Proc. Natl. Acad. Sci. USA* 2008, 105, 3690-3695.

¹⁰ Park S., Gildersleeve, J. C., Blixt O., Shin, I., Carbohydrate microarrays, *Chem. Soc. Rev.* 2013, DOI: 10.1039/C2CS35401B.

¹¹ Rillahan C. D., Paulson J. C., Glycan microarrays for decoding the glycome. *Ann. Rev. Biochem.* 2011, 80, 797-823 and references therein.

widely used assay for diagnostic purposes. Its simplicity, high sensitivity and low cost make ELISA a reliable competitor of newer screening methods for diagnosis such as printed glycan microarray technology. Although the comparison between glycan microarrays technology and conventional ELISA for evaluation of anti-carbohydrate antibodies led to contrasting opinions about sensitivity^{9, 12} the importance of both techniques as complementary screening methods has prompted the development of new immobilization strategies to improve their performance. For example, a new type of microarray based on silica glyconanoparticles has recently been described to study glycan-lectin interactions.¹³

In this chapter we describe the development of a fast and highly sensitive serology method, in which commercially available ELISA plates are directly coated with two nanometer gold glyconanoparticles (GNPs) carrying carbohydrate antigens. We demonstrate that anti-carbohydrate antibodies can be detected in the nanomolar range by performing GNP-ELISA with the purified anti-HIV human monoclonal antibody 2G12 and with serum from mice immunized against *Streptococcus pneumoniae*. Moreover, we show that GNPs can be employed in a solid phase assay to profile the carbohydrate-binding of human cells and to profile lectins affinities on a highly multivalent surface. GNPs allow the introduction of a high number of carbohydrates on a nanometric gold scaffold¹⁴ and the combination of different molecules on the same nanoparticle in a controlled way and with varying density.^{15, 16} We reasoned that the high number of carbohydrates on the GNPs (60-100 molecules) and their high molecular weight (around 50 kD) make GNPs very suitable for the ELISA plate coating in order to improve the sensitivity of the anti-carbohydrate antibody detection and study other carbohydrate-binding proteins.

¹² Pochechueva T., Jacob F., Goldstein D. R., Huflejt M. E., Chinarev A., Caduff R., Fink D., Hacker N., Bovin N. V., Heinzelmann-Schwarz V., Comparison of printed glycan array, suspension array and ELISA in the detection of human anti-glycan antibodies, *Glycoconj J.* 2011, 28, 507-517.

¹³ Tong Q., Wang X., Wang H., Kubo T., Yan M., Fabrication of glyconanoparticle microarrays, *Anal. Chem.* 2012, 84, 3049-3052.

¹⁴ de La Fuente J. M., Barrientos A. G., Rojas T. C., Rojo J., Cañada J., Fernández A., Penadés, S., Gold glyconanoparticles as water-soluble polyvalent models to study carbohydrate interactions, *Angew. Chem. Int. Ed.* 2001, 40, 2257-2261.

¹⁵ Ojeda R., de Paz J. L., Barrientos A. G., Martín-Lomas M, Penadés S., Preparation of multifunctional glyconanoparticles as a platform for potential carbohydrate-based anticancer vaccines, *Carbohydr. Res.* 2007, 342, 448-459.

¹⁶ Marradi M., Martín-Lomas M., Penadés S., Glyconanoparticles: Polyvalent tools to study carbohydrate-based interactions, *Adv. Carbohydr. Chem. Biochem.* 2010, 64, 211-290.

Design and preparation of GNPs

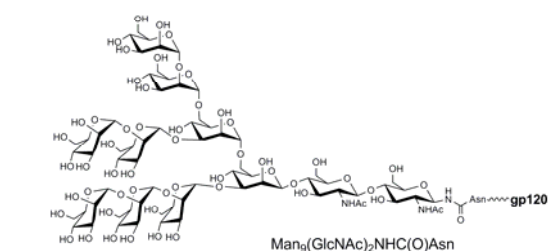
To validate the GNP-ELISA we have selected as antigens a panel of GNPs (Fig. 1) that we have previously prepared to investigate glycan/protein interactions and as a carrier for carbohydrate-based vaccine candidates: Two of them (Fig. 1A) carry the disaccharide Man(α 1-2)Man(α 1 \rightarrow) (DiMan-GNP) or the tetrasaccharide Man(α 1-2)Man(α 1-2)Man(α 1-3)Man(α 1 \rightarrow) (TetraMan-GNP) that are present in the high-mannose type glycans of HIV glycoprotein gp120 (see chapter-2).¹⁷ Another set (Fig. 1B) is formed by GNPs that carry the tetrasaccharide Gal(β 1-4)Glc(β 1-6)[Gal(β 1-4)]GlcNAc(1 \rightarrow) epitope of the *S. pneumoniae* type 14 polysaccharide, alone (TetraPn-GNP) or in combination with the small peptide OVA₃₂₃₋₃₃₉ of ovalbumin (TetraPnOv-GNP) (see chapter-3).¹⁸ As a control (Fig. 1C), GNPs bearing only glucose (Glc-GNP) or galactose (Gal-GNP) were also included. The oligosaccharides are conjugated to the same aglycon, a thiol-ending amphiphilic linker to attach them to the gold surface. A glucose conjugate is incorporated as inner component to modulate the density of the antigenic oligosaccharides on the surface.¹⁹ Nunc MaxiSorp plates were selected for the GNP-ELISA, as similar modified polystyrene slides were previously used to prepare microarrays of polysaccharides and proteoglycans.²⁰

¹⁷ Martínez-Avila O., Hijazi K., Marradi M., Clavel C., Campion C., Kelly C., Penadés S., Gold manno-glyconanoparticles: multivalent systems to block HIV-1 gp120 binding to the lectin DC-SIGN, *Chem. Eur. J.* 2009, 15, 9874-9888.

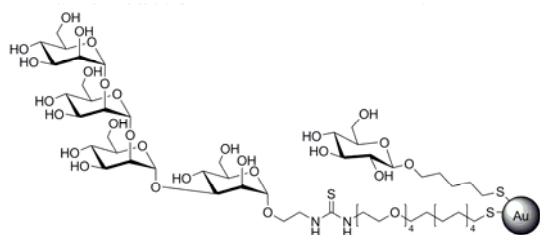
¹⁸ Safari D., Marradi M., Chiodo F., Dekker H. A. T., Shan Y., Adamo R., Oscarson S., Rijkers G. T., Lahman M., Kamerling J. P., Penadés S., Snippe H., Gold nanoparticles as carriers for a synthetic *Streptococcus pneumoniae* type 14 conjugate vaccine, *Nanomedicine UK* 2012, 7, 651-662.

¹⁹ Barrientos A. G., de la Fuente J. M., Rojas T. C., Fernández A., Penadés S. (). Gold glyconanoparticles: synthetic polyvalent ligands mimicking glycocalyx-like surfaces as tools for glycobiological studies, *Chem. Eur. J.* 2003, 9, 1909-1921.

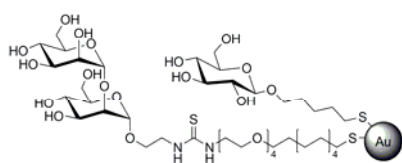
²⁰ Willats W. G., Rasmussen S. E., Kristensen T., Mikkelsen J. D., Knox, J. P., Sugar-coated microarrays: A novel slide surface for the high-throughput analysis of glycans, *Proteomics* 2000, 2, 1879-1883.

A Undecasaccharide of HIV gp120 and related GNPs

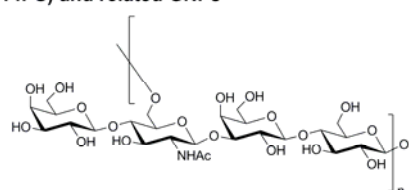
GNPs incorporating gp120 high-mannose



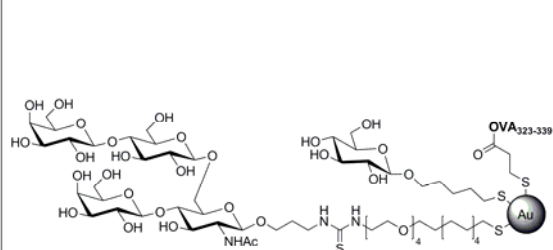
TetraMan-GNP: 90% Glc
10% $\text{Man}_\alpha 1-2\text{Man}_\alpha 1-2\text{Man}_\alpha 1-3\text{Man}_\alpha$



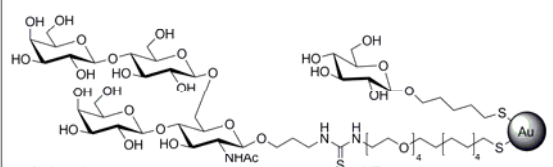
DiMan-GNP: 90% Glc
10% $\text{Man}_\alpha 1-2\text{Man}_\alpha$

B *S. pneumoniae* type 14 capsular polysaccharide (Pn14PS) and related GNPs

GNPs incorporating a single repeat unit of Pn14PS



TetraPnOv-GNP: 50% Glc
45% $\text{Gal}(\beta 1-4)\text{Glc}(\beta 1-6)[\text{Gal}(\beta 1-4)]\text{GlcNAc}(\beta 1-O)$
5% $\text{OVA}_{323-339}$



TetraPn-GNP: 50% Glc
50% $\text{Gal}(\beta 1-4)\text{Glc}(\beta 1-6)[\text{Gal}(\beta 1-4)]\text{GlcNAc}(\beta 1-O)$

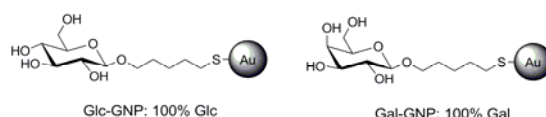
C Control GNPs

Figure 1: Gold glyconanoparticles used in this chapter to coat ELISA plates for anti-carbohydrate-antibodies detection: **A)** High-mannose type undecasaccharide present on the HIV gp120 surface and GNPs carrying the tetramannoside (TetraMan) or dimannoside (DiMan), partial structures of the viral gp120 high-mannose undecasaccharide to detect 2G12 antibody. **B)** Repeated unit of *S. pneumoniae* type 14 capsular polysaccharide and GNPs carrying the tetrasaccharide epitope (TetraPn) of the *S. pneumoniae* Pn14PS and the T-helper $\text{OVA}_{323-339}$. **C)** GNPs carrying glucose or galactose as control.

Detection of anti-HIV monoclonal antibody 2G12

As a proof of principle, we set up a GNP-ELISA for the detection of the anti-HIV human monoclonal antibody 2G12. The 2G12 antibody is one of the broadly neutralizing antibodies against HIV-1 and binds to a conserved high-mannose cluster on HIV gp120.²¹ GNPs carrying

²¹ Scanlan C. N., Pantophlet R., Wormald M. R., Ollmann Saphire E., Stanfield R., Wilson I.A., Katinger H., Dwek R. A., Rudd P. M., Burton D. R., The broadly neutralizing anti-human immunodeficiency virus type

selected gp120 high-mannose oligosaccharides were previously shown to bind 2G12 and to compete with 2G12/gp120 binding as demonstrated by surface plasmon resonance (SPR), NMR, and cellular neutralization experiments (see chapter-2).²²

Following the standard procedure for ELISA antigens coating, the wells were coated with a solution of TetraMan-GNP, DiMan-GNP, and Glc-GNP at different concentrations (100, 10, and 1 $\mu\text{g mL}^{-1}$). Glc-GNP was included as a negative control. We observed in our experiments that multiple Tween washes decreased the sensitivity of the detection, so we decided to wash the plate with PBS (10 mM, pH 7.4) before blocking with 1% BSA. Next, 2G12 was added at 2.4 $\mu\text{g mL}^{-1}$ (16.5 nM) concentration and incubated for 1 h at room temperature followed by detection with horseradish peroxidase (HRP)-conjugated goat anti-human IgG.

Figure 2A shows the concentration-dependent response of 2G12 towards the GNPs measuring the optical density (OD) at 450 nm. Even at 1 $\mu\text{g mL}^{-1}$ of coating, TetraMan-GNP was able to induce a significant signal (OD \sim 0.5) after incubation with 2G12. However, 2G12 did not interact with the DiMan-GNP at the tested concentrations. The negative response of the DiMan-GNP excluded non-specific interactions (due to the linker or gold) between 2G12 and the gold nanoparticles. Glc-GNP was not recognized by the antibody (Fig. 2) excluding also non-specific interactions because both TetraMan-GNP and DiMan-GNP have 90% of Glc conjugate on their surface. 2G12 recognized neither GNPs coated with OVA₃₂₃₋₃₃₉ nor GNPs bearing a branched high-mannose pentasaccharide. When the monomeric TetraMan oligosaccharide conjugated to 2-aminoethyl linker was employed to coat the Nunc MaxiSorp plate under the same conditions as those for GNPs coating, no 2G12 response was detected as expected.

1 antibody 2G12 recognizes a cluster of α 1 \rightarrow 2 mannose residues on the outer face of gp120, J. Virol. 2002, 76, 7306–7321.

²² Marradi M., Di Gianvincenzo P., Enríquez-Navas P. M., Martínez-Ávila O. M., Chiodo F., Yuste E., Angulo J., Penadés S., Gold nanoparticles coated with oligomannosides of HIV-1 glycoprotein gp120 mimic the carbohydrate epitope of antibody 2G12, J. Mol. Biol. 2011, 410, 798-810.

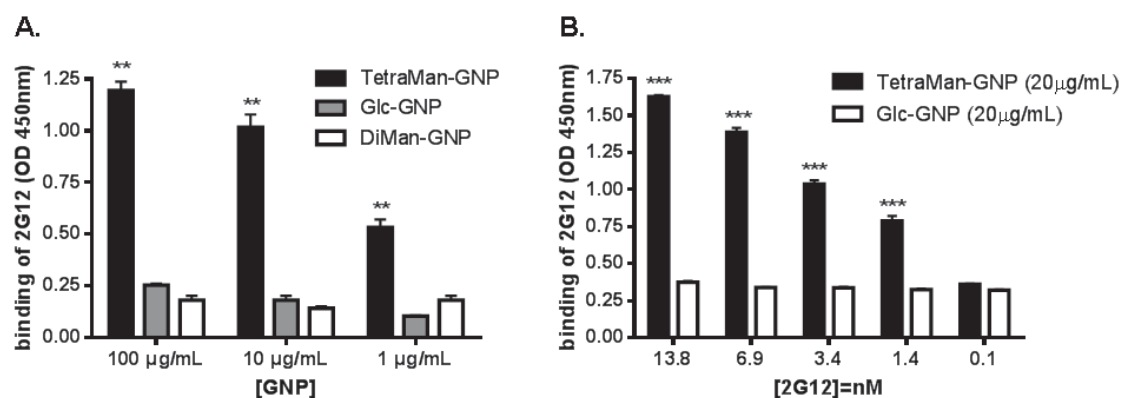


Figure 2: Detection of anti-HIV monoclonal antibody 2G12 by GNP-ELISA. **A)** TetraMan, DiMan and Glc-GNP at different concentrations (100, 10, and 1 $\mu\text{g}\cdot\text{mL}^{-1}$) were used for ELISA plates coating. Antibody 2G12 (2.4 $\mu\text{g}\cdot\text{mL}^{-1}$) recognizes TetraMan-GNP in a coating-concentration dependent manner, while DiMan-GNP and Glc-GNP are not recognized. Differences between TetraMan-GNP and both control GNPs are significant, as indicated with two asterisks ($p < 0.01$). **B)** Limit of 2G12 detection with TetraMan-GNP: 20 $\mu\text{g}/\text{mL}$ of GNPs were used to coat the plate and subsequently incubated with different concentrations of 2G12 (13.8 to 0.1 nM). Error bars represent the standard deviation of three different experiments. Differences between TetraMan-GNP and both control GNPs are significant, as indicated with three asterisks ($p < 0.001$).

To get a deeper insight on the sensitivity of the GNP-ELISA, 20 $\mu\text{g mL}^{-1}$ of GNPs were used to coat the ELISA plates and different concentrations of 2G12 (from 13.8 nM to 0.1 nM) were subjected to analysis (Fig. 2B). The GNP-ELISA with TetraMan-GNP allowed the detection of 2G12 at 1.4 nM (0.2 $\mu\text{g mL}^{-1}$). Considering that the concentration of 2G12 in plasma (in animal models) ranges between 1200 to 49 $\mu\text{g mL}^{-1}$,²³ our results indicated that GNP-ELISA is a valid method for the detection of very low levels of anti-carbohydrate antibodies that could be also applied for biological samples.

To correlate the 2G12 response with the increase of carbohydrates copies on the gold surface, GNPs carrying 50% of TetraMan instead of 10% were also used to coat ELISA plate. The 50% TetraMan-GNP led to a more sensitive 2G12 detection in comparison to the 10% TetraMan-GNP (Fig. 3). These results suggest that the multivalent high-mannose presentation on the gold nanoparticles, used as antigens in the ELISA coating, provides high selectivity and sensitivity for the detection of 2G12.

²³ Hessel A. J., Rakasz E. G., Pognard P., Hangartner L., Landucci G., Forthal D.N., Koff W.C., Watkins D. I., Burton D. R., Broadly neutralizing human anti-HIV antibody 2G12 is effective in protection against mucosal SHIV challenge even at low serum neutralizing titers, PLoS Pathog. 2009, 5, e1000433.

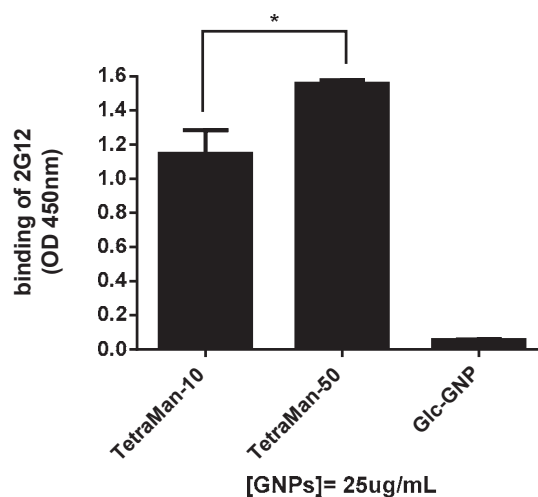


Figure 3: GNPs carrying 10% or 50% of TetraMan were compared to coat ELISA plate. The 50% TetraMan-GNPs led to a more sensitive 2G12 detection in comparison to the 10 % TetraMan-GNPs. No detection was observed for Glc-GNPs.

Our GNPs add a new multivalent tool to the described glycan arrays of covalently coupled oligomannose dendrons⁹ and virus capsids glycoconjugates uses in ELISA as antigens²⁴ for 2G12 detection.

GNP-ELISA for the detection of anti-carbohydrates antibodies in mice

The next step was to verify the method for the detection of anti-carbohydrate IgG antibodies in a more complex biological sample. We have previously demonstrated in chapter-3 that TetraPnOv-GNP bearing 40 % of the synthetic epitope TetraPn, which corresponds to the single repeating unit of the *S. pneumoniae* type 14 capsular polysaccharide (Pn14PS),²⁵ and 5 % of the T-cell epitope OVA₃₂₃₋₃₃₉ (Fig. 1) are able to evoke functional anti-carbohydrate IgG antibodies in mice against Pn14PS.¹⁸ In chapter-3, the detection of the specific IgGs was performed by coupling the tetrasaccharide epitope (Tetra-Pn) to BSA and running a “classic” ELISA for IgG antibodies diluting mice sera from 1:10 to 1:1000. Here, TetraPnOv-GNP (25 $\mu\text{g mL}^{-1}$) was directly used to coat ELISA plates for the IgG detection (Fig. 4). TetraPn-GNP carrying 50 % of tetrasaccharide and 50% glucose was also tested in the ELISA in order to exclude sera

²⁴ Astronomo R. D., Kaltgrad E., Udit A. K., Wang S. K., Doores K. J., Huang C. Y., Pantophlet R., Paulson J. C., Wong C. H., Finn M. G., Burton D. R., Defining criteria for oligomannose immunogens for HIV using icosahedral virus capsid scaffolds, *Chem. Biol.* 2010, 17, 357-370.

²⁵ Safari D., Dekker H. A., Joosten J. A., Michalik D., de Souza A. C., Adamo R., Lahmann M., Sundgren A., Oscarson S., Kamerling J. P., Snippe H., Identification of the smallest structure capable of evoking opsonophagocytic antibodies against *Streptococcus pneumoniae* type 14, *Infect. Immun.* 2008, 76, 4615-4623.

interactions with the OVA₃₂₃₋₃₃₉ peptide. TetraMan-GNP, DiMan-GNP, Glc-GNP, and Gal-GNP were used as control. Sera from mice immunized with TetraPnOv-GNP were diluted 1:30,000. Specific IgGs against TetraPn recognized TetraPnOv- and TetraPn-GNPs on the ELISA plate with high OD at 450 nm (Fig. 4A). High levels of IgGs were detected in serum of mice immunized with the TetraPnOv-GNP (OD > 1) and significant signal (~0.8 OD) was also detected for TetraPn-GNP.

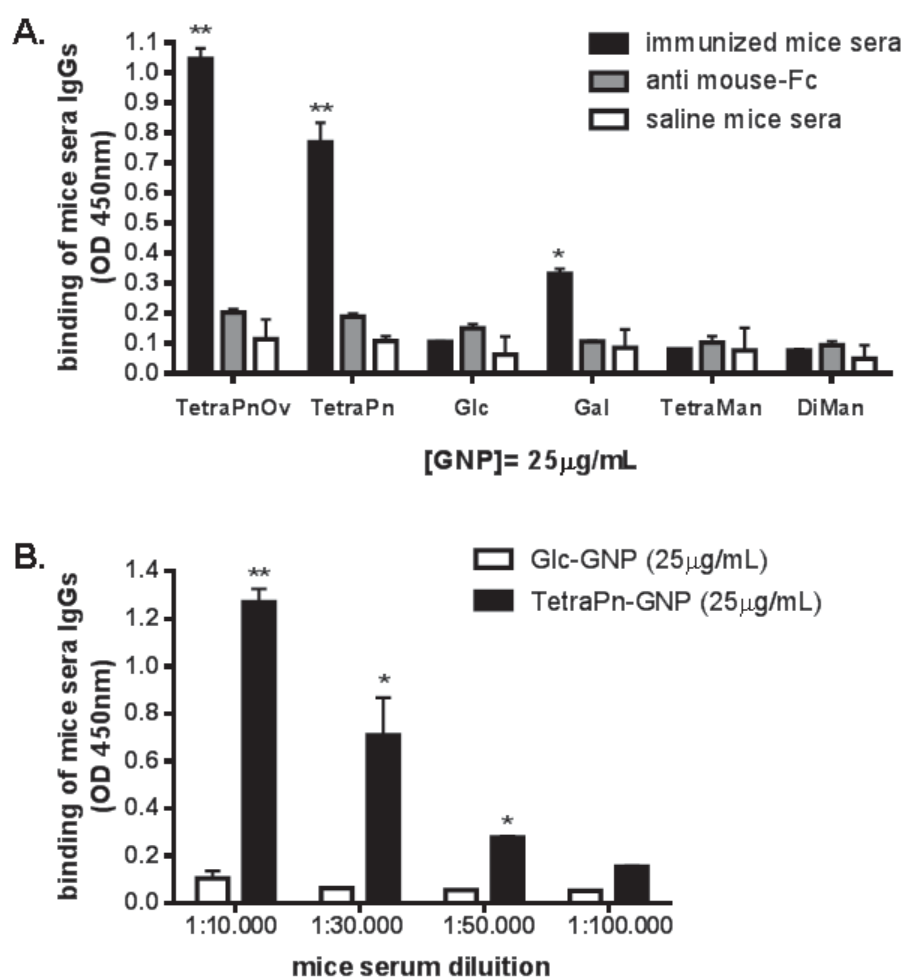


Figure 4: GNP-ELISA for the detection of anti-carbohydrates antibodies from mice immunized with TetraPnOv-GNP: **A)** Detection of specific IgG by GNPs carrying different carbohydrates. TetraPnOv- and TetraPn-GNPs show strong binding to mice serum at a 1:30,000 dilution. Detectable binding was also observed for Gal-GNP. Glc-, TetraMan-, and DiMan-GNPs were not recognized by the sera's IgG. Non-specific interactions of the secondary anti-mouse IgG with the GNPs were excluded performing the GNP-ELISA in the absence of 2G12. Sera of mice immunized with saline were used as negative control. Differences between sera from immunized mice and control samples are significant, as indicated with one ($p < 0.05$) or two asterisks ($p < 0.01$); **B)** ELISA plate coated with 25 µg/mL of TetraPn-GNP carrying *S. pneumoniae* or Glc-GNP (control) were used to determine the detection limit for anti-TetraPn antibodies in mice sera. GNP-ELISA was able to detect antibodies up to 1:50,000 dilutions of sera. Differences between TetraMan-GNP and Glc- GNP are significant, as indicated with one ($p < 0.05$) or two asterisks ($p < 0.01$).

No response was detected after coating the ELISA plate with Glc-GNP, indicating the absence of significant titers of anti-glucose antibodies in the serum of mice immunized with the TetraPnOv-GNP (that contains 50% of glucose). A weak positive but significant signal ($OD > 0.2$) was observed for Gal-GNP, in agreement with the molecular structure of the biantennary TetraPn (Fig. 1) that presents a terminal galactose in both antennas. As expected, serum antibodies showed no affinity for mannosides, as both TetraMan- and DiMan-GNPs were not able to capture any component of sera from mice immunized with TetraPnOv-GNP. Sera from mice immunized with saline were used as negative control and gave no signal ($OD < 0.2$) in the GNP-ELISA (Fig. 4A). The secondary anti-mouse IgG antibody did not react with any of the GNPs, so that non-specific interactions were excluded. In order to define the detection limit of this methodology, serial dilutions (1:10,000 to 1:100,000) of sera from mice immunized with TetraPnOv-GNP were analyzed on plates coated with $25 \mu\text{g mL}^{-1}$ of TetraPn-GNP (Fig. 4B). The OD at 450 nm coming from the specific anti-carbohydrate IgGs binding was detected up to 1:50,000 dilution, indicating a $\sim 3,000$ -fold increase of detection in comparison to the classical ELISA used in our previous chapter-3 (Fig. 5).¹⁸

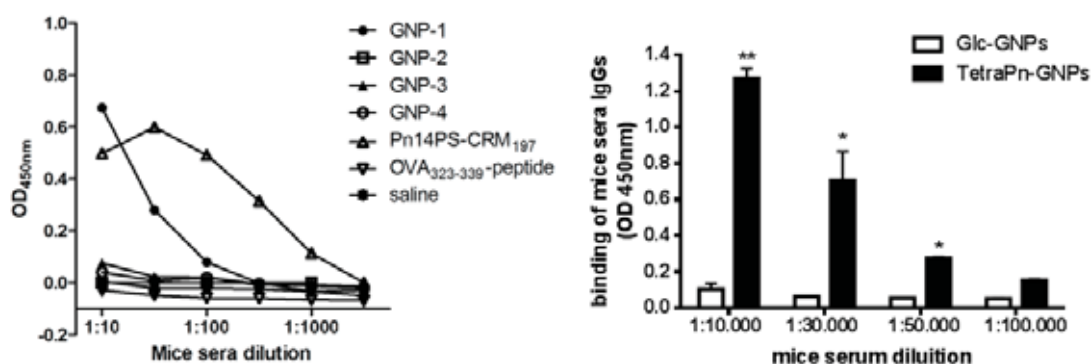


Figure 5: Comparison between BSA-TetraPn conjugate and TetraPn-GNP as antigens for ELISA in the detection of specific IgG in mice. Left: detection of IgG against BSA-TetraPn used as antigen to coat ELISA plates (see chapter-3).¹⁸ Mice immunized with Pn14PS-CRM and mice immunized with GNP-1 (TetraPn-GNPs in this chapter) showed high amount of specific IgG diluting mice sera from 1:10 to 1:100. Right: detection of IgG against TetraPn-GNPs used as antigen to coat ELISA plates. Mice immunized with TetraPn-GNPs showed high amount of specific IgG diluting mice sera from 1:10,000 to 1:50,000. The comparison clearly shows a ~ 3000 fold improvement of the IgG detection. Same mice sera, same coating conditions, same buffers, same detection procedure and same equipments were used.

GNPs bearing 5 % of OVA peptide and 95% of glucose were not detected by mice sera IgGs (Fig. 6).

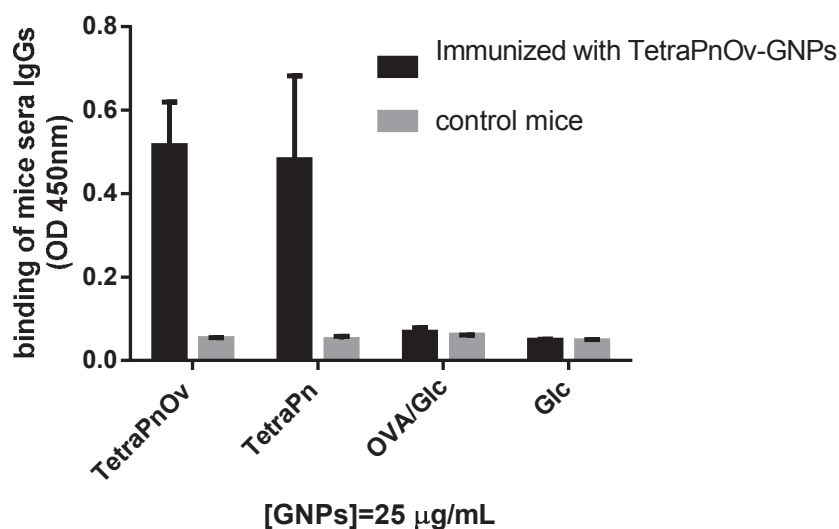


Figure 6: Detection of anti-carbohydrates antibodies from mice immunized with TetraPnOv-GNP: Detection of specific IgG by GNPs carrying different carbohydrates. TetraPnOv- and TetraPn-GNP show strong binding to mice serum at a 1:30,000 dilution. OVA/Glc-GNPs (GNP carrying 5% of OVA₃₂₃₋₃₃₉, like on the TetraPnOVA-GNPs, and 95% of glucose) and Glc-GNPs were not recognized by the sera's IgG. Sera of mice immunized with saline were used as negative control.

The presence of specific IgGs against TetraPn was also detected in mice immunized with Pn14PS conjugated to cross reactive material from diphtheria toxin (Pn14PS-CRM)¹⁸ (Fig. 7).

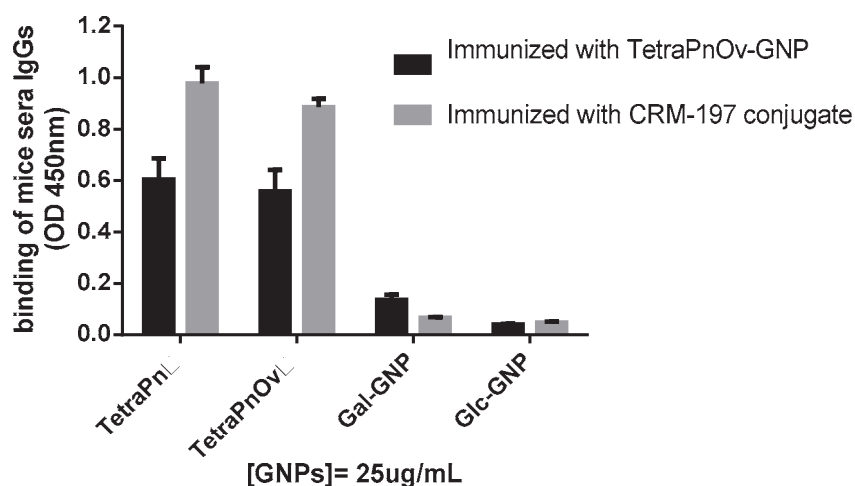


Figure 7: Sera from mice immunized with TetraPnOv-GNP or Pn14PS conjugated to cross reactive material from diphtheria toxin (Pn14PS-CRM, CRM-197 conjugate) were diluted 1:30,000. Specific IgGs against TetraPn recognized TetraPnOv- and TetraPn-GNPs on the ELISA plate with high OD at 450 nm. IgGs levels in serum of mice immunized with the Pn14PS-CRM were higher than in serum of mice immunized with TetraPnOv-GNP.

These results demonstrate that the GNP-ELISA represents a novel, straightforward screening method for detecting anti-carbohydrate antibodies evoked by carbohydrate-based vaccines.

The method could be extended to screen the affinity of any carbohydrate, once tailored onto the multivalent GNP nanoplatform. The GNP-technique is more sensitive than ELISA based on glycoconjugation to proteins, probably due to the higher glycan density on the 3D surface of the gold nanoclusters. This new approach also affords an easier and faster procedure to monitor the antibody titers during animal immunization studies as the same GNP construct can be used both for the immunization and for screening the antibody titers in ELISA. The GNP-ELISA approach may also allow multiple screening of complex samples for the detection of anti-carbohydrate antibodies by using GNPs displaying different carbohydrate antigens.

Dendritic cells adhesion assay using GNP-ELISA

The application of the multivalent GNP-coated surface was extended to an adhesion assay with human dendritic cells (DC). DC are antigen-presenting cells that display calcium-dependent glycan-binding proteins (C-type lectins) on their surface, which function in the recognition and internalization of pathogens.²⁶ One of the C-type lectin expressed in DC is DC-SIGN (Dendritic Cell Specific Intracellular Adhesion Molecule Grabbing Non-integrin) with dual specificity for mannose- and fucose-containing glycans.^{27, 28} To evaluate binding of DC to different GNPs, ELISA wells were coated with Glc-GNP, DiMan-GNP, and Gal-GNP. It has been previously shown that DiMan-GNP inhibits gp120(CN54) binding to DC-SIGN in the nanomolar range.¹⁷ Binding of moDC was determined using a calcium and magnesium containing buffer in the absence and presence of ethylene glycol tetra acetic acid (EGTA) or the anti DC-SIGN blocking mAbs AZN-D1.²⁹ This antibody was previously shown to block the DC internalization of fluorescent-GNPs carrying oligomannosides.³⁰ The GNP-modified plate was incubated with calcein-labeled monocyte-derived DC (moDC) following a protocol commonly used to investigate the binding

²⁶ García-Vallejo J. J., van Kooyk, Y., Endogenous ligands for C-type lectin receptors: the true regulators of immune homeostasis, *Immunol. Rev.* 2009, 230, 22-37.

²⁷ Appelmelk B. J., van Die I., van Vliet S. J., Vandenbroucke-Grauls C. M., Geijtenbeek T. B. H., van Kooyk Y., Cutting edge: carbohydrate profiling identifies new pathogens that interact with dendritic cell-specific ICAM-3-grabbing nonintegrin on dendritic cells, *J. Immunol.* 2003, 170, 1635-1639.

²⁸ van Liempt E., Bank C. M., Mehta P., García-Vallejo J. J., Kwar Z. S., Geyer R., Alvarez R. A., Cummings R. D., van Kooyk Y., van Die I., Specificity of DC-SIGN for mannose- and fucose-containing glycans, *FEBS Lett.* 2006, 580, 6123-6131.

²⁹ Geijtenbeek T. B., Torensma R., van Vliet S. J., van Duijnhoven G. C., Adema G. J., van Kooyk Y., Figdor C. G., Identification of DC-SIGN, a novel dendritic cell-specific ICAM-3 receptor that supports primary immune responses, *Cell* 2000, 100, 575-585.

³⁰ Arnáiz B., Martínez-Ávila O., Falcon-Perez J. M., Penadés S., Cellular uptake of gold nanoparticles bearing HIV gp120 oligomannosides, *Bioconjugate Chem.* 2011, 23, 814-825.

of moDC with glycoconjugates.³¹ The moDC showed a specific carbohydrate-dependent binding to the selected GNPs, as shown in Figure 8. DiMan-GNP exhibited the highest affinity for moDC (around 40 % binding), while a weak binding (~15%) was detected for Gal-GNP. This low binding is in agreement with the reported low adhesion of DC to PAA-coupled galactose.³¹ The significant signal detected for Glc-GNP (30 %) can be explained by the previous evidence that glucose at high concentrations inhibits the binding of high-mannose glycoproteins to DC-SIGN.³²

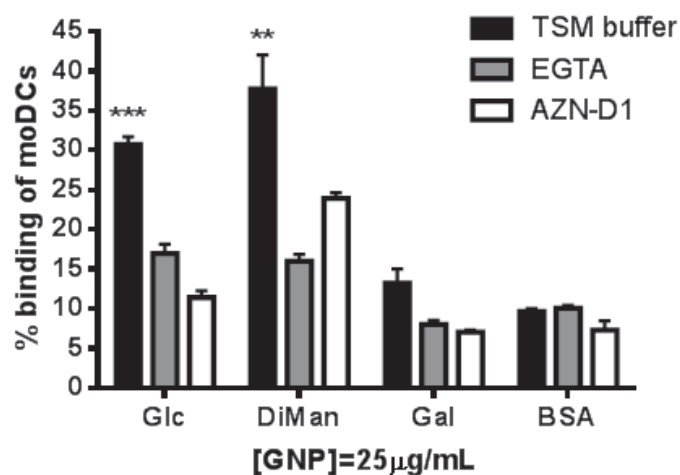


Figure 8: Dendritic cells adhesion assay using GNP-ELISA. Dendritic cells show different carbohydrate-affinity. Binding of moDC to GNPs in calcium and magnesium containing buffer, was determined using plate adhesion assay in the presence or absence of EGTA (3.75 nM) or anti-DC-SIGN antibody AZN-D1 (10 µg mL⁻¹). These experiments were performed at least four times with similar results. Each experiment was performed in triplicate. Error bars indicate standard deviations. The binding to the GNPs was significantly decreased when treated with EGTA or AZN-D1, as indicated with one (p<0.05) or two asterisks (p<0.01).

The presence of EGTA 3.75 mM blocked the binding of the moDC to both DiMan-GNP and Glc-GNP, indicating the involvement of calcium-dependent C-type lectins (Fig. 8, grey bars). Pre-

³¹ van Vliet S. J., van Liempt E., Saeland E., Aarnoudse C. A., Appelmelk B., Irimura T., Geijtenbeek T. B. H., Blixt O., Alvarez R., van Die I., van Kooyk Y., Carbohydrate profiling reveals a distinctive role for the C-type lectin MGL in the recognition of helminth parasites and tumor antigens by dendritic cells, *Int. Immunol.* 2005, 17, 661-669.

³² Ilyas R., Wallis R., Soilleux E. J., Townsend P., Zehnder D., Tan B. K., Sim R. B., Lehnert H., Randeve H. S., Mitchell D. A., High glucose disrupts oligosaccharide recognition function via competitive inhibition: a potential mechanism for immune dysregulation in diabetes mellitus, *Immunobiology* 2011, 216, 126-131.

treatment of moDC with AZN-D1 (10 µg/mL) significantly decreases their binding to Glc-GNP and, in a less extent, to DiMan-GNP. This result suggests that DC-SIGN is involved in the binding of moDC to DiMan and Glc-GNPs.

DC-SIGN binding to GNPs

To extend the GNP-ELISA to other carbohydrate-binding proteins, the binding of a recombinant chimera protein DC-SIGN-Fc to different sugar-coated GNPs was tested (Fig. 9). DC-SIGN-Fc was produced in Chinese hamster ovary K1 cells by co-transfection of DC-SIGN-Sig-pIgG1 Fc (20 µg) and pEE14 (5 µg) vector. DC-SIGN-Fc consists of the extracellular portion of DC-SIGN (residues 64 to 404) fused at the C-terminus to a human IgG1/Fc fragment into the Sig-pIgG1-Fc vector.³³ DC-SIGN-Fc bound to TetraMan-, DiMan- and PentaMan-GNPs in presence of calcium and magnesium containing buffer (TSM). The binding of DC-SIGN to DiMan-GNP, TetraMan and PentaMan-GNPs was very high (OD>1) in agreement with the carbohydrate-specificity of this lectin.^{17, 28} Glc-GNP exhibited significant lower binding (OD~0.3) than the mannoside GNPs, while no binding was detected for Gal-GNP (OD<0.1) and BSA. No binding was detected in PBS. This result indicates that DC-SIGN is involved in the adhesion of DC to the carbohydrate-modified plate and validate the GNP-ELISA for lectin detection and interactions. The selective adhesion of DCs and recombinant lectin to GNPs confirms also the coating of the ELISA surface with the multivalent GNPs and indicates that GNP-ELISA can be used in solid-phase assays to explore glycan-binding properties of lectins as well as whole cells. The binding of bacteria³⁴ and mammalian cells³⁵ to carbohydrates have been also probed in microarray systems and our new ELISA approach can contribute to cellular studies on solid-phase.

³³ Fawcett J., Holness C. L., Needham L. A., Turley H., Gatter K. C., Mason D. Y., Simmons D. L., Molecular cloning of ICAM-3, a third ligand for LFA-1, constitutively expressed on resting leukocytes, *Nature* 1992, 360, 481-484.

³⁴ Disney M. D., Seeberger P. H. The use of carbohydrate microarrays to study carbohydrate-cell interactions and to detect pathogens, *Chem. Biol.* 2004, 11, 1701-1707.

³⁵ Nimrichter L., Gargir A., Gortler M., Altstock R. T., Shtevi A., Weissshaus O., Fire E., Dotan N., Schnaar R. L., Intact cell adhesion to glycan microarrays, *Glycobiology* 2004, 14, 197–203.

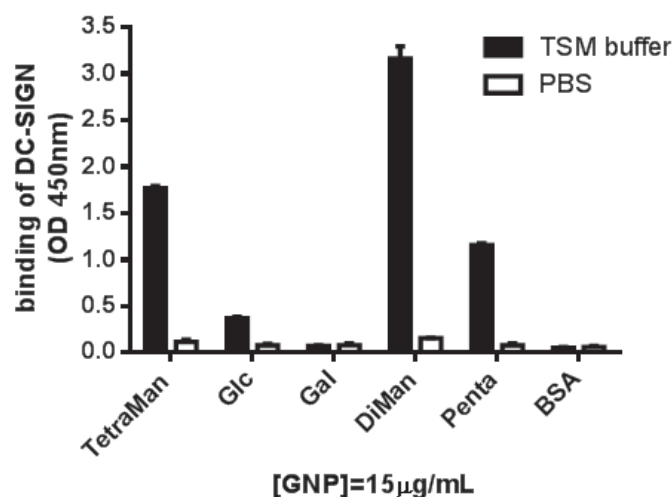


Figure 9: DC-SIGN-Fc binding to GNP. Binding was determined using GNP-ELISA in PBS and in calcium and magnesium containing buffer (TSM). These experiments were performed in triplicate at least three times with similar results. Error bars indicate standard deviations.

Conclusions

A new fast and sensitive method (GNP-ELISA) for the detection of anti-carbohydrates antibodies and other glycan-binding proteins has been developed by using multivalent and high molecular weight GNPs as solid-phase coating. GNPs are three-dimensional systems that allow a high valency in the presentation of selected glycans (up to 100 copies per nanoparticle) on a 2 nm gold nanoclusters. The possibility of varying density and type of carbohydrate antigen on the nanoparticles³⁶ makes the GNP-ELISA a versatile and sensitivity method for multiplex detection of carbohydrate-binding partner comparable to printed glycan-array. We first showed the selectivity of GNP-ELISA for detecting the multivalent interaction between a tetramannoside of the high-type mannose glycan expressed on HIV glycoprotein gp120 and the human antibody 2G12 at the nM range. Furthermore, we have successfully used GNP-ELISA to highly improve the detection (~3,000-fold) of specific IgGs against *S. pneumoniae* in mice sera respect to the BSA-based ELISA. Finally, we showed that the GNP-ELISA can be used in solid phase cellular binding assays, as demonstrated by the selective binding of human moDC, and the lectin DC-SIGN on a multivalent surface. The simplicity, the high sensitivity and versatility of this GNP-ELISA method, represent a new approach that can facilitate basic studies of protein-carbohydrate interactions and be especially useful in vaccination studies and in clinical identification of biomarkers.

³⁶ Marradi M., Chiodo F., García I., Penadés, S., Glyconanoparticles as multifunctional and multimodal carbohydrate systems, Chem. Soc. Rev. 2013DOI:10.1039/C2CS35420A.

Experimental part

Materials

All chemicals were purchased as reagent grade from Sigma-Aldrich, except chloroauric acid (Strem Chemicals), and were used without further purification. Anti HIV-1 gp120 Monoclonal Antibody 2G12 was kindly supplied by Dr D. Katinger (Polymun Scientific, Vienna, Austria).

Preparation of GNPs

GNPs were prepared in a one-step reaction by reducing a gold salt with sodium borohydride in the presence of a mixture of thiol-functionalized glycoconjugates in the desired molar ratio following an established procedure.³⁷ GNPs bearing 10% of a thiol-ending conjugate of dimannoside $\text{Man}(\alpha 1-2)\text{Man}(\alpha 1\rightarrow)$ (DiMan), tetramannoside $\text{Man}(\alpha 1-2)\text{Man}(\alpha 1-2)\text{Man}(\alpha 1-3)\text{Man}(\alpha 1\rightarrow)$ (TetraMan) or $\text{Man}(\alpha 1-2)\text{Man}(\alpha 1-3)[\text{Man}(\alpha 1-2)\text{Man}(\alpha 1-6)]\text{Man}(\alpha 1\rightarrow)$ (Penta) and 90% of 5-(mercapto)pentyl β -D-glucopyranoside as inner component were prepared as previously reported (see chapter-2).¹⁷ GNPs carrying $\text{Gal}(\beta 1-4)\text{Glc}(\beta 1-6)[\text{Gal}(\beta 1-4)]\text{GlcNAc}(1\rightarrow)$ (TetraPn) and OVA₃₂₃₋₃₃₉ peptide were prepared following a protocol previously described (see chapter-3).¹⁸ The ratio of the different ligands on the nanocluster surface was determined by quantitative ¹H NMR. Transmission electron microscopy showed an average gold core diameter of 2 nm.

GNP-ELISAs

50 μL of GNPs solution (25 $\mu\text{g}/\text{mL}$ or the reported concentration in the manuscript) in the coating buffer (50mM Na_2CO_3 , pH=9.7) were used to coat the Nunc MaxiSorp plate, overnight at 4°C or 2h at room temperature. After discarding the GNPs solutions and washing with PBS (10mM, pH=7.4) (2x200 μL), the wells were blocked with 200 μL of 1% BSA (Sigma-Aldrich, lyophilized powder, $\geq 96\%$, agarose gel electrophoresis) in PBS at room temperature for 30 min. The wells were discarded, and 100 μL of 2G12 (from 13.8 to 0.13nM) or 100 μL of mice serum at different dilution in assay buffer (0.5% BSA) were added in the plate that was shaken for 1 h at 500rpm. After washing the wells with PBS (3x200 μL), 100 μL of anti-human horseradish peroxidase (0.8 $\mu\text{g}/\text{mL}$, life technologies, Novex[®] Goat anti-Human IgG-HRP) or 100 μL of anti-mouse horseradish peroxidase (0.8 $\mu\text{g}/\text{mL}$, life technologies, Novex[®] Rabbit anti-Mouse IgG-HRP) were added for 2G12 or mice serum IgG detection, respectively. After 30 min of shaking at 500 rpm, the wells were washed with PBS (3x200 μL). Finally, 100 μL of substrate solution (3,3',5,5'-Tetramethylbenzidine, TMB, in citric/acetate buffer, pH=4, and H_2O_2) was added and after 3 min incubation at room temperature the reaction was stopped with 50 μL of H_2SO_4 (0.8 M) and the optical density was measured at 450 nm in an ELISA reader. These experiments were always performed in triplicate.

In vitro generation and culture of human DCs

Immature DCs were generated from human peripheral blood mononuclear cells (PBMCs) as described previously³⁸ from buffy coats of healthy donors (Sanquin). Monocytes were prepared from PBMCs by centrifugation over Percoll and incubated for 5 days in RPMI supplemented with 10% heat inactivated fetal calf serum, 2.4 mM L-glutamine, 100 U/ml penicillin-streptomycin (all from Gibco), 800 U/ml of human recombinant granulocyte-

³⁷ Di Gianvincenzo P., Chiodo F., Marradi M., Penadés S., Gold manno-glyconanoparticles for intervening in HIV gp120 carbohydrate-mediated processes, *Methods Enzymol.* 2012, 509, 21-40.

³⁸ Sallusto F., Lanzavecchia A., Efficient presentation of soluble antigen by cultured human dendritic cells is maintained by granulocyte/macrophage colony-stimulating factor plus interleukin 4 and downregulated by tumor necrosis factor alpha, *J. Exp. Med.* 1994, 179, 1109-1118.

macrophage colony-stimulating factor and 500 U/ml of human recombinant IL-4 (both from Schering-Plough, Brussels, Belgium).

Cellular binding

Ninety-six-well plates (Nunc MaxiSorp®) were coated at room temperature for 2 h with GNPs (25 µg/mL) and afterwards blocked with 1% BSA. Calcein AM (Molecular Probes) was used to label moDC following a reported protocol.³¹ Then, calcein pre-treated moDC were incubated on the ELISA wells (40,000 cells/well) for 2 h at 37°C in calcium and magnesium containing TSM buffer (20 mM tris(hydroxymethyl)aminomethane (Tris)-HCl, pH 8.0; 150 mM NaCl; 1 mM CaCl₂; 2 mM MgCl₂). The cells were added for 1.5 h at 37°C in the presence or absence of 3.75 mM EGTA or 10 µg/mL of mAbs AZN-D1. Non-adherent cells were removed by gentle washing. After that, adherent cells were lysed and the binding was correlated with the calcein absorption. The fluorescence was quantified on a Fluorostar spectrofluorimeter (BMG Labtech, Offenburg, Germany).

DC-SIGN binding

Nunc MaxiSorp plates were coated with 50 µL GNPs (15 µg/mL in coating buffer) for 2 h at room temperature. The wells were washed twice with TSM (2x200µL) and blocked with 100 µL TSM with 1% of BSA for 30 min at room temperature. After 1x200µL wash with PBS, the wells were incubated at 37°C with 50 µL DC-SIGN-Fc (3 µg/mL) in TSM with 1% of BSA for 1 h. The wells were washed four times with TMS (4x200µL) and incubated at room temperature with 50 µL of Goat-anti human HRP (0.8 µg/mL) in TSM with 1% of BSA for 30 min. After four washes with TMS (4x200µL), 100 µL of substrate solution (3,3',5,5'-Tetramethylbenzidine, TMB, in citric/acetate buffer, pH=4, and H₂O₂) were added and after 4 min at room temperature the reaction was stopped with 50 µL of H₂SO₄ (0.8M) and the plate was read at 450 nm ELISA reader. All the experiments were performed in triplicate.

Statistical methods

Multiple t-test was used to determine differences between the experiments and the control conditions. P-value ≤0.05 is considered to be statistically significant (Graphad Prism 6.00). One asterisk indicates a P-value < 0.05; two asterisks indicate a P-value < 0.01 and three asterisks indicate a P-value < 0.001.

Part-2

GNPs as tool to study the role of carbohydrates in the dendritic cell- mediated innate immunity

Introduction

In the previous part of this Thesis (**chapter 2 and 3**), we explored the potential application of gold nanoparticles as carriers for multiple glycan epitopes related to HIV and *S. pneumoniae*. The specific production of antibodies against the carbohydrate structures of these parasites demonstrates the usefulness of GNPs to evoke an adaptive immune response against carbohydrate antigens. To expand our knowledge on the potentiality of GNPs in the so-called glyco-immunology field, we have been also explored GNPs as an interesting carbohydrate multivalent system to study the dendritic cells-mediated innate immune response to carbohydrates.

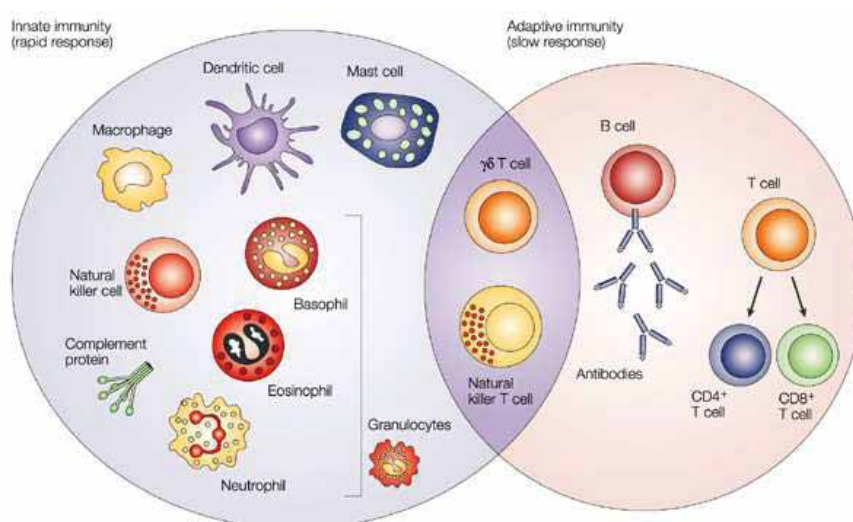


Figure 1: Cells involved in the innate (left) and adaptive (right) immune responses. Naïve T-cells are on the borderline between both immune responses. (From reference 1).

The immune system can be divided into two branches that are strictly connected: the innate and the adaptive systems (Fig. 1). The evolutionary conserved innate branch of the immune system is responsible for the detection of well known pathogen-associated molecular patterns (PAMPs). PAMPs are molecules associated with groups of pathogens that are recognized by cells of the

¹ Dranoff G., Cytokines in cancer pathogenesis and cancer therapy, Nat. Rev. Cancer 2004 4, 11-22.

innate immune system like granulocytes, nature killer-cells, macrophages and dendritic cells. These molecules are small molecular motifs conserved within a class of microbes. They are recognized by Toll-like receptors (TLRs) and other pattern recognition receptors (PRRs) expressed on the cells of the innate immune system. PAMPs activate innate immune responses, protecting the host from infection, by identifying some evolutionary conserved non-self molecules like bacterial lipopolysaccharides (LPS), endotoxins founded on the bacterial cell membrane of bacteria. LPS is specifically recognised by TLR 4, one of the recognition receptors of the innate immune system.

The adaptive branch of the immune system includes the activation and the related proliferation of specific T and B-cells against pathogens. T cells (thymus cells) and B cells (bursa of Fabricius-derived cells) are the major cellular components of the adaptive immune response. T cells are involved in the so called cell-mediated immunity, whereas B cells are responsible for the so called humoral immunity (related to antibodies production). The function of T cells and B cells is to recognize specific non-self antigens, during a process known as antigen presentation. Once they have identified an “invader”, these cells generate specific responses to eliminate pathogens and pathogen-infected cells. The B cells response to pathogens is to produce antibodies which then neutralize foreign parasites like bacteria and viruses. In response to pathogens some T cells, called T helper cells, are able to produce cytokines that stimulate the immune response. T-cells express a unique T-cell receptor (TCR) that recognizes specific antigens when presented in the major-histocompatibility complexes (MHC). The antigen-MHC complexes are expressed on the cellular membrane of antigen-presenting cells (APC). The function of APCs is to recognize the antigens and present them to the naïve T-cell in the so-called immunological synapse (Fig. 2).

Dendritic cells (DCs) are APCs able to induce and modulate specific immune responses after pathogens recognition.² The signalling induced by parasites after the interaction with the conserved receptors of DCs is crucial for triggering adaptive immune response to pathogens. The pathogens-promoted signalling is able to induce DCs maturation and their migration to the lymph node where the naïve T-cell will be educated to trigger an effective adaptive immune response.³

² Steinman R. M., The dendritic cell system and its role in immunogenicity, *Annu. Rev. Immunol.* 1991, 9 271–296.

³ Kapsenberg M. L., Dendritic-cell control of pathogen-driven T-cell polarization, *Nat. Rev. Immunol.* 2003, 3, 984-993.

DCs express different pattern recognition receptors (PRRs) able to recognize the conserved PAMPs that can induce an innate signalling directly related to their nature: peptides, lipids, nucleotides and carbohydrates are different classes of PAMPs that induce a specific signalling to the DCs that will influence the instruction to give to the naïve T cells by the production of different cytokines (Fig. 2).

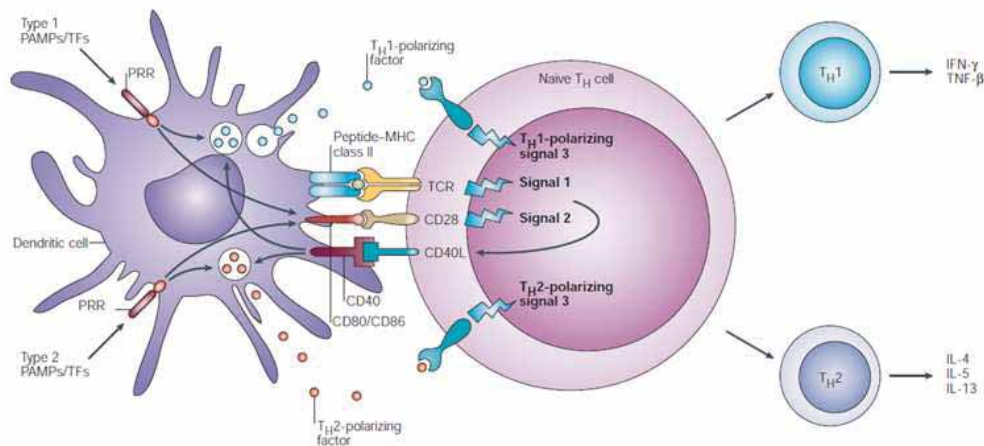


Figure 2: Cross-talk between a DC and a naïve $CD4^+$ T-cell in the immunological synapse: **Signal 1** is the antigen-specific signal that is mediated through T-cell receptor (TCR) and MHC class-II-associated peptides processed from pathogens after internalization through specialized pattern recognition receptors (PRRs). **Signal 2** is the co-stimulatory signal, mainly mediated by CD28 complex with CD80 and CD86 that are expressed by dendritic cells (DCs) after ligation of PRRs, such as Toll-like receptors (TLRs) that are specialized to sense infection through recognition of pathogen-associated molecular patterns (PAMPs). **Signal 3** is the polarizing signal that is mediated by various soluble or membrane-bound factors, such as interleukins that promote the development of Th1 or Th2 cells. The nature of signal 3 depends on the activation of particular PRRs by PAMPs. The profile of T-cell-polarizing factors is primed by recognition of PAMPs and the optimal expression of this profile often requires feedback stimulation by CD40 ligand expressed by T cells after activation by signals 1 and 2. (From reference 3)

After the antigen-recognition between the DCs MHC-complexes (including the antigen) and specific the T-cell receptor (TCR) signal-1, DCs develop phenotypic changes up-regulating their surface co-stimulatory molecules (proteins CD80 and CD86, signal-2) with a process called DCs maturation. This process allows DCs to migrate to the lymph node where they will interact with naïve T-cells. These phenotypic changes and the correlated interleukins production (signal-3) allow

DCs to cross-talk with the naïve T-cells that will be educated by DCs to become effector CD4⁺ T-helper cells. Under the influence of the local cytokines, effector CD4⁺ T-helper cells (Th cells) can differentiate into T-helper 1 (Th1) or T-helper 2 (Th2). Th1-cells produce interferon gamma, IFN- γ , and are crucial for cellular immunity against intracellular pathogens such as viruses or some bacteria or protozoa. Th2-cells produce interleukins IL-4, IL-5 and IL-13. The Th2 response is essential for nematode infections and allergies. DCs are able to educate the effector CD4⁺ T-helper cells to become immuno-suppressive T-cells called T-regulatory cells (Treg). Stimulated by IL-10, Treg are essential for the prevention of chronic immune response, allergies and transplant-rejection. All these balanced behaviours of the immune system have been conserved by evolution to avoid hyper-responses to antigens that could damage tissues and vital organs.

Through the binding with lectins (the PRR for carbohydrates), **carbohydrates participate in the modulation of innate immunity driving the routing for the MHC II presentation to prime antigen-specific CD4⁺ T cell responses.**^{4, 5} Carbohydrates are a complex class of PAMPs that are well recognized by DCs lectins especially when presented in a multivalent way.⁶ In this Thesis, GNPs have been explored as carbohydrates-multivalent systems to study **the DC-mediated innate immune response** (Fig. 2), e.g. the role of carbohydrates in the cross-talk between DCs and T-cells.

In chapter-5, GNP carrying galactofuranaose (Gal β) will be prepared and their effect on the DCs behavior will be studied. Gal β is a non-self ancient PAMP expressed in a multivalent way on several pathogens like *A. niger* and *M. tuberculosis*. We will exploit GNPs carrying Gal β to study if this monosaccharide could play a role during the interaction between parasites and DCs. To define the immunomodulatory effects of Gal β on DCs, we incubated DCs with Gal β -GNPs and measured the surface expression of the maturation markers (CD86 and CD80). The interleukins profile of DCs was also studied after their interaction with DCs (Fig. 3).

⁴ van Kooyk Y., Rabinovich G. A., Protein-glycan interactions in the control of innate and adaptive immune responses, *Nat. Immunol.* 2008, 9, 593-601.

⁵ Rabinovich G. A., van Kooyk Y., Cobb B. A., Glycobiology of immune responses, *Ann. N. Y. Acad. Sci.* 2012, 1253, 1-15.

⁶ García-Vallejo J. J., van Kooyk Y., Endogenous ligands for C-type lectin receptors: the true regulators of immune homeostasis, *Immunol. Rev.* 2009, 230, 22-37.

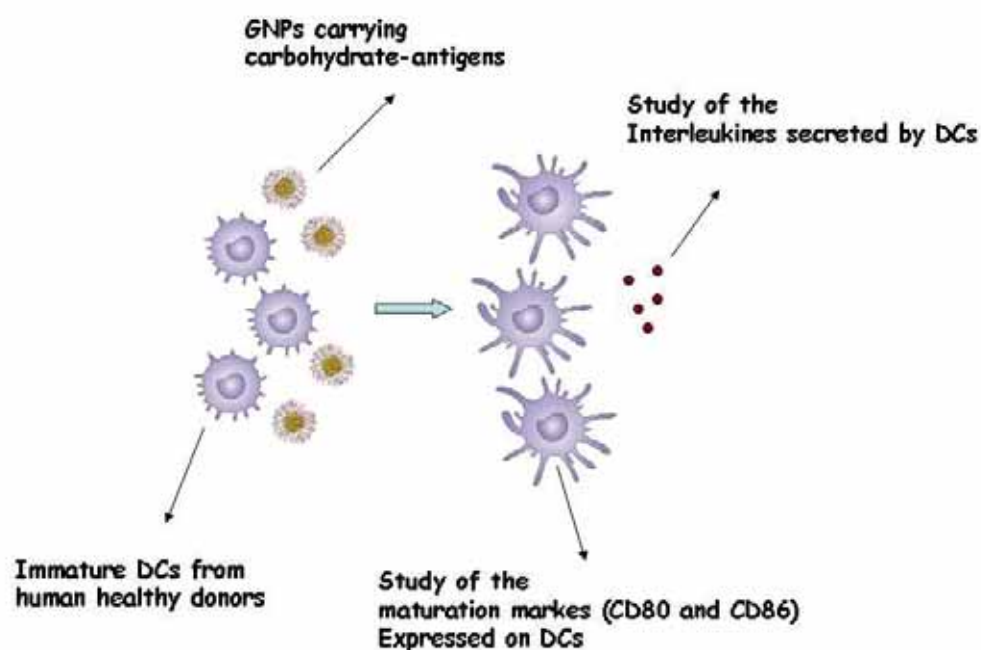


Figure 3: Immature human dendritic cells (DC) were incubated with selected GNPs carrying non-self Gal β and the innate immune response triggered on DC was studied (chapter-5).

In chapter-6, we designed GNPs carrying Lewis and high-mannoses glycans to achieve the efficient down modulation of T-cell responses after their interaction with GNPs. Lewis and high-mannoses are conserved self-glycans structures that interact with human lectins allowing the internalization of certain type of parasites like HIV and *Schistosoma mansoni*. In 2009 the notion that different glycans, interacting with the same lectin, can trigger different signalization processes to the naïve T-cells, opened new prospective in the study of the innate immune system.⁷ High mannose and Lewis X-GNPs were incubated with DCs and the interleukins profile of DCs was studied. Then we studied if the signaling induced by the GNPs on the DCs could be able to educate and modulate the CD4⁺ naïve T cell in a carbohydrates-dependent manner (Fig. 4).

⁷ Gringhuis S. I., den Dunnen J., Litjens M., van der Vlist M., Geijtenbeek T. B., Carbohydrate-specific signaling through the DC-SIGN signalosome tailors immunity to *Mycobacterium tuberculosis*, HIV-1 and *Helicobacter pylori*, Nat. Immunol. 2009, 10, 1081-1088.

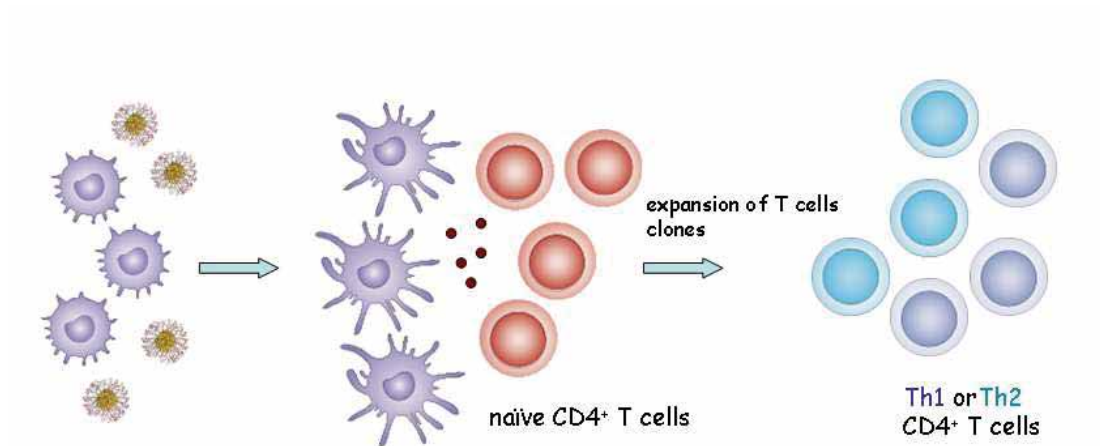


Figure 4: High mannose and Lewis X-GNPs were incubated with DCs and the interleukin profile of DCs was studied. The cross-talk between the DCs and T-cells was also studied after the interaction with this type of GNPs (chapter 6).

Maturation markers and interleukins production were studied on human DCs after their interaction with the described GNPs. The cellular experiments of this part of the Thesis were performed during a six months stay in the Molecular Cell Biology and Immunology department (MCBI) of Vrije University Medical Center (VUmc) (Amsterdam). The work presented in Chapter-5 was performed in the laboratory of Irma van Die with the help of the people from her group. The work presented in Chapter-6 was performed in the laboratory of Yvette van Kooyk with the help of the people from her group.

Chapter-5

Gold nanoparticles coated with galactofuranose elicit a pro-inflammatory response in human monocytes-derived dendritic cells and interact with C-type lectins

In collaboration with the Glycobiology and immune regulation group, MCBI, VUmc, Amsterdam

As described in the introduction of this Thesis, polysaccharides and glycoconjugates play important roles in many biological events. Typically, they are present at the cell membrane, cell wall, or are secreted in the extracellular space, where they form the interface between a cell or organism and its environment enabling cell-cell interactions and signalling events.¹ A number of glycans, including α and β -glucans, chitin, galactomannan and galactosaminoglycan, mediate the fungal adherence to the host cells. Glycoconjugates containing terminal galactofuranose (Galf) residues have been found in many microorganisms including trypanosomatids, fungi and bacteria (Fig. 1 left).²

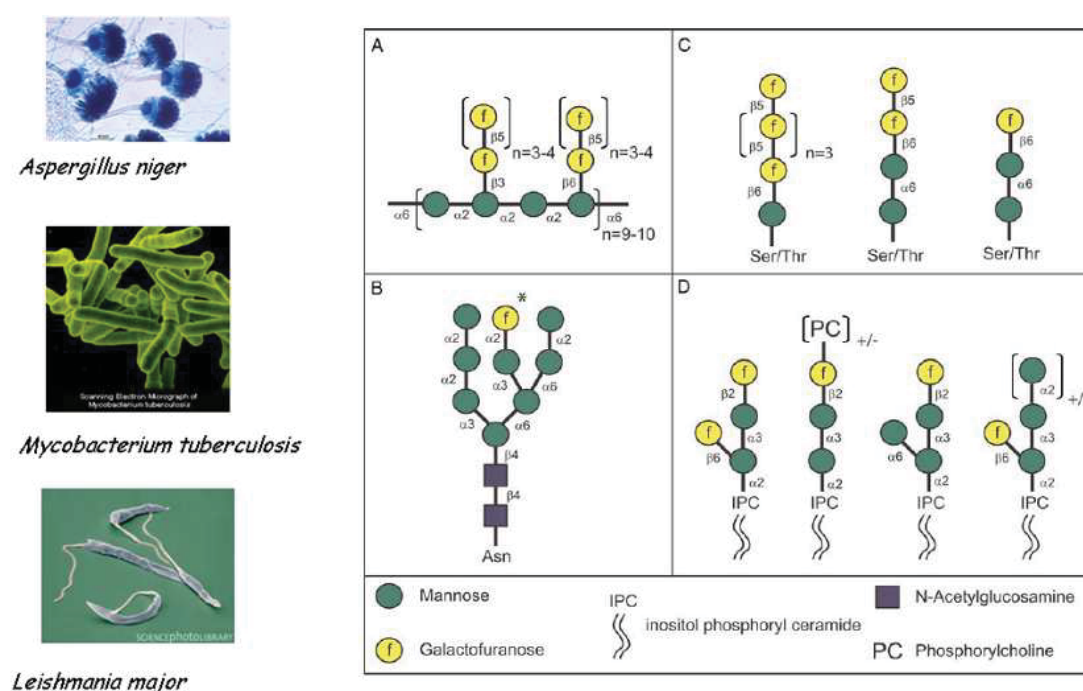


Figure 1: Parasites and corresponding glycoconjugates exposing terminal Galf units on their surface. **Left:** Parasites exposing Galf as terminal unit of their glycoconjugate. **Right:** Different Galf-containing glycoconjugates found in different parasites. Glycoside linkages are indicated and monosaccharides are represented by the conventional symbols as defined in the figure. Galactomannan (A) has been found in a soluble form, covalently bound to β -glucan and attached to a GPI anchor. N-glycans, containing Galf (B), are covalently linked to the protein backbone via an asparagine (Asn) residue. An N-glycan containing eight mannose residues is depicted here, but shorter N-glycans with 5, 6 or 7 mannoses have also been characterized. The asterisk indicates that β -linked Galf have also been found on N-glycans. Galf-containing O-glycans (C) are covalently linked to the protein backbone via a serine (Ser) or threonine (Thr) residue. Galf-containing glycosphingolipids (D) identified in *A. fumigatus*. +/- indicates that this moiety can be present or absent. Figure from reference 2.

¹ Dwek R. A., Glycobiology: Toward Understanding the Function of Sugars, Chem. Rev. 1996, 96, 683-720

² Tefsen B., Ram A. F., van Die I., Routier F. H., Galactofuranose in eukaryotes: aspects of biosynthesis and functional impact, Glycobiology 2012, 22, 456-469.

Different Galf-containing polysaccharides, *N*- and *O*-glycoproteins and glycosphingolipids have been identified in *A. fumigatus*, *M. tuberculosis* and *L. major* (Fig. 1 right).

As Galf is frequently found in pathogens, there is a scientific debate on its functional role and it has been hypothesized that it may be advantageous to express Galf as an important element for pathogen survival and reproduction in the host.^{2,3} Galf deficiency has been associated with important changes in the morphology of the cell wall that influence the sensitivity of these mutants to drugs and other perturbation agents. The lack of Galf on the galactomannan structure was also correlated with the virulence of some eukaryotic pathogens like *L. major*.³ Interestingly, absence of Galf in *A. niger* results in morphological abnormalities and an impaired cell wall function, resulting in hypersensitivity to drugs and a constitutive osmotic stress phenotype.⁴ Above that, Galf-deficient *A. fumigatus* mutants also display an attenuated virulence.⁵ Since Galf has never been found in mammals, Galf-biosynthetic pathways have raised interest as targets for drug development to combat parasitic and fungal infections.⁶

Galactose is a common monosaccharide, which is found in mammals exclusively in the hexopyranosyl form (Galp) (Fig. 2). By contrast, in several other non-mammalian organisms depicted in figure 1, galactose is frequently found as a five-membered ring form of galactose, galactofuranose (Galf) (Fig. 2).

³ Kleczka B., Lamerz A. C., van Zandbergen G., Wenzel A., Gerardy-Schahn R., Wiese M., Routier F. H., Targeted gene deletion of *Leishmania major* UDP-galactopyranose mutase leads to attenuated virulence, *J. Biol. Chem.* 2007, 282, 10498-10505.

⁴ Damveld R. A., Franken A., Arentshorst M., Punt P. J., Klis F. M., van den Hondel C. A., Ram A. F., A novel screening method for cell wall mutants in *Aspergillus niger* identifies UDP-galactopyranose mutase (UgmA) as an important protein in fungal cell wall biosynthesis, *Genetics* 2008, 178, 873-881.

⁵ a) Schmalhorst P. S., Krappmann S., Vervecken W., Rohde M., Müller M., Braus G. H., Contreras R., Braun A., Bakker H., Routier F. H., Contribution of Galactofuranose to the Virulence of the Opportunistic Pathogen *Aspergillus fumigatus*, *Eukaryot. Cell* 2008, 7, 1268-1277.

b) Engel J., Schmalhorst P. S., Dörk-Bousset T., Ferrières V., Routier F. H., A single UDP-galactofuranose transporter is required for galactofuranosylation in *Aspergillus fumigatus*, *J. Biol. Chem.* 2009, 284, 33859-33868.

⁶ a) Splain R. A., Kiessling L. L., Synthesis of galactofuranose-based acceptor substrates for the study of the carbohydrate polymerase GlfT2, *Bioorg. Med. Chem.* 2010, 18, 3753-3759.

b) de Lederkremer R. M., Colli W., Galactofuranose-containing glycoconjugates in trypanosomatids, *Glycobiology* 1995, 5, 547-552.

c) Pedersen L. L., Turco S. J., Galactofuranose metabolism: a potential target for antimicrobial chemotherapy, *Cell Mol. Life Sci.* 2003, 60, 259-266.

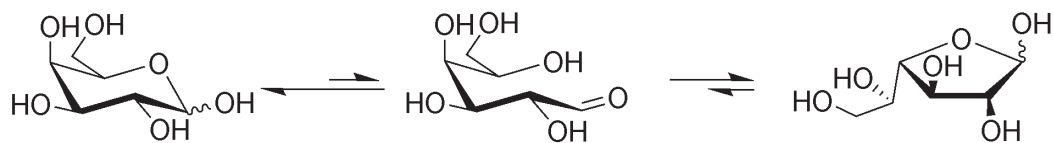


Figure 2: The equilibrium in water between Galp (left) and Galf (right). The equilibrium is energetically in favour of the hexapyranose Galp form.

To study the specific role of Galf with different cells of the host's immune system is complicated by the presence of many other molecules on the surface of the pathogens carrying this carbohydrate. Some of these molecules interact with Toll-like receptors (TLRs) or C-type lectin receptors (CLRs) and thereby direct the outcome of the immune response. Galf might participate in the regulation of this innate immune response, but a new perspective is needed to investigate this hypothesis.

As we have presented in the Introduction of this PhD Thesis, carbohydrate-mediated interactions are generally very weak and the low affinity has to be compensated by multivalent presentation of the ligands. Glycochemistry allows the design and preparation of well-defined glyco-conjugates that can be exploited to study the role of a specific carbohydrate in glycobiology. In this Thesis, gold glyconanoparticles (GNPs) have been presented and exploited as a multivalent system to study carbohydrate-mediated processes (see Chapters 2, 3 and 4). We now reasoned that multivalent Galf-conjugates could mimic the natural carbohydrates presentation of Galf-containing glycoconjugates of parasites (Fig. 1) and interfere with their adhesion to the host cells. Seminal studies employed well-defined synthetic fragments containing β -interlinked galactofuranosyl units to determine the immunodominant structure of polysaccharides from different strains of *Penicillium* and *Aspergillus*.⁷ The penta-, hexa and heptamer of the β -(1 \rightarrow 5)-interlinked galactofuranosides were able to link antibodies against extracellular polysaccharides from *Penicillium* and *Aspergillus*. As described in this seminal work, the number of Galf units present on that polymeric structure plays a fundamental role in the competition with the antibodies against the parasite polysaccharides.⁷

⁷ Notermans S., Veeneman G. H., van Zuylen C. W., Hoogerhout P., van Boom J. H., (1 \rightarrow 5)-linked β -D-galactofuranosides are immunodominant in extracellular polysaccharides of *Penicillium* and *Aspergillus* species, *Mol. Immunol.* 1988, 25, 975-979.

In this chapter, we describe the synthesis of gold nanoparticles carrying multiple copies (around 10 copies of Gal β per GNP) of Gal β (Gal β -GNPs) to study the role of this non-self monosaccharide in dendritic cells-mediated innate immune response (Fig. 4). Gal β -GNPs are one of the first examples of a well-defined multivalent system containing Gal β -moieties. We show that the anti-Gal β antibody EB-A2, that is widely used to detect galactomannan in the serum of Aspergillosis patients, specifically recognizes these Gal β -GNPs, as measured by GNP-ELISA (see chapter 4). Furthermore, we demonstrate that human dendritic cells (DCs) bind to Gal β -GNPs probably via a C-type lectin. We also demonstrate that lectin DC-SIGN bind to these nanoparticles. Finally, we show that Gal β -GNPs are capable of eliciting a pro-inflammatory response in DCs, as demonstrated by the up-regulation of surface maturation markers and secretion of pro-inflammatory cytokines. This latter result suggests that Gal β is a pathogen molecular pattern (PAMP) that is recognized by the human innate immune system. In conclusion, multivalent Gal β -GNPs are an interesting tool to better understand the role of Gal β in host-pathogen interactions and could be used for future functional experiments.

Synthesis of thiol-ending conjugates and Galf-GNPs

The synthesis of Galf- β -1-ethyl-3-(23-mercapto-3,6,9,12-tetraoxatricosyl)thiourea (**1**) was the first step to be achieved and has been carried out following a described protocol (Fig. 4)^{6a}.

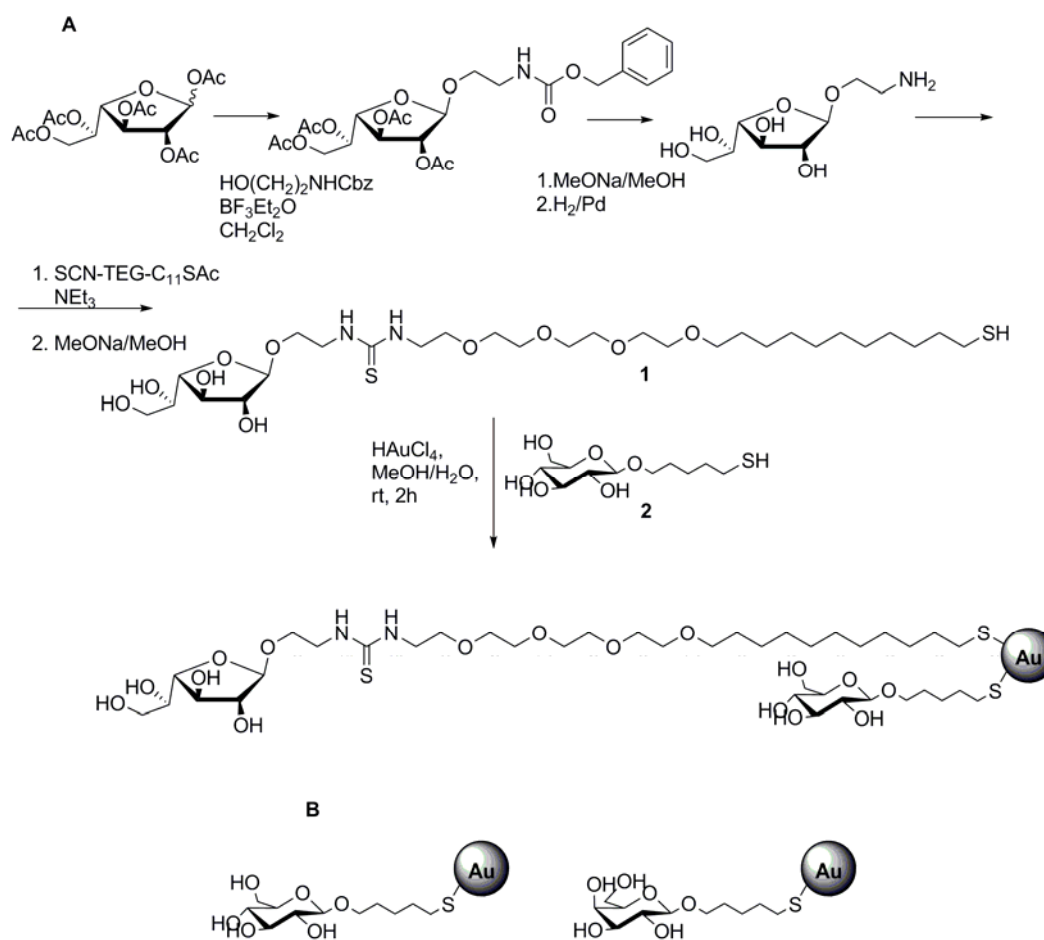


Figure 4: Glycoconjugates and GNPs prepared and tested in this work: **A**) Synthesis of thiol-ending conjugates and Galf-GNPs. Peracetylated Galf was first glycosylated with Benzyl-*N*-(2-hydroxyethyl)carbamate using $\text{BF}_3\text{Et}_2\text{O}$ as Lewis acid^{6a}; after deprotection, the amino Galf conjugate was coupled to a linker having a thio-acetyl and an isothiocyanate functionality at the terminal ends (SCN-TEG-C₁₁-S-Ac) in the presence of triethylamine; deacetylation was then performed with MeONa . The prepared Galf conjugate **1** was mixed in $\text{MeOH/H}_2\text{O}$ with glucose conjugate **2** in 1:9 ratio. HAuCl_4 was added to the ligands solution and NaBH_4 was added; after 2 h of shaking the solid Galf-GNPs were washed and purified by dialysis. **B**) Glc and Gal β -GNPs prepared in this work and used as control GNPs.

To favour the presentation of the carbohydrate of interest (Gal β in this case), we decided to conjugate Gal β to a long amphiphilic linker in order to assure ligand flexibility and to make Gal β protruding above the gold surface.⁸ 5-(Thio)pentyl β -D-glucopyranoside (**2**), having a short aliphatic linker, was chosen as ligand partner to modulate the density of Gal β on the GNPs. To prepare Gal β -GNPs, a solution of tetrachloroauric acid 0.025 M (1 equiv.) in water was added to a 0.012 M (3 equiv.) methanolic solution of the mixture of 10% thiol-ending conjugate **1** and 90% of conjugate **2** (Fig. 4). An aqueous solution of NaBH₄ 1M (21 equiv.) was then added in four portions, with vigorous shaking. The black suspension formed was shaken for 2 hours at 25°C. After that, the supernatant was removed and analysed. The residue was dissolved in a minimal volume of Nanopure water and purified by dialysis. The prepared Gal β -GNPs were freeze-dried and stored at 4°C. In these conditions Gal β -GNPs can be stored for months maintaining their bio-physical properties. The ratio of the ligands on the GNPs was evaluated by quantitative NMR (qNMR) by integrating the signals of an internal standard (Trimethylsilyl propionate, TSP) and the anomeric protons of **1**. The results of the ligands quantification on the gold surface led to an estimation of 10% of Gal β on the GNPs and 90% of inner glucose. The particle size distribution (average gold diameter) of the gold nanoparticles was determined from the transmission electron microscopy (TEM) micrographs and the average diameter was founded to be ~2nm. Glc-GNPs and Gal α -GNPs were prepared as previously described.⁸

Recognition of Gal β -GNPs by the anti-Gal β EB-A2 antibody

To test the biological functionality of the Gal β moiety on the Gal β -GNPs, we used of a rat monoclonal antibody (EB-A2) that recognizes Gal β -moieties on biologically derived molecules. EB-A2 is widely used to early detect circulating galactomannan (a Gal β -containing polysaccharide) in the serum of Aspergillosis patients⁹ through the double-sandwich enzyme-linked immunosorbent assay Platelia *Aspergillus* (Bio-Rad, Marnes-La-Coquette, France). The immunogenic epitope recognized by EB-A2 is the β (1-5)-linked galactofuranosyl side chain of the *Aspergillus*

⁸ Martínez-Avila O., Hijazi K., Marradi M., Clavel C., Campion C., Kelly C., Penadés S., Gold manno-glyconanoparticles: multivalent systems to block HIV-1 gp120 binding to the lectin DC-SIGN, Chem. Eur. J. 2009, 15, 9874-9888.

⁹ Stynen D., Goris A., Sarfati J., Latgé J. P., A new sensitive sandwich enzyme-linked immunosorbent assay to detect galactofuran in patients with invasive aspergillosis, J. Clin. Microbiol. 1995, 33, 497-500.

galactomannan.¹⁰ We used EB-A2 linked to HRP (from the Platelia assay kit) for detection of Gal β -GNPs in an GNP-ELISA assay (see chapter 4 of this Thesis). ELISA wells were coated with Gal β -GNPs, Glc-GNPs and galactopyranose-coated GNPs (Gal β -GNPs) at different concentrations and the interaction with EB-A2-HRP was measured at 450 nm (Figure 5A). EB-A2 was able to detect Gal β -GNPs used as antigen in the ELISA wells in a concentration dependent manner, whereas Glc-GNPs and Gal β -GNPs were not recognized by this antibody.

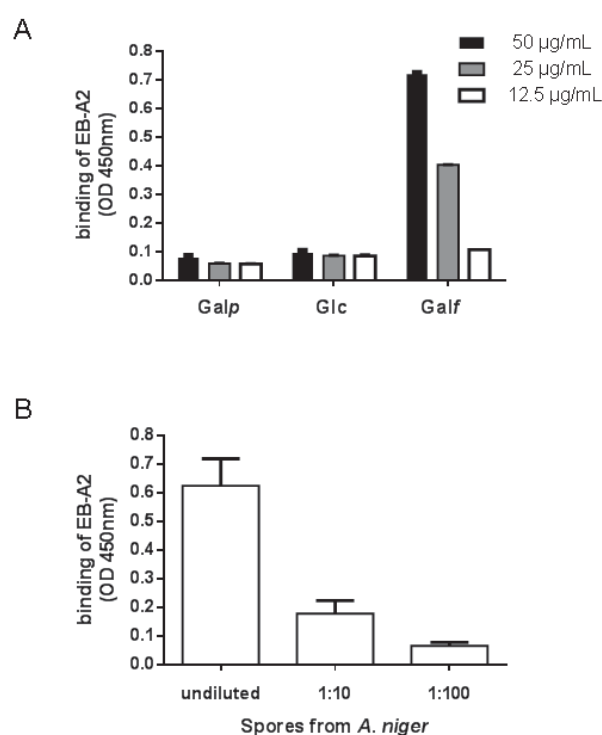


Figure 5: Anti-Gal β antibody EB-A2 recognizes Gal β -GNPs: **A)** The indicated concentrations of Gal β -GNPs, Glc-GNPs and Gal β -GNPs were used for coating an ELISA plate and subsequent detection with EB-A2. Experiments were performed five times and depicted here is one representative experiment performed in duplicate (error bars are barely detectable). **B)** Heat-killed spores from *A. niger* were coated in different concentrations (undiluted is $5 \cdot 10^7$ spores/mL) to 96-wells Nunc Maxisorp plate and immunodetection with EB-A2 was performed. Shown here is a typical experiment performed in duplicate.

¹⁰ Latgé J. P., Kobayashi H., Debeaupuis J. P., Diaquin M., Sarfati J., Wieruszkeski J. M., Parra E., Bouchara J. P., Fournet B., Chemical and immunological characterization of the extracellular galactomannan of *Aspergillus fumigatus*, *Infect. Immun.* 1994, 62, 5424-5433.

To compare Gal α -GNPs with a natural Gal α -containing molecule, we coat ELISA plates with heat-killed spores from wild type *A. niger*, and detected Gal α with EB-A2. Also in these experiments the Gal α containing glycoconjugates from *A. niger* spores were recognized by the antibody in a concentration-dependent manner (Figure 5B).

DCs bind to Gal α -GNPs

We aimed at looking the interaction of Gal α -GNPs with immune cells that will encounter Gal α -containing structures in the human host. For this reason, we selected human dendritic cells.

As described in the introduction of Part-2, DCs are a class of antigen-presenting cells that express a multitude of well conserved pattern recognition receptors (PRRs) on their membrane responsible for the recognition of pathogen-associated molecular patterns (PAMPs). Gal α is an ancient PAMP expressed on several pathogens, but the mechanism by which the host responds to this monosaccharide is not well known. In our work, we checked whether Gal α could play a role during the interaction between parasites and DCs.

We first showed in a cell adhesion assay, that DCs have a high affinity for the Gal α -GNPs and this binding was abolished in the presence of EGTA (Figure 6A). This calcium dependence of the DC binding with the Gal α -GNPs indicates that C-type lectin receptors (CLRs) on the DCs are able to interact with Gal α . Indeed, lectin DC-SIGN is involved in the interaction of the DCs with Gal α -GNPs because a significant decrease in the interaction was observed by using the anti-DC-SIGN antibody AZN-D1. DCs also bound to Glc-GNPs, as expected on the basis of previous results with DC-SIGN (see chapter-4), although to a lesser extent compared to Gal α -GNPs. It was previously demonstrated the alveolar DCs are able to interact with *A. fumigatus* spores through the C-type lectin DC-SIGN^{11,12} and recently, the C-type lectin Dectin-1 and DC-SIGN polymorphism were associated with invasive pulmonary aspergillosis infection.¹³

¹¹ Serrano-Gómez D, Domínguez-Soto A., Ancochea J., Jimenez-Heffernan J. A., Leal J. A., Corbí A. L., Dendritic cell-specific intercellular adhesion molecule 3-grabbing nonintegrin mediates binding and internalization of *Aspergillus fumigatus* conidia by dendritic cells and macrophages, *J. Immunol.* 2004, 173, 5635-5643.

¹² Heesemann L., Kotz A., Echtenacher B., Broniszewska M., Routier F., Hoffmann P., Ebel F., Studies on galactofuranose-containing glycostructures of the pathogenic mold *Aspergillus fumigates*, *Int. J. Med. Microbiol.* 2011, 30, 523-530.

¹³ Sainz J., Lupiáñez C. B., Segura-Catena J., Vazquez L., Ríos R., Oyonarte S., Hemminki K., Försti A., Jurado M., Dectin-1 and DC-SIGN Polymorphisms Associated with Invasive Pulmonary Aspergillosis Infection, *PLoS One* 2012, 7, e32273.

The described interactions between DC-SIGN and the natural *Gal*f-containing glycoconjugates and the results from the cellular adhesion assay with *Gal*f-GNPs lead us to study the direct binding of *Gal*f-GNPs with a chimeric DC-SIGN-Fc. In our GNPs-ELISA experiments, the chimeric-DC-SIGN showed higher affinity for *Gal*f-GNPs than *Glc*-GNPs in the presence of a calcium and magnesium containing buffer, like as the cellular adhesion assay (Fig. 6A and 6B). Although other glyconanoparticles carrying high-mannose and Lewis type glycans show a better affinity for DC-SIGN (see chapter-4), the presence of *Gal*f entities on the *Glc*-GNPs increase the binding with DC-SIGN.

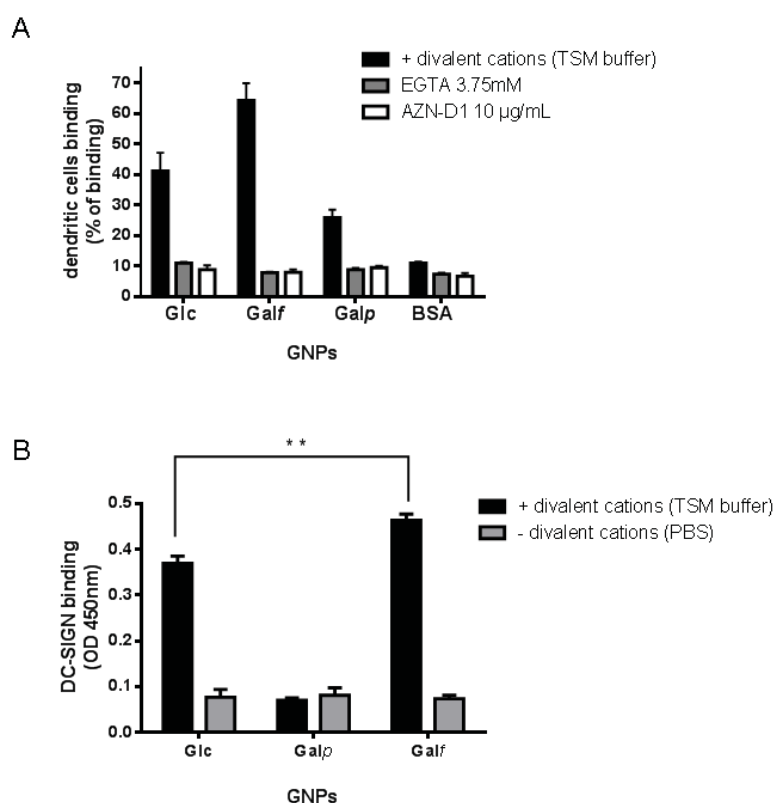


Figure 6: *Gal*f-GNPs binding to DCs and DC-SIGN-Fc. **A)** The indicated GNPs were adsorbed in a 96-wells Nunc Maxisorp plate and incubated with DCs that were previously labeled with calcein. The assay was performed in the presence or absence of the calcium-chelator EGTA and the anti DC-SIGN-specific antibody AZN-D1. These experiments were performed at least four times with similar results. The experiments were performed in triplicate, with error bars indicating standard deviations. All the P values between the bars of normal experiments and the EGTA/AZN-D1 ones are <0.0001. The differences in the BSA group are not significant. **B)** The indicated GNPs were coated in a concentration of 10 µg/ml in a NUNC Maxisorp plate and incubated with 3 µg/ml DC-SIGN-Fc, followed by detection with an HRP-conjugated anti-human Fc antibody.

Incubation of Gal β -GNPs with human DCs leads to up-regulation of maturation markers and production of pro-inflammatory cytokines

To define the putative immunomodulatory effects of Gal β on DCs, we incubated DCs with Glc- and Gal β -GNPs (10 μ g/mL) for 16 h and subsequently measured the surface expression of the maturation markers CD86, CD80 and HLA-DR by flow cytometry analysis (Figure 7A). These surface molecules are up-regulated on DCs in response to pathogenic stimuli and are required for proper antigen presentation to T-cells in the lymph node (see intro to this part of the Thesis).

Human DCs from healthy donors treated with Gal β -GNPs up-regulated the expression of all these maturation markers, especially CD86 (Figure 7A). DCs treated with Glc-GNPs and Gal ρ -GNPs showed no changes in their surface maturation markers compared to cells that were given only PBS as a negative control. GNPs carrying 10% of the dimannoside Man α 1-2Man (prepared with the same linker and conditions of Gal β -GNPs, see chapter-2) were not able to up-regulate the CD86 of the DCs at the tested concentration (5-10 μ g/mL).

Next, a panel of pro-inflammatory cytokines secreted by the DCs that were incubated with the different GNPs was measured by sandwich ELISA. DCs treated with 10 μ g/mL of Gal β -GNPs produced high amounts of IL-6 (Figure 7B) and tumor necrosis factor alpha (TNF- α) (Figure 7C) comparable with the cells treated with LPS. Glc-GNPs did not promote these effects (Figure 7BC) and Gal ρ -GNPs were only tested as negative control for the CD86 maturation showing no ability to up-regulate this maturation marker.

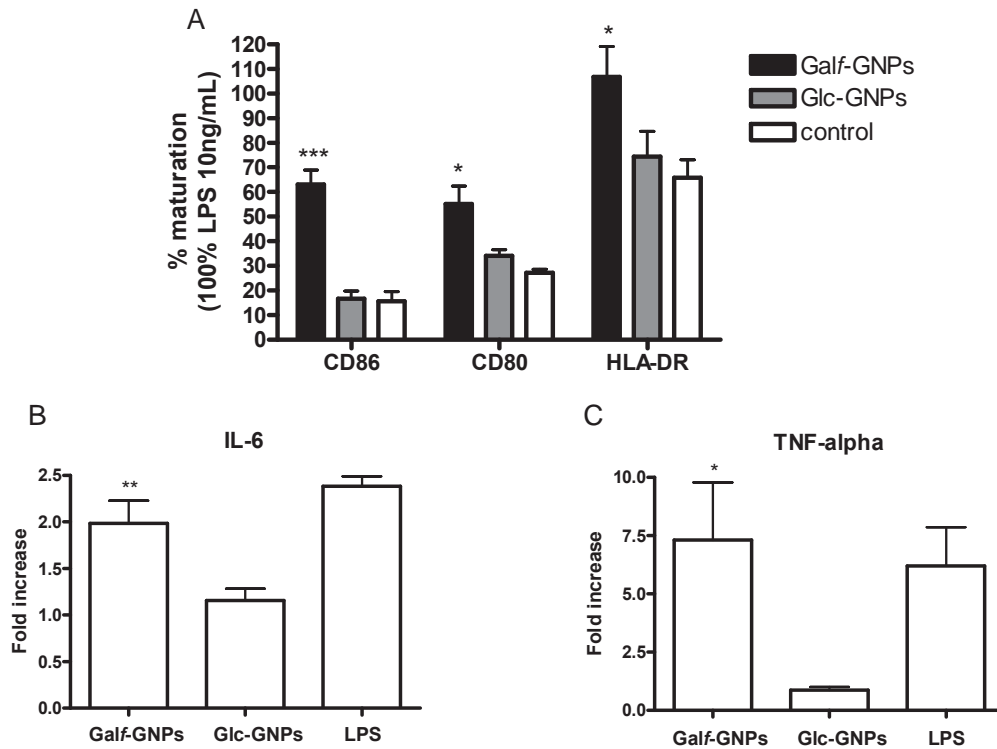


Figure 7: DC maturation and cytokine production after incubation with Galf-GNPs: A) Surface expression of the maturation markers CD86, CD80 and HLA-DR by FACS analysis staining with the corresponding antibodies. DCs from different healthy human donors were incubated for 16 h with the indicated GNPs (10 μ g/mL) in the presence of LPS (10 ng/mL) or with media (control). The graph shows the percentage of maturation. The percentage of maturation was normalized to the DCs treated with 10 ng/mL LPS. For CD86, the results of six donors are shown; for CD80 and HLA-DR, the results for three donors are shown. One asterisk indicates that the P value between the bars and the control is <0.05 and three asterisks indicate that the P value is <0.0001. B) IL-6 production by DCs treated with 10 μ g/mL of different GNPs for 16 h and LPS for comparison. Data depicted here shows the fold increase over the untreated DCs for three donors. Two asterisks indicate that the P value between the Galf and Glc-GNPs is <0.001. C) TNF α production by DCs treated with 10 μ g/mL of different GNPs for 16 h and LPS for comparison. Depicted is the fold increase over the untreated DCs for three donors. One asterisk indicates that the P value between the Galf and Glc-GNPs is <0.05.

To exclude lipopolysaccharide (LPS) contamination of the GNPs that would interfere in our studies, we have conducted a *Limulus* Amoebocyte Lysate (LAL) test. LAL is an aqueous extract of blood cells (amoebocytes) from the horseshoe crab, *Limulus polyphemus*. LAL reacts with bacterial endotoxin or LPS. This reaction is the basis of the LAL test, which is used for the detection and

quantification of bacterial endotoxins.¹⁴ All GNPs used in this study contained less LPS (< 0.65 ng LPS/mL) than could be detected with the LAL test. To confirm that LPS is not causing the maturation of the DCs seen with Gal β -GNPs, the maturation experiments with the Gal β -GNPs were also performed once in the presence of the antibiotic polymyxin B (PX), which inhibits maturation of DCs by LPS.¹⁵ CD86 was similarly up-regulated on DCs that were treated with Gal β -GNPs, irrespective of the presence of polymyxin B, while DCs treated with LPS and polymyxin B together did not up-regulated CD86 on their surface (Fig. 8). These experiments exclude LPS contamination indicating that Gal β -GNPs are the inducing factor for the up-regulation of the maturation markers.

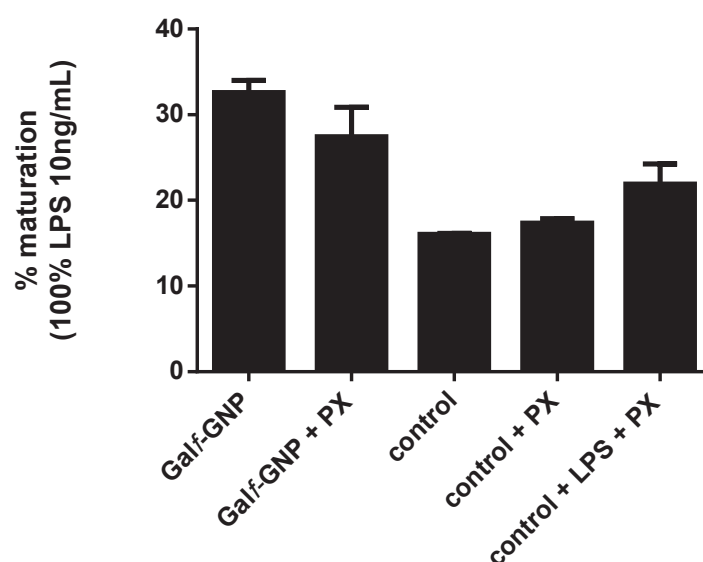


Figure 8: CD86 expression on DCs after co-incubation of GNPs and Polymyxin B (PX). 10ng/mL of LPS was set as 100% of DCs maturation expressed as CD86 expression) CD86 was similarly up-regulated on DCs that were treated with Gal β -GNPs, irrespective of the presence of polymyxin B (~30% of maturation). The DCs treated with LPS and polymyxin B together up-regulated CD86 on their surface around ~25% of maturation confirming the effectiveness of polymyxin B.

¹⁴ <http://www.fda.gov/Drugs/GuidanceComplianceRegulatoryInformation/Guidances/ucm314718.htm>

¹⁵ Cardoso L. S, Araujo M. I, Góes A. M, Pacífico L. G, Oliveira R. R., Oliveira S. C., Polymyxin B as inhibitor of LPS contamination of *Schistosoma mansoni* recombinant proteins in human cytokine analysis, Microb. Cell Fact. 2007, 6, 1.

Carbohydrate-specific signalling through DC-SIGN triggers a cytokine production in response to distinct pathogens¹⁶ and the signalling cascade seems to be carbohydrate-dependent. In this work, the addition of 10% of Gal_f-moieties on the GNPs is able to induce a pro-inflammatory immune response by the DCs that is not seen with the Glc-GNPs. More experiments are needed to understand the mechanism behind these observations. An alternative explanation could be that another, unidentified (lectin-) receptor specifically reacts to Gal_f-GNPs is involved in the up-regulation of the maturation markers and pro-inflammatory cytokines like IL-6 and TNF- α .

Anti-Gal_f antibody detection in human sera (preliminary results)

The detection of specific IgG in human sera is a well known procedure to detect the exposure to some parasites. Galactofuranose is a well conserved structure in the parasite word² and infected people showed specific anti-carbohydrates IgG against parasites structures. GNPs carrying galactofuranose were used to coat ELISA plate for Ab detection in human serum from patients affected by tuberculosis. Seminal works showed that a Galactofuranose containing disaccharide (6-O- β -D-galactofuranosyl-D-galactose) was one of the immunoadjuvant fractions of the *Mycobacterium tuberculosis* cell wall.¹⁷

A preliminary assay was performed using serum samples of tuberculosis (TBC) infected patients trying to detect low amount of anti-galactofuranose IgG. People that never were in contact with galactofuranose-expressing parasites should not have in their blood anti Gal_f IgGs (Fig. 9). The data showed differences between the human samples and the only known patient that was infected by TBC (sample number 10, see Fig. 9). Although this is a very preliminary and incomplete result, it can be considered a proof on principle for the further application of Gal_f-GNPs as coating for ELISA plates in the detection of important biomarkers evoked by parasites.

¹⁶ Gringhuis S. I., den Dunnen J., Litjens M., van der Vlist M., Geijtenbeek T. B., Carbohydrate-specific signaling through the DC-SIGN signalosome tailors immunity to *Mycobacterium tuberculosis*, HIV-1 and *Helicobacter pylori*, Nat. Immunol. 2009, 10, 1081-1088.

¹⁷ Vilkas E., Amar C., Markovits J., Vliegenthart J. F. G., Kamerling J. P., Occurrence of a galactofuranose disaccharide in immunoadjuvant fractions of *Mycobacterium tuberculosis* (Cell walls and wax D), Biochim. Biophys. Acta. 1973, 297, 423-435.

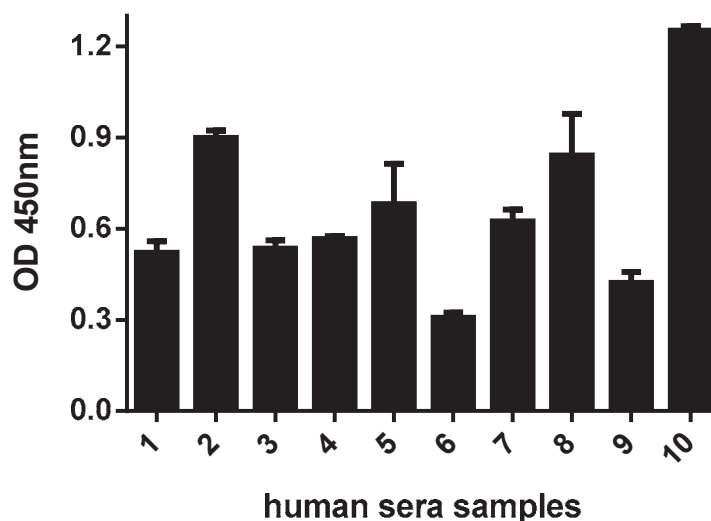


Figure 9: Anti galactofuranose antibodies in human sera samples affected by TBC were detected by Gal f -GNPs on the ELISA plate. These preliminary results show significant differences between the samples. Sample number 9 was the negative control and sample number 10 was the positive control.

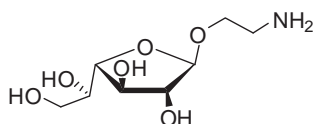
The described Gal f -GNPs were exploited in this work to study the role of Gal f in the dendritic cells mediated innate immune response, but they could be also explored to identify and study the Gal f receptors (PRR) present on antigen presenting cells. In addition Gal f -GNPs could be exploited as glycomimetic compounds able to inhibit the enzymes related to the Gal f biosynthesis and for the serodiagnosis of pathogens that cause serious diseases like Aspergillosis, Cryptococcosis or Tuberculosis in developing countries.

Gal f -GNPs are one of the first examples of a well-defined multivalent system containing Gal f -moieties. We show that the anti-Gal f antibody EB-A2, that is widely used to detect galactomannan in the serum of Aspergillosis patients, specifically recognizes these Gal f -GNPs, as measured by ELISA. Furthermore, we demonstrate that human dendritic cells (DCs) bind to Gal f -GNPs probably via a C-type lectin. We also demonstrate that lectin DC-SIGN bind to these nanoparticles. Finally, we show that Gal f -GNPs are capable of eliciting a pro-inflammatory response in DCs, as demonstrated by the upregulation of surface maturation markers and secretion of pro-inflammatory cytokines. The latter result suggests that Gal f is a pathogen molecular pattern (PAMP) that is recognized by the human innate immune system. In conclusion, multivalent Gal f -GNPs are an interesting tool to better understand the role of Gal f in host-pathogen interactions and could be used in the future for a range of functional experiments.

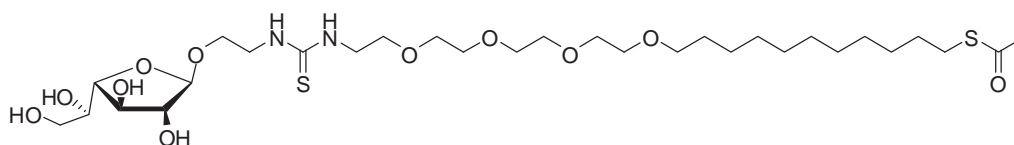
Experimental section

Materials

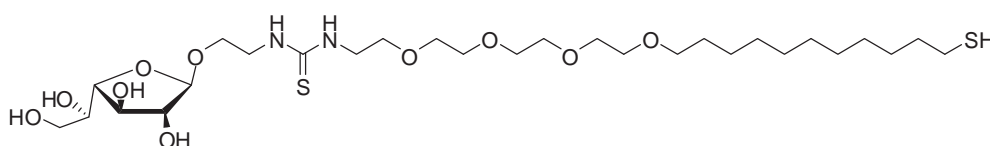
1,2,3,5,6-Penta-O-acetyl-D-galactofuranose were purchased from Carbosynth. All other chemicals were purchased as reagent grade from Sigma-Aldrich and used without further purification, unless otherwise stated. TLC was performed on 0.25 mm pre-coated silica gel glass plates or aluminum backed sheets (Merck silica gel 60 F₂₅₄) with detection by UV-light (254 nm) and/or heating at over 200°C after staining either with 10 % sulfuric acid (aqueous solution) or *p*-anisaldehyde solution consisting of 25 mL *p*-anisaldehyde, 25 mL H₂SO₄, 450 mL EtOH, and 1 mL CH₃COOH. Organic solvents were removed by rotary evaporation under reduced pressure at approximately 40°C (water bath). Silica gel (0.041–0.063 mm, Amicon and 0.063-0.200 mm, Merck) was used for flash column chromatography. Size-exclusion column chromatography was performed on Sephadex LH-20 (GE Healthcare). NMR spectra were recorded at 500 MHz (Bruker) (¹H) or 125 MHz (¹³C) at 25°C. If not otherwise stated, chemical shifts (δ) are given in ppm relative to the residual solvent signal. Infrared spectra (IR) were recorded from 4000 to 400 cm⁻¹ with a Nicolet 6700 FT-IR spectrometer (Thermo Spectra-Tech), solids were pressed into KBr pellets. Mass spectrometric data was obtained from a Waters LCT Premier XE instrument with a standard ESI source by direct injection. The instrument was operated with a capillary voltage of 1.0 kV and a cone voltage of 200 V. Cone and desolvation gas flow were set to 50 and 500 L/h, respectively; source and desolvation temperatures were 100°C. High resolution mass was determined using glycocholic acid (Sigma) as an internal standard (2 M+Na⁺, *m/z* = 953.6058). MALDI-Tof spectra were recorded on a Bruker Reflex IV using 2',4',6'-trihydroxy-acetophenone monohydrate (THAP) as matrix.



Gal_f-NH₂^{6a}: Peracetylated galactofuranose (222mg, 0.56mmol, 1equiv.) was dissolved in dry CH₂Cl₂ (3mL) and glycosylated by treatment with benzyl 2-hydroxyethylcarbamate (333mg, 1.7mmol, 3equiv.) in the presence of BF₃·Et₂O (288 μL, 2.3mmol, 4equiv.) under dry conditions. After 12h, the reaction was worked up and the crude was purified by column chromatography (AcOEt/Hex = 1/1) to obtain the β-glycosylated and peracetylated Gal_f-NHCBz (256mg, 0.4mmol, 86%). This compound (162mg, 0.3mmol, 1equiv.) was dissolved in MeOH (8mL) and MeONa (16mg, 0.3mmol) was added. After 4h, NMR of the crude showed no signals from the acetyl groups and the reaction was quenched with Amberlite to pH=6. The resulting deacetylated Gal_f-NHCBz was dissolved in 4mL of MeOH/HOOCH (95/5) in presence of 140mg of Pd on activated carbon. N₂ was first flushed in the flask followed by H₂. After 12h, the reaction was filtered over celite and concentrated under vacuum. The crude material was purified by Sephadex LH-20 chromatography (column: diameter = 2 cm; height = 45 cm) using as eluent MeOH/ H₂O = 9/1 to afford the Gal_f-NH₂ conjugate (formate salt) as a white solid after lyophilisation (58mg, 0.26 mmol). ¹H NMR of the amino ethyl derivative: (500 MHz, D₂O) δ 5.02 (d, *J* = 1.1, 1H), 4.09 (m, 2H), 4.01 – 3.92 (m, 2H), 3.84 – 3.79 (m, 1H), 3.78 – 3.72 (m, 1H), 3.67 (m, 2H), 3.30 – 3.17 (m, 2H, CH₂NH₃⁺).

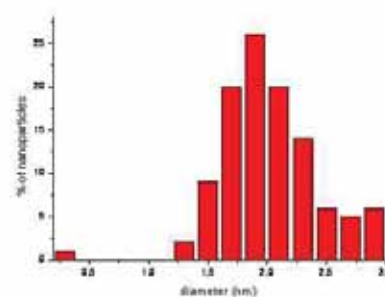
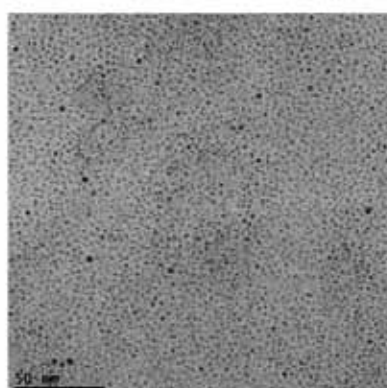
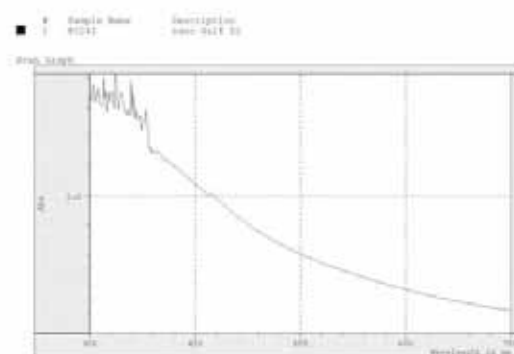
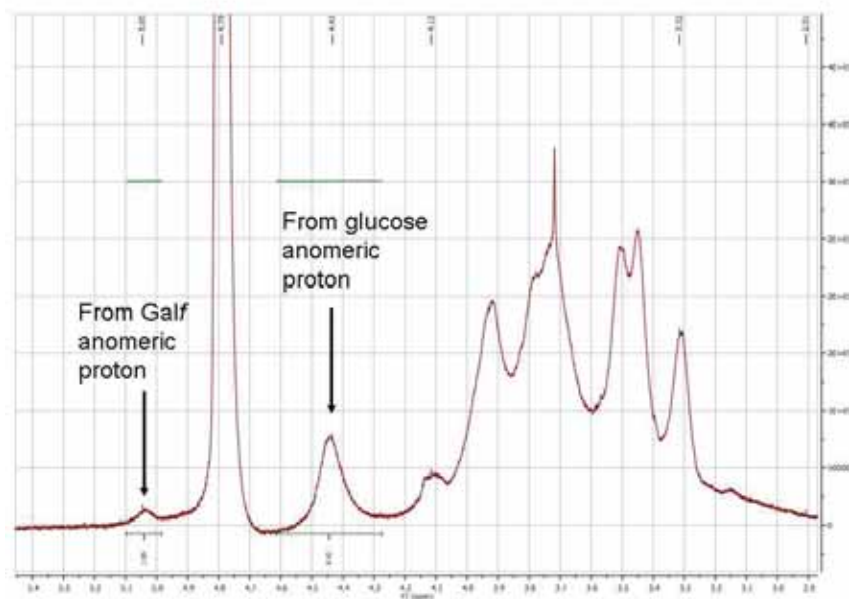
Galf-NH(CS)NH-TEG-C₁₁-SAc

A solution of isothiocyanate linker (13.2 mg, 28.5 μmol , 1.1 equiv.) in H_2O - i -PrOH- CH_3CN (1:1:1, v/v/v, 0.5 mL) was added to a solution of 3-aminopropyl Galf conjugate (5.79 mg, 26 μmol , 1 equiv.) in H_2O - i -PrOH- CH_3CN (1:1:1, v/v/v, 0.5 mL) and the pH was set to basic by addition of triethylamine (10 μL , 78 μmol , 3 equiv.). The mixture was stirred at room temperature for 17 h and then evaporated. The crude material was kept in high vacuum to remove the residual triethylamine and then triturated with Et_2O (5 x 1 mL) in order to get rid of the excess of the linker. The S-protected Galf conjugate was directly used for the next reaction after NMR and MALDI characterization (8 mg, 26 μmol). ^1H NMR (500 MHz, CD_3OD) δ = 4.89 (bs, 1H), 4.03-3.95 (m, 3H), 3.82-3.78 (m, 1H), 3.74-3.62 (m, 20H), 3.60-3.57 (m, 2H), 3.47 (t, J =6.6, 2H), 2.86 (t, J =7.3, 2H), 2.30 (s, 3H, SAc), 1.59 – 1.53 (m, 4H), 1.40 – 1.28 (m, 14H).

Galf-thiol ending conjugate (1).

Sodium methoxide (1.4 mg, 26 μmol , 1 equiv.) was added to a solution of Galf-NH-SCN-TEG-C₁₁-SAc (8 mg, 26 μmol , 1 equiv.) in MeOH (2 mL). The mixture was stirred at room temperature for 12 hours and then evaporated. The crude material was concentrated and purified by Sephadex LH-20 chromatography (column: diameter = 2 cm; height = 45 cm) using as eluent MeOH/ H_2O = 9/1 to afford the Galf conjugate as a white solid after lyophilisation (9mg, 0.014 mmol): ^1H NMR (500 MHz, CD_3OD) δ = 4.92 (bs, 1H), 4.03-3.96 (m, 3H), 3.83-3.78 (m, 1H), 3.75-3.63 (m, 20H), 3.62-3.56 (m, 2H), 3.50 (t, J =6.6, 2H), 2.69 (t, J =7.2, 0.65H), 2.47 (t, J =7.2, 1.35H), 1.75 – 1.56 (m, 4H), 1.47 – 1.31 (m, 14H). ^1H , ^{13}C HSQC (125 MHz, CD_3OD) δ = 108.1 (d, 1C, C-1), 83.1 (d, 1C), 81.6 (d, 1C), 77.1 (d, 1C), 71.3 (t, 1C), 70.9, 69.9, 66.3, 66.2, 62.7, 28.9, 28.7, 28.5; CH_2S not detected. HR-MS: calcd for $\text{C}_{28}\text{H}_{56}\text{N}_2\text{O}_{10}\text{S}_2\text{Na}^+$: 666.3196 $[\text{M}+\text{Na}]^+$; found 666.3166.

Galf-GNPs: Reaction of a 1:9 mixture **1** (1.5mg) and **2** (5.9mg) with HAuCl_4 and NaBH_4 gave 1.54mg of Galf-GNPs as a dark-brown powder. TEM (average diameter): 2.0 ± 0.4 nm. Quantitative ^1H NMR: 1.54mg of Galf-GNPs were dissolved in 700 μL of 0.75% TSP in D_2O and 0.07 μmoles of Galf were found. NMR (500 MHz, D_2O /internal standard TSP) only significant peaks are reported: δ = 5.05 (s, from Galf-conjugate anomeric proton), 4.43 (s, from Glc-conjugate anomeric proton), 4.12-3.32 (m), 2-1.38 (m); ratio between Galf and Glc signals \sim 1 to 8.42. These results are in agreement with the estimation of 10% of Galf on the GNPs. Molar ratio of conjugates per nanoparticle was also determined by analyzing the mixtures using NMR before and after nanoparticle formation. Estimated average molecular weight for $(\text{C}_{28}\text{H}_{56}\text{N}_2\text{O}_{10}\text{S}_2)_7(\text{C}_{11}\text{H}_{21}\text{O}_6\text{S})_{59}\text{Au}_{116}$: \sim 44 kDa. IR (KBr): ν = \sim 3600–3100 (br), 2912, 2851, 2378, 1648, 1075, 1030. UV/Vis (H_2O , 0.1 mg/mL): surface plasmon band not observed. (Fig. 10).



Diameter = 2.0 ± 0.4

Figure 10: Characterization of Galf-GNPs: *Upper panel:* ^1H NMR spectrum of Galf-GNPs in D_2O at 500 MHz. The signals from the anomeric protons of the glycoconjugates on the GNPs are clearly observed between 5.0 and 5.5 ppm. *Bottom panel:* UV-Vis spectra of a 0.1 mg/mL solution of the Galf-GNPs in water; TEM micrograph and size-distribution histogram obtained from analysis of TEM micrographs.

Galp-GNPs and Glc-GNPs were prepared with a short aliphatic derivative of glucose and galactopyranose. Both GNPs were fully covered by the corresponding glycoconjugate. Glc-GNPs was prepared as previously described.⁸

Galp-GNPs: GalC₅SH (4.6 mg, 0.014 mmol, 3 eq.) were dissolved in MeOH (1.5 mL). HAuCl₄ (1.6 mg, 0.0048 mmol, 1 eq.), NaBH₄ (4.9 mg, 0.1 mmol, 21 eq.) After freeze-drying, 1.4 mg of a brown solid was obtained. TEM: 1.8 ± 0.1 nm. ¹H NMR (D₂O, 500 MHz) Only significant peaks are reported δ 4.40 (bd, from anomeric galactose proton), 3.95-3.54 (bm, from the galactose protons), 2.04-1.48 (bm, aliphatic signals from the linker).

Characterization of Galf-GNPs

For the analysis of the number of Galf-ligands on the Galf-GNPs, ¹H NMR spectra of the initial mixture and of the supernatant after GNPs formation were recorded. The ligands ratio was evaluated by qNMR with TSP as internal standard and was also evaluated by integrating the signals of the anomeric protons of **1** and **2**. The particle size distribution (average gold diameter) of the gold nanoparticles was determined from the transmission electron microscopy (TEM) micrographs: a single drop (10 µL) of the aqueous solution (ca. 0.1 mg/mL in milliQ water) of the GNPs was placed onto a copper grid coated with a carbon film (Electron Microscopy Sciences). The grid was left to dry in air for several hours at room temperature. TEM analyses were carried out in a Philips JEOL JEM-2100F microscope working at 200 kV. The average number of gold atoms was calculated on the basis of the average diameter obtained by TEM micrographs, and molecular formulas of the GNPs were estimated according to a previous work.⁸

ELISA with anti galactofuranose antibody EB-A2 or DC-SIGN-Fc

50 µL of GNPs solution (50, 25 and 12.5 µg/mL) in buffer (50mM Na₂CO₃, pH=9.7) were used to coat a NUNC Maxisorp plate 2 h at ambient temperature or over night at 4°C. After washing with PBS (2x200µL), 1% BSA (fatty acid free, Calbiochem) in PBS was used for blocking at ambient temperature for 30 min. Subsequently, 70 µL of antibody EB-A2-HRP (Platelia Aspergillus EIA kit, Bio-Rad) diluted 1:3 in assay buffer (0.5% BSA) was added and the plate was shaken at 500 rpm for 1 h. The wells were discarded and washed with PBS (3x200µL) and 100 µL of substrate solution (TMB in citric/acetate buffer) was added. The reaction was stopped with 50 µL of 0.8 M H₂SO₄ and binding was measured at an OD of 450 nm.

DC-SIGN-Fc¹⁸ was used for detection at a final concentration of 3 µg/mL and after washing, an incubation step with the secondary antibody, peroxidase-coupled goat anti-human IgG (Dako) in a 1:1000 dilution, was added to the procedure described above.

In vitro generation and culture of human DCs

Immature DCs were generated from human peripheral blood mononuclear cells (PBMCs) from buffy coats of healthy donors (Sanquin) as described previously¹⁹. Monocytes were prepared from

¹⁸ Geijtenbeek T. B., van Duijnhoven G. C., van Vliet S. J., Krieger E., Vriend G., Figdor C. G., van Kooyk Y., Identification of different binding sites in the dendritic cell-specific receptor DC-SIGN for intercellular adhesion molecule 3 and HIV-1, *J. Biol. Chem.* 2002, 277, 11314-11320.

¹⁹ Sallusto F., Lanzavecchia A., Efficient presentation of soluble antigen by cultured human dendritic cells is maintained by granulocyte/macrophage colony-stimulating factor plus interleukin 4 and downregulated by tumor necrosis factor alpha, *J. Exp. Med.* 1994, 179, 1109-1118.

PBMCs by centrifugation over Percoll and incubated for 5 days in RPMI supplemented with 10% heat inactivated fetal calf serum, 2.4 mM L-glutamine, 100 U/ml penicillin-streptomycin (all from Gibco), 800 U/ml of human recombinant granulocyte-macrophage colony-stimulating factor and 500 U/ml of human recombinant IL-4 (both from Schering-Plough, Brussels, Belgium).

LAL-test

LAL-test was performed in duplicate using the QCL-1000 Endpoint Chromogenic LAL assay as described by manufacturer's protocol (Lonza) on all GNPs used in this study. Control LPS samples and GNP samples gave expected values, whereas non-spiked GNPs contained less LPS than was detectable with this method (< 0.65 ng/ml).

Cellular binding

Ninety-six-well plates (NUNC Maxisorp) were coated at room temperature for 2 h with GNPs (25 µg/mL) and afterwards blocked with 1% BSA. Calceine AM-labeled DCs (Molecular Probes) were added for 1.5 h at 37°C in the presence or absence of 3.75 mM EGTA or 10 µg/mL mAb AZN-D1. Non-adherent cells were removed by gentle washing. Adherent cells were lysed and fluorescence was quantified on a Fluorostar spectrofluorimeter (BMG Labtech, Offenburg, Germany).

Flow cytometry analysis of DC surface molecules and cytokine production Suspensions of 100 µL immature DCs ($1 \cdot 10^6$ cells/mL) were stimulated by addition of GNPs (10 µg/mL) in 96-well plates. 10 ng/ml LPS (*Salmonella typhi*, Sigma-Aldrich) served as a control. DCs were incubated for 16-20 hours at 37°C in the presence of 5% CO₂. Hereafter, cells were collected by centrifugation, washed with 1% BSA in phosphate-buffered saline and incubated with 1 µl mouse anti-human CD80, mouse anti-human HLA-DR or mouse anti-human CD86, all conjugated with phycoerythrin (PE, BD Pharmingen, San Diego, CA). After 30 min incubation at 4°C, cells were washed and analyzed using a FACScan flow cytometer (Becton Dickinson). Supernatants of stimulated DCs were analyzed for the presence of IL-6 and TNFα by ELISA using the Human Cytosets (Biosource).

Chapter-6

Gold glyconanoparticles bearing Lewis and high-mannose-type self-glycans for the modulation of T-cell responses

In collaboration with the Dendritic cell immunobiology group, MCBI, VUmc, Amsterdam

The modulation of the immune system is a key strategy to intervene in vaccine development and autoimmune disease. Carbohydrate-mediated signalling is an archetypical response of innate immunity that can be exploited for the modulation of T cell immune reactivity.¹ Dendritic cells (DCs) are antigen presenting cells that have a high specificity for carbohydrates such as high-mannose and Lewis-type structures. The mechanisms of dendritic cells behaviour are important to understand and manipulate the immune system. Dendritic cells have a sentinel role that allow the capture and presentation of antigens; they have a migratory function to the lymphoid organs where they will collaborate with naive T cells by inducing activation of specific T-cell immune response.² Recent developments in the understanding of dendritic cell (DC) biology³ have generated an enormous interest in the use of these cells as targets for the immunotherapy of autoimmune diseases and cancer.^{4,5,6} A wide variety of DC subsets⁷ reside at peripheral tissues with an immature phenotype.⁸ This state is characterized by an elevated expression of receptors that are specialized in the recognition and uptake of antigens and, therefore, confers DCs the capacity to sample the environment for pathogens. Receptors such as C-type lectins (for self and non-self glycans) and Toll-like receptors (for Gram-positive and Gram-negative bacteria, DNA and RNA viruses, fungi, and protozoa)⁹ allow the detection of invading pathogens, their capture for proper processing and presentation and the initiation of intracellular signaling that induces the migration of DCs to the lymph node and a phenotypic change on DCs known as maturation.² As described in the introduction of this part of the Thesis, the maturation process is characterized by the up-regulation of the expression of the co-stimulatory molecules (signal 2) and cytokines (signal 3) that are required for T-cell activation.¹⁰ A crucial point for the success of DC-targeting vaccination strategies is the balance of signals achieved during maturation, since this determines the differentiation of

¹ Geijtenbeek T. B, Gringhuis S. I., Signalling through C-type lectin receptors: shaping immune responses, *Nat. Rev. Immunol.* 2009, 9, 465-479.

² Steinman R. M., The dendritic cell system and its role in immunogenicity, *Annu. Rev. Immunol.* 1991, 9, 271-296.

³ Steinman, R. M., Decisions about dendritic cells: past, present, and future, *Annu. Rev. Immunol.* 2012, 30, 1-22.

⁴ Palucka K. K., Banchereau J. J., Cancer immunotherapy via dendritic cells, *Nat. Rev. Cancer.* 2012, 12, 265-277.

⁵ Unger W. W. J., van Kooyk Y., "Dressed for success" C-type lectin receptors for the delivery of glyco-vaccines to dendritic cells, *Curr. Opin. Immunol.* 2011, 23, 131-137.

⁶ Tacken P. J., de Vries I. J., Torensma R., Figdor C. G., Dendritic-cell immunotherapy: from *ex vivo* loading to in vivo targeting, *Nat. Rev. Immunol.* 2007, 7, 790-802.

⁷ Merad M., Manz M. G., Dendritic cell homeostasis, *Blood* 2009, 113, 3418-3427.

⁸ Mellman I., Steinman R. M., Dendritic cells: specialized and regulated antigen processing machines, *Cell* 2001, 106, 255-258.

⁹ Iwasaki A., Medzhitov R., Regulation of adaptive immunity by the innate immune system, *Science* 2010, 327, 291-295.

¹⁰ Steinman R. M., Banchereau J., Taking dendritic cells into medicine, *Nature* 2007, 449, 419-426.

antigen-specific T cells.¹¹ DCs express different receptors able to recognize PAMPs (pathogen associate molecular patterns) that are able to induce an innate signalling directly related to their nature. Peptides, lipids, nucleotides and carbohydrates are different classes of PAMPs that induce a specific signalling to the DCs, which will influence the instruction to give to the naive T cells by the production of different cytokines.

The signaling induced by C-type lectin receptors is not as strong as that of other pattern-recognition receptors and it has often been observed that C-type lectin receptors modulate the signaling elicited by TLRs.¹² The existence of a fine signaling balance between C-type lectin receptors and TLRs signaling has been demonstrated for several C-type lectin receptors and specially for DC-SIGN, a C-type lectin that does not only modulate TLR signaling¹³, but also trigger different responses depending on the type of glycan recognized.¹⁴ The use of DC-SIGN-ligands (glycans) for DC-targeting provides a clear advantage over monoclonal antibody-based approaches since, even when humanized, monoclonal antibodies may still elicit adverse immune reactions that can decrease the efficiency of the immunotherapy but also may induce severe autoimmune side effects.¹⁵ The natural ligands of DC-SIGN comprise high-mannose-type glycans and Lewis-type epitopes, such as Lewis X (Le^X), Lewis Y (Le^Y), Lewis a (Le^a) and Lewis b (Le^b).^{16,17}

To investigate this type of carbohydrate-mediated processes, we made use of gold glyconanoparticles (GNPs) functionalized with DC-targeting glycans. In this part of the Thesis, we demonstrated that GNPs functionalized with high-mannose-type oligosaccharides and Lewis X (Le^X) conjugates are able to induce a series of immunosuppressive responses in DC-mediated processes. Our previous works have demonstrated that the multivalent presentation

¹¹ Zhu J., Paul W. E., CD4 T cells: fates, functions, and faults, *Blood* 2008, 112, 1557-1569.

¹² Sancho D., Reis E Sousa C., Signaling by myeloid C-type lectin receptors in immunity and homeostasis, *Annu. Rev. Immunol.* 2012, 30, 491-529.

¹³ Gringhuis S. I., den Dunnen J., Litjens M., van Het Hof B., van Kooyk Y., Geijtenbeek T. B., C-type lectin DC-SIGN modulates toll-like receptor signaling via Raf-1 kinase-dependent acetylation of transcription factor NF-kappa B, *Immunity* 2007, 26, 605-616.

¹⁴ Gringhuis S. I., den Dunnen J., Litjens M., van der Vlist M., Geijtenbeek T. B., Carbohydrate-specific signaling through the DC-SIGN signalosome tailors immunity to *Mycobacterium tuberculosis*, HIV-1 and *Helicobacter pylori*, *Nat. Immunol.* 2009, 10, 1081-1088.

¹⁵ Wang J., Zou Z. H., Xia H. L., He J. X., Zhong N. S., Tao A. L., Strengths and weaknesses of immunotherapy for advanced non-small-cell lung cancer: a meta-analysis of 12 randomized controlled trials, *PLoS ONE* 2012, 7, e32695.

¹⁶ Appelmelk B. J., van Die I., van Vliet S. J., Vandenbroucke-Grauls C. M., Geijtenbeek T. B., van Kooyk Y., Cutting edge: carbohydrate profiling identifies new pathogens that interact with dendritic cell-specific ICAM-3-grabbing nonintegrin on dendritic cells, *J. Immunol.* 2003, 170, 1635-1639.

¹⁷ van Liempt E., Bank C. M., Mehta P., Garcíá-Vallejo J. J., Kawar Z. S., Geyer R., Alvarez R. A., Cummings R. D., van Kooyk Y., van Die I., Specificity of DC-SIGN for mannose- and fucose-containing glycans, *FEBS Lett* 2006, 580, 6123-6131.

of oligomannosides on the GNPs increases the affinity for the DC-SIGN receptor¹⁸ and inhibits DC-SIGN mediated HIV *trans*-infection of human T cells at nanomolar concentration.¹⁹ Other multivalent systems (glycodendrimers) have also shown to compete for the recognition of several DC-SIGN-specific pathogens.²⁰ In this study, we use multivalent DC-SIGN-targeting GNPs functionalized with the antigen Lewis X, Gal β 1-4[Fuc α 1-3]GlcNAc β 1, (Le^X-GNP); the dimannoside Man α 1-2Man (D-GNPs), the tetramannoside Man α 1-2Man α 1-2Man α 1-3Man α (Tetra-GNPs, presented in chapter-2), and with a mixture of both Le^X and Te (Le^X/Te-GNP) aiming to achieve efficient down modulation of T cell responses through the DC-SIGN targeting of DCs (Fig. 1).

¹⁸ Martínez-Avila O., Hijazi K., Marradi M., Clavel C., Campion C., Kelly C., Penadés S., Gold manno-glyconanoparticles: multivalent systems to block HIV-1 gp120 binding to the lectin DC-SIGN, *Chem. Eur J.* 2009, 15, 9874-9888

¹⁹ Martínez-Avila O., Bedoya L. M., Marradi M., Clavel C., Alcamí J., Penadés S., 2009. Multivalent *manno*-Glyconanoparticles Inhibit DC-SIGN-Mediated HIV-1 Trans-Infection of Human T Cells, *ChemBioChem* 2009, 10, 1806-1809.

²⁰ a) Garcia-Vallejo J. J., Koning N., Ambrosini M., Kalay H., Vuist I., Sarrami-Forooshani R., Geijtenbeek T. B., van Kooyk Y., Glycodendrimers prevent HIV-transmission via DC-SIGN on dendritic cells. *Int. Immunol.* 2013, *in press*

b) Berzi A., Reina J. J., Ottria R., Sutkevičiūtė I., Antonazzo P., Sanchez-Navarro M., Chabrol E., Biasin M., Trabattoni D., Cetin I., Rojo J., Fieschi F., Bernardi A., Clerici M., A glycomimetic compound inhibits DC-SIGN-mediated HIV infection in cellular and cervical explant models, *AIDS* 2012, 26, 127-137.

c) Sattin S., Daggetti A., Thépaut M., Berzi A., Sánchez-Navarro M., Tabarani G., Rojo J., Fieschi F., Clerici M., Bernardi A., Inhibition of DC-SIGN-mediated HIV infection by a linear trimannoside mimic in a tetravalent presentation, *ACS Chem. Biol.* 2010, 5, 301-312.

d) Luczkowiak J., Sattin S., Sutkevičiūtė I., Reina J. J., Sánchez-Navarro M., Thépaut M., Martínez-Prats L., Daggetti A., Fieschi F., Delgado R., Bernardi A., Rojo J., Pseudosaccharide functionalized dendrimers as potent inhibitors of DC-SIGN dependent Ebola pseudotyped viral infection, *Bioconjug. Chem.* 2011, 22, 1354-1365.

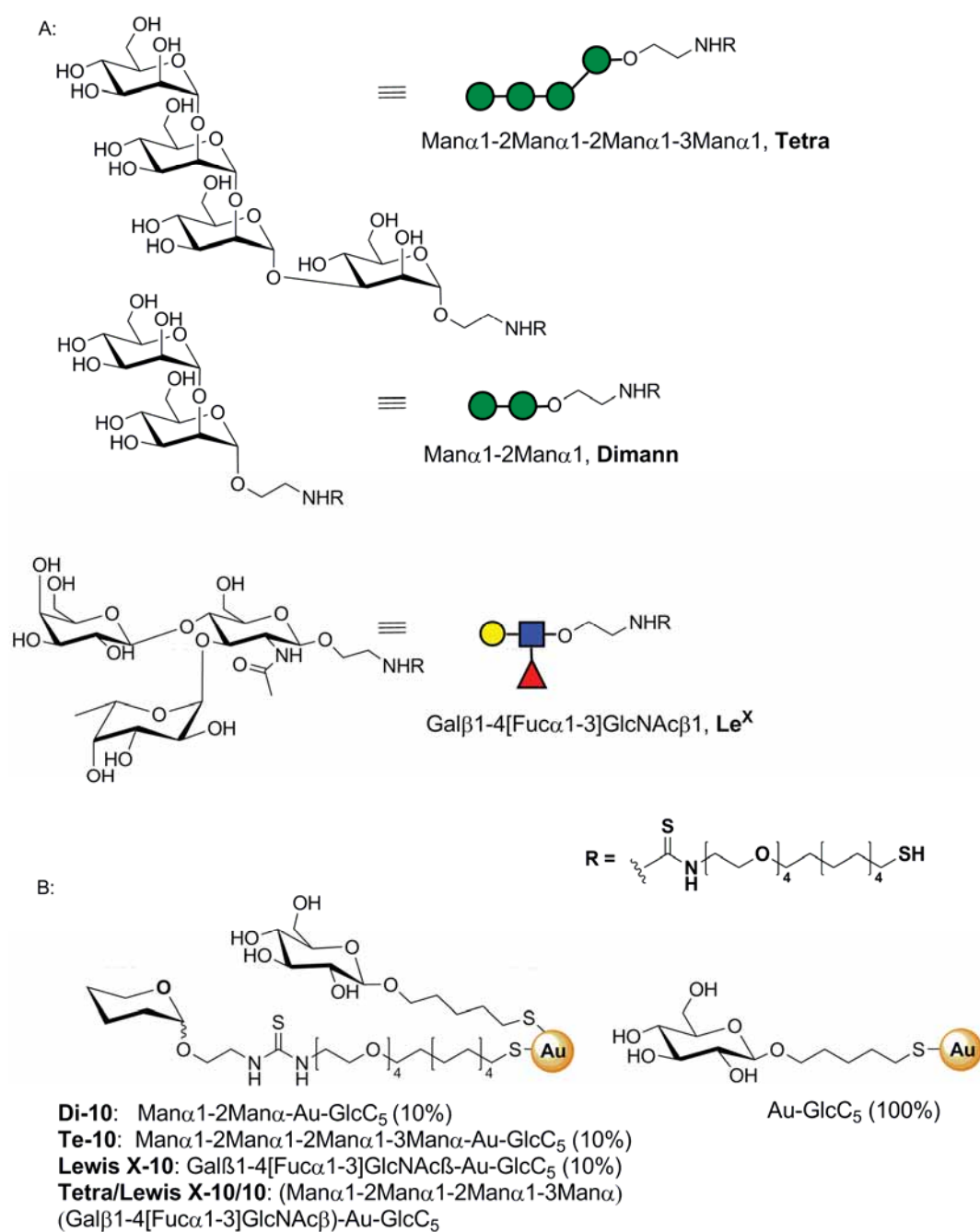
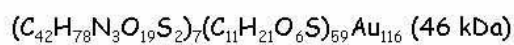
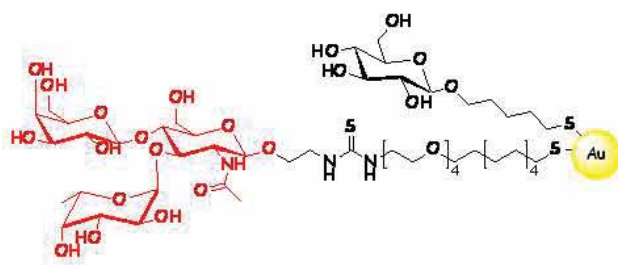


Figure 1: A) Thiol-ending glycoconjugates prepared to functionalize GNPs; B) GNPs prepared with different type of oligosaccharides.

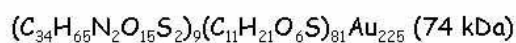
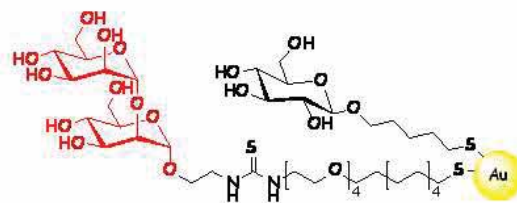
GNPs bearing 10 % of Lewis X, dimannoside and tetramannoside were prepared as mimicking system of the glycocalix of some parasites (*S. mansoni* and HIV) (Fig. 2). We selected Le^X-GNPs as tool to study the role of Le^X in the induction of immune responses on T-cells because it is known that some glycoprotein secreted by the parasitic helminth *S. mansoni* (containing the

Le^X antigen), induces strong Th2 responses both *in vitro* and *in vivo*.²¹ The GNPs bearing dimannoside (D-GNP) and tetramannosides (Te-GNP), described in chapter-2 as interesting mimetics of gp120 high-mannose glycan clusters on the HIV gp120, were also selected to study the role of high-mannoses type glycans in the induction of immune suppressive responses on DCs. It has been reported that HIV-1 gp120 high-mannose glycans induce immune suppressive responses on human dendritic cells.²² In addition to Le^X-GNP, D-GNP, and Te-GNP, we test also GNPs carrying Le^X and Te simultaneously (Te/Le^X-GNP) to evaluate whether a synergistic effect is observed due to the presence of the two antigens on the same GNP. As control, GNPs coated only with glucose were used.

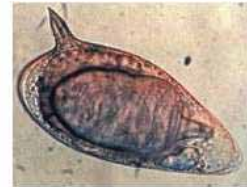
Lewis X and Di-GNPs



LeX-GNPs = 10% Lewis X and 90% Glucose

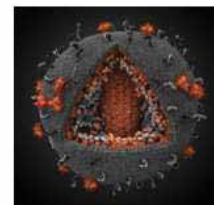


Di-GNP = 10% Dimann and 90% Glucose



Schistosoma mansoni egg

Eur. J. Immunol., 2010, 40, 1525



HIV

PLoS Pathogens, 2007, 3, 1637

Figure 2: Lewis X and dimannose-GNPs were prepared as mimicking system of the glycocalyx of some parasites able to induce an immune suppressive state on DCs cause of a carbohydrate-induced signalling. The Te-GNPs (Fig. 1B) was also prepared as mimicking of gp120 oligomannoside-clusters. In red the carbohydrate-structures involved in the described immune responses.

²¹ Everts B., Smits H. H., Hokke C. H., Yazdanbakhsh M., Helminths and dendritic cells: sensing and regulating via pattern recognition receptors, Th2 and Treg responses, Eur. J. Immunol. 2010, 40, 1525-1537.

²² Shan M., Klasse P. J., Banerjee K., Dey A. K., Iyer S. P., Dionisio R., Charles D., Campbell-Gardener L., Olson W. C., Sanders R. W., Moore J. P., HIV-1 gp120 mannoses induce immunosuppressive responses from dendritic cells, PLoS Pathog. 2007, 3, e169.

Preparation of GNPs

GNPs bearing 10% of thiol-ending conjugate of dimannoside (Man α 1-2Man α 1) and tetramannoside (Man α 1-2Man α 1-2Man α 1-3Man α) conjugates and 90% of 5-(mercapto)pentyl β -D-glucopyranoside as inner component were prepared as described.¹⁸ The preparation of the oligomannose derivatives following a standard procedure²³ is reported in appendix 2.

However, for the preparation of GNPs bearing 10% of Gal β 1-4[Fuc α 1-3]GlcNAc β 1 (Lewis X antigen) and 90% of 5-(mercapto)pentyl β -D-glucopyranoside derivative, the synthesis of the Le^X conjugate was first addressed.

Synthesis of the Le^X conjugate to prepare GNPs

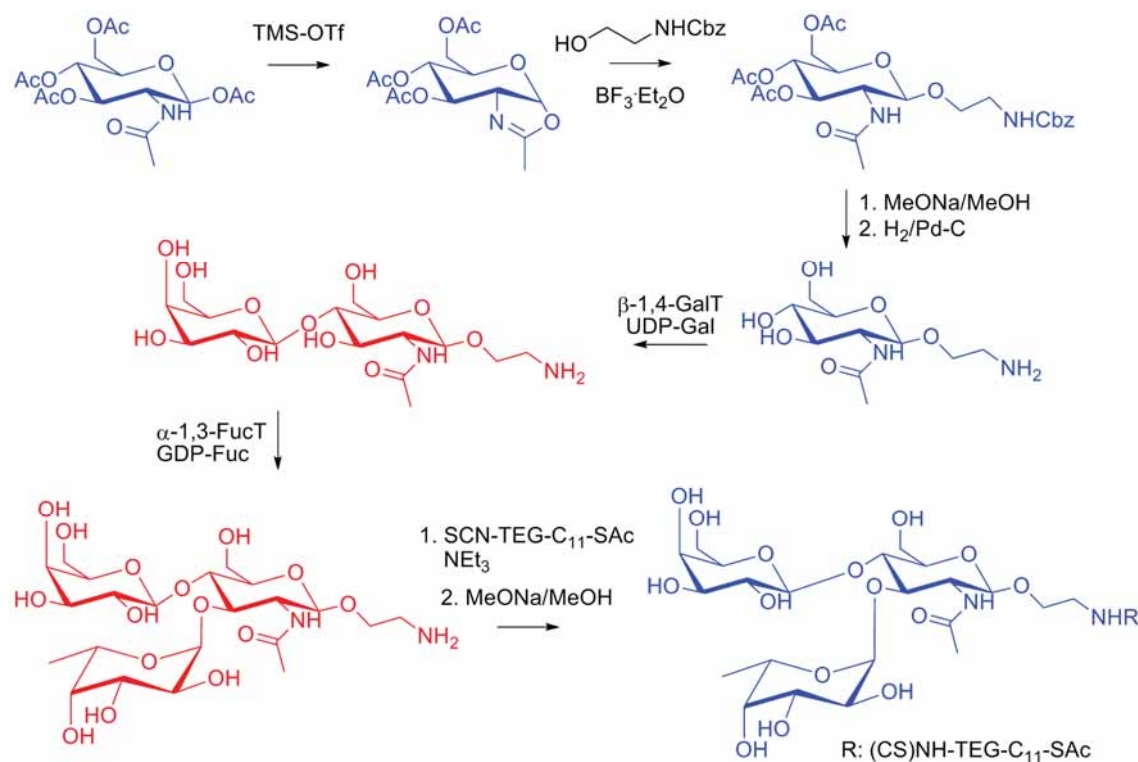
In order to prepare a suitable Le^X thiol-ending glycoconjugate a chemo-enzymatic synthesis was performed. Protected 2-aminoethyl β -D-N-acetyl-glucosamine derivative was prepared in two steps following a reported procedure.²⁴ After deprotection, two enzymatic steps (galactose and fucose glycosylations) were performed in water by enzymatic reactions following reported procedures²⁵ (scheme 1) under the supervision of Dr. S. Serna. The Le^X amino derivative was then coupled with a long isothiocyanate linker ending with a thiol group in order to allow its coupling on the GNPs (same method used in this Thesis for the GNPs preparation, see intro). The thiol-ended Le^X conjugate was used for the preparation of Le^X-GNP and Le^X/Te-GNP.

²³ Lee H. K., Scanlan C. N., Huang C. Y., Chang A. Y., Calarese D. A., Dwek R. A., Rudd P. M., Burton D. R., Wilson I. A., Wong C. H., Reactivity-based one-pot synthesis of oligomannoses: defining antigens recognized by 2G12, a broadly neutralizing anti-HIV-1 antibody, *Angew. Chem. Int. Ed.* 2004, 43, 1000-1003.

²⁴ Sardzík R., Noble G. T., Weissenborn M. J., Martin A., Webb S. J., Flitsch S. L., Preparation of aminoethyl glycosides for glycoconjugation, *Beilstein J. Org. Chem.* 2010, 6, 699-703.

²⁵ a) DeBose-Boyd R. A., Nyame A. K., Cummings R. D., Molecular cloning and characterization of an alpha1,3 fucosyltransferase, CEFT-1, from *Caenorhabditis elegans*, *Glycobiology* 1998, 8, 905-917.

b) Nguyen K., van Die I., Grundahl K. M., Kawar Z. S., Cummings R. D., Molecular cloning and characterization of the *Caenorhabditis elegans* alpha1,3-fucosyltransferase family, *Glycobiology* 2007, 17, 586-599



Scheme 1: Chemo-enzymatic synthesis for the preparation of the thiol-ending Le^x derivative. In blue the chemical steps; in red the enzymatic ones. 30% yield from the first three chemical steps. 88% yield from the two enzymatic steps and 72% yield from the last isothiocyanate and thiol-deprotection steps.

GNPs induce an immunosuppressive state on dendritic cells

General overview on the cellular experiments

To study the role of the different carbohydrates present on the GNPs in the modulation of the T cell immune response, different cellular experiments were performed. We first investigated on the ability of GNPs to trigger a lectin mediated signaling on DCs that led to the production of the anti-inflammatory cytokine IL-10. GNPs were incubated with human DCs from healthy donors and the cytokines produced in the cellular media were analyzed by ELISA after 16h.

Once demonstrated that the GNPs were able to trigger a carbohydrate-mediated IL-10 production in DCs, we investigated the effect of these DCs-signaling in naïve T-cells. GNPs were incubated by DCs and then co-incubated with naïve CD4⁺ T-cells from another donor. After the expansion of the T-cells clones, intracellular markers for T-helper subsets were determined by flow cytometry to prove that the GNPs-induced signaling on DCs was able to educate naïve T-cells to switch in their different subsets (Th1 or Th2).

Finally a functional assay called mixed leukocyte reaction (MLR) was designed to validate the induction of a tolerance mechanism (anergy) on T-cells triggered by the GNPs on DCs. MLR is an *in vitro* experiment to validate the CD4⁺ T-cells proliferation. When allogeneic (different donors with different MHC) lymphocytes are cultured together, CD4⁺ T-cell populations expand. The total proliferation of lymphocytes from the allogeneic strains is measured by adding [³H]-thymidine to the culture medium monitoring its uptake (the uptake occurs during each cell division and the [³H] signal is related with the cellular proliferation).

Effects of GNPs on cytokine IL-10 production by DCs

It was previously shown that triggering of DC-SIGN in the context of simultaneous activation through Toll-like receptor 4 (TLR-4) results in a synergistic up regulation in the expression of the anti-inflammatory interleukine IL-10.¹³ TLR-4 detects lipopolysaccharide from Gram-negative bacteria and is thus important in the activation of the innate immune system. Because GNPs are highly multivalent and bind with high affinity to DC-SIGN,^{19,26} we speculated that they could induce the modulation of TLR4 signaling leading to IL-10 up regulation.

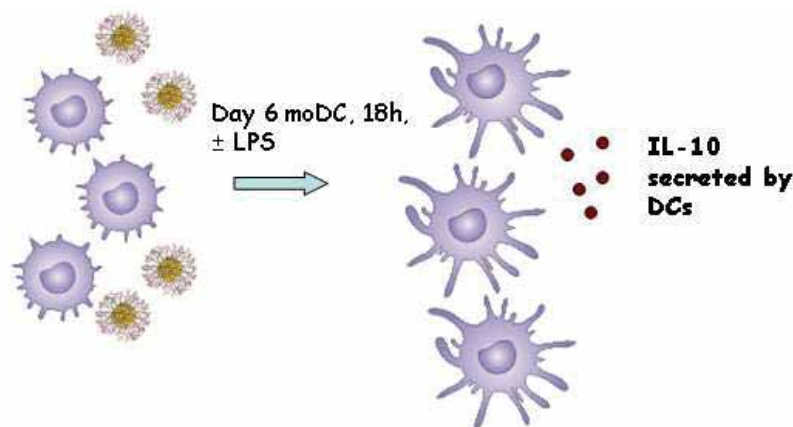


Figure 3: Schematic overview of the experiment performed for the detection of IL-10.

Day 6 monocyte-derived DCs (moDC) (50.000 cells/well) were stimulated in presence of 1 µg/mL of GNPs and LPS (10 ng/mL). After 16 h the cells were centrifuged and the presence of IL-10 in the supernatant was detected by ELISA (Fig. 3). GNPs carrying dimannosides (D), tetramannosides (Te), and Le^x, were able to enhance the LPS-mediated secretion of IL-10, while control Glc-GNPs did not (Figure 4).

²⁶ Arnáiz B., Martínez-Ávila O., Falcon-Perez J. M., Penadés S., Cellular uptake of gold nanoparticles bearing HIV gp120 oligomannosides, *Bioconjug. Chem.* 2012, 23, 814-825.

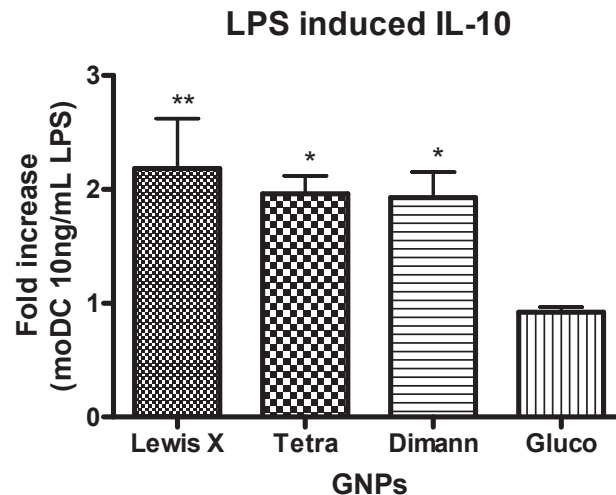


Figure 4. Effect of GNPs in the LPS induced IL-10 secretion in the cellular media. The maximum amount of IL-10 that can be secreted by DCs after LPS interaction by the TLR route is set by 1. Le^x, Te- and D-GNPs were able to up-regulate the IL-10 production when co-incubated with LPS. Glc-GNP did not improve the amount of IL-10. The ~2 fold increase respect to the IL-10 production in presence of LPS, indicates that GNPs are able to induce a C-type lectin mediated IL-10 production triggering a signaling route that involves TLR and lectins.

As described previously, IL-10 is an anti-inflammatory cytokine produced to control the activation of antigen presenting cells after a specific exogenous ligand interaction. The up-regulation of IL-10 in the presence of LPS is a typical response of TLR4 against pathogen endotoxins. The cross-talk between lectins and TLR-4 seems to be related to the nature of the carbohydrates-induced signaling. Interesting, we also appreciated clear differences between different human donors. We think that it may be a category of donors more reactive to Le^x-GNPs and another category more reactive to the D-GNPs. These differences on the human donors are preliminary results that need a further study to confirm that there are Le^x or mannoses human responders. These different behaviors between the donors could be related to different lectins subsets on the human genome.

T cell polarization assay : Th1/Th2 balance

Because the cytokine production of DCs affects the differentiation of T cells, we addressed whether pulsing DCs with our GNPs would affect their capacity to induce Th1/Th2 responses. Monocyte derived dendritic cells (moDC, 200.000 cells/well) were incubated with the GNPs (4µg/mL) for 48h (Fig. 5). After washing, moDC were co-cultured with naive CD4+ T cells (from fresh blood donors). The T cell expansion was followed for 5 days with the addition of IL-2, which is necessary for the growth, proliferation, and differentiation of T cells to become

'effector' T cells. IL-2 is normally produced by T cells during an immune response.²⁷ The CD4+ T cells were stained for intracellular INF- γ (Th1 marker) and IL-4 (Th2 marker).

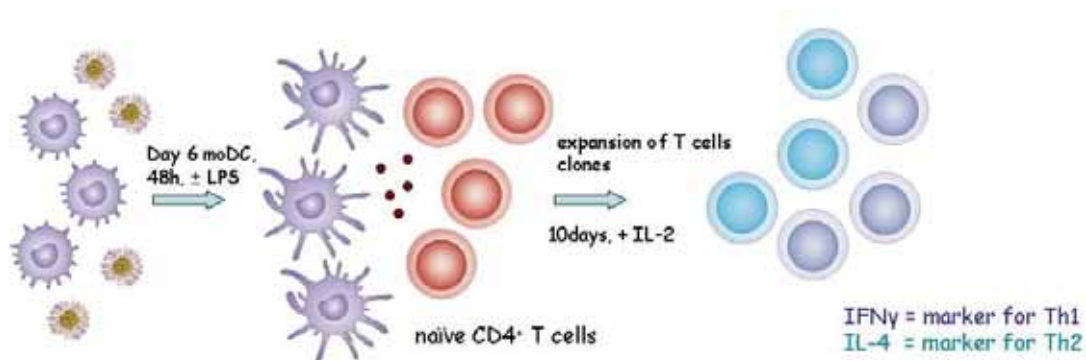


Figure 5: General overview on the experiment designed to evaluate the ability of GNPs to modulate the behavior of naïve T-cells after thought a DC-mediated signaling. Dark circles in the middle of the figure represent interleukins.

The CD4+ T cells that were incubated with the Le^X-GNPs-treated moDC switch their characteristics to Th2 and clearly decreased the Th1 population (Figure 6). As described previously, Lewis X containing proteins are able to condition moDC in vitro to drive Th2 polarization.²¹ Using Le^X-GNPs we were able to induce a clear Th2 polarization and Th1 reduction. D-GNPs were also able to induce a clear Th2 polarization, while the glucose and tetra GNPs-treated moDC were not able to switch the CD4+ naïve T cell balance. Although D-, Te-, and Le^X-GNPs were able to induce a C-type lectin induced IL-10 production (Fig. 4), only Le^X and the dimannoside educated the CD4+ naïve T cell in a carbohydrate-dependent to switch the CD4+ naïve T cell to the Th2 population in this last experiment.

²⁷ Smith K. A., Interleukin-2: inception, impact, and implications, Science 1988, 240, 1169-1176.

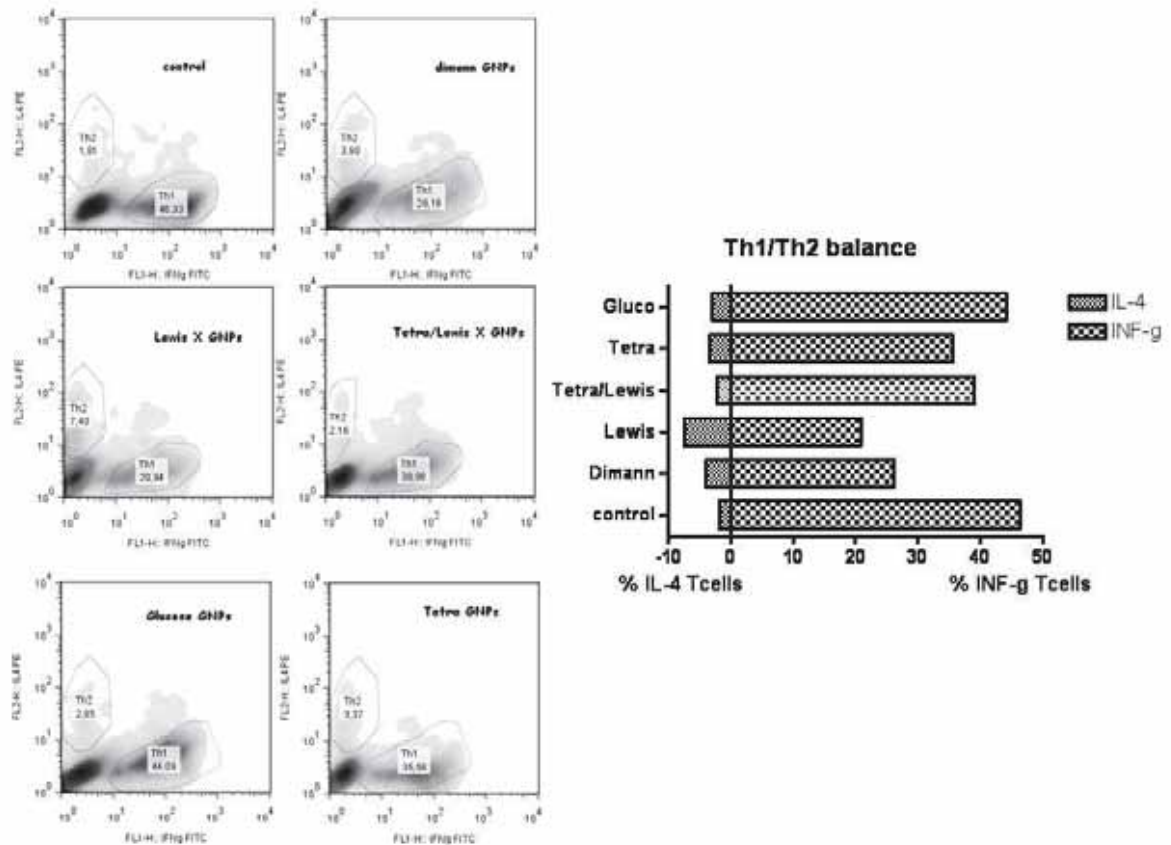


Figure 6: Intracellular detection of IFN- γ (marker for Th1) and IL-4 (marker for Th2) on the clones of CD4⁺ T-cells that were incubated with the DCs stimulated with GNPs. Left: flow cytometry analysis to detect the Th1 or Th2 markers. Right: graph bars representing the cytometry results. Lewis and dimannoside GNPs clearly decrease the Th1 population and increase the Th2 population.

To evaluate the effect of the simultaneous presence on the GNPs of mannoside and Lewis type antigens the Th2 polarization, a GNP carrying both Lewis X and tetramannoside was prepared. The presence of the Te on the Le^X-GNP decreased the Lewis capacity to polarize the CD4⁺ T cell to Th2 (Figure 6).

Effects of GNPs on the generation of regulatory T-cells (Treg) and induction of tolerance mechanism (anergy)

As described in the introduction to this part of the Thesis, Treg are a subpopulation of T cells which modulate the immune system, maintain tolerance to self-antigens, and abrogate autoimmune disease. Mouse models have suggested that modulation of Tregs can treat autoimmune disease and cancer, and facilitate organ transplantation. IL-10 has been considered as a mediator of the regulatory T-cells (Treg) induced suppression.²⁸ The increase of IL-10 production previously observed, lead us to design a functional assay to demonstrate that the carbohydrate-induce signalling on the moDC may induce a tolerance mechanics (anergy) on T-cells. Anergy is a tolerance mechanism by which a subset of lymphocytes (Treg) is functionally inactivated, but remains alive for an extended period of time in a hypo responsive state.²⁹ An allogeneic mixed leukocytes reaction (MLR) was performed by incubation of moDC (200.000 cells/well) with 4µg/mL of the GNPs. After 16h the DCs were co-cultured with peripheral blood leucocytes (PBL)-derived CD4⁺ naive T cells (Fig. 7).

The CD4⁺ T cells were expanded and cultured for 5 days with the addition of IL-2, IL-7 and IL-15 to maintain the proliferative state of the cells. After the expansion, the CD4⁺ T cells were exposed again with the moDC of day 1 and the reproduction of cells was monitored by the incorporation of ³H-thymidine into dividing cells.

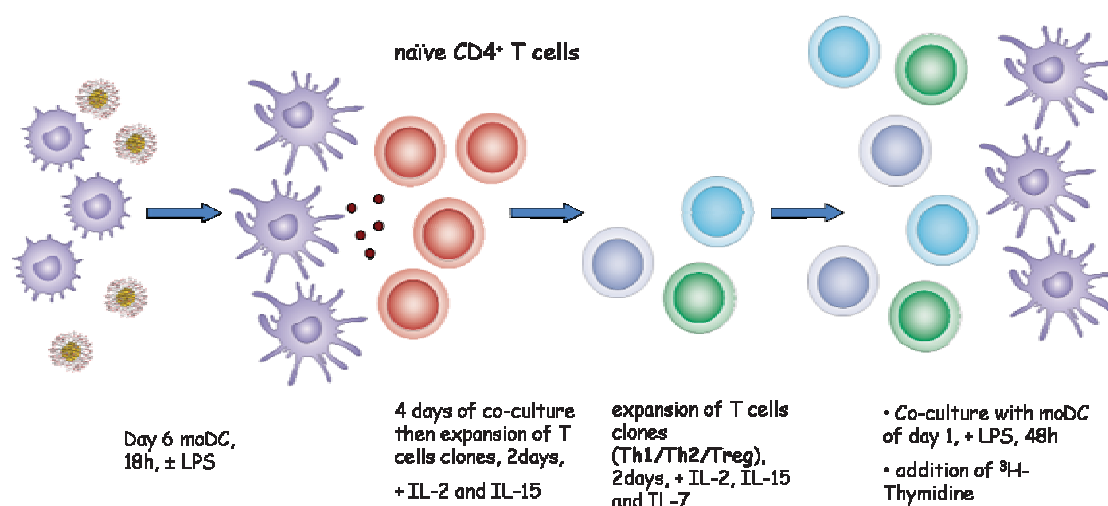


Figure 7: MLR experiment designed as functional assay to validate the tolerance mechanism induced on naïve T-cells (anergy).

²⁸ Chaudhry A., Samstein R. M., Treuting P., Liang Y., Pils M. C., Heinrich J. M., Jack R. S., Wunderlich F. T., Brüning J. C., Müller W., Rudensky A. Y., Interleukin-10 signaling in regulatory T cells is required for suppression of Th17 cell-mediated inflammation, *Immunity*. 2011, 34, 566-578.

²⁹ Schwartz R. H., T cell anergy, *Annu. Rev. Immunol.* 2003, 21, 305-334.

The CD4⁺ T cells that were cultured with the Lewis X GNPs-treated moDC showed a clear suppression in their replication when exposed to the day 1 moDC (Figure 8). Probably, the signalling triggered by the Lewis X GNPs is able to release in the medium an appropriate amount of IL-10 that switch the CD4⁺ naive T cell to be Treg. The carbohydrate-specific signalling induced by the moDC was able to educate the CD4⁺ naive T cell to an anergic state that was evinced by the decrease in the replication count of the T cells after the day 1 moDC exposure. The presence of the tetramannoside on the Lewis X GNPs induced a higher T cells replication, decreasing the anergic effect of the Lewis X. The dimannoside GNPs also showed an anergic state of the moDC, but no as strong as the Le^X-GNPs. The GNPs carrying only glucose or tetramannoside were not able to induce the anergic effect on the T cells.

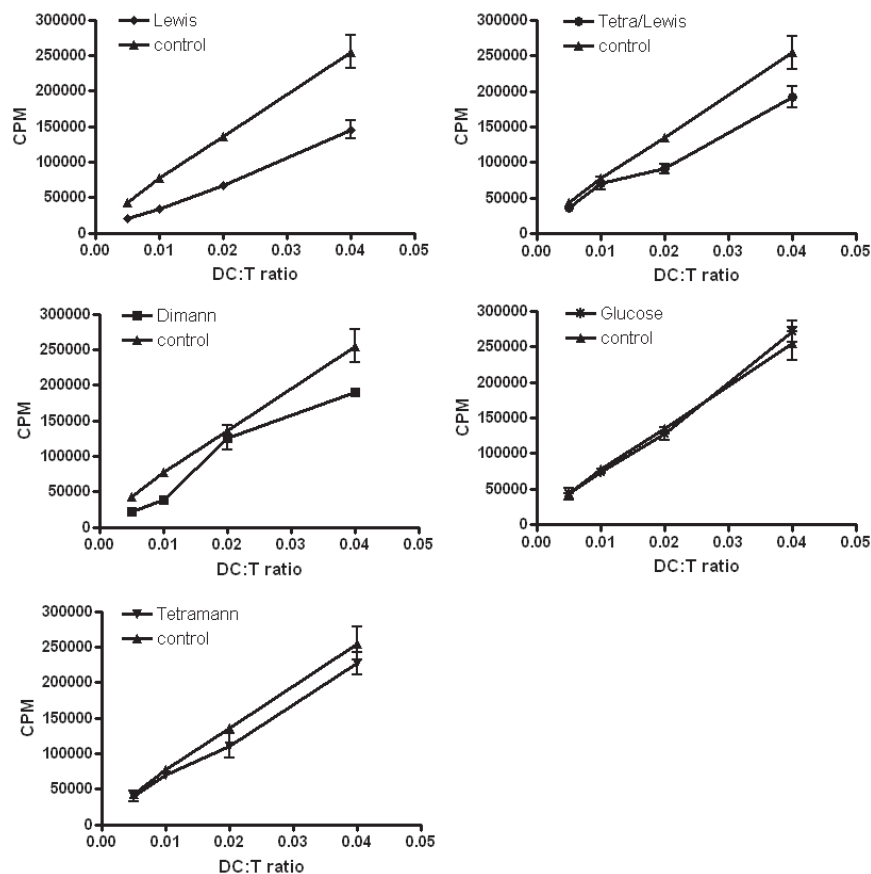


Figure 8: Influence of GNPs in the MLR experiment. Incorporation of ³H-thymidine into clones of dividing T-cells at different DC/T ratio was monitored by counting the rate of counts per unit time (CPM, counts per minute) registered by scintillography. Triangles showed the replication of T-cells that were co-incubated with not stimulated DCs. T-cells co-incubated with DCs treated with Le^X (rhombs) or dimannose-GNPs (squares) at day one decreased their replication rate. GNPs carrying glucose and tetramannoside were not able to induce the anergic effect on the T cells (stars or inverted triangle).

Conclusions

Targeting antigen presenting cells with carbohydrates is a well established strategy to improve drugs³⁰ or vaccines response³¹. The seminal work of Geijtenbeek¹⁴ showed that parasites carrying different type of carbohydrates were able to interact with DC-SIGN triggering different immuno-pathways in a carbohydrate-dependent manner. Differences in the DC-SIGN signalling were described also using multivalent carbohydrate functionalised polymers (PAA-Le^X and PAA-mannose).¹⁴ Lewis X-containing molecules are known to polarize the CD4+ naive T cells to a Th2 phenotype²¹ and the gp120 high-mannoses are associated to an IL-10 production by moDC.²²

Based on these results, we have designed and prepared multivalent GNPs carrying Lewis X and oligomannoside antigens. Well-defined glycoconjugates can help in understanding the role of carbohydrates in the innate immune response and their application in autoimmune diseases and immune-adjuvant administration. High mannose type oligosaccharide and Lewis X GNPs were able to induce a C-type lectin mediated IL-10 production on moDC that was able to educate and modulate the CD4+ naive T cell in a carbohydrate-dependent manner. The carbohydrates signalling induced by DC on T cells could be exploited to manipulate the immune homeostasis: Different GNPs could be prepared to activate a specific C-type lectin signalling that will be able to attenuate the response to parasites or prevent autoimmune diseases. The DCs-induced immunological tolerance observed with our GNPs seems to be sensitive to the lectin-induced signalling, triggering a T cells response in a carbohydrate-specific manner.

This is one of the first examples of carbohydrate-multivalent systems (without any peptide entity), able to interact with DCs in a carbohydrate-dependent manner, triggering different lectin-pathways that influence the T-cells behaviour. These results encourage the use of GNPs to study the role of different carbohydrates in the innate immune response. This work extends the knowledge on DC-SIGN targeting by using a 2nm gold scaffold that can be designed in future to modulate response to pathogens or to prevent autoimmune diseases. The information that could be gained from this type of studies will add important information for the glyco-induced vaccination strategy.

³⁰ Barratt G., Tenu J. P., Yapo A., Petit J. F., Preparation and characterization of liposomes containing mannosylated phospholipids capable of targeting drugs to macrophages, *Biochim. Biophys. Acta*, 1986, 862, 153-164.

³¹ Cruz L. J., Tacken P. J., Pots J. M., Torensma R., Buschow S. I., Figdor C. G., Comparison of antibodies and carbohydrates to target vaccines to human dendritic cells via DC-SIGN, *Biomaterials* 2012, 33, 4229-4239.

Experimental section

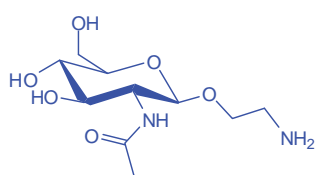
Materials

All chemicals were purchased as reagent grade from Sigma-Aldrich and used without further purification, unless otherwise stated. TLC was performed on 0.25 mm pre-coated silica gel glass plates or aluminium backed sheets (Merck silica gel 60 F₂₅₄) with detection by UV-light (254 nm) and/or heating at over 200 °C after staining either with 10 % sulfuric acid (aqueous solution) or *p*-anisaldehyde solution [*p*-anisaldehyde (25 mL), H₂SO₄ (25 mL), EtOH (450 mL), and CH₃COOH (1 mL)]. Organic solvents were removed by rotary evaporation under reduced pressure at approximately 40 °C (water bath). Silica gel (0.041–0.063 mm, Amicon and 0.063–0.200 mm, Merck) was used for flash column chromatography (FCC). Size-exclusion column chromatography was performed on Sephadex LH-20 (GE Healthcare). NMR spectra were recorded at 500 MHz (Bruker) (¹H) or 125 MHz (¹³C) at 25 °C. If not otherwise stated, chemical shifts (δ) are given in ppm relative to the residual solvent signal. Infrared spectra (IR) were recorded from 4000 to 400 cm⁻¹ with a Nicolet 6700 FT-IR spectrometer (Thermo Spectra-Tech), solids were pressed into KBr pellets. Mass spectrometric data was obtained from a Waters LCT Premier XE instrument with a standard ESI source by direct injection. The instrument was operated with a capillary voltage of 1.0 kV and a cone voltage of 200 V. Cone and desolvation gas flow were set to 50 and 500 L/h, respectively; source and desolvation temperatures were 100°C. High resolution mass was determined using glycocholic acid (Sigma) as an internal standard (2M+Na⁺, *m/z* = 953.6058). MALDI-Tof spectra were recorded on a Bruker Reflex IV using 2',4',6'-trihydroxy-acetophenone monohydrate (THAP) as matrix.

β-1,4-Galactosyltransferase from bovine milk, uridine 5'-diphosphogalactose disodium salt (UDP-Gal), guanosine 5'-diphospho-β-L-fucose sodium salt (GDP-Fuc) were purchased from Sigma Aldrich. *Pichia pastoris* clones expressing *C. elegans* α-1,3-fucosyltransferase (CeFUT6) were kindly provided by Professor Dr. Iain B. H. Wilson, Department für Chemie, Universität für Bodenkultur, Vienna.

Chemo-enzymatic synthesis of Lewis X amino derivative (see scheme 1)

Chemical steps: ²⁴



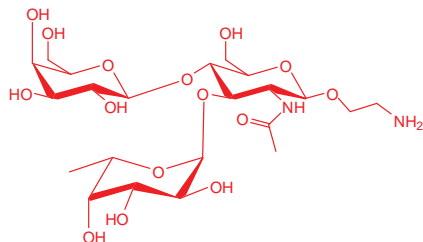
GlcNAc-NH₂: Peracetylated GlcNAc (468mg, 1.2mmol, 1equiv.) was dissolved in dry CH₂Cl₂. TMS-OTf (651 μL, 3.6mmol, 3eq) was added and the mixture heated at reflux at 50° C for 12h. After a fast silica gel chromatography purification (AcOEt/Hex = 3/1) the resulting oxazolidine was directly glycosylated with benzyl 2-hydroxyethylcarbamate (550mg, 3mmol, 2equiv.) in presence of

BF₃·Et₂O (280 μL, 2.2mmol, 1.5equiv.) under dry conditions (5mL dry CH₂Cl₂ and 500mg mol. sieves). After 2h, the reaction was directly purified by column chromatography (AcOEt/Hex = 3/1) and the first fraction containing the peracetylated GlcNAc-NHCbz was directly used for the next reaction.

Peracetylated GlcNAc-NHCbz (42mg, 80 μmol, 1 equiv.) was dissolved in MeOH (3mL) followed by the addition of MeONa (4.3mg, 80 μmol, 1 equiv.). After 3h, NMR of the crude showed no signals from the acetyl groups and the reaction was quenched with HCl 1M to pH=3. The solution was evaporated and the product was dissolved in 3mL of MeOH/HOOCH (95/5) in the presence of 65mg of Pd on activated carbon. N₂ was first flushed in the flask followed by H₂. After 12h, the reaction was filtered over celite and concentrated under vacuum. The crude material was purified by Sephadex LH-20 chromatography (column: diameter = 2 cm; height = 45 cm) using as eluent MeOH/ H₂O = 9/1 to afford the **GlcNAc-NH₂** conjugate as a white solid after lyophilisation (13mg, 50 μmol).

^1H NMR (500 MHz, D_2O): δ (ppm) = 2.05 (s, 3H, COCH_3), 2.69–2.85 (m, 2H, CH_2NH_2), 3.34–3.52 (m, 2H, 4-H, 5-H), 3.52–3.59 (m, 1H, 3-H), 3.59–3.67 (m, 1H, $\text{CHaHbCH}_2\text{NH}_2$), 3.71–3.80 (m, 2H, 2-H, 6-Ha), 3.87–4.01 (m, 2H, 6-Hb, $\text{CHaHbCH}_2\text{NH}_2$), 4.53 (d, $J = 8.4$ Hz, 1H, 1-H).

Enzymatic steps: ²⁵

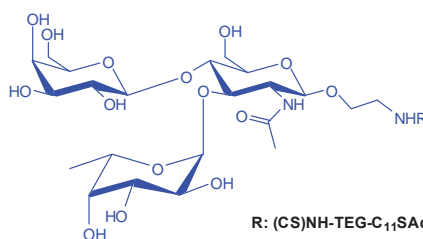


$\text{Le}^{\text{X}}\text{-NH}_2$: GlcNAc- NH_2 (2.4mg, 8 μmol), UDP-Gal (Uridine 5'-diphosphogalactose disodium salt) (6.2 mg, 8.8 μmol), bovine serum albumin BSA (1 mg), 100 μL of 1U/mL of bovine milk β -1,4-galactosyltransferase, 50 μL of 10mU/ μL of alkaline phosphatase and MnCl_2 (10 mM) in 1mL HEPES buffer (50 mM, pH=7.4), was incubated at 37 $^\circ\text{C}$ for 2 h. The resulting mixture was heated at 95 $^\circ\text{C}$ for 5

minutes. The white precipitate was centrifuged and the solution was purified by column chromatography in Biogel P2 with NH_4HCO_3 (40 mM). Fractions were analyzed by MALDI-TOF and the compound-containing fractions were pooled and freeze-dried to obtain the disaccharide **Gal-GlcNAc- NH_2** as a white powder (3.5 mg, 88 %).

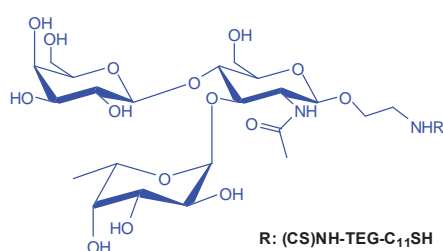
Gal-GlcNAc- NH_2 (3.4mg, 8 μmol), GDP-Fucose (4mg, 8.8 μmol), *C. elegans* α -1,3 FucT (CeFUT6) (12mU from 0.24mU/ μL solution) and MnCl_2 (20 mM) in MES buffer (80 mM, pH=6.5) was incubated at room temperature for 12 h. The resulting mixture was heated at 95 $^\circ\text{C}$ for 5 minutes, centrifuged and the solution was purified by column chromatography in Biogel P2 with NH_4HCO_3 (40 mM). Fractions were analyzed by MALDI-TOF, the compound-containing fractions were pooled and freeze-dried to obtain **Gal-[Fuc]-GlcNAc- NH_2 ($\text{Le}^{\text{X}}\text{-NH}_2$)** as a white powder (2.8 mg, 4.9 μmol , 80 %).

^1H NMR (500 MHz, D_2O) $\delta = 5.13$ (d, $J=3.9$, 1H), 4.84 (m, 1H), 4.57 (d, $J=8.4$, 1H), 4.47 (d, $J=7.8$, 1H), 4.02 (m, 1H), 3.98 – 3.84 (m, 7H), 3.80 (d, $J=2.4$, 1H), 3.78 – 3.64 (m, 5H), 3.61 (m, 2H), 3.51 (m, 1H), 2.90 (m, 2H), 2.06 (s, 3H), 1.19 (d, $J=6.6$, 3H).



$\text{Le}^{\text{X}}\text{-NH(CS)NH-TEG-C}_{11}\text{-SAc}$: A solution of isothiocyanate linker (2.5 mg, 5.39 μmol , 1.1 equiv.) in $\text{H}_2\text{O-iPrOH-CH}_3\text{CN}$ (1:1:1, v/v/v, 0.5 mL) was added to a solution of 3-aminopropyl Lewis X conjugate (2.8 mg, 4.9 μmol , 1 equiv.) in $\text{H}_2\text{O-iPrOH-CH}_3\text{CN}$ (1:1:1, v/v/v, 0.5 mL) and the pH was set to basic by addition of triethylamine (2 μL , 15 μmol , 3 equiv.). The mixture was stirred at room

temperature for 12 h and then evaporated. The crude material was kept in high vacuum to remove the residual triethylamine and then triturated with Et_2O (4 x 1 mL) in order to get rid of the excess of the linker. In the ^1H NMR spectrum of the crude, a singlet at 2.30 ppm (C(O)CH_3) integrates 3H just like the methyl group of the fucose moiety at 1.18 ppm (d, $J=6.5$, 3H, CH_3) indicating that the coupling reaction was successful. The S-acetyl protected Lewis X conjugate was directly used for the next reaction after NMR and MALDI characterization (3 mg, 4.9 μmol).



$\text{Le}^{\text{X}}\text{-NH(CS)NH-TEG-C}_{11}\text{-SH}$. Sodium methoxide (0.2 mg, 4.9 μmol , 1 equiv.) was added to a solution of $\text{Le}^{\text{X}}\text{-NH(CS)NH-TEG-C}_{11}\text{-SAc}$ (3 mg, 4.9 μmol , 1 equiv.) in MeOH (2 mL). The mixture was stirred at room temperature for 12 hours and then evaporated. The crude material was concentrated and purified by Sephadex LH-20 chromatography (column: diameter = 2 cm; height = 45 cm) using as eluent $\text{MeOH/ H}_2\text{O} = 9/1$ to afford the Lewis X conjugate as a white solid after lyophilisation (2mg, 2 μmol). ^1H NMR (500 MHz, MeOD) $\delta = 5.05$ (d, $J=3.9$,

1H), 4.84 (q, J = 6.6, 1H), 4.49 (d, J=8.2, 1H), 4.42 (d, J=7.5, 1H), 3.98-3.47 (m, 37H), 2.69 (t, J=7.2, 2H, CH₂S), 1.98 (s, 3H, NAc), 1.74 – 1.67 (m, 2H), 1.63 – 1.56 (m, 2H), 1.45-1.31 (m, 14H), 1.18 (d, J=6.5, 3H, CH₃ fucose moiety). ¹H, ¹³C HSQC (125 MHz, CD₃OD) δ = 104.0 (d, 1C), 102.5 (d, 1C), 100.3 (d, 1C), 77.0, 76.6, 75.1, 74.9, 73.6, 72.4, 71.4, 70.9, 69.9, 69.6, 67.5 (d, 1C), 62.6 (t, 1C), 61.2 (t, 1C), 57.1 (d, 1C), 39.6 (t, 1C, CH₂S), 30.6, 30.5, 30.2, 23.1 (q, 1C, NAc), 16.2 (q, 1C, CH₃ fucose moiety). HR-MS: calcd for C₄₂H₇₉N₃O₁₉S₂Na⁺: 1015.4568 [M+Na]⁺; found 1015.4645.

For the oligomannosides synthesis see appendix 2.

Preparation and Characterization of GNPs

General synthesis and characterization of GNPs

A solution of tetrachloroauric acid (HAuCl_4 , Strem Chemicals, 0.025 M, 1 equiv.) in water was added to a 0.012 M (3 equiv.) methanolic solution of the mixture of 10% thiol-ending conjugates and 90% of glucose-conjugate. An aqueous solution of NaBH_4 1M (21 equiv.) was then added in four portions, with vigorous shaking. The black suspension formed was shaken for an additional 2 h at 25°C after which the supernatant was removed and analysed. The residue was dissolved in a minimal volume of Nanopure water and purified by dialysis.

Dimann, Tetramann and glucose GNPs were prepared as previously described, chapter-2.¹⁸

Lewis X GNPs: Reaction of a 1:9 mixture of 1mg Lewis X conjugate and 2.55mg of GlcC5S with HAuCl_4 and NaBH_4 gave 0.73mg of Lewis X-GNPs as a dark-brown powder. TEM (average diameter): 1.8 ± 0.4 nm. Quantitative ^1H NMR: 0.73mg of Lewis X-GNPs were dissolved in 700 μL of 0.75% TSP in D_2O and 0.07 μmoles of Lewis X were founded.

NMR (500 MHz, D_2O /internal standard TSP) only significant peaks are reported: $\delta = 5.13$ (s, from Lewis X conjugate, anomeric proton), 4.44 (bs, from Glucose conjugate), 2.10 (s, NAc of Lewis X conjugate), 1.20 (bs, fucose $-\text{CH}_3$ of Lewis X conjugate); ratio between Lewis X and Glucose signals $\sim 1:8$. These results are in agreement with the estimation of 10% of Lewis X on the GNPs. Molar ratio of conjugates per nanoparticle was also determined by analyzing the mixtures using NMR before and after nanoparticle formation. Estimated average molecular weight for $(\text{C}_{42}\text{H}_{78}\text{N}_3\text{O}_{19}\text{S}_2)_7(\text{C}_{11}\text{H}_{21}\text{O}_6\text{S})_{59}\text{Au}_{116}$: ~ 46 kDa. IR (KBr): $\nu = \sim 3600\text{--}3100$ (br), 2919, 2848, 2365, 2343, 1654, 1381, 1069. UV/Vis (H_2O , 0.1 mg/mL): surface plasmon band not observed.

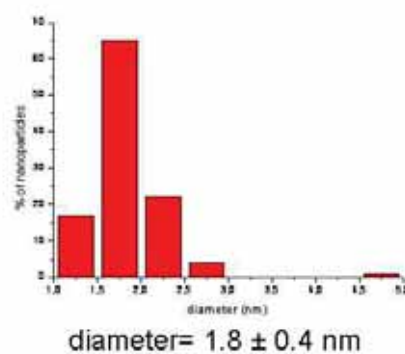
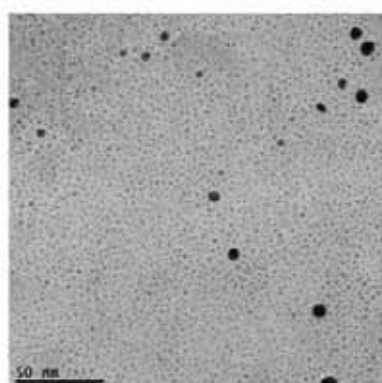
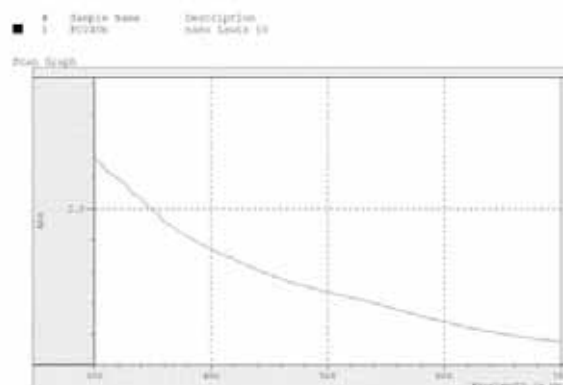
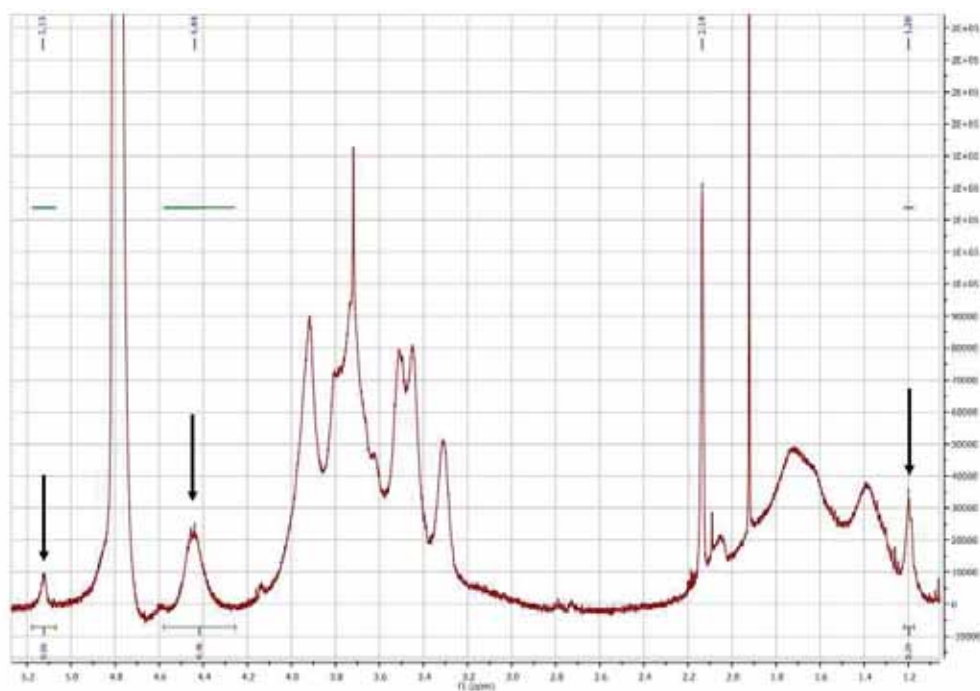


Figure 9: Characterization of Le^X-GNPs: *Upper panel:* ¹H NMR spectrum of Le^X-GNPs in D₂O at 500 MHz. The signals from the anomeric protons of the glycoconjugates on the GNPs are clearly observed between 5.0 and 5.5ppm. *Bottom panel:* UV-Vis spectra of a 0.1 mg/mL solution of the Le^X-GNPs in water; TEM micrograph and size-distribution histogram obtained from analysis of TEM micrographs

Tetra/Lewis X GNPs: Reaction of a 1:1:8 mixture of 0.60mg of Lewis X conjugate, 0.68mg of Tetramann conjugate and 1.36mg of GlcC5S with HAuCl_4 and NaBH_4 gave 0.520mg of Tetra/Lewis X-GNPs as a dark-brown powder. TEM (average diameter): 1.8 ± 0.3 nm. Quantitative ^1H NMR: 0.52mg of Tetra/Lewis X-GNPs were dissolved in 700 μL of 0.75% TSP in D_2O and 0.08 μmoles of Lewis X and 0.07 μmoles were founded. NMR (500 MHz, D_2O /internal standard TSP) only significant peaks are reported: $\delta = 5.38$ (s, from Tetramann anomeric proton), 5.32 (s, from Tetramann anomeric proton), 5.12 (s), 5.07 (s), 4.59 (s, from Lewis X anomeric proton), 4.48 (s, from glucose anomeric proton), 2.05 (s, NAC of Lewis X conjugate), 1.20 (bs, fucose $-\text{CH}_3$ of Lewis X conjugate); ratio between Lewis X, Tetramann and Glucose signals $\sim 1:0.7:10$. These results are in agreement with the estimation of 10% of Lewis X and 10% of Tetramann on the GNPs. Molar ratio of conjugates per nanoparticle was also determined by analyzing the mixtures using NMR before and after nanoparticle formation. Estimated average molecular weight for $(\text{C}_{46}\text{H}_{85}\text{N}_2\text{O}_{25}\text{S}_2)_7(\text{C}_{42}\text{H}_{78}\text{N}_3\text{O}_{19}\text{S}_2)_7(\text{C}_{11}\text{H}_{21}\text{O}_6\text{S})_{52}\text{Au}_{116}$: ~ 49 kDa. IR (KBr): $\nu = \sim 3600\text{--}3100$ (br), 2906, 2845, 1638, 1094. UV/Vis (H_2O , 0.1 mg/mL): surface plasmon band not observed.

Human monocyte-derived dendritic cells

Monocytes were isolated from the blood of healthy donors (Sanquin, The Netherlands) through a sequential Ficoll/Percoll gradient centrifugation. Isolated monocytes (purity, > 85 %) were cultured in RPMI 1640 (Invitrogen, USA) supplemented with 10% FCS (BioWhittaker, USA), 1,000 U/ml penicillin (BioWhittaker, USA), 1,000 U/ml streptomycin (BioWhittaker, USA), and 2 mM glutamine (BioWhittaker, USA) in the presence of interleukin-4 (IL-4) (500 U/ml; BioSource, Belgium) and granulocyte-macrophage colony-stimulating factor (GM-CSF) (800 U/ml; BioSource, Belgium) for 7 days. ³²DC differentiation was confirmed by flow cytometric analysis (FACScan, BD biosciences, USA) of the expression of DC-SIGN using the monoclonal antibody AZN-D1³³ followed by staining with a secondary FITC-labeled anti-mouse antibody (Zymed, San Francisco, CA).

Cytokine ELISA

For the detection of cytokines, culture supernatants were harvested 24 h after DC stimulation and frozen at -80°C until analysis. Cytokines were measured by ELISA using antibody pairs from eBioscience (The Netherlands) and according to manufacturer's protocols.

T cell polarization assay

To determine T cell polarization, 5×10^3 48 h-pulsed DCs were co-cultured with 2×10^4 naive T cells that were purified using a human CD4+CD45RO- column kit (R&D Systems) in the presence of 10 pg/ml staphylococcal enterotoxin B (Sigma-Aldrich) in 96-well flat-bottom plates (Corning). On day 5, 10 U/ml of IL-2 (R&D Systems) was added, and the cultures were expanded for another 7 days. For intracellular cytokine production, the primed CD4+ T cells were restimulated with 50 ng/ml PMA plus 2 µg/ml ionomycin for 6 h. 10 µg/ml brefeldin A was added during the last 2 h (all Sigma-Aldrich). The cells were stained with a combination of PE-labeled anti-IL-4 and FITC-labeled anti-IFN γ antibodies.

TReg/anergy induction assays

Briefly, 10^6 untouched CD4⁺CD45⁺ T cells purified using a kit from Invitrogen (The Netherlands), were cultured with allogeneic 10^5 stimulated DC in 24-well plates in IMDM medium supplemented with 10 % human AB serum (HS; PAA laboratories) for 6 days. Primed T cells were recovered, washed and allowed to rest for three days in the presence of IL-7 (10 ng/ml) and IL-15 (5 ng/ml). On day 9 after primary stimulation, primed T cells were washed and restimulated by co-culturing 10^5 T cells with LPS-activated moDC from the original donor at different ratios in 96-well plates. After 6 days plates were pulsed with [3H]-thymidine (0,5 µCi/well, Amersham Biosciences). After an additional 18 h of incubation, [3H]-thymidine incorporation was measured on a Wallac-LKB Betaplate 1205 (LKB) liquid scintillation counter.

³² Sallusto F., Lanzavecchia A., Efficient presentation of soluble antigen by cultured human dendritic cells is maintained by granulocyte/macrophage colony-stimulating factor plus interleukin 4 and downregulated by tumor necrosis factor alpha, *J. Exp. Med.* 1994, 179, 1109-1118.

³³ Geijtenbeek T. B, Torensma R., van Vliet S. J., van Duijnhoven G. C., Adema G. J., van Kooyk Y., Figdor C. G., Identification of DC-SIGN, a novel dendritic cell-specific ICAM-3 receptor that supports primary immune responses, *Cell* 2000, 100, 575-585.

Appendix

1. Design, Preparation and Characterization of Gold Glyco Nanoparticles

There are essentially two strategies for the preparation of gold glyconanoparticles: direct gold(III) salt reduction in the presence of thiol-ending ligands in aqueous solution and ligand-exchange on pre-formed gold nanoclusters (Fig. 1).¹

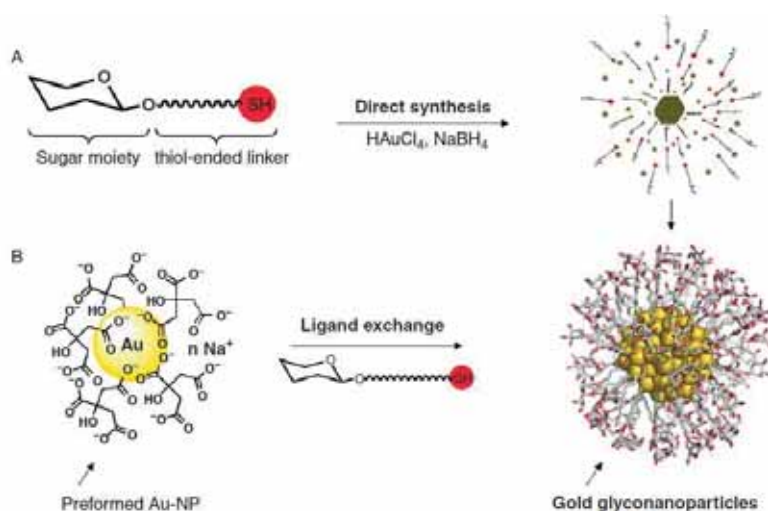


Figure 1: Main methods for the preparation of gold GNPs. **A)** Direct synthesis based on the reduction of a Au(III) salt and in situ protection of the nascent gold nanocluster with thiol-armed glycoconjugates. **B)** Ligand exchange reactions based on the treatment of preformed gold nanoparticles with thiol-derivatized glycoconjugates.

GNPs were prepared by direct synthesis using a modified protocol of the Brust-Schiffrin method.² Preparation of GNPs requires conjugation of the glycans to a spacer ending in a thiol (mercapto) group. To prepare the neoglycoconjugates diverse types of spacers have been used with hydrophobic and/or hydrophilic nature: aliphatic chains (five carbon atoms) to provide rigidity to

¹ Marradi M., Martín-Lomas M., Penadés S., Glyconanoparticles polyvalent tools to study carbohydrate-based interactions, *Adv. Carbohydr. Chem. Biochem.* 2010, 64, 211-290.

² Brust M., Fink J., Bethell D., Schiffrin D. J., Kiely C., Synthesis and reactions of functionalized gold nanoparticles, *J. Chem. Soc. Chem. Commun.* 1995, 1655–1656.

the ligands on the GNP or an amphiphilic mixed aliphatic/tetraethyleneglycol linker to provide flexibility to the glycans on the GNPs. GNPs coated with variable density of glycans (10%, 50% and 100%) were prepared to assess the effect of presentation on the cluster in their interactions. The glycan density on the gold surface can be controlled by incorporating a second thiol-ending ligand on the surface. Glucose conjugate (GlcC₅S) was selected as inner component to control the density of more complex glycans on the GNPs.

General preparation of GNPs

(Partially published in the attached publication Di Gianvincenzo P. et al. 2012)³

The first step for the direct GNPs formation was the preparation of a solution of the thiol-ending neoglycoconjugates that has to be linked to the gold surface. ¹H NMR spectrum of the neoglycoconjugates mixture were registered to confirm the ligands ratio. Methanol and water were used as solvents for the direct GNPs preparation. Usually, pear-shaped flasks were used. However, 2.5 mL eppendorfs were preferably used for thiol-ending ligand concentration below 10 μmol.

As a typical GNPs preparation, the protocol for Te-50 GNP having a 1:1 ratio of tetramannoside conjugate (Te or Man₄) and glucose conjugate was carried out as follows: To a methanolic solution of thiol-ending glycoconjugates in the desired ratio (total concentration 0.012M; 3 eq), HAuCl₄ (0.025M in H₂O; 1 eq) was added. A freshly prepared water solution of NaBH₄ (1M; 21 eq) was added in 4 times to the mixture under gentle shaking. It is convenient to perform some holes in the top of the reaction vessel, to avoid overpressure caused by the exothermic reaction of NaBH₄ with H₂O that produces H₂. Mixture was left 2 h under shaking at room temperature and, after centrifugation (5 min, 10000 rpm), the dark solid washed 4-5 times with methanol (or ethanol). Supernatants containing unreacted ligands were collected and purified on Sephadex LH-20 (MeOH/H₂O 9/1 as eluent). GNPs were dissolved in the minimum volume of NANOPURE water (18.2 MΩ-cm obtained by a Thermo Scientific Barnstead NANOpure Diamond Water System), and purified by dialysis. Briefly, GNPs solution was loaded into 5-10 cm segments of SnakeSkin pleated dialysis tubing (Pierce, 3500 MWCO) and placed in a 3 L beaker full of H₂O under gentle stirring. Water was changed 7-8 times in 72h; afterwards the solution was freeze-dried. The dry dark solid

³ Di Gianvincenzo P., Chiodo F., Marradi M., Penadés S., Gold manno-glyconanoparticles for intervening in HIV gp120 carbohydrate-mediated processes, *Methods Enzymol.* 2012, 509, 21-40.

can be stored under Argon, in a dark dry place 5°C. It is better to avoid the use of gloves handling the dry solid GNPs (weight them with a Teflon spatula) because of electrostatic charges.

General characterization of GNPs

The gold core of GNPs was characterized by UV/Vis, transmission electron microscopy (TEM). The organic ligands were determined by $^1\text{H-NMR}$ and elemental analysis as previously reported^{4,5}. The UV/Vis spectra gave an indication of the GNPs dimensions: small GNPs, with a diameter below 2 nm, do not show the plasmon absorption band at 520 nm at 0.1 mg/mL in water. (Fig. 2)

UV/Vis spectra were registered in a Beckman Coulter DU 800 spectrophotometer. IR on KBr pellet is a qualitative technique that helps especially when small amounts of ligands are attached on the gold surface. A GNPs spatula tip is enough to run IR spectra. Infrared spectra (IR) were recorded from 4000 to 400 cm^{-1} with a Nicolet 6700 FT-IR spectrometer (Thermo Spectra-Tech).

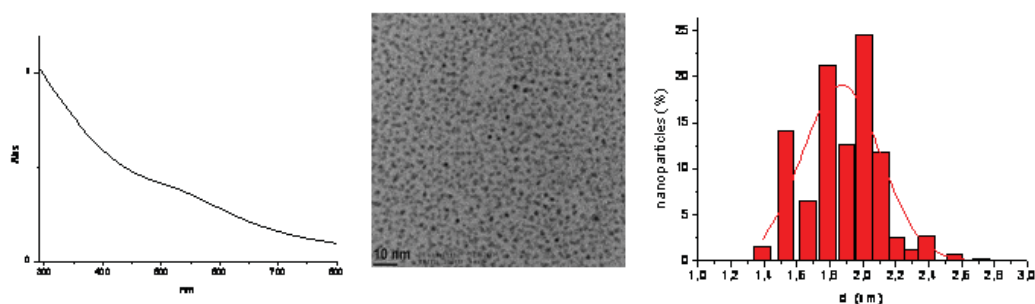


Figure 2: Characterization of *manno*-GNPs : UV/Vis spectrum; TEM micrograph in H_2O ; size-distribution histogram of Te-50.

⁴ Barrientos A. G., de la Fuente J.M., Rojas T. C., Fernández A., Penadés S., Gold glyconanoparticles: synthetic polyvalent ligands mimicking glycocalyx-like surfaces as tools for glycobiological studies, *Chem. Eur. J.* 2003, 9, 1909-1921.

⁵ Carvalho de Souza A., Halkes K. M, Meeldijk J. D, A. J. Verkleij, Vliegenthart J. F. G., Kamerling J. P., Synthesis of gold glyconanoparticles: Possible probes for the exploration of carbohydrate-mediated self-recognition of marine sponge cells, *Eur. J. Org. Chem.* 2004, 4323–4339.

In order to determine the diameter of the gold nucleus, TEM analyses were performed. A drop of a GNPs solution (10 μ L; 0.1 mg/mL in milliQ water) was placed onto a copper grid coated with a carbon film (Electron Microscopy Sciences) and left drying on air over night at room temperature. TEM analyses were carried out in a Philips JEOL JEM-2100F microscope working at 200 kV. Statistical determination of gold dimension was performed over 200 GNPs using ImageJ program (Java-based image processing program developed at the National Institutes of Health, NIH). The diameter of the gold core can be correlated to the number of ligands present on the GNP.⁶ The total amount of organic ligands was determined by elemental analysis when the sample amount was enough or estimated by analogy. The ratio of different neoglycoconjugates on the same GNP can be deduced from ¹H NMR spectrum. ¹H NMR of the mixture of unreacted ligands after purification compared to ¹H NMR of reactants before the reaction gave a good qualitative indication about the ratio of different neoglycoconjugates on the GNPs. In the case of *manno*-GNPs the ratio between mannose and glucose ligands in the GNPs was deduced by comparing integration of the mannoside anomeric protons signals with respect to those of glucoside, as shown in figure 3.

⁶ Hostetler M. J., Templeton A. C., Murray R. W., Dynamics of place-exchange reactions on monolayer-protected gold cluster molecules, *Langmuir* 1999, 15, 3782–3789.

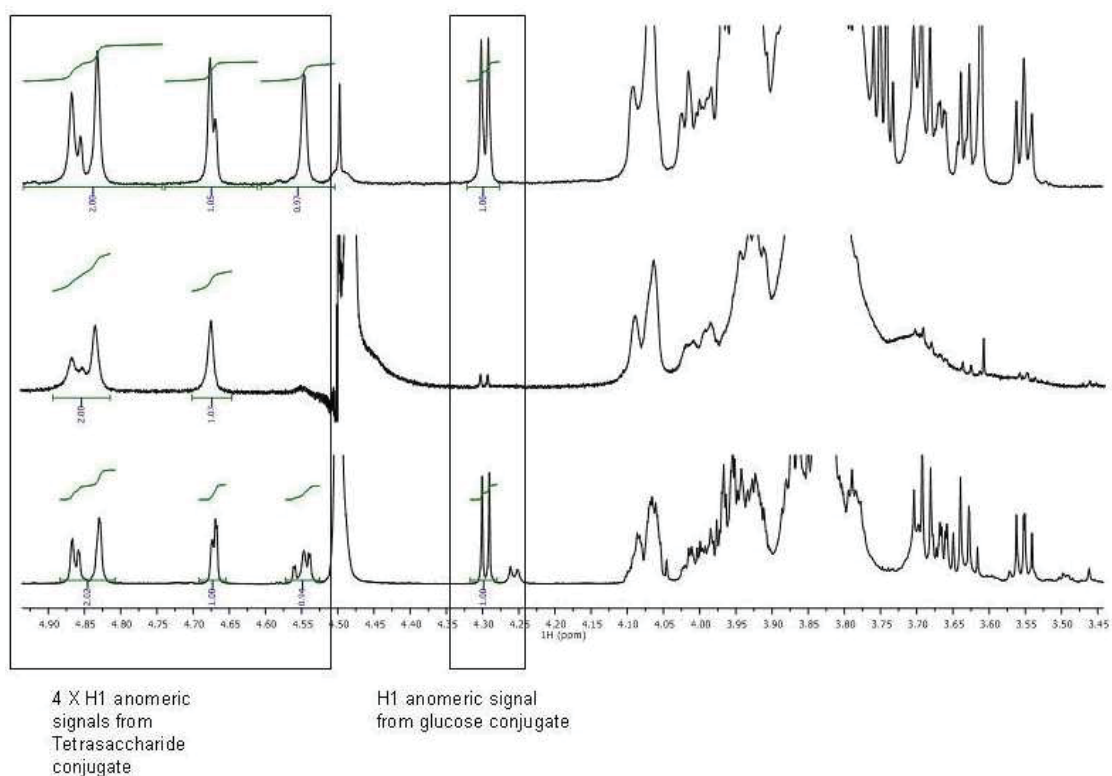


Figure 3: $^1\text{H-NMR}$ of neoglycoconjugates ratio before and after GNPs preparation. *Top panel:* $^1\text{H-NMR}$ (500 MHz, CD_3OD) of the mixture of tetrasaccharide Te/glucose conjugates used to prepare GNP. Integration of selected signals shows that the ratio between tetrasaccharide and glucose conjugate is about 1:1. *Middle panel:* $^1\text{H-NMR}$ (500 MHz, D_2O , water suppression) of Te-50 GNP. The selected signals show the presence of the two components in the same nanoparticle. *Bottom panel:* $^1\text{H-NMR}$ (500 MHz, CD_3OD) of the mixture used to prepare GNP after GNPs preparation. Integration of selected signals shows that the ratio between tetrasaccharide and glucose conjugates is 1:1.

By combining together TEM, elemental analysis and $^1\text{H-NMR}$ data it was possible to calculate an average molecular formula for each *manno*-GNP. As an example, we show the characterization steps of Te-10 GNP. From TEM micrographs the diameter found was 1.4 ± 0.7 nm which corresponds to a gold nanocluster of 116 gold atoms which theoretically can arrange around 53 ligands.⁶ From NMR the ligands ratio of tetrasaccharide and glucose (before and after GNPs preparation) was 1:9. From these data the calculated molecular formula was $(\text{C}_{46}\text{H}_{85}\text{N}_2\text{O}_{25}\text{S}_2)_7(\text{C}_{11}\text{H}_{21}\text{O}_6\text{S})_{59}\text{Au}_{116}$, which correspond to an average molecular weight of 47KDa and a calculated elemental composition of C 24.63%, H 3.90%, N 0.41%, S 4.94%. The elemental analysis obtained for the Te-10 GNP was: C 24.40%, H 4.36%, N 0.77%, S 4.53% that fitted well with the calculated one. From the obtained molecular formula, an average yield can be calculated.

The yield of GNPs reaction calculated based on “active” gold atoms (6.8 μmol of surface gold atoms) is around 35%. The yield based on consumed neoglycoconjugate is 11 %, but the no-reacted glycoconjugates can be recovered.

Quantitative NMR (qNMR) on GNPs

D₂O containing 0.75% (w/w) of Trimethylsilyl propionate (TSP) can also be used as a solvent/internal standard to perform a quantitative NMR (qNMR) on the intact nanoparticles.⁷ The signals of the molecules attached to the nanoparticle can be integrated and compare with internal standard. This non destructive approach is very useful to know the moles of ligands per mg of GNP. It works very well with long linker-attached molecules. The TSP can be removed by dialysis after the qNMR quantification.

⁷ Polito L., Colombo M., Monti D., Melato S., Caneva E., Prospero D., Resolving the structure of ligands bound to the surface of superparamagnetic iron oxide nanoparticles by high-resolution magic-angle spinning NMR spectroscopy, J. Am. Chem. Soc. 2008, 130, 12712-12724.

2. Synthesis of Oligomannosides

The Man α 1-2Man containing oligosaccharides have been prepared, with a minimal number of building block, following the Wong's one-pot self-condensation synthesis (Fig. 4)⁸.

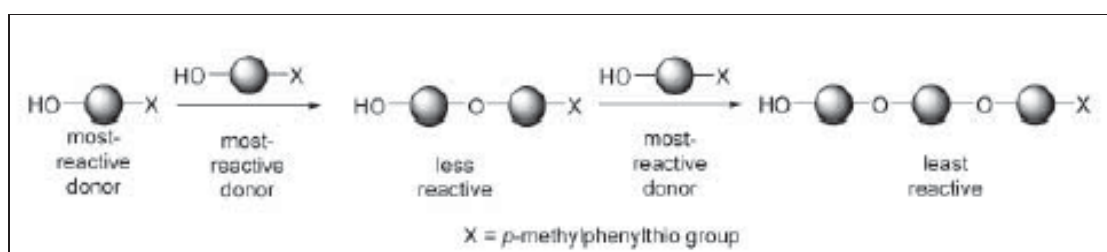


Figure 4: The programmable reactivity-based one-pot method for oligosaccharide synthesis⁹ has been successfully applied to the synthesis of several biologically significant oligosaccharides (which include Globo H¹⁰ Lewis Y¹¹ and fucosyl-GM1¹²), before been applied to the synthesis of Man α 1-2Man containing oligosaccharides.

⁸ Lee H. K., Scanlan C. N., Huang C. Y., Chang A. Y., Calarese D. A., Dwek R. A., Rudd P. M., Burton D. R., Wilson I. A., Wong C. H., Reactivity-based one-pot synthesis of oligomannoses: defining antigens recognized by 2G12, a broadly neutralizing anti-HIV-1 antibody, *Angew. Chem. Int. Ed.* 2004, 43, 1000-1003.

⁹ Wu C. Y., Wong C. H., Programmable one-pot glycosylation, *Top. Curr. Chem.* 2011, 301, 223-252.

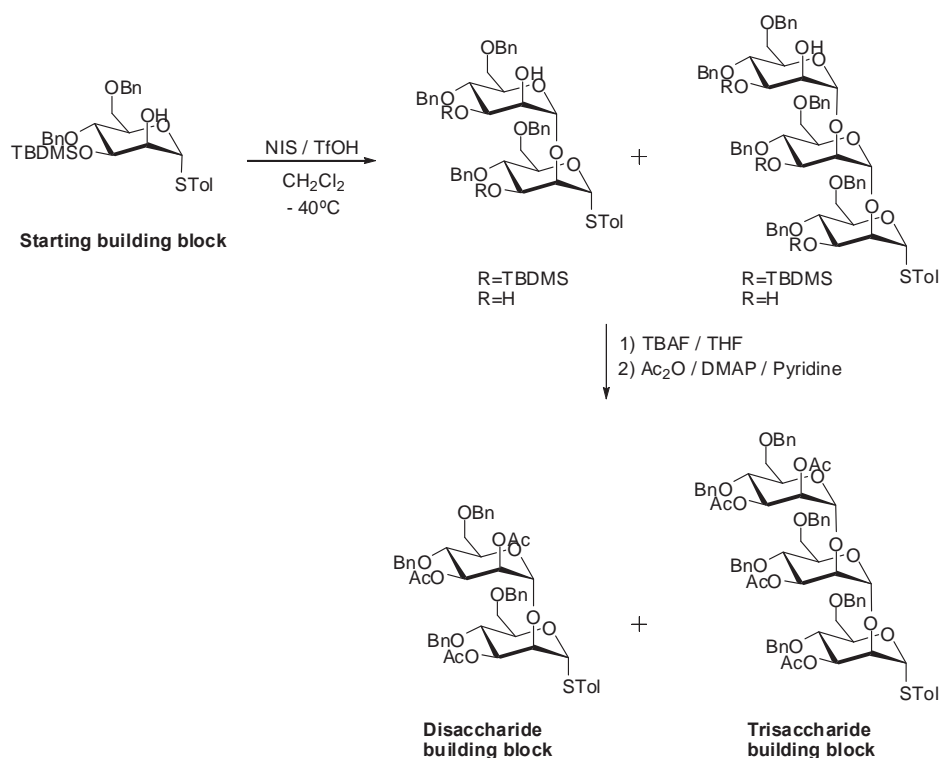
¹⁰ Burkhardt F., Zhang Z. Y., Wacowich-Sgarbi S., Wong C. H., Synthesis of the Globo H Hexasaccharide Using the Programmable Reactivity-Based One-Pot Strategy, *Angew. Chem.* 2001, 113, 1314-1317.

¹¹ Mong K. K. T., Wong C. H., Reactivity-Based One-Pot Synthesis of a Lewis Y Carbohydrate Hapten: A Colon-Rectal Cancer Antigen Determinant, *Angew. Chem.* 2002, 114, 4261-4264.

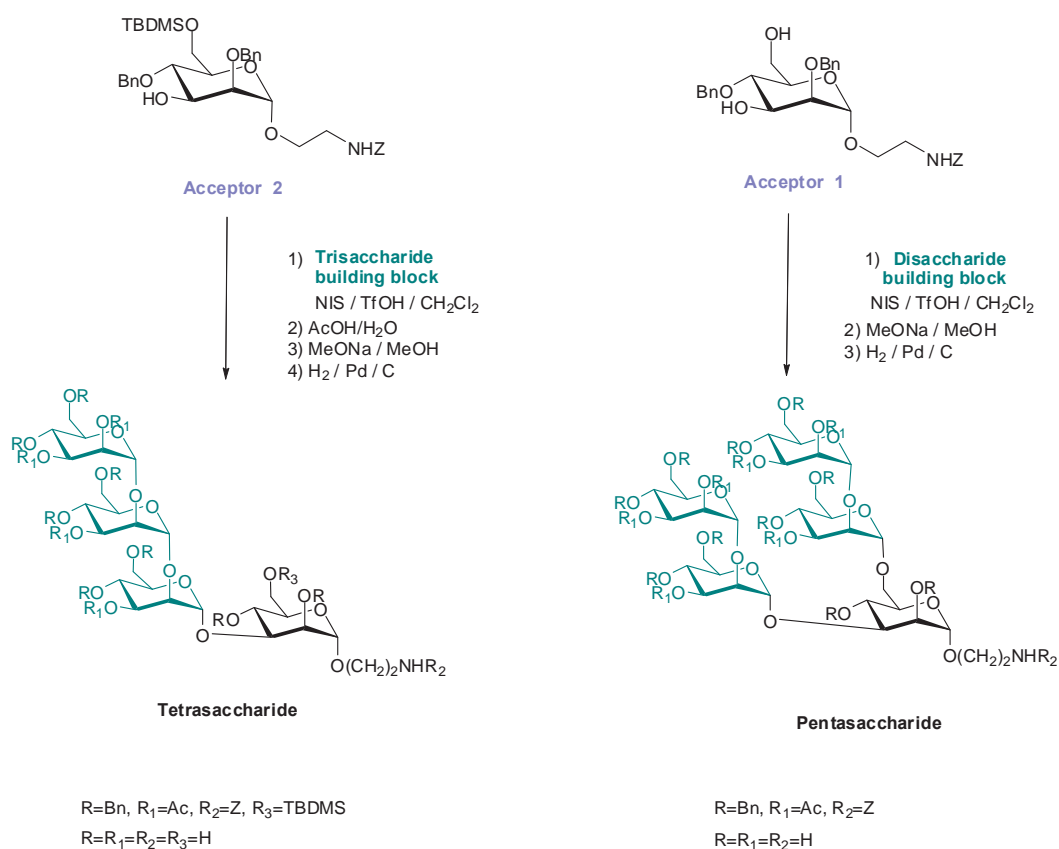
¹² Mong K. K. T., Lee H. K., DurKn S. G., Wong C. H., Reactivity-based one-pot total synthesis of fucose GM1 oligosaccharide: a sialylated antigenic epitope of small-cell lung cancer, *Proc. Natl. Acad. Sci. USA* 2003, 100, 797-802.

One pot self condensation

The most reactive monomer (**starting building block**) undergoes self-condensation to give a less-reactive dimer. The dimer then serves as an acceptor for another monomer molecule, which leads to formation of the trimer. The reaction temperature is a key parameter for the degree of self-condensation. At -50°C , dimer is formed almost exclusively (70%); whereas at -40°C , a mixture of dimer (38%) and trimer (30%) can be obtained one-pot (scheme 1). Subsequent removal of the TBDMS group and acetylation gave **disaccharide building block** and **trisaccharide building block** (scheme 1). They were coupled to **acceptor 1** and **acceptor 2** to obtain aminoethyl pentamannoside and tetramannoside after complete deprotection (scheme 2).



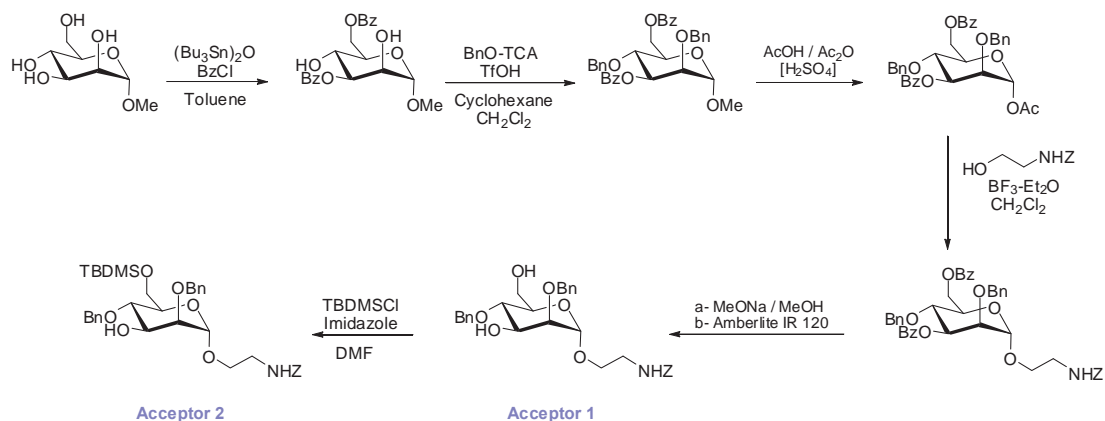
Scheme 1



Scheme 2

Synthesis of acceptors

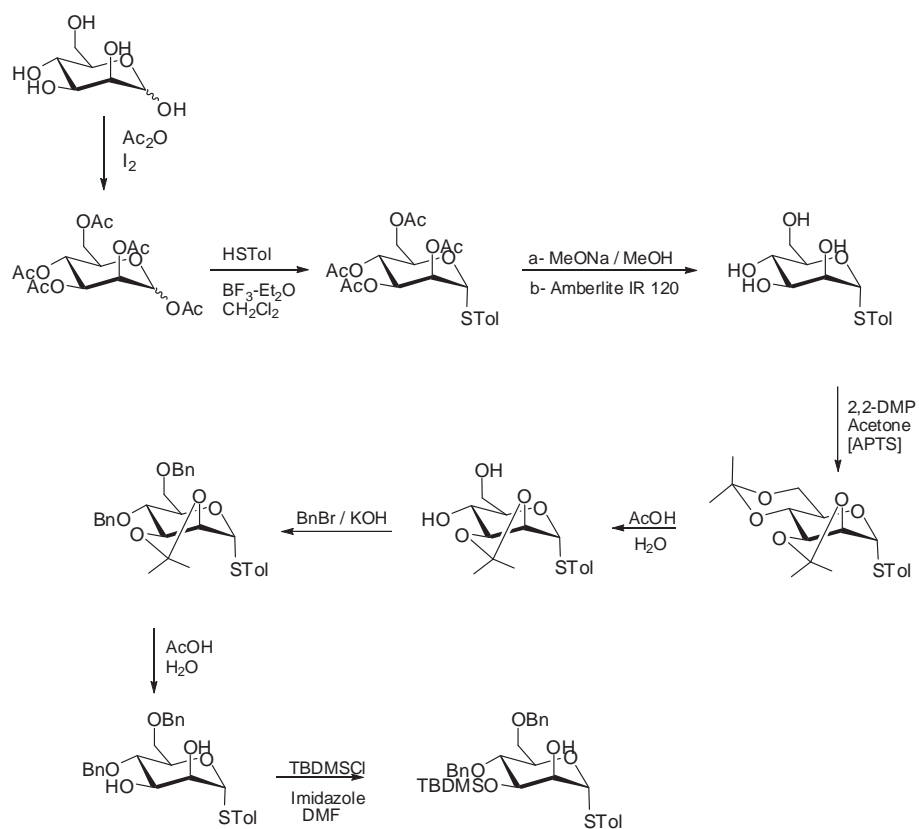
From the commercial peracetylated mannose, the 1-O-methyl-3,6-di-O-**benzoyl**-2,4-di-O-**benzyl**- α -D-mannopyranoside was prepared in 2 steps (overall yield 40%). After anomeric O-acetylation, the protected mannoside derivative was glycosylated in presence of 2-benzoyloxycarbonylaminoethanol and the following selective deprotection strategy lead to the 2,4-selectively protected mannoside (**acceptor 1**). Subsequent protection of 6-OH with TBDMSCI led to **acceptor 2**. (scheme 3)



Scheme 3

Synthesis of starting building block for Wong's one pot self-condensation

The **starting building block** has been prepared in 8 steps (scheme 4), following the same synthetic route as the one described by Wong. The mannose *p*-methoxythioglycoside was obtained in 3 steps (acetylation, glycosidation and deacetylation) from commercial mannose. 2,3:4,6-Di-*O*-isopropylidene was synthesised in standard conditions and then the 4,6-isopropylidene protecting group was selectively opened to yield the 2,3-isopropylidene-protected mannoside with a 40% overall yield in the 4 last steps. This compound was benzylated at position 4 and 6 to yield 90% of the fully protected mannose derivative. The desired **starting building block** was finally obtained after removal of the 2,3-isopropylidene group and subsequent selective silylation at position 3 with a 70% overall yield on the 2 steps.



Starting building block

Scheme 4

GOLD MANNO-GLYCONANOPARTICLES FOR INTERVENING IN HIV GP120 CARBOHYDRATE-MEDIATED PROCESSES

Paolo Di Gianvincenzo,^{*} Fabrizio Chiodo,^{*} Marco Marradi,^{*,†} and Soledad Penadés^{*,†}

Contents

1. Introduction	22
2. Design, Preparation, and Characterization of <i>manno</i> -GNPs	23
2.1. Preparation of <i>manno</i> -GNPs	25
2.2. Characterization of <i>manno</i> -GNPs	25
3. Evaluation of <i>manno</i> -GNPs as Inhibitors of Carbohydrate-Mediated gp120 Interactions	28
3.1. Binding study of <i>manno</i> -GNPs to 2G12 by SPR	28
3.2. Study of the 2G12/GNP interaction by STD-NMR	30
4. Validation of <i>manno</i> -GNPs as Inhibitors of HIV-1/Cell Infection	33
4.1. Effect of <i>manno</i> -GNPs on HIV-1 neutralization by 2G12 in cellular models	33
4.2. Inhibition of DC-SIGN-mediated HIV-1 trans-infection of human T cells by <i>manno</i> -GNPs	35
Acknowledgments	37
References	37

Abstract

After nearly three decades since the discovery of human immunodeficiency virus (HIV) (1983), no effective vaccine or microbicide is available, and the virus continues to infect millions of people worldwide each year. HIV antiretroviral drugs reduce the death rate and improve the quality of life in infected patients, but they are not able to completely remove HIV from the body. The glycoprotein gp120, part of the envelope glycoprotein (Env) of HIV, is responsible for virus entry and infection of host cells. High-mannose type glycans that decorate gp120

^{*} Laboratory of GlycoNanotechnology, Biofunctional Nanomaterials Unit, CIC biomaGUNE, San Sebastián, Spain

[†] Biomedical Research Networking Center in Bioengineering, Biomaterials and Nanomedicine (CIBER-BBN), San Sebastián, Spain

are involved in different carbohydrate-mediated HIV binding. We have demonstrated that oligomannoside-coated gold nanoparticles (*manno*-GNPs) are able to interfere with HIV high-mannose glycan-mediated processes. In this chapter, we describe the methods for the preparation and characterization of *manno*-GNPs and the experiments performed by means of SPR and STD-NMR techniques to evaluate the ability of *manno*-GNPs to inhibit 2G12 antibody binding to gp120. The antibody 2G12-mediated HIV neutralization and the lectin DC-SIGN-mediated HIV trans-infection in cellular systems are also described.

1. INTRODUCTION

In the fight against the transmission of the human immunodeficiency virus (HIV), strategies are being developed to prevent (vaccines and microbicides) or to eliminate infection (antiretrovirals, therapeutic vaccines). None of these strategies have yet eradicated HIV infection or prevented transmission. A renewed effort is needed to understand the molecular basis of the complex mechanism of virus infection. The recent development of biofunctional nanoparticles and their applications in biomedicine has opened new opportunities to address this problem.

A remarkable feature of HIV is the dense carbohydrate coating of the envelope glycoprotein gp120 (Allan *et al.*, 1985; Barin *et al.*, 1985). This protein is heavily glycosylated with *N*-linked high-mannose type glycans (Feizi and Larkin, 1990; Geyer *et al.*, 1988; Mizuochi *et al.*, 1988). The glycans account for about 50% of the mass of this viral protein, the densest array of carbohydrates observed among human glycoproteins. The carbohydrate coating promotes HIV infection by its interaction with the dendritic cell-specific ICAM 3-grabing nonintegrin (DC-SIGN) expressed in dendritic cells (DCs). The C-type lectin DC-SIGN plays a crucial role in the entry and dissemination of HIV-1 from the mucosal site to T-cell areas in lymphoid tissues (Engering *et al.*, 2002; Fenouillet *et al.*, 1994; Geijtenbeek *et al.*, 2000). The glycan coat also protects the virus from potential immunogenic response. In spite of this role, the broadly neutralizing human antibody 2G12 that binds oligomannoside clusters of gp120 with nanomolar affinity was isolated from infected patients (Sanders *et al.*, 2002; Scanlan *et al.*, 2002; Trkola *et al.*, 1996). The crystal structure of the Fab fragment of 2G12 with oligosaccharide Man₉GlcNAc₂ and disaccharide Man α 1-2Man was determined (Calarese *et al.*, 2003). The X-ray structure, supported by electron microscopic data, showed that the 2G12 Fab arms are locked together through the variable heavy domain, forming a previously uncharacterized dimer interface region for multivalent interaction with oligomannosides on gp120.

The multivalent presentation of the high-mannose glycans on the gp120 is fundamental for establishing both gp120/DC-SIGN binding and gp120/2G12

interactions. Mimicking the cluster presentation of gp120 high-mannose oligosaccharides is a strategy for designing carbohydrate-based antiviral agents and vaccines. Many different scaffolds were used to multimerize mannose oligosaccharides: Cholic acid (Li and Wang, 2004), galactose (Wang *et al.*, 2004), peptides (Dudkin *et al.*, 2004; Krauss *et al.*, 2007; Wang *et al.*, 2007), dendrons (Kabanova *et al.*, 2010; Wang *et al.*, 2008), and icosahedral virus capsids (Astronomo *et al.*, 2010). Our laboratory has developed a methodology based on gold nanoclusters as a scaffold to present carbohydrates in a multivalent display (glyconanoparticles) (de la Fuente *et al.*, 2001). The carbohydrate ligands are linked to the metallic nucleus by a stable Au—S bond. The carbohydrate molecules confer water solubility and biological functionality to the inorganic core of the nanomaterial. The nanometric size (1–3 nm) of these biofunctional materials is in the same order of magnitude of biological macromolecules such as proteins and nucleic acids, and allows the study, at the molecular level, of biorecognition processes where carbohydrates are involved (de la Fuente and Penadés, 2006; García *et al.*, 2010).

To interfere with gp120 carbohydrate-mediated processes, gold glyconanoparticles presenting different structural motifs of the *N*-linked high-mannose glycans of gp120 (oligomannoside-coated gold nanoparticle, *manno*-GNP) were designed and prepared (Fig. 2.1; Martínez-Ávila *et al.*, 2009a). The *manno*-GNPs were designed to mimic the carbohydrate cluster of gp120. The calcium-dependent lectin DC-SIGN and the antibody 2G12 that bind gp120 through mannose oligosaccharides were chosen as molecular targets to study the efficacy of *manno*-GNPs. We found that oligomannoside-functionalized gold glyconanoparticles are able to inhibit the HIV-1 DC-SIGN-mediated trans-infection of T cells at nanomolar concentrations (Martínez-Ávila *et al.*, 2009b), which validates *manno*-GNPs as an antiadhesive barrier at an early stage of HIV-1 infection.

In this chapter, we describe the design, preparation, and characterization of a set of *manno*-GNPs and methods to study their efficacy as inhibitors of gp120 binding to DC-SIGN or 2G12. We also describe their use as inhibitors of antibody 2G12-mediated HIV neutralization and DC-SIGN-mediated HIV trans-infection in a cellular system that mimics the natural route of infection of T-lymphocytes by DCs.

2. DESIGN, PREPARATION, AND CHARACTERIZATION OF MANNO-GNPs

There are essentially two strategies for the preparation of gold glyconanoparticles: direct gold salt reduction in the presence of thiol-ending ligands in aqueous solution, and ligand exchange on preformed gold nanoclusters (Marradi *et al.*, 2010).

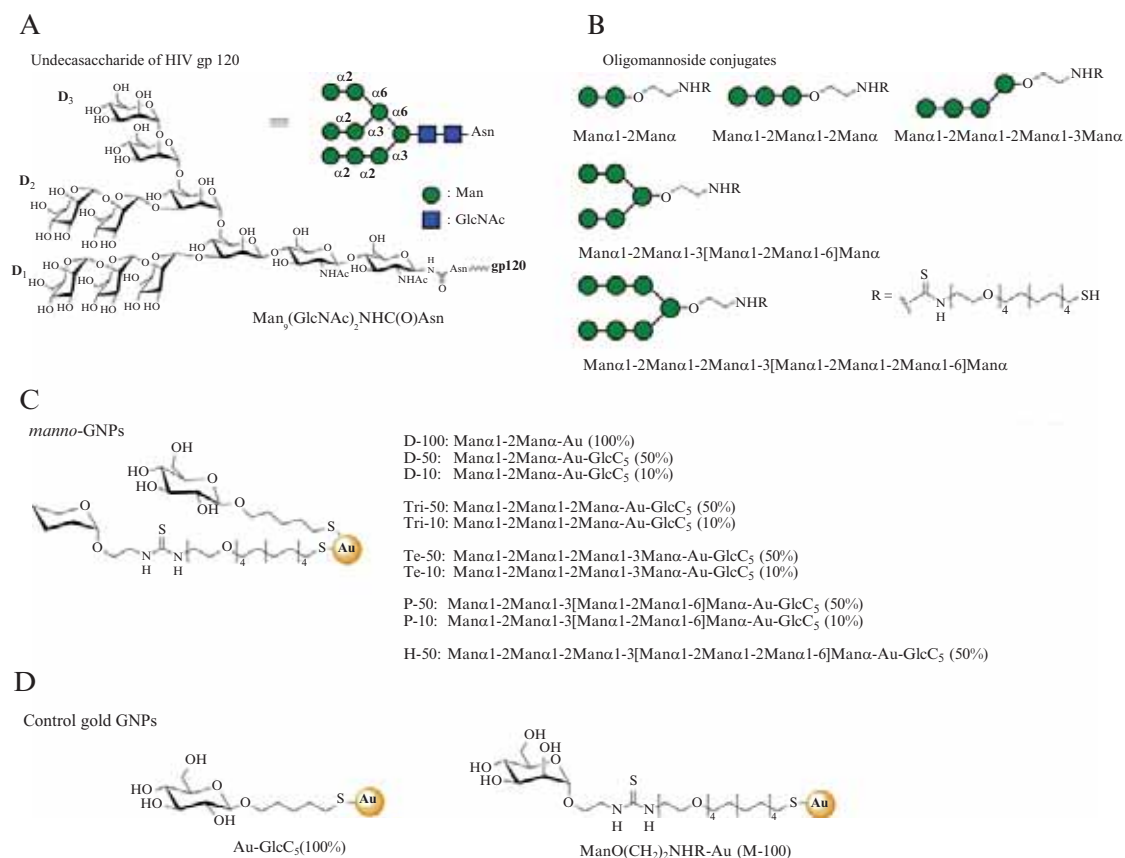


Figure 2.1 (A) gp120 N-glycan undecasaccharide; (B) thiol-ending oligomannoside conjugates used for *manno*-GNP preparation; (C) *manno*-GNPs. D, T, Te, P, and H stand for di-, tri-, tetra-, penta-, and heptamannoside conjugates, respectively; the numbers indicate the percentages of oligomannosides on GNP, the rest being the 5-(mercapto)pentyl β -D-glucopyranoside (GlcC₅) component; (D) control GNPs bearing glucose and mannose conjugates.

manno-GNPs are prepared by direct synthesis (Martinez-Ávila *et al.*, 2009a) using a modified protocol of the Brust-Schiffrin method (Brust *et al.*, 1994). Preparation of *manno*-GNPs require conjugation of the oligomannosides to a spacer ending in a mercapto group. The selected oligosaccharides are structural motifs of the gp120 undecasaccharide Man₉(GlcNAc)₂, except for a heptasaccharide that results from adding two mannose residues to the pentasaccharide (Fig. 2.1). To prepare the glycoconjugates, diverse types of spacers have been used with a hydrophobic and/or hydrophilic nature: aliphatic chains (five carbon atoms) to provide rigidity to the sugars on GNP or an amphiphilic mixed aliphatic/polyethyleneglycol linker to provide flexibility and solubility to the nanoparticle. The detailed protocols for the synthesis of the thiol-ending glycoconjugates have been described (Martinez-Ávila *et al.*, 2009a). *manno*-GNPs coated with variable density of oligomannosides (10%, 50%, and 100%) are prepared to assess the effect of presentation on the cluster in their interactions. Gold clusters of 2 nm size can bear up to 100 units of oligomannosides (Barrientos *et al.*, 2003). The mannoside density on the gold surface can be controlled by incorporating a second thiol-ending ligand on the surface.

A glucose conjugate (GlcC₅S) is used as a stealth component to control the density of oligomannosides on the *manno*-GNPs. GNPs fully covered by glucose or mannose thiol-ending conjugate are prepared and used as GNP controls. The oligomannoside conjugates and *manno*-GNPs are shown in Fig. 2.1.

2.1. Preparation of *manno*-GNPs

The first step for the direct *manno*-GNPs formation is the preparation of a solution of the thiol-ending neoglycoconjugates that will be linked to the gold surface. The ¹H-nuclear magnetic resonance (NMR) spectrum of the neoglycoconjugates mixture is registered to confirm the ligand ratio. Methanol and water are used as solvents for the direct GNP preparation. Usually, peer-shaped flasks are used. However, 2.5 mL Eppendorf tubes are preferably used for thiol-ending ligand amount below 10 μmol.

A typical *manno*-GNP preparation with tetramannoside conjugate and glucose conjugate is carried out as follows: To a methanolic solution of thiol-ending glycoconjugates in the desired ratio (total concentration 0.012 M; 3 eq), HAuCl₄ (0.025 M in H₂O; 1 eq) is added.

A freshly prepared water solution of NaBH₄ (1 M; 21 eq) is added in four times to the mixture under gentle shaking. It is convenient to perform some holes in the top of the reaction vessel, to avoid overpressure caused by the exothermic reaction of NaBH₄ with H₂O that produces H₂. Mixture is left 2 h under shaking at room temperature and, after centrifugation (5 min, 10000 rpm), the dark solid is washed four to five times with methanol (or ethanol). Supernatants containing unreacted ligands are collected and purified on Sephadex LH-20 (MeOH/H₂O 9/1 as eluent). GNPs are dissolved in the minimum volume of NANOPURE water (18.2 MΩ-cm obtained by a Thermo Scientific Barnstead NANOpure DIamond Water System), and purified by dialysis. Briefly, the GNP solution is loaded into 5–10 cm segments of SnakeSkin pleated dialysis tubing (Pierce, 3500 MWCO) and placed in a 3-L beaker full of H₂O under gentle stirring. Water is changed seven to eight times in 72 h; afterward the solution is freeze-dried. The dry dark solid can be stored under Argon, in a dark dry place at 5 °C. It is better to avoid the use of gloves handling the dry solid GNPs (weight them with a Teflon spatula) because of electrostatic charges.

2.2. Characterization of *manno*-GNPs

The gold core of *manno*-GNPs is characterized by UV/Vis spectroscopy and, transmission electron microscopy (TEM). The organic ligands are determined by ¹H-NMR and elemental analysis as previously reported (Barrientos *et al.*, 2003; Carvalho de Souza and Kamerling, 2006). The UV/Vis spectra gave an indication of the GNPs' dimensions: small GNPs, with a diameter below 2 nm, do not show the plasmon absorption band at

520 nm at 0.1 mg mL^{-1} in water. UV/Vis spectra are registered in a Beckman Coulter DU 800 spectrophotometer. Infrared spectra (IR) on KBr pellet is a qualitative technique that helps especially when small amounts of ligands are attached on the gold surface. A GNP's spatula tip is enough to run IR spectra. IR were recorded from 4000 to 400 cm^{-1} with a Nicolet 6700 FT-IR spectrometer (Thermo Spectra-Tech).

In order to determine the diameter of the gold nucleus, TEM analysis is performed. A drop of a GNP's solution ($10 \text{ }\mu\text{L}$; 0.1 mg mL^{-1} in milliQ water) was placed onto a copper grid coated with a carbon film (Electron Microscopy Sciences) and left drying on air over night at room temperature. TEM analyses are carried out in a Philips JEOL JEM-2100F microscope working at 200 kV. Statistical determination of gold dimension is performed over 200 GNP's using ImageJ program (Java-based image processing program developed at the National Institutes of Health, NIH) (Fig. 2.2). The diameter of the gold core can be correlated to the number of ligands present on the GNP (Hostetler *et al.*, 1998). The total amount of organic ligands is determined by elemental analysis. The ratio of different neoglycoconjugates on the same GNP can be deduced from $^1\text{H-NMR}$ spectrum. $^1\text{H-NMR}$ of the mixture of unreacted ligands after purification compared to $^1\text{H-NMR}$ of reactants before the reaction gave a good qualitative indication about the ratio of different neoglycoconjugates on the GNP's. In the case of *manno*-GNP's the ratio between mannose and glucose ligands in the GNP's is deduced by comparing integration of the mannoside anomeric protons signals with respect to those of glucoside, as shown in Fig. 2.3.

By combining together TEM, elemental analysis and $^1\text{H-NMR}$ data, it is possible to calculate an average molecular formula for each *manno*-GNP. As an example, we show the characterization steps of Te-10 GNP. From TEM micrographs the diameter found is $1.4 \pm 0.7 \text{ nm}$ that corresponds to a gold nanocluster of 116 gold atoms which theoretically can arrange around 53 ligands (Hostetler *et al.*, 1998). From NMR, the ligands ratio of tetrasaccharide and glucose (before and after the preparation of GNP's) is 1:9. From these data,

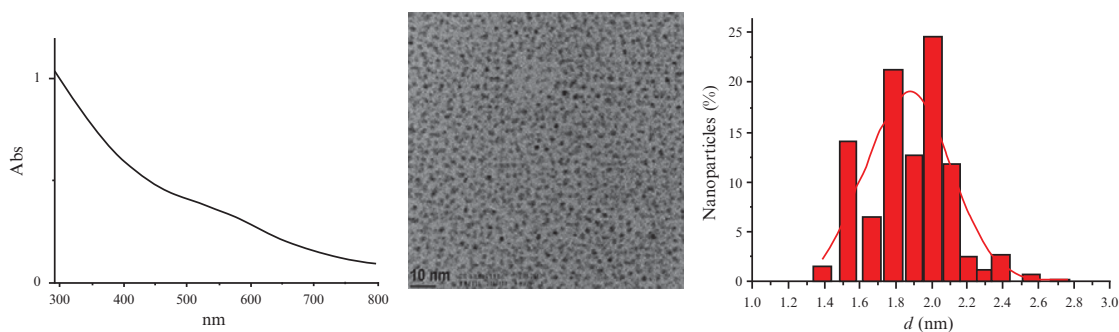


Figure 2.2 Characterization of *manno*-glyconanoparticles: UV/Vis spectrum, TEM micrograph in H_2O , and size-distribution histogram of Te-50.

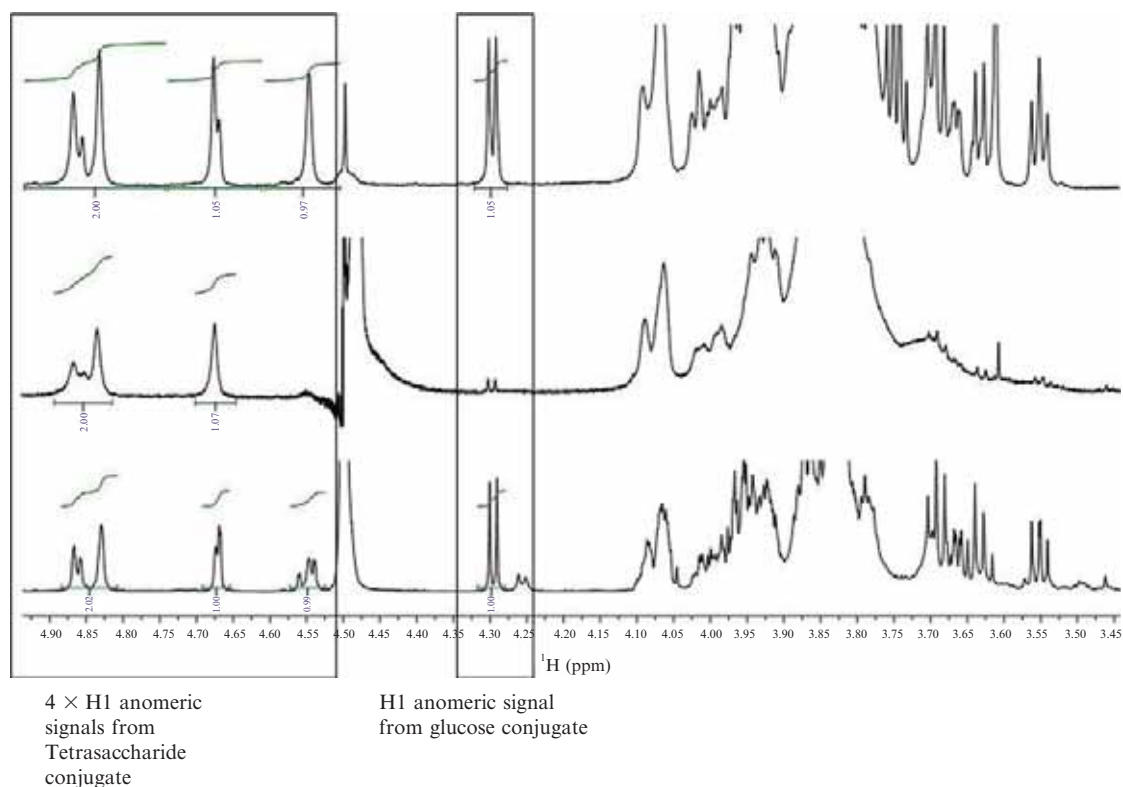


Figure 2.3 ^1H -NMR of neoglycoconjugates ratio before and after GNP preparation. *Top panel:* ^1H -NMR (500 MHz, CD_3OD) of the mixture of tetrasaccharide/glucose conjugates used to prepare GNP. Integration of selected signals show that the ratio between tetrasaccharide and glucose conjugate is about 1:1. *Middle panel:* ^1H -NMR (500 MHz, D_2O , water suppression) of Te-50 GNP. The selected signals show the presence of the two components in the same nanoparticle. *Bottom panel:* ^1H -NMR (500 MHz, CD_3OD) of the mixture used to prepare GNP after GNPs preparation. Integration of selected signals show that the ratio between tetrasaccharide and glucose conjugates is 1:1.

the calculated molecular formula was $(\text{C}_{46}\text{H}_{85}\text{N}_2\text{O}_{25}\text{S}_2)_7(\text{C}_{11}\text{H}_{21}\text{O}_6\text{S})_{59}\text{Au}_{116}$, which correspond to an average molecular weight of 47 KDa and a calculated elemental composition of C 24.63%, H 3.90%, N 0.41%, and S 4.94%. The elemental analysis obtained for the Te-10 GNP was: C 24.40%, H 4.36%, N 0.77%, and S 4.53% that fitted well with the calculated one. From the obtained molecular formula, an average yield can be calculated. The yield of GNPs reaction calculated based on “active” gold atoms (surface gold atoms) is around 35%. The yield based on consumed neoglycoconjugate is 11%, but the unreacted glycoconjugates can be recovered.

The use of enzymes to determine the amount of specific ligands attached to the gold surface is a destructive technique that have been used for the quantification of sialyl Lewis X attached to iron oxide nanoparticles (van Kasteren *et al.*, 2009). However, it has been observed that degradation of lactose GNPs by β -galactosidase does not take place completely due probably to the ligand presentation on the gold surface (Barrientos *et al.*, 2009).

3. EVALUATION OF *MANNO*-GNPs AS INHIBITORS OF CARBOHYDRATE-MEDIATED GP120 INTERACTIONS

The potency of the multimerized oligomannoside as inhibitors of the gp120 binding to 2G12 is evaluated by biosensor and magnetic resonance techniques. Biosensors with surface plasmon resonance (SPR) detectors have become an established method of measuring molecular interactions (Rich and Miszka, 2000). Many SPR studies are carried out in order to understand the molecular basis of HIV viral life cycle, HIV drug discovery, and anti-HIV mAb characterization (Rich and Miszka, 2003). *manno*-GNPs were already evaluated by means of SPR in competition experiments as inhibitors of gp120 binding to DC-SIGN (Martinez-Ávila *et al.*, 2009a). *manno*-GNPs bearing disaccharide Man α 1-2Man α inhibited gp120/DC-SIGN binding 20,000-fold more efficiently than the free oligosaccharide.

NMR has been widely used to study the interactions between biological macromolecules (usually proteins and antibodies) and their small ligands in solution. Transferred nuclear Overhauser effect enhancement experiments provide dynamic information about a macromolecule–ligand interaction (Jiménez-Barbero and Peters, 2003). An advance in this technique has been achieved by saturation transfer difference (STD) experiments (Berger and Braun, 2004; Mayer and Meyer, 1999; Meyer and Peters, 2003), where selective irradiation of proton signals of protein side chains in a spectral region free of small ligands proton signals causes a magnetization transfer to the protons of the ligands that make closer contacts with the protein. These protons can be identified because they yield more intense signals than remote ones in the final difference spectrum and quantitative information of the binding can be obtained. We found that *manno*-GNPs are synthetic mimics of the 2G12 epitope using SPR technology and STD-NMR spectroscopy. We demonstrated the ability of *manno*-GNPs to bind 2G12 and to inhibit 2G12/gp120 binding, proving that the oligomannosides maintain their functionality and enhance their ability to interact with this antibody when clustered onto gold nanoparticles (Marradi *et al.*, 2011). We describe now SPR and STD experiments which have been carried out to evaluate the direct binding of *manno*-GNPs to 2G12 and the ability to inhibit gp120 binding to 2G12.

3.1. Binding study of *manno*-GNPs to 2G12 by SPR

3.1.1. Direct binding of *manno*-GNPs to 2G12

Interaction measurements are carried out using ProteOn XPR36 biosensor with research-grade GLC sensor chips. Due to its unique technological features, ProteOn is able to process 36 binding events simultaneously

(Bravman *et al.*, 2006). Antibody 2G12 was kindly supplied by Dr D. Katinger (Polymun Scientific, Vienna, Austria). Recombinant gp120 from HIV-1 CN54 clone (repository reference ARP683) was obtained from the Centre for AIDS Reagents, NIBSC HPA UK (by Prof. Ian Jones, Reading University, UK). ProteOn GLC sensor chips are washed with a short pulse of NaOH (50 mM), HCl (100 mM), and SDS (0.5%) before using. Channel activation is performed at 25 °C using phosphate-buffered saline (PBS)–Tween 20 as running buffer (PBS, 10 mM Na₃PO₄ and 150 mM NaCl, pH 7.4) with 0.005% of the surfactant Tween 20. Sensor chip channels are activated with 1-ethyl-3-(3-dimethylaminopropyl) carbodiimide (EDC, 16 mM) and *N*-hydroxysulfosuccinimide (sulfo-NHS, 4 mM). Thirty microliters of a 1:1 mixture of EDC/sulfo-NHS are injected (contact time: 60 s; flow rate: 30 μL min⁻¹). In channel 1, after activation, 120 μL of a 2G12 solution in acetate buffer pH 5.5 (50 μg mL⁻¹, 10 mM) are injected (240 s, 30 μL min⁻¹) until 2600 RU. Channel 2 is used as control and only PBS–Tween 20 buffer is injected. Both channels are then saturated with 100 μL of 1 M ethanolamine HCl (200 s, 30 μL min⁻¹). Binding experiments are performed at 25 °C using *tris*(hydroxymethyl)amino methane buffer (Tris-buffered saline: 10 mM Tris and 150 mM NaCl, pH 7.4) containing 0.005% Tween 20, as running buffer. This buffer is also used to prepare *manno*-GNPs solutions at different concentrations. Six dilutions for each analyte are prepared (1, 0.5, 0.25, 0.125, 0.06, and 0.03 μg mL⁻¹) and injected simultaneously. Each analyte (*manno*-GNPs and control GNPs) is injected under the same conditions (flow rate: 30 μL min⁻¹; contact time: 300 s; dissociation: 300 s). Sensorgrams are obtained by automatic subtraction of the reference channel signal from the 2G12 channel signal. After every injection, channels are regenerated with a short pulse of 3.5 M MgCl₂ (flow rate: 100 μL min⁻¹; contact time: 30 s). The affinity of gp120 to 2G12 is also evaluated to verify the binding features of the antibody after immobilization on the sensor chip. 2G12 activity slightly decreased after the regeneration conditions due to the instability of the antibody for long periods. To compare the interactions of *manno*-GNPs to 2G12, sensorgrams corresponding to the highest concentration tested (1 μg mL⁻¹) are used. Data shown in Table 2.1 indicate that at this concentration the response of most of the *manno*-GNPs is similar to the gp120 used.

When comparing at the same oligomannoside concentration (0.1 μM), the highest and similar binding affinities for 2G12 correspond to Te-10 and Te-50 (Marradi *et al.*, 2011).

3.1.2. Competition experiments

gp120 is immobilized on a GLC sensor chip (around 8000 RU) using the same methodology described above for 2G12. Antibody 2G12 (final concentration, 100 nM) is incubated with five different concentrations of *manno*-GNPs for 10 min at 25 °C in Tris-buffered saline. 2G12/*manno*-GNP complexes and 2G12 (control) are injected simultaneously onto

Table 2.1 Direct binding of GNPs ($1 \mu\text{g mL}^{-1}$) and gp120 ($1.6 \mu\text{g mL}^{-1}$) to 2G12

<i>manno</i> -GNP	Binding [Ru] ^a	Mannoside chains	GNP conc. [μM] ^b	Mannoside conc. [μM] ^c
D-10	<2	9	0.014	0.13
D-50	77	22	0.025	0.55
D-100	26	59	0.016	0.94
Tri-10	<5	13	0.012	0.16
Tri-50	66	62	0.010	0.62
Te-10	85	7	0.021	0.15
Te-50	113	56	0.008	0.45
P-10	<5	5	0.017	0.09
P-50	39	28	0.010	0.28
<i>gp120</i>	20 ^d	–	0.011	–
M-100	0	40	0.024	0.96
Au-GlcC ₅	0	0	0.027	0

^a Taken at 150-s in the association phase of the sensorgrams.

^b Calculated using the average molecular formulas.

^c Calculated from the number of oligomannosides per GNP.

^d The lower SPR response of gp120 with respect to *manno*-GNPs can be due to the gold colloid SPR-enhancing effects.

gp120 and reference channels (flow rate: $30 \mu\text{L min}^{-1}$; contact time: 300 s; dissociation: 300 s). The sensor surface between runs is regenerated with a short pulse of 0.1 M HCl. In repeated experiments, gp120 shows a slight loss of activity due to HCl regeneration phases. Te-10 and Te-50 GNPs showed the best binding activity to 2G12 (Marradi *et al.*, 2011). The other *manno*-GNPs showed slight effects (D-50 and Tri-50) to moderate effects (D-100 and P-50) at the tested concentrations.

3.2. Study of the 2G12/GNP interaction by STD-NMR

The dissociation constants (K_D) of monovalent 1-aminoethyl oligomannoside/2G12 complex have been previously determined by STD-NMR (Enríquez-Navas *et al.*, 2011) following an improved protocol for single-ligand STD-NMR titrations based on the initial slopes of the build-up curves of the STD amplification factor against ligand concentration (Angulo *et al.*, 2010). The study of the direct interaction between *manno*-GNPs and 2G12 in STD experiments is hampered by the fact that both the antibody and the nanoparticles are macromolecules. We overcame this impasse by carrying out indirect competition experiments in which 2G12-oligomannoside mixtures were titrated with *manno*-GNPs. The displacement of a monovalent oligomannoside from the 2G12 binding sites resulted in a significant reduction of its STD signal. This effect

has been used to obtain qualitative and quantitative information on the affinity of *manno*-GNPs for antibody 2G12, as it will be shown in detail in the following section.

3.2.1. Titration of 2G12-oligomannoside mixtures with *manno*-GNPs

For the STD-NMR titration experiments in isotropic solution, the aminoethyl oligomannosides and *manno*-GNPs are lyophilized twice against D₂O (99.9% purity, Sigma-Aldrich). Antibody 2G12 (400 μ L at 11.69 mg mL⁻¹, in 2 mM acetic acid, 10% maltose-sterile, no preservatives) is dialyzed (10 \times 10 mL in the reservoir, 30 min each) against 10 mM phosphate buffer (pH 6.7) using a membrane with 100,000 MWCO (Float-A-Lyzer of 5 mm diameter and 500 μ L volume, Spectrum Laboratories, Inc.) following the manufacturer's instructions. Unlike SPR experiments, this step is necessary to remove the excess of maltose. To verify whether 2G12 remained inside the membrane, the dialysate is subjected to a Bradford-type protein assay (Bradford, 1976).

3.2.2. 2G12 deuteration

After 2G12 dialysis with 10 mM phosphate buffer (pH 6.7), three additional dialyses (3 \times 10 mL, 30 min each) are performed with deuterated buffer. To deuterate the buffer 35 mL of the phosphate buffer is freeze-dried and then subjected to three solubilization-lyophilization cycles against 10 mL of D₂O (99% purity, Sigma-Aldrich) before final dissolution in 35 mL of D₂O (99% purity, Sigma-Aldrich). After dialysis with deuterated buffer, 2G12 is carefully recovered from the membrane and lyophilized twice against D₂O (99.9% purity, Sigma-Aldrich).

3.2.3. Competition experiments

For the inhibition experiments, we selected as monovalent ligands the aminoethyl tetramannoside and aminoethyl trimannoside because they have a high affinity for 2G12 ($K_D = 400 \mu$ M, Enríquez-Navas, *et al.*, 2011). STD-NMR titration experiments are recorded at 25 °C in a Bruker DRX 500-MHz spectrometer with a broadband inverse probe using 1 K scans and 32 dummies scans without suppression of the residual HDO signal. The broad signals of the antibody are eliminated by adding a $T_{1\rho}$ filter to the pulse sequence (stdiff3, Bruker). Selective irradiation of the aromatic side chains of 2G12 is achieved by using a typical train of 50 ms Gaussian pulses (Mayer and Mayer, 1999), each one with a total saturation time of 2 s. The absence of aromatic protons in the *manno*-GNPs and in the aminoethyl oligomannosides allowed the selective excitation of antibody aromatic protons without affecting the signals of the ligands.

In a typical experiment, special NMR tubes (3 mm \times 100 mm, Bruker) adaptable to a Bruker MATCHTM holder are charged with 180 μ L containing

2G12 (25 μM) and aminoethyl tetramannoside (8 mM) in 10 mM deuterated potassium phosphate buffer (pH 6.7). The high ligand/antibody ratio is set up so that more than 90% of the 2G12 binding sites are occupied, fulfilling the condition of competitive inhibition titrations (Cheng and Prusoff, 1973). Increasing volumes (0.6, 2.46, 6.33, 7.85, 9.0, and 18.0 μL) of solution of Te-50 GNP (733 μM in tetramannoside) in D_2O are added to the 180 μL solution of 2G12/aminoethyl tetramannoside mixture. The decrease in the STD signals intensity of the anomeric proton at the nonreducing mannose of aminoethyl tetramannoside is monitored. The STD signal intensity of this proton decreased up to 60% of its original value (in the absence of GNPs) in a dose-dependent way, as shown in Fig. 2.4. This indicates that Te-50 GNP efficiently displaces the free tetramannoside ligand from the binding site of 2G12. Similar results are found with Te-10 GNP, proving that this tetramannoside clustered onto gold nanoparticles enhances its ability to interact with 2G12.

3.2.4. Calculation of the dissociation constant

To calculate the dissociation constant K_D of the oligomannosides multi-merised onto the *manno*-GNPs, the STD data obtained from the titrations experiments with Te-10 and Te-50 GNPs are mathematically fitted to Eq. (2.1) (Benie *et al.*, 2003). Equation (1) describes a competitive model and derives from the seminal Cheng–Prusoff equation (Cheng and Prusoff, 1973).

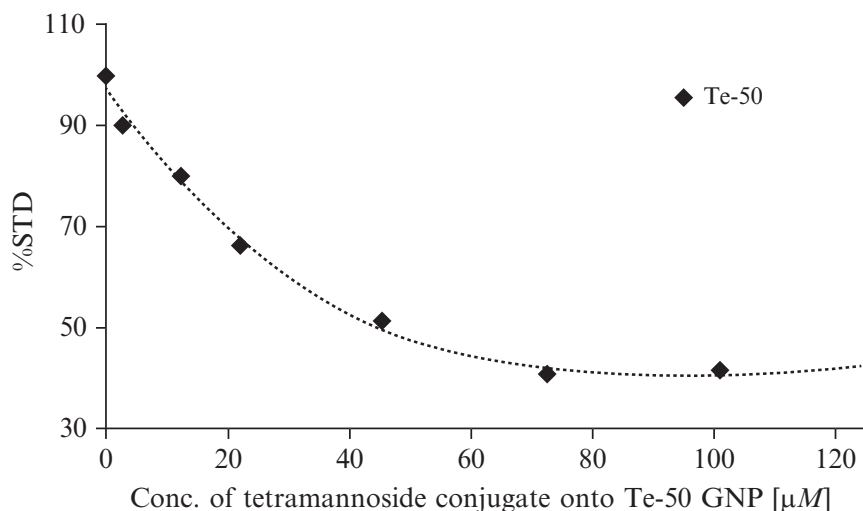


Figure 2.4 Competitive titration of 2G12/aminoethyl tetramannoside complex with Te-50 GNP. The decrease in the STD intensity of the anomeric proton H1 of the mannose ring at the nonreducing end of aminoethyl tetramannoside was monitored as a function of the GNP concentration expressed in terms of tetramannoside. The concentration of the monovalent aminoethyl tetramannoside was set to 8 mM . Symbols correspond to experimental data. Lines represent a three-order polynomial fitting (for visualization purposes).

$$I_{\text{STD}} = 100 \left(1 - \frac{[K_{\text{D}}/L_0][I_0/K_{\text{I}}]}{1 + [K_{\text{D}}/L_0][1 + (I_0/K_{\text{I}})]} \right). \quad (2.1)$$

In Eq. (2.1), I_{STD} is the monitored STD ^1H intensity of the monovalent ligand, K_{D} is the dissociation constant of the monovalent ligand, L_0 is the concentration of the monovalent ligand in the sample, I_0 is the concentration of the inhibitor (in these cases, the oligomannosides onto the *manno*-GNPs), and K_{I} is the dissociation constant of the oligomannoside onto *manno*-GNPs. The calculated inhibition constants of Te-10 and Te-50 GNPs are 4.2 ± 0.5 and $3.6 \pm 0.6 \mu\text{M}$ (expressed in terms of tetramannoside), respectively. This indicates that the affinity of the monovalent aminoethyl tetramannoside for 2G12 ($K_{\text{D}} = 400 \mu\text{M}$) was enhanced ~ 100 -fold by the multimerization of tetramannoside onto gold nanoparticles (Marradi *et al.*, 2011).

4. VALIDATION OF MANNO-GNPs AS INHIBITORS OF HIV-1/CELL INFECTION

4.1. Effect of *manno*-GNPs on HIV-1 neutralization by 2G12 in cellular models

The inhibitory effect of Te-10 and Te-50 GNPs on the 2G12-mediated neutralization of a replication-competent HIV infection of TZM-bl cells was also demonstrated by competition neutralization assay under conditions that resemble the ones in which normal serum prevents infection of the target cells (Marradi *et al.*, 2011).

4.1.1. Determination of 2G12 neutralizing concentration

Before testing the *manno*-GNPs, experiments to find the conditions in which antibody 2G12 neutralizes the HIV-1 infection of TZM-bl cells is performed. TZM-bl is a luciferase reporter HeLa cell line (Derdeyn *et al.*, 2000; Platt *et al.*, 1998; Wei *et al.*, 2002) that stably expresses CD4, CCR5, and CXCR4 (viral receptor and coreceptors) and also contains separate integrated copies of the luciferase and β -galactosidase genes under the control of the HIV-1 promoter. We used a neutralization assay (see below for further details) that has been previously validated by comparison with the current standardized pseudotype assays and a good agreement is found (Fenyo *et al.*, 2009; Garcia-Perez *et al.*, 2007). Different concentrations of 2G12 are tested against an HIV-1 strain NL4-3 laboratory isolate (Fang *et al.*, 1999; Salminen *et al.*, 1995) to find the optimal conditions for inhibiting the HIV infection of TZM-bl cells (Fig. 2.5A). At $29 \mu\text{g mL}^{-1}$, 2G12 could efficiently inhibit the infectivity of the NL4-3

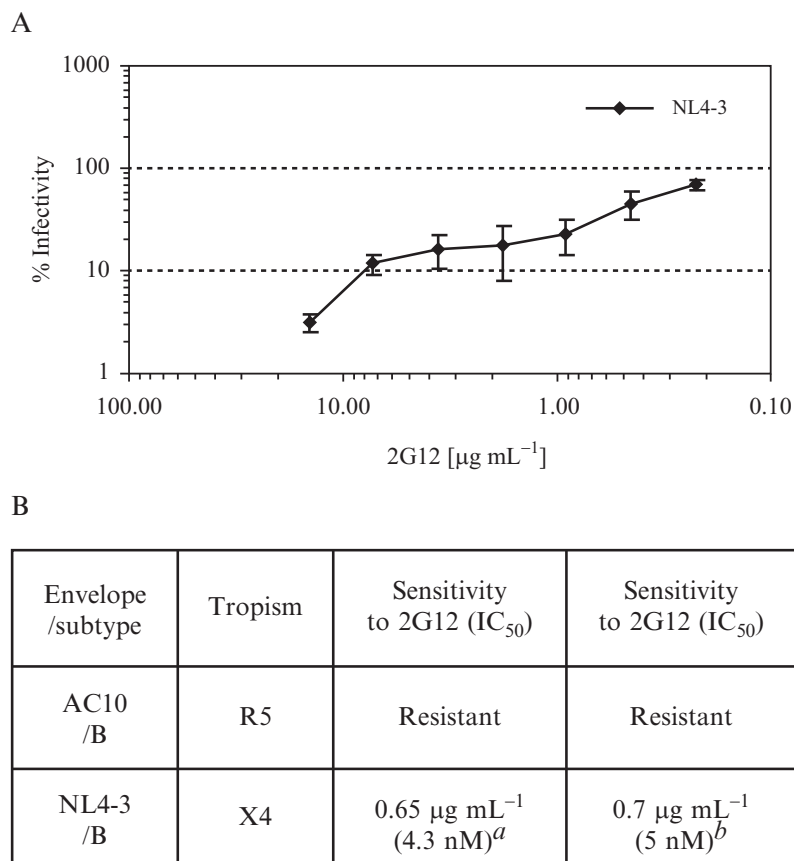


Figure 2.5 (A) Sensitivity of HIV-1 NL4-3 to 2G12-mediated neutralization using TZM-bl cells. 2G12 was used at 29.2, 14.6, 7.3, 3.65, 1.83, 0.91, 0.46, and 0.23 µg mL⁻¹. (B) IC₅₀ of 2G12-mediated neutralization of HIV-1 infection of TZM-bl cells, in the absence of *manno*-GNPs (^aFour independent measurements; ^bPublished by Binley *et al.*, 2004 using a different assay, but the same viral envelopes).

HIV-1 so that this concentration is used in the inhibition assays with the *manno*-GNPs. The data reported in Fig. 2.5A are also used to calculate the concentration of antibody 2G12 which is required to reduce by 50% the HIV-1 infection of TMZ-bl cells in the absence of *manno*-GNPs (IC₅₀, Fig. 2.5B). The obtained IC₅₀ (0.65 µg mL⁻¹) is in agreement with the literature (Binley *et al.*, 2004).

4.1.2. Inhibition of *manno*-GNPs of 2G12-mediated HIV-1 neutralization

Serial dilutions of GNP Te-10 and Te-50 GNP (the highest concentration being 125 µg mL⁻¹) are preincubated with antibody 2G12 (58 µg mL⁻¹) to a final volume of 50 µL in culture media, in triplicate, for 30 min at 37 °C. The GNP-2G12 solution is then added (1:1, by volume) to the HIV-1 virus (4 ng of p24, NL4-3 strain) and the mixture is incubated for 1 h at 37 °C. At this point, the concentration of 2G12 (29 µg mL⁻¹) is able to

neutralize the virus (see Fig. 2.5). The virus–GNP–antibody mixture is added (1:1, by volume) to 10,000 TZM-bl cells (final volume 200 μ L). The plate is then placed in a humidified chamber within a CO₂ incubator at 37 °C. Luciferase activity is measured from cell lysates when levels are sufficiently over background to give reliable measurements (at least 10-fold) using the Luciferase Assay System (Promega) and following the manufacturer's recommendations. Virus equivalent to 4 ng of the p24 capsid protein (quantified by an antigen-capture assay; Innogenetics, Belgium) of the NL4-3 strain of HIV-1 is chosen as the lowest level of viral input sufficient to give a clear luciferase signal within the linear range on day 3 postinfection. Neutralization activity is measured in triplicate and reported as the percentage of luciferase activity compared to the luciferase activity corresponding to the wells with virus and no antibody. The 2G12 concentration required to inhibit 50% of viral infectivity (IC₅₀) is determined for each GNP at different concentrations. Competition is observed when the addition of GNPs resulted in a decrease in the neutralizing capacity of the antibody (higher IC₅₀).

It is found that Te-10 and Te-50 GNPs caused a reproducible inhibition of 2G12 neutralization within the micromolar range in experiments using TZM-bl cells. Te-10 GNPs could efficiently inhibit the 2G12-mediated neutralization of the NL4-3 strain at 5.5 μ M (37 μ M of tetrasaccharide). At this concentration of Te-10 GNP, the amount of 2G12 required to reduce 50% of viral infectivity (IC₅₀) is three times higher (13.3 nM) than the one required in the absence of GNPs (4.3 nM; Fig. 2.5). When Te-50 GNP is used, similar results were observed (Marradi *et al.*, 2011).

4.2. Inhibition of DC-SIGN-mediated HIV-1 trans-infection of human T cells by *manno*-GNPs

DC-SIGN mediates interactions between DCs and resting T cells, by binding ICAM-3 (Geijtenbeek *et al.*, 2000). DCs in mucosal tissues capture HIV-1 through DC-SIGN–gp120 interactions. After migration to lymphoid organs, DCs promote efficient trans-infection of T cells through DC-SIGN, resulting in a vigorous viral replication.

The *manno*-GNPs are designed to target DC-SIGN receptors present on DCs by mimicking the clustered carbohydrate display of gp120. We found that oligomannoside-functionalized gold glyconanoparticles are able to inhibit the HIV-1 DC-SIGN-mediated trans-infection of T cells at nanomolar concentrations and they could be an antiadhesive barrier at an early stage of HIV-1 infection, preventing viral attachment to DC-SIGN-expressing cells (Martinez-Ávila *et al.*, 2009b).

For trans-infection experiments, Raji DC-SIGN transfected lymphoblastoid B cells are used. *manno*-GNPs are nontoxic to Raji DC-SIGN+ and to human-activated PBMCs at concentrations of 100 mg mL⁻¹, as

determined by the CellTiter cell viability assay. The activities of *manno*-GNPs against R5 or X4 HIV-1 are evaluated through an original DC-SIGN transfer assay in which inhibition of HIV-1 infection by GNPs is assessed by use of recombinant viruses carrying the Renilla reporter genes in their genomes (Garcia-Perez *et al.*, 2007). Inhibition of viral replication is proportional to Renilla-luciferase activity in cell lysates.

4.2.1. Cell culture and preparation of PBMCs from blood

Raji cells were kindly provided by Dr. Alfredo Toraño (Instituto de Salud Carlos III, Madrid, Spain), and Raji DC-SIGN+ cells are kindly provided by Dr. Fernando Arenzana-Seisdedos (Institut Pasteur, Paris, France). Both cell lines are cultured in RPMI 1640 medium containing fetal bovine serum (10% v/v), l-glutamine (2 mM), penicillin (50 IU mL⁻¹), and streptomycin (50 mg mL⁻¹; all from Whittaker M.A. Bio-Products, Walkerville, MD, USA). The 293T cells (used for the production of recombinant viruses) are cultured in Dulbecco's modified Eagle's medium (DMEM) containing fetal bovine serum (10% v/v), l-glutamine (2 mM), penicillin (50 IU mL⁻¹), and streptomycin (50 mg mL⁻¹). The 293T cells are cultured at 37 °C in a humidified atmosphere with CO₂ (5%) and split twice a week. PBMCs are obtained from buffy coats from healthy donors. PBMCs are harvested from buffy coats by centrifugation over Lymphoprep (Sigma-Aldrich) gradient by standard procedures, stimulated with interleukin-2 (300 IU mL⁻¹; Chiron) and phytohaemagglutinin (5 mg mL⁻¹), and incubated at 37 °C under humidified CO₂ (5%) for 48 h.

4.2.2. Trans-infection assay

Raji or Raji DC-SIGN+ cells (10⁵ cells per well) are incubated with GNPs for 1 h prior to addition of either R5 or X4 tropic recombinant viruses (JR-Renilla or NL4.3-Renilla, respectively; both 200 ng p24 per well) and left for 2 h at 37 °C for efficient adsorption. Cells are washed extensively with PBS and preactivated PBMCs (10⁵ per well) are added. Viral replication is followed by measurement of Relative luminescence unit (RLU) activity in cell lysates. Briefly, cells are harvested and lysed after 48 h and sample activity is measured with the Renilla-luciferase assay system (Promega) according to the manufacturer's protocol. RLUs are obtained by using a luminometer (Berthold Detection Systems, Pforzheim, Germany) after the addition of substrate to cells extracts. All the experiments are performed in parallel with Raji cells as control. IC₅₀ values are calculated with GraphPad Prism Software (Sigmoidal dose-response analysis). The results are representative of at least three independent experiments and are shown in Fig. 2.6.

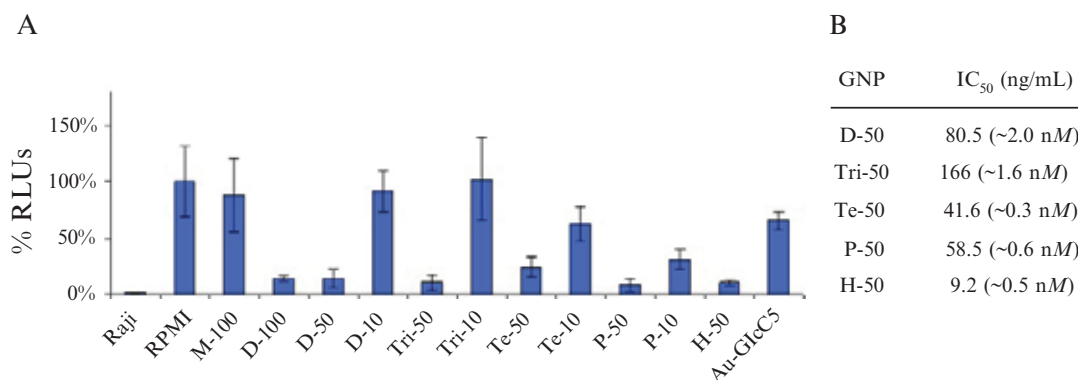


Figure 2.6 (A) Anti-HIV evaluation of *manno*-GNPs at 1 mg mL^{-1} in DC-SIGN-mediated trans-infection of human T cells. HIV-1 recombinant viruses JR-Renilla R5 was used. Raji cells not expressing DC-SIGN (Raji DC-SIGN⁻) were used as control. Results are expressed as percentages of infection related to untreated control. (B) IC₅₀ of selected *manno*-GNPs in ng mL^{-1} and nM concentration of oligomannosides.

ACKNOWLEDGMENTS

We thank the Spanish Ministry of Science and Innovation MICINN (grant CTQ2008-04638/BQU), the European Union (CHAARM grant Health-F3-2009-242135, EMPRO LSHP-CT2003-503558, Glycogold MRTN-CT2004-005645), and the Department of Industry of the Basque Country (grant ETORTEK2009) for financial support. Antibody 2G12 was kindly supplied by Dr D. Katinger (Polymun Scientific, Vienna, Austria). Recombinant gp120 from HIV-1 CN54 clone (repository reference ARP683) was obtained from the Program EVA Centre for AIDS Reagents, NIBSC HPA UK, supported by the EC FP6/7 Europrise Network of Excellence, and NGIN consortia, and the Bill and Melinda Gates GHRC-CAVD Project and was donated by Prof. I. Jones (Reading University, UK). T2M-bl was obtained from Dr. J. C. Kappes, Dr. X. Wu, and Tranzyme, Inc., through the National Institutes of Health AIDS Research and Reference Reagent Program, Division of AIDS, National Institute of Allergy and Infectious Diseases. We thank all the members of the group and collaborators who have contributed to the work described here. Dr. P. M. Enríquez-Navas and Dr. E. Yuste are acknowledged for revising [Sections 3.2 and 4.1](#), respectively.

REFERENCES

- Allan, J. S., Coligan, J. E., Barin, F., McLane, M. F., Sodroski, J. G., Rosen, C. A., Haseltine, W. A., Lee, T. H., and Essex, M. (1985). Major glycoprotein antigens that induce antibodies in AIDS patients are encoded by HTLV-III. *Science* **228**, 1091–1094.
- Angulo, J., Enríquez-Navas, P. M., and Nieto, P. M. (2010). Ligand–receptor binding affinities from saturation transfer difference (STD) NMR spectroscopy: The binding isotherm of STD initial growth rates. *Chem. Eur. J.* **16**, 7803–7812.
- Astronomo, R. D., Kaltgrad, E., Udit, A. K., Wang, S. K., Doores, K. J., Huang, C. Y., Pantophlet, R., Paulson, J. C., Wong, C. H., Finn, M. G., and Burton, D. R. (2010). Defining criteria for oligomannose immunogens for HIV using icosahedral virus capsid scaffolds. *Chem. Biol.* **17**, 357–370.

- Barin, F., McLane, M. F., Allan, J. S., Lee, T. H., Groopman, J. E., and Essex, M. (1985). Virus envelope protein of HTLV-III represents major target antigen for antibodies in AIDS patients. *Science* **228**, 1094–1096.
- Barrientos, A. G., de la Fuente, J. M., Rojas, T. C., Fernandez, A., and Penadés, S. (2003). Gold glyconanoparticles: Synthetic polyvalent ligands mimicking glycocalyx-like surfaces as tools for glycobiological studies. *Chem. Eur. J.* **9**, 1909–1921.
- Barrientos, A. G., de la Fuente, J. M., Jiménez, M., Solís, D., Cañada, F. J., Martín-Lomas, M., and Penadés, S. (2009). Modulating glycosidase degradation and lectin recognition of gold glyconanoparticles. *Carbohydr. Res.* **344**, 1474–1478.
- Benie, A. J., Moser, R., Bäuml, E., Blaas, D., and Peters, T. (2003). Virus–ligand interactions: Identification and characterization of ligand binding by NMR spectroscopy. *J. Am. Chem. Soc.* **125**, 14–15.
- Berger, S., and Braun, S. (2004). 200 and More NMR Experiments. Wiley-VCH, Verlag GmbH & Co. KGaA, Weinheim Ch. 8, Exp. 8.13, pp. 298–301.
- Binley, J. M., Wrin, T., Korber, B., Zwick, M. B., Wang, M., Chappey, C., Stiegler, G., Kunert, R., Zolla-Pazner, S., Katinger, H., Petropoulos, C. J., and Burton, D. R. (2004). Comprehensive cross-clade neutralization analysis of a panel of anti-human immunodeficiency virus type 1 monoclonal antibodies. *J. Virol.* **78**, 13232–13252.
- Bradford, M. M. (1976). Rapid and sensitive method for the quantitation of microgram quantities of protein utilizing the principle of protein–dye binding. *Anal. Biochem.* **72**, 248–254.
- Bravman, T., Bronner, V., Lavie, K., Notcovich, A., Papalia, G. A., and Miszka, D. G. (2006). Exploring “one-shot” kinetics and small molecule analysis using the ProteOn XPR36 array biosensor. *Anal. Biochem.* **358**, 281–288.
- Brust, M., Walker, M., Bethell, D., Schiffrin, D. J., and Whyman, R. (1994). Synthesis of thiol derivatised gold nanoparticles in a two-phase liquid/liquid system. *J. Chem. Soc. Chem. Commun.* **7**, 801–802.
- Calarese, D. A., Scanlan, C. N., Zwick, M. B., Deechongkit, S., Mimura, Y., Kunert, R., Zhu, P., Wormald, M. R., Stanfield, R. L., Roux, K. H., Kelly, J. W., Rudd, P. M., *et al.* (2003). Antibody domain exchange is an immunological solution to carbohydrate cluster recognition. *Science* **300**, 2065–2071.
- Carvalho de Souza, A., and Kamerling, J. P. (2006). Analysis of carbohydrate–carbohydrate interactions using gold glyconanoparticles and oligosaccharide self-assembling monolayers. *Methods Enzymol.* **417**, 221–243.
- Cheng, Y. C., and Prusoff, W. H. (1973). Relationship between the inhibition constant (K_i) and the concentration of inhibitor which causes 50 per cent inhibition (I_{50}) of an enzymatic reaction. *Biochem. Pharmacol.* **22**, 3099–3108.
- de la Fuente, J. M., and Penadés, S. (2006). Glyconanoparticles: Types, synthesis and applications in glycoscience, biomedicine and material science. *BBA* **1760**, 636–651.
- de la Fuente, J. M., Barrientos, A. G., Rojas, T. C., Rojo, J., Canada, J., Fernandez, A., and Penadés, S. (2001). Gold glyconanoparticles as water-soluble polyvalent models to study carbohydrate interactions. *Angew. Chem. Int. Ed.* **40**, 2258–2261.
- Derdeyn, C. A., Decker, J. M., Sfakianos, J. N., Wu, X., O’Brien, W. A., Ratner, L., Kappes, J. C., Shaw, G. M., and Hunter, E. (2000). Sensitivity of human immunodeficiency virus type 1 to the fusion inhibitor T-20 is modulated by coreceptor specificity defined by the V3 loop of gp120. *J. Virol.* **74**, 8358–8367.
- Dudkin, V. Y., Orlova, M., Geng, X., Mandal, M., Olson, W. C., and Danishefsky, S. J. (2004). Toward fully synthetic carbohydrate-based HIV antigen design: On the critical role of bivalency. *J. Am. Chem. Soc.* **126**, 9560–9562.
- Engering, A., van Vliet, S., Geijtenbeek, T. B., and van Kooyk, Y. (2002). Subset of DC-SIGN dendritic cells in human blood transmits HIV-1 to T lymphocytes. *Immunobiology* **100**, 1780–1786.

- Enriquez-Navas, P. M., Marradi, M., Padro, D., Angulo, J., and Penadés, S. (2011). A solution NMR study of the interactions of oligomannosides and the anti-HIV-1 2G12 antibody reveals distinct binding modes for branched ligands. *Chem. Eur. J.* **17**, 1369–1707.
- Fang, G., Weiser, B., Visosky, A., Moran, T., and Burger, H. (1999). PCR-mediated recombination: A general method applied to construct chimeric infectious molecular clones of plasma-derived HIV-1 RNA. *Nat. Med.* **5**, 239–242.
- Feizi, T., and Larkin, M. (1990). AIDS and glycosylation. *Glycobiology* **1**, 17–23.
- Fenouillet, E., Gluckman, J. C., and Jones, I. M. (1994). Functions of HIV envelope glycans. *Trends Biochem. Sci.* **19**, 65–70.
- Fenyo, E. M., Heath, A., Dispinseri, S., Holmes, H., Lusso, P., Zolla-Pazner, S., Donners, H., Heyndrickx, L., Alcamí, J., Bongertz, V., Jassoy, C., Malnati, M., *et al.* (2009). International network for comparison of HIV neutralization assays: The NeutNet report. *PLoS One* **4**, e4505.
- García, I., Marradi, M., and Penadés, S. (2010). Glyconanoparticles: Multifunctional nanomaterials for biomedical applications. *Nanomedicine* **5**, 777–792.
- García-Pérez, J., Sánchez-Palomino, S., Pérez-Olmeda, M., Fernández, B., and Alcamí, J. (2007). A new strategy based on recombinant viruses as a tool for assessing drug susceptibility of human immunodeficiency virus type 1. *J. Med. Virol.* **79**, 127–137.
- Geijtenbeek, T. B., Kwon, D. S., Torensma, R., van Vliet, S. G., van Duinshoven, G. C., Middel, J., Cornelissen, I. L., Nottet, H. S., KewalRamani, V. N., Littman, D. R., Figdor, C. G., and van Kooyk, Y. (2000). DC-SIGN, a dendritic cell-specific HIV-1-binding protein that enhances trans-infection of T cells. *Cell* **100**, 587–597.
- Geyer, H., Holschbach, C., Hunsmann, G., and Schneider, J. (1988). Carbohydrates of human immunodeficiency virus-structure of oligosaccharides linked to the envelope glycoprotein-120. *J. Biol. Chem.* **263**, 11760–11767.
- Hostetler, M. J., Wingate, J. E., Zhong, C.-J., Harris, J. E., Vachet, R. W., Clark, M. R., Londono, J. D., Green, S. J., Stokes, J. J., Wignall, G. D., Glish, G. L., Porter, M. D., *et al.* (1998). Alkanethiolate gold cluster molecules with core diameters from 1.5 to 5.2 nm: Core and monolayer properties as a function of core size. *Langmuir* **14**, 17–30.
- Jiménez-Barbero, J., and Peters, T. (2003). TR-NOE experiments to study carbohydrate-protein interactions. In “NMR Spectroscopy of Glycoconjugates,” (J. Jiménez-Barbero and T. Peters, eds.), Wiley-VCH, Verlag GmbH & Co. KGaA, Weinheim.
- Kabanova, A., Adamo, R., Proietti, D., Berti, F., Tontini, M., Rappuoli, R., and Costantino, P. (2010). Preparation, characterization and immunogenicity of HIV-1 related high-mannose oligosaccharides-CRM197 glycoconjugates. *Glycoconj. J.* **27**, 501–513.
- Krauss, I. J., Joyce, J. G., Finnefrock, A. C., Song, H. C., Dudkin, V. Y., Geng, X., Warren, J. D., Chastain, M., Shiver, J. W., and Danishefsky, S. J. (2007). Fully synthetic carbohydrate HIV antigens designed on the logic of the 2G12 antibody. *J. Am. Chem. Soc.* **129**, 11042–11044.
- Li, H., and Wang, L. X. (2004). Design and synthesis of a template-assembled oligomannose cluster as an epitope mimic for human HIV-neutralizing antibody 2G12. *Org. Biomol. Chem.* **2**, 483–488.
- Marradi, M., Martín-Lomas, M., and Penadés, S. (2010). Glyconanoparticles: Polyvalent tools to study carbohydrate-based interactions. *Adv. Carbohydr. Chem. Biochem.* **64**, 212–270.
- Marradi, M., Di Gianvincenzo, P., Enriquez-Navas, P. M., Martínez-Ávila, O. M., Chiodo, F., Yuste, E., Angulo, J., and Penadés, S. (2011). Gold nanoparticles coated with oligomannosides of HIV-1 glycoprotein gp120 mimic the carbohydrate epitope of antibody 2G12. *J. Mol. Biol.* **410**, 798–810.
- Martínez-Ávila, O., Hijazi, K., Marradi, M., Clavel, C., Champion, C., Kelly, C., and Penadés, S. (2009a). Gold manno-glyconanoparticles: Multivalent system to block HIV-1 gp120 binding to the lectin DC-SIGN. *Chem. Eur. J.* **15**, 8974–9888.

- Martinez-Ávila, O., Bedoya, Luis M., Marradi, M., Clavel, C., Alcamí, J., and Penadés, S. (2009b). Multivalent manno-glyconanoparticles inhibit DC-SIGN mediated HIV-1 trans-infection of human T cells. *Chembiochem* **10**, 1806–1809.
- Mayer, M., and Meyer, B. (1999). Characterization of ligand binding by saturation transfer difference NMR spectra. *Angew. Chem. Int. Ed.* **38**, 1784–1788.
- Meyer, B., and Peters, T. (2003). NMR spectroscopy techniques for screening and identifying ligand binding to protein receptors. *Angew. Chem. Int. Ed.* **42**, 864–890.
- Mizuochi, T., Spellman, M. W., Larkin, M., Solomon, J., Basa, L. J., and Feizi, T. (1988). Carbohydrate structures of the human-immunodeficiency-virus (HIV) recombinant envelope glycoprotein gp120 produced in chinese ovary cells. *Biochem. J.* **254**, 599–603.
- Platt, E. J., Wehrly, K., Kuhmann, S. E., Chesebro, B., and Kabat, D. (1998). Effects of CCR5 and CD4 cell surface concentrations on infections by macrophagetropic isolates of human immunodeficiency virus type 1. *J. Virol.* **72**, 2855–2864.
- Rich, R. L., and Miszka, D. G. (2000). Advances in surface plasmon resonance biosensor analysis. *Curr. Opin. Biotechnol.* **11**, 54–61.
- Rich, R. L., and Miszka, D. G. (2003). Spying on HIV with SPR. *Trends Microbiol.* **11**, 124–133.
- Salminen, M. O., Koch, C., Sanders-Buell, E., Ehrenberg, P. K., Michael, N. L., Carr, J. K., Burke, D. S., and McCutchan, F. E. (1995). Recovery of virtually full-length HIV-1 provirus of diverse subtypes from primary virus cultures using the polymerase chain reaction. *Virology* **213**, 80–86.
- Sanders, R. W., Venturi, M., Schiffner, L., Kalyanaraman, R., Katinger, H., Lloyd, K. O., Kwong, P. D., and Moore, J. P. (2002). The mannose-dependent epitope for neutralizing antibody 2G12 on human immunodeficiency virus type 1 glycoprotein gp120. *J. Virol.* **76**, 7293–7305.
- Scanlan, C. N., Pantophlet, R., Wormald, M. R., Saphire, E. O., Stanfield, R., Wilson, I. A., Katinger, H., Dwek, R. A., Rudd, P. M., and Burton, D. R. (2002). The broadly neutralizing anti-HIV-1 antibody 2G12 recognizes a cluster of 132 mannose residues on the outer face of gp120. *J. Virol.* **76**, 7306–7321.
- Trkola, A., Purtscher, M., Muster, T., Ballaun, C., Buchacher, A., Sullivan, N., Srinivasan, K., Sodroski, J., Moore, J. P., and Katinger, H. (1996). Human monoclonal antibody 2G12 defines a distinctive neutralization epitope on the gp120 glycoprotein of human immunodeficiency virus type 1. *J. Virol.* **70**, 1100–1108.
- van Kasteren, S. I., Campbell, S. J., Serres, S., Anthony, D. C., Sibson, N. R., and Davis, B. G. (2009). Glyconanoparticles allow pre-symptomatic in vivo imaging of brain disease. *Proc. Natl. Acad. Sci. USA* **106**, 18–23.
- Wang, L. X., Ni, J., Singh, S., and Li, H. (2004). Binding of high-mannose-type oligosaccharides and synthetic oligomannose clusters to human antibody 2G12: Implications for HIV-1 vaccine design. *Chem. Biol.* **11**, 127–134.
- Wang, J., Li, H., Zou, G., and Wang, L. X. (2007). Novel template-assembled oligosaccharide clusters as epitope mimics for HIV-neutralizing antibody 2G12. Design, synthesis, and antibody binding study. *Org. Biomol. Chem.* **5**, 1529–1540.
- Wang, S. K., Liang, P. H., Astronomo, R. D., Hsu, T. L., Hsieh, S. L., Burton, D. R., and Wong, C. H. (2008). Targeting the carbohydrates on HIV-1: Interaction of oligomannose dendrons with human monoclonal antibody 2G12 and DC-SIGN. *Proc. Natl. Acad. Sci. USA* **105**, 3690–3695.
- Wei, X., Decker, J. M., Liu, H., Zhang, Z., Arani, R. B., Kilby, J. M., Saag, M. S., Wu, X., Shaw, G. M., and Kappes, J. C. (2002). Emergence of resistant human immunodeficiency virus type 1 in patients receiving fusion inhibitor (T-20) monotherapy. *Antimicrob. Agents Chemother.* **46**, 1896–1905.

ACKNOWLEDGEMENTS

I want to thank my boss, Soledad, who bet on me in October 2008, and gave me the opportunity to learn about Glyco-sciences and who let me play with glyco-nanotechnology applying it to different scientific fields...Grazie Marco, per ogni insegnamento chiave, per avermi fatto crescere, per ogni discussione, e per ogni giorno in cui mi hai sostenuto...Thank you to the Director (Manuel) of biomaGUNE for all the facilities and funding I exploited during these years...I had the opportunity to be surrounded by a lot of great young-scientists during these years in biomaGUNE, and really, thank you to all you...Thank you to all the non-scientific supports I found in biomaGUNE (administration, maintenance, informatic etc)...Thank you to Javi for the help in the analytical parts of this Thesis...Thank you to Europe and Spain who paid me during these years with Public money that I tried to respect every day...Thank you all my friends who support me with natural simplicity during my studies in San Sebastian...Thank you to all the people from the Glyco-nanotechnology Lab...During these years I had the opportunity to meet at the International conferences a lot of brilliant glyco-scientists from whom I learn a lot...Following the order of the chapters presented in this Thesis I have to thank the co-workers who made this story better: Miguel Angel, Javi and Elisa for the drugs project...Eloisa for the drugs project and HIV-glycans one...Pedro Miguel y Jesús, para todas las discusiones y trabajos relacionados con el 2G12...Sonia y Juan por los glycan-arrays...Sonia again for the enzymatic reactions...Dodi, Harm, Martina and Hans, for their fundamental help and great ideas during the *S. pneumoniae* story...I had the opportunity to spend six months at the MCBi Department in Amsterdam, and really, it was an incredible experience... Thank you to all the people from the Red groups especially to the ones that are now my Friends...Gracias Juan...para haberme enseñado mucho, Maestro...Thank you Boris and Irma, for your interest on my work, for your help and for the ELISA story and the Galf one...Thank you Yvette for the glyco-immunology story and for the great impact in my life of the glyco-science you are doing ...Thank you Ron and Maria to be the first scientists who invited me for a seminar and for your scientific suggestions...Grazie ai miei vecchi Maestri...dal Liceo all'Università...Thank you to all my Motivations and to the Muse who inspired my days...Gracias Yury y Vicente...por motivarme:

"...Uno no puede ser científico si no siente la satisfacción de arrancarle algún secreto a la naturaleza por el bien colectivo"[cit.]...

CURRICULUM VITAE

PERSONAL INFORMATION

Name: FABRIZIO CHIODO
Address: Lungomare Cristoforo Colombo 3641, 90149, Palermo
Telephone: +393397829357, +34690079570
Fax: +34943005314
E-mail: chiodo.fabrizio@gmail.com
Nationality: Italian
Date of birth: 26-02-1985

WORK EXPERIENCE

- From 01/10/2006 to 01/07/2008 preparation of Master experimental Thesis in the department of Pharmaceutical technology at the University of Palermo, Italy.
Supervisor: L. I. Giannola
- From 01/10/2007 to 01/04/2008 stage at the Pharmacy of the Hospital "Ospedale Civico" in Palermo, Italy
- From 01/10/2008 to 01/04/2009 PhD student in CIC BiomaGUNE, San Sebastian, Spain, European fellowship Marie-Curie related with GLYCOGOLD project. Supervisors: S. Penadés and M. Marradi
- From 01/09/2009 to 01/03/2013 PhD student in CIC BiomaGUNE, San Sebastian, Spain, with national Spanish fellowship FPI, project CTQ2008-04638, Biofunctional nanoparticles for biosensors. Supervisors: S. Penadés and M. Marradi.
- From 01/10/2011 to 01/04/2012 Guest PhD student at the VU medical center, Amsterdam. Supervisor: Y. van Kooyk
- From 01/10/2011 to 01/04/2012 Guest PhD student at the VU medical center, Amsterdam. Supervisor: I. van Die

MAIN ACTIVITIES AND RESPONSIBILITIES

- Preparation and characterization of liposomes containing trehalose and studies of cell cryopreservation in association with the transplantation center ISMETT
- Synthesis of pro-drugs to increase the passage of BBB for Parkinson and Alzheimer diseases
- Galenic and advanced pharmaceutical formulations (microspheres and liposomes)
- Synthesis of complex oligomannosides related with HIV gp120 envelope glycoprotein and Lewis-type oligosaccharides by chemo-enzymatic synthesis

- Preparation of gold glyconanoparticles as anti HIV agents and drugs delivery system (contribution to European project CHAARM, Combined Highly Active Anti-retroviral Microbicides)
- Preparation of gold glyconanoparticles as carbohydrate-based vaccines platform against *S. pneumoniae* and HIV
- Behavior of human dendritic cells and T-cells in front of multivalent nano glycoconjugates: study of maturation markers and cytokines production

EDUCATION AND TRAINING

- 2003 – Diploma di maturità scientifica (High school diploma). Five years (Experimental class of Natural sciences) – Liceo scientifico statale Galileo Galilei, Palermo (100/100)
- 2008 – Degree and Master (300 ECTS) in Chemistry and Pharmaceutical Technologies, Faculty of Pharmacy, University of Palermo, 110/110 *cum laude*

PRINCIPAL SUBJECTS/OCCUPATIONAL SKILLS COVERED

- Multivalent Glycoconjugates.
- Glyco-nanotechnology (from carbohydrates synthesis to nanomaterials preparation and characterization).
- Glyco-immunology (dendritic cells mediated innate immunity).

PERSONAL SKILLS AND COMPETENCES

MOTHER TONGUE Italian

OTHER LANGUAGES

English

- Reading skills Excellent
- Writing skills Good
- Verbal skills Good

French (mother of Belgian origins)

- Reading skills Excellent
- Writing skills Basic
- Verbal skills Excellent

Spanish (European diplome D.E.L.E., Level B1)

- Reading skills Excellent
- Writing skills Good
- Verbal skills Excellent

SOCIAL SKILLS AND COMPETENCES

- 2001-2003 Leader of a young political party
- 2002-2003 Delegate of students at High school (Liceo scientifico Galileo Galilei)
- 2005-2008 Delegate of students at the Faculty of Pharmacy
- 2007-2008 Chairman and speaker at some public debates against mafia
- 2000-2005 Captain of an amateur football team

TECHNICAL SKILLS AND COMPETENCES

- Good skills in window, Microsoft word, Power point, Microsoft excel, Prezi
- Carbohydrate chemistry and related characterization techniques
- Gold nanoparticles preparation and characterization
- TEM microscopy user at CIC biomaGUNE
- FACS and ELISA
- Basic cell-culture laboratory

ARTISTIC SKILLS AND COMPETENCES

- Flute player
- Author of different political essays

SCIENTIFIC CONTRIBUTIONS

Conferences contributions

Authors: G. Giandalia, V. De Caro, M. G. Siragusa, F. Chiodo, L. Cordone, B. Gridelli, M. D'Amato, F. Triolo, L. I. Giannola

Title: Inclusion of trehalose into liposomes to regulate uptake of this cryoprotectant into human hepatocytes

Contribution type: Poster

Conference: Young pharmaceutical scientists, Nice, France, 7-8 June 2009

Publication: book of abstracts, p. 27

Authors: F. Chiodo, D. Safari, M. Marradi, H. A. Th. Dekker, Y. Shan, R. Adamo, S. Oscarson, G. Rijkers, M. Lahmann, J. P. Kamerling, H. Snippe, S. Penadés

Title: Gold nanoparticles coated with a synthetic epitope of *Streptococcus pneumoniae* capsular polysaccharide induce carbohydrate-specific immune response

Contribution type: Poster

Conference: "Glycomarkers for Disease" conference, Wierzba, Poland, 12-15 September 2010

Publication: book of abstracts, p. 43 (P2)

Authors: F. Chiodo, D. Safari, M. Marradi, H. Snippe, S. Penadés
Title: Immune response against gold glyconanoparticles
Contribution type: Poster
Conference: X Jornadas de Carbohidratos, Granada, Spain, 15-18 September 2010
Publication: book of abstracts, p. 105

Authors: F. Chiodo, D. Safari, M. Marradi, H. A. Th. Dekker, Y. Shan, R. Adamo, G. Rijkers, M. Lahmann, J. P. Kamerling, H. Snippe, S. Penadés
Title: A fully synthetic carbohydrate vaccine based on gold nanoparticles
Contribution type: Poster
Conference: Imagenenano, Bilbao, Spain, 11-14 April 2011
Publication: book of abstracts, p. 25

Authors: F. Chiodo, D. Safari, M. Marradi, H. A. Th. Dekker, Y. Shan, R. Adamo, S. Oscarson, G. Rijkers, M. Lahmann, J. P. Kamerling, H. Snippe, S. Penadés
Title: A Fully Synthetic Carbohydrate Vaccine Candidate Based on Gold Nanoparticles
Contribution type: **Oral**
Conference: XVI European Carbohydrate Symposium, Sorrento (Italy), 3-7 July 2011
Publication: book of abstracts, OL144

Authors: F. Chiodo, D. Safari, M. Marradi, H. A. Th. Dekker, Y. Shan, R. Adamo, S. Oscarson, G. Rijkers, M. Lahmann, J. P. Kamerling, H. Snippe, S. Penadés
Title: Towards a new synthetic carbohydrate-vaccine candidate based on gold glyconanoparticles
Contribution type: Poster
Conference: 21st International symposium on glycoconjugates, Vienna, Austria, 21-26 August 2011
Publication: Glycoconjugate Journal, 28, 5, p. 35

Authors: F. Chiodo, J. J Garcia-Vallejo, M. Marradi, S. Penadés, Y. van Kooyk
Title: Glyconanoparticles (GNPs) as a tool for study the role of carbohydrates in dendritic cells mediated innate immunity
Contribution type: **Oral**
Conference: 10th Jenner Glycobiology and Medicine Symposium, Den Haag, 31 March - 3 April 2012
Publication: book of abstracts

Authors: F. Chiodo, M. Marradi, J. J Garcia-Vallejo, M. Lahmann, J.P. Kamerling, H. Snippe, Y. van Kooyk, S. Penadés
Title: Glyco gold nanoparticles: new tool for glycoimmunology studies
Contribution type: **Oral**
Conference: Increasing the Impact of Glycoscience through New Tools and Technologies, San Sebastian, 19-21 July 2012
Publication: book of abstracts (F8)

Authors: F. Chiodo, J. J Garcia-Vallejo, M. Marradi, S. Bruijns, S. Penadés, Y. van Kooyk
Title: Synthetic Gold Glyconanoparticles induce an immunosuppressive state on dendritic cells
Contribution type: **Oral**
Conference: 26th International Carbohydrate Symposium (ICS 2012), Madrid, 22-27 July 2012.
Publication: book of abstracts (OC31)

Invitations

Seminar title: Glyco gold nanoparticles: an interesting tool to mimic carbohydrate antigens
Place: Leiden Medical center (LUMc), Parasitology Department
Date: 30.03.2012
Invited by: C. H. Hokke and M. Yazdanbakhsh

Publications

Authors: M. Marradi, F. Chiodo, I. García, S. Penadés
Title: Glycoliposomes and metallic glyconanoparticles in glycoscience, chapter 10
Journal/Book title: Synthesis and biological applications of glycoconjugates, Edited by O. Renaudet; Co-Edited by N. Spinelli, Bentham eBooks, ISBN: 978-1-60805-277-6.
Date of publication: 2011

Authors: M. Marradi, P. Di Gianvincenzo, P. M. Enríquez-Navas, O. M. Martínez-Ávila, F. Chiodo, E. Yuste, J. Angulo, S. Penadés
Title: Gold Nanoparticles Coated with High Mannose-Type Oligosaccharides Bind the HIV-1 Broadly Neutralizing Antibody 2G12 and Inhibit its Interaction with the Viral Envelope Glycoprotein gp120 and with the Virus
Journal/Book title: Journal of Molecular Biology, 410, 5, 798-810
Date of publication: 2011

Authors: D. Safari, M. Marradi, F. Chiodo, H. A. Th. Dekker, Y. Shan, R. Adamo, S. Oscarson, G. Rijkers, M. Lahmann, J. P. Kamerling, H. Snippe, S. Penadés
Title: Gold nanoparticles as carriers for a synthetic *S. pneumoniae* type 14 conjugate vaccine
Journal/Book title: Nanomedicine, 7, 5, 651–662
Date of publication: 2012

Authors: P. Di Gianvincenzo, F. Chiodo, M. Marradi, S. Penadés
Title: Gold manno-Glyconanoparticles for Intervening in HIV gp120 Carbohydrate-Mediated Processes
Journal/Book title: *Methods in Enzymology*, 509, 21-40
Date of publication: 2012

Authors: P. M. Enríquez-Navas*, F. Chiodo*, M. Marradi, J. Angulo, S. Penadés
Title: STD NMR Study of the Interaction between Antibody 2G12 and Synthetic Oligomannosides That Mimic Selected Branches of gp120 Glycans
Journal/Book title: *ChemBioChem*, 13, 1357-1365
Date of publication: 2012
* Authors contributed equally to this work

Authors: J. J. García-Vallejo, M. Ambrosini, A. Overbeek, H. van Riel, K. Bloem, W. W. J. Unger, F. Chiodo, J. G. Bolscher, K. Nazmi, H. Kalay, Y. van Kooyk
Title: Multivalent glycopeptide dendrimers for the targeted delivery of antigens to dendritic cells
Journal/Book title: *Mol. Immunol.*, *in press*
Data of publication: 2013

Authors: M. Marradi, F. Chiodo, I. García, S. Penadés
Title: Glyconanoparticles as multifunctional and multimodal carbohydrate systems
Journal/Book title: *Chem. Soc. Rev.*, *in press*
Data of publication: 2013

Authors: R. Murray, Y. Qiu, F. Chiodo, M. Marradi, S. Penadés, S. E. Moya
Title: A Quantitative Study of Intracellular Dynamics of Fluorescently Labelled Gold Nanoparticles via Fluorescence Correlation Spectroscopy
Journal/Book title: *Submitted*

Authors: F. Chiodo*, M. Marradi, B. Tefsen, H. Snippe, I. van Die, S. Penadés
Title: High Sensitive Detection of Carbohydrate Binding Proteins on an ELISA-Solid Phase Assay based on Multivalent Glyconanoparticles
Journal/Book title: *Submitted*
*Corresponding author

Authors: F. Chiodo, M. Marradi, J. Park, A. F. J. Ram, S. Penadés, I. van Die, B. Tefsen
Title: Galactofuranose-coated gold nanoparticles elicit a pro-inflammatory response in human monocyte-derived dendritic cells and interact with C-type lectins
Journal/Book title: *Manuscript in preparation*

Authors: F. Chiodo, J. J. Garcia-Vallejo, M. Marradi, S. Bruijns, S. Penades, Y. van Kooyk.
Title: DC-SIGN targeting glycan nanoparticles for effective modulation of T cells responses
Journal/Book title: *Manuscript in preparation*

Awards

2010: First price for the best poster in the field of experimental work in the Glycomarkers for disease conference, Wierzba, Poland, 12-15 September 2010

2011: Best poster prize in the 21st International symposium on glycoconjugates, Vienna, Austria, 21-26 August 2011

2012: Prize for one of the best Oral Communication presented by Young Investigators in the 26th International Carbohydrate Symposium (ICS 2012), Madrid, 22-27 July 2012

